Methods and Protocols
in Food Science

Springer Protocols

Cinthia Baú Betim Cazarin *Editor*

Basic Protocols in Foods and Nutrition

Humana Press

Methods and Protocols in Food Science

Series Editor
Anderson Sant'Ana
University of Campinas
Campinas, Brazil

For further volumes:
http://www.springer.com/series/16556

Methods and Protocols in Food Science series is devoted to the publication of research protocols and methodologies in all fields of food science.

Volumes and chapters will be organized by field and presented in such way that the readers will be able to reproduce the experiments in a step-by-step style. Each protocol will be characterized by a brief introductory section, followed by a short aims section, in which the precise purpose of the protocol will be clarified.

Basic Protocols in Foods and Nutrition

Edited by

Cinthia Baú Betim Cazarin

School of Food Engineering, University of Campinas, Campinas, São Paulo, Brazil

Humana Press

Editor
Cinthia Baú Betim Cazarin
School of Food Engineering
University of Campinas
Campinas, São Paulo, Brazil

ISSN 2662-950X ISSN 2662-9518 (electronic)
Methods and Protocols in Food Science
ISBN 978-1-0716-2344-2 ISBN 978-1-0716-2345-9 (eBook)
https://doi.org/10.1007/978-1-0716-2345-9

This Humana imprint is published by the registered company Springer Science+Business Media, LLC, part of Springer Nature.
The registered company address is: 1 New York Plaza, New York, NY 10004, U.S.A.

Preface to the Series

Methods and Protocols in Food Science series is devoted to the publication of research protocols and methodologies in all fields of food science. The series is unique as it includes protocols developed, validated, and used by food and related scientists as well as theoretical bases for each protocol. Aspects related to improvements in the protocols, adaptations, and further developments in the protocols may also be approached.

Methods and Protocols in Food Science series aims to bring the most recent developments in research protocols in the field as well as very well established methods. As such the series targets undergraduates, graduates, and researchers in the field of food science and correlated areas. The protocols documented in the series will be highly useful for scientific inquiries in the field of food sciences, presented in such way that the readers will be able to reproduce the experiments in a step-by-step style.

Each protocol will be characterized by a brief introductory section, followed by a short aims section, in which the precise purpose of the protocol is clarified. Then, an in-depth list of materials and reagents required for employing the protocol is presented, followed by a comprehensive and step-by-step procedures on how to perform that experiment. The next section brings the dos and don'ts when carrying out the protocol, followed by the main pitfalls faced and how to troubleshoot them. Finally, template results will be presented and their meaning/conclusions addressed.

The Methods and Protocols in Food Science series will fill an important gap, addressing a common complain of food scientists, regarding the difficulties in repeating experiments detailed in scientific papers. With this, the series has a potential to become a reference material in food science laboratories of research centers and universities throughout the world.

Campinas, São Paulo, Brazil — *Anderson S. Sant'Ana*

Preface

Nutrition is a science that studies the physiological effects of food intake for health promotion and disease prevention. The knowledge about food composition and the effects of bioactive compounds on health has grown increasingly in the last few years. Research in different areas has contributed to understanding how nutrients and non-nutrients impact and protect the body against aging and the development of some diseases, especially non-communicable diseases. The COVID-19 pandemic reinforced the importance of having good health and a good lifestyle, including healthy nutrition and exercise. The use of standardized procedures to evaluate the food intake and predict the individual's nutritional status is mandatory to establish the proper clinical procedures and compare data with databases, guidelines, and other studies. In this way, the book *Basic Protocols in Foods and Nutrition* makes a part of the book series Methods and Protocols in Food Science. This book is presented in two parts: the first part deals with protocols used in experimental studies with rats and mice, and the second part focuses on protocols applied in clinical trials.

This book aims to help researchers design and execute their research using standardized protocols that facilitate the application of fundamental concepts and make comparisons with the literature. In the first part, you will find protocols on how to prepare experimental diets and monitor food intake and weight gain, as well as many protocols that help you to evaluate biological samples and predict physiological changes, and the final chapter of this part shows you a protocol that can be used to evaluate the bioavailability of bioactive compounds. In the second part, you will find protocols used in clinical practice that will permit you to establish the nutritional status of the individual or population studied. In this way, protocols about anamnesis, evaluation of food intake and appetite, measuring the metabolic rate, assessing the body composition, assessing glucose homeostasis, and monitoring the metabolomic pathways are presented. Finally, I would thank all the authors who contributed with their expertise to this book; our main goal with this book is to spread our knowledge and contribute to the development of nutrition science.

Campinas, São Paulo, Brazil ***Cinthia Baú Betim Cazarin***

Contents

Preface to the Series . . . . . *v*
Preface . . . . . *vii*
Contributors . . . . . *xi*

PART I ANIMAL EXPERIMENTATION

1 Experimental Diets (Normocaloric and Hypercaloric Diets) 3
Laís Marinho Aguiar, Juliana Kelly da Silva-Maia, and Cinthia Baú Betim Cazarin

2 Measures of Food Intake, Body Weight Gain, and Energy Efficiency in Mice 17
Cíntia Reis Ballard and Cinthia Baú Betim Cazarin

3 The Assessment of Glucose Homeostasis in Rodents: Glucose, Insulin and Pyruvate Tolerance Tests 33
Nathalia Romanelli Vicente Dragano and Edward Milbank

4 Histopathological Evaluation of Steatohepatitis in Animal Experiments 53
Yoshihisa Takahashi, Erdenetsogt Dungubat, Hiroyuki Kusano, and Toshio Fukusato

5 Quantification of Short-Chain Fatty Acids in Feces 73
Mirella Romanelli Vicente Bertolo and Stanislau Bogusz Junior

6 Quantification of Non-esterified Fatty Acids in Serum and Plasma 93
Mirella Romanelli Vicente Bertolo and Stanislau Bogusz Junior

7 Lipid Peroxidation (TBARS) in Biological Samples 107
Lilian Regina Barros Mariutti

8 Extraction of Bile Acids from Biological Samples and Quantification Using Ultra-High-Performance Liquid Chromatography-Orbitrap Mass Spectrometry 115
Shota Hori, Hongxia Liu, Riho Yamada, Shun Ichitsubo, Ayana Sakaguchi, Fumika Yokoyama, and Satoshi Ishizuka

9 Glycogen Measurement 129
Cláudia Regina Cavaglieri, Carlos Alberto da Silva, and Celene Fernandes Bernardes

10 Evaluation of the Minerals and Trace Elements in the Biological Samples 145
Duygu Aydemir and Nuriye Nuray Ulusu

11 Microbiome Evaluation 169
Alba Rodríguez-Nogales, Antonio Jesús Ruiz-Malagón, Jose Alberto Molina-Tijeras, Maria Elena Rodríguez-Cabezas, and Julio Gálvez

12 The GSH Colorimetric Method as Measurement of Antioxidant Status in Serum and Rodent Tissues 187
Milena Morandi Vuolo, Juliana Kelly da Silva-Maia, and Ângela Giovana Batista

13 Guidance for Designing a Preclinical Bioavailability Study of Bioactive Compounds 195
Helena Dias de Freitas Queiroz Barros, Cinthia Baú Betim Cazarin, and Mario Roberto Maróstica Junior

Part II Clinical Trials

14 Protocols Related to Nutritional Anamnesis in Head and Neck Cancer Patients 209
Judith Büntzel and Jens Büntzel

15 Food Diary, Food Frequency Questionnaire, and 24-Hour Dietary Recall 223
Luisa Saravia, Paula Moliterno, Estela Skapino, and Luis A. Moreno

16 The Use of Questionnaires to Measure Appetite 249
James H. Hollis

17 Protocols for the Use of Indirect Calorimetry in Clinical Research 265
Katherine L. Ford, Camila L. P. Oliveira, Stephanie M. Ramage, and Carla M. Prado

18 Anthropometric Assessment Methods for Adults and Older People 293
Thalita Cremonesi Pereira and Cinthia Baú Betim Cazarin

19 MRI-Based Body Composition Analysis 307
Magnus Borga, André Ahlgren, and Sarah Weston

20 Functional Tests for Assessing Human Beta-Cell Function and Insulin Sensitivity 335
Marcelo Miranda de Oliveira Lima and Bruno Geloneze

21 Maximum Oxygen Consumption: $\dot{V}O_{2\ max}$ Laboratory Assessment 367
Mara Patrícia Traina Chacon-Mikahil, Alex Castro, Danilo dos Santos Caruso, and Arthur Fernandes Gáspari

22 Muscle and Fat Biopsy and Metabolomics 381
Cláudia Regina Cavaglieri, Mara Patrícia Traina Chacon-Mikahil, Renata Garbellini Duft, Ivan Luiz Padilha Bonfante, Arthur Fernandes Gáspari, and Alex Castro

Index 407

Contributors

Laís Marinho Aguiar • *Department of Food Science and Nutrition, School of Food Engineering, University of Campinas (UNICAMP), Campinas, São Paulo, Brazil*

André Ahlgren • *AMRA Medical AB, Linköping, Sweden*

Duygu Aydemir • *Koc University, School of Medicine, Department of Medical Biochemistry, Sariyer, Istanbul, Turkey; Koç University Research Center for Translational Medicine (KUTTAM), Sariyer, Istanbul, Turkey*

Cíntia Reis Ballard • *Department of Food Science and Nutrition, School of Food Engineering, University of Campinas (UNICAMP), Campinas, São Paulo, Brazil*

Ângela Giovana Batista • *Department of Food and Nutrition, Universidade Federal de Santa Maria (UFSM), Palmeira das Missões, RS, Brazil*

Celene Fernandes Bernardes • *Faculty of Chemistry, Pontifical Catholic University of Campinas (PUC-C), Campinas, São Paulo, Brazil*

Mirella Romanelli Vicente Bertolo • *University of São Paulo (USP), São Carlos Institute of Chemistry (IQSC), São Carlos, São Paulo, Brazil*

Stanislau Bogusz Junior • *University of São Paulo (USP), São Carlos Institute of Chemistry (IQSC), São Carlos, São Paulo, Brazil*

Ivan Luiz Padilha Bonfante • *Exercise Physiology Laboratory (FISEX), School of Physical Education, University of Campinas (UNICAMP), Campinas, São Paulo, Brazil; Federal Institute of Education, Science and Technology of São Paulo - IFSP, Hortolândia, São Paulo, Brazil*

Magnus Borga • *Department of Biomedical Engineering, Linköping University, Linköping, Sweden; AMRA Medical AB, Linköping, Sweden*

Jens Büntzel • *Department of Otorhinolaryngology, Head Neck Surgery, Suedharz Klinikum Nordhausen, Nordhausen, Germany*

Judith Büntzel • *Department of Hematology & Medical Oncology, University Hospital Göttingen, Göttingen, Germany*

Alex Castro • *Exercise Physiology Laboratory (FISEX), School of Physical Education, University of Campinas (UNICAMP), Campinas, São Paulo, Brazil; Nuclear Magnetic Resonance Laboratory, Department of Chemistry, Federal University of São Carlos (UFSCar), São Carlos, São Paulo, Brazil*

Cláudia Regina Cavaglieri • *Exercise Physiology Laboratory (FISEX), School of Physical Education, University of Campinas (UNICAMP), Campinas, São Paulo, Brazil*

Cinthia Baú Betim Cazarin • *Department of Food Science and Nutrition, School of Food Engineering, University of Campinas (UNICAMP), Campinas, São Paulo, Brazil*

Mara Patrícia Traina Chacon-Mikahil • *Exercise Physiology Laboratory (FISEX), School of Physical Education, University of Campinas (UNICAMP), Campinas, São Paulo, Brazil*

Nathalia Romanelli Vicente Dragano • *Department of Physiology, CiMUS, University of Santiago de Compostela-Instituto de Investigación Sanitaria, Santiago de Compostela, Spain*

Renata Garbellini Duft • *Exercise Physiology Laboratory (FISEX), School of Physical Education, University of Campinas (UNICAMP), Campinas, São Paulo, Brazil*

Erdenetsogt Dungubat • *Department of Pathology, School of Medicine, International University of Health and Welfare, Narita, Japan*
Katherine L. Ford • *Human Nutrition Research Unit, Department of Agricultural, Food & Nutritional Science, University of Alberta, Edmonton, AB, Canada*
Helena Dias de Freitas Queiroz Barros • *Department of Food Science and Nutrition, School of Food Engineering, University of Campinas (UNICAMP), Campinas, São Paulo, Brazil*
Toshio Fukusato • *General Medical Education and Research Center, Teikyo University, Tokyo, Japan*
Julio Gálvez • *CIBER-EHD, Department of Pharmacology, Center for Biomedical Research (CIBM), University of Granada, Granada, Spain; Instituto de Investigación Biosanitaria de Granada (ibs.GRANADA), Granada, Spain*
Arthur Fernandes Gáspari • *Exercise Physiology Laboratory (FISEX), School of Physical Education, University of Campinas (UNICAMP), Campinas, São Paulo, Brazil; Brazilian Sport Climbing Association, São Paulo, Brazil; Sidia Institute of Science and Technology, Manaus, Amazonas, Brazil*
Bruno Geloneze • *Laboratory of Investigation in Metabolism and Diabetes (LIMED), Faculty of Medical Sciences, University of Campinas, Campinas, São Paulo, Brazil; Obesity and Comorbidities Research Center (OCRC), University of Campinas, Campinas, São Paulo, Brazil; National Council for Scientific and Technological Development (CNPq), National Institute of Science and Technology of Obesity and Metabolism, Campinas, São Paulo, Brazil*
James H. Hollis • *Department of Food Science and Human Nutrition, Iowa State University, Ames, IA, USA*
Shota Hori • *Research Faculty of Agriculture, Hokkaido University, Sapporo, Hokkaido, Japan*
Shun Ichitsubo • *Research Faculty of Agriculture, Hokkaido University, Sapporo, Hokkaido, Japan*
Satoshi Ishizuka • *Research Faculty of Agriculture, Hokkaido University, Sapporo, Hokkaido, Japan*
Hiroyuki Kusano • *Department of Pathology, School of Medicine, International University of Health and Welfare, Narita, Japan*
Hongxia Liu • *Research Faculty of Agriculture, Hokkaido University, Sapporo, Hokkaido, Japan*
Lilian Regina Barros Mariutti • *Department of Food Science and Nutrition, School of Food Engineering, University of Campinas (UNICAMP), Campinas, São Paulo, Brazil*
Mario Roberto Maróstica Junior • *Department of Food Science and Nutrition, School of Food Engineering, University of Campinas (UNICAMP), Campinas, São Paulo, Brazil*
Edward Milbank • *Department of Physiology, CiMUS, University of Santiago de Compostela-Instituto de Investigación Sanitaria, Santiago de Compostela, Spain*
Jose Alberto Molina-Tijeras • *CIBER-EHD, Department of Pharmacology, Center for Biomedical Research (CIBM), University of Granada, Granada, Spain; Instituto de Investigación Biosanitaria de Granada (ibs.GRANADA), Granada, Spain*
Paula Moliterno • *Departamento de Nutrición Clínica, Escuela de Nutrición, Universidad de la República, Montevideo, Uruguay*
Luis A. Moreno • *GENUD (Growth, Exercise, Nutrition and Development) Research Group, University of Zaragoza, Instituto Agroalimentario de Aragón (IA2), Instituto de Investigación Sanitaria de Aragón (IIS Aragón), Zaragoza, Spain; Centro de Investigación Biomédica en Red de Fisiopatología de la Obesidad y Nutrición (CIBEROBN), Instituto de Salud Carlos III, Madrid, Spain*

Camila L. P. Oliveira • *Human Nutrition Research Unit, Department of Agricultural, Food & Nutritional Science, University of Alberta, Edmonton, AB, Canada*
Marcelo Miranda de Oliveira Lima • *Laboratory of Investigation in Metabolism and Diabetes (LIMED), Faculty of Medical Sciences, University of Campinas, Campinas, São Paulo, Brazil*
Thalita Cremonesi Pereira • *Department of Food Science and Nutrition, School of Food Engineering, University of Campinas (UNICAMP), Campinas, São Paulo, Brazil*
Carla M. Prado • *Human Nutrition Research Unit, Department of Agricultural, Food & Nutritional Science, University of Alberta, Edmonton, AB, Canada*
Stephanie M. Ramage • *Human Nutrition Research Unit, Department of Agricultural, Food & Nutritional Science, University of Alberta, Edmonton, AB, Canada*
Maria Elena Rodríguez-Cabezas • *CIBER-EHD, Department of Pharmacology, Center for Biomedical Research (CIBM), University of Granada, Granada, Spain; Instituto de Investigación Biosanitaria de Granada (ibs.GRANADA), Granada, Spain*
Alba Rodríguez-Nogales • *CIBER-EHD, Department of Pharmacology, Center for Biomedical Research (CIBM), University of Granada, Granada, Spain; Instituto de Investigación Biosanitaria de Granada (ibs.GRANADA), Granada, Spain; Servicio de Digestivo, Hospital Universitario Virgen de las Nieves, Granada, Spain*
Antonio Jesús Ruiz-Malagón • *CIBER-EHD, Department of Pharmacology, Center for Biomedical Research (CIBM), University of Granada, Granada, Spain; Instituto de Investigación Biosanitaria de Granada (ibs.GRANADA), Granada, Spain*
Ayana Sakaguchi • *Research Faculty of Agriculture, Hokkaido University, Sapporo, Hokkaido, Japan*
Danilo dos Santos Caruso • *Laboratory of Exercise Physiology, School of Physical Education, University of Campinas (UNICAMP), Campinas, São Paulo, Brazil; Brazilian Sport Climbing Association (ABEE), São Paulo, Brazil*
Luisa Saravia • *Centro de Posgrado, Escuela de Nutrición, Universidad de la República, Montevideo, Uruguay*
Carlos Alberto da Silva • *Paulista University (UNIP), Campinas, São Paulo, Brazil; University Center UNIMETROCAMP Wyden, Campinas, São Paulo, Brazil*
Juliana Kelly da Silva-Maia • *Department of Nutrition, Federal University of Rio Grande do Norte (UFRN), Natal, RN, Brazil*
Estela Skapino • *Departamento de Nutrición Clínica, Escuela de Nutrición, Universidad de la República, Montevideo, Uruguay*
Yoshihisa Takahashi • *Department of Pathology, School of Medicine, International University of Health and Welfare, Narita, Japan*
Nuriye Nuray Ulusu • *Koc University, School of Medicine, Department of Medical Biochemistry, Sariyer, Istanbul, Turkey; Koç University Research Center for Translational Medicine (KUTTAM), Sariyer, Istanbul, Turkey*
Milena Morandi Vuolo • *Department of Food Science and Nutrition, School of Food Engineering, University of Campinas (UNICAMP), Campinas, São Paulo, Brazil*
Sarah Weston • *AMRA Medical AB, Linköping, Sweden; Edinburgh Imaging Academy, University of Edinburgh, Edinburgh, UK*
Riho Yamada • *Research Faculty of Agriculture, Hokkaido University, Sapporo, Hokkaido, Japan*
Fumika Yokoyama • *Research Faculty of Agriculture, Hokkaido University, Sapporo, Hokkaido, Japan*

Part I

Animal Experimentation

Chapter 1

Experimental Diets (Normocaloric and Hypercaloric Diets)

Laís Marinho Aguiar, Juliana Kelly da Silva-Maia, and Cinthia Baú Betim Cazarin

Abstract

Animal models are widely used in scientific research to understand human and animal anatomy and physiology, pathology, and pharmacology. Animal selection (species, lineage, sex, age, etc.) and the diet offered to them are fundamental to the experimentation. The high obesity rates and the outcomes associated with increased adipose tissue led many researchers to investigate mechanisms and molecular pathways activated in this condition. The literature has proposed diet formulations to simulate different obesity-related outcomes. This chapter describes the step-by-step formulation of a normocaloric diet used as a control diet and two options of hypercaloric ones.

Key words Experimental diets, Formulated diets, Diet-induced obesity, Obesity

1 Introduction

Eating habits have a strong impact on health and, thus, on diverse chronic complications. Considering the association between diet and the development and prevention of pathologies, its composition is a relevant factor for study [1]. The high obesity rates and the outcomes associated with increased adipose tissue led many researchers to investigate mechanisms and molecular pathways activated in this condition.

Animal models are widely used in scientific research to understand human and animal anatomy, as well as physiology, pathology, and pharmacology [2]. Note that studies in nutrition that seek to assess the metabolic and physiological consequences of excessive weight gain widely use animal experimentation. Beyond obesity studies, changing the diet formulation by adding or excluding compounds can help to understand the effect of nutrients and non-nutrients in health or disease conditions. In this way, nutritionally adequate and standardized diets for laboratory animals

Cinthia Baú Betim Cazarin (ed.), *Basic Protocols in Foods and Nutrition*,
Methods and Protocols in Food Science, https://doi.org/10.1007/978-1-0716-2345-9_1,

reduce variations and biases in the studies and facilitate interpretation and comparison of results among experiments [3].

The protocols published by the American Nutrition Institute (AIN), through an *ad hoc* committee, with the purified diet for rodents have guided experimental research around the world since 1976. Despite the critics of the AIN formulation, this diet is widely used as a control normocaloric diet. Also, adding or removing ingredients can easily modify this formulation [3].

After its first publication in 1976, a modified version, AIN-93, was published in 1993. The formulation of these purified diets specifically considers the life stage requirements: the AIN-93G is proper to support growth, lactation, and pregnancy phases; and the AIN-93 M is for the adult stage when the requirements are for maintenance only. The AIN-93 M diet has a lower protein and fat content compared with AIN-93G [3].

Corn starch, maltodextrin, sucrose, and cellulose stand out as the carbohydrate sources in the AIN-93 formulation. The previous formulation, AIN-76, contained a higher sucrose concentration. However, studies observed that large amounts of sucrose contribute to adverse effects, such as hyperlipidemia and liver damage [4]. Thus, the AIN-93 formulation incorporated corn starch as the main carbohydrate source, with sucrose added only to promote palatability and disperse vitamins and minerals. The protein source is casein due to its amino acid composition and relatively low cost. Soy oil is fat source due to the supply of essential fatty acids: linoleic and linolenic. Despite not being an essential nutrient for rodents, the formulation also contains fibers to modulate the animal's microbiota. Vitamins and minerals are also added to prevent oxidation, renal calcification, and to act as essential cofactors on metabolic processes [5].

The literature describes several diet formulations for experimental studies. For obesity induction, for example, some hypercaloric and hyperlipidic diet formulations are widely used due to their similarity to the eating habits currently observed in the population and to the efficiency presented in studies.

Researchers have analyzed the amount of fat necessary to induce obesity in animals, which is between 30% and 60% of the total energy value – including saturated, monounsaturated, and polyunsaturated fats [6, 7]. Thus, using a high-fat diet with animal fat and low content of vegetable oils rich in omega 3, 6, and 9 fatty acids could be a viable option [8].

Offering the animals, a diet rich in fat is associated with the consequences of a diet with poor nutritional value, like those observed in overeating and sedentary humans, the two main risk factors for developing metabolic syndrome [8, 9]. Data from National Health and Nutrition Examination Survey (NHANES 2015–2016) also shows that the American diet consists of 49% of carbohydrates, 35% of lipids, and 16% of protein, which is very

similar to the high-fat diet proposed in this chapter, with 46% of carbohydrates, 35% of lipids, and 14% of protein [10]. This type of diet contributes to increased energy storage and fat depots in organs, such as the liver, muscle, and heart [11, 12]. Also, the increment on adipose tissue increases the release of pro-inflammatory cytokines and adipokines, contributing to the pro-inflammatory status associated with obesity.

In experimental nutrition studies, lard is one of the main saturated fat sources for high-fat diets [13–15]. The intake of saturated fatty acid, especially palmitic acid, is associated with a decrease in insulin signaling in the central nervous system, leading to insulin resistance (IR) in the brain and obesity [16]. The consumption of saturated fatty acids increases LDL-cholesterol (low--density lipoprotein) concentrations, thus explaining its association with an increased risk of developing cardiovascular diseases [17].

Note that the type and proportion of fatty acids in the diet impact health and body physiology [18]. Studies reported that consuming ω-3 polyunsaturated fatty acids is more beneficial to health than ω-6 polyunsaturated fatty acids since the former is anti-inflammatory while the second is pro-inflammatory [19].

Sucrose and fructose (simple sugars) consumption has also been associated with increased weight gain. Sucrose provides considerable amounts of carbohydrates that are quickly absorbed, contributing to overeating, weight gain, and the development of the metabolic syndrome. On the other hand, fructose, which has been used to replace sucrose in industrial products due to its sweetness and lower cost, favors lipogenesis and may contribute to hyperlipidemia. Fructose also does not reduce the levels of ghrelin, a hunger-signaling hormone, nor does it stimulate the release of insulin and leptin, related to satiety, contributing to a positive energy balance [20–23].

Thus, the use of diets rich in lipids and simple sugars to simulate the pattern observed in the human population is advised especially in studies that focus on obesity and metabolic disorders associated with the consumption of an unhealthy diet.

Given the above, the study with animals becomes a valuable tool since it allows controlling variables, such as diets, which can contribute to understanding the pathways related to the development of chronic diseases. Therefore, this chapter shows the step-by-step preparation of three kinds of experimental diets used as control normocaloric and hypercaloric diets.

2 Normocaloric and Normolipid Diet – AIN-93G and AIN-93 M

2.1 Material

Table 1 shows a list of ingredients for the AIN-93G and AIN-93 M diets (per kilogram of diet) [5], which should be of the greatest quality and purchased from reputable suppliers. First, separate the

Table 1
Composition of normocaloric and normolipid purified diets described by the American Institute of Nutrition

Ingredients	AIN-93G g/kg diet	AIN-93 M
Cornstarch	397.486	465.692
Casein (≥85% protein)	200.000	140.000
Dextrinized cornstarch (90–94%)	132.000	155.000
Sucrose	100.000	100.000
Soybean oil (no additives)	70.000	40.000
Fiber (cellulose)	50.000	50.000
Mineral mix (AIN-93 M-MV)	35.000	35.000
Vitamin mix (AIN-93-Vx)	10.000	10.000
L-cystine	3.000	1.800
Choline bitartrate (41.1% choline)	2.500	2.500
Tert-butylhydroquinone	0.014	0.014

Adapted from Reeves et al. [3]
AIN-93G diet for growth, lactation, and pregnancy stages of rodents, *AIN-93 M* diet for maintenance of adult rodents

ingredients, beakers, bowls, sieves, and scale and calculate the necessary amount for the experiment according to the following equation:

$$\text{Diet}(g) = N \times \text{DI} \times \text{EP}$$

N = number of animals.
DI = diet ingestion (g/day).
EP = experimental period (days).

The necessary instruments are:

- Bowl.
- Analytical and semi-analytical scale.
- Sieve (6–7 mesh).
- Air-circulation oven.
- Thermometer.
- Refrigerator or freezer.

Although some suppliers dedicated to animal experimentation sell mineral and vitamin mixes, they can be found in veterinary manipulation pharmacies or prepared in the laboratory if all the ingredients are available (Tables 2 and 3). Both mixes can be stored between −20 °C to −80 °C for 6 months. Vitamins should be stored in a dark package or dark bottle to avoid oxidation.

Table 2
Mineral mix for purified diets

Ingredients	AIN-93G-MX g/kg	AIN-93 M-MX
Essential mineral element		
Calcium carbonate, anhydrous, 40.04% ca	357.00	357.00
Potassium phosphate, monobasic, 22.76% P; 28.73% K	196.00	250.00
Potassium citrate, tri-potassium, monohydrate, 36.16% K	70.78	28.00
Sodium chloride, 39.34% Na; 60.66% cl	74.00	74.00
Potassium sulfate, 44.87% K; 18.39% S	46.60	46.60
Magnesium oxide, 60.32% mg	24.00	24.00
Ferric citrate, 16.5% Fe	6.06	6.06
Zinc carbonate, 57.47% Zn	1.65	1.65
Manganous carbonate, 47.79% Mn	0.63	0.63
Cupric carbonate, 57.47% cu	0.30	0.30
Potassium iodate, 59.3% I	0.01	0.01
Sodium selenate, anhydrous, 41.79% se	0.01025	0.01025
Ammonium paramolybdate, 4 hydrate, 54.34% Mo	0.00795	0.00795
Potentially beneficial mineral element		
Sodium meta-silicate, 9 hydrate, 9.88% Si	1.45	1.45
Chromium potassium sulfate, 12 hydrate, 10.42%	0.275	0.275
Lithium chloride, 16.38% li	0.0174	0.0174
Boric acid, 17.5% B	0.0815	0.0815
Sodium fluoride, 45.24% F	0.0635	0.0635
Nickel carbonate, 45% Ni	0.0318	0.0318
Ammonium vanadate, 43.55% V	0.0066	0.0066
Powdered sucrose	221.026	209.806

Adapted from Reeves et al. [3]

2.2 Preparation of the Normocaloric and Normolipid Diet

1. Check if casein protein content is over 85% by proximate composition before the preparation. The protein concentration of casein is required to ensure that the final diet composition corresponds to the protocol (around 17% in AIN-93G, and 12% in AIN-93 M).
2. Calculate the amounts of the ingredients necessary to prepare the diet for your experiment (*see* **Note 1**).

Table 3
Vitamin mix for AIN-93G and AIN-93 M

Vitamin	g/kg
Nicotinic acid	3.000
Ca pantothenate	1.600
Pyridoxine-HCl	0.700
Thiamin-HCl	0.600
Riboflavin	0.600
Folic acid	0.200
D-biotin	0.020
Vitamin B-12 (cyanocobalamin) (0.1% in mannitol)	2.500
Vitamin E (all-rac-α-tocopheryl acetate) (500 IU/g)	15.00
Vitamin A (all-trans-retinyl palmitate) (500,000 IU/g)	0.800
Vitamin D3 (cholecalciferol) (400,000 IU/g)	0.250
Vitamin K (phylloquinone)	0.075
Powdered sucrose	974.655

Adapted from Reeves et al. [3]

3. Prepare the diet under low-light conditions to minimize vitamin degradation.
4. Weigh all ingredients according to the amount of diet required for the experiment (Table 1) (*see* **Notes 2** and **3**).
5. Mix all the ingredients manually in a bowl in descending order of quantity (the smaller quantities first), except the oil.
6. Mix the ingredients slowly to reduce dust.
7. Sieve the diet powder 3 times in a 6- to 7-mesh sieve to mix and homogenize the formulation.
8. Add the oil slowly, mixing the entire diet.
9. Sieve the diet powder 3 times in a 6- to 7-mesh sieve to mix and homogenize the formulation (*see* **Note 4**).
10. Place the diet on plastic bags, identify, and store at 4–10 °C until pelletization.
11. Determine analytically the powder diet proximate composition (lipid, protein, ashes, humidity, and carbohydrates) to check the nutrient distribution (*see* **Notes 5** and **6**).
12. Pelletize the AIN diet powder either by extrusion or manually.
13. Add water gradually until forming a dough, then roll it into a cylinder and cut each 2–3 cm for manual pelletizing.

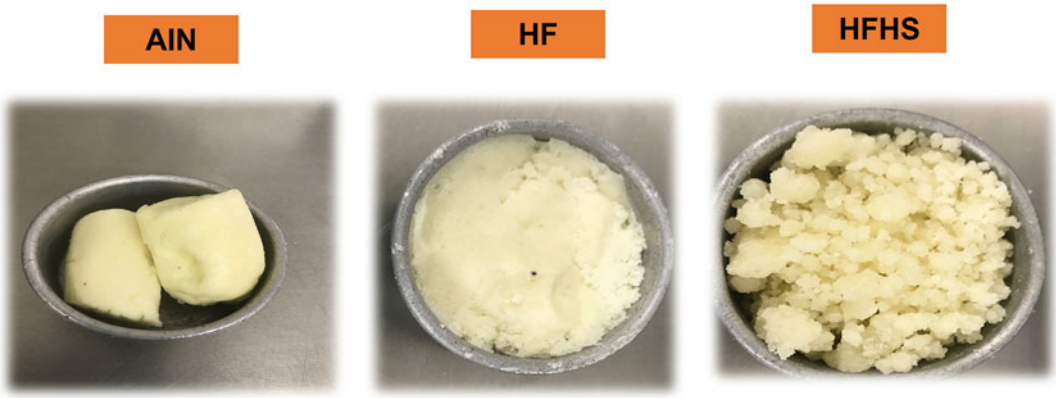

Fig. 1 Samples of the normocaloric diet AIN-93G, and both hypercaloric diets (high-fat diet and high-fat high-sucrose). (Source: Photos from the personal archive of Laís Aguiar Marinho)

14. Place the pellets onto trays to dry in the air-circulation oven at 40–50 °C (Fig. 1).
15. Store the diet in lidded plastic containers at 4 °C for 3 months or frozen for 6 months.
16. Monitor deterioration.

3 Hyperlipidic Diet (High-Fat Diet or HF Diet)

Largely used as a diet-induced obesity (DIO) model, the high-fat diet is adequate to promote weight gain, hyperinsulinemia, hyperglycemia, and hypertension in C57BL/6 J mouse compared with the cafeteria diet (another DIO model) [24].

The literature proposed many HF diet formulations with different concentrations of lipids as an incremental energy source [8]. This chapter will describe the step-by-step formulation of an HF diet with 35% of energy from lipid sources – 31% from lard and 4% from soy oil.

3.1 Material

All the ingredients described in the AIN diet are used to prepare this formulation, including lard. The literature has evidence that a diet rich in saturated fatty acids has more accentuated pro-inflammatory effects than one rich in polyunsaturated sources [25].

The necessary instruments are:

- Bowl.
- Analytical and semi-analytical scale.
- Sieve (6–7 mesh).

- Air-circulation oven.
- Thermometer.
- Refrigerator or freezer.

3.2 Methods

1. Check if casein protein content is over 85% by proximate composition before preparing the diet. The protein concentration of casein is required to ensure the protein concentration in the diet.
2. Calculate the amounts of the ingredients necessary to prepare the diet for your experiment (*see* **Note 1**).
3. Prepare the diet under low-light conditions to minimize vitamin degradation.
4. Weigh all ingredients according to the amount of diet required for the experiment (Table 4) (*see* **Notes 2** and **3**).
5. Mix all the ingredients manually in a bowl in descending order of quantity (the smaller quantities first), except the oil and lard.
6. Mix the ingredients slowly to reduce dust.
7. Sieve the diet powder 3 times in a 6- to 7-mesh sieve to mix and homogenize the formulation.
8. Add the oil slowly, mixing the entire diet.

Table 4
Formulation of HF diet

Ingredients	(g/1000 g)
Corn starch	221.00
Casein	140.00
Maltodextrin	90.00
Sucrose	100.00
Soybean oil	40.00
Lard	310.00
Microcrystalline cellulose	50.00
Mineral mix	35.00
Vitamin mix	10.00
L-cystine	1.80
Choline Bitartrate (41.1% choline)	2.50
T-butyl-hydroquinone	0.008
Total	**1000 g**

9. Sieve the diet powder 3 times in a 6- to 7-mesh sieve to mix and homogenize the formulation (*see* **Note 4**).
10. Add the lard to the diet and homogenize manually (*see* **Note 7**).
11. Place the diet on plastic bags, identify, and store at 4–10 °C (this diet is not pelletized).
12. Determine analytically the powder diet proximate composition (lipid, protein, ashes, humidity, and carbohydrates) to check the nutrient distribution (*see* **Notes 5** and **6**).
13. Store the diet in lidded plastic containers at 4 °C for 3 months or frozen for 6 months at most.
14. Monitor deterioration.

4 Hypercaloric Diet (High-Fat and High-Sucrose Diet or HFHS)

The high-fat and high-sucrose diet (HFHS diet) better resemble modern human food consumption patterns. Simple carbohydrates, such as sucrose, and fat are incorporated in its formulation to achieve a typical fast-food diet [26].

The World Health Organization (WHO) recommends reducing the daily consumption of free sugars to less than 10% of the total energy value since higher intake may contribute to adverse effects, such as overweight, obesity, insulin resistance, and diabetes [27–30].

4.1 Material

The literature proposes several HFHS diet formulations. We will present three options: one of them prepared by our research group and two commercially available. The main goal of this diet is to increase the sources of simple carbohydrates and fat to make a hyperglicidic and hyperlipidic diet. The HFHS diet has the same ingredients as the AIN-93 diet but in different proportions (Table 5).

- Bowl.
- Analytical and semi-analytical scale.
- Sieve (6–7 mesh).
- Air-circulation oven.
- Thermometer.
- Refrigerator or freezer.

Table 5
Formulation of three HFHS diets

Ingredients	Proposed (g/1000 g)	D12451	TD.88137
Corn starch	112.49	84.80	150.00
Casein	145.00	233.00	195.00
Maltodextrin	132.00	116.50	–
Sucrose	300.00	201.40	341.46
Soybean oil	210.00	29.00	–
Lard	–	207.00	–
Anhydrous milkfat (ghee)	–	–	210.00
Cholesterol	–	–	1.50
Microcrystalline cellulose	50.00	58.30	50.00
Mineral mix	35.00	11.70[a]	35.00[c]
Calcium carbonate	–	6.40	4.00
Di-calcium phosphate	–	15.10	–
Potassium citrate monohydrate	–	19.20	–
Vitamin mix	10.00	11.70[b]	10.00[d]
L-cystine	3.00	3.50	–
DL-methionine	–	–	3.00
Choline bitartrate (41.1% choline)	2.50	2.30	–
T-butyl-hydroquinone	0.014	–	–
Ethoxyquin	–	–	0.04
Total	**1000 g**	**1000 g**	**1000 g**

D12451 is commercialized by Research Diets, Inc. (https://www.researchdiets.com/formulas/d12451) and TD.88137 is commercialized by Envigo Teklad Custom Diets (https://insights.envigo.com/hubfs/resources/data-sheets/88137.pdf)

[a] Mineral Mix S10026 formulated by Research Diets, Inc.
[b] Vitamin Mix V10001 formulated by Research Diets, Inc.
[c] Mineral Mix proposed by AIN-76
[d] Vitamin Mix, Teklad (40060) formulated by Teklad Custom Diets

4.2 Methods

All ingredients must be weighed dry on a calibrated analytical or semi-analytical scale. Vitamins are unstable; thus, the preparation and the storage of the diet need attention. A low-light environment is recommended due to the vulnerability of riboflavin and vitamin K to degradation.

The HFHS diet proposed by our research group was adapted from the AIN-93G diet to reach 30% sucrose and 21% fat, which characterizes it as a diet rich in simple sugars and lipids. This diet is prepared following the steps described below:

1. Check if casein protein content is over 85% by proximate composition before all else.
2. Calculate the amounts of ingredients necessary to prepare the diet for your experiment (*see* **Note 1**).
3. Prepare the diet under low-light conditions to minimize the degradation of vitamins.
4. Weigh all ingredients according to the amount of diet required for the experiment (Table 1) (*see* **Notes 2** and **3**).
5. Mix all the ingredients manually in a bowl in descending order of quantity (the smaller quantities first), except the oil.
6. Mix the ingredients slowly to reduce dust.
7. Sieve the diet powder 3 times in a 6- to 7-mesh sieve to mix and homogenize the formulation.
8. Add the oil slowly, mixing the entire diet.
9. Sieve the diet powder 3 times in a 6- to 7-mesh sieve to mix and homogenize the formulation (*see* **Note 4**).
10. Determine analytically the powder diet proximate composition (lipid, protein, ashes, humidity, and carbohydrates) to check the nutrient distribution (*see* **Notes 5** and **6**).
11. We could not pelletize this diet manually and dry it in the oven since the high amount of sucrose and oil kept its consistency as neither a powder, like AIN-93G, nor a dough, observed with the HF diet (Fig. 1).
12. Store the diet in lidded plastic containers at 4 °C for 3 months or frozen for 6 months.
13. Monitor deterioration.

5 Notes

1. Double-check the calculation of the necessary diet before initiating the preparation.
2. Keep a list of the quantity of the ingredients and check each one after the weighing step.
3. Identify the beakers to avoid mistakes (i.e., beaker 1 = casein, beaker 2 = starch, etc.)
4. The mixer can also be used; in this case, place the ingredients in the bowl with a cap, keeping vitamins and minerals separated. Mix for 5 minutes at a slower speed; after slowly adding the oil and mix for 15 minutes.
5. If the diet composition, mainly the protein content, is too low, the concentration can be corrected by adding casein. On the other hand, if it is above the expected value, fix the

concentration by adding other ingredients (e.g., starch or maltodextrin) in the appropriate proportion to promote the appropriate distribution of the macronutrients.

6. The proximate composition of the diet can be determined using the methodologies described by the AOAC [31] for moisture, ash, proteins by the micro Kjeldahl methodology, and for total lipids by Bligh & Dyer [32]. The carbohydrate content is, in general, calculated by the percentile difference from all the other constituents.
7. Put the lard in a beaker and liquefy it in the microwave. This procedure will ease the incorporation into the diet.

Acknowledgments

The authors thank Espaço da Escrita – Pró-Reitoria de Pesquisa - UNICAMP – for the language services provided. This study was financed in part by the Coordenação de Aperfeiçoamento de Pessoal de Nível Superior - Brasil (CAPES) - Finance Code 001.

References

1. Miller V et al (2017) Fruit, vegetable, and legume intake, and cardiovascular disease and deaths in 18 countries (PURE): a prospective cohort study. Lancet 390(10107):2037–2049
2. Andersen ML, Winter LMF (2019) Animal models in biological and biomedical research – experimental and ethical concerns. An Acad Bras Cienc 91(Suppl. 1):e20170238
3. Reeves PG, Nielsen FH, Fahey GC Jr (1993) AIN-93 purified diets for laboratory rodents: final report of the American Institute of Nutrition ad hoc writing committee on the reformulation of the AIN-76A rodent diet. J Nutr 123(11):1939–1951
4. Medinsky MA et al (1982) Development of hepatic lesions in male Fischer-344 rats fed AIN-76A purified diet. Toxicol Appl Pharmacol 62(1):111–120
5. Reeves PG (1997) Components of the AIN-93 diets as improvements in the AIN-76A diet. J Nutr 127(5 Suppl):838S–841S
6. Buettner R, Schölmerich J, Bollheimer LC (2007) High-fat diets: modeling the metabolic disorders of human obesity in rodents. Obesity (Silver Spring) 15(4):798–808
7. Hulbert AJ et al (2005) Dietary fats and membrane function: implications for metabolism and disease. Biol Rev Camb Philos Soc 80(1): 155–169
8. Hariri N, Thibault L (2010) High-fat diet-induced obesity in animal models. Nutr Res Rev 23(2):270–299
9. James AM et al (2012) Mitochondrial oxidative stress and the metabolic syndrome. Trends Endocrinol Metab 23(9):429–434
10. USDA (2016) Agricultural Research Service. Nutrient intakes from food and beverages: mean amounts consumed per individual, by gender and age, What We Eat in America, NHANES 2013–2014
11. Després JP, Lemieux I (2006) Abdominal obesity and metabolic syndrome. Nature 444(7121):881–887
12. White PJ, Marette A (2014) Potential role of omega-3-derived resolution mediators in metabolic inflammation. Immunol Cell Biol 92(4): 324–330
13. Gallou-Kabani C et al (2007) C57BL/6J and a/J mice fed a high-fat diet delineate components of metabolic syndrome. Obesity (Silver Spring) 15(8):1996–2005
14. Poussin C et al (2011) Oxidative phosphorylation flexibility in the liver of mice resistant to high-fat diet-induced hepatic steatosis. Diabetes 60(9):2216–2224
15. Lionetti L et al (2014) High-lard and high-fish-oil diets differ in their effects on function

and dynamic behaviour of rat hepatic mitochondria. PLoS One 9(3):e92753–e92753

16. Benoit SC et al (2010) Palmitic acid mediates hypothalamic insulin resistance by altering PKC-q subcellular localization in rodents. J Clin Invest 120(1):394–394
17. Siri-Tarino PW et al (2010) Saturated fat, carbohydrate, and cardiovascular disease. Am J Clin Nutr 91(3):502–509
18. Ratnayake WM, Galli C (2009) Fat and fatty acid terminology, methods of analysis and fat digestion and metabolism: a background review paper. Ann Nutr Metab 55(1–3):8–43
19. Siriwardhana N et al (2012) N-3 and n-6 polyunsaturated fatty acids differentially regulate adipose angiotensinogen and other inflammatory adipokines in part via NF-κB-dependent mechanisms. J Nutr Biochem 23(12): 1661–1667
20. Havel PJ (2005) Dietary fructose: implications for dysregulation of energy homeostasis and lipid/carbohydrate metabolism. Nutr Rev 63(5):133–157
21. Bizeau ME, Pagliassotti MJ (2005) Hepatic adaptations to sucrose and fructose. Metabolism 54(9):1189–1201
22. Tappy L et al (2010) Fructose and metabolic diseases: new findings, new questions. Nutrition 26(11–12):1044–1049
23. Roglans N et al (2007) Impairment of hepatic Stat-3 activation and reduction of PPARalpha activity in fructose-fed rats. Hepatology 45(3): 778–788
24. Lang P et al (2019) Effects of different diets used in diet-induced obesity models on insulin resistance and vascular dysfunction in C57BL/6 mice. Sci Rep 9(1):19556
25. Wang X et al (2013) Differential effects of high-fat-diet rich in lard oil or soybean oil on osteopontin expression and inflammation of adipose tissue in diet-induced obese rats. Eur J Nutr 52(3):1181–1189
26. Parks BW et al (2013) Genetic control of obesity and gut microbiota composition in response to high-fat, high-sucrose diet in mice. Cell Metab 17(1):141–152
27. World Health Organization (2015) Guideline: sugar intake for adults and children. World Health Organization, Geneva
28. Blouet C et al (2007) Dietary cysteine alleviates sucrose-induced oxidative stress and insulin resistance. Free Radic Biol Med 42(7): 1089–1097
29. Busserolles J et al (2002) Rats fed a high sucrose diet have altered heart antioxidant enzyme activity and gene expression. Life Sci 71(11):1303–1312
30. Feillet-Coudray C et al (2009) Oxidative stress in rats fed a high-fat high-sucrose diet and preventive effect of polyphenols: involvement of mitochondrial and NAD(P)H oxidase systems. Free Radic Biol Med 46(5):624–632
31. AOAC (2005) Official Methods of Analysis of Association of Official Analytical Chemists., A.o.O.A. Chemists, Editor. Association of Official Analytical Chemists
32. Bligh EG, Dyer WJ (1959) A rapid method of total lipid extraction and purification. Can J Biochem Physiol 37(8):911–917

Chapter 2

Measures of Food Intake, Body Weight Gain, and Energy Efficiency in Mice

Cíntia Reis Ballard and Cinthia Baú Betim Cazarin

Abstract

Developing and validating accurate methods to quantify food intake (FI) and body weight gain (BWG) is a growing need considering the number of studies on the deregulation of nutritional status, especially malnutrition, obesity, or energy balance. These methods are also relevant for gaining additional insights on the use of the ingested energy by the metabolism through energy efficiency. Quantifying these variables remains a challenge in rodents since minor errors diminish scientific data quality. Although traditional methods of manual weighing are still the most used by researchers, automated systems have been improving over the past few decades, and some are open source. Some technologies require animals' training, whereas others do not quantify FI or BWG but analyze feeding behavior. This chapter aims to provide guidance on measuring FI, BWG, and energy efficiency, highlighting the techniques, advantages, and limitations.

Key words Food intake, Feed efficiency, Body weight, Rodent, Metabolism, NutritionKey words, Obesity, Malnutrition

1 Importance of Food Intake, Body Weight Gain, and Energy Efficiency in Mice Studies

Experimental animal models play a key role in elucidating biological phenomena related to metabolism, nutrition, chronic diseases, medication dosage, and surgical techniques [1–3]. Rodents, especially *Mus musculus* (mice), have been the most universally used animal in preclinical studies in vivo for many years [4]. Mice are easy to handle, have a short lifespan and different strains, and have relative genome and physiology in similarity with humans [5]. When planning a study to test a scientific hypothesis, the animal model's choice is critical since an inadequate model may compromise the analysis and the interpretation of the results, consequently, their extrapolation for human beings.

Regarding this, preclinical studies in vivo require optimized planning with clinical trials' scientific rigor to improve the

Cinthia Baú Betim Cazarin (ed.), *Basic Protocols in Foods and Nutrition*,
Methods and Protocols in Food Science, https://doi.org/10.1007/978-1-0716-2345-9_2,

relevance, translation, and reproduction of their results [6]. A recurring concern is the animals' baseline characteristics and nutritional status monitoring. The animal's baseline characteristics, which include data on sex, body weight, age, housing conditions, and others depending on the project, may directly influence the results, contributing to bias in the intervention responses if randomization fails [7]. In turn, nutritional status monitoring confirms the coverage of physiological needs for nutrients [8], and unassessed changes in this status may also contribute to biases since they directly affect the animals' growth, reproduction, and longevity [9]. Thus, meeting the specific nutritional demands of an animal model is one of the central factors in its survival.

The simplest way to assess nutritional status is to measure food intake (FI) and body weight gain (BWG). Currently, a sizable number of studies on deregulation of nutritional status, mainly malnutrition, obesity, or energy balance, pressure the development of precise methods to quantify these variables since accurately quantifying them also determines the strength of association with other biological and non-biological parameters – like energy efficiency. Energy efficiency evaluates the animal's ability to convert food energy consumed into body weight [10], providing additional information on energy intake and assessing whether changes in energy expenditure or nutrient absorption contribute to BWG.

Although quantifying FI and BWG seems simple, several factors may negatively impact these variable values directly or indirectly. Environmental and non-environmental stressors, such as noise, temperature, smells, procedures, and transport, affect a series of biological functions, and consequently FI and BWG [11]. Similarly, the daily routine has inherent difficulties, for example, nutritional consistency type (e.g., liquid, powder, solid, gel), food grinding (e.g., solid diet), housing (e.g., pairs, groups, individually), handling (e.g., type, frequency), and equipment (e.g., type, displacements, miscalibration) [12–17]. Limitations may lead to quantification errors, requiring the establishment of the correct approaches in protocols. Our goal is to guide the reader on measuring FI, BWG, and energy efficiency, highlighting the techniques, advantages, and limitations.

1.1 Food Intake, Body Weight Gain, and Energy Efficiency Measurement Techniques

The techniques used in any experimental animal model must guarantee animal welfare and scientific data quality [18, 19]. A well-trained laboratory team helps to achieve adequate animal care, equipment preservation, and results in optimization regardless of the chosen method. Identifying sources of variability or conditions that can potentially influence the results and manage them to minimize possible confounding factors is also essential. Thus, we recommend performing FI and BWG measurements on the same equipment and work area for more reproducible studies free from the researcher's bias, according to the ARRIVE guidelines [20],

and keeping detailed reports for adequate control of the FI and BWG variation estimates.

Another key point is the stress inherent in the animal's laboratory life. Acute stressful conditions are considered beneficial since they can lead to resilience to future stressors [21]. In contrast, chronic stress can negatively impact metabolism and, consequently, FI and BWG [22]. Cold stress, for example, can increase food consumption [23]. The hypothalamus-pituitary-adrenal axis (HPA) regulates the stress response by secreting glucocorticoids like corticosterone [24]. Thus, we suggest estimating corticosterone as the primary measure of axis activity to certify homogeneity among the experimental units studied [25]. The laboratory team must provide practical solutions to reduce possible stressors according to current animal experimentation regulations and protocols.

An eventual point concerns the temporal resolution of FI and BWG measurement techniques. Mice have a circadian behavior associated with the 24-hour light-dark cycle, consuming most food during the dark period (~70%), with short moments of feeding during the light period [26]. More effective temporal resolution improves FI details by the quantitative data on consumption, duration, frequency of meals, and BWG by the quantitative data on possible weight fluctuations during the light-dark cycle. A better understanding of feeding behavior and body mass gain in preclinical studies in vivo contributes to future clinical trials on obesity reduction and other food-related illnesses.

Many FI and BWG monitoring mechanisms have been developed in recent decades [27]. First, we will examine the four most common quantifying FI methods: manual weighing, automated weighing scales, pellet dispensers, and video-based procedures. Second, we will review the manual and automatic weighing scales used for BWG. Each instrument has different degrees of invasiveness and accuracy. Automated mechanisms monitor FI and BWG fluctuations during the 24-hour light-dark cycle, aiding with energy balance and food behavior studies [28–33]. Pellet dispensers respond to the animal's training or to an infrared beam [34–40]. The video-based tool is more suitable for research feeding behavior since it only quantifies energy when combined with another procedure [41–43]. Finally, we will analyze the energy efficiency calculation.

1.1.1 FI Methods

Manual Weighing

Manual weighing is the technique most used by researchers, consisting of calculating the difference between the weight of the food initially put into the hopper and the weight that remains with an accuracy of ~100 mg after a time interval – minutes, hours, days – defined by the project (Fig. 1) [10]. This approach requires low-cost equipment and is performed on conventional cage racks and with diets with different consistency [27]. However, it presents various issues related to housing (individual or social), waste

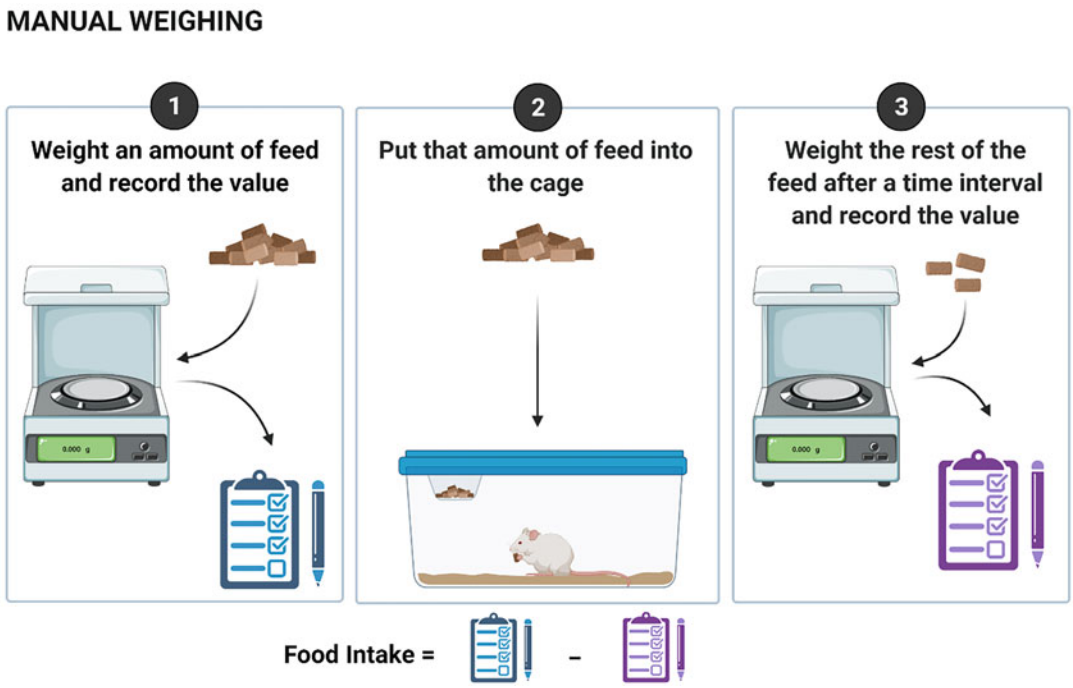

Fig. 1 Scheme of FI manual weighing. (Created with BioRender.com)

material formation, and low temporal resolution, which we will discuss along ways to reduce possible measurement errors.

Mice are a species with a complex social organization, and the number of animals per accommodation may impact variables of interest. A recent meta-analysis demonstrates that individual housing, which is the condition of the mice in most feeding behavior studies, can favor increased FI without changing BWG, mainly due to rodents' emotional stress [15], which can be mitigated with environmental enrichment strategies [12–14]. On the other hand, socially housed animals can establish a hierarchical relationship; consequently, subordinate and dominant animals have different food consumption patterns and BWG [44]. Therefore, considering the animal group as an experimental unit is appropriate [45].

The production of crumbs in mice's natural process feeding (spillage), food grinding behavior; and data with a low temporal resolution are other limitations to this method [16]. Always checking the crumbs and considering them before estimating FI to control waste material is crucial, all while discarding from quantification any diet residue in contact with urine or feces. The lack of hardness of the diet or genetic factors producing fragments called orts are the most common causes of the food grinding behavior [18, 35]. Failure to consider orts can lead to 31.8% FI errors varying with diet or animal strain – the high-fat diets common in diet-induced obesity studies need particular attention since they usually have a lower degree of hardness, facilitating ort production

[16]. The temporal resolution may improve by shortening the FI measurement interval, generating more data for the same study period; nevertheless, it lessens practicality due to the number of animals in the study.

Automated Weighing Scales

Automated weighing scales (AWS) allow for long-term FI assessment with many systems – differing in composition, monitoring, and accuracy – available from several companies since the 1990s [28–32]. The mechanism comprises chambers supported by sensitive and precise weighing sensors (load cell) or scales with a computer interface. Food is continuously weighed, generating FI computer data with accuracy up to ~1 mg. Food is accessed through a feeding tunnel (adjacent compartment) or directly from the home cage floor (Fig. 2). These systems even automatically resume data acquisition after power outages.

The AWS allow for minimum handling, high temporal resolution, variety in diet types, reduced workload, and variability in results between experiments [27]. Some commercial AWS analyze the quantity, time, duration, and frequency of FI, and fasting periods between meals on a 24-hour light-dark cycle [28]. Furthermore, other feeding devices can be adapted into AWS, helping research on dietary preferences and patterns (e.g., food restriction, intermittent fasting). Comprehensive FI data contribute to studies on feeding behavior and its impact on health, besides those assessing the effectiveness and specificity of agents that stimulate or inhibit appetite [29–32].

The high cost is the main limitation to AWS since it requires adequate equipment (specialized cage) and takes up more space for laboratory implantation. Some systems also lack means of accurately accounting for spillage, and others need special care for calibration [27]. Most AWS is limited in monitoring multiple animals simultaneously, and only some of them specify the maximum housing time. Although these systems promote a reduction in handling, we suggest corticosterone measurement to check the HPA axis activation for reasons other than the stress from human handling.

Pellet Dispensers

Pellet dispensers are mechanical devices that release a known mass of pellets through different mechanisms (Fig. 3), such as animal behavior conditioned to an operational task, infrared beam detection, or both [34–40]. The FI record has high temporal resolution with computer monitored recording of the time and date of delivery of the pellets. Some open-source options have information for building an adjustable automatic feeder [35–37, 40], and accuracy is approximately 20–300 mg, depending on pellet size [27]. These systems cost less than AWS and can be used in domestic cages [35–37, 39]. Studies on rehabilitation after neurological disorders also use pellet dispensers to reach and seize a single pellet [40].

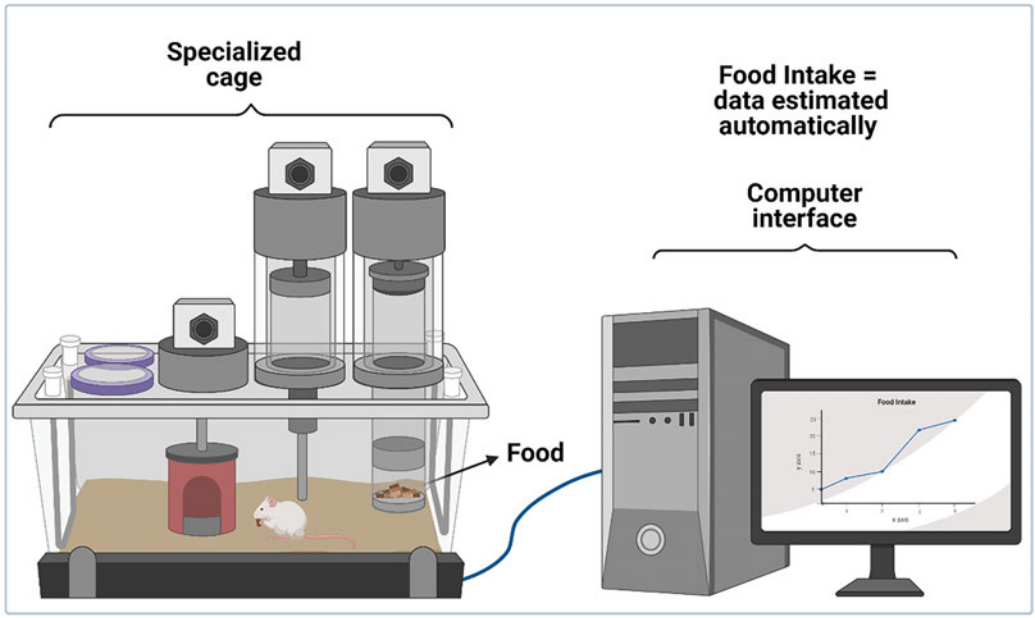

Fig. 2 Scheme of FI automated weighing scale. (Created with BioRender.com)

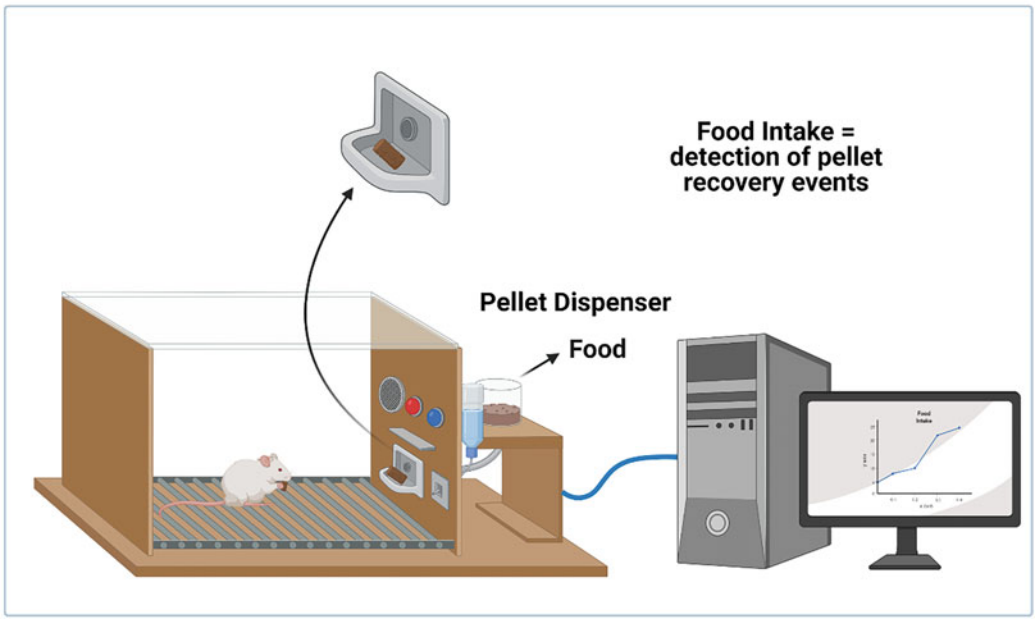

Fig. 3 Scheme of pellet dispenser. (Created with BioRender.com)

The main limitations of this method are clogging in the equipment or crumb accumulation preventing a new pellet release [27]. Regularly monitoring and cleaning the device is vital to reduce FI measurement errors and increase data accuracy. The specificity of the diets (size, composition, consistency) for each dispenser is another issue since several commercial dispensers available are specific to species and types of diet. High-fat diets are incompatible with most of these devices for they contain soft pellets [27], thus, coating high-fat pellets with alternative materials to make them firmer may solve this issue. We again suggest checking the activation of the HPA axis by corticosterone measurement since a final concern is the possibility of the animal training and the noise produced by dispensers increasing the animal's stress level.

Video-Based Systems

Video-based systems are non-invasive approaches involving visual methods with a computer interface to study feeding behavior patterns reliably and consistently over long periods (Fig. 4). It allows for high resolution without interference from the observer's fatigue or drift and quantification of the animal's interactions with food both in cages for individual and for social housing [41–43].

However, video-based systems are expensive systems (depending on the vision algorithms, camera position, light effects) and hard to adapt to the domestic cage [27]. Despite being an efficient method to visualize feeding behavior, it lacks real FI quantification unless integrated with another of the systems discussed above. As with previous systems, we suggest quantifying corticosterone as a stress marker even with reduced human interaction.

1.1.2 BWG Methods

Manual Weighing

Like with the FI, manual weighing is the most used technique for BWG measurement. It equals to estimating body weight after a defined time interval – minutes, hours, days – by an electronic scale with an accuracy of ~10 mg [10]. Dynamic weighing scales are the better option since the measurement is the average estimate of an animal in motion (Fig. 5). This approach has the advantage of requiring easy-to-use, low-cost equipment.

The main limitation is the low temporal resolution, which is improved by increasing the number of BWG measurements per time interval. However, this will increase animal handling, which, depending on handling type and frequency, may affect the animals' behavior and even the experimental results [46]. For example, handling laboratory mice by grabbing the tails' base between thumb and forefinger has increased stress and anxiety [47] more than non-aversive mice handling procedures, such as tunnels or cupping them on the open hand [48]. Knowing that chronic stress can affect FI and BWG, choosing handling tools that avoid it is preferable [49, 50]. Search at Weiss [51] to clarify doubts about handling types. Given this limitation, we suggest checking corticosterone as a stress marker.

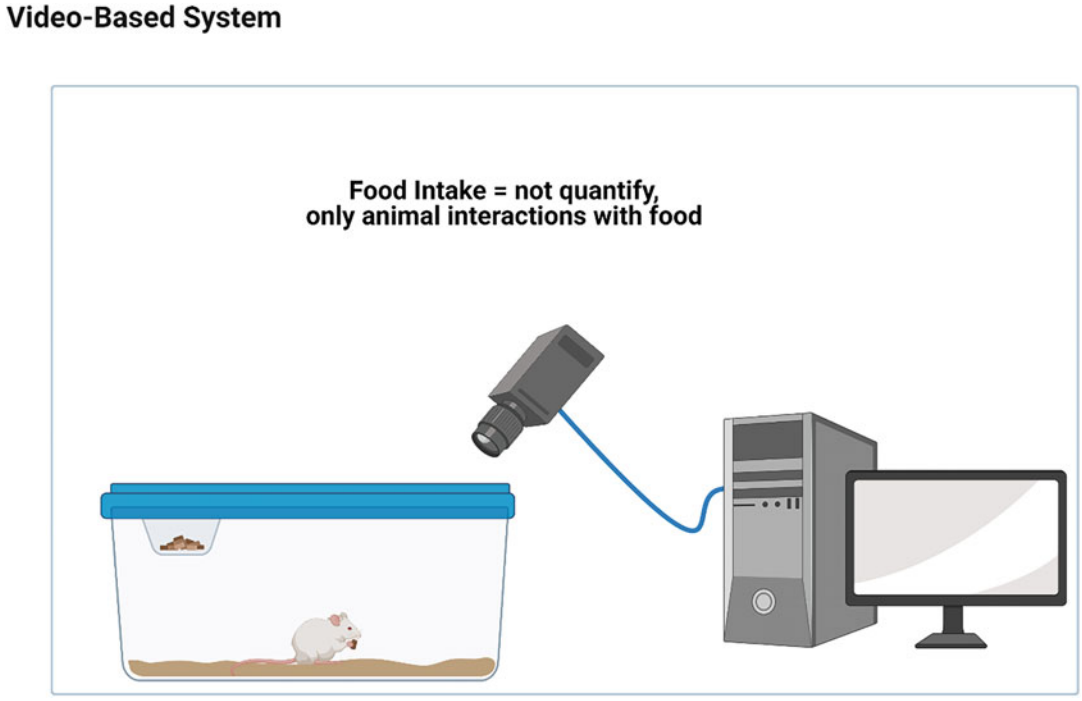

Fig. 4 Scheme of FI video-based system. (Created with BioRender.com)

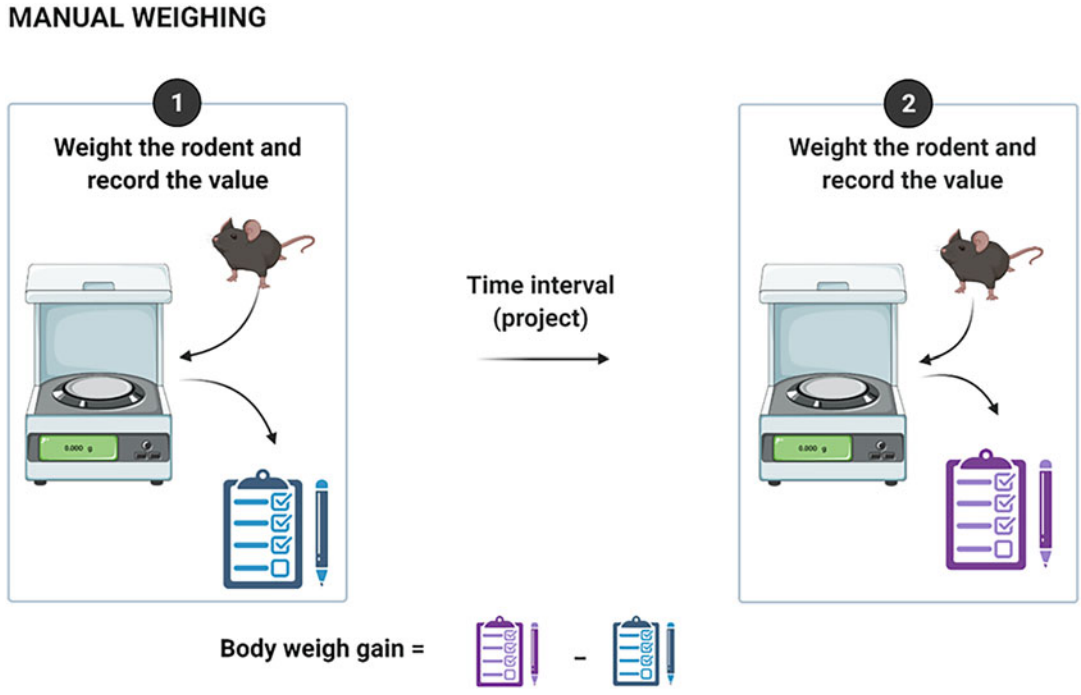

Fig. 5 Scheme of BWG manual weighing. (Created with BioRender.com)

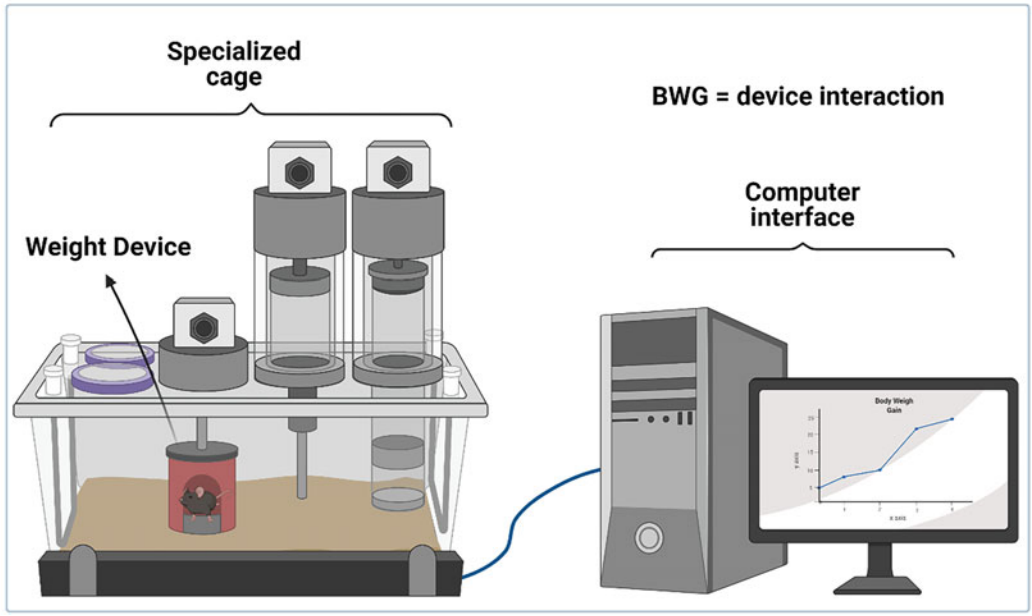

Fig. 6 Scheme of BWG automated weighing scale. (Created with BioRender.com)

Automated Weighing Scales

The AWS estimates body weight in chambers supported by load cells with a computer interface (Fig. 6). In most commercial systems, a nesting compartment inside specialized cages for individual animal housing rests over sensitive and accurate weighing sensors [29, 52]. The BWG is monitored real-time when the rodent interacts with the device. Some open-source systems are developed in domestic cages and estimate the BWG of the animals in social housing with microchips and radiofrequency technology [33, 53]. The average readability is 100 mg, varying among models [33]. AWS has a high temporal resolution that contemplates weight fluctuations during the 24 h of the light-dark cycle, reducing animal handling and workload. However, the cost is still an impediment since most available systems demand specialized cages and more space in the laboratory. The measurement of corticosterone as a stress marker also remains a suggestion in using this approach for FI reasons.

These FI and BWG quantification methods have advantages and features to cope with their limitations. However, increasing the number of systems for animals housed in groups is a challenge, and studying how the social context influences eating behavior is needed [54]. Identifying animals by microchips and radiofrequency is a promising alternative with promising results alongside pellet dispensers, AWS, and video-based systems, reducing the number of cages, costs, and prioritizing the social aspects of FI [53, 55, 56].

Different home-cage monitoring systems facilitate handling-free evaluation and improve the FI and BWG estimation. However, studies with varying rodent strains are scarce and, several mechanisms are available for study. Therefore, we recommend that researchers examine the advantages and limitations discussed above for commercial or open-source systems and validate newly created mechanisms. This protocol describes a step-by-step procedure for manual weighing of FI, BWG, and calculation of energy efficiency.

2 Materials

2.1 Animal

Mice strains or lineage, after weaning, matched for age, sex, and genetic background strain individually housed under controlled environmental conditions (e.g., temperature, noise, humidity).

2.2 Diet

Solid consistency diets under *ad libitum* regime (*see* **Note 1**).

2.3 Equipment and Record Sheet

Scale and record sheet for monitoring BWG and FI. Scale with ±0.001-gram readability for weighing food and ± 0.01 gram for mice.

3 Method

All procedures are performed during the light phase of the 24-hour light-dark cycle and must be approved by the institutions' Institutional Animal Care and User Committee (IACUC). We emphasize the need for collecting the FI and BWG measurements on the same equipment and work area (*see* **Note 2**).

3.1 Procedure of FI Manual Weighing

I. Check the balance calibration at the start of the study (*see* **Note 3**).

II. Weigh and record ~25 g of diet to three decimal places and put into the hopper for *ad libitum* access of individually housed mice (initial quantity) (*see* **Note 4**).

III. Measure the rest of the diet and record it on the sheet (three decimal places). At the previously set day and time. This protocol covers three FI quantifications in the week (e.g., Monday, Wednesday, and Friday). Weigh food at the same time of day to ensure reproducibility.

IV. Complete up to ~25 g of diet, recorded to three decimal places, and replace it for animals' access (*see* **Note 5**).

V. Calculate the FI by subtracting the remaining food weight from the initial value.

VI. Divide the weight difference by the number of days since the last weighing of the food to estimate a per day value.

3.2 Procedure of BWG Manual Weighing

I. Check the balance calibration at the start of the study (*see* **Note 3**).

II. Record the mice's body weight to two decimal places 2 to 3 times a week throughout the experimental period (*see* **Note 6**).

III. Calculate the BWG by subtraction of the body weight from a day by its antecedent.

IV. Divide the body weight difference by the number of days to estimate a BWG per day value.

3.3 Energy Efficiency

The calculation of energy efficiency depends on the FI values in calories and BWG in grams. The proportion of energy consumed is divided by body weight gain over a specific time (e.g., day, week).

$$\text{Energy efficiency(g/Kcal)} = (\text{body weight gain/week})/(\text{food intake/week})$$

4 Conclusion

The improvement of the current methods and the emergence of new ones to increase FI and BWG estimate's accuracy will help understanding public health problems related to food and nutrition. However, the cost of automated systems is still impeditive to their popularization. Furthermore, comparing the equivalence of results of these systems is also necessary.

We look forward to future systems with the possibility of group accommodation and more accessibility for installation. The manual weighing of FI and BWG has limitations, mainly temporal resolution, despite being the most widely used and accessible method.

5 Notes

1. A*d libitum* regime → Rodents have access to a continuous supply of food. Diets are properly prepared and free from chemical and microbial contaminants and their compositions depend on the project proposal (e.g., diet-induced obesity, supplemented diets, standard diets).
2. Estimates in the dark period under red light are ideal for studies focusing on hyperphagia episodes, satiety, or tests of compounds that can affect FI since about 70% of rodents' food consumption occurs in the dark phase.

3. Scale calibration is essential for accurate weighing results. Environmental changes can also increase random errors which degrade the scale performance.
4. The daily food intake among mice of different strains and ages varies from 3 to 6 g/day [57]. Observe spilled diet and add it back to the hopper. Discard from quantification diet residues in contact with urine or feces.
5. Discard small pellets that may fall through the hopper. Weigh a more significant amount of diet (~50 g) if the FI is not being measured on the weekend. Renew food every 3 days to ensure the organoleptic properties.
6. Use non-invasive methods to remove the animal from the cage (tunnels or cupping them on the open hand). Weigh the animal on the same day, at the same time of day throughout the experimental period.

Acknowledgments

The authors thank Espaço da Escrita – Pró-Reitoria de Pesquisa - UNICAMP – for the language services provided. This study was financed in part by the Coordenação de Aperfeiçoamento de Pessoal de Nível Superior - Brasil (CAPES) - Finance Code 001.

References

1. Ballard CR, dos Santos EF, Dubois M-J, Pilon G, Cazarin CBB, Maróstica Junior MR et al (2020) Two polyphenol-rich Brazilian fruit extracts protect from diet-induced obesity and hepatic steatosis in mice. Food Funct 11: 8800–8810. https://doi.org/10.1039/D0FO01912G
2. Takaoka N, Sanoh S, Okuda K, Kotake Y, Sugahara G, Yanagi A et al (2018) Inhibitory effects of drugs on the metabolic activity of mouse and human aldehyde oxidases and influence on drug–drug interactions. Biochem Pharmacol 154:28–38. https://doi.org/10.1016/j.bcp.2018.04.017
3. Paish HL, Reed LH, Brown H, Bryan MC, Govaere O, Leslie J et al (2019) A bioreactor technology for modeling fibrosis in human and rodent precision-cut liver slices. Hepatology 70:1377–1391. https://doi.org/10.1002/hep.30651
4. Hickman DL, Johnson J, Vemulapalli TH, Crisler JR, Shepherd R (2017) Commonly used animal models. Princ Anim Res, Elsevier:117–175. https://doi.org/10.1016/B978-0-12-802151-4.00007-4
5. Vandamme TF (2015) Rodent models for human diseases. Eur J Pharmacol 759:84–89. https://doi.org/10.1016/j.ejphar.2015.03.046
6. Muhlhausler BS, Bloomfield FH, Gillman MW (2013) Whole animal experiments should be more like human randomized controlled trials. PLoS Biol 11. https://doi.org/10.1371/journal.pbio.1001481
7. Laajala TD, Jumppanen M, Huhtaniemi R, Fey V, Kaur A, Knuuttila M et al (2016) Optimized design and analysis of preclinical intervention studies in vivo. Sci Rep 6:30723. https://doi.org/10.1038/srep30723
8. Picó C, Serra F, Rodríguez AM, Keijer J, Palou A (2019) Biomarkers of nutrition and health: new tools for new approaches. Nutrients 11. https://doi.org/10.3390/nu11051092
9. Curfs J, Chwalibog A, Savenije B, Ritskes-Hoitinga M (2010) Nutrient requirements, experimental design, and feeding schedules in animal experimentation. In: Handbook of laboratory animal science, vol 1, 3rd edn. CRC Press, pp 307–342. https://doi.org/10.1201/b10416-12

10. Moir L, Bentley L, Cox RD (2016) Comprehensive energy balance measurements in mice. Curr Protoc Mouse Biol 6:211–222. https://doi.org/10.1002/cpmo.13
11. Castelhano-Carlos MJ, Baumans V (2009) The impact of light, noise, cage cleaning and in-house transport on welfare and stress of laboratory rats. Lab Anim 43:311–327. https://doi.org/10.1258/la.2009.0080098
12. Bayne K (2018) Environmental enrichment and mouse models: current perspectives. Anim Model Exp Med 1:82–90. https://doi.org/10.1002/ame2.12015
13. Bailoo JD, Murphy E, Boada-Saña M, Varholick JA, Hintze S, Baussière C et al (2018) Effects of cage enrichment on behavior, welfare and outcome variability in female mice. Front Behav Neurosci 12:1–20. https://doi.org/10.3389/fnbeh.2018.00232
14. Morano R, Hoskins O, Smith BL, Herman JP (2019) Loss of environmental enrichment elicits Behavioral and physiological dysregulation in female rats. Front Behav Neurosci 12:287. https://doi.org/10.3389/fnbeh.2018.00287
15. Schipper L, Harvey L, van der Beek EM, van Dijk G (2018) Home alone: a systematic review and meta-analysis on the effects of individual housing on body weight, food intake and visceral fat mass in rodents. Obes Rev 19:614–637. https://doi.org/10.1111/obr.12663
16. Cameron KM, Speakman JR (2010) The extent and function of 'food grinding' in the laboratory mouse (Mus musculus). Lab Anim 44:298–304. https://doi.org/10.1258/la.2010.010002
17. Fischer AW, Cannon B, Nedergaard J (2018) Optimal housing temperatures for mice to mimic the thermal environment of humans: an experimental study. Mol Metab 7:161–170. https://doi.org/10.1016/j.molmet.2017.10.009
18. National Research Council (US) (2011) Guide for the care and use of laboratory animals. National Academies Press, Washington, D.-C. https://doi.org/10.17226/12910
19. Russel W, Burch R (1959) The principles of humane experimental technique. Methuen & Co. Ltda. [Reissued: 1992; Potters Bar: Universities Federation for Animal Welfare. 238p.], London
20. du Sert NP, Ahluwalia A, Alam S, Avey MT, Baker M, Browne WJ et al (2020) Reporting animal research: explanation and elaboration for the arrive guidelines 2.0. PLoS Biol 18:e3000411. https://doi.org/10.1371/journal.pbio.3000411
21. Brivio P, Sbrini G, Riva MA, Calabrese F (2020) Acute stress induces cognitive improvement in the novel object recognition task by transiently modulating Bdnf in the prefrontal cortex of male rats. Cell Mol Neurobiol 40:1037–1047. https://doi.org/10.1007/s10571-020-00793-7
22. Kamakura R, Kovalainen M, Leppaluoto J, Herzig K-H, Makela KA (2016) The effects of group and single housing and automated animal monitoring on urinary corticosterone levels in male C57BL/6 mice. Physiol Rep 4. https://doi.org/10.14814/phy2.12703
23. Gaskill BN, Garner JP (2017) Stressed out: providing laboratory animals with behavioral control to reduce the physiological effects of stress. Lab Anim (NY) 46:142–145. https://doi.org/10.1038/laban.1218
24. Gjerstad JK, Lightman SL, Spiga F (2018) Role of glucocorticoid negative feedback in the regulation of HPA axis pulsatility. Stress 21:403–416. https://doi.org/10.1080/10253890.2018.1470238
25. Mesa-Gresa P, Ramos-Campos M, Redolat R (2016) Corticosterone levels and behavioral changes induced by simultaneous exposure to chronic social stress and enriched environments in NMRI male mice. Physiol Behav 158:6–17. https://doi.org/10.1016/j.physbeh.2016.02.027
26. Ellacott KLJ, Morton GJ, Woods SC, Tso P, Schwartz MW (2010) Assessment of feeding behavior in laboratory mice. Cell Metab 12:10–17. https://doi.org/10.1016/j.cmet.2010.06.001
27. Ali MA, Kravitz AV (2018) Challenges in quantifying food intake in rodents. Brain Res 1693:188–191. https://doi.org/10.1016/j.brainres.2018.02.040
28. Robinson L, Riedel G (2014) Comparison of automated home-cage monitoring systems: emphasis on feeding behaviour, activity and spatial learning following pharmacological interventions. J Neurosci Methods 234:13–25. https://doi.org/10.1016/j.jneumeth.2014.06.013
29. Tilston TW, Brown RD, Wateridge MJ, Arms-Williams B, Walker JJ, Sun Y et al (2019) A novel automated system yields reproducible temporal feeding patterns in laboratory rodents. J Nutr 149:1674–1684. https://doi.org/10.1093/jn/nxz116
30. Hulsey MG, Martin RJ (1991) A system for automated recording and analysis of feeding behavior. Physiol Behav 50:403–408. https://doi.org/10.1016/0031-9384(91)90086-4

31. Meguid MM, Kawashima Y, Campos ACL, Gelling PD, Hill TW, Chen T-Y et al (1990) Automated computerized rat eater meter: description and application. Physiol Behav 48: 759–763. https://doi.org/10.1016/0031-9384(90)90222-P
32. Minematsu S, Hiruta M, Taki M, Fujii Y, Aburada M (1991) Automatic monitoring system for the measurement of body weight, food and water consumption and spontaneous activity of a mouse. J Toxicol Sci 16:61–73. https://doi.org/10.2131/jts.16.61
33. Noorshams O, Boyd JD, Murphy TH (2017) Automating mouse weighing in group homecages with raspberry pi micro-computers. J Neurosci Methods 285:1–5. https://doi.org/10.1016/j.jneumeth.2017.05.002
34. Gill K, Mundl WJ, Cabilio S, Amit Z (1989) A microcomputer controlled data acquisition system for research on feeding and drinking behavior in rats. Physiol Behav 45:741–746. https://doi.org/10.1016/0031-9384(89)90288-6
35. Nguyen KP, O'Neal TJ, Bolonduro OA, White E, Kravitz AV (2016) Feeding experimentation device (FED): a flexible open-source device for measuring feeding behavior. J Neurosci Methods 267:108–114. https://doi.org/10.1016/j.jneumeth.2016.04.003
36. Nguyen KP, Ali MA, O'Neal TJ, Szczot I, Licholai JA, Kravitz AV (2017) Feeding experimentation device (FED): construction and validation of an open-source device for measuring food intake in rodents. J Vis Exp 2017: 55098. https://doi.org/10.3791/55098
37. Oh J, Hofer R, Fitch WT (2017) An open source automatic feeder for animal experiments. HardwareX 1:13–21. https://doi.org/10.1016/j.ohx.2016.09.001
38. Acosta-Rodríguez VA, de Groot MHMM, Rijo-Ferreira F, Green CB, Takahashi JS, Acosta-Rodriguez VA et al (2017) Mice under caloric restriction self-impose a temporal restriction of food intake as revealed by an automated feeder system. Cell Metab 26: 267–277.e2. https://doi.org/10.1016/j.cmet.2017.06.007
39. Rainwater A, Sanz E, Palmiter RD, Quintana A (2017) Striatal GPR88 modulates foraging efficiency. J Neurosci 37:7939–7947. https://doi.org/10.1523/JNEUROSCI.2439-16.2017
40. Torres-Espín A, Forero J, Schmidt EKA, Fouad K, Fenrich KK (2018) A motorized pellet dispenser to deliver high intensity training of the single pellet reaching and grasping task in rats. Behav Brain Res 336:67–76. https://doi.org/10.1016/j.bbr.2017.08.033
41. Salem GH, Dennis JU, Krynitsky J, Garmendia-Cedillos M, Swaroop K, Malley JD et al (2015) SCORHE: a novel and practical approach to video monitoring of laboratory mice housed in vivarium cage racks. Behav Res Methods 47:235–250. https://doi.org/10.3758/s13428-014-0451-5
42. Spink AJ, Tegelenbosch RAJ, Buma MOS, Noldus LPJJ (2001) The EthoVision video tracking system – a tool for behavioral phenotyping of transgenic mice. Physiol Behav 73: 731–744. https://doi.org/10.1016/S0031-9384(01)00530-3
43. Noldus LPJJ, Spink AJ, Tegelenbosch RAJ (2001) EthoVision: a versatile video tracking system for automation of behavioral experiments. Behav Res Methods Instrum Comput 33:398–414. https://doi.org/10.3758/BF03195394
44. Tamashiro KLK, Nguyen MMN, Ostrander MM, Gardner SR, Ma LY, Woods SC et al (2007) Social stress and recovery: implications for body weight and body composition. Am J Physiol Integr Comp Physiol 293: R1864–R1874. https://doi.org/10.1152/ajpregu.00371.2007
45. Lazic SE, Clarke-Williams CJ, Munafò MR (2018) What exactly is 'N' in cell culture and animal experiments? PLoS Biol 16:e2005282. https://doi.org/10.1371/journal.pbio.2005282
46. Sensini F, Inta D, Palme R, Brandwein C, Pfeiffer N, Riva MA et al (2020) The impact of handling technique and handling frequency on laboratory mouse welfare is sex-specific. Sci Rep 10:1–9. https://doi.org/10.1038/s41598-020-74279-3
47. Clarkson JM, Dwyer DM, Flecknell PA, Leach MC, Rowe C (2018) Handling method alters the hedonic value of reward in laboratory mice. Sci Rep 8. https://doi.org/10.1038/s41598-018-20716-3
48. Gouveia K, Hurst JL (2019) Improving the practicality of using non-aversive handling methods to reduce background stress and anxiety in laboratory mice. Sci Rep 9:1–19. https://doi.org/10.1038/s41598-019-56860-7
49. Coccurello R, Romano A, Giacovazzo G, Tempesta B, Fiore M, Giudetti AM et al (2018) Increased intake of energy-dense diet and negative energy balance in a mouse model of chronic psychosocial defeat. Eur J Nutr 57: 1485–1498. https://doi.org/10.1007/s00394-017-1434-y
50. Carneiro-Nascimento S, Opacka-Juffry J, Costabile A, Boyle CN, Herde AM, Ametamey SM et al (2020) Chronic social stress in mice

alters energy status including higher glucose need but lower brain utilization. Psychoneuroendocrinology 119:104747. https://doi.org/10.1016/j.psyneuen.2020.104747

51. Weiss T, Bürge T (2012) Handling and restraint. Lab Mouse, Elsevier:697–708. https://doi.org/10.1016/B978-0-12-382008-2.00029-5
52. Soto JE, Burnett CML, Ten Eyck P, Abel ED, Grobe JL (2019) Comparison of the effects of high-fat diet on energy flux in mice using two multiplexed metabolic phenotyping systems. Obesity 27:793–802. https://doi.org/10.1002/oby.22441
53. Ahloy-Dallaire J, Klein JD, Davis JK, Garner JP (2019) Automated monitoring of mouse feeding and body weight for continuous health assessment. Lab Anim 53:342–351. https://doi.org/10.1177/0023677218797974
54. Higgs S, Thomas J (2016) Social influences on eating. Curr Opin Behav Sci 9:1–6. https://doi.org/10.1016/j.cobeha.2015.10.005
55. Holley DC, Said B, Howard A, Ward-Dolkas P (2003) Monitoring lab animal feeding by using subcutaneous microchip transponders: validation of use with group-housed rats. Contemp Top Lab Anim Sci 42:26–28
56. Bains RS, Cater HL, Sillito RR, Chartsias A, Sneddon D, Concas D et al (2016) Analysis of individual mouse activity in group housed animals of different inbred strains using a novel automated home cage analysis system. Front Behav Neurosci 10:106. https://doi.org/10.3389/fnbeh.2016.00106
57. Bachmanov AA, Reed DR, Beauchamp GK, Tordoff MG (2002) Food intake, water intake, and drinking spout side preference of 28 mouse strains. Behav Genet 32:435–443. https://doi.org/10.1023/A:1020884312053

Chapter 3

The Assessment of Glucose Homeostasis in Rodents: Glucose, Insulin and Pyruvate Tolerance Tests

Nathalia Romanelli Vicente Dragano and Edward Milbank

Abstract

Medical management of obese and type II diabetes patients has improved greatly in the last century. However, even with technological advances, the underlying cause of glucose intolerance and insulin resistance remains unclear, limiting the development of efficient pharmacotherapies. In this sense, preclinical studies are highly valuable and necessary. However, the huge number of available animal models, experimental procedures, and variability in performing or analyzing metabolic tests can easily lead to misunderstanding and misinterpretation. Reliability and reproducibility of experimental procedures are of critical importance for any pre- or clinical study, independently of the investigation field. Thus, in order to ensure harmonization, we provide detailed protocols to perform glucose (GTT), insulin (ITT), and pyruvate (PTT) tolerance tests. Additionally, other important considerations mainly related to species and strain, age, sex, housing/handling, environment, stress, and recovery are discussed to obtain reliable and relevant results that could help to unravel the complexity of metabolic pharmacotherapies.

Key words Diet-induced obesity, Type 2 diabetes, Glucose intolerance, Insulin resistance, Rodents

1 Introduction

The prevalence of obesity worldwide has nearly tripled in the last 40 years, reaching epidemic proportions, and is now regarded as a major health issue in contemporary society [1]. Overweight and obesity represent an increased risk of developing multiple disease conditions, such as type 2 diabetes (T2DM), cardiovascular diseases, mental health abnormalities, and some types of cancer, thereby reducing both life quality and expectancy [2].

The strong association between obesity and T2DM has given birth to the "diabesity" term, which describes the combined adverse health effects of obesity and T2DM [3]. In fact, the majority (85–90%) of patients with T2DM are overweight or obese, and even a slight reduction in body weight (between 5% and 10%) could minimize diabetes-associated complications [4–6]. Although

Cinthia Baú Betim Cazarin (ed.), *Basic Protocols in Foods and Nutrition*,
Methods and Protocols in Food Science, https://doi.org/10.1007/978-1-0716-2345-9_3,

increased adiposity is an established risk factor for T2DM, only a relatively small fraction of obese individuals will develop T2DM over time [7, 8].

Although the primary cause of obesity is a long-term energy imbalance between energy intake and energy expenditure, both obesity and T2DM have a highly complex etiology that involves interplay between genetic, physiological, environmental, and lifestyle-related factors [9, 10]. The multifactorial aspect of these diseases represents a major challenge for the complete understanding of the underlying molecular and biochemical mechanisms and translating them into effective treatment strategies.

In an effort to better understand these mechanisms, recent years have seen a rise in the use of genetically engineered mouse models in basic science research to study the role of specific genes or molecular pathways that could be involved in the development of obesity and T2DM in humans, thereby facilitating the identification of therapeutic targets [11]. However, as one of the main drivers of the actual obesity pandemic is overnutrition, the most common approach used in preclinical studies is the dietary induction of obesity (DIO) in polygenetically susceptible animals, such as the C5BL/6 J mouse and Sprague-Dawley rats, since it mimics better the etiology of obesity and T2DM in humans than the most of genetic/transgenic models [12]. Nevertheless, the choice of a specific animal model for studying metabolic phenotypes depends on the experimental design and the purpose of the study [13].

Numerous high-energy diets have been employed to induce obesity and related metabolic disorders in rodent models. Typically, DIO modeling involves the use of experimental high-fat diets (HFD, ~45–60% of energy from fat, especially dietary fats from an animal source, such as lard) feeding for prolonged periods. The onset of the obese phenotype during the feeding period is gradual. Although an increase in body weight can be observed after 1 or 2 weeks of the diet, other metabolic disturbances, such as glucose intolerance, insulin resistance, hepatic steatosis, and systemic inflammation, can be detected only after several weeks of HFD feeding (8–20 weeks) [12, 14]. Moreover, it is important to highlight that the phenotypic response to HFD feeding can be very heterogeneous within a strain of mice, as it has been reported for Wistar/Sprague-Dawley rats and C57BL/6 J mice [15–17].

Due to the increasing development and availability of animal models to study metabolic diseases, numerous experimental methods to characterize them are needed [11]. Body weight, food intake, and body composition can be routinely measured without major concerns by researchers and technicians, despite being carried out at the same time of day (or night). Several metabolic tolerance tests were also designed to identify glucose metabolism dynamics attributable to genetic or dietary manipulations in rodents [18]. The use of these metabolic techniques – Glucose,

Insulin, and Pyruvate Tolerance Tests and Glucose Clamp Experiments – in animal models has resulted in important advances in understanding obesity-associated T2DM progression.

Glucose homeostasis in rodents, as in humans, is determined by two main factors: (i) the rate of insulin secretion from the pancreatic β-cells in response to glucose and (ii) the sensitivity of the target tissues to insulin action. A proper balance between these two factors determines the ability of the animals to maintain glucose levels within the normal physiological range upon a load [19]. Long-term DIO rodents exhibit glucose homeostasis alterations such as glucose intolerance, reduced insulin sensitivity, and compensatory hyperinsulinemia, all of them being known as previous steps for T2DM onset, characterized by pancreatic β-cell dysfunction and insufficient insulin secretion [20, 21].

In this chapter, we describe the most commonly used methods for assessing glucose tolerance in preclinical studies –Glucose and Insulin Tolerance Tests – as well as the Pyruvate Tolerance Test, which is a supplementary metabolic assay normally used to assess hepatic gluconeogenesis, which is helpful to characterize impaired glucose homeostasis in rodents properly. We also include some basic considerations and specific recommendations, based on our practical experience, that should be taken into account in the experimental design to obtain reproducible and reliable data.

2 Metabolic Tolerance Tests (MTTs): Basic Considerations for Experimental Design and Execution

Although these tests are relatively easy to perform and do not require any specific animal handling practices, investigators should consider some factors when performing MTTs, regardless of the conducted test.

These observations include factors mainly related to animal model and housing conditions (e.g., strain, sex, age, animal per cage, environmental stress) as well as other factors related to experimental procedures (such as fasting, blood glucose measurements, glucose/insulin/pyruvate doses, and route of administration).

2.1 Animal Model and Housing Conditions

Animal Models of Obesity and T2DM In the last 30 years, genetic and dietary-induced obese rodent models, including rats and mice, have been used as important tools to study the complex pathways and genetic basis of energy homeostasis regulation and human metabolic pathophysiology. Each of these models exhibits a distinct metabolic phenotype which has been extensively reviewed [12, 20]. This section focused more on DIO models since it is the most widely used paradigm to study gene-diet interactions in obesity research.

The susceptibility of mice and rats to DIO depends on their respective strain. Typically, the inbred C57BL/6 J polygenic mouse strain is widely used as a DIO model as they are prone to develop obesity and related complications, such as glucose intolerance and insulin resistance [22]. However, only 60% of DIO C57BL/6 J mice will present a significant increase in body weight [23, 24] and will rarely develop β-cell atrophy and frank hyperglycemia when fed with an obesogenic diet [20]. Other inbred strains, including SWR/J, Balb/cJ, and A/J mice, are less susceptible to DIO and display preserved glucose tolerance and insulin action under HFD [25]. There are also important differences in metabolic phenotypes of the C57BL/6 J (J, for Jackson Laboratory, referred to as 6 J) and the C57BL/6 N (N, for National Institutes of Health, 6 N) substrains of the C57BL/6 mice, regardless of the type of diet consumed. For example, the 6 J (under chow or HFD) presents higher glucose levels and lower insulin secretion after intravenous Glucose Tolerance Test (GTT) than the 6 N [26, 27]. Significant disparities in the effects of HFD feeding on C57BL/6 J-related substrains should also be considered in the design of animal DIO studies [22].

Regarding DIO rats, outbred Sprague-Dawley is the most commonly used rat strain as a polygenic model of obesity, which presumably better resembles the common form of human obesity [28]. Nevertheless, experiments using outbred rats (i.e., all animals of the same strain are not genetically identical) usually require a higher number of animals per group than ones using inbred animals, as they show greater differences in response to treatment [29]. For example, when exposed to HFD, only ~50% of outbred Sprague-Dawley rats develop obesity (named as DIO-prone), whereas others have a body weight gain trajectory similar to chow diet-fed controls (named as DIO-resistant) [30].

As in most DIO approaches, rats and mice rarely progress from insulin resistance to T2DM with β-cell failure, new experimental protocols have been established to mimic the slow pathogenesis of T2DM that occurs in humans. A typical procedure is to combine HFD feeding with subsequent injection of low doses of streptozotocin to initiate the β-cell dysfunction in rodents. This approach represents a suitable non-genetic preclinical model for T2DM studies that recapitulate the natural history of the disease progression (from insulin resistance to pancreatic β-cell dysfunction) [31–33]. Besides all the above considerations, choosing a specific animal model will mainly depend on the aim of the research, on the experimental design, and on the desirable phenotypes by which each model will develop obesity, glucose intolerance, insulin resistance, and T2DM.

Sex and Age In different rodent models of obesity-induced glucose intolerance, insulin resistance, and diabetes, males show a stronger phenotype than females. Studies suggest that the propensity toward the development of obesity and its negative metabolic

outcomes is mainly due to sex-based hormonal differences (testosterone versus estradiol and progesterone) and their differential effect on fat distribution and content. For example, when submitted to a dietary challenge (e.g., HFD), age-matched males gained weight and increased their adiposity percentage in a higher proportion than females. Conversely, ovariectomy is known to induce (i) a significant increase in the percentage of adiposity, specifically localized in the gonadal/intra-abdominal depots (comparable to typical male fat distribution), as well as (ii) an increased susceptibly to develop diet-induced insulin resistance [34–36]. Although male animals in preclinical biomedical studies are generally preferred, the inclusion of both sexes should drive important outcomes in basic research that aim to prevent or reverse obesity or treat T2DM besides improving their translational value [20, 37].

Age is another factor that has a substantial effect on metabolic parameters in rodents. In C57BL/6 J mice, the body weight increases gradually over time, reaching a plateau at 36 weeks [38], and 2-year-old mice are significantly heavier than young mice (3 months), mostly due to an increase in their fat mass despite having a significant decrease in lean mass. Additionally, it has been described that old mice could develop discrete glucose intolerance [39]. However, when comparing adult (8 months) and old (24 months-old) mice with similar body composition, it seems that age did not induce any detrimental effect on plasma glucose, insulin levels, or glucose tolerance. Thus, aging-associated glucose intolerance is most likely due to increased adiposity of old C57BL/6 J mice.

Conversely, aged mice fed with chow or HFD exhibited impaired insulin sensitivity and reduced insulin clearance [40, 41]. Thus, insulin resistance appears to be adiposity-independent metabolic effects of aging in mice. Intriguingly, 24 months-old Sprague-Dawley male rats also present glucose intolerance in addition to increased body weight and whole-body insulin resistance when compared with 6 months rats, indicating that the glucose homeostasis in rats seems to be more affected by aging than mice [42].

Another important consideration is the age at which rodents start to be fed with HFD, which will significantly impact the development and severity of obesity-associated metabolic perturbations [43]. The most common protocol for the onset of HFD in rodents is between 6 and 8 weeks of age, and the typical length of HFD feeding is 8–16 weeks [44]. In general, HFD induces higher changes in body weight and glucose metabolism in older (6 months) than young mice (<6 weeks). Importantly, mice younger than 6 weeks can develop potential age-dependent adaptive mechanisms to HFD. For example, young mice respond to HFD by increasing β-cell mass and proliferation and maintaining

normoglycemia, whereas older mice did not display any increases in β-cell proliferation before developing T2DM [45]. Therefore, it is mandatory that all studies of glucose homeostasis need to be performed in age-matched animals of the same sex and strain.

Housing and Environment Conditions Although rodents are typically bred and housed under highly controlled environmental conditions (12:12-hour light/dark cycles, room temperature of 21 ± 2 °C, ad libitum access to food and water), some environmental factors can affect their normal physiology and behaviors. In metabolic characterization studies, mice and rats are often individually housed to allow more precise quantification of food intake, energy expenditure, and other parameters relevant to energy balance regulation at an individual level [46]. However, mice that are housed in groups (5/cage) can show more significant phenotypic variance in body composition parameters when compared with individually housed mice of the same inbred strain, likely due to the effect of behavioral/social interactions, such as subordination and social hierarchies, on the phenotype [47]. In general, while housing does not affect body weight, both food intake and visceral adipose tissue mass are significantly higher individually compared with socially housed animals; such consequences are attributed to a combination of social isolation stress and increased thermogenesis due to a lack of social thermoregulation (reviewed by 47). Taking this into account, it is recommendable to have the same number of animals per cage during the whole experimental period; besides that, changes in social housing conditions within an experiment should be avoided.

Another important consideration is related to the time of the day at which the metabolic tests have to be conducted. The circadian rhythm plays an essential role in the regulation of glucose homeostasis. Over a 24-hour interval both rodents and humans experience variations in glucose and metabolic hormone levels. For instance, in rats, plasma glucose concentration displays circadian variation, with the highest levels toward the beginning of the activity period (dark phase) [48, 49]. Therefore, to allow a better interpretation and reproducibility of the results, all MTTs in a given study should be carried out at the same time of day.

It is also important to minimize some environmental conditions that can generate stress responses in experimental animals when performing MTTs. A common feature of a stress response is a rapid increase of circulating glucose mediated by augmented glucocorticoid synthesis and release from the adrenal glands through the activation of the autonomic nervous system (SNS) and hypothalamic-pituitary-adrenal (HPA) axis [50]. The detrimental influence of stress during glucose assessment protocols can be potentially reduced with acclimatization of animals to regular

handling (i.e., at least once a week) [51]. It is also advisable to transport rats or mice to the experimental room in their home cages at least 2 hours before starting metabolic testing.

2.2 Experimental Procedures-Related Factors

Fasting In rodents, all MTTs are routinely performed following a certain period of fasting to reduce variability and obtain more standardized blood glucose measurements from the different included animals. In experimental research, it is fairly common to withdraw food the night before (overnight fasting, 14–18 hours) or 5–6 hours before (also known as a morning or daytime fast), starting early in the morning (6–8 am), preferably as soon as the light period begins. There is no consensus in the literature about which fasting duration is the most appropriate; however, some considerations about rodent behavior and physiology should be taken into account. As rats and mice are nocturnal, they consume approximately 70% of their food during the dark cycle; consequently, they are already in a low-consumption state at the beginning of overnight fasting (generally around 6–7 pm). Thus, researchers have to keep this in mind when planning the experiment, as overnight fasting is a relatively long time of food deprivation for rodents. For example, it was described that in lean mice, overnight fasting could induce a significant body weight loss (5% and 16% in 5-hour and 18-hour fasted mice, respectively) associated with a decrease in lean and fat masses and hepatic glycogen contents but resulted in enhanced insulin sensitivity compared with 5-h fasting [52]. Thus, considering the well-being of the animals and the reliability of the results, fasting animals for a shorter interval appears to be more physiological and results in reduced metabolic stress [53]. A 5- to 6-hour fasting is considered adequate to determine whether fasting glucose levels are in normal ranges and to perform MTTs in rodents. However, as overnight fasting nearly depletes liver glycogen contents in mice, this can lead to lower variability in baseline blood glucose measurements which can be useful in some experiments. Nevertheless, while both fasting protocols have their one advantages/disadvantages, once one is elected, it should be kept constant throughout the study [17].

Blood Glucose Measurements All MTT protocols presented below involve multiple measurements of blood glucose concentration over a 2-hour interval following the administration of a bolus of glucose (for the Glucose Tolerance Test), insulin (for the Insulin Tolerance Test), or pyruvate (for the Pyruvate Tolerance Test). Typically, small tail-tip amputation (using sharp scissors or scalpel blade) is commonly performed to obtain blood samplings in rodents, mainly because it permits rapid and repeated sampling with minimal pain or invasiveness and does not require anesthesia or analgesia. Portable glucose monitors (glucometers) are commonly used to measure the blood glucose levels in animal models

since these devices are inexpensive, easy to use, and provide fast and reliable results from very small volumes of blood (typically 3–5 μl) [51, 53]. Although most of the available models of whole-blood glucose monitors are designed for the measurement of glucose in humans, except for the AlphaTRAK® (Abbot Laboratory), which is the only glucometer calibrated for the use in rodents, these devices are routinely used in preclinical research to assess glycemia of rats and mice [54]. Importantly, given the differences between glucometers in terms of glucose measurement range, sample size, accuracy, and precision, investigators should not change the monitor's brand throughout the whole experimental period. When using a new glucometer brand/model, it is advisable to carefully check the device by measuring the same animal's glycemia 3 times in a row and analyzing the deviation between the measurements. It is also recommendable to calibrate glucometers following the manufacturer's instructions regularly. Many devices also require new calibration each time a different lot of test strips are used.

3 Assessing Glucose Homeostasis in Rodents

MTTs are designed to identify glucose metabolism derangements in rodents due to genetic or dietary manipulation or to analyze whether a specific treatment is able to induce metabolic or glycemic homeostasis regulation improvements. However, before performing any MTT, we recommend that researchers firstly measure glucose and insulin levels in fasting rodents as primary screening for glucose metabolism disorders. If the glucose or insulin concentrations suggest that glucose intolerance or insulin resistance exist, Glucose (GTT), Insulin (ITT), and Pyruvate (PTT) Tolerance Tests should then be performed. This section describes these 3 protocols in detail, providing guidelines for experimental design and data analysis (also reviewed by [44, 51, 53]).

3.1 Glucose Tolerance Tests (GTT)

The GTT is the easiest and usually the first test to be performed in an animal model. GTT provides a physiological overview of any changes in glucose tolerance [19, 51]. Basically, it measures the clearance by the body of a glucose load, commonly administered orally (OGTT) or intraperitoneal injection (ipGTT). Although both routes of administration are suitable, there are differences in the dynamics of glucose and insulin excursion response to oral and intraperitoneal delivery that should be considered. OGTT represents the most physiological route of glucose entry since the glucose load is administered directly into the stomach via catheter-gavage or feeding needle. The clearance of glucose during OGTT is influenced by several factors, including the rate of gastric emptying and, most importantly, the "incretin effect", which is mediated by

the release of gastrointestinal hormones (i.e., GLP-1 and GIP) that potentiates glucose-dependent insulin secretion. Accordingly, oral glucose delivery results in an elevated insulin secretory response (peaking at 15 min) with lower blood glucose levels than intraperitoneally glucose injection, where the incretin effect is absent [19, 55]. It is worth mentioning that although the oral route is more physiological and more similar to the GTT performed in humans, it frequently introduces significant inconsistency due to variable rates of gastric emptying as well as common technical complications. Some of the oral gavage complications are increased stress and incomplete glucose retention in rodents, even when performed by experienced personnel. Particularly, other research groups and we usually prefer to conduct ipGTT rather than OGTT, thereby in the detailed description of the GTT test presented below, the intraperitoneal route of administration was chosen as a basic method [51, 53].

The standard approach when performing GTTs is to base the glucose doses to inject on the body weight of the animal: 1–2 g of glucose/kg of body weight are commonly administered. However, it is important to note that genetic or DIO rodent models are characterized by increased body weight, predominantly due to increased body fat mass, without differences in lean mass, which is actually the major site of glucose disposal (muscle, brain, and liver). Consequently, HFD-fed animals could be misdiagnosed as glucose intolerants simply because they receive more glucose in absolute terms compared to chow-fed animals. Thus, it is recommendable to calculate the glucose dose based on lean mass (not on total body weight) in experiments involving groups of different body weight or fat pad weights [51, 53, 55, 56].

Briefly, after 6-hour fasting, the rodents receive an intraperitoneal injection of glucose (2 g/kg of body weight). Blood samples are collected from the tail vein of the animal (as described above) for the measurement of blood glucose using a glucometer device at different times: 0 (before intraperitoneal injection), 15, 30, 45, 60, and 120 min after glucose administration. The GTT results are frequently presented as (i) a time course of absolute blood glucose measurements (mg/dL) and (ii) as the area under the curve (AUC). When fasting glucose levels differ between two groups, a calculation of the AUC above glucose baseline should be performed to validate the results [56].

It is important to emphasize that GTT's data only allow a drawn conclusion related to the presence or absence of glucose tolerance in rodents without determining any causative mechanisms. Although a glucose load can stimulate insulin release from β-cells to induce glucose uptake by peripheral tissues and inhibit hepatic glucose production, which in turn indicates insulin secretion and insulin sensibility, these parameters are not directly

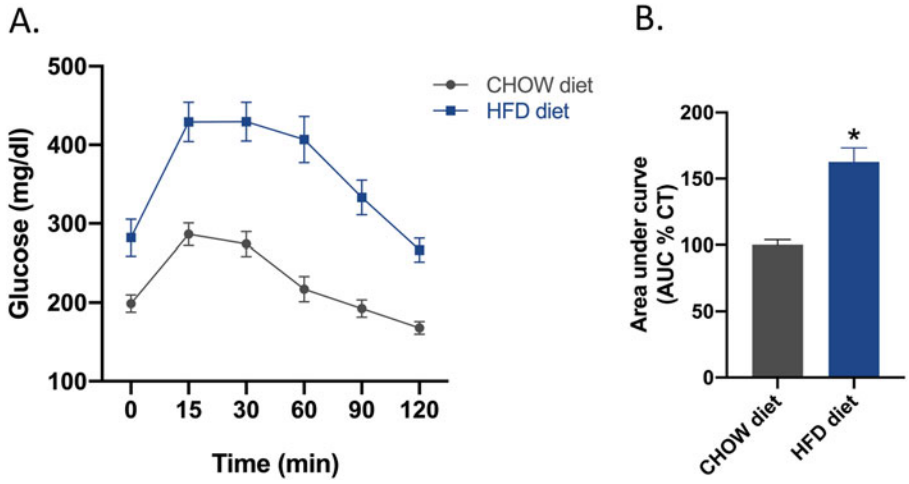

Fig. 1 Representative results of ipGTT performed in chow-fed and 8 weeks HFD-fed C57BL6/J mice. After 6 hours fast, basal glycemia (mg/dl) was assessed. Then, the mice received an intraperitoneal injection of glucose (2 g/kg), and blood glucose levels were measured at different time points. The glycemic values were plotted vs. time after injection (**a**), and the AUC was calculated (**b**). Results are mean ± SEM. *$p < 0.05$

assessed during a GTT and require other tests to be specifically evaluated.

Representative ipGTT results obtained from chow-fed and 8 weeks HFD-fed C57BL6/J mice are presented in Fig. 1. Typically, chow-fed glucose tolerant mice present a characteristic rapid increase in blood glucose 15 minutes after the glucose administration, followed by a gradual decrease of the blood glucose concentration before reaching the basal levels after approximately 60–90 min (Fig. 1a). On the contrary, long-term consumption of HFD induced a significantly impaired glucose tolerance in mice as indicated by both elevated glucose levels through the time course curve and higher adjusted AUC compared with lean controls (Fig. 1b). The lower rate of glucose disappearance in obese mice suggests impairments in the first phase of glucose-induced insulin release, which is characteristic of the early onset of T2DM. Thus, measuring insulin and C-peptide levels during a GTT might provide valuable insulin secretion information [44, 51, 55].

3.2 Insulin Tolerance Test (ITT)

To further characterize the glucose homeostasis in rodents, measurements of insulin resistance are usually performed in addition to glucose tolerance measurements, generally when data obtained from GTT suggest changes in the whole-body insulin sensitivity. There are numerous approaches for assessing insulin resistance in vivo ranging from simple surrogate indexes for insulin sensitivity/resistance (e.g., homeostasis model assessment of insulin resistance: HOMA-IR and the quantitative insulin check index of insulin sensitivity: QUICKI) to the ITT and to the

hyperinsulinemic-euglycemic clamp technique which is widely accepted as being the reference standard for the direct evaluation of insulin sensitivity in both humans and animals [19, 57].

Nevertheless, the ITT is the most used experimental protocol to assess whole-body insulin action in rodents since it is relatively easy to perform and minimally invasive compared with clamp experiments. This test evaluates insulin sensitivity by monitoring endogenous glucose disappearance over time in response to an intraperitoneal injection of human recombinant insulin. The degree by which blood glucose concentration decays following the insulin bolus indicates whole-body insulin action, mostly in the liver and skeletal muscle [17, 51].

Some of the technical issues regarding the GTT test can also be applied to ITT; however, some other important points should be highlighted. When performing ITT experiments, fasting periods ranging between 2 and 6 hours are recommended in order to reduce the possibility of hypoglycemic events (such as tremors, intensified anxiety or apathy, paresthesia, loss of consciousness, and convulsions) in animals subjected to prolonged fasting (e.g., overnight fasting) [51]. The insulin dose is also based on the animal body weight after fasting, and the changes in body composition should also be considered to determine the appropriate dose of insulin to inject for an ITT [53]. For instance, obese mice may receive higher insulin doses than lean mice, even they likely have a very similar amount of lean mass, leading to the following misinterpretation: obese mice are more insulin sensitive, while they are only responding to higher amounts of insulin. For this reason, as explained above for the GTT, normalizing the insulin dose to the lean body mass rather than to the body weight of the animal is the most accurate option. The insulin dose applied in ITT ranges from 0.5 to 2.0 U/kg, usually for lean and chow-fed animals; the dose used is 0.75–1.0 U/kg, while for obese (>40 g) or HFD-fed animal, the dose can be increased up to 2.0 U/kg [51].

Another experimental parameter that requires consideration is the duration of the ITT since insulin has a short plasma half-life in rodents (around 10 min in mice and 3 to 5 min in rats [58, 59] we recommend that blood glucose measurements from the tail vein have to be taken at times 0 (before insulin administration), 5, 10, 15, 30, 45, 60, and 90 min following intraperitoneal injection. Alternatively, other laboratories perform glucose measurements at 0, 5, 10, 15, 20, 25, and 30 min after insulin injection [60]. Importantly, glucose excursions at later time points (i.e., beyond 30 minutes after the insulin bolus) are likely related to the counterregulatory response to hypoglycemia (glucagon, catecholamines, and cortisol) rather than variations in insulin sensitivity [44]. The glucose threshold for increased counterregulatory hormone release in mice is around 80 mg/dl; however, this can vary

depending on the stimulus intensity, nutritional status, and animal models used [61].

The results from ITT should be presented as a time course of absolute blood glucose measurements in addition to inverse AUC below glucose baseline or percentual changes in fasting glucose calculations. The latter can only be applied if the compared groups have similar basal glucose levels. The rate of glucose disappearance constant (kITT) can also be calculated as the slope of the decline in blood glucose is plotted logarithmically (Ferreira, 2012). To determine the kITT of each animal, the values of blood glucose obtained after the initial decrease in response to insulin administration are converted to a logarithmic scale (Y = Ln (Y)). Subsequently, the linear slope (resulting from the logarithm of glycemia vs. time) is calculated and, the obtained values are multiplied by 100 in a module, resulting in the glucose disappearance constant value. This parameter has been described to be closely correlated with insulin sensitivity parameters made by hyperinsulinemic euglycemic clamp [62, 63].

Representative ITT results for lean and DIO mice are shown in Fig. 2. Obese mice developed whole-body insulin resistance as evidenced by higher glucose levels after the insulin injection (Fig. 2a) and lower kITT values (Fig. 2b) compared to control mice.

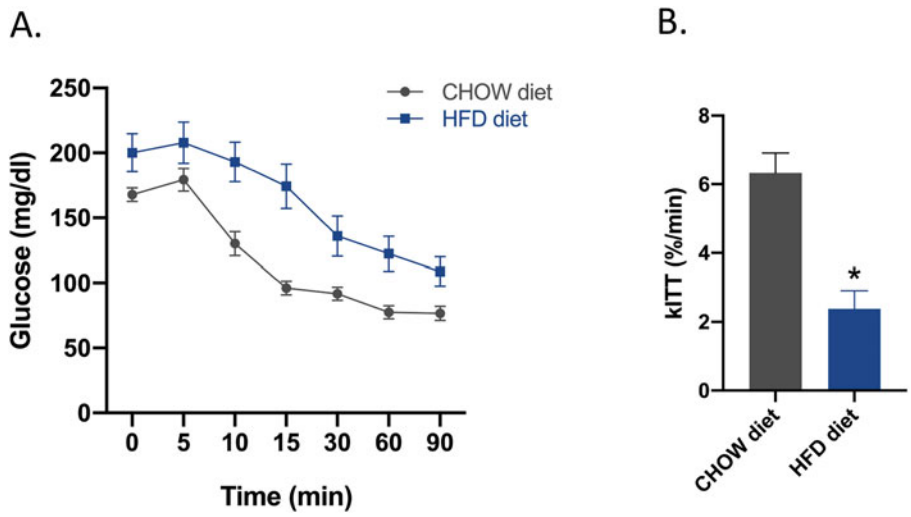

Fig. 2 Representative results of ipITT performed in lean and long-term DIO mice. Mice fasted for 4 h and glucose response to intraperitoneal insulin administration (1 UI/kg) was measured at 5, 10, 15, 30, 60, and 90 min after injection. The glycemic values were plotted vs. time after the injection (**a**), and the KITT was calculated (**b**). Results are mean ± SEM. *$p < 0.05$

The ITT only provides information about the presence or absence of insulin resistance. For example, a lower rate of glucose disappearance during the test is indicative of insulin resistance, however, we cannot properly distinguish the specific site of the defect of insulin action, i.e., either there are impairments in whole-body glucose disposal (mainly accounted by defective insulin-stimulated muscle glucose uptake) or in insulin-induced suppression hepatic glucose production (HGP) or both. Furthermore, it is important to note that ITT is not a very sensitive test; a lack of differences between the groups when performing this test does not imply that the animals have comparable insulin sensitivity levels. More refined experiments (such as a hyperinsulinemic-euglycemic clamp, hyperglycemic clamp, and even in vitro studies on β-cells function) should be considered to better define the mechanisms underlying glucose intolerance and insulin resistance in rodents [44].

3.3 Pyruvate Tolerance Test (PTT)

In addition to GTT and ITT, PTT can also be performed to evaluate the glucose homeostasis in rodents. This test measures the extension of the whole-body conversion of pyruvate into glucose and allows the assessment of the gluconeogenesis rate, which is an important component of HGP. Increased HGP rates have been reported to contribute to hyperglycemia and glucose intolerance in obese mice [60].

The PTT is technically very similar to the ipGTT as it involves monitoring blood glucose levels over time but in response to pyruvate administration rather than glucose loading. Basically, rats or mice are fasted for 6 to 12 hours and then receive an intraperitoneal pyruvate injection (2 g/kg). As performed for GTT or ITT, glucose levels are determined using the blood collected from the tail vein before (0 min) and 15, 30, 60, 90, 120, and 150 min after pyruvate administration. Importantly, once again, all the technical issues regarding how GTTs should be performed are also applied to PTT.

The PTT data are presented as a time course of absolute blood glucose measurements (mg/dL) and as the AUC of glycemia vs. time curve, which is calculated above each individual baseline (basal glycemia) to estimate the total glucose synthesized from pyruvate [60]. Representative PTT results obtained from lean and DIO mice are presented in Fig. 3. As expected, pyruvate injection increased blood glucose levels in both lean and DIO mice, with a greater effect in the latter (Fig. 3a, b), consistent with their common insulin-resistant state and increased gluconeogenesis [64].

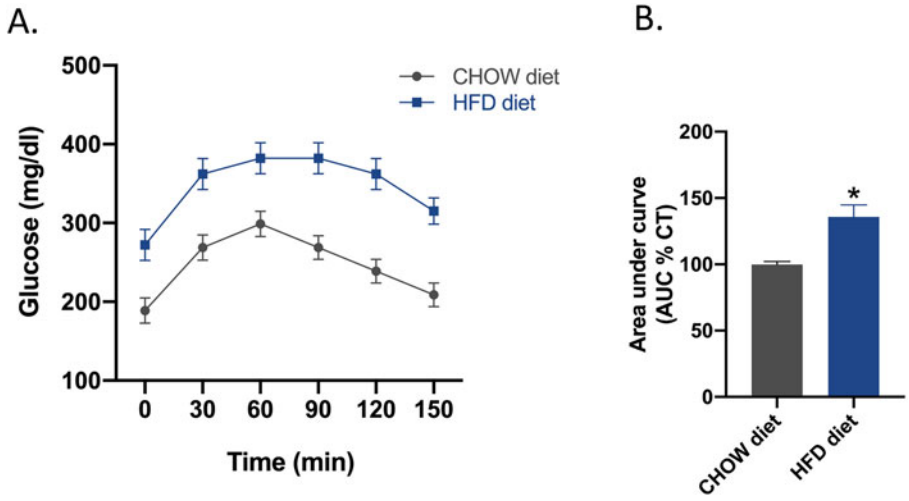

Fig. 3 Representative results of PTT were performed in chow-fed and 8 weeks HFD-fed C57BL6/J mice. Blood glucose was measured before (0 min) and 15, 30, 60, 90, 120, and 150 min after pyruvate injection. The glycemic values were plotted vs. time after injection (**a**), and the AUC was calculated (**b**). Results are mean ± SEM. *$p < 0.05$

4 General Experimental Procedure to Conduct GTT, ITT, and PTT in Rodents

4.1 Materials

Before starting any MTT, be sure that all the material, equipment, and solutions are available for their use.

- Experimental record sheet.
- Laboratory balance and plastic beaker.
- Sharp scissors or scalpel blade.
- Glucometers and glucose test strips.
- Timer.
- 1 mL syringes and 23 g or 25 g needles for intraperitoneal injections in rats and mice, respectively. Insulin syringes can also be used.

All the required work solutions should be prepared the day of the experiment (just prior to use) and should be kept at room temperature (24 °C).

For GTT 20% (w/v) glucose solution (dissolve 2 g of D-glucose in 10 mL of sterile saline solution and sterilize the solution by 0.2 μm filtration).

Calculate the glucose injection volume based on body weight. For a dosage of 2 g/kg, use the formula:

$$20\%\text{glucose solution (}\mu\text{l)} = \text{Body weight (g)} \times 10$$

For ITT 0.25 IU insulin stock solution (dilute 25 μl of rapid-acting human insulin (100UI/ml) in 9975 mL of sterile saline solution, vortex and sterilize the solution by 0.2 μm filtration). Additionally, prepare 20% glucose solution (as above) to be administered if the animals become hypoglycemics.

Calculate the insulin injection volume based on body weight. For a dosage of 1 UI/kg, use the formula:

$$0.25\ \text{IU stock insulin solution}\ (\mu l) = \text{Body weight}\ (g) \times 4$$

For PTT 20% (w/v) pyruvate solution (dissolve 2 g of sodium pyruvate in 10 mL of sterile saline solution and sterilize the solution by 0.2 μm filtration).

Calculate the pyruvate injection volume based on body weight. For a dosage of 2 g/kg, use the formula:

$$20\%\text{sodium pyruvate solution}\ (\mu l) = \text{Body weight}\ (g) \times 10$$

4.2 Experimental Pre-Settings

We recommend performing the metabolic studies at approximately the same time of the day; thereby, fasting periods should be kept constant throughout the study. For overnight fasting, remove food just before the dark cycle starts, and the MTT should be performed in the early morning. For morning fasting (6 h), remove food just after the light cycle starts.

- Regardless of the fasting scheme adopted, place the animals in a clean cage with fresh bedding and free access to drinking water.
- Take the animals to the experimental room in their home cages, preferentially 2 hours before starting a metabolic test in order to acclimate them and reduce stress, which can provoke hyperglycemia affecting the basal glucose measurement.
- The animals should not be individualized at the time of the experiment because it represents a new stress source. In case the animals are housed in groups, they must be clearly identified (e.g., by ear punches or marking the tail with permanent markers) to avoid mistakes when performing the MTTs.
- It is also recommended to individually perform the tests on no more than 15 animals within the same experimental setup to have at least 1 min handling-time per animal and avoid overlapping of timings in the blood glucose measurements. The time left between the injections between one animal and another will also depend on the previous experience of the personnel.
- Do not forget to calibrate the blood glucose monitor as described in the manufacturer's user manual of the device before performing the MTTs.

4.3 Experimental Protocol

1. After the fasting period, measure the body weight of each animal.
2. Based on the body weight, depending on the test to be performed, calculate and annotate in the experimental sheet the volume of glucose, insulin, or pyruvate solution required for intraperitoneal injection.
3. Prepare syringes loaded with the required volume of the specific solution for each animal.
4. Leave separately the number of glycemia strips needed for all tests (calculate an average of 10% more strips due to possible errors in the glucometer readings). Duplicate glucose measurements and using previously calibrated glucometers are recommended.
5. Measure the basal glucose levels (time point = 0) of each animal by carefully cutting off 1–2 mm of the tail tip using sharp scissors or scalp scalpel blade. To obtain the blood drop, gentle squeeze the tail and apply the drop directly to the test strip inserted into the glucometer. We always advise wiping off the first drop of blood before taking new blood samples for blood glucose determination.
6. Slowly inject the appropriate amount of glucose, insulin, or pyruvate solution into the intraperitoneal cavity and start the timer immediately after the first animal is injected. In the experimental sheet, record the exact time in which the first injection was performed to properly control the further times of glucose measurements.
7. Repeat the blood glucose measurements at the appropriate times according to the selected test following the same order in which each animal was injected (e.g., for GTTs, glycemia is measured at times 15, 30, 45, 60, 90, and 120 minutes after glucose injection). When necessary, remove the scab from the tail tip and massage the tail to facilitate blood sampling during the glucose measurements. All blood glucose measurements and their respective time have to be recorded in the experimental sheet.

   Note: When performing ITT, closely monitor the animals for hypoglycemia signs or when blood glucose drops below 40 mg/dL. In case an episode occurs, immediately inject 150ul of 20% glucose intraperitoneal and let the animal recover. Remove the animal of the experiment and observe them during the following 2 hours.
8. At the end of the experiment, place animals in a clean cage with food and water available ad libitum for recovery. Since the MTT are very exhausting for the animals, wait at least 1 week before performing another metabolic test.
9. Plot the data and analyze them according to the recommendations described in the previous section.

5 Conclusions

Obesity and its associated metabolic diseases such as T2DM are now regarded as major health issues in contemporary society. While much progress was made during the last 20 years in managing of these patients improving their condition and well-being, the needs to develop effective pharmacotherapies remain high. Important progress was made to establish suitable preclinical animal models able to mimic clinical courses to protect healthy volunteers and patients included in clinical studies. Due to the high number of animal models available and to respect ethical concerns, choosing the most appropriate one regarding the species, environmental conditions, and genetic background is of critical importance for any study. This chapter summarized the key information about the preclinical rodent models that can be used for obesity and T2DM metabolic research. The reliability and reproducibility also rely on other important factors (sex, age, strains, housing, environment mainly), which were also discussed. Apart from these considerations in the preclinical study setting, depending on the selected MTT, different results and interpretations of one or different parameters will be obtained, possibly leading to misinterpretations. In order to ensure harmonization, we provided a detailed description of the different available MTTs with their application and advantages. Additionally, easy-to-follow experimental procedures were also presented, allowing skilled and young scientists to obtain reliable evidence on obesity and T2DM pharmacotherapies.

References

1. Abarca-Gómez L, Abdeen ZA, Hamid ZA et al (2017) Worldwide trends in body-mass index, underweight, overweight, and obesity from 1975 to 2016: a pooled analysis of 2416 population-based measurement studies in 128·9 million children, adolescents, and adults. Lancet 390:2627–2642. https://doi.org/10.1016/S0140-6736(17)32129-3
2. Dragano NRV, Fernø J, Diéguez C et al (2020) Reprint of: recent updates on obesity treatments: available drugs and future directions. Neuroscience 447:191–215. https://doi.org/10.1016/j.neuroscience.2020.08.009
3. Diabesity: the combined burden of obesity and diabetes on heart disease and the role of imaging | Nature Reviews Cardiology. https://www.nature.com/articles/s41569-020-00465-5. Accessed 12 Feb 2021
4. Obesity and overweight. https://www.who.int/news-room/fact-sheets/detail/obesity-and-overweight. Accessed 12 Feb 2021
5. Colagiuri S (2010) Diabesity: therapeutic options. Diabetes Obes Metab 12:463–473. https://doi.org/10.1111/j.1463-1326.2009.01182.x
6. Apovian CM, Okemah J, O'Neil PM (2019) Body weight considerations in the management of type 2 diabetes. Adv Ther 36:44–58. https://doi.org/10.1007/s12325-018-0824-8
7. Eckel RH, Kahn SE, Ferrannini E et al (2011) Obesity and type 2 diabetes: what can be unified and what needs to be individualized? J Clin Endocrinol Metab 96:1654–1663. https://doi.org/10.1210/jc.2011-0585
8. Malone JI, Hansen BC (2019) Does obesity cause type 2 diabetes mellitus (T2DM)? Or is it the opposite? Pediatr Diabetes 20:5–9. https://doi.org/10.1111/pedi.12787
9. Bhupathiraju Shilpa N, Hu FB (2016) Epidemiology of obesity and diabetes and their cardiovascular complications. Circ Res 118:

1723–1735. https://doi.org/10.1161/CIRCRESAHA.115.306825

10. Blüher M (2019) Obesity: global epidemiology and pathogenesis. Nat Rev Endocrinol 15: 288–298. https://doi.org/10.1038/s41574-019-0176-8
11. Hughey CC, Wasserman DH, Lee-Young RS, Lantier L (2014) Approach to assessing determinants of glucose homeostasis in the conscious mouse. Mamm Genome 25:522–538. https://doi.org/10.1007/s00335-014-9533-z
12. Lutz TA, Woods SC (2012) Overview of animal models of obesity. Curr Protoc Pharmacol Chapter 5(Unit5):61. https://doi.org/10.1002/0471141755.ph0561s58
13. King AJ (2012) The use of animal models in diabetes research. Br J Pharmacol 166: 877–894. https://doi.org/10.1111/j.1476-5381.2012.01911.x
14. Buettner R, Schölmerich J, Bollheimer LC (2007) High-fat diets: modeling the metabolic disorders of human obesity in rodents. Obesity (Silver Spring) 15:798–808. https://doi.org/10.1038/oby.2007.608
15. Levin BE, Dunn-Meynell AA (2002) Defense of body weight depends on dietary composition and palatability in rats with diet-induced obesity. Am J Physiol Regul Integr Comp Physiol 282:R46–R54. https://doi.org/10.1152/ajpregu.2002.282.1.R46
16. Burcelin R, Crivelli V, Dacosta A et al (2002) Heterogeneous metabolic adaptation of C57BL/6J mice to high-fat diet. Am J Physiol Endocrinol Metab 282:E834–E842. https://doi.org/10.1152/ajpendo.00332.2001
17. Ayala JE, Samuel VT, Morton GJ et al (2010) Standard operating procedures for describing and performing metabolic tests of glucose homeostasis in mice. Dis Model Mech 3: 525–534. https://doi.org/10.1242/dmm.006239
18. Vinué Á, González-Navarro H (2015) Glucose and insulin tolerance tests in the mouse. Methods Mol Biol 1339:247–254. https://doi.org/10.1007/978-1-4939-2929-0_17
19. Bowe JE, Franklin ZJ, Hauge-Evans AC et al (2014) Metabolic phenotyping guidelines: assessing glucose homeostasis in rodent models. J Endocrinol 222:G13–G25. https://doi.org/10.1530/JOE-14-0182
20. Kleinert M, Clemmensen C, Hofmann SM et al (2018) Animal models of obesity and diabetes mellitus. Nat Rev Endocrinol 14:140–162. https://doi.org/10.1038/nrendo.2017.161
21. Cerf ME (2013) Beta cell dysfunction and insulin resistance. Front Endocrinol (Lausanne) 4. https://doi.org/10.3389/fendo.2013.00037
22. Siersbæk MS, Ditzel N, Hejbøl EK et al (2020) C57BL/6J substrain differences in response to high-fat diet intervention. Sci Rep 10:14052. https://doi.org/10.1038/s41598-020-70765-w
23. Schwartz MW, Porte D (2005) Diabetes, obesity, and the brain. Science 307:375–379. https://doi.org/10.1126/science.1104344
24. Nishikawa S, Yasoshima A, Doi K et al (2007) Involvement of sex, strain and age factors in high fat diet-induced obesity in C57BL/6J and BALB/cA mice. Exp Anim 56:263–272. https://doi.org/10.1538/expanim.56.263
25. West DB, Boozer CN, Moody DL, Atkinson RL (1992) Dietary obesity in nine inbred mouse strains. Am J Phys 262:R1025–R1032. https://doi.org/10.1152/ajpregu.1992.262.6.R1025
26. Fontaine DA, Davis DB (2016) Attention to background strain is essential for metabolic research: C57BL/6 and the international knockout mouse consortium. Diabetes 65: 25–33. https://doi.org/https://doi.org/10.2337/db15-0982
27. Simon MM, Greenaway S, White JK et al (2013) A comparative phenotypic and genomic analysis of C57BL/6J and C57BL/6N mouse strains. Genome Biol 14:R82. https://doi.org/10.1186/gb-2013-14-7-r82
28. Levin BE, Dunn-Meynell AA, Balkan B, Keesey RE (1997) Selective breeding for diet-induced obesity and resistance in Sprague-Dawley rats. Am J Phys 273:R725–R730. https://doi.org/10.1152/ajpregu.1997.273.2.R725
29. Festing MFW (2014) Evidence should trump intuition by preferring inbred strains to outbred stocks in preclinical research. ILAR J 55:399–404. https://doi.org/10.1093/ilar/ilu036
30. Levin BE, Dunn-Meynell AA (2000) Defense of body weight against chronic caloric restriction in obesity-prone and -resistant rats. Am J Physiol Regul Integr Comp Physiol 278: R231–R237. https://doi.org/10.1152/ajpregu.2000.278.1.R231
31. Kasuga M (2006) Insulin resistance and pancreatic β cell failure. J Clin Invest 116: 1756–1760. https://doi.org/10.1172/JCI29189
32. Srinivasan K, Viswanad B, Asrat L et al (2005) Combination of high-fat diet-fed and low-dose

streptozotocin-treated rat: a model for type 2 diabetes and pharmacological screening. Pharmacol Res 52:313–320. https://doi.org/10.1016/j.phrs.2005.05.004

33. Barrière DA, Noll C, Roussy G et al (2018) Combination of high-fat/high-fructose diet and low-dose streptozotocin to model long-term type-2 diabetes complications. Sci Rep 8: 424. https://doi.org/10.1038/s41598-017-18896-5
34. Macotela Y, Boucher J, Tran TT, Kahn CR (2009) Sex and depot differences in adipocyte insulin sensitivity and glucose metabolism. Diabetes 58:803–812. https://doi.org/10.2337/db08-1054
35. Grove KL, Fried SK, Greenberg AS et al (2010) A microarray analysis of sexual dimorphism of adipose tissues in high-fat-diet-induced obese mice. Int J Obes 34: 989–1000. https://doi.org/10.1038/ijo.2010.12
36. Palmer BF, Clegg DJ (2015) The sexual dimorphism of obesity. Mol Cell Endocrinol 0:113–119. https://doi.org/10.1016/j.mce.2014.11.029
37. Beery AK (2018) Inclusion of females does not increase variability in rodent research studies. Curr Opin Behav Sci 23:143–149. https://doi.org/10.1016/j.cobeha.2018.06.016
38. van der Heijden RA, Bijzet J, Meijers WC et al (2015) Obesity-induced chronic inflammation in high fat diet challenged C57BL/6J mice is associated with acceleration of age-dependent renal amyloidosis. Sci Rep 5:16474. https://doi.org/10.1038/srep16474
39. Elahi D, Muller DC, Andersen DK et al (1985) The effect of age and glucose concentration on insulin secretion by the isolated perfused rat pancreas. Endocrinology 116:11–16. https://doi.org/10.1210/endo-116-1-11
40. Leiter EH, Premdas F, Harrison DE, Lipson LG (1988) Aging and glucose homeostasis in C57BL/6J male mice. FASEB J 2:2807–2811. https://doi.org/10.1096/fasebj.2.12.3044905
41. Ehrhardt N, Cui J, Dagdeviren S et al (2019) Adiposity-independent effects of aging on insulin sensitivity and clearance in mice and humans. Obesity (Silver Spring) 27:434–443. https://doi.org/10.1002/oby.22418
42. Li Q-X, Xiong Z-Y, Hu B-P et al (2009) Aging-associated insulin resistance predisposes to hypertension and its reversal by exercise: the role of vascular vasorelaxation to insulin. Basic Res Cardiol 104:269–284. https://doi.org/10.1007/s00395-008-0754-8
43. Lai M, Chandrasekera PC, Barnard ND (2014) You are what you eat, or are you? The challenges of translating high-fat-fed rodents to human obesity and diabetes. Nutr Diabetes 4: e135–e135. https://doi.org/10.1038/nutd.2014.30
44. Alquier T, Poitout V (2018) Considerations and guidelines for mouse metabolic phenotyping in diabetes research. Diabetologia 61: 526–538. https://doi.org/10.1007/s00125-017-4495-9
45. Tschen S-I, Dhawan S, Gurlo T, Bhushan A (2009) Age-dependent decline in β-cell proliferation restricts the capacity of β-cell regeneration in mice. Diabetes 58:1312–1320. https://doi.org/10.2337/db08-1651
46. Schipper L, van Heijningen S, Karapetsas G et al (2020) Individual housing of male C57BL/6J mice after weaning impairs growth and predisposes for obesity. PLoS One 15: e0225488. https://doi.org/10.1371/journal.pone.0225488
47. Nagy TR, Krzywanski D, Li J et al (2002) Effect of group vs. single housing on phenotypic variance in C57BL/6J mice. Obes Res 10:412–415. https://doi.org/10.1038/oby.2002.57
48. Bizot-Espiard JG, Doublé A, Guardiola-Lemaitre B et al (1998) Diurnal rhythms in plasma glucose, insulin, growth hormone and melatonin levels in fasted and hyperglycaemic rats. Diabetes Metab 24:235–240
49. Jensen T, Kiersgaard M, Sørensen D, Mikkelsen L (2013) Fasting of mice: a review. Lab Anim 47:225–240. https://doi.org/10.1177/0023677213501659
50. Ghosal S, Nunley A, Mahbod P et al (2015) Mouse handling limits the impact of stress on metabolic endpoints. Physiol Behav 150: 31–37. https://doi.org/10.1016/j.physbeh.2015.06.021
51. Benedé-Ubieto R, Estévez-Vázquez O, Ramadori P et al (2020) Guidelines and considerations for metabolic tolerance tests in mice. In: Diabetes, metabolic syndrome and obesity: targets and therapy. https://www.dovepress.com/guidelines-and-considerations-for-metabolic-tolerance-tests-in-mice-peer-reviewed-article-DMSO. Accessed 12 Feb 2021
52. Ayala JE, Bracy DP, McGuinness OP, Wasserman DH (2006) Considerations in the design of hyperinsulinemic-euglycemic clamps in the conscious mouse. Diabetes 55:390–397. https://doi.org/10.2337/diabetes.55.02.06.db05-0686

53. McGuinness OP, Ayala JE, Laughlin MR, Wasserman DH (2009) NIH experiment in centralized mouse phenotyping: the Vanderbilt experience and recommendations for evaluating glucose homeostasis in the mouse. Am J Physiol Endocrinol Metab 297:E849–E855. https://doi.org/10.1152/ajpendo.90996.2008
54. Togashi Y, Shirakawa J, Okuyama T et al (2016) Evaluation of the appropriateness of using glucometers for measuring the blood glucose levels in mice. Sci Rep 6:25465. https://doi.org/10.1038/srep25465
55. Andrikopoulos S, Blair AR, Deluca N et al (2008) Evaluating the glucose tolerance test in mice. Am J Physiol Endocrinol Metab 295: E1323–E1332. https://doi.org/10.1152/ajpendo.90617.2008
56. Nagy C, Einwallner E (2018) Study of in vivo glucose metabolism in high-fat diet-fed mice using Oral Glucose Tolerance Test (OGTT) and Insulin Tolerance Test (ITT). JoVE (Journal of Visualized Experiments):e56672. https://doi.org/10.3791/56672
57. Lee S, Muniyappa R, Yan X et al (2008) Comparison between surrogate indexes of insulin sensitivity and resistance and hyperinsulinemic euglycemic clamp estimates in mice. Am J Physiol Endocrinol Metab 294:E261–E270. https://doi.org/10.1152/ajpendo.00676.2007
58. Cresto JC, Lavine RL, Buchly ML et al (1977) Half life of injected 125I-insulin in control and Ob/Ob mice. Acta Physiol Lat Am 27:7–15
59. Cañas X, Fernández-López JA, Ardévol A et al (1995) Rat insulin turnover in vivo. Endocrinology 136:3871–3876. https://doi.org/10.1210/endo.136.9.7649094
60. Ferreira DS, Amaral FG, Mesquita CC et al (2012) Maternal melatonin programs the daily pattern of energy metabolism in adult offspring. PLoS One 7. https://doi.org/10.1371/journal.pone.0038795
61. Jacobson L, Ansari T, McGuinness OP (2006) Counterregulatory deficits occur within 24 h of a single hypoglycemic episode in conscious, unrestrained, chronically cannulated mice. Am J Physiol Endocrinol Metab 290:E678–E684. https://doi.org/10.1152/ajpendo.00383.2005
62. Bonora E, Manicardi V, Zavaroni I et al (1987) Relationships between insulin secretion, insulin metabolism and insulin resistance in mild glucose intolerance. Diabete Metab 13:116–121
63. Borai A, Livingstone C, Ferns GAA (2007) The biochemical assessment of insulin resistance. Ann Clin Biochem 44:324–342. https://doi.org/10.1258/000456307780945778
64. Soto M, Orliaguet L, Reyzer ML et al (2018) Pyruvate induces torpor in obese mice. PNAS 115:810–815. https://doi.org/10.1073/pnas.1717507115

Chapter 4

Histopathological Evaluation of Steatohepatitis in Animal Experiments

Yoshihisa Takahashi, Erdenetsogt Dungubat, Hiroyuki Kusano, and Toshio Fukusato

Abstract

Fatty liver is a medical condition in which excessive neutral fats accumulate in the liver; its main causes are nonalcoholic fatty liver disease (NAFLD) and alcoholic liver disease (ALD). Both NAFLD and ALD comprise a spectrum of liver diseases ranging from simple steatosis to steatohepatitis, fibrosis, and cirrhosis. NAFLD is currently a major cause of liver cirrhosis and hepatocellular carcinoma, and it is a major indication for liver transplantation. ALD has also emerged as a serious medical and social problem worldwide. Studies using animal models are very useful for elucidating the pathogenesis of and establishing treatment modalities for NAFLD and ALD. In this chapter, we first introduce animal models of NAFLD and ALD that are most commonly used at present, with an emphasis on their advantages and disadvantages. Next, we describe prevalent methodologies used for histopathological evaluation of steatohepatitis in studies using these animal models.

Key words Nonalcoholic fatty liver disease, Nonalcoholic steatohepatitis, Alcoholic liver disease, Animal model, Histopathology

1 Introduction

Fatty liver is a condition in which excessive neutral fats accumulate in the liver; its main causes are nonalcoholic fatty liver disease (NAFLD) and alcoholic liver disease (ALD). Both NAFLD and ALD comprise a spectrum of liver diseases ranging from a mild lesion in which the only steatosis is observed (simple steatosis) to more severe lesions accompanied by necroinflammatory reactions (steatohepatitis), fibrosis and cirrhosis, and finally hepatocellular carcinoma (HCC) [1–3]. Nonalcoholic steatohepatitis (NASH) is histologically characterized by steatosis, lobular inflammation, and hepatocellular ballooning and is often accompanied by fibrosis [4, 5]. Steatosis in human NAFLD is usually macrovesicular and begins in zone 3 [4]. Fibrosis in NASH is characterized by a

Cinthia Baú Betim Cazarin (ed.), *Basic Protocols in Foods and Nutrition*,
Methods and Protocols in Food Science, https://doi.org/10.1007/978-1-0716-2345-9_4,

perisinusoidal/pericellular (chicken wire) pattern that typically begins in zone 3 [4]. The histological appearance of alcoholic steatohepatitis (ASH) resembles that of NASH, but the necroinflammatory activity of ASH is generally more severe than that of NASH, with a higher incidence of canalicular cholestasis, numerous and well-formed Mallory-Denk bodies (eosinophilic irregular-shaped aggregates in the cytoplasm of hepatocytes), prominent ductular reaction, and acute inflammation and fibrosis in the portal tract [4, 6].

NAFLD/NASH is a hepatic manifestation of the metabolic syndrome that is associated with obesity, dyslipidemia, hyperinsulinemia, type 2 diabetes, and hypertension [7, 8]. Insulin resistance (IR), oxidative stress, proinflammatory cytokines, and intestinal flora are considered to be associated with NAFLD's development and progression [3, 9]. In line with the increased prevalence of obesity, NAFLD/NASH incidence is also rapidly increasing across the world. In a recent meta-analysis, NAFLD's global prevalence was estimated to be as high as 25% [10]. NAFLD/NASH is currently a major cause of liver cirrhosis and HCC, and it is a major indication for liver transplantation [11–14]. ALD has also emerged as a serious medical and social problem worldwide. Alcohol-attributable liver cirrhosis was responsible for 0.9% of all global deaths and 47.9% of all deaths associated with liver cirrhosis in 2010 [15].

In light of this global burden, detailed information on the pathogenesis of and effective treatment modalities for NAFLD and ALD are urgently needed. However, the mechanisms of occurrence and progression of NAFLD and ALD have not been completely elucidated, and pharmacotherapy for NAFLD and treatments for ALD other than abstinence have not yet been established. Human NAFLD and ALD occurrence and progression span many years, and administration of drugs and collection of histological samples in human studies have ethical limitations. Therefore, it is very useful to study these diseases using animal models. An ideal animal model should accurately reflect both the disease's pathophysiological and histopathological characteristics, as observed in human subjects. This chapter introduces animal models of NAFLD and ALD that are most commonly used at present, referring to their advantages and disadvantages. Next, we describe the methods of histopathological evaluation of steatohepatitis in studies using these animal models.

2 Animal Models of NAFLD/NASH (Table 1)

2.1 Dietary Models

2.1.1 High-Fat Diet (HFD)

An HFD was developed to induce NAFLD/NASH in experimental animals via diet since the disease is associated with obesity. Forty-five to 75% of the total calories in HFDs are derived from fat

Table 1
Main features of commonly used rodent models of NAFLD/NASH

Models	Obesity	IR	Steatosis	Steatohepatitis	Fibrosis
Dietary models					
HFD	Yes	Yes	Yes	Yes (slight)	Yes (slight)
High-fructose diet	Yes/no	Yes	Yes	Yes/no	No
Cholesterol and cholate	Weight loss	Hepatic IR only	Yes	Yes	Yes
MCD diet	Weight loss	Hepatic IR only	Yes	Yes (severe)	Yes
CDAA diet	No	No	Yes	Yes	Yes
Genetic models					
Ob/Ob mice	Yes	Yes	Yes	No	No (resistant)
Db/Db mice	Yes	Yes	Yes	No	No
Foz/Foz mice	Yes	Yes	Yes	Yes/no	Yes/no

NAFLD nonalcoholic fatty liver disease, *NASH* nonalcoholic steatohepatitis, *IR* insulin resistance, *HFD* high-fat diet, *MCD* methionine- and choline-deficient, *CDAA* choline-deficient L-amino acid-defined

[16]. In many cases, HFDs are administered *ad libitum* to experimental animals. In the model developed by Lieber et al. [17], male Sprague-Dawley rats were fed a high-fat liquid diet (71% of energy from fat, 11% from carbohydrates, 18% from protein) *ad libitum*. After 3 weeks, panlobular steatosis and mononuclear inflammation were observed in the liver accompanied by increased levels of hepatic tumor necrosis factor (TNF)-alpha mRNA expression and oxidative stress. Plasma insulin levels were also elevated, reflecting the development of IR. In a more recent study, male C57BL/6 mice were fed the same HFD for up to 16 weeks, leading to hepatic steatosis, hepatocyte ballooning, Mallory-Denk body formation, increased serum glucose, and decreased adiponectin levels [18].

It is notable that the severity of NAFLD lesions caused by HFDs depends on the experimental animal's species and strain. For example, BALB/c male mice were reported to accumulate more hepatic lipids than C57BL/6 J male mice maintained on HFD [19].

The advantage of the HFD model is that the model's pathophysiology resembles that of human NAFLD with obesity and IR. However, the histological changes observed in the model are mild, representing a substantial disadvantage. When a large amount of HFD is administered to the experimental animal via an implanted gastrostomy tube, more severe hepatic lesions are induced compared to *ad libitum* administration; however, specialized techniques and equipment are necessary for this method [20].

Diet composition is important in the HFD model. In particular, *trans* fats are considered to be effective in the induction of NAFLD. Tetri et al. [21] developed a model in which high-fat chow containing *trans* fats was combined with relevant amounts of a high-fructose corn syrup equivalent in drinking water (American Lifestyle-Induced Obesity Syndrome (ALIOS) mouse model). Male C57BL/6 mice fed this diet became obese and developed severe hepatic steatosis with associated necroinflammatory changes by 16 weeks. Furthermore, glucose intolerance and impaired fasting glucose levels developed within 2 and 4 weeks, respectively, in these animals.

2.1.2 High-Fructose Diet

Fructose is a monosaccharide primarily metabolized in the liver [9, 22]. Fructose consumption is a risk factor for NAFLD development [23] and is associated with severe fibrosis in patients with NAFLD [24]. In our previous study, male Wistar rats fed a high-fructose (70%) diet for 5 weeks developed macrovesicular hepatic steatosis and lobular inflammation. The distribution of steatosis was predominant in zone 1, unlike the usual human NAFLD pattern [25, 26]. In studies from other groups, simple steatosis was induced when water supplemented with 20% or 30% fructose was administered to mice or rats for 8 weeks [27, 28]. The high-fructose diet model is a natural model reflecting the dietary habits of patients with NAFLD, but it suffers from the caveat that a single administration of fructose does not necessarily induce NASH in experimental animals, while it does induce hepatic steatosis. Fructose administration is sometimes combined with administering other nutrients such as fat to induce a more severe lesion. Kohli et al. [29] administered HFD (58% of calories from fat) and water supplemented with 55% fructose and 45% sucrose (w/v) to male C57BL/6 mice for 16 weeks and were successful in inducing obesity, IR, oxidative stress, and a NASH-like phenotype with fibrosis.

2.1.3 High-Cholesterol Diet

Excessive consumption of cholesterol is associated with hepatic steatosis and inflammation [30–32]. However, mice maintained solely on a high-cholesterol (1%) diet showed only simple steatosis [32]. Cholesterol and cholate are known for their atherogenic properties [33]. Mice fed for 24 weeks with an atherogenic diet containing 1.25% cholesterol and 0.5% cholate induced dyslipidemia, lipid peroxidation, oxidative stress, and hepatic stellate cell (HSC) activation in the liver, resulting in pre-cirrhotic steatohepatitis with cellular ballooning. The addition of a high-fat component to the atherogenic diet caused hepatic IR and further accelerated steatohepatitis pathology [34]. This atherogenic diet model's advantage is that the hepatic histopathology is similar to that of human NASH, but the metabolic status differs appreciably from human NASH. In particular, this animal model is characterized by

decreased body weight and plasma triglyceride levels and the development of small epididymal fat pads. Furthermore, systemic IR is not observed.

Recently, diets combining cholesterol with various nutrients have been developed. Savard et al. [32] administered a high-fat high-cholesterol diet (15% fat and 1% cholesterol) to male C57BL/6 J mice for 30 weeks. As a result, obesity, hypercholesterolemia, steatohepatitis with perisinusoidal fibrosis, adipose tissue inflammation, and decreased plasma adiponectin levels were induced in the animals. Charlton et al. [35] fed mice a fast-food diet containing 40% energy as fat (12% saturated fatty acids and 2% cholesterol) supplemented with high fructose for 6 months, and the authors observed the development of obesity, IR, and steatohepatitis with pronounced ballooning and progressive fibrosis (stage 2). A diet high in *trans* fats, fructose, and cholesterol is known to induce NASH with fibrosis effectively, and it is designated as the Amylin liver NASH model (AMLN) [36, 37].

2.1.4 Methionine- and Choline-Deficient (MCD) Diet

The MCD diet is high in sucrose and moderate in fat content (40% sucrose and 10% fat) but deficient in methionine and choline, which are essential for hepatic β-oxidation and very-low-density lipoprotein (VLDL) production [3, 38]. Serum alanine aminotransferase (ALT) levels are consistently increased in mice administered the MCD diet [39]. Steatohepatitis occurs on day 10, and perisinusoidal fibrosis is observed by 8–10 weeks in these mice [40, 41]. Oxidative stress, endoplasmic reticulum stress, and autophagy deregulation are more prominent in the MCD diet model than in the western diet model [42].

As in HFD, the severity of NASH lesions caused by the MCD diet depends on the experimental animal's species, strain, and sex. Kirsch et al. [43] administered the MCD diet to males and females Wistar, Long-Evans, and Sprague-Dawley rats and C57BL/6 mice. As a result, the Wistar strain and the male sex were associated with the greatest steatosis degree in rats. Among the groups studied, male C57BL/6 mice developed the most inflammation and necrosis, lipid peroxidation, and ultrastructural injury, and they most closely mimicked the histological features of NASH.

The advantage of the MCD diet model is that severe histopathology of NASH is induced in a short period, whereas the disadvantage is that the metabolic profile is quite different from human NAFLD. In fact, experimental animals fed an MCD diet are insulin-sensitive and show significant weight loss. Serum glucose, cholesterol, triglyceride, insulin, and leptin levels are decreased, and adiponectin levels are unchanged or increased [44–48]. Therefore, this model is inappropriate for evaluating NAFLD/NASH's pathophysiology but is suitable for evaluating hepatic histopathology. The MCD diet is occasionally administered to genetically obese mice (e.g., *ob/ob* and *db/db* mice) to improve this disadvantage.

2.1.5 Choline-Deficient L-Amino Acid-Defined (CDAA) Diet

The semisynthetic CDAA diet resembles the MCD diet with respect to choline deficiency. However, in the CDAA diet, proteins are substituted with an equivalent and corresponding L-amino acid mixture [9, 49]. Similar to the MCD diet, mice fed the CDAA diet show oxidative stress, increased lipid synthesis, inflammation, and fibrosis in the liver [3, 38]. The CDAA diet requires a longer time to induce these histopathological changes, but the NASH degree is the same or more severe compared to the MCD diet [3, 9, 50]. Although animals fed the CDAA diet do not experience the weight loss observed with the MCD diet, human NAFLD's metabolic features still fail to appear when used in the same time frame as the MCD diet [9, 38, 50]. A CDAA diet with high-fat (CDAHFD) was therefore established to improve the model. Male C57BL/6 J mice fed CDAHFD maintained or gained weight and developed enlarged fatty liver with fibrosis by week 6, but they failed to elicit metabolic syndrome features [51]. Work from our group also confirmed that male C57BL/6 J mice fed CDAHFD for 7 weeks developed NASH with fibrosis (Figs. 1 and 2). Both the CDAA diet and CDAHFD are inappropriate for examining the metabolic profile of NAFLD/NASH. Notably, male C57BL/6 J mice fed the CDAA diet for 84 weeks developed hepatocellular adenomas and carcinomas with an incidence of 66.7% and 20.8%, respectively [52]. CDAHFD more rapidly induced hepatocellular adenomas and carcinomas in male C57BL/6 J mice (from 36 weeks) [53].

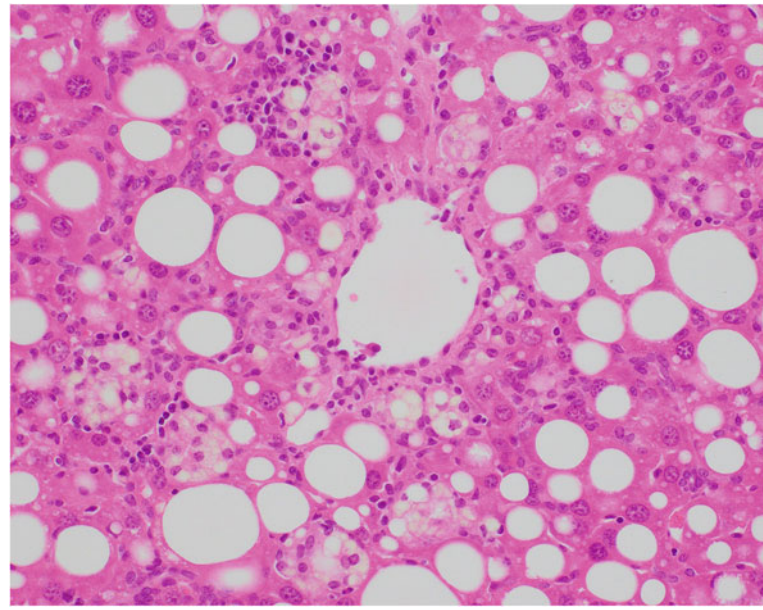

Fig. 1 Histological appearance of a male C57BL/6 J mouse's liver maintained on CDAHFD for 7 weeks. Findings of NASH are clearly observed. (H&E staining, original magnification: 200×)

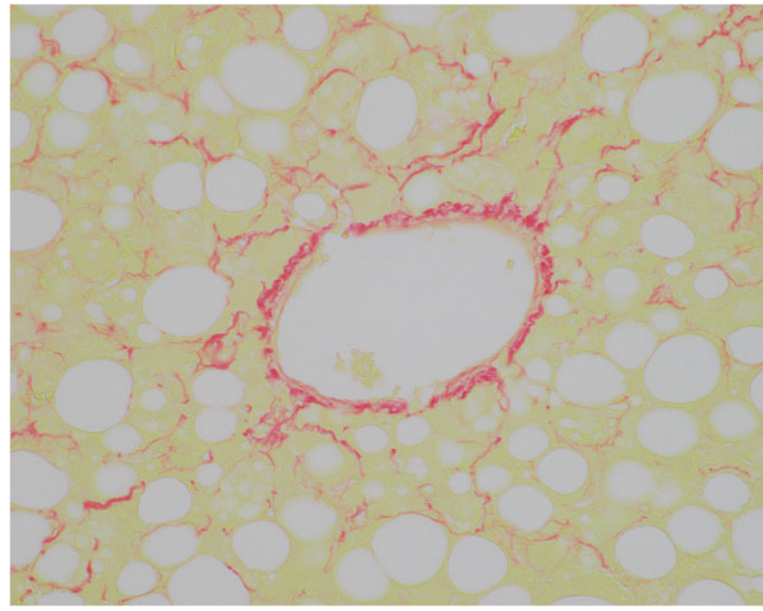

Fig. 2 Sirius Red staining slide of the same mouse as in Fig. 1. Centrilobular fibrosis is clearly confirmed. (Original magnification: 200×)

2.2 Genetic Models

2.2.1 ob/ob *Mice*

Leptin is an adipokine produced by white adipose tissue. It exerts an anorexic effect by acting on the hypothalamus and plays an important role in regulating energy balance. The *ob/ob* mice are leptin-deficient due to a spontaneous mutation of the leptin gene. They are hyperphagic, inactive, and very obese and exhibit hyperlipidemia, hyperglycemia, hyperinsulinemia, and IR [54]. The *ob/ob* mice develop hepatic steatosis but do not spontaneously develop NASH [26]. Additional stimuli such as HFD, MCD diet, or lipopolysaccharide administration are necessary to induce NASH in *ob/ob* mice [55]. Leptin is considered essential for hepatic fibrosis, and *ob/ob* mice are resistant to hepatic fibrosis [56]. However, Kristiansen et al. [57] reported that male *ob/ob* mice fed an AMLN diet for 12 weeks developed NASH with considerable fibrosis, and the fibrosis stage was significantly more advanced than in C57BL/6 J mice fed the same diet for 26 weeks.

This model has the advantage that it has a metabolic status similar to that of human NAFLD, including obesity and IR. However, observational clinical studies have shown higher or similar leptin levels in simple steatosis and NASH compared to controls in humans [58]; therefore, *ob/ob* mice do not reflect the leptin status in human NAFLD.

2.2.2 db/db *Mice*

The db/db mice possess a spontaneous point mutation in the leptin receptor gene. Therefore, leptin levels in *db/db* mice remain normal or increase, but the mice are resistant to leptin. Similar to *ob/ob* mice, *db/db* mice are hyperphagic, inactive, and very obese and

exhibit hyperlipidemia, hyperglycemia, hyperinsulinemia, and IR. They develop hepatic steatosis but do not spontaneously develop steatohepatitis. Additional stimuli such as HFD, MCD diet, or iron overload are necessary to induce NASH in *db/db* mice [26, 59–61]. Unlike *ob/ob* mice, *db/db* mice develop fibrosis when administered the MCD diet [62]. Rats with an analogous mutation are called *fa/fa* rats (also known as Zucker rats) and show similar features to *db/db* mice [9].

2.2.3 foz/foz *Mice*

Alström syndrome 1 (Alms1) is a protein encoded by the *Alms1* gene in humans. Alms1 is a ubiquitous protein that is essential for proper primary cilia function. Although its function has not yet been fully elucidated, it is thought to be crucial in intracellular transport and appetite regulation. The *foz/foz* mice are Alms1-deficient due to a truncating mutation in the *Alms1* gene. Similar to *ob/ob* and *db/db* mice, *foz/foz* mice are hyperphagic and obese and exhibit IR, hyperglycemia, dyslipidemia, and hepatic steatosis [63, 64]. When *foz/foz* mice are maintained on HFD, they develop severe steatohepatitis with hepatocyte ballooning and fibrosis [65]. NAFLD lesions in *foz/foz* mice are dependent on the background strain. Farrell et al. [66] fed *foz/foz* BALB/c and C57BL/6 J mice HFD or control diet for 24 weeks and reported that all *foz/foz* mice turned obese. Hepatomegaly, hyperinsulinemia, hyperglycemia, and hypoadiponectinemia occurred only in *foz/foz* C57BL/6 J mice, whereas *foz/foz* BALB/c mice formed more adipose tissues. Serum ALT levels, steatosis, ballooning, liver inflammation, and NAFLD activity score (NAS) were worse in C57BL/6 J mice. In HFD-fed mice, fibrosis was severe in *foz/foz* C57BL/6 J mice but absent in *foz/foz* BALB/c mice.

As mentioned above, certain genetic models of NAFLD do not spontaneously progress to NASH, and these are often used in combination with a special diet such as HFD and MCD diet. In experiments using these combination models, more severe NASH lesions are induced in a shorter period, and pathophysiology more similar to that in human NAFLD is obtained compared to ordinary animals maintained on a special diet. However, the financial cost associated with the former studies is higher.

3 Animal Models of ALD (Table 2)

3.1 Ad Libitum Feeding

The advantage of *ad libitum* feeding of ethanol via drinking water is that it is easy to perform and is the closest to the human condition of alcohol drinking. Therefore, this method was used in the earliest animal experiments of ALD. However, sufficient blood alcohol levels and severe hepatic lesions cannot be induced using this method since rodents show aversion to ethanol's taste or smell and they exhibit rapid rates of alcohol catabolism [67].

Table 2
Main features of commonly used rodent models of ALD

Models	Steatosis	Inflammation	Fibrosis	Advantages and disadvantages
Ad libitum alcohol in drinking water	Yes/no	No	No	Easy to perform Minimal elevation of ALT levels and mild or no steatosis
Ad libitum alcohol in a liquid diet	Yes	Yes/no	No	Easy to perform Steatosis is induced, but severe steatohepatitis is not
Chronic and binge feeding	Yes	Yes	Yes	Cost- and time-efficient Steatohepatitis is induced
Enteral feeding (Tsukamoto-French model)	Yes	Yes	Yes	Difficult to perform, and intensive care is required Steatohepatitis is induced

ALD alcoholic liver disease, *ALT* alanine aminotransferase

To overcome this limitation, Lieber et al. [68] developed a method of *ad libitum* feeding of ethanol in a liquid diet (Lieber-DeCarli liquid diet). In this method, a liquid diet containing ethanol is the only energy source, with the animals not being supplied with any other food or drink. The optimal amount of ethanol for the liquid diet for rats was found to be 5 g/dl or 36% of the total energy [69]. In this method, blood alcohol levels mimicking clinical conditions and alcoholic fatty liver are induced in rats. However, severe steatohepatitis is generally not observed.

3.2 Chronic and Binge Feeding

Chronic alcohol drinkers commonly experience one or multiple cycles of binge drinking. An animal model reflecting such a drinking habit of humans was developed. Bertola et al. [70] administered mice the Lieber-DeCarli ethanol liquid diet *ad libitum* for 10 days followed by a single binge ethanol feeding, and the animals were euthanized 9 h later. This protocol for chronic-plus-single-binge ethanol feeding was found to synergistically induce liver injury, inflammation, and fatty liver, which mimicked the acute-on-chronic alcoholic liver injury in patients. This feeding protocol can also be extended to chronic feeding for more extended periods up to 8 weeks plus single or multiple binges.

3.3 Enteral Feeding (Tsukamoto-French Model)

One of the methods to circumvent the aversion of experimental animals toward ethanol involves forced administration of ethanol. Tsukamoto et al. [71] administered male Wistar rats ethanol and a nutritionally defined low-fat liquid diet via continuous intragastric infusion for 15 to 85 days. Ethanol intake was progressively increased from 32% to 41.4% of total calories. As a result, high blood alcohol levels were maintained, and severe and progressive fatty infiltration was induced in the liver. After 30 days of

intoxication, one-third of the animals showed focal necrosis with mononuclear cell infiltration in the liver's centrilobular areas. This was correlated with markedly elevated levels of serum aspartate aminotransferase (AST) and ALT. The addition of fat or iron to this diet and an extension of the administration period led to the induction of liver fibrosis or cirrhosis [72, 73]. This method's advantage is that more severe hepatic histopathology could be generated compared to *ad libitum* ethanol feeding. Also, accurate control of diet delivery is possible with this method. However, this method requires advanced technical skills and specialized equipment since a tube is placed in the stomach through the skin. In addition, extensive and stringent postoperative care is essential.

4 Materials

4.1 Euthanization of Experimental Animals

Body weight is usually measured before the euthanization of experimental animals, and electronic weighing instruments for experimental animals are commercially available. Inhalation anesthetics are frequently used for anesthesia before euthanization of experimental animals, and specialized apparatus for this procedure is also commercially available. If such apparatus cannot be obtained, an anesthesia bottle may be used instead. Blood-collecting needles for experimental animals are commercially available and convenient when blood is to be collected from the heart, jugular vein, aorta, or vena cava. If blood is to be collected by decapitation, a decapitator should be prepared. When the liver and other tissues are excised, dissecting scissors and tweezers designed for experimental animals should be used. A razor is convenient for cutting excised tissues. Frozen samples for molecular analyses should be snap frozen using liquid nitrogen or other freezing agents and preserved in tubes or bags of appropriate size. For this, commercially available nucleic acid protectants may be useful.

4.2 Preparation of Histological Slides

Ten percent neutral buffered formalin is usually used for the fixation of tissues. This can be prepared by diluting formalin solution with a buffer solution; however, the conditioned ready-to-use solution is commercially available. Ten percent neutral buffered formalin is placed in a sample bottle, and tissues are immersed in it. Ethanol and xylene are the most frequently used dehydration agents. A paraffin melter and hard paraffin are necessary for embedding the tissue. A microtome and slide glasses are necessary to make paraffin sections.

Trays, an optimal cutting temperature (OCT) compound (embedding medium for frozen samples) and a freezing agent are necessary to obtain samples for frozen sections. Liquid nitrogen or dry ice-isopentane is frequently used as the freezing agent.

A styrene foam reserving box, or a beaker, should be prepared to contain the freezing agent. A cryostat and slide glasses are necessary to prepare the frozen sections.

Xylene, ethanol, hematoxylin solution, eosin solution, and a mounting medium are necessary for hematoxylin and eosin (H&E) staining. Staining baskets to place slide glasses, staining vats to store xylene or ethanol, and cover glasses for sealing should also be prepared. In addition to these, picric acid and Sirius Red are necessary to perform Sirius Red staining, and isopropyl alcohol and Oil Red O powder are necessary to perform Oil Red O staining. To perform immunohistochemical staining, appropriate antibodies and staining kits should be prepared.

4.3 Histopathological Evaluation and Image Analysis

Usually, histopathological evaluation can be performed using an ordinary microscope. Equipment for taking photomicrographs and software for image analysis are necessary to perform image analysis. Furthermore, a scanner, an image storage system, image viewer software, and a monitor are necessary for image analysis using whole slide imaging (WSI) (virtual microscopy).

5 Methods

5.1 Euthanization of Experimental Animals

In general, experimental animals are anesthetized, and their body weight is measured just before euthanization. Inhalation anesthetics such as isoflurane and sevoflurane are frequently used. Although diethyl ether was frequently used as an inhalation anesthetic earlier, it is rarely used at present because it is flammable and may cause excessive respiratory secretion and laryngeal spasms.

If biochemical examinations of the serum are scheduled, blood is collected at the time of the euthanization of experimental animals. In experiments using mice, as much blood as possible should be collected since the total amount of blood in mice is very small. In many cases, blood is collected from the heart, jugular vein, aorta, or vena cava, and 0.5–1 and 2–10 mL of blood can be collected from mice and rats, respectively, using those methods. However, if the experimentalist is not skillful, sufficient biochemical analysis of the serum may not be possible due to the low amount of collected blood and/or hemolysis. Blood collection via decapitation under deep anesthesia is the easiest method, and a large amount of blood can be collected this way with relatively mild hemolysis.

After blood collection, the liver is excised and weighed. The epididymal adipose tissue is occasionally excised and weighed in NAFLD/NASH studies since the disease is associated with metabolic syndrome, and the inflammation of adipose tissue and adipokines production are known to be important in the pathogenesis. Next, samples for formalin-fixed paraffin-embedded (FFPE) sections and frozen sections are collected from the excised liver.

Frozen sections are necessary for performing fat staining. It is desirable that samples for FFPE sections are fixed in 10% neutral buffered formalin for one to several days. After that, these could be embedded in paraffin to prepare paraffin blocks. Automatic embedding devices have been developed for this purpose. Samples for frozen sections are placed in trays, embedded in an OCT compound, quickly frozen using liquid nitrogen or other freezing agents, and stored at −80 °C. If molecular analyses are scheduled, frozen hepatic tissues are also collected from the euthanized animals and stored.

5.2 Preparation of Histological Slides

First, 3–5 μm histological sections are prepared using the paraffin blocks and a microtome, and the generated sections are attached to slide glasses. Next, the slide glasses are placed in a staining basket and immersed sequentially in xylene, 99% ethanol, 90% ethanol, 80% ethanol, and 70% ethanol (stored in each staining vat) for 5–10 min each (deparaffinization step).

5.2.1 H&E Staining

After deparaffinization, the sections are washed in running water for approximately 5 min and stained with hematoxylin for 3–5 min. Next, the sections are again washed in running water for more than 20 min and stained with eosin for 1–3 min.

Sections after eosin staining are dehydrated by treating with an alcohol series. This step is performed by sequentially immersing the H&E stained sections in 70% ethanol (for several seconds), 80% ethanol (for several seconds), 90% ethanol (for 3 min), 99% ethanol (for several seconds), and 100% ethanol (twice, for several seconds each). Next, the sections are permeated by immersing in xylene (twice, for several minutes each). Finally, the sections are sealed with cover glasses (Fig. 1). In many laboratories, the entire process from deparaffinization to sealing has been automated, with machines developed to perform the method.

5.2.2 Sirius Red Staining

Histological staining methods to evaluate hepatic fibrosis include Masson staining, Azan staining, and Sirius Red staining. The collagen fibers are stained blue in Masson and Azan staining, and they are stained red in Sirius Red staining. Here, we explain the method of Sirius Red staining (Fig. 2).

Picro Sirius Red solution is prepared by mixing 100 mL of a saturated aqueous solution of picric acid and 5 mL of 1% (w/v) aqueous Sirius Red solution. After deparaffinization and washing, similar to those required for H&E staining, the sections are stained with the Picro Sirius Red solution for 20 min and quickly washed with distilled water. Next, dehydration, permeation, and sealing are performed similarly to the H&E staining protocol. Various kits for performing Sirius Red staining are commercially available.

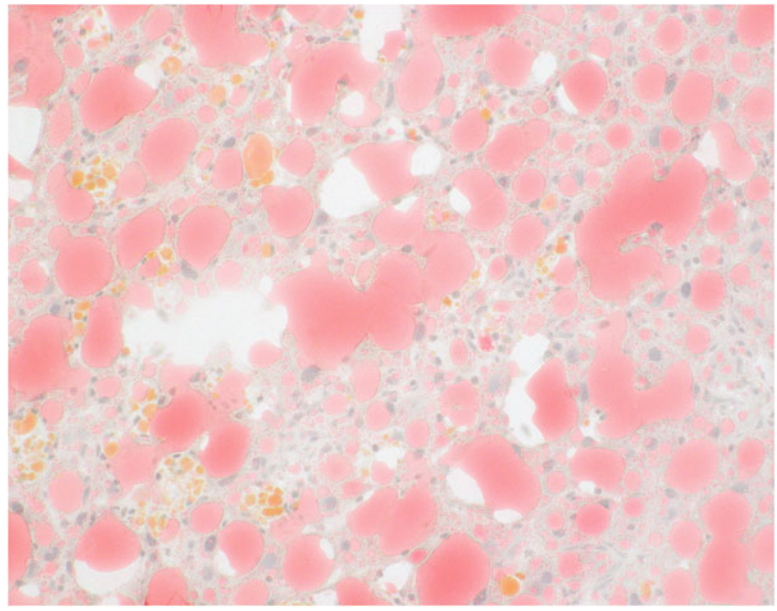

Fig. 3 Oil Red O staining slide of fatty liver. Neutral fat is stained red. (Original magnification: 200×)

5.2.3 Oil Red O Staining

Fat staining includes Sudan III, Sudan IV, Sudan Black B, and Oil Red O staining. Neutral fat is stained orange in Sudan III, orange-red in Sudan IV, black in Sudan Black B, and red in Oil Red O staining. Here, we describe the protocol for Oil Red O staining (Fig. 3).

A 100 mL aliquot of 99% isopropyl alcohol and 0.3 g of Oil Red O powder are placed in a closed vessel and kept overnight at 60 °C with occasional shaking to prepare the saturated solution. The solution is allowed to cool to room temperature (*approximately 20° C*) and kept as a preservative solution. This preservative solution and purified water are mixed at a ratio of 6:4 and shaken hard, kept for 10 min, and filtered to prepare the working solution.

Frozen sections of 5–10 μm thickness are attached to slide glasses and washed lightly in running water before washing with purified water. Next, the sections are sequentially immersed in 60% isopropyl alcohol (for 1 min), Oil Red O staining solution (at 37 °C for 10–15 min), and 60% isopropyl alcohol (for 2 min). The sections are washed lightly in running water before washing with purified water. Next, the sections are stained with hematoxylin for 3–5 min, washed twice in running water, and washed with purified water. Finally, the sections are sealed with a water-soluble permanent mounting medium.

5.2.4 Immunohistochemical Staining

Immunohistochemical staining is useful for determining the type of inflammatory cells and evaluating activated HSCs that are associated with fibrogenesis in the liver. Representative antibodies used for determining the type of inflammatory cells in steatohepatitis studies include CD45 (a marker of leukocytes), CD3 (a marker of T lymphocytes), CD4 and CD8 (useful for identification of the type of T lymphocytes), CD20 (a marker of B lymphocytes), myeloperoxidase (a marker of myeloid cells), and CD68 (a marker of monocytes/macrophages/Kupffer cells). Alpha-smooth muscle actin is employed as a marker of activated HSCs. Various antibodies and kits for immunohistochemical staining have been developed, and staining is basically performed according to the manufacturer's instructions. Automated immunostaining devices are currently used for this purpose in many laboratories.

5.3 Histopathological Evaluation

In general, histopathological evaluation of steatohepatitis is performed using both H&E staining slides and specialized staining slides such as Sirius Red, Masson, or Azan staining slides. When the effects of a test substance or genetic manipulation are examined, semi-quantitative histopathology analysis is not necessarily required if the effect is very clear. However, if the histological change is not so clear, semi-quantitative analysis followed by statistical analysis is a powerful tool to explore the effect under study. A semi-quantitative analysis for NAFLD was developed by Kleiner et al. [74], with this method being frequently applied to animal experiments as well as human studies. The semi-quantitative analysis is summarized as follows. Steatosis grade is classified by low- to medium-power evaluation of parenchymal involvement by steatosis as 0 (<5%), 1 (5–33%), 2 (>33–66%), or 3 (>66%). Fibrosis stage is classified as 0 (none), 1 (perisinusoidal or periportal), 2 (perisinusoidal and portal/periportal), 3 (bridging fibrosis), or 4 (cirrhosis). Lobular inflammation is graded by an overall assessment of all inflammatory foci as 0 (no foci), 1 (<2 foci per 200× field), 2 (2–4 foci per 200× field), or 3 (>4 foci per 200× field). Portal inflammation is assessed at low magnification and classified as 0 (none to minimal) or 1 (greater than minimal). Hepatocellular ballooning is classified as 0 (none), 1 (few balloon cells), or 2 (many cells/prominent ballooning). NAS is calculated as the sum of the steatosis (0–3), lobular inflammation (0–3), and hepatocellular ballooning (0–2) scores.

5.4 Image Analysis

Image analysis is useful for the objective evaluation of histopathological conditions. In particular, image analysis of steatosis using fat staining, that of fibrosis using Sirius Red or another specialized staining, and that of inflammatory cell infiltration or activated HSCs using immunohistochemical staining are frequently performed. Statistically significant differences are commonly observed in image analysis, even if that is not the case with semi-quantitative

analysis. While performing image analysis, photomicrographs of several randomly selected microscopic fields are generally taken for each histological slide, and the frequency of the positively stained area is calculated using image analysis software. Various kinds of image analysis software are commercially available, and specific image analysis protocols are available from the respective manufacturers. In this context, WSI represents an emerging modality for more accurate image analysis [75]. Furthermore, recent advances in deep learning have revolutionized image analysis, and automated deep learning-based scores reportedly agree with scores assigned by a human pathologist in the histological evaluation of animal models of NASH [76].

5.5 Other Analyses

Triglyceride and cholesterol quantification is possible if frozen hepatic tissues are collected during experimental animal euthanasia. The Folch method is widely used to extract lipids [77], and various kits are commercially available to measure the amount of extracted lipids. NAFLD/NASH is associated with IR [3, 9], and adiponectin, a type of adipokine, is known to inhibit NAFLD [78]. Therefore, serum insulin and adiponectin quantification is often performed in studies of NAFLD/NASH. Enzyme-linked immunosorbent assay (ELISA) is the most common method to achieve this, with various commercially available kits. In addition, analysis of expression patterns of cytokine and receptor genes using real-time reverse transcription-polymerase chain reaction (RT-PCR) or western blotting is useful for elucidating the mechanisms of the effects of drug administration or genetic manipulation. However, the detailed methodology of these biochemical and molecular analyses is beyond the scope of this chapter.

6 Notes

In this section, we list some points to be noted while performing animal experiments on steatohepatitis:

1. There are no complete animal models of NAFLD/NASH or ALD. The most appropriate animal model should be selected based on the purpose, period, and budget of the study, equipment available in the researcher's laboratory, and technical skills. For example, the MCD diet model is inappropriate for a study on the pathophysiology of NAFLD.
2. In many animal experiments of ALD, the ethanol dosage is small to begin with, and is gradually increased. Before performing any experiment, the researcher should check available literature in detail or perform a preliminary experiment to determine the best administration protocol.

3. Subtle differences in diet composition, laboratory environment, species, strain, and sex of the experimental animal can cause appreciable differences in the experimental results. The researcher should perform a preliminary experiment when using an untried animal model.
4. If blood glucose or serum insulin measurement is scheduled, a sufficiently long fasting period should be included before euthanizing the experimental animals.
5. There are no established rules concerning the sampling site and size of FFPE liver tissue. Our group usually makes a cross-section of the two large liver lobes along the long axis to prepare slides for histological examination. The recommended size of the liver tissue for frozen sections is approximately 5 mm in diameter. Liver tissues for DNA or RNA examination should be cut into 2–3 mm-sized blocks before freezing.
6. Some antibodies for immunohistochemical staining can only be used for human tissues. Therefore, the researcher must confirm whether the antibody can be used for the experimental animal tissues before acquiring it. The optimum staining conditions may vary based on the combination of the antibody, kit, and laboratory equipment. Therefore, while performing initial immunohistochemical staining, we recommend that the researcher tries several antigen retrieval methods and antibody dilution ratios to determine the optimal staining condition.
7. Macrovesicular steatosis is predominant in most human NAFLD cases, but microvesicular steatosis may be predominant in experimental animals' NAFLD. Differentiation between microvesicular steatosis and clear cell change of hepatocytes may be difficult to perform with H&E staining slides. In such cases, fat staining is very useful.
8. Differentiation between the portal tracts and central veins in mice and rats' liver tissue may be difficult since the amount of collagen fibers in the portal tracts is small in these animals. The presence of the bile duct is useful as a reference for this distinction.
9. The criteria for semi-quantitative analysis of NAFLD/NASH's histopathology reported by Kleiner et al. [74] may be modified depending on the animal model used.
10. The microscopic fields and magnification should be determined according to the purpose while acquiring photomicrographs for image analysis, and image acquisition conditions should be kept constant. For example, when evaluating centrilobular fibrosis, the photomicrograph should contain a central vein at the central part, and it should not contain portal tracts. In evaluating immunohistochemical staining slides, counting positively stained cells in the photomicrograph (instead of image analysis) is permitted if the number of positively stained cells is small.

References

1. Farrell GC, Larter CZ (2006) Nonalcoholic fatty liver disease: from steatosis to cirrhosis. Hepatology 43(2 Suppl 1):S99–S112
2. Lamas-Paz A, Hao F, Nelson LJ et al (2018) Alcoholic liver disease: utility of animal models. World J Gastroenterol 24:5063–5075
3. Zhong F, Zhou X, Xu J, Gao L (2020) Rodent models of nonalcoholic fatty liver disease. Digestion 101(5):522–535
4. Takahashi Y, Fukusato T (2014) Histopathology of nonalcoholic fatty liver disease/nonalcoholic steatohepatitis. World J Gastroenterol 20:15539–15548
5. Beddosa P (2017) Pathology of non-alcoholic fatty liver disease. Liver Int 37(Suppl 1):85–89
6. Tiniakos DG (2010) Nonalcoholic fatty liver disease/nonalcoholic steatohepatitis: histological diagnostic criteria and scoring systems. Eur J Gastroenterol Hepatol 22:643–650
7. Machado M, Cortez-Pinto H (2006) Non-alcoholic steatohepatitis and metabolic syndrome. Curr Opin Clin Nutr Metab Care 9:637–642
8. Haas JT, Francque S, Staels B (2016) Pathophysiology and mechanisms of nonalcoholic fatty liver disease. Annu Rev Physiol 78: 181–205
9. Van Herck MA, Vonghia L, Francque SM (2017) Animal models of nonalcoholic fatty liver disease – a starter's guide. Nutrients 9: 1072
10. Younossi ZM, Koenig AB, Abdelatif D, Fazel Y, Henry L, Wymer M (2016) Global epidemiology of nonalcoholic fatty liver disease - meta-analytic assessment of prevalence, incidence, and outcomes. Hepatology 64:73–84
11. El-Serag HB (2011) Hepatocellular carcinoma. N Engl J Med 365:1118–1127
12. Wong RJ, Cheung R, Ahmed A (2014) Nonalcoholic steatohepatitis is the most rapidly growing indication for liver transplantation in patients with hepatocellular carcinoma in the U.S. Hepatology 59:2188–2195
13. Wong RJ, Aguilar M, Cheung R et al (2015) Nonalcoholic steatohepatitis is the second leading etiology of liver disease among adults awaiting liver transplantation in the United States. Gastroenterology 148:547–555
14. Brunt EM, Wong VW, Nobili V et al (2015) Nonalcoholic fatty liver disease. Nat Rev Dis Primers 1:15080
15. Rehm J, Samokhvalov AV, Shield KD (2013) Global burden of alcoholic liver diseases. J Hepatol 59:160–168
16. Jacobs A, Warda AS, Verbeek J, Cassiman D, Spincemaille P (2016) An overview of mouse models of nonalcoholic steatohepatitis: from past to present. Curr Protoc Mouse Biol 6: 185–200
17. Lieber CS, Leo MA, Mak KM et al (2004) Model of nonalcoholic steatohepatitis. Am J Clin Nutr 79:502–509
18. Eccleston HB, Andringa KK, Betancourt AM et al (2011) Chronic exposure to a high-fat diet induces hepatic steatosis, impairs nitric oxide bioavailability, and modifies the mitochondrial proteome in mice. Antioxid Redox Signal 15: 447–459
19. Nishikawa S, Yasoshima A, Doi K, Nakayama H, Uetsuka K (2007) Involvement of sex, strain and age factors in high fat diet-induced obesity in C57BL/6J and BALB/cA mice. Exp Anim 56:263-272
20. Deng QG, She H, Cheng JH et al (2005) Steatohepatitis induced by intragastric overfeeding in mice. Hepatology 42:905–914
21. Tetri LH, Basaranoglu M, Brunt EM, Yerian LM, Neuschwander-Tetri BA (2008) Severe NAFLD with hepatic necroinflammatory changes in mice fed trans fats and a high-fructose corn syrup equivalent. Am J Physiol Gastrointest Liver Physiol 295:G987–G995
22. Lowette K, Roosen L, Tack J, Berghe PV (2015) Effects of high-fructose diets on central appetite signaling and cognitive function. Front Nutr 2:5
23. Ouyang X, Cirillo P, Sautin Y et al (2008) Fructose consumption as a risk factor for non-alcoholic fatty liver disease. J Hepatol 48: 993–999
24. Abdelmalek MF, Suzuki A, Guy C et al (2010) Increased fructose consumption is associated with fibrosis severity in patients with nonalcoholic fatty liver disease. Hepatology 51: 1961–1971
25. Kawasaki T, Igarashi K, Koeda T et al (2009) Rats fed fructose-enriched diets have characteristics of nonalcoholic hepatic steatosis. J Nutr 139:2067–2071
26. Takahashi Y, Soejima Y, Fukusato T (2012) Animal models of nonalcoholic fatty liver disease/nonalcoholic steatohepatitis. World J Gastroenterol 18:2300–2308
27. Spruss A, Kanuri G, Wagnerberger S, Haub S, Bischoff SC, Bergheim I (2009) Toll-like receptor 4 is involvled in the development of fructose-induced hepatic steatosis in mice. Hepatology 50:1094–1104

28. Mamikutty N, Thent ZC, Suhaimi FH (2015) Fructose-drinking water induced nonalcoholic fatty liver disease and ultrastructural alteration of hepatocyte mitochondria in male Wistar rat. Biomed Res Int 2015:895961
29. Kohli R, Kirby M, Xanthakos SA et al (2010) High-fructose, medium chain trans fat diet induces liver fibrosis and elevates plasma coenzyme Q9 in a novel murine model of obesity and nonalcoholic steatohepatitis. Hepatology 52:934–944
30. Wouters K, Van Gorp PJ, Bieghs V et al (2008) Dietary cholesterol, rathan than liver steatosis, leads to hepatic inflammation in hyperlipidemic mouse models of nonalcoholic steatohepatitis. Hepatology 48:474–486
31. Subramanian S, Goodspeed L, Wang S et al (2011) Dietary cholesterol exacerbates hepatic steatosis and inflammation in obese LDL receptor-deficient mice. J Lipid Res 52: 1626–1635
32. Savard C, Tartaglione EV, Kuver R et al (2013) Synergistic interaction of dietary cholesterol and dietary fat in inducing experimental steatohepatitis. Hepatology 57:81–92
33. Santhekadur PK, Kumar DP, Sanyal AJ (2018) Preclinical models of non-alcoholic fatty liver disease. J Hepatol 68:230–237
34. Matsuzawa N, Takamura T, Kurita S et al (2007) Lipid-induced oxidative stress causes steatohepatitis in mice fed an atherogenic diet. Hepatology 46:1392–1403
35. Charlton M, Krishnan A, Viker K et al (2011) Fast food diet mouse: novel small animal model of NASH with ballooning, progressive fibrosis, and high physiological fidelity to the human condition. Am J Physiol Gastrointest Liver Physiol 301:G825–G834
36. Trevaskis JL, Griffin PS, Wittmer C et al (2012) Glucagon-like peptide −1 receptor agonism improves metabolic, biochemical, and histopathological indices of nonalcoholic steatohepatitis in mice. Am J Physiol Gastrointest Liver Physiol 302:G762–G772
37. Clapper JR, Hendricks MD, Gu G et al (2013) Diet-induced mouse model of fatty liver diseae and nonalcoholic steatohepatitis reflecting clinical disease progression and methods of assessment. Am J Physiol Gastrointest Liver Phhysiol 305:G483–G495
38. Ibrahim SH, Hirsova P, Malhi H, Gores GJ (2016) Animal models of nonalcoholic steatohepatitis: eat, delete, and inflame. Dig Dis Sci 61:1325–1336
39. Pena AD, Leclercq I, Field J, George J, Jones B, Farrell G (2005) NF-kappaB activation, rather than TNF, mediates hepatic inflammation in a murine dietary model of steatohepatitis. Gastroenterology 129: 1663–1674
40. Leclercq IA, Farrell GC, Field J, Bell DR, Gonzalez FJ, Robertson GR (2000) CYP2E1 and CYP4A as microsomal catalysts of lipid peroxides in murine nonalcoholic steatohepatitis. J Clin Invest 105:1067–1075
41. Ip E, Farrell G, Hall P, Robertson G, Leclercq I (2004) Administration of the potent PPARalpha agonist, Wy-14,643, reverses nutritional fibrosis and steatohepatitis in mice. Hepatology 39:1286–1296
42. Machado MV, Michelotti GA, Xie G et al (2015) Mouse models of diet-induced nonalcoholic steatohepatitis reproduce the heterogeneity of the human disease. PLoS One 10: e0127991
43. Kirsch R, Clarkson V, Shephard EG et al (2003) Rodent nutritional model of non-alcoholic steatohepatitis: species, strain and sex difference studies. J Gastroenterol Hepatol 18:1272–1282
44. Nagasawa T, Inada Y, Nakano S et al (2006) Effects of bezafibrate, PPAR pan-agonist, and GW501516, PPARdelta agonist, on development of steatohepatitis in mice fed a methionine- and choline-deficient diet. Eur J Pharmacol 536:182–191
45. Larter CZ, Yeh MM, Williams J, Bell-Anderson KS, Farrell GC (2008) MCD-induced steatohepatitis is associated with hepatic adiponectin resistance and adipogenic transformation of hepatocytes. J Hepatol 49:407–416
46. Rinella ME, Elias MS, Smolak RR, Fu T, Borensztajn J, Green RM (2008) Mechanisms of hepatic steatosis in mice fed a lipogenic methionine choline-deficient diet. J Lipid Res 49:1068–1076
47. Itagaki H, Shimizu K, Morikawa S, Ogawa K, Ezaki T (2013) Morphological and functional characterization of non-alcoholic fatty liver disease induced by a methionine-choline-deficient diet in C57BL/6 mice. Int J Clin Exp Pathol 6: 2683–2696
48. Sanches SC, Ramalho LN, Augusto MJ, Da Silva DM, Ramalho FS (2015) Nonalcoholic steatohepatitis: a search for factual animal models. Biomed Res Int 2015:574832
49. Nakae D, Mizumoto Y, Andoh N et al (1995) Comparative changes in the liver of female Fischer-344 rats after short-term feeding of a semipurified or a semisynthetic L-amino acid-defined choline-deficient diet. Toxicol Pathol 23:583–590
50. Ishioka M, Miura K, Minami S, Shimura Y, Ohnishi H (2017) Altered gut microbiota

composition and immune response in experimental steatohepatitis mouse models. Dig Dis Sci 62:396–406

51. Matsumoto M, Hada N, Sakamaki Y et al (2013) An improved mouse model that rapidly develops fibrosis in non-alcoholic steatohepatitis. Int J Exp Pathol 94:93–103
52. Denda A, Kitayama W, Kishida H et al (2002) Development of hepatocellular adenomas and carcinomas associated with fibrosis in C57BL/6J male mice given a choline-deficient, L-amino acid-defined diet. Jpn J Cancer Res 93:125–132
53. Ikawa-Yoshida A, Matsuo S, Kato A et al (2017) Hepatocellular carcinoma in a mouse model fed a cholne-deficient, L-amino acid-defined, high-fat diet. Int J Exp Pathol 98: 221–233
54. Lindström P (2007) The physiology of obese-hyperglycemic mice [*Ob/Ob* mice]. Sci World J 7:666–685
55. Hansen HH, Feigh M, Veidal SS, Rigbolt KT, Vrang N, Fosgerau K (2017) Mouse models of nonalcoholic steatohepatitis in preclinical drug development. Drug Discov Today 22: 1707–1718
56. Leclercq IA, Farrell GC, Schriemer R, Robertson GR (2002) Leptin is essential for the hepatic fibrogenic response to chronic liver injury. J Hepatol 37:206–213
57. Kristiansen MNB, Veidal SS, Rigbolt KTG et al (2016) Obese diet-induced mouse models of nonalcoholic steatohepatitis – tracking disease by liver biopsy. World J Hepatol 8:673–684
58. Polyzos SA, Kountouras J, Mantzoros CS (2015) Leptin in nonalcoholic fatty liver disease: a narrative review. Metabolism 64:60–78
59. Takahashi Y, Soejima Y, Kumagai A, Watanabe M, Uozaki H, Fukusato T (2014) Inhibitory effects of Japanese herbal medicines sho-saiko-to and juzen-taiho-to on nonalcoholic steatohepatitis in mice. PLoS One 9: e87279
60. Takahashi Y, Soejima Y, Kumagai A, Watanabe M, Uozaki H, Fukusato T (2014) Japanese herbal medicines shosaikoto, inchinkoto, and juzentaihoto inhibit high-fat diet-induced nonalcoholic steatohepatitis in *db/db* mice. Pathol Int 64:490–498
61. Handa P, Morgan-Stevenson V, Maliken BD et al (2016) Iron overload results in hepatic oxidative stress, immune cell activation, and hepatocellular ballooning injury, leading to nonalcoholic steatohepatitis in genetically obese mice. Am J Physiol Gastrointest Liver Physiol 310:G117–G127
62. Sahai A, Malladi P, Pan X et al (2004) Obese and diabetic *db/db* mice develop marked liver fibrosis in a model of nonalcoholic steatohepatitis: role of short-form leptin receptors and osteopontin. Am J Physiol Gastrointest Liver Physiol 287:G1035–G1043
63. Heydet D, Chen LX, Larter CZ et al (2013) A truncating mutation of *Alms1* reduces the number of hypothalamic neuronal cilia in obese mice. Dev Neurobiol 73:1–13
64. Poekes L, Legry V, Farrell G, Leclercq I (2014) Role of ciliary dysfunction in a new model of obesity and non-alcoholic steatohepatitis: the *Foz/Foz* mice. Arch. Public Health 72(Supple 1):07
65. Arsov T, Larter CZ, Nolan CJ et al (2006) Adaptive failure to high-fat diet characterizes steatohepatitis in *Alms1* mutant mice. Biochem Biophys Res Commun 342:1152–1159
66. Farrell GC, Mridha AR, Yeh MM et al (2014) Strain dependence of diet-induced NASH and liver fibrosis in obese mice is linked to diabetes and inflammatory phenotype. Liver Int 34: 1084–1093
67. Takahashi Y, Fukusato T (2017) Animal models of liver diseases. In: Conn PM (ed) Animal models for the study of human disease, 2nd edn. Academic Press/Elsevier, Cambridge
68. Lieber CS, Jones DP, DeCarli LM (1965) Effects of prolonged ethanol intake: production of fatty liver despite adequate diets. J Clin Invest 44:1009–1021
69. Lieber CS, DeCarli LM (1989) Liquid diet technique of ethanol administration: 1989 update. Alcohol Alcohol 24:197–211
70. Bertola A, Mathews S, Ki SH, Wang H, Gao B (2013) Mouse model of chronic and binge ethanol feeding (the NIAAA model). Nat Protoc 8:627–637
71. Tsukamoto H, French SW, Benson N et al (1985) Severe and progressive steatosis and focal necrosis in rat liver induced by continuous intragastric infusion of ethanol and low fat diet. Hepatology 5:224–232
72. French SW, Miyamoto K, Tsukamoto H (1986) Ethanol-induced hepatic fibrosis in the rat: role of the amount of dietary fat. Alcohol Clin Exp Res 10(6 Suppl):13S–19S
73. Tsukamoto H, Horne W, Kamimura S et al (1995) Experimental liver cirrhosis induced by alcohol and iron. J Clin Invest 96:620–630
74. Kleiner DE, Brunt EM, Van Natta M et al (2005) Design and validation of a histological scoring system for nonalcoholic fatty liver disease. Hepatology 41:1313–1321

75. Melo RCN, Raas MWD, Palazzi C, Neves VH, Malta KK, Silva TP (2020) Whole slide imaging and its applications to histopathological studies of liver disorders. Front Med (Lausanne) 6:310
76. Heinemann F, Birk G, Stierstorfer B (2019) Deep leaning enables pathologist-like scoring of NASH models. Sci Rep 9:18454
77. Folch J, Lees M, Sloane Stanley GH (1957) A simple method for the isolation and purification of total lipids from animal tissues. J Biol Chem 226:497–509
78. Finelli C, Tarantino G (2013) What is the role of adiponectin in obesity related non-alcoholic fatty liver disease? World J Gastroenterol 19: 802–812

Chapter 5

Quantification of Short-Chain Fatty Acids in Feces

Mirella Romanelli Vicente Bertolo and Stanislau Bogusz Junior

Abstract

Short-chain fatty acids (SCFA) have attracted the attention of researchers due to their positive physiological effects on health. SCFA are involved directly or indirectly in many physiologic responses correlated to the modulation of inflammatory processes, anti-carcinogenic effects, and cardiovascular disease risk-reducing. Besides that, SCFA have a regulatory role in the gut environment and hepatic and whole-body glucose homeostasis. Chemically, SCFA are carboxylic acids with an aliphatic chain containing two to six carbons. They are the primary products of gut fermentation of dietary fiber. Therefore, a quantitative analysis of SCFA in feces is necessary to evaluate the impact of fiber-rich foods on health. This chapter aims to provide some of the principal basic protocols for extracting, separating, and quantifying SCFA in feces.

Key words Short-chain fatty acids, Sample preparation, Quantitative analysis

1 Introduction

1.1 Short-Chain Fatty Acids in Feces

Short-chain fatty acids (SCFA) are a class of volatile carboxylic acids with a saturated aliphatic chain containing between two and six carbons [1, 2]. SCFA include acetic acid ($C_2H_4O_2$), propionic acid ($C_3H_6O_2$), butyric acid ($C_4H_8O_2$), isobutyric acid ($C_4H_8O_2$), valeric acid ($C_5H_{10}O_2$), isovaleric acid ($C_5H_{10}O_2$), caproic acid ($C_6H_{12}O_2$), and heptanoic acid ($C_7H_{14}O_2$). Nevertheless, acetic acid, propionic acid, and butyric acid together account for more than 95% of the SCFA found in the colon and feces [2, 3].

SCFA appear as the primary product of the fermentation of dietary fibers [4, 5]. The dietary fibers are polymers derived primarily from edible parts of foods and can be grouped in: (i) non-digestible oligosaccharides such as fructooligosaccharides, galactooligosaccharides, inulin, and pectin oligosaccharides; (ii) non-digestible polysaccharides such as pectin, gum, cellulose, hemicellulose, mucilage, chitin, β-glucan, resistant starch, and resistant dextrin; and (iii) non-carbohydrate fiber like lignin [6].

Cinthia Baú Betim Cazarin (ed.), *Basic Protocols in Foods and Nutrition*,
Methods and Protocols in Food Science, https://doi.org/10.1007/978-1-0716-2345-9_5,

The extent of fermentation (and, consequently, the rate of SCFA production) will depend on the type of dietary fiber that is consumed [7]. For example, insoluble fibers such as cellulose and lignin are more resistant to intestinal microbiota and suffer from 5% to 20% fermentation, the unfermented fiber contributing to the formation of the fecal mass. On the other hand, water-soluble fibers such as pectin are less resistant to bacterial action and, because of that, are practically 100% fermented [6, 8].

The importance of SCFA for health begins in the intestinal environment: among their main actions are the contribution to the normal function of the gut and to the muscles and vasculature of the colon [4]. Furthermore, with the increase of SCFA, the intestinal pH decreases modulating the gut microbiota's composition and reducing colonization by pathogenic species [6, 9, 10].

SCFA also acts as nutrients for colon cells, stimulating their proliferation and increasing blood flow [11, 12]. Still in the intestine, the high production of SCFA contributes to the absorption of water and minerals, leading to faster recovery from diarrhea and contributing to avoiding a mineral deficiency [13]. Furthermore, SCFA are involved in several other physiological aspects of the host, including immunological processes in the body, in addition to presenting anticarcinogenic action and reducing the risk of cardiovascular diseases [2, 14, 15].

Acetic acid is one of the most abundant SCFA and may be formed from pyruvate by acetogenic bacteria that utilize H_2 to reduce CO_2 to acetic acid [6]. A wide range of gut microbes, e.g., *Bacteroides*, *Bifidobacterium*, *Clostridium*, and *Ruminococcus* species, produce acetic acid. After the production, acetic acid manages to cross the blood barrier in the brain and act as an appetite regulator, using a homeostatic mechanism [16]. Acetic acid has also proven to be able to reduce the cholesterol levels in the blood [3, 17].

Propionic acid may be produced in the gut by carbohydrate fermentation, either by the succinate or acrylate pathway. The conversion of succinate to methylmalonate and the further release of CO_2 results in propionic acid by *Bacteroides*, *Prevotella*, *Alistipes*, *Ruminococcus*, *Phascolarctobacterium*, *Dialister*, and *Akkermansia* species [18]. Propionic acid can also inhibit cholesterol production in the liver, reducing intrahepatic levels of triglycerides [2, 13]. In addition, propionic acid and acetic acid can directly activate G protein-coupled receptors, which implies activation of signal transduction pathways and reduces the host's blood pressure [19].

Butyric acid is generated by various gut bacteria, particularly the gram-positive anaerobic bacteria, *Faecalibacterium*, *Eubacterium*, and *Roseburia* species [18, 20, 21]. These bacteria condense two molecules of acetyl-CoA to acetoacetyl-CoA, which subsequently converts to β-hydroxybutyryl-CoA and crotonyl-CoA. The final product is butyryl-CoA. Butyryl-CoA may be further

converted to butyric acid by a butyryl-CoA:acetate Co-A transferase or phosphorylated to butyryl-phosphate and converted to butyric acid by a butyrate kinase [6]. The produced butyric acid is extremely important in preventing and treating colon diseases such as colon cancer and colitis, as it acts as an energy source for the enterocytes and to the intestinal epithelial cells, and also promotes apoptosis in tumoral cells [4, 16].

1.2 In Vivo *and* In Vitro *SCFA Studies*

Given the importance of SCFA for health due to their diverse physiological functions, many studies in the literature aim to isolate, identify, and quantify these compounds using the most diverse analytical methods. To obtain SCFA, both *in vivo* and *in vitro* studies can be conducted, each one with its peculiarities, advantages, and disadvantages.

Dobrowolska-Iwanek et al. [4] developed a study with fecal samples collected from a 35-year-old male subject, who underwent physical and laboratory analysis prior to the collection, involving his permission and consent to conduct the study. The subject, who had not administered any probiotics or antibiotics for at least 1 year, was kept on a controlled low-fat and low-energy diet for a week before collecting feces.

Although the collection of human samples is workable, the number of studies involving mice and rats is much greater given the advantages of being small mammals, with rapid reproduction and biological processes similar to those of humans [2]. Marques et al. [2] described a study involving a total of 26 female rats, maintained at controlled temperature and light. They were divided into three groups, all of which were fed with a commercial diet. Two of these groups received water for 14 days, and one of them received jaboticaba (*Plinia cauliflora*) aqueous extract. Then, the water and the extract were replaced with dextran sodium sulfate (DSS) to induce colitis in the animals. The animal's weight, blood in the feces, and feces consistency were monitored daily throughout the experiment. After 2 weeks, the animals were euthanized under anesthesia, and their fecal contents were collected and stored at −80 °C until the SCFA analysis.

Despite involving simpler procedures for obtaining samples, *in vivo* assays are severely criticized by some studies in the literature, which claim that their quantification is inaccurate since the total SCFA in the gut must be a balance between what was produced and what was absorbed in the colon (about 80–90%) [15, 22–24]. Thus, these studies develop different strategies to induce fermentation *in vitro*, under strict control over the production of SCFA.

In these *in vitro* studies, animals are used only as donors of the intestinal microbiota: Wang et al. [15] used the content collected from the cecum of six male rats to prepare suspensions of intestinal bacteria (10%, w/v). For that, they prepared a culture medium with

nutrients in fixed concentrations such as arabinogalactan (1 g/L), pectin (2 g/L), xylan (1 g/L), starch (4.2 g/L), glucose (0.4 g/L), yeast extract (3 g/L), peptone (1 g/L), mucin (4 g/L), and cysteine (0.5 g/L) and controlled pH (5.5). The suspensions were incubated for 2 h at 37 °C under slow continuous shaking of 50 rpm to enable the bacteria to adapt to the new physical-chemical conditions and the new nutritional medium. After the adaptation of the bacteria, the authors conduct a fermentation for 24 h at 37 °C and 50 rpm. SCFA contents were measured at 0, 12, and 24 h.

Moreover, one of the most recent and well-validated models of *in vitro* studies for the analysis of SCFA is the so-called human intestinal microbial ecosystem simulator (SHIME). This dynamic and multi-compartmental model simulates the gastrointestinal environment by adjusting some validated parameters, such as the pH of the different compartments, as well as the diet and temperature of the intestinal microbiota that will be inoculated into the system [24, 25]. Douny et al. [24] adapted SHIME to simulate the gastrointestinal tract of piglets. They used a first bioreactor mimicking stomach, duodenum/jejunum, a second bioreactor for ileum, and finally, a third bioreactor for the proximal colon. The medium used to feed the gastrointestinal system was prepared to make it closer to piglet feed using: mucin (6.0 g/L), protease-peptone (1.0 g/L), potato starch (1.0 g/L), L-cysteine hydrochloride (0.2 g/L), and a post-weaning diet (8.0 g/L) that contained mainly barley (30%), soy (29%), wheat (14%), maize (5%), and oat flakes (5%). That culture medium was previously autoclaved for 35 min at 121 °C. For the SHIME first vessel, the pH was adjusted at 3.0. Moreover, for the intestinal vessel, the authors use a pancreatic juice made with sodium hydrogen carbonate (2.5 g/L), pancreatin (0.9 g/L), and Oxgall (4.0 g/L). The system was inoculated with the microbiota of the healthy weaned piglet of 35 days old, and a stabilization period of 2 weeks had been applied. After the stabilization, they collected 20 samples of the different fermentation liquids for the SCFA determination.

2 Sample Preparation for Quantification of SCFA in Feces

2.1 Sample Preparation Techniques for SCFA Analysis

Considering how *in vivo* tests are carried out to determine SCFA in feces, a crucial step after collecting the samples is the sample preparation step, that is, their conversion to an appropriate form that can be analyzed with the analytical tools available in the laboratory. In general, aspects such as sample preparation time, consumption of solvents, concentration and volatility of the analytes, and risk of contamination must be considered when selecting the best sample preparation method. Regardless of the method chosen, it must be able to remove as many as possible the interferants from the sample matrix in an acceptable time for recovery of the analytes of interest

present in the sample. Furthermore, since SCFA are volatile components present in samples in limited quantities, their sample preparation should be as simplified as possible. The next item details some of the most recommended sample preparation methods for SCFA recovery.

2.1.1 Centrifugation and Filtration

In most procedures involving samples collected *in vivo*, the sample preparation covers simple steps of dilution, centrifugation, and filtration. For that, the fecal samples are weighed and suspended in water (~20% w/w), followed by homogenization (by vortex or preferably in an Ultra Turrax). Next, the formed fecal suspensions have their pH adjusted to values between 2 and 3 (by adding 5 M hydrochloric acid or 0.3 M formic acid) and are then centrifuged (20 min at 3698 × g and 4 °C) to the obtention of clear supernatants. Sometimes, filters with controlled pore sizes are used to filtrate the supernatant (0.45 or 0.2 μm membrane), which proceeds to the subsequent techniques of SCFA separation and quantification [2, 13, 15].

2.1.2 Liquid-Liquid Extraction

Liquid-liquid extraction (LLE) is one of the most common sample preparation methods, and it consists of solvent extraction and partitioning, based on the relative solubilities of the analytes in two different immiscible liquids, usually water (polar) and an organic solvent (non-polar). De Baere et al. [26] developed an LLE sample preparation step to determine SCFA and lactic acid produced in supernatant from intestinal bacterial cultures during *in vitro* fermentation. The authors used diethyl ether and an acid environment (obtained by the use of 100 μL of concentrate HCl) to extract the analytes from the sample supernatant. After the extraction, the diethyl ether containing the SCFA and lactic acid was cleaned up by centrifugation providing good recoveries of the analytes (34–94%). Despite being a more error-prone method, which depends a lot on the mode of operation of the analyst, LLE is also more direct and faster, dispensing volatilization and derivatization steps and making it possible to analyze a larger number of samples in a shorter time (~100 samples/day) [26]. In addition, LLE does not require the use of special extraction filters, cartridges, or columns.

2.1.3 Solid-Phase Extraction

Solid-phase extraction (SPE) consists of miniaturization of classical liquid chromatography, based on the principle of adsorption of analytes in a stationary phase and their greater or lesser retention according to their affinity for the mobile phase. In some situations, SPE is more advantageous than LLE for avoiding the formation of emulsions and incomplete phase separation. For the analysis of SCFA by SPE, the fecal samples are passed through a C_{18} cartridge pre-conditioned with 5 mL of methanol and 5 mL of Clark and Lubbs buffer (KCl/HCl) at pH 2.0. Then, SCFA are eluted from

the sorbent with the use of an appropriate buffer (0.05 M phosphate buffer, pH 7.0) for subsequent filtration (0.45 μm membrane) analysis [27].

2.1.4 Miniaturized Extraction Techniques

Although the techniques described above are very useful and widely used for the recovery of SCFA in feces, the use of miniaturized extraction techniques has been gaining prominence, presenting as a major advantage the low, or even non-existent, solvent consumption. As SCFA are volatile compounds, one of the most efficient techniques for miniaturized extraction is the solid phase microextraction (SPME). In the SPME extraction, the volatile metabolites are captured by the coated polymeric fibers, that can be used in direct mode (DI-SPME) (i.e., when the SPME fiber is dipped into the sample solution) or in the headspace mode (HS-SPME) (i.e., when the SPME fiber is placed above the sample and the cap of the vial) [28]. In the HS-SPME mode, it is usual to heat the vial containing the sample, to increase the volatilization of the SCFA to the HS for the SPME extraction and concentration [24]. There are several kinds of commercial SPME fiber coatings. However, these coatings can be grouped into two major types: polymeric films for absorption of analytes and particles embedded in polymeric films for adsorption of analytes. The absorbent coating includes polydimethylsiloxane (PDMS), polyacrylate (PA), and polyethylene glycol (PEG).

On the other hand, the adsorbent coating can contain porous particles, such as divinylbenzene (DVB), carboxen (CAR), or a combination of DVB and CAR [28]. Once the analytes are absorbed or adsorbed in the fiber coating, the desorption can be performed on the gas chromatograph (GC) injection port without using solvents [29]. In some situations, it is also possible to use an appropriate solvent in small volume (some μL) for desorption of SCFA from the SPME for analysis by high-performance liquid chromatography (HPLC) or by capillary electrophoresis (CE) [24, 30].

Another microextraction technique that has been highlighted in the extraction of SCFA from feces is liquid-phase microextraction (LPME). A microextraction technique is based on a traditional LLE, but uses a small amount of organic solvent as an extractant (typically 1–100 μL) [31]. One example of the use of LPME is the work of Tan et al. [32], that developed and optimized a method using a drop of organic solvent, suspended from the tip of a syringe needle exposed to the headspace above a stirred sample (HS-LPME), for extraction of SCFA from plasma. Unfortunately, this very elegant sample preparation technic is not yet applied to the extraction of SCFA from feces. However, in our opinion, as HS-LPME works for the extraction of SCFAs from plasma, we hypothesized that it would work for feces samples as well.

The hollow-fiber liquid-phase microextraction (HF-LPME) is a variant of LPME in which the solvent is immobilized into the wall of a hollow porous fiber, usually polypropylene (Accurel® PP Q3/2). The membrane is filled with a receptor solvent, and this entire system is placed in the sample containing analytes, which are extracted by the organic solvent in the membrane. Then with the aid of a microsyringe, the receiving solution is removed from the hollow fiber and directly injected into the HPLC or CE [1].

2.1.5 Derivatization of SCFA

Most sample preparation methods for SCFA analysis described in the literature involve direct injection (without derivatization) of the analytes after SCFA extraction, concentration, and clean-up. However, in some situations where it is necessary to improve peak symmetry, peak separation, and detector response, an additional step called derivatization may be necessary [33]. Derivatization is the process of chemically modifying a compound to produce a new derivative compound, which has properties that are appropriate for the analysis [34]. However, the derivatization is not always the best choice to achieve these objectives, since it involves the use of organic solvents and other compounds which use can be a hazard for the analyst (i.e., toxic, caustic, volatile, explosive, etc.); in addition, the derivatization steps usually increase the analysis time and configure itself as another step subjected to contamination and errors [16, 35, 36].

Hoving et al. [37] recommended the use of alkylation reagent pentafluorobenzyl bromide (PFBBr) for derivatization of SCFA because the benzyl bromide group of alkylation reagent reacts with the carboxylic acid group to form an ester, allowing analysis as pentafluorobenzyl ester; this ester is ideal for electron-capture negative ionization and detection in the single ion monitoring mode on quadrupole-based mass spectrometers. He et al. [35] reported a GC-MS analysis of SCFA after derivatization by PFBBr alkylation reaction, reaching an extremely lower SCFA detection limit (0.244–0.977 μM/g). The optimal derivatization conditions reported by the authors were derivatization time of 90 min, temperature of 60 °C, pH 7, and $(CH_3)_2CO$:H_2O ratio 2:1 (v:v).

Liebisch et al. [38] reported SCFA quantification in fecal samples by liquid chromatography-tandem mass spectrometry (LC-MS/MS) upon derivatization to 3-nitrophenylhydrazones. This derivatization step gave a lower SCFA detection limit (0.003–1.9 μM/g). In brief, these authors used 50 μL of supernatant of feces homogenate (2 mg/mL), 20 μL of 200 mM 3-nitrophenylhydrazine hydrochloride, and 20 μL of 120 mM N-(3-dimethylaminopropyl)-N′-ethylcarbodiimide hydrochloride. The derivatization time was 30 min and the derivatization temperature was 40 °C.

2.2 Separation Techniques for SCFA Analysis

Once the SCFA of the feces have been recovered by one of the sample preparation methods listed above, the next step is to proceed with their separation, identification, and quantification. The techniques most used and well consolidated in the literature for SCFA separation are GC, HPLC, and CE, coupled with the most diverse detectors for identification and quantification of the analytes (i.e., flame ionization detector, mass spectrometry detector, refractive index detector, and ultraviolet detector, among others).

2.2.1 Gas Chromatography

GC is the most used technique for analyzing SCFA since they are volatile analytes, a basic requirement for a sample to be analyzed by this type of chromatography [39]. In addition, the advantages of using polar GC capillary columns, especially bonded acid-modified polyethylene glycol phases, give good selectivity, sensitivity, and resolution in most SCFA analysis by GC. Furthermore, the fact that the mobile phase is a carrier gas, with greater diffusion power than liquids in general, leads to a very reduced analysis time compared to HPLC, another advantage that is considered for SCFA analysis. The most common detectors to which GC can be coupled are the flame ionization detectors (FID), which are very useful for the analysis and quantification of organic compounds, and the mass spectrometer detectors (MS), which provide a more precise structural identification with the mass spectrum of the analytes, enhancing the selectivity and sensitivity of the method [15, 16, 24, 35].

2.2.2 Liquid Chromatography (LC)

Most of the LC procedures employed in the analysis of SCFA use liquid extracts from feces or liquid extracts from *in vitro* fermentation of intestinal bacteria as samples; the column applied for their separation is commonly constituted by a C_{18} stationary phase operating in the reverse-phase mode, with mixtures of water and solvents such as acetonitrile as a mobile phase.

The challenges of employing LC arise when choosing the detector: the most common are the ultraviolet detector (LC-UV) and the mass spectrometer detector (LC-MS). However, SCFA do not have significant chromophore groups which absorb in the UV (only the carboxylic group), and their largest molar absorptions occur at small wavelength values (205–210 nm), compromising the selectivity of UV detection. In the case of MS, the major challenge concerns the low molar masses of SCFA, which result in isotopic ions with masses smaller than the scanning range of most MS analyzers. Thus, it is necessary to use derivatization reactions for the analysis of SCFA by LC, either for the insertion of chromophore groups that improve UV absorption, or for the increase of the molar mass of the analytes that MS will be analyzed. As previously described in this chapter, Subheading 2.1.5, the most recent works in the literature develop new derivatization methods and reactions that simplify the process and make LC analysis more suitable [26, 38].

2.2.3 Capillary Electrophoresis (CE)

CE is a separation technique whose use for the separation of SCFA and other analytes in biological fluids has been growing recently. It is a technique based on the movement of electrically charged particles present in a liquid medium when an electric voltage is applied. Among the several advantages that capillary electrophoresis has in relation to the other chromatographic techniques are its extremely high resolution of separation, the lower cost and the shorter time of analysis, the need for smaller amounts of sample and solvents, the lesser tendency of enlargement of peaks, and the minimum or none sample pretreatment. In most cases, CE is coupled to a UV detector since the maximum absorption wavelength of the SCFA chromophore group, 200–210 nm, can be easily used in CE detection [2, 40]. Some studies have also reported the coupling of CE to capacitively coupled contactless conductivity detector (C^4D) [1].

2.2.4 Quantification Approaches

Once the main techniques for SCFA separation have been discussed, it is necessary to present all possible standardization methods for their quantification after the analysis: external standardization, internal standardization, standard addition method, and internal normalization. Furthermore, the analyst must know how to report the results concisely and accurately, with all the necessary information.

Absolute Response Factor (*R*)

The absolute response factor is defined as the ratio between the peak area of the analyte (A_a) and its mass (m_a), as indicated in Eq. 1:

$$R = \frac{A_a}{m_a} \tag{1}$$

External Standardization

One of the most common quantification methods in the chromatographic analysis is the use of external standard solutions with the aid of a calibration curve. For this purpose, several analyte solutions to be quantified in the sample are prepared in a range of concentrations and injected individually, obtaining a series of chromatograms. A linear calibration curve is constructed, relating the concentration of the standard samples to the area obtained in each chromatogram. For the quantification to be reliable, some requirements must be considered: the range of concentrations adopted for the standards must cover the concentration at which the analyte is expected to be present in the sample. In addition, standard solutions must be injected in the same operating conditions as the sample. Therefore, the injection should be as reproducible as possible, and the use of autosamplers is highly recommended. For the quantification of the analyte using a single calibration point, the peak areas in the chromatograms can be related to the concentrations (known and desired), following Eq. 2:

$$C_a = \frac{C_{std} \times A_a}{A_{std}} \tag{2}$$

In the equation, C_a is the desired concentration of the analyte, C_{std} is the standard concentration, A_a is the area of the analyte from the sample chromatogram, and A_{std} is the area of the analyte from the standard chromatogram. Another way of quantifying is based on the equation obtained by the constructed calibration curve.

Internal Standardization

The internal standardization method involve the use of a substance that is not originally present in the sample, but which has properties similar to the analytes to be quantified, such as melting point, boiling point, and chemical structure. The internal standard must be of high purity, cannot co-elute with any analyte of interest, and must form a single, well-resolved peak in the sample chromatogram. For quantification using this method, it is necessary to calculate the relative response factor, RRF, which relates the absolute response factors of the analyte of interest (R_a) and the internal standard (R_{is}), as shown in Eq. 3:

$$\mathrm{RRF} = \frac{R_a}{R_{is}} \tag{3}$$

To determine the mass of the analyte present in the sample after adding the internal standard, use the calculated RRF (Eq. 4):

$$m_a = \frac{A_a}{A_{is}} \times \frac{m_{is}}{\mathrm{RRF}} \tag{4}$$

In practice, a series of solutions for each analyte is prepared over a range of concentrations, and the same known amount of internal standard is added to each one. The calibration curve is constructed by relating the ratio of the analyte areas and the internal standard (A_a/A_{is}) to the mass ratio (m_a/m_{is}). When chromatographing the sample in which it is desired to determine the concentrations of the analytes, the ratio between the areas obtained is interpolated, and m_a is determined using the value of m_i added to the sample.

Standard Addition Method

The standard addition method is recommended if the analyte of interest is present in low concentrations in the sample. Initially, the sample is chromatographed, determining the area A of the analyte. Then, a known mass of the analyte is added to the sample, which is injected again, determining the area B of the analyte peak. The addition of new quantities of analyte to the sample is performed successively until a line is drawn between the points (area versus mass graph) so that by extrapolation, the original analyte mass present in the sample can be determined.

Internal Normalization

Internal normalization consists of expressing the results as % area of the analyte and should only be applied when using an internal standard is unnecessary or impracticable. This type of normalization leads to overestimated results since it assumes that all analytes originally present in the sample were eluted and detected. To

determine the % of the analyte of interest, just divide its area in the chromatogram (A_a) by the sum of the areas of all the eluted peaks (A_i), according to Eq. 5.

$$\%\text{analyte} = \frac{A_a}{\sum A_i} \times 100 \tag{5}$$

If it is possible to determine the absolute response factors (R) for all analytes, the % can be calculated from Eq. 6, with the correction of the areas:

$$\%\text{analyte} = \frac{R_a A_a}{\sum (R_i A_i)} \times 100 \tag{6}$$

2.2.5 Results Report

In addition to its clarity and conciseness, a results report must also pass all the necessary information on the analysis so that anyone can reproduce the experiments if necessary. Thus, according to IOFI [41], the essential items of a report are:

1. Basic information, such as analyst name, date, and place of analysis
2. Identification of the analyzed samples and the standards used, with their indicated purity
3. Details of the method used, with information about the equipment (name and brand), column, temperature, solvent flow, mobile phase used, carrier gas flow, total analysis time, and number of analysis replicates
4. The results obtained, duly validated with the figures of merit, expressed using figures and tables for better understanding and with their appropriate units
5. Finally, it should detail any deviations from the procedure, unusual events, or problems that occurred during the analysis

2.3 Method Validation for SCFA in Feces

For the experiments carried out to have a reliable result, which can be reported and reproduced in accordance with the requirements of the analytical applications, the validation procedure is extremely important. For this validation to be conducted, the equipment must be properly calibrated, and the analysts must be qualified and trained for the analysis. The main figures of merit used for the validation of analytical methods are detailed below, according to National Health Surveillance Agency [42], applied in Brazil.

2.3.1 Specificity and Selectivity

Selectivity is the ability of the method to measure a specific analyte in the midst of other compounds, such as impurities, matrix components, or degradation products. For the quantitative measure of selectivity, the results obtained from non-contaminated samples can be compared with samples contaminated with known amounts of impurity to demonstrate that they do not interfere with the test result.

2.3.2 Linearity

Linearity ensures that the analytical methodology developed is capable of obtaining results proportional to the concentration of the analyte in the sample within an adopted and specified range. For that, at least five different concentrations of the sample are used, and when plotting the results (y-axis) as a function of the concentration (x-axis), the correlation coefficient (r) of the formed line must be greater than 0.99.

2.3.3 Concentration Range

The concentration range adopted in the tests is the interval between the upper and lower limits of quantification of a method. It is derived from linearity, and its scope depends on the intended application with the analysis.

2.3.4 Precision

Precision measures how close are the results obtained in multiple measurements from the same sample. For this, it is considered at three different levels:

Repeatability (Intra-Run Precision)

Repeatability is determined with three replicates of three different analyte concentrations (low, medium, and high), in a short period, with the same analyst and the same instrumentation.

Intermediate Precision (Inter-Race Precision)

Inter-race precision evaluates the agreement between results obtained in the same laboratory, but with different analysts and/or equipment, with a minimum of 2 different days and 2 different analysts.

Reproducibility (Inter-Laboratory Precision)

Reproducibility measures the agreement between the data obtained in different laboratories, which participate in collaborative studies as for the standardization of analytical methodologies.

Regardless of the level at which precision is being obtained, it can be expressed as the relative standard deviation (RSD) (also known as the coefficient of variation, CV) of a series of results, according to Eq. 7:

$$\mathrm{RSD} = \frac{\mathrm{SD}}{\mathrm{AC}} \times 100 \tag{7}$$

SD is the standard deviation in the equation, and AC is the average concentration determined.

2.3.5 Limits of Detection (LOD) and Quantification (LOQ)

The limit of detection, or sensitivity, is the smallest amount of analyte present in the sample that can be detected but not necessarily quantified with the method employed. For that, solutions of known and decreasing concentrations of the analyte are prepared, close to the supposed limit of quantification, and injected under the same conditions of analysis of the sample. Then, at least three calibration curves are constructed for the analyte so that the LOD can be calculated following Eq. 8:

$$\mathrm{LOD} = \frac{\mathrm{SD} \times 3}{S} \tag{8}$$

In the equation, SD is the standard deviation between the linear coefficients obtained on the three calibration curves, and S is the slope of the calibration curve.

The limit of quantification, in turn, is the smallest amount of analyte that can be determined with acceptable precision and accuracy. For this purpose, the same solutions prepared for the determination of the LOD are used, and the LOQ is calculated according to Eq. 9:

$$\mathrm{LOQ} = \frac{\mathrm{SD} \times 10}{S} \tag{9}$$

2.3.6 Accuracy

Accuracy measures how close the results of an analytical method are to the true value. It can be calculated as the percentage recovery of the known amount of analyte added to the sample or as the percentage difference between the averages obtained and the accepted true value, plus the confidence intervals. At least nine determinations must be performed, with three replicates at each of the concentration levels (low, medium, and high) to determine accuracy, using Eq. 10:

$$\text{Accuracy} = \frac{\text{Experimental mean concentration}}{\text{Theoretical concentration}} \times 100 \tag{10}$$

2.3.7 Robustness

Robustness measures the ability of the analytical method to withstand slight variations in the analytical parameters, which can result in variation in the method's response. Among these variations, we can mention the stability of analytical solutions, different batches or column manufacturers, the flow of the mobile phase, and temperature, among others.

3 Protocol for Determination of SCFA in Feces

3.1 Determination of SCFA in Feces by GC-FID

3.1.1 Injection

The injection is one of the crucial steps in the separation techniques since it must allow the entry of controlled quantities of sample and guarantee its immediate vaporization (in the case of GC) in the form of bands as narrow as possible, ensuring resolution and efficiency. The injection volume must be chosen carefully, especially when it comes to capillary columns: the evaporation of volumes in the order of microliters of liquid samples leads to sufficient amounts of steam to occupy a good part of the internal volume of the capillary column and can even saturate the stationary phase, depending on the thickness of its film.

The two injection modes most used for SCFA samples in GC are split and splitless. In the split mode, the injected sample is immediately vaporized in the hot injection port, and the steam is

divided into known ratios (ranging from 20:1 to 200:1), with only about 1% of the sample going to the column. In the case of splitless injection, the injector used is basically the same, but the split valve remains closed for a determined time after injection and vaporization; when it is opened, practically 100% of the sample goes to the column.

While the split mode guarantees narrower bands by using very small amounts of the sample, in the splitless, almost the whole sample is entering the column, which makes necessary its coupling with some band reduction mechanism, such as the cold trapping and the solvent focusing. For this purpose, the column temperature is programmed to a value much lower than the injector temperature, causing the vaporized compounds and the solvent to condense at the column entrance. When the temperature starts to rise, vaporization of the solvent begins (usually more volatile than the analytes), and the analytes become increasingly concentrated in a narrow band until their vaporization.

As the sensitivity of the splitless is higher, very concentrated samples must be diluted for injection. When compared to the split, one disadvantage is that it is a slower process since the oven must be cooled before each injection. However, splitless overcomes one of the main disadvantages of the split mode: the lack of linearity since compounds with a high boiling point can be lost during the split. In either mode, the thermal degradation of the sample can occur when in contact with the metal surface of the injector; therefore, the use of ultra-inert or silanized liners is highly recommended, as they minimize the loss of analytes and maximize the sample transfer from the injector to the column.

3.1.2 Separation

After the injection, the SCFA separation will occur within the chromatographic column, according to their greater or lesser affinity for the stationary phase. Thus, choosing the right column with appropriate polarity and dimensions is important, which allows a proper separation.

A class of columns widely used for SCFA analysis is that based on silicones, since a greater or lesser polarity is obtained according to the substituents attached to the silicon atoms. Columns with polar stationary phases are more suitable for SCFA separation, as these compounds have a certain polarity due to their carboxylic group (−COOH). The OV-225 (50% cyanopropyl methyl, 50% phenylmethyl polysiloxane) is an example of a polar stationary phase based on silicones. Another class of polar stationary phases are those based on polyethylene glycol, usually known as Carbowax 20 M. PEG can also be modified with nitroterephthalic acid to obtain columns of very high polarity, known as OV-351 or FAAP, designed precisely to analyze volatile fatty acids and phenols. It is worth pointing that all the aforementioned stationary phases are

bonded and crosslinked, which increases their lifetime and stability in the column, and prevents them from being easily detached by washing with solvents.

Regarding the dimensions of the columns, GC capillary columns are available in basically three different internal diameters: 0.25, 0.32, and 0.53 mm. The smaller internal diameter of the column gives greater separation efficiency and a shorter analysis time. However, smaller amounts of the sample must be injected to avoid saturation. As for the size, the greater the length of the columns (from 15 to 105 m), the greater the resolution, but the analysis time also increases. Another factor to be considered is the film thickness of the stationary phase: "fat" films (greater than 0.3 μm) increase retention for analytes; however, they are less efficient and can promote greater bleeding. In turn, thin films (less than 0.1 μm) present less bleeding and analysis time, but a lower capacity. Therefore, it is recommended to use standard films (usually 0.25 μm) with low bleed, good resolution, and good capacity.

3.1.3 Detection

Once the stationary phase has been chosen, the mobile phase will be a high purity inert carrier gas responsible for carrying the sample analytes along the column. The carrier gases most used in GC are hydrogen, helium, and nitrogen, often chosen according to their compatibility with the detector to be used. As stated earlier, one of the most used detectors in coupling with GC is the flame ionization detector (FID), selective for organic compounds. The carrier gases hydrogen and nitrogen are compatible with FID, and their flow must be strictly controlled for the analysis to be reproducible. The injection of standard solutions of alkanes allows the calculation of the analyte's retention index for correct identification and quantification.

Another widely used detector is the mass spectrometer (MS), which allows spectral identification of the analytes through their mass-to-charge ratios (m/z), in addition to the identification by the retention time. The carrier gas most used with MS is helium, which must also have its flow controlled throughout the analysis. Moreover, the temperatures of the MS ionization source (usually by electron impact, EI, or chemical ionization, CI) and the ion analyzer (usually a quadrupole) need to be controlled. Finally, it is also necessary to specify in which mode the data is being obtained: the scan mode registers the abundance of ions within a pre-established m/z range, while the SIM mode (selected ion monitoring) analyzes target compounds, as a quantitative ion (present in greater quantity in the analyte), and two other qualitative ions.

3.2 Determination of SCFA in Feces by LC

3.2.1 Injection

Sample injection is also a crucial step in liquid chromatography; in general, precision, resolution, and accuracy are influenced by the injection technique and equipment, as well as by the user if the injection is manual. The most common and simple modes of LC

injection involve the use of syringes and valves. However, despite the advantage of allowing great flexibility in terms of the volume injected and being less expensive, syringes do not present much reproducibility in injections. The valves, in turn, allow greater reproducibility and are relatively easy to automate; basically, the sample fills the sampling loop in the loading position and is injected into the column by changing the rotor to the injection position.

Autosamplers allow the automatic analysis of a larger number of samples, with guaranteed reproducibility. Therefore, the injection temperature must also be controlled and specified. The injection volume, in turn, must be kept to a minimum to ensure adequate sensitivity without causing the sample to spread and, consequently, to widen the peaks. Regardless of the injection system adopted, it is necessary to take extra care with its washing since it is very common in LC the so-called carryover effect, that is, the residual presence of a sample in the injection system that can interfere in subsequent analysis.

3.2.2 Separation

As in gas chromatography, in LC, the separation occurs in the column, according to the greater or lesser affinity of the analytes to the stationary phase, in relation to the mobile phase. The dimensions of the column, as well as the polarity of the stationary phase that comprises it also interfere with the efficiency of the chromatographic separation. As already seen, SCFA are polar compounds; thus, their separation in LC will occur in the so-called reverse phase, that is, employing a nonpolar stationary phase, with polar solvents as a mobile phase that elute the analytes.

The stationary phase most used in reverse phase LC is the C18, composed of ultra-inert silica to which a hydrophobic chain with 18 carbons (octadecyl silyl groups, ODS) has been added to the surface. The size of the particles that compose the stationary phase of the packed columns also influences the separation: smaller particles lead to a greater number of plates and, consequently, to greater efficiency. As a result, the exchange of analytes between the mobile phase and the small particle of the stationary phase occurs faster, resulting in narrower peaks.

In LC, high pressures are common to propel the solvents of the mobile phase through the column in a reproducible way, overcoming the obstacles of the packed particles. The analytes elution can be carried out in the isocratic mode, when the composition of the mobile phase remains constant throughout the chromatographic run, or in the gradient mode, when the composition is changed during the run. The gradient mode improves the separation efficiency since it allows the combination of two or more solvents of different polarities and, consequently, retention forces. For SCFA separation, combining two polar solvents in the gradient mode is common, such as water, methanol, or acetonitrile.

3.2.3 Detection

As mentioned in Subheading 2.2.2, the most common detectors for SCFAs separated by LC are the UV-Vis with photodiode array detector (also known as DAD) and the MS detector. However, when it comes to MS, it is worth noting that there are two other modes of data acquisition, in addition to the SIM mode already described in Subheading 3.1.3. These two modes, common in LC-MS for the analysis of SCFAs, are the selected reaction monitoring mode (SRM) and the multiple reaction monitoring mode (MRM). In SRM mode, data is acquired only for specific ion products produced by precursor ions whose *m/z* had been previously selected. In MRM mode, the selected reaction monitoring is applied for multiple products from one or more precursor ions. Moreover, regardless of the mode in which the data is being obtained, it is necessary to specify which reactions are being monitored, with their specified *m/z* ratios, and which SCFAs they involve.

Despite the aforementioned problems involving the existence of insufficient chromophore groups in SCFAs for adequate detection in ultraviolet, many studies choose the UV detector for its simplicity and efficiency. It is, therefore, necessary to adopt the use of derivatization reactions for the analysis of SCFAs and specify at which wavelength the analytes are being detected.

3.3 Determination of SCFA in Feces by CE

In capillary electrophoresis, the separation occurs according to the difference in the migration speed of the analytes when the sample is submitted to an electric field. For this purpose, a capillary column is used filled with suitable electrolytes, which are in contact with electrodes from a high voltage source. The injection of the sample in the electrophoresis system can be performed in two modes: hydrodynamic or electrokinetic. In the first mode, a pressure difference is applied between the reservoir containing the electrolyte and the capillary; thus, the amount of sample injected will depend on the pressure applied, the capillary size, and the sample's viscosity and can vary from 1 to 50 nL.

3.3.1 Injection

On the other hand, the electrokinetic injection mode is based on applying an electrical voltage, being simpler and not involving any additional equipment. However, the volume to be injected will depend on the electrophoretic mobility of each analyte, discriminating ionic species of greater or lesser mobility.

3.3.2 Separation

The capillaries used in CE are usually open, consisting of fused silica and externally coated with polymers that give them flexibility and resistance, such as polyamides and polyacrylates. The silanol groups (−SiOH) of the fused silica, when in contact with the aqueous medium, ionize and become negatively charged; when an electric field is applied, a unilateral movement of ions begins toward the electrode of opposite charge from the high voltage source, originating the so-called electroosmotic flow, responsible for the migration and separation of the analytes.

The electric field applied in the system can end up generating heating, and to minimize this effect on the capillaries is necessary to keep them always at a constant temperature through the circulation of liquids or air. Therefore, it is also mandatory to specify the size of the capillary being used: CE capillaries can vary from 10 to 100 cm, with 10 to 200 μm of internal diameter. Moreover, it is necessary to differentiate the total capillary length from its effective length, which consists of the distance from the sample injection point to the detection point. The effective length determines the total analysis time and migration, while the total length determines the applied electric field.

Before the injection of the sample and between different runs, it is necessary to carry out the conditioning of the capillary; for this, usually are used sodium hydroxide solution, ultrapure water, and background electrolyte solution (BGE), a saline buffer whose function is to maintain constant the analysis conditions for the sample analytes during their migration.

3.3.3 Detection

As mentioned earlier, the most common detector applied with CE is the UV-Vis detector. However, compared to the use of the same detector in HPLC, it is necessary to point out that its sensitivity is impaired in CE, due to the shortest optical path of the capillaries. Therefore, the beam must be well focused on the capillary to avoid the dispersion of the light, and the analyte absorptivity will be dictated by Beer-Lambert's law (Eq. 11).

$$\text{Abs} = b.C.\varepsilon \tag{11}$$

In the equation, b is the optical path, C is the molar concentration, and ε is the molar absorptivity of the analyte. Two UV detection modes can be conducted in CE: the direct, suitable for analytes that have absorption in the ultraviolet and/or visible region, such as the SCFAs, and the indirect, applied for analytes that do not present this absorption. In this case, it is necessary to use a chromophore group in the electrolyte.

4 Conclusions

In conclusion, all the most common techniques for analyzing and determining SCFAs in feces have been explored and can be applied both *in vivo* and *in vitro* studies. As they have several singularities regarding injection, separation, and detection of the samples, the analyst must determine which is the most appropriate according to the analysis objectives, always taking into consideration analysis time and cost, and equipment availability. The protocols suggested in this chapter must be accompanied by an adequate sample preparation step, with the removal of interferences from the matrix, and complete validation of the method, with the writing of clear and reproducible analysis reports.

Acknowledgements

The authors would like to thank the São Paulo Research Foundation (FAPESP—Ph.D. grant for M.R.V.B., 2019/18748-8) and to Coordination for the Improvement of Higher Education Personnel (CAPES Foundation—Brazil) Financing Code 001.

References

1. Kong J et al (2018) Tributyl phosphate assisted hollow-fiber liquid-phase microextraction of short-chain fatty acids in microbial degradation fluid using capillary electrophoresis-contactless coupled conductivity detection. J Pharm Biomed Anal 154:191–197
2. Marques L et al (2019) Determination of short chain fatty acids in mice feces by capillary electrophoresis. J Braz Chem Soc 30(6): 1326–1333
3. den Besten G et al (2013) The role of short-chain fatty acids in the interplay between diet, gut microbiota, and host energy metabolism. J Lipid Res 54(9):2325–2340
4. Dobrowolska-Iwanek J et al (2016) Procedure optimization for extracting short-chain fatty acids from human faeces. J Pharm Biomed Anal 124:337–340
5. Zhou L et al (2021) Gut microbiota-related metabolome analysis based on chromatography-mass spectrometry. TrAC Trends Anal Chem 143:116375
6. Blanco-Pérez F et al (2021) The dietary fiber pectin: health benefits and potential for the treatment of allergies by modulation of gut microbiota. Curr Allergy Asthma Rep 21(10): 43
7. Tomasova L et al (2021) The impact of gut microbiota metabolites on cellular bioenergetics and cardiometabolic health. Nutr Metab (Lond) 18(1):72
8. Cook SI, Sellin JH (1998) Review article: short chain fatty acids in health and disease. Aliment Pharmacol Ther 12(6):499–507
9. Cherrington CA et al (1991) Short-chain organic acids at pH 5.0 kill Escherichia coli and Salmonella spp. without causing membrane perturbation. J Appl Bacteriol 70(2): 161–165
10. Walker AW et al (2005) pH and peptide supply can radically alter bacterial populations and short-chain fatty acid ratios within microbial communities from the human colon. Appl Environ Microbiol 71(7):3692–3700
11. Nyman M (2002) Fermentation and bulking capacity of indigestible carbohydrates: the case of inulin and oligofructose. Br J Nutr 87(Suppl 2):S163–S168
12. Hajiagha MN et al (2022) Gut microbiota and human body interactions; its impact on health: a review. Curr Pharm Biotechnol 23(1):4–14
13. Zhao G, Nyman M, Jönsson JA (2006) Rapid determination of short-chain fatty acids in colonic contents and faeces of humans and rats by acidified water-extraction and direct-injection gas chromatography. Biomed Chromatogr 20(8):674–682
14. Lattimer JM, Haub MD (2010) Effects of dietary fiber and its components on metabolic health. Nutrients 2(12):1266–1289
15. Wang LL et al (2017) Comprehensive evaluation of SCFA production in the intestinal bacteria regulated by berberine using gas-chromatography combined with polymerase chain reaction. J Chromatogr B Analyt Technol Biomed Life Sci 1057:70–80
16. Han X et al (2018) A fast and accurate way to determine short chain fatty acids in mouse feces based on GC-MS. J Chromatogr B Analyt Technol Biomed Life Sci 1099:73–82
17. Ohira H, Tsutsui W, Fujioka Y (2017) Are short chain fatty acids in gut microbiota defensive players for inflammation and atherosclerosis? J Atheroscler Thromb 24(7):660–672
18. Louis P, Flint HJ (2017) Formation of propionate and butyrate by the human colonic microbiota. Environ Microbiol 19(1):29–41
19. Natarajan N et al (2016) Microbial short chain fatty acid metabolites lower blood pressure via endothelial G protein-coupled receptor 41. Physiol Genomics 48(11):826–834
20. Barcenilla A et al (2000) Phylogenetic relationships of butyrate-producing bacteria from the human gut. Appl Environ Microbiol 66(4): 1654–1661
21. De Vuyst L, Leroy F (2011) Cross-feeding between bifidobacteria and butyrate-producing colon bacteria explains bifdobacterial competitiveness, butyrate production, and gas production. Int J Food Microbiol 149(1):73–80
22. Minekus M et al (1999) A computer-controlled system to simulate conditions of

the large intestine with peristaltic mixing, water absorption and absorption of fermentation products. Appl Microbiol Biotechnol 53(1): 108–114

23. Macfarlane S, Macfarlane GT (2003) Regulation of short-chain fatty acid production. Proc Nutr Soc 62(1):67–72
24. Douny C et al (2019) Development of an analytical method to detect short-chain fatty acids by SPME-GC-MS in samples coming from an in vitro gastrointestinal model. J Chromatogr B Analyt Technol Biomed Life Sci 1124: 188–196
25. Venema K, van den Abbeele P (2013) Experimental models of the gut microbiome. Best Pract Res Clin Gastroenterol 27(1):115–126
26. De Baere S et al (2013) Development of a HPLC–UV method for the quantitative determination of four short-chain fatty acids and lactic acid produced by intestinal bacteria during in vitro fermentation. J Pharm Biomed Anal 80:107–115
27. Horspool LJ, McKellar QA (1991) Determination of short-chain fatty acids in equine caecal liquor by ion exchange high performance liquid chromatography after solid phase extraction. Biomed Chromatogr 5(5):202–206
28. Pawliszyn J, Vuckovic D, Risticevic S (2012) *Handbook of solid phase microextraction*. Elsevier
29. Fiorini D et al (2016) A quantitative headspace-solid-phase microextraction-gas chromatography-flame ionization detector method to analyze short chain free fatty acids in rat feces. Anal Biochem 508:12–14
30. Dixon E et al (2011) Solid-phase microextraction and the human fecal VOC metabolome. PLoS One 6(4):e18471
31. Prosen H (2014) Applications of liquid-phase microextraction in the sample preparation of environmental solid samples. Molecules 19(5):6776–6808
32. Tan L et al (2005) Headspace liquid-phase microextraction of short-chain fatty acids in plasma, and gas chromatography with flame ionization detection. Chromatographia 62(5): 305–309
33. Bizkarguenaga E et al (2013) In-port derivatization after sorptive extractions. J Chromatogr A 1296:36–46
34. Parkinson D (2012) Analytical derivatization techniques. In: Pawliszyn J (ed) Comprehensive sampling and sample preparation. Academic Press, pp 559–595
35. He L et al (2018) Simultaneous quantification of straight-chain and branched-chain short chain fatty acids by gas chromatography mass spectrometry. J Chromatogr B Analyt Technol Biomed Life Sci 1092:359–367
36. Scortichini S et al (2020) Development and validation of a GC-FID method for the analysis of short chain fatty acids in rat and human faeces and in fermentation fluids. J Chromatogr B Analyt Technol Biomed Life Sci 1143: 121972
37. Hoving LR et al (2018) GC-MS analysis of short-chain fatty acids in feces, cecum content, and blood samples. Methods Mol Biol 1730: 247–256
38. Liebisch G et al (2019) Quantification of fecal short chain fatty acids by liquid chromatography tandem mass spectrometry-investigation of pre-analytic stability. Biomol Ther 9(4):121
39. Primec M, Mičetić-Turk D, Langerholc T (2017) Analysis of short-chain fatty acids in human feces: a scoping review. Anal Biochem 526:9–21
40. Garcia A et al (2008) Capillary electrophoresis for short chain organic acids in faeces Reference values in a Mediterranean elderly population. J Pharm Biomed Anal 46(2):356–361
41. IOFI Working Group on Methods of Analysis (2011) Guidelines for the quantitative gas chromatography of volatile flavouring substances, from the Working Group on Methods of Analysis of the International Organization of the Flavor Industry (IOFI). Flavour Fragr J 26(5):297–299
42. National Health Surveillance Agency (2003) Guide for validation of analytical and bioanalytical methods analytical methods. Resolution – RE No. 899

Chapter 6

Quantification of Non-esterified Fatty Acids in Serum and Plasma

Mirella Romanelli Vicente Bertolo and Stanislau Bogusz Junior

Abstract

Non-esterified fatty acids (NEFA) are the main components of triglycerides and are related to an adequate body energy balance. NEFA concentration is a direct indicator of the lipolysis rate of the body, and their deficiency in serum and blood plasma can lead to several physiological disorders, such as diabetes and insulin resistance. Therefore, determining and monitoring NEFA concentration is extremely valuable for diagnosing and controlling such diseases, and there are numerous analytical techniques for this purpose, each one with its peculiarities, benefits, and drawbacks. This chapter aims to bring the most common techniques for determining NEFAs in serum and plasma, detailing all the steps necessary for developing an analytical method, from sample preparation to method validation.

Key words Non-esterified fatty acids, Sample preparation, Quantitative analysis

1 Introduction

1.1 Non-esterified Fatty Acids (NEFA) in Serum

Non-esterified fatty acids (NEFA), also known as free fatty acids, are the major components of triglycerides, lipid molecules made up of three fatty acids linked to a glycerol backbone. They act as a vehicle for the transportation of triglycerides from the adipose tissue to the utilization sites [1]. The enzyme lipase promotes the hydrolysis of triglycerides and the consequent release of NEFA, which are transported through the bloodstream bound to albumin [2, 3]. NEFA make up about 10% of the total fatty acids in blood plasma, with their usual concentration (i.e., in a healthy individual) around 0.1–1.8 mmol/L [4].

Biologically, the importance of NEFA is related to adequate energy intake: under accelerated conditions of energy consumption, as in an individual with diabetes and insulin deficiency, the main sources of NEFA are the stored fats of the body and no longer the triglycerides ingested in the diet, which leads to a negative energy imbalance. Therefore, the levels of NEFA in blood plasma

Cinthia Baú Betim Cazarin (ed.), *Basic Protocols in Foods and Nutrition*,
Methods and Protocols in Food Science, https://doi.org/10.1007/978-1-0716-2345-9_6,

and serum are a direct indicator of the body's lipolysis rate and are related to the existence of physiological disorders, such as diabetes, obesity, diabesity, and skeletal muscle insulin resistance [3, 5, 6].

Moreover, high levels of NEFA in serum are one of the main contributors to the development of insulin resistance [1]; the concentration of NEFA in the blood can also be used as an early diagnosis for the identification of type 2 diabetes (T2D), even before insulin resistance develops [5]. The importance of NEFA is not exclusive to humans: in dairy cows, the determination of NEFA in serum acts as a straight indicator of the risks of postpartum diseases and the dry cow nutritional management; diseases such as ketosis and retained placentas have already been associated with excessive increases in NEFA plasma levels in the last 3 weeks of cows pregnancy [7].

For all the biological importance that NEFA play, both determining and monitoring their concentration in biological fluids are extremely important, not only in clinical but also in experimental conditions. Monitoring the levels of NEFA in the blood during metabolic and biological processes can assist in diagnosing diseases and ensure means of prevention and/or control [5, 8]. For this reason, several methods of detecting and quantifying NEFA in serum have been developed since the late 1950s [9]. This chapter aims to detail all the most known and useful methods for this purpose, highlighting their advantages, limitations, and procedures.

1.2 Methods to Quantify NEFA in Serum

The first methods developed for the quantification of NEFA in blood date from the late 1950s and continue throughout the 1960s; they are basically based on the extraction of lipids with organic solvents in order to eliminate compounds of no interest, such as volatile fatty acids [10, 11]. Following extraction, a titration of the NEFA carboxylic acids is performed, in the presence of a pH indicator. Then, by calculating the concentration of carboxylic acids present in the sample, a correlation is made to the concentration of NEFA. The determination can also be colorimetric, based on the complexation of NEFA with divalent metal ions such as Cu^{2+} or Co^{2+} [5, 12].

However, despite the simplicity of the titrimetric and colorimetric techniques for determining NEFA, they present some inherent problems that make their results unreliable; in addition to being excessively time-consuming, they also have low specificity, with the interference of non-lipid compounds in the final concentration value. The results are generally overestimated, with concentrations higher than reality, and give no information about the NEFA pattern [5, 13].

Thus, the development and use of chromatographic and spectrometric techniques for the analysis and determination of NEFA in plasma and serum have been carried out in order to overcome the

limitations mentioned above: many methods have been developed in recent years using liquid chromatography coupled with mass spectrometry (LC-MS) and gas chromatography coupled to mass spectrometry (GC-MS) techniques [3, 6, 14], which gain a lot in selectivity when compared to the techniques of titration and complexation [5, 6]. Nevertheless, even these chromatographic techniques have some limitations regarding NEFA analysis: in addition to also consuming a lot of analysis time, they require sample preparation prior to analysis, with an extra extraction/derivatization step [15, 16].

One technique that has stood out to those mentioned above, due to its greater selectivity and specificity, is based on enzymatic methods for the determination of NEFA: with direct and colorimetric detection, without the need of extraction prior to analysis, and with the possibility of being adapted to tests on a micrometric scale, saving reagents and time consumption, enzymatic assays gained space and importance. They are fast, reproducible, sensitive, and applied to serum and plasmas of various animals [17]. Their detection mechanism is based on the conversion of NEFA to acyl-coenzyme A, in the presence of the enzyme acyl-CoA synthetase. Next, acyl-coenzyme A is oxidized to acyl-CoA oxidase, forming hydrogen peroxide (H_2O_2). The peroxide will then undergo oxidative condensation and form a blue/purple pigment, which can be quantified with a UV-spectrometer [5].

Currently, some commercial enzyme kits are used extensively in quantifying NEFA in blood serum, all automated and based on the reactions described above, pioneered by Shimizu et al. [18]. For example, the enzyme kit from Wako diagnostics is based on the quantification of oleic acid (HR Series NEFA-HR (2)), and the one from Roche determines palmitic acid (Free fatty acids, Half-micro test). Detection is performed at wavelengths of 550 and 546 nm, respectively, and in both cases, the extraction step is unnecessary.

Finally, it is also worth mentioning that some electrochemical methods for detecting NEFA, developed as an alternative to enzymatic kits, are not routinely used outside the laboratory despite being effective. Sode et al. [19] developed an electrochemical sensor based on the consumption of dissolved oxygen by the two enzymatic reactions that occur with NEFA; Kang et al. [5] went further and produced carbon screen-printed electrodes with the two enzymes (acyl-CoA synthetase and acyl-CoA oxidase), monitoring the oxidation current of hydrogen peroxide produced by the enzymatic reactions. Veerapandian et al. [20] manufactured ruthenium-graphene oxide electrodes in which they immobilized the enzyme lipoxygenase, which can oxidize the NEFA and allow their rapid determination.

Thus, numerous techniques are employed for the study and quantification of NEFA in serum, each with its advantages, disadvantages, and peculiarities. When choosing one of them for use in

the laboratory, we must seek reliability of results and effectiveness. Over the next sections, we will discuss in detail the walkthrough of most of the techniques mentioned above.

2 Materials

2.1 Sample Preparation for NEFA in Serum

As mentioned earlier, the sample preparation step is necessary for some of the NEFA determination techniques. Despite being an extra step that demands time and reagents consumption, it is indispensable because it guarantees a purer sample with fewer interferents that can harm the concentration result. The simplest and fastest methods of sample preparation use organic solvents to extract NEFA; the HIA method (heptane-isopropanol-sulfuric acid) consists of extracting 1 mL of serum with 5 mL of the heptane-isopropanol-sulfuric acid mixture, in the ratios of 10/40/1, v/v/v. Then, heptane-saturated nitrogen is bubbled into the solution for 10 s, after which the top layer is removed for washing with 0.05% sulfuric acid [10, 12].

Another method, the ES (di-isopropylic ether-silicic acid), consists of extracting 1 mL of plasma with 20 mL of di-isopropylic ether in the presence of 3 g of silicic acid. The advantage of this method is the removal of phospholipids, possible interferents [21]. After removing the solvent by evaporation, the NEFA are dissolved in the solvent appropriate to the method to be applied in their determination.

The sample preparation process can also be miniaturized to determine NEFA using chromatographic techniques. Pavicevic et al. [22] reported the extraction of NEFA and their determination by high-performance thin-layer chromatography (qTLC) and gas chromatography (GC); for this purpose, 250 μL of an aliquot of serum was added to 800 μL of acidified copper (II) sulfate reagent (0.5 mol/L copper (II) sulfate with 1 mol/L orthophosphoric acid), and vortexed before adding 100 μL of a mixture of n-heptane and chloroform (4:1, v/v). The mixture was incubated for 10 min and then centrifuged to remove the n-heptane upper layer containing the NEFA. An additional derivatization step was also necessary for GC analysis: NEFA had to be trans-methylated to FAs methyl esters (FAME), which were extracted with hexane and analyzed.

Another miniaturized method of sample preparation for NEFA extraction was proposed by Dole et al. [11] and continues to be applied: Kopf & Schmitz [6] used it to extract serum NEFA and their subsequent analysis by GC-MS. Briefly, 50 μL of plasma or serum was added to 50 μL of methanol containing internal standards C13:0 and C21:0; the sample was diluted with water to 500 μL, and 2.5 mL of the Dole solution (2-propanol/n-hexane, 8:2 v/v, and H_2SO_4 0.1%) was added to the diluted mixture. Then,

1.5 mL of n-hexane and 1.0 mL of water were added, and the system was vortexed for 30 s. After separating the hexane phase and its evaporation, the residue was dissolved in 2 mL of chloroform, and it was passed through a column of SPE preconditioned with 4 mL of n-hexane. The neutral lipids were eluted with a mixture of chloroform and 2-propanol, while the NEFA were eluted with a mixture of diethyl ether and glacial acetic acid (2 mL, 99:1 v/v). For FAME derivatization, they added the extracted NEFA to a mixture of methanol, acetyl-chloride, and n-hexane, and the system was stirred overnight. A 6% potassium carbonate solution was added, and the sample was then vortexed and centrifuged for later removal and injection of the n-hexane phase [23].

The sample preparation step is usually suppressed when using automated enzymatic kits to determine NEFA, since the reagents in the kit are already appropriate for extracting fatty acids. Miksa et al. [7] reported the use of a commercial enzyme kit (NEFA C, Wako Chemicals Inc., Richmond, VA), both on a regular scale and on a scale adapted to a 96-well plate. They prepared the reagents A (acyl-CoA synthetase, ascorbate oxidase, CoA, adenosine triphosphate [ATP], 4-animoantipyrine), and B (acyl-CoA oxidase and peroxidase) according to the kit instructions; in the miniaturized procedure, 10 μL of the plasma samples were incubated with 200 μL of reagent A for 10 min, and re-incubated with 400 μL of reagent B. Then, 250 μL of the mixtures were transferred to a 96-well plate for later absorbance reading.

Finally, it is worth emphasizing the matter of the stability and storage time of NEFA, for samples that cannot be analyzed immediately after their separation. Menéndez et al. [17] developed a complete study evaluating the storage effect of NEFA extracted from plasma and serum prior to enzymatic determination since different studies in the literature reported different results and storage modes. They concluded that the stability of NEFA proved to be particularly good during 14 days of storage at −20 °C, without significant changes in their concentration. Furthermore, the results at −20 °C were more satisfactory than at room temperature and at 4 °C.

2.2 Procedures for NEFA Analysis in Serum

2.2.1 Titrimetric and Colorimetric

The titrimetric and colorimetric procedures were the first to be developed to analyze NEFA in plasma and serum, as previously mentioned. In the titration procedure, the fraction extracted from NEFA in hexane (from the sample preparation step) is titrated with a NaOH solution of known concentration. It is necessary to use an indicator, such as thymol blue, to announce the turning point of the solution, in which all NEFA carboxylic groups will have been consumed. From the spent volume of the basic solution and the concentrations used, the concentration of carboxylic groups present in the NEFA sample is calculated [10–12]. However, like all titration procedures, it is an experiment very dependent on the

operator and subject to more errors. In addition, it should be noted that the result found for the concentration of NEFA does not exclude possible interferents that may have remained in the matrix even after sample preparation.

As for colorimetric procedures, the most usual is to perform reactions of NEFA with metal ions to form colored complexes, with absorbance measured by UV-Vis spectrophotometer. For example, in the red phenol method (PR), the solutions of NEFA in heptane coming from the sample preparation step are mixed with a colored reagent based on red phenol and sodium barbital, under CO_2 flow; the conversion of the basic red phenol to its yellow acid form allows reading at 560 nm [24]. In the copper soap method (CS), NEFA react with copper forming copper soaps, which subsequently react with zinc dibenzyl-dithiocarbamate to form complexes, whose absorbance is measured at 440 nm [21]. This method is still widely used today: Sellin et al. [25] used an adaptation of the method proposed by Tinnikov and Boonstra [26] to determine NEFA in plasma samples from *Drosophila* using multiwell plates.

2.2.2 Chromatographic

Chromatographic techniques started to be used to analyze NEFA in blood plasma and serum more recently, in relation to titrimetric and colorimetric techniques. Gas chromatography coupled with mass spectrometry (GC-MS) is extremely useful for identifying the individual profile of NEFA (or FAME, since they need to be derivatized for GC-MS analysis) and is therefore widely used, with several methodologies already developed [6, 27, 28]. As it is a more robust technique than those previously described, more details about it must be explored since they directly influence the analysis result.

First, the dimensions of the column must be previously chosen and analyzed carefully since they impact the separation of the molecules: the total length of the column has a direct impact on its efficiency (or the number of theoretical plates), the internal diameter influences the separation resolution, and the film thickness of the stationary phase, responsible for the retention of the analytes, interferes with the mass transfer. Another important point of optimization is the volume of sample injected, as well as the injection mode and temperature: the split mode prevents previous column saturation, and the most common split ratio for FAME injection is 1:100 [6]. During the chromatographic run, an oven heating ramp also helps separate the analytes. Finally, the nature of the carrier gas (usually helium) and its linear velocity throughout the run are also important.

To detect FAME, it is usual to adopt the scan mode in qualitative analysis, when only the identification of the compounds is performed, and the SIM mode (selected ion fragments) in quantitative analysis, to calculate the concentration of the fragments with

higher intensities. For quantitative determination, it is also necessary to use internal standards, such as the C21: 0 iso, the most common for FAME analysis [6].

Although the methods developed for FAME analysis by GC-MS are satisfactory and provide good results, gas chromatography remains a time-consuming technique, especially due to the need to derivatize NEFA to their methyl esters prior to the analysis [16]. Many studies developed methodologies based on liquid chromatography coupled with electrospray ionization tandem mass spectrometry (LC-EI-MS) to analyze fatty acids without derivatization [16, 29, 30]. The gas-phase ionization mechanism ensures no matrix effects, a challenge to be overcome in liquid chromatography, and allows the ions to be analyzed in SIM mode during the chromatographic run.

In liquid chromatography, it is necessary to choose a mobile phase of suitable composition, with an optimized percolation gradient that guarantees the highest possible selectivity. The injection volume of the sample is also important, and the gas phase ionization occurs through the formation of an aerosol by a nebulizer under high vacuum conditions. As a disadvantage of the technique in relation to GC, there is the fact that only NEFA with small and medium chains can be ionized in this process, that is, compounds with low molecular weight and volatile enough to be ionized [16]. Long-chain NEFA, on the other hand, cannot be analyzed by LC-EI-MS, and GC-MS is the most appropriate chromatographic technique in their case.

2.2.3 Enzymatic Kits

Enzymatic kits to determine NEFA in blood serum and plasma have been established as a good alternative to chromatographic analysis since they do not require the sample preparation step [5, 7, 31]. The reagents necessary for the determination of NEFA are prepared on the spot, following the manufacturer's instructions. Generally, the whole procedure occurs in a few steps: (1) in the first reagent (which will react directly with the NEFA), there is ATP, coenzyme A (CoA), and the enzyme acyl-coenzyme A synthetase, which will promote the conversion of CoA into acyl-coenzyme A. In a second reaction step (2), acyl-coenzyme A will be oxidized in the presence of acyl-coenzyme A oxidase, generating hydrogen peroxide.

The peroxide will then react with 4-aminoantipyridine or 4-aminoantipyrine (3), depending on the kit, in the presence of the peroxidase enzyme, to form a chromophore dye through oxidation condensation with 2,4,6-tribromo-3-hydroxy-benzoic-acid (TBHB) or 3-methyl-N-ethyl-N-(betahydroxyethlyl)-aniline (MEHA). According to the reagents used, the dyes may be red or purple/blue; reading their absorbance (4) then allows the concentration of NEFA in the samples to be calculated [5, 18]. Another

advantage of commercial kits is that they can be adapted for smaller sample volumes, thus allowing more samples to be analyzed in the same kit, optimizing the analysis time, and reducing the analysis cost [7].

2.3 Method Validation for NEFA in Serum and Results Report

Once we discussed the most common and used techniques for determining NEFA in blood serum and plasma, it is necessary to explore the means of reporting the results in a validated and suitable method for use, according to the analytical applications. Regardless of the adopted technique, a validation study is required before its subsequent use in other samples. Furthermore, the validated method to be applied to a type of sample matrix, such as serum, cannot be applied to determine NEFA in another matrix (such as milk, for example) without a new validation step, since chemical and analytical methods are specific not only to the analyte but also to its matrix [32].

Usually, the validation of a method with a new type of matrix occurs through the replicate analysis of a large set of internal standards in the sample to determine the precision and accuracy of the method [32]. Precision measures how close are the results obtained in different measurements for the same sample, while accuracy measures how close these results are to the real value [33]. The internal standards are substances of high purity, which are not necessarily present in the sample but resemble many analytes to be quantified in terms of their physicochemical properties.

Other important figures of merit can be determined during the validation of the method, according to the technique applied for the analysis of NEFA: linearity, for example, measures the ability of the analytical technique to generate results proportional to the concentration of analytes in the sample, over a given range of concentrations. In addition, the limits of detection (LOD) and quantification (LOQ) are also important, especially when it comes to chromatographic techniques: they measure, respectively, the smallest amount of analyte in the sample that can be detected (and not necessarily quantified), and the smallest amount of analyte in the sample that can be quantified with acceptable precision and accuracy [33].

Kopf & Schmitz [6] validated the NEFA SPE-separation method that they developed prior to their analysis by GC-MS. For that, they selected the 13 fatty acids of highest occurrence in the test samples, both short and long chain, and added them to the plasma samples in three levels, low, medium, and high (from 5 to 20 μg/mL). As variables, they analyzed recovery and accuracy, which they believed to be directly influenced during the recovery of NEFAs by SPE. As a validation criterion, they established a variation coefficient (CV) of less than 15% between five replicates for each level of concentration adopted. Of the 13 fatty acids used in the validation study, 12 met this criterion, demonstrating that the developed method was successfully validated.

In turn, Kang et al. [5] developed an electrochemical method for the determination of NEFA based on the detection of hydrogen peroxide produced by enzymatic reactions of oleic acid, chosen because it is one of the most abundant in plasma. To validate the developed method, they compared it to the enzymatic method of the Wako commercial kit for different concentrations of oleic acid (from 0 to 0.9 mmol/L). Each concentration was measured three times by each method, and a calibration curve was constructed to validate the linearity of the electrochemical method.

The results found by the validated methods can be expressed in two modes, relative and absolute. In relative mode, the units are given as % of the weight of total fatty acids (%, wt:wt, or even g/100 g); in this type of result, the variability is usually lower than in the results expressed in absolute terms, in which we report the concentration of NEFA in the fluids, such as serum or plasma, as mg NEFA/mL of fluid [32, 34]. Regardless of how the results are reported, it is important that all necessary data for their interconversion are provided, in order to report a method with reproducible results.

According to IOFI (2011), the essential items of a clear, concise, and reproducible report are:

- The basics information: who performed the analysis, where and when.
- The names of the samples and the standards, with information regarding their origin, composition, and purity.
- The details of the method adopted in the analysis include the reagents used in a titrimetric NEFA determination, the enzymatic kit purchased for an enzymatic determination, or the column, temperature, and equipment used in a chromatographic analysis, total analysis time, and the number of analysis replicates.
- A summary of the results obtained, with figures and tables, besides the validation procedure adopted.
- In the last place, any deviations from the procedure, unusual events or problems during the analysis.

3 Methods

Once all the details for the development of a method for determining NEFA in serum and plasma have been elucidated, such as the type of analysis that can be adopted, the possible sample preparation step before analysis, and the validation of the method developed, below we present suggestions of protocols to be followed, according to studies in the literature that applied the techniques

explored in this work. It is important to emphasize the need for sample replicates, as well as the use of internal standards when necessary.

3.1 Determination of NEFA in Serum by Titrimetric and Colorimetric Analysis

1. Protocol for NEFA determination by titration, adapted from Chilliard et al. [10]:
   (a) Separate a known volume of the NEFA sample extracted earlier, in the sample preparation step;
   (b) Prepare a standardized 0.01 N solution of NaOH in isopropanol and a 0.1% solution of blue thymol indicator in isopropanol.
   (c) Titrate in a burette or microburette of known precision, with sample agitation, until the turning point occurs.
   (d) Note the volume of basic solution spent; calculate the concentration of carboxylic acids in the NEFA solution according to the reaction stoichiometry and the equation:

$$C_{NaOH}\, V_{NaOH} = C_{COOH}\, V_{COOH}.$$

2. Protocol for NEFA determination by the colorimetric copper soap method, adapted from Sellin et al. [25]:
   (a) Separate a known volume of the NEFA sample extracted earlier, in the sample preparation step.
   (b) Evaporate the organic solvent in which the NEFA were extracted, and add the same volume of phosphate buffer.
   (c) Prepare glass vials with 500 μL of chloroform/heptane (4:3) for each sample.
   (d) Add 25 μL of the samples to the mixture of chloroform and heptane, vortex intensely for 2 min, let stand for 15 min and centrifuge for 10 min at 2000 g at room temperature.
   (e) Prepare 250 μL of copper TEA solution: 1 M triethanolamine (TEA) (Cu-TEA solution) for each sample and add 300 μL of the solvent phase of the samples to the solution. Vortex and centrifuge again for phase separation.
   (f) Separate 150 μL of the top phase, evaporate the solvent, and add 150 μL of ethanol for dissolution.
   (g) Add 30 μL of the diphenylcarbazide/-bazone solution to each sample and standard, vortex for 10 s and incubate in the dark for 15 min; transfer to a 96-well plate and measure absorbance at 550 nm.
   (h) Subtract the absorbance from the blank and calculate the concentration of NEFA with the aid of the calibration curve built with the standards.

3.2 Determination of NEFA in Serum by Chromatographic Analysis

1. Protocol for NEFA determination by GC-MS, adapted from Kopf & Schmitz [6]:
   (a) Separate 100 μL of the NEFA solution obtained after sample preparation and derivatization [23].
   (b) For a BPX70 column (dimensions: 10 m length, 0.10 mm diameter, 0.20 μm film thickness, coated with 70% cyanopropyl polysilphenyl-siloxane), in a Shimadzu 2010 GC-MS system:
      (i) Inject 1 μL of the sample and use a programmed temperature vaporizer (PTV) in 1:20 split mode for 3 s; switch to the splitless mode for 1.3 min and use the 1:100 split ratio until the end of the chromatographic run.
      (ii) Set the injection temperature to 72 °C for 3 s and increase by 240 °C min^{-1} to 250 °C, remaining for 15 min.
      (iii) Set the oven temperature to 50 °C for 0.75 min, and increase 40 °C min^{-1} to 155 °C, 6 °C min^{-1} to 210 °C, and 15 °C min^{-1} to 250 °C, staying for 2 min.
      (iv) Use helium as carrier gas at 50 cm/s.
      (v) For detection, set the temperature to 250 °C; use the scan mode to identify the ions, and the SIM mode in specifics *m/z* for the most saturated ions.

3.3 Determination of NEFA in Serum with Enzymatic Kits

1. Protocol for NEFA determination with an enzymatic kit, adapted from Miksa et al. [7]:
   (a) Prepare the reagents, the blank, and the stock solutions according to the kit instructions.
   (b) Pipette different volumes of stock solutions into 10 μL of plasma samples.
   (c) Add 200 μL of reagent A to all solutions and incubate at 37 °C for 10 min.
   (d) Add 400 μL of reagent B and re-incubate.
   (e) Leave the samples to stand at room temperature for 5 min, and transfer 250 μL of each solution to a 96-well microplate; read the absorbance of the samples at 550 nm.
   (f) Subtract the absorbance from the blank and calculate the concentration of NEFA with the aid of the calibration curve built with the standards.

4 Conclusions

In conclusion, several analytical techniques are available for the determination of NEFA in blood serum and plasma. The operator must choose which technique best fits his objectives, analyzing aspects such as time, cost of analysis and reliability of the results. Colorimetric and titrimetric techniques can be useful if no chromatographic equipment or enzyme kit is available. Gas chromatography coupled with mass spectrometry will provide a complete fatty acid profile but requires derivatization of the sample and a trained user for analysis. The enzymatic kits are a versatile and faster alternative; however, they are more expensive, and their cost is only worthwhile with miniaturization of the process for the analysis of several samples. Thus, regardless of the method of choice, the operator must keep in mind all the necessary precautions when developing it, such as the proper preparation of sample (when necessary), the development of the method with certified and pure standards, and the writing of a clear, concise, and reproducible analysis report.

Acknowledgments

The authors would like to thank the São Paulo Research Foundation (FAPESP—Ph.D. grant for M.R.V.B., 2019/18748-8) and Coordination for the Improvement of Higher Education Personnel (CAPES Foundation—Brazil) Financing Code 001.

References

1. Karpe F, Dickmann JR, Frayn KN (2011) Fatty acids, obesity, and insulin resistance: time for a reevaluation. Diabetes 60(10):2441–2449
2. eClinpath (2020) [cited November 24, 2020]. Available from: eClinpath: https://eclinpath.com/chemistry/energy-metabolism/non-esterified-fatty-acids/
3. Gonçalves-de-Albuquerque CF et al (2019) Serum albumin saturation test based on non-esterified fatty acids imbalance for clinical employment. Clin Chim Acta 495:422–428
4. Roden M (2004) How free fatty acids inhibit glucose utilization in human skeletal muscle. News Physiol Sci 19:92–96
5. Kang J et al (2014) Electrochemical detection of non-esterified fatty acid by layer-by-layer assembled enzyme electrodes. Sens Actuators B Chem 190:535–541
6. Kopf T, Schmitz G (2013) Analysis of non-esterified fatty acids in human samples by solid-phase-extraction and gas chromatography/mass spectrometry. J Chromatogr B Analyt Technol Biomed Life Sci 938:22–26
7. Miksa IR, Buckley CL, Poppenga RH (2004) Detection of nonesterified (free) fatty acids in bovine serum: comparative evaluation of two methods. J Vet Diagn Invest 16(2):139–144
8. Christmass MA et al (1998) A semiautomated enzymatic method for determination of nonesterified fatty acid concentration in milk and plasma. Lipids 33(10):1043–1049
9. Carlson LA (1958) A colorimetric method of determining unesterified fatty acids in plasma. Scand J Clin Lab Invest 10(4):407–414
10. Chilliard Y, Bauchart D, Barnouin J (1984) Determination of plasma non-esterified fatty acids in herbivores and man: a comparison of values obtained by manual or automatic chromatographic, titrimetric, colorimetric and

enzymatic methods. Reprod Nutr Dev 24(4): 469–482

11. Dole VP, Meinertz H (1960) Microdetermination of long-chain fatty acids in plasma and tissues. J Biol Chem 235:2595–2599
12. Trout DL, Estes EH Jr, Friedberg SJ (1960) Titration of free fatty acids of plasma: a study of current methods and a new modification. J Lipid Res 1:199–202
13. Rogiers V (1977) The application of an improved gas-liquid chromatographic method for the determination of the long chain non-esterified fatty acid pattern of blood plasma in children. Clin Chim Acta 78(2): 227–233
14. Chu X et al (2009) Determination of 13 free fatty acids in pheretima using ultra-performance LC-ESI-MS. Chromatographia 69(7):645–652
15. Costa CG et al (1998) Simultaneous analysis of plasma free fatty acids and their 3-hydroxy analogs in fatty acid beta-oxidation disorders. Clin Chem 44(3):463–471
16. Trufelli H et al (2011) Profiling of non-esterified fatty acids in human plasma using liquid chromatography-electron ionization mass spectrometry. Anal Bioanal Chem 400(9):2933–2941
17. Menéndez LG et al (2001) Effect of storage of plasma and serum on enzymatic determination of non-esterified fatty acids. Ann Clin Biochem 38(Pt 3):252–255
18. Shimizu S et al (1979) Acyl-CoA oxidase from Candida tropicalis. Biochem Biophys Res Commun 91(1):108–113
19. Sode K et al (1989) Sensor for free fatty acids based on acyl coenzyme-a synthetase and acyl coenzyme-a oxidase. Anal Chim Acta 220: 251–255
20. Veerapandian M, Hunter R, Neethirajan S (2016) Lipoxygenase-modified Ru-bpy/graphene oxide: electrochemical biosensor for on-farm monitoring of non-esterified fatty acid. Biosens Bioelectron 78:253–258
21. Antonis A (1965) Semiautomated method for the colorimetric determination of plasma free fatty acids. J Lipid Res 6:307–312
22. Pavićević ID et al (2016) Quantification of total content of non-esterified fatty acids bound to human serum albumin. J Pharm Biomed Anal 129:43–49
23. Ecker J et al (2012) A rapid GC-MS method for quantification of positional and geometric isomers of fatty acid methyl esters. J Chromatogr B Analyt Technol Biomed Life Sci 897: 98–104
24. Baird JD, Black MW, Faulkner DE (1967) Semi-automated method for the determination of free fatty acids in plasma. J Clin Pathol 20(6):905–909
25. Sellin J et al (2020) Free fatty acid determination as a tool for modeling metabolic diseases in Drosophila. J Insect Physiol 126:104090
26. Tinnikov AA, Boonstra R (1999) Colorimetric micro-determination of free fatty acids in plasma using microplate readers. Clin Chim Acta 281(1–2):159–162
27. Bicalho B et al (2008) Creating a fatty acid methyl ester database for lipid profiling in a single drop of human blood using high resolution capillary gas chromatography and mass spectrometry. J Chromatogr A 1211(1–2): 120–128
28. Marangoni F, Colombo C, Galli C (2004) A method for the direct evaluation of the fatty acid status in a drop of blood from a fingertip in humans: applicability to nutritional and epidemiological studies. Anal Biochem 326(2): 267–272
29. Pulfer M, Murphy RC (2003) Electrospray mass spectrometry of phospholipids. Mass Spectrom Rev 22(5):332–364
30. Sommer U et al (2006) LC-MS-based method for the qualitative and quantitative analysis of complex lipid mixtures. J Lipid Res 47(4): 804–814
31. Balogh O et al (2018) Effect of maternal metabolism on fetal supply: glucose, non-esterified fatty acids and beta-hydroxybutyrate concentrations in canine maternal serum and fetal fluids at term pregnancy. Anim Reprod Sci 193:209–216
32. Brenna JT et al (2018) Best practices for the design, laboratory analysis, and reporting of trials involving fatty acids. Am J Clin Nutr 108(2):211–227
33. National Health Surveillance Agency (2003) Guide for validation of analytical and bioanalytical methods analytical methods. Resolution – RE No. 899
34. Mocking RJ et al (2012) Statistical methodological issues in handling of fatty acid data: percentage or concentration, imputation and indices. Lipids 47(5):541–547

Chapter 7

Lipid Peroxidation (TBARS) in Biological Samples

Lilian Regina Barros Mariutti

Abstract

This chapter describes a simple and easy-to-do protocol to assay the level of lipid peroxidation in biological samples by a colorimetric method. The estimate of malonaldehyde, a secondary product of lipid oxidation, can be carried out by the TBARS assay, which measures the amount of thiobarbituric acid reactive substances forming a red complex with maximum absorbance at 532 nm against a calibration curve built with malonaldehyde.

Key words Lipid oxidation, Malondialdehyde, Spectrophotometry, Colorimetry, TBARS

1 Introduction

Lipid oxidation and oxidative stress are major contributors to the development of several non-communicable diseases, including obesity, type 2 diabetes, and cardiovascular diseases [1–3]. The mechanisms of lipid oxidation have been extensively studied, and the major products of these reactions are well known [3, 4].

Malonaldehyde (MDA) is an aldehyde formed as a major secondary product of the oxidation of polyunsaturated fatty acids possessing three or more double bonds and is recognized as a biological marker of oxidative damage [4, 5]. Several methods can be used to determine MDA in biological samples by using diverse techniques such as HPLC, GC, and CE; however, visible spectrophotometry after a colorimetric reaction (commonly known as thiobarbituric acid reactive substances (TBARS assay)) is by far the most used one [5].

The TBARS assay is widely used to indicate the oxidative state of lipids in biological systems and can also be considered an indirect method to estimate the antioxidant capacity despite taking a long time to be performed than the more traditional antioxidant assays, such as ORAC, DPPH, ABTS, or FRAP. In this assay, MDA reacts

Cinthia Baú Betim Cazarin (ed.), *Basic Protocols in Foods and Nutrition*,
Methods and Protocols in Food Science, https://doi.org/10.1007/978-1-0716-2345-9_7,

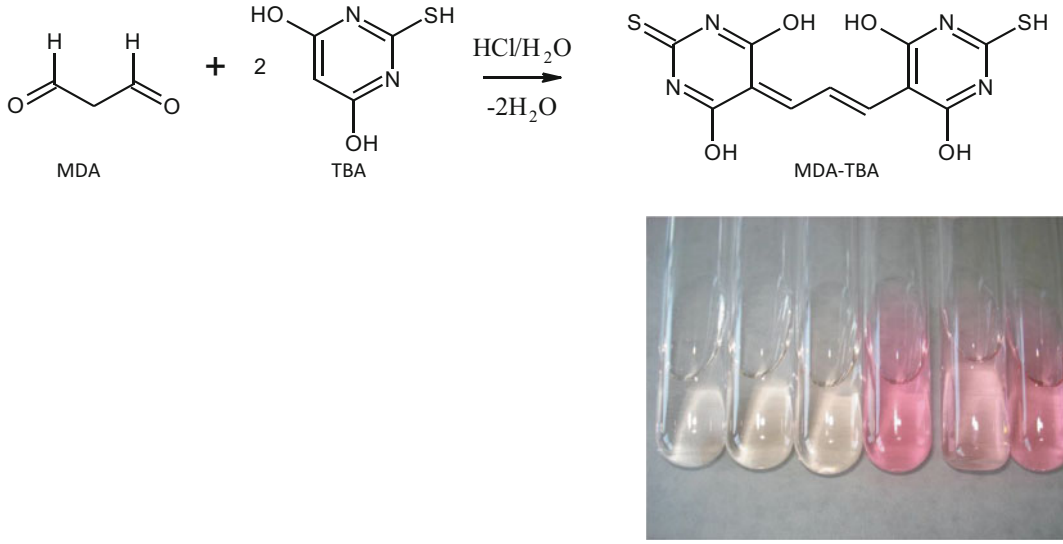

Fig. 1 The reaction between malonaldehyde (MDA) and thiobarbituric acid (TBA) forms a colored adduct

with TBA in its monoenolic form by attacking the methylene groups generating an adduct with maximum absorption at 532–535 nm (Fig. 1).

This colorimetric method has been constantly criticized due to its limitations; however, it was proposed in 1944 by Kohn and Liversedge and finds wide application until today. The most important limitation is that the TBARS assay does not measure the content of MDA; it measures the amount of all the compounds that form a colored (red/pink) adduct with TBA with the same UV-visible spectrum as MDA. Another drawback is the possible overestimate of TBARS content due to the presence of interferents such as bile, amino acids, sugars, and other products from lipid oxidation that can produce adducts with TBA that significantly overlap the MDA-TBA spectrum in its maximum absorption wavelength [5, 6].

Quantification can be done by plotting a calibration curve. For this purpose, MDA is usually generated by acid hydrolysis of commercially available standards of 1,1,3,3-tetramethoxypropane (TMP, also called malondialdehyde bis(dimethyl acetal)), 1,1,3,3-tetraethoxypropane (TEP), malondialdehyde tetrabutylammonium salt, and malonaldehyde bis(phenylimine) monohydrochloride (Fig. 2).

2 Materials

Unless indicated otherwise: Prepare all solutions using distilled water and analytical grade reagents and store all reagents at room temperature (24 °C).

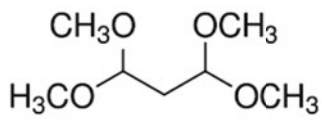

1,1,3,3-Tetramethoxypropane or
Malondialdehyde bis(dimethyl acetal)

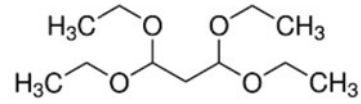

1,1,3,3-Tetraethoxypropane

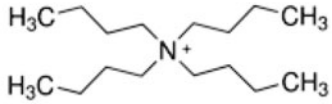

Malondialdehyde tetrabutylammonium salt

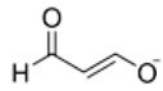

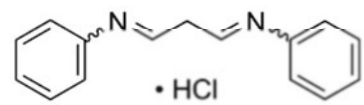

Malonaldehyde bis(phenylimine) monohydrochloride

Fig. 2 Compounds used as standards to generate malonaldehyde by acid hydrolysis

Follow the waste disposal regulations of reagents and other materials from your country.

- *20% Acetic acid solution*: Gently add 100 mL of glacial acetic acid to a beaker containing 350 mL of water under magnetic stirring. After complete dissolution, bring the final volume to 500 mL.
- *200 μM Malonaldehyde standard intermediate solution*: Dilute 726 μL of malonaldehyde standard stock solution in 1274 μL of water. Prepare a fresh solution for each batch of samples.
- *550 μM Malonaldehyde standard stock solution*: Dilute 92 μL of malonaldehyde bis(dimethyl acetal) in 1 L of water. This solution can be stored at 4 °C for 30 days (*see* **Note 1**).
- *3.5 M Sodium acetate buffer pH 4.0*: Firstly, gently add 100 mL of glacial acetic acid to a beaker containing 350 mL of water under magnetic stirring. In a polyethylene beaker placed in a cold-water bath, dissolve 13 g of sodium hydroxide (NaOH) beads in 50 mL of water. Carefully add about 46 mL of the NaOH solution to the acetic acid solution mixing with a stir bar, check the pH of the solution while mixing until it reaches 4.0. Bring the final volume to 500 mL with water (*see* **Note 2**).
- *0.9% Sodium chloride solution*: Weight 0.9 g of sodium chloride (NaCl) and dissolve it in 85–90 mL of water using a magnetic stirring. After NaCl is completely dissolved, bring the solution to a final volume of 100 mL.
- *8.1% Sodium dodecyl sulfate (SDS) solution*: Weight 8.1 g of SDS and dissolve in 85–90 mL of water using a magnetic stirring in slow rotation to avoid foam formation. After the SDS is completely dissolved, bring the solution to a final volume of 100 mL (*see* **Note 3**).

- *0.8% Thiobarbituric acid (TBA) aqueous solution*: Weight 0.8 g of SDS and dissolve in 85–90 mL of water using a magnetic stirring or in an ultrasonic bath. After the TBA is completely dissolved, bring the solution to a final volume of 100 mL. Prepare a fresh solution for each batch of samples (*see* **Note 4**).
- Spectrophotometer or Microplate reader.
- Centrifuge.

3 Methods

1. Sample preparation.
   (a) Tissue [7].
      (i) Harvest the tissue (brain, heart, lung, liver, kidney, adrenal gland, testis), wash with 0.9% sodium chloride solution and store properly until analysis (*see* **Note 5**).
      (ii) Prepare the tissue homogenate: Macerate the frozen tissue in liquid nitrogen and sonicate it in acetate buffer (pH 3.5) in an ice bath in a concentration of 10 mg of tissue/mL.
   (b) Plasma [8].
      (i) Collect the blood sample in tubes, flux with nitrogen, and store properly until analysis (*see* **Note 6**).
2. Calibration curve.
   (a) Prepare the solutions for the calibration curve as described in Table 1.
   (b) Proceed to **step 3** to perform the reaction with the MDA standard solutions.
3. Reaction and absorbance measurement [6–9].
   (a) Pipette the reaction mixture in a glass tube with a tide cap as follows: 100 µL of sample (plasma or tissue homogenate) or standard solution (*see* Table 1), 200 µL 8.1% SDS, 1500 µL 20% acetic acid solution, and 1500 µL 0.8% TBA aqueous solution (*see* **Note 8**).
   (b) Prepare a blank control without adding the sample (B), add 100 µL of water instead.
   (c) Made up the volume of the reaction mixture to 4.0 mL with distilled water.
   (d) Heat the test tubes in boiling water for 60 min (*see* **Note 9**).
   (e) Cool the test tubes in an ice bath for 10 min.
   (f) Centrifuge the test tubes at 10,000 g at 4 °C for 10 min.
   (g) Read the absorbance of the supernatant at 532 nm at room temperature (*see* **Notes 10–13**).

Table 1
Preparation of solutions for the calibration curve of MDA (*see* Note 7)

Concentration (μM)	Volume of MDA intermediate solution (μL)	Volume of water (μL)
0	0	1000
2.5	12.5	987.5
5	25	975
10	50	950
20	100	900
40	200	800
80	400	600
160	800	200

Adapted from De Leon and Borges [9]

4. Calculations.
   (a) Plot a calibration curve by subtracting the blank control (B) the known concentration of each standard (*x*-axis) vs. absorbance readings at 532 nm (*y*-axis) (*see* Table 1).
   (b) Fit the data using linear regression and obtain the linear regression equation ($y = ax + b$), where y is the absorbance at 532 nm, x is MDA the concentration, a is the slope, and b is the intercept.
   (c) Calculate the MDA concentration in the samples using the linear regression equation:

$$\text{TBARS/MDA } (\mu\text{M}) = \frac{\text{Absorbance 532 nm} - \text{intecept}}{\text{Slope}}$$

4 Notes

1. This solution can also be prepared by the acid hydrolysis of other MDA salts (Fig. 2).
2. Always check the pH of the sodium acetate buffer before use.
3. Preferentially prepare only the amount of solution needed for the number of samples that will be analyzed. Each sample requires 200 μL of 8.1% SDS solution.
4. Do not heat the mixture to dissolve the TBA. Instead, prepare only the amount of solution needed for the number of samples that will be analyzed. Each sample requires 1500 μL of TBA solution.

5. Tissues will be well preserved if immediately after washing they were frozen under liquid nitrogen, vacuum-packed, and stored at −80 °C.
6. Plasma will be well preserved if immediately frozen under liquid nitrogen and stored at −80 °C.
7. These solutions can be prepared in a 1.5 mL Eppendorf tube. One hundred microliters will be necessary for each replicate of each point of the calibration curve.
8. At least triplicate analysis of each sample or concentration of the calibration curve is recommended.
9. Pay attention if the caps are well-tight to avoid water evaporation and volume changes.
10. The reaction product is stable for up to 3 h at room temperature (24 °C) under room light.
11. If a microplate reader is used for absorbance measurements, transfer 150 μL of the supernatant for a well (Fig. 3). Use 96-well white polystyrene microplates for visible spectrophotometric measurements.

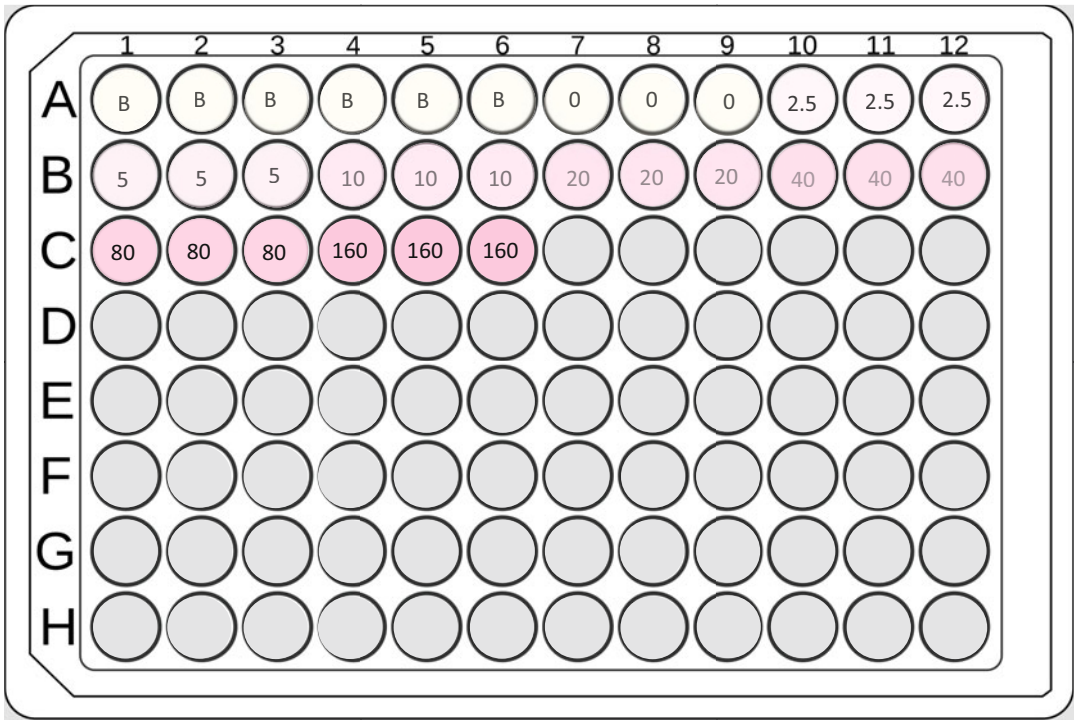

Fig. 3 The suggestion of 96-well microplate organization. Legend: B = blank assay (at least 6–8 replicates to allow the determination of your limit of detection); 0, 2.5, 5, 10, 20, 40, 80, and 160 μM = standard solutions to build the calibration curve (triplicate analysis is recommended); empty wells should be filled with samples in triplicate (grey color). (The microplate template file is available under the Creative Commons CC0 1.0 Universal Public Domain Dedication)

12. If a regular spectrophotometer is used, read the absorbance of the supernatant at room temperature; otherwise, condensation water may form on the spectrophotometer glass or quartz cuvette.
13. Absorbance values must be within 0.2 and 0.8 and fit the analytical curve linear interval. If necessary, dilute the supernatant with distilled water and consider this dilution in your calculations.

References

1. Seyedsadjadi N, Grant R (2020) The potential benefit of monitoring oxidative stress and inflammation in the prevention of non-communicable diseases (NCDs). Antioxidants (Basel) 10:15. https://doi.org/10.3390/antiox10010015
2. Nediani C, Giovannelli L (2020) Oxidative stress and inflammation as targets for novel preventive and therapeutic approaches in non-communicable diseases. Antioxidants (Basel) 9:290. https://doi.org/10.3390/antiox9040290
3. Pisoschi AM, Pop A, Iordache F, Stanca L, Predoi G, Serban AI (2021) Oxidative stress mitigation by antioxidants – an overview on their chemistry and influences on health status. Eur J Med Chem 209:112891. https://doi.org/10.1016/j.ejmech.2020.112891
4. Del Rio D, Stewart AJ, Pellegrini N (2005) A review of recent studies on malondialdehyde as toxic molecule and biological marker of oxidative stress. Nutr Metab Cardiovasc Dis 15:316–328. https://doi.org/10.1016/j.numecd.2005.05.003
5. Mariutti LRB, Bragagnolo N (2015) Analysis methods for thiobarbituric acid reactive substances and malonaldehyde in food and biological samples. In: Advances in chemistry research, vol 29, 1st edn. Nova Science Publishers, New York, pp 100–130
6. Ohkawa H, Ohishi N, Yagi K (1979) Assay for lipid peroxides in animal tissues by thiobarbituric acid reaction. Anal Biochem 95:351–358. https://doi.org/10.1016/0003-2697(79)90738-3
7. Cazarin CBB, Silva JK, Colomeu TC et al (2015) Intake of *Passiflora edulis* leaf extract improves antioxidant and anti-inflammatory status in rats with 2,4,6-trinitrobenzenesulphonic acid induced colitis. J Funct Foods 17:575–586. https://doi.org/10.1016/j.jff.2015.05.034
8. Batista AG, Lenquiste SA, Cazarin CBB et al (2014) Intake of jaboticaba peel attenuates oxidative stress in tissues and reduces circulating saturated lipids of rats with high-fat diet-induced obesity. J Funct Foods 6:450–461. https://doi.org/10.1016/j.jff.2013.11.011
9. De Leon JAD, Borges CR (2020) Evaluation of oxidative stress in biological samples using the thiobarbituric acid reactive substances assay. J Vis Exp 159:e61122. https://doi.org/10.3791/61122

Chapter 8

Extraction of Bile Acids from Biological Samples and Quantification Using Ultra-High-Performance Liquid Chromatography-Orbitrap Mass Spectrometry

Shota Hori, Hongxia Liu, Riho Yamada, Shun Ichitsubo, Ayana Sakaguchi, Fumika Yokoyama, and Satoshi Ishizuka

Abstract

Bile acid (BA) has attracted significant attention because it is considered a metabolic regulator in the body. BA metabolism is modulated by dietary intervention and disease conditions. Here, we present a comprehensive BA measurement system used to enable an understanding of the BA distribution in the body. We also focused on BA extraction methods, such as organ, fluid, or semisolid samples, depending on sample characteristics. To precisely measure the BA composition, we introduced an ultra-high-performance liquid chromatography/orbitrap-mass spectrometry (UHPLC-Orbitrap MS) technique for BA analysis. This method enabled us to measure BA concentrations in various biological samples derived from experimental animals and humans similarly, and would be a useful tool for investigating the roles of BA in physiological and pathological events.

Key words Bile acids, Ultra-high-performance liquid chromatography, Orbitrap mass spectrometry

1 Introduction

Bile acids (BAs) are characterized as amphipathic molecules that contribute to the absorption of dietary lipids and reportedly demonstrate functions as signaling molecules for specific receptors [1]. BAs are involved in various metabolic processes [2], and BA metabolism is modulated by dietary interventions [3–5]. Presently, researchers have reported investigations conducted to elucidate the precise metabolic roles of BAs in disease conditions and dietary interventions.

In humans, two types of primary BAs are synthesized in the liver, namely cholic acid (CA) and chenodeoxycholic acid (CDCA). CA possesses a hydroxyl group at position 12α in the steroid ring, but CDCA does not possess a hydroxyl group at the position. They are produced in conjugated forms with taurine or glycine and are

Cinthia Baú Betim Cazarin (ed.), *Basic Protocols in Foods and Nutrition*,
Methods and Protocols in Food Science, https://doi.org/10.1007/978-1-0716-2345-9_8,

secreted into the duodenum [2]. Almost all BAs are hydroxylated at position 3α, and a prevailing clinical kit to measure BAs has been designed to detect 3α-hydroxylated BAs. Conjugated BAs contribute to lipid absorption as a lipid emulsifier in the intestine and are reabsorbed by the ileal epithelial cells via specific BA transporters [6]. After reabsorption, they are released into the portal blood and incorporated into the liver. This type of BA circulation in the liver, intestine, and portal blood is called enterohepatic circulation. In the intestine, a few conjugated CA and CDCA are subjected to deconjugation and dihydroxylation via the activity of intestinal bacteria. Such processes enable the production of secondary BAs, such as deoxycholic acid (DCA) and lithocholic acid (LCA) [7]. In certain cases, the hydroxyl groups in the BAs undergo conversion to oxo forms [8]. In rodents, 6-hydroxylated BAs, α- or β-muricholic acid (MCA), are frequently observed as the primary BAs [9]. These 6-hydroxylated BAs also undergo epimerization or dihydroxylation via the activity of gut bacteria, following which ωMCA and hyodeoxycholic acid (HDCA) are produced [10]. Such a diverse range of BA metabolites present different chemical characteristics that modulate various cellular functions via BA receptors [1].

Owing to the pleiotropic roles of BAs observed in metabolism, establishing a comprehensive analytical method is necessary to understand the metabolic roles of BAs. In this chapter, we have introduced the BA extraction method in samples obtained from experimental animals and humans and have described an analytical method using ultra-high-performance liquid chromatography (UHPLC)-Orbitrap mass spectrometry (MS) as a revised version of our previously reported method [11]. This method is categorized as an omics-like approach in BA analysis [12]; however, we did not analyze BAs at trace levels or less common unusual BAs using this method. This approach aimed to survey the BA environment under specific conditions, such as dietary intervention or metabolic disorders. More details in technical aspects of BA analysis have been reviewed by Griffith and Sjövall [12].

Before the conduction of BA extraction, the samples were lyophilized and finely ground, if necessary, to optimize extraction using ethanol via a reduction in the water content present in the samples. The BAs in the lyophilized samples were extracted with ethanol according to the methods reported by Locket and Gallaher [13], with minor modifications. The extracted fraction was purified via solid-phase extraction, following which they were separated via UHPLC and were analyzed using Orbitrap MS. This method enables the measurement of BAs present in organs, body fluid (blood plasma, bile, and urine), and semisolid samples (intestinal contents and feces). The BA concentration can be calculated and expressed as mol/L or mol/g, depending on the sample characteristics, by which we can estimate the BA distribution in the body. BA

concentrations determined using this method have already been published in our previous papers [3, 4, 14–23] on rat studies (such as bile, liver, blood plasma, intestinal contents, and feces). This method was also adopted in a clinical study (blood sera and feces) [24].

2 Materials

2.1 Chemicals

1. Standards of primary and secondary BAs are shown in Tables 1 and 2, respectively.
2. BA internal standard: 23-nor-5β-cholanic acid-3α,12α-diol (23-nordeoxycholic acid, NDCA) (Steraloids).
3. Standard mixture solution including the BAs mentioned above. A calibration curve was constructed using the standard mixture solution.

2.2 Reagents

1. Ion-exchanged and redistilled water.
2. High-grade ethanol.
3. 10 mM ammonium acetate (NH_4Ac) in water.

Table 1
Primary BA standards

Systematic name	Trivial name	Abbreviation
12αOH BAs		
5β-cholanic acid-3α,7α,12α-triol	Cholic acid	CA
5β-cholanic acid-3α,7α,12α-triol-*N*-(2-sulfoethyl)-amide	Taurocholic acid	TCA
5β-cholanic acid-3α,7α,12α-triol-*N*-(carboxymethyl)-amide	Glycocholic acid	GCA
Non-12αOH BAs		
5β-cholanic acid-3α,7α-diol	Chenodeoxycholic acid	CDCA
5β-cholanic acid-3α,6α,7α-triol	Hyocholic acid	HCA
5β-cholanic acid-3α,6β,7α-triol	α-Muricholic acid	αMCA
5β-cholanic acid-3α,6β,7β-triol	β-Muricholic acid	βMCA
5β-cholanic acid-3α,6β,7α-triol-*N*-(2-sulfoethyl)-amide	Tauro-α-muricholic acid	TαMCA
5β-cholanic acid-3α,6β,7β-triol-*N*-(2-sulfoethyl)-amide	Tauro-β-muricholic acid	TβMCA
5β-cholanic acid-3α,7α-diol-*N*-(2-sulfoethyl)-amide	Taurochenodeoxycholic acid	TCDCA
5β-cholanic acid-3α,7α-diol-*N*-(carboxymethyl)-amide	Glycochenodeoxycholic acid	GCDCA

Table 2
Secondary BA standards

Systematic name	Trivial name	Abbreviation
12αOH BAs		
5β-cholanic acid-3α,12α-diol	Deoxycholic acid	DCA
5β-cholanic acid-3α,12α-diol-*N*-(2-sulfoethyl)-amide	Taurodeoxycholic acid	TDCA
5β-cholanic acid-3α,12α-diol-*N*-(carboxymethyl)-amide	Glycodeoxycholic acid	GDCA
5β-cholanic acid-3α,12α-diol-7-one	7-Oxo-deoxycholic acid	7oDCA
5β-cholanic acid-3α-ol-12-one	12-Oxo-lithocholic acid	12oLCA
5β-cholanic acid-12α-ol-3-one	–	3o12α
5β-cholanic acid-3α,7β,12α-triol	Ursocholic acid	UCA
Non-12αOH BAs		
5β-cholanic acid-3α-ol	Lithocholic acid	LCA
5β-cholanic acid-3α,6α-diol	Hyodeoxycholic acid	HDCA
5β-cholanic acid-3α,7β-diol	Ursodeoxycholic acid	UDCA
5β-cholanic acid-3α-ol-7-one	7-Oxo-lithocholic acid	7oLCA
5β-cholanic acid-3α,6α,7β-triol	ω-Muricholic acid	ωMCA
5β-cholanic acid-3α-ol-*N*-(2-sulfoethyl)-amide	Taurolithocholic acid	TLCA
5β-cholanic acid-3α-ol-*N*-(carboxymethyl)-amide	Glycolithocholic acid	GLCA
5β-cholanic acid-3α,6α-diol-*N*-(2-sulfoethyl)-amide	Taurohyodeoxycholic acid	THDCA
5β-cholanic acid-3α,6α-diol-*N*-(carboxymethyl)-amide	Glycohyodeoxycholic acid	GHDCA
5β-cholanic acid-3α,7β-diol-*N*-(2-sulfoethyl)-amide	Tauroursodeoxycholic acid	TUDCA
5β-cholanic acid-3α,7β-diol-*N*-(carboxymethyl)-amide	Glycoursodeoxycholic acid	GUDCA
5β-cholanic acid-3α,6α,7β-triol-*N*-(2-sulfoethyl)-amide	Tauro-ω-muricholic acid	TωMCA

4. HPLC-grade acetonitrile.
5. HPLC-grade methanol.
6. Solvent A: acetonitrile/water (20:80, v/v) containing 10 mM NH_4Ac.
7. Solvent B: acetonitrile/water (80:20, v/v) containing 10 mM NH_4Ac (*see* **Note 1**).

2.3 Instruments

1. 2-mL microtubes.
2. Freeze dryer (FDU-1000, Tokyo Rikakikai, Tokyo, Japan).
3. Homogenizer (Dispergieramtrieb T10 basic, IKA, Staufen, Germany).

4. Ultrasonic homogenizer (VP-050, Taitec Corp., Saitama, Japan).
5. Water bath (NT-1400, Tokyo Rikakikai).
6. Vortex mixer (Cute Mixer CM-100 Tokyo Rikakikai).
7. Centrifuge (Centrifuge 5415 R, Eppendorf, Hamburg, Germany).
8. Centrifugal concentrator (VC-96N, Taitec Corp.).
9. Oasis HLB cartridge 1 cc/10 mg (Waters, Milford, MA, USA).
10. Dionex UltiMate 3000 UHPLC system (Thermo Fisher Scientific, San Jose, CA, USA).
11. BEH C18 column (1.7 μm, 100 mm × 2.0 mm i.d.; Waters).
12. Q Exactive Plus Orbitrap mass spectrometer (Thermo Fisher Scientific).

3 Methods

Biological samples, including blood plasma, bile, liver, intestinal mucosa, intestinal contents, and feces, were lyophilized before extraction to eliminate moisture to the most considerable possible extent. This step is advantageous for increasing the extraction efficiency to eliminate unwanted substances. In the cases of feces and liver, the lyophilized samples were ground thoroughly to increase the extraction efficiency further. The samples were then extracted using ethanol and purified via solid-phase extraction. The extraction methods are described in detail below. The required amounts of various tissues, body fluids, intestinal contents, and feces are shown in Table 3. Additionally, a tube containing only 15 μL of 500 μM or 5 mM NDCA, depending on the sample source, was also used for extraction. By calculating the final NDCA concentration, we can determine the extraction efficiency, which can be used to determine the BA concentration in the sample.

3.1 Bile Acid Extraction from Biological Samples

3.1.1 Blood Plasma, Urine, and Bile

1. Blood plasma (100 μL), urine (100 μL), or bile samples (50 μL) collected in a 2-mL tube covered with paper (*see* **Note 2**) were incubated at −80 °C overnight.
2. The samples were lyophilized without heating for 48 h (Fig. 1a).
3. Next, 1 mL of ethanol was added to the lyophilized samples.
4. Then, 15 μL of 500 μM NDCA in ethanol was added to each sample for blood plasma (7.5 nmol/tube), urine (7.5 nmol/tube), or 5 mM for bile (75 nmol/tube) as an internal standard, and the mixture was vortexed thoroughly (*see* **Note 3**).

Table 3
Required amounts of biological samples and dilution of the extracts for BA analysis

Sample	Amount	MeOH for purification[a]	Dilution[b]	HLB purification[c]	MeOH for LC[d]
Aortic plasma	100 μL	0.3 mL	–	100 μL	0.2 mL
Portal plasma	100 μL	0.5 mL	–	100 μL	2 mL
Urine (gall bladder)	100 μL	0.3 mL	–	100 μL	0.2 mL
Bile	50 μL	1 mL	10	100 μL	0.5 mL
Liver	100 mg (dry)	0.5 mL	–	100 μL	1 mL
Renal cortex	100 mg (dry)	0.3 mL	–	100 μL	0.2 mL
Intestinal mucosa	100 mg (wet)	0.5 mL	–	100 μL	2 mL
Feces	100 mg (dry)	1 mL	20	100 μL	1 mL
Jejunal and ileal contents	200 mg (wet)	1 mL	25	100 μL	1 mL
Cecal contents	200 mg	1 mL	10	100 μL	1.5 mL
Colonic contents	200 mg	1 mL	20	100 μL	1 mL

[a]Volume of MeOH to be added to the dried extracts
[b]Dilution ratio of the extracts in MeOH
[c]Amount of MeOH extracts for HLB cartridge purification
[d]Volume of MeOH to be added to the purified extracts

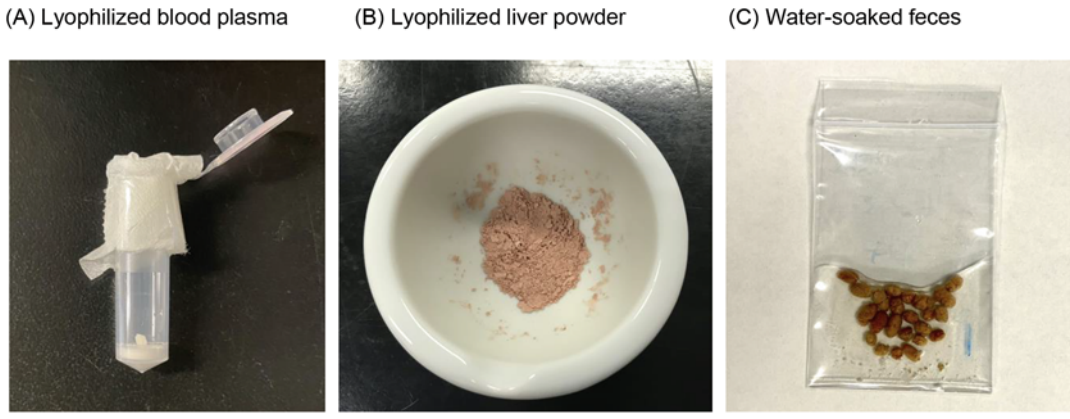

Fig. 1 Sample preparations for BA analysis. (**a**) Blood plasma was subjected to lyophilization in a tube covered with paper. (**b**) Lyophilized rat liver was ground with a pestle and mortar. (**c**) Fecal samples were soaked in water for a day and were then ground before freezing

5. The samples were sonicated on ice (POW SET 30%, START PWM 30%, twice for 10 s).
6. The samples were then heated at 60 °C for 30 min in a water bath and were then heated at 100 °C for 3 min in a water bath (*see* **Note 4**).
7. After cooling the samples to room temperature, they were vortexed thoroughly.
8. The samples were centrifuged at 2300 × *g* for 10 min at 4 °C.
9. The supernatants were collected into a new tube and subjected to evaporation.
10. Next, 1 mL of ethanol was added to the precipitates.
11. The samples were vortexed thoroughly.
12. Then, centrifugation was performed at 9300 × *g* for 1 min at 4 °C.
13. The supernatants were transferred into the tubes collected from **step 9**.
14. The extraction steps (*see* **steps 10–13**) were repeated once again.
15. The pooled extracts were then subjected to evaporation.
16. Then, the samples were stored at −40 °C until analysis.

3.1.2 Liver and Renal Cortex

1. The collected liver or renal cortex samples were placed in a plastic pack and stored at −80 °C overnight.
2. The samples were subjected to lyophilization for 48 h (*see* **Note 5**).
3. The lyophilized sample was ground thoroughly with a mortar and pestle (Fig. 1b).
4. Then, 1 mL of ethanol was added to a 2-mL tube containing 100 mg of the ground samples.
5. Next, 15 μL of 500 μM NDCA in ethanol (7.5 nmol/tube) was added as an internal standard to each sample, and the mixture was vortexed thoroughly (*see* **Note 3**).
6. **Steps 5–16** were followed, as shown in Subheading 3.1.1.

3.1.3 Intestinal Mucosa

1. Intestinal luminal contents were rinsed using cold saline. Segments were opened longitudinally, and the mucosa was scraped. Mucosal scrapings (100 mg) in a 2-mL tube were stored at −80 °C overnight.
2. The samples were subjected to lyophilization for 48 h (*see* **Note 5**).
3. Then, 1 mL of ethanol was added to the lyophilized samples.

4. Next, 15 μL of 500 μM NDCA in ethanol (7.5 nmol/tube) was added as an internal standard to each sample, and the mixture was vortexed thoroughly (*see* **Note 3**).
5. The samples were homogenized at maximum speed.
6. **Steps 5–16** were followed, as shown in Subheading 3.1.1.

3.1.4 Feces

1. Fecal samples collected for a period of 24 h were placed in a plastic pack and soaked in water for 24 h at 4 °C (Fig. 1c).
2. The samples were ground in the plastic pack using a stick and placed at −80 °C overnight.
3. The samples were subjected to lyophilization for 48 h (*see* **Note 5**).
4. The samples were ground the lyophilized thoroughly with a pestle and mortar.
5. Then, 1 mL of ethanol was added to 100 mg of the ground samples.
6. Next, 15 μL of 5 mM NDCA in ethanol (75 nmol/tube) was added as an internal standard to each sample, and the mixture was vortexed thoroughly (*see* **Note 2**).
7. **Steps 5–16** were followed, as shown in Subheading 3.1.1.

3.1.5 Intestinal Contents (Jejunal, Ileal, Cecal, and Colonic Contents)

1. First, 100 mg of the intestinal content (jejunal, ileal, cecal, and colonic content) was collected in a 2-mL tube covered with paper and stored at −80 °C overnight.
2. The samples were subjected to lyophilization for 48 h (*see* **Note 5**).
3. Then, 1 mL of ethanol was added to the samples.
4. Next, each sample added 15 μL of 5 mM NDCA in ethanol (75 nmol/tube) as an internal standard, and the mixture was vortexed thoroughly (*see* **Note 3**).
5. The samples were subjected to homogenization at maximum speed.
6. **Steps 5–16** were followed, as shown in Subheading 3.1.1.

3.2 Solid-Phase Extraction

1. First, 1 mL of methanol was added to the evaporated extracts, and the contents were mixed well (Table 3) (*see* **Notes 6** and 7).
2. Next, 100-μL samples from the methanol solutions were purified using an HLB cartridge, according to the manufacturer's instructions (*see* **Note 8**).
3. The recovered eluates were then subjected to evaporation.
4. Next, 1 mL of methanol was added to evaporated eluents and suspended thoroughly.
5. The dissolved extracts were then analyzed via LC.

3.3 LC Settings

1. The column oven and the autosampler were maintained at 40 °C and 15 °C, respectively (*see* **Note 9**). The solvent flow rate was 400 μL/min, and the sample injection volume was 3 μL.
2. The gradient program was as follows: 5% solvent B from 0 to 5 min, linear ramp to 15% solvent B over 10 min, linear ramp to 25% solvent B over 5 min, and linear ramp to 75% solvent B over 2 min. Solvent B was maintained at 75% for 1 min and was then decreased linearly to 5% over 1 min. Solvent B was maintained at 5% for 3 min.
3. The column eluent was then analyzed via MS.

3.4 MS Settings

1. MS was performed using an Orbitrap MS equipped with an electrospray ionization probe in the negative-ion mode. Full-scan MS spectral data (from m/z 200 to 700) were acquired using an Orbitrap analyzer after accumulation to achieve a target value of 1e6 in the linear ion trap. The resolution of the Orbitrap system was set to $r = 17{,}500$. Standard mass spectrometric conditions for all experiments were as follows: spray voltage, 3.8 kV; sheath gas flow rate, 35 L/h; aux gas flow rate, 10 L/h; heated capillary temperature, 250 °C; aux gas heater temperature, 450 °C; s-lens RF level, 100%.
2. Each BA was detected by performing extraction of the ions produced from the deprotonated molecule $[M–H]^-$, as shown in Fig. 2a. The exact masses of all BAs are shown in Tables 4 and 5.
3. Individual BAs' concentration was calculated by comparing the area under the peak of each BA with that of the BA and the value is adjusted with extraction efficiency with NDCA.
4. A chromatogram of BAs in the liver is shown in Fig. 2b.

4 Notes

1. In the preparation of solvents, A and B, it is advised to perform prior dissolution of NH_4Ac in water, followed by subsequent mixing of acetonitrile with water containing NH_4Ac (NH_4Ac cannot be dissolved in acetonitrile).
2. The tubes were covered with a piece of paper to prevent the samples from spilling out (Fig. 1a).
3. The amount of NDCA should be adjusted appropriately because the dilution ratio depends on the actual BA concentration in the samples.
4. Cap holders should be used to avoid the opening of caps during heating.

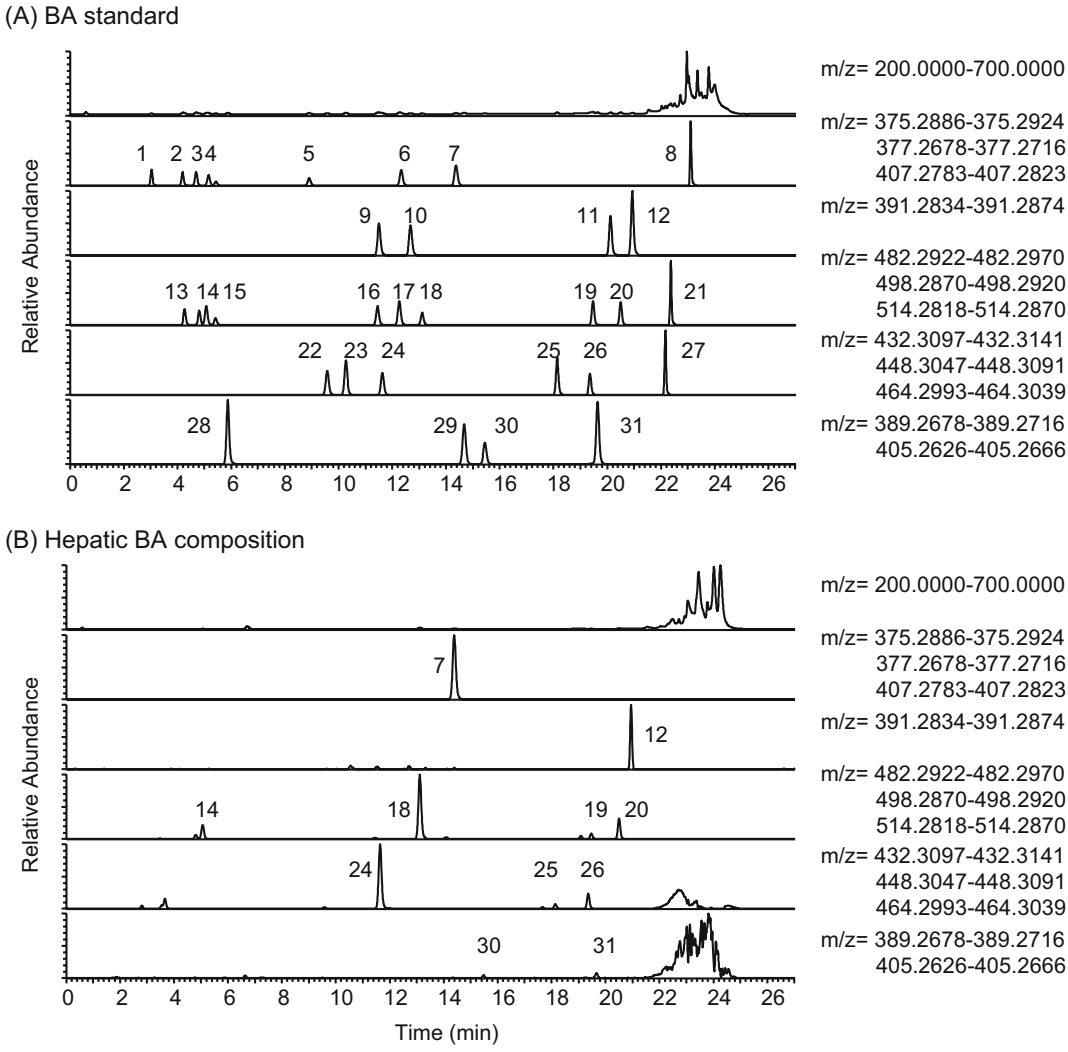

Fig. 2 Chromatograms of BA standard (**a**) and rat hepatic BA composition (**b**). (1) UCA, (2) ωMCA, (3) αMCA, (4) βMCA, (5) HCA, (6) CA, (7) NDCA (internal standard), (8) LCA, (9) UDCA, (10) HDCA, (11) CDCA, (12) DCA, (13) TωMCA, (14) TαMCA, (15) TβMCA, (16) TUDCA, (17) THDCA, (18) TCA, (19) TCDCA, (20) TDCA, (21) TLCA, (22) GUDCA, (23) GHDCA, (24) GCA, (25) GCDCA, (26) GDCA, (27) GLCA, (28) 7oDCA, (29) 7oLCA, (30) 12oLCA, and (31) 3o12α

5. The sample weight before and after lyophilization was recorded to calculate the sample's water content.
6. A centrifugation step can be included if a disturbance in extracting liquid with floating substances in the tube after adding methanol is encountered.
7. The amount of MeOH used to dissolve the dried EtOH extract can be reduced to obtain a suitable concentration for relatively low-concentration samples, such as plasma, liver, and urine

Table 4
Exact mass of primary BAs and NDCA

	$[M-H]^-$	Correlation coefficient
12αOH BAs		
CA	407.280	0.9998
TCA	514.284	1.0000
GCA	464.302	0.9999
Non-12αOH BAs		
CDCA	391.285	1.0000
HCA	407.280	1.0000
αMCA	407.280	1.0000
βMCA	407.280	0.9997
TαMCA	514.284	1.0000
TβMCA	514.284	0.9998
TCDCA	498.289	1.0000
GCDCA	448.307	0.9999
Internal standard		
NDCA	377.270	0.9998

Each correlation coefficient is calculated by analyzing BA standard mixture (0.025, 0.25, 2.5, and 25 μM)

(Table 3). On the other hand, highly concentrated samples such as feces, bile, and intestinal contents should be appropriately diluted (Table 3).

8. Although the sample used for injection is normally dissolved in the same solvent as that used for cartridge equilibration, the samples are usually dissolved in methanol. Briefly, after conditioning the cartridges with 1 mL of methanol, we used 1 mL of 10 mM NH_4Ac as an equilibration step. Then, 1 mL of 10 mM NH_4Ac was added to the cartridge. Next, 100 μL of the sample in methanol (described in **step 1** in Subheading 3.2) was added and gently mixed with the NH_4Ac solution on the top of the cartridge. By considering this procedure, the sample can be used almost entirely with the NH_4Ac solution. Add 1 mL of NH_4Ac solution again and wait for 1 h. Then, add 1 mL of MeOH and collect all the eluates. Finally, the remaining unpurified samples were evaporated and stored at −40 °C for reuse after reconstitution.
9. The temperature in the autosampler was maintained at 15 °C under default conditions in the LC. However, the methanol evaporation in the samples is strictly limited because the vials are tightly closed with a cap.

Table 5
Exact mass of secondary BAs

	$[M–H]^-$	Correlation coefficient
12αOH BAs		
DCA	391.285	0.9998
TDCA	498.289	1.0000
GDCA	448.307	1.0000
7oDCA	405.265	0.9996
12oLCA	389.270	0.9997
3o12α	389.270	0.9996
UCA	407.280	0.9998
Non-12αOH BAs		
LCA	375.290	0.9997
HDCA	391.285	0.9999
UDCA	391.285	0.9999
7oLCA	389.270	0.9999
ωMCA	407.280	1.0000
TLCA	482.295	0.9999
GLCA	432.312	0.9996
THDCA	498.289	1.0000
GHDCA	448.307	0.9999
TUDCA	498.289	0.9999
GUDCA	448.307	1.0000
TωMCA	514.284	0.9999

Each correlation coefficient is calculated by analyzing BA standard mixture (0.025, 0.25, 2.5, and 25 μM)

References

1. Fiorucci S, Distrutti E (eds) (2019) Bile acids and their receptors. Springer, Cham
2. de Aguiar Vallim TQ, Tarling EJ, Edwards PA (2013) Pleiotropic roles of bile acids in metabolism. Cell Metab 17:657–669
3. Yoshitsugu R, Kikuchi K, Iwaya H, Fujii N, Hori S, Lee DG, Ishizuka S (2019) Alteration of bile acid metabolism by a high-fat diet is associated with plasma transaminase activities and glucose intolerance in rats. J Nutr Sci Vitaminol 65:45–51
4. Lee DG, Hori S, Kohmoto O, Kitta S, Yoshida R, Tanaka Y, Shimizu H, Takahashi K, Nagura T, Uchino H, Fukiya S, Yokota A, Ishizuka S (2019) Ingestion of difructose anhydride III partially suppresses the deconjugation and 7α-dehydroxylation of bile acids in rats fed with a cholic acid-supplemented diet. Biosci Biotechnol Biochem 83:1329–1335
5. Hori S, Abe T, Lee DG, Fukiya S, Yokota A, Aso N, Shirouchi B, Sato M, Ishizuka S (2020) Association between 12α-hydroxylated bile acids and hepatic steatosis in rats fed a high-fat diet. J Nutr Biochem 83:108412
6. Kramer W, Stengelin S, Baringhaus KH, Enhsen A, Heuer H, Becker W, Corsiero D, Girbig F, Noll R, Weyland C (1999) Substrate

specificity of the ileal and the hepatic Na^+/bile acid cotransporters of the rabbit. I. Transport studies with membrane vesicles and cell lines expressing the cloned transporters. J Lipid Res 40:1604–1617

7. Ridlon JM, Kang DJ, Hylemon PB (2006) Bile salt biotransformations by human intestinal bacteria. J Lipid Res 47:241–259
8. Marion S, Studer N, Desharnais L, Menin L, Escrig S, Meibom A, Hapfelmeier S, Bernier-Latmani R (2019) *In vitro* and *in vivo* characterization of *Clostridium scindens* bile acid transformations. Gut Microbes 10:481–503
9. Takahashi S, Fukami T, Masuo Y, Brocker CN, Xie C, Krausz KW, Wolf CR, Henderson CJ, Gonzalez FJ (2016) Cyp2c70 is responsible for the species difference in bile acid metabolism between mice and humans. J Lipid Res 57: 2130–2137
10. Eyssen HJ, De Pauw G, Van Eldere J (1999) Formation of hyodeoxycholic acid from muricholic acid and hyocholic acid by an unidentified gram-positive rod termed HDCA-1 isolated from rat intestinal microflora. Appl Environ Microbiol 65:3158–3163
11. Hagio M, Matsumoto M, Ishizuka S (2011) Bile acid analysis in various biological samples using ultra performance liquid chromatography/electrospray ionization-mass spectrometry (UPLC/ESI-MS). Methods Mol Biol 708: 119–129
12. Griffiths WJ, Sjövall J (2010) Bile acids: analysis in biological fluids and tissues. J Lipid Res 51: 23–41
13. Locket PL, Gallaher DD (1989) An improved procedure for bile acid extraction and purification and tissue distribution in the rat. Lipids 24:221–223
14. Hagio M, Matsumoto M, Fukushima M, Hara H, Ishizuka S (2009) Improved analysis of bile acids in tissues and intestinal contents of rats using LC/ESI-MS. J Lipid Res 50: 173–180
15. Hagio M, Matsumoto M, Yajima T, Hara H, Ishizuka S (2010) Voluntary wheel running exercise and dietary lactose concomitantly reduce proportion of secondary bile acids in rat feces. J Appl Physiol 109:663–668
16. Hagio M, Shimizu H, Joe GH, Takatsuki M, Shiwaku M, Xu H, Lee JY, Fujii N, Fukiya S, Hara H, Yokota A, Ishizuka S (2015) Diet supplementation with cholic acid promotes intestinal epithelial proliferation in rats exposed to γ-radiation. Toxicol Lett 232:246–252
17. Islam KB, Fukiya S, Hagio M, Fujii N, Ishizuka S, Ooka T, Ogura Y, Hayashi T, Yokota A (2011) Bile acid is a host factor that regulates the composition of the cecal microbiota in rats. Gastroenterology 141: 1773–1781
18. Lee Y, Yoshitsugu R, Kikuchi K, Joe GH, Tsuji M, Nose T, Shimizu H, Hara H, Minamida K, Miwa K, Ishizuka S (2016) Combination of soya pulp and *Bacillus coagulans* lilac-01 improves intestinal bile acid metabolism without impairing the effects of prebiotics in rats fed a cholic acid-supplemented diet. Br J Nutr 116:603–610
19. Yoshitsugu R, Kikuchi K, Hori S, Iwaya H, Hagio M, Shimizu H, Hira T, Ishizuka S (2020) Correlation between 12α-hydroxylated bile acids and insulin secretion during glucose tolerance tests in rats fed a high-fat and high-sucrose diet. Lipids Health Dis 19:9
20. Yoshitsugu R, Liu H, Kamo Y, Takeuchi A, Joe GH, Tada K, Kikuchi K, Fujii N, Kitta S, Hori S, Takatsuki M, Iwaya H, Tanaka Y, Shimizu H, Ishizuka S (2021) 12-α-Hydroxylated bile acid enhances accumulation of adiponectin and immunoglobulin A in the rat ileum. Sci Rep 11:12939
21. Hori S, Satake M, Kohmoto O, Takagi R, Okada K, Fukiya S, Yokota A, Ishizuka S (2021) Primary 12α-hydroxylated bile acids lower hepatic iron concentration in rats. J Nutr 151:523–530
22. Lee JY, Shimizu H, Hagio M, Fukiya S, Watanabe M, Tanaka Y, Joe GH, Iwaya H, Yoshitsugu R, Kikuchi K, Tsuji M, Baba N, Nose T, Tada K, Hanai T, Hori S, Takeuchi A, Furukawa Y, Shirouchi B, Sato M, Ooka T, Ogura Y, Hayashi T, Yokota A, Ishizuka S (2020) 12-α-Hydroxylated bile acid induces hepatic steatosis with dysbiosis in rats. Biochim Biophys Acta Mol Cell Biol Lipids 1865:158811
23. Maegawa K, Koyama H, Fukiya S, Yokota A, Ueda K, Ishizuka S (2021) Dietary raffinose ameliorates hepatic lipid accumulation induced by cholic acid via modulation of enterohepatic bile acid circulation in rats. Br J Nutr:1–10. https://doi.org/10.1017/S0007114521002610
24. Hashimoto N, Matsui I, Ishizuka S, Inoue K, Matsumoto A, Shimada K, Hori S, Lee DG, Yasuda S, Katsuma Y, Kajimoto S, Doi Y, Yamaguchi S, Kubota K, Oka T, Sakaguchi Y, Takabatake Y, Hamano T, Isaka Y (2020) Lithocholic acid increases intestinal phosphate and calcium absorption in a vitamin D receptor dependent but transcellular pathway independent manner. Kidney Int 97:1164–1180

Chapter 9

Glycogen Measurement

Cláudia Regina Cavaglieri, Carlos Alberto da Silva, and Celene Fernandes Bernardes

Abstract

Glycogen is a branched polysaccharide consisting of glucose units found primarily in animals, fungi, and bacteria. In humans, glycogen is the main storage form of glucose and the primary means of nonoxidative glucose disposal into muscle and liver tissues. However, significant amounts are found elsewhere, such as in the brain and kidney. Glycogen is a ubiquitous fuel source stored in the cytosol of cells. During times of need, glycogen is rapidly broken down to produce glucose. In the liver, the breakdown of glycogen during fasting conditions contributes to hepatic glucose production that is crucial for maintaining blood glucose levels and supporting other tissues' needs. Almost all tissues contain some glycogen, but the relative amounts of glycogen vary considerably. Glycogen synthesis and degradation are highly regulated multi-step processes involving distinct sets of enzymatic reactions. The concentration of glycogen can be carried out in various cell tissues and using different experimental techniques.

Key words Glycogen, Liver, Muscle, Glycogen measurement

1 Introduction

Glycogen is a branched polysaccharide consisting of glucose units found primarily in animals, fungi, and bacteria [1]. The discovery of liver glycogen in 1857 is attributed to Claude Bernard [2]. Over 150 years of research on this macromolecule has led to many Nobel prizes in physiology. The first was in 1947, awarded to Carl Ferdinand Cori and Gerty Theresa Cori for their work on the catalytic conversion of glycogen [3, 4]. The second Earl Wilbur Sutherland in 1971 demonstrated how epinephrine initiates a signal cascade to trigger glycogen breakdown [5, 6]. Finally, Edmond Henri Fischer and Edwin Gerhard Krebs in 1992 demonstrated how reversible protein phosphorylation could control glycogen phosphorylase activity [7, 8].

In humans, glycogen is the main storage form of glucose and the primary means of nonoxidative glucose disposal into muscle and liver tissues [9]. However, significant amounts are also found

Cinthia Baú Betim Cazarin (ed.), *Basic Protocols in Foods and Nutrition*,
Methods and Protocols in Food Science, https://doi.org/10.1007/978-1-0716-2345-9_9,

elsewhere, such as the brain and kidney [1]. Glycogen is a ubiquitous fuel source stored in the cytosol of cells, occupying 2% of the volume of cardiac cells [10], 1–2% of the volume of skeletal muscle cells, and 5–6% of the volume of liver cells [11]. The glycogen particles in liver cells can be 10 times larger than those in skeletal muscle cells, with each particle containing >50,000 glucose molecules [1, 12]. Each gram of glycogen is stored with at least 3 g of water [13, 14]. During times of need, glycogen is rapidly broken down to produce glucose. This muscle serves as an immediate and important energy source for exercise during the first 30 minutes [15]. In the liver, the breakdown of glycogen during fasting conditions contributes to hepatic glucose production that is crucial for maintaining blood glucose levels, for supporting other tissues' needs [16]. Although glycogen is mobilized during fasting in both the liver, the latter tissue lacks key metabolic enzymes to transport glucose back into the bloodstream. On the other hand, the rapid weight loss due to carbohydrate-restricted diets promotes the breakdown of glycogen and excretion of water in the urine. Interestingly, neither short-term fasting nor prolonged sedentary behavior affects muscle glycogen stores [16].

Almost all tissues contain some glycogen, but the relative amounts of glycogen vary considerably. Glycogen levels found in the adult rat under physiological conditions are as follows: liver > skeletal muscle > cardiac muscle > brain > kidney [17]. In addition to human muscle and liver cells, glycogen is stored in small amounts in brain cells, heart cells, smooth muscle cells, kidney cells, red and white blood cells, and even adipose cells [18]. Glucose is a critical energy source for neurons in the brain and throughout the body [19], and under normal circumstances, glucose is the only fuel the neurons use to produce ATP; at rest, approximately 60% of the glucose found in the blood is metabolized by the brain [20]. Also, a small amount of glycogen is stored in brain tissue (100 less than the glycogen content of muscle cells), specifically in astrocytes, non-neuronal glial cells that play an important role stabilizing, insulating, and nourishing neurons [19, 21–23]. Whole-body glycogen content is approximately 600 g, and the content of glycogen in liver cells varies throughout each day depending upon the carbohydrate content of the diet, the time between meals, and the intensity and duration of recent physical activity.

Glycogen synthesis and degradation are highly regulated multistep processes involving distinct sets of enzymatic reactions [1]. The new glycogen granule synthesis is thought to be initiated by glycogen [24, 25]. An enzyme that forms a complex with glycogen synthase links uridine diphosphate–glucose molecules to create a glycogen particle [25]. Glycogen synthase and branching enzyme then work in concert to enlarge the glycogen particle. Glycogen synthase produces 1,4-glycosidic linkages to create a strand of glucose molecules, and the branching enzyme establishes

α-1,6 bonds between glucose molecules to create branches every 8–12 glucose molecules; the branches increase the density, solubility, and surface area of the glycogen particle [1, 25]. Glycogen particles have been categorized into two forms based upon their size: (1) proglycogen and (2) macroglycogen [26]. Proglycogen particles comprise roughly 15% of total glycogen content, are sensitive to dietary carbohydrates, and are first to add glucose units after glycogen depletion; additional glucose units are then more slowly added to create the larger macroglycogen particles. This observation may explain glycogen repletion's biphasic nature: rapid for the first few hours and more slowly after that.

The breakdown of glycogen occurs through two distinct pathways, one occurring in the cytosol (glycogenolysis) and another in the lysosomes (glycogen autophagy or glycophagy). Glycogenolysis is carried out by the enzyme glycogen phosphorylase (GP), which catalyzes the release of glucose-1-phosphate (G1P) from the ends of glycogen branches [27]. As with GS, the activity of GP is also regulated allosterically and by phosphorylation. The G1P produced can then be converted to glucose-6-phosphate (G6P) and funneled through glycolysis and other metabolic pathways [28]. UTP is consumed at the glucose UDP pryophosphorylation step of glycogen synthesis such that the shuttling of each glucose moiety on and off glycogen requires one ATP equivalent.

Individual glycogen molecules are too small to be detected by normal light microscopy. Histochemical staining for glycogen in cells or tissues can therefore only reveal conglomerates of glycogen particles. However, electron microscopy is large enough to detect glycogen molecules and has been described as rosette-like β-particles in muscle and larger α-particles in the liver [29]. In addition, hepatic glycogen can be purified by size exclusion chromatography techniques [30].

2 Method for Analysis of Glycogen Concentration in Muscle and Liver Tissue

The concentration of glycogen can be performed in various cellular tissues and using different experimental techniques. The classical analysis was initially developed for skeletal muscles, including tissue digestion techniques with potassium hydroxide, glycogen separation with ethyl alcohol, and colorimetric analysis after treatment with sulfuric phenol [31, 32].

Some adaptations were later performed, such as the addition of saturated sodium sulfate after hot tissue digestion with potassium hydroxide, for glycogen analysis in liver and muscle tissue [33].

Other methodologies were proposed, such as the enzymatic hydrolysis of glycogen with amyloglucosidase enzyme and subsequent glucose analysis resulting from hydrolysis with colorimetric enzymatic reagents [34, 35]. These methodologies do not eliminate the initial stage of alkaline tissue hydrolysis. Recently, the

techniques that use alkaline hydrolysis [36] and enzymatic hydrolysis [37] for muscle tissues and liver are the most used.

The colorimetric analysis of glycogen treated with phenol and sulfuric acid is based on dehydration of carbohydrates by sulfuric acid and subsequent formation of the complex with phenol. The developed color complex is proportional to the carbohydrate concentration and can be determined by spectrophotometry using the 490 nm wavelength range. The glycogen concentration is obtained using a standard curve and expressed in mg of glycogen per g of tissue weight.

2.1 Equipments

- Precision milligram scale.
- Boiling water bath.
- Ice bath.
- Centrifuge.
- Visible spectrophotometer.
- Pipettes.
- Test tubes.

2.2 Reagents

- Potassium hydroxide – solution of 30 g of KOH in 100 mL of distilled water.
- Sodium sulfate – saturated solution.
- Ethyl alcohol 95%.
- Phenol – solution of 800 mg phenol in 200 μL of distilled water.
- Pure concentrated sulfuric acid for analysis.
- Glucose – solution of 200 mg of glucose in 100 mL of distilled water.

2.3 Method

2.3.1 Collecting the Sample

1. Remove (macroscopically) visible fat, connective tissue, and blood.
2. Weigh 200 mg of muscle or liver samples.
3. Transfer the sample with a clamp to a test tube and cap.
4. Freeze the sample immediately; liquid nitrogen is recommended.
5. Keep the sample deep-frozen until the moment of use.

2.3.2 Extraction of Glycogen from Tissues

1. Add 1 mL of KOH 30 g% solution for the muscle or liver samples (TIP: keep the sample fully submerged in the solution).
2. Heat in boiling water bath, for 20 to 30 minutes or until checking homogeneous solution (TIP: use tubes that remain with the mouth out of the boiling water, being careful not to get water in the tube).

3. Remove the tube from boiling water and cool it in cold water.
4. Add 100 μL of saturated sodium sulfate solution to the muscle and liver samples.
5. Add 3.5 mL of 95% ethanol to the muscle and liver samples for precipitation of glycogen after alkaline tissue digestion.
6. Keep the sample on ice for 30 minutes.
7. Centrifuge at 840 g for 30 minutes.
8. Separate the supernatant by aspiration.
9. Dissolve the precipitate containing the glycogen in 5 mL of distilled water for the muscle and liver samples (TIP: instead of large volume trials, of 5 mL, serial dilutions to achieve a 5× diluted solution can be used, be aware that the analytical error may be greater).

2.3.3 Preparation of the Standard Curve

1. Prepare a glucose stock solution at a concentration of 50 mg/dL.
2. Dilute the stock solution in the standard proportions indicated below:
   - P1 = 1 mg/dL: 20 μL stock solution +980 μL distilled water.
   - P2 = 2 mg/dL: 40 μL stock solution +960 μL distilled water.
   - P3 = 4 mg/dL: 80 μL stock solution +920 μL distilled water.
   - P4 = 6 mg/dL: 120 μL stock solution +880 μL distilled water.
3. Prepare test tubes containing 1 mL of each standard solution P1, P2, P3, and P4.
4. Add 10 μL of phenol solution to each tube.
5. Then add 2.5 mL of sulfuric acid.
6. Leave the tubes to stand for 10 minutes.
7. Shake the solutions.
8. Put for 10 minutes in a boiling water bath.
9. Cool in a water bath at room temperature (24 °C).Calibrate the spectrophotometer, in 490 nm of wavelength, with the calibration solution composed of 1 mL of distilled water, 10 μL of phenol solution, and 2.5 mL of sulfuric acid.
10. Check the absorbance of the standard solutions.

2.3.4 Quantitative Analysis of Glycogen with Phenol-Sulfuric

1. Collect an aliquot of 200 μL of muscle or 50 μL of liver from the solutions prepared according to the previous item and place in test tubes.

Table 1
Synthesis of the steps of the glycogen dosing technique in liver and muscle

		Alíquo	Water	Phenol	H_2SO_4
Samples	Muscle	200 μL	800 μL	10 μL	2.5 mL
	Liver	50 μL	950 μL	10 μL	2.5 mL
Standards	1 mg/dL	1000 μL	0	10 μL	2.5 mL
	2 mg/dL	1000 μL	0	10 μL	2.5 mL
	4 mg/dL	1000 μL	0	10 μL	2.5 mL
	6 mg/dL	1000 μL	0	10 μL	2.5 mL
Calibrator	0	0	1000 μL	10 μL	2.5 mL

2. Complete the 1 mL volume with distilled water by placing 800 μL in the tube containing the muscle sample and 950 μL in the tube containing the liver sample.
3. Add 10 μL of phenol solution.
4. Then add 2.5 mL concentrated sulfuric acid (TIP: add the acid quickly and directly onto the tube solution instead of against the side of the test tube to ensure adequate mixing).
5. Leave the tube to stand for 10 minutes.
6. Shake the solution.
7. Put for 15 minutes in a boiling water bath.
8. Cool in a water bath at room temperature (24 °C).
9. Calibrate the spectrophotometer, in 490 nm of wavelength, with the calibration solution composed of 1 mL of distilled water, 10 μL of phenol solution, and 2.5 mL of sulfuric acid.
10. Check the absorbance of the sample solution.
11. Determine the concentration of glycogen using the standard curve prepared according to **item 2.3.3** (Table 1).

2.3.5 Calculations

The concentration of glycogen in liver and muscle samples can be determined using the formula below. The concentration of glycogen will be expressed in mg of glycogen in g of sample.

$$[\text{GLYCOGEN}]\ (\text{mg/dL}) = \frac{[\text{Standard}] \times \text{Absorbance sample} \times \text{dilution}}{\text{Standard Absorbance}}$$

1. Calculate the arithmetic mean of the glycogen concentration values in the standard solutions. [Standard] = (1 + 2 + 4 + 6)/4 = 3.25 mg/dL.
2. Calculate the mean of the absorbance values verified for the standard solutions. Consider "Standard Absorbance" in the formula described above.

3. Consider the dilution of 5 for the muscle sample and 20 for the liver sample, dilution resulting from the addition of water in the precipitated glycogen aliquot.
4. Convert the concentration of hepatic glycogen, from mg/dL to mg in 5 mL, considering that the precipitated glycogen from liver and muscle samples were dissolved in 5 mL of water.
5. The mass of hepatic glycogen in 5 mL solution corresponds to the mass of glycogen (mg) in the total sample (g) of liver or muscle samples digested.

Example:

Liver sample = 200 mg.

Absorbance of the liver sample = 0.30.

Average concentration of standards = 3.25 mg/dL.

Mean absorbance of standards = 0.325.

Dilution of the liver glycogen sample = 20

$$[\text{GLYCOGEN}]\ (\text{mg/dL}) = \frac{[\text{Standard}] \times \text{Absorbance sample} \times \text{dilution}}{\text{Standard absorbance}}$$

$$[\text{GLYCOGEN}]\ (\text{mg/dL}) = \frac{3.25 \times 0.30 \times 20}{0.325} = 60\ \text{mg/dL}$$

60 mg of glycogen in 100 mL of solution.

The glycogen solution precipitated from the liver sample was dissolved in 5 mL of water; therefore:

3 mg of glycogen in 5 mL of sample solution.

As in the sample solution, 200 mg of the liver was placed, 3 mg of glycogen in 200 mg of the liver, which corresponds to 15 mg of glycogen per gram of liver sample.

3 Method for Analysis of Glycogen Concentration in Erythrocytes

The erythrocytes use as an energetic source, mainly the glucose that is metabolized by the Embden-Meyerhoff route. The hexose is decomposed until lactate, which is considered a common value between 6 and 8 μmoles of glucose per g of hemoglobin per hour. Besides, a small fraction of the glucose-6-phosphate formed is metabolized via the hexose phosphate route, producing reduced nicotinamide adenine dinucleotide phosphate [38].

Within the aspects of the analysis of the dynamics of glucose uptake by red blood cells, it should be noted that this is a much higher uptake rate than consumption. The uptake of hexose is the responsibility of a refined system that involves membrane proteins with easy transport activity, being called GLUT 1 (glucose

transporter 1), which has the characteristic of transferring glucose from the extracellular medium to the cytosol in a way that does not depend on insulin [39].

Molecular analyses aimed at evaluating the population of this class of carriers estimated that the population of GLUT1 is approximately 3×10^5, making up 3.5% of membrane proteins, a much more considerable amount, if compared to the presence of Na+/K+ pumps, is only 200 per human red blood cell. It has also been demonstrated that the transport of glucose in the human red blood cell far exceeds the cell's metabolic needs, which makes erythrocytes one of the most important glucose consumers (carrying 40% of plasma glucose) after the brain [40, 41].

It is a consensus that in erythrocytes, the glucose uptake is high and fast enough to follow the changes in plasma concentration in the time of a capillary transit. In humans, the transit time in the lung capillary bed is only 0.75 s at rest and an average flow velocity of 0.3 mm/s, and slower in systemic capillaries due to a more extensive cross-section where the average transit time is 2.5 s [41].

Regarding glucose in the metabolism of human red blood cells, it has already been described that the glycolysis rate is 1,1 $mmol.h^{-1}.1^{-1}$ cells at pH of 7.4. In short, the maximum transport of glucose in the erythrocytes in the 5 mM glycemia is 315 $mmol.h^{-1}.1^{-1}$, value 12,350 times the glycolytic rate.

To identify and quantify the glycogen reserves, the method that has the acid hydrolysis of the hot tissue followed by the enzymatic analysis of the resulting glucose was used; followed by the enzymatic hydrolysis with amylo-α-1,4-α-1,6-glucosidase and again the quantified glucose. The degradation of glycogen with phosphorylase and coupled debranching complex is performed, and the resulting glucose is evaluated; however, it was verified that the results were not satisfactory in the evaluation performed in leucocytes [42].

The above studies demonstrated that the erythrocytes could store glucose through an amyloglucosidase-sensitive system, an enzyme used to quantify glycogen. The presence of the enzyme amylo-1,6-glucosidase has already been described, which catalyzes glycogen phosphorylase's debranching limiting dextrin, thus releasing glucose in human erythrocytes [43]. In the absence of other tests sensitive enough to detect small amounts of glycogen and as no other form is known to react to this enzyme, it has been suggested that it is glycogen [44].

It should be noted that the traditional methods that use the chemical digestion of liver or muscle tissue under heating for extraction and quantification of glycogen present low sensitivity if applied to samples of erythrocytes, suggesting the need for improvement of methods for application in these cells. Thus, the following procedure was applied: blood was collected and centrifuged (2000 rpm, 10 min) to separate plasma and cells, then the

cells were washed three times with cold saline and under refrigeration. A sample of the erythrocytes was submitted to osmotic shock, and, using the amyloglucosidase method, glycogen is transformed into glucose. The total glucose from glycogen could be measured by the hexokinase method. This method was able to detect glucose concentrations as low as 200 ng [45].

Ferrannini and Bjorkman [46] conducted a study in the 1980s that showed that erythrocytes could accumulate large reserves of glucose in the postprandial period and release it into circulation in case of hypoglycemia, suggesting that this enormous amount of glucose is in the form of glycogen reserves. In this aspect and the same period, Guarner and Alvarez-Buylla [47] demonstrated that the erythrocytes reserve glycogen when incubated in hyperglycemic and release glucose when in hypoglycemic. A fact also described *in vivo* when an arterio-venous difference in erythrocytes' glycogen content was verified, indicating glucose distribution during the passage through the blood capillaries. Molecular studies have described the presence of β-adrenergic receptors in the erythrocyte membrane, with activity identical to the receptors described in hepatocytes [47–49]. In this line of reasoning, besides the globules releasing oxygen in the capillary transit, they would release glucose, being stored promptly mobilized in the arteriovenous transition supplying the tissues' energetic needs.

In the 1990s, it was proposed a micro method for evaluation of glycogen reserves in erythrocytes, based on evidence that the previously published methods used the precipitation of glycogen in ethanol, a condition that, for evaluation of the glycogen content in erythrocytes, presents less potential for extraction, quantification, and evaluation of glycogen reserves. Thus, a methodology for replacing ethanol with isopropyl alcohol was developed, allowing improvement and development of an erythrocyte assay for glycogen with a sensitivity of 0.1 μg of glycogen (5 μg glycogen/g hemoglobin) with 95% confidence [50].

3.1 Equipments

- Visible spectrophotometer.
- Ultrasonic shakerRefrigerated centrifuge.
- Peripheral blood collection material.
- Vortex shaker.
- Water bath at 37 °C and 50 °C.
- Test tubes and pipettes.

3.2 Reagents

- Sodium chloride 0.15 mol/L – 0.9 g in 100 mL of distilled water.
- Perchloric acid 0.6 mol/L – 50 mg perchloric acid in 1 liter of distilled water.
- Isopropyl alcohol.

- Sodium acetate buffer 0.1 mol/L pH 4.8.
- Glycogen 50 mg/dL – 50 mg in 100 mL of distilled water.
- Amyloglucosidase reagent (4 U) – Amyloglucosidase enzyme – pure standard for quantitative analysis, for example, from *Aspergillus niger*; amylo-α-1,6-α-1,4 glucosidase, EC 3.2.1.3.
- Hexokinase reagent for determining glucose concentration. The reagent consists of a hexokinase enzyme (D-hexose-6-phosphotransferase, EC 2.7.1.1); glucose d-phosphate dehydrogenase enzyme (D-glucose-6-phosphate: NADP l-oxidoreductase, EC 1.1.1.49); phosphate buffer 70 mmol/L, pH 7.7 and magnesium solutions (4 mmol/L), NADP (1.3 mmol/L) and ATP (1.3 mmol/L). The reagent is found ready in commercial kits for glucose measurement.

In the hexokinase method for glucose dosage, glucose is phosphorated to glycose-6-phosphate by the phosphate originated from ATP, catalyzed by hexokinase. The glycose-6-phosphate is oxidized to 6-phosphorus gluconate in a reaction catalyzed by the glycose-6-phosphate dehydrogenase and, concomitantly, the oxidized adenine nucleotide (NAD^+) is reduced to NADH. NADH's absorbance can be determined at 340 nm and is directly proportional to the concentration of glucose in the sample.

3.3 Method

3.3.1 Experimental Animals

In procedures with experimental animals, it is proposed to be performed under fasting for 12 hours, and if anesthesia is necessary, sodium pentobarbital can be used at a concentration of 30 mg/kg, applied intraperitoneally.

3.3.2 Sample Collection

A hypodermic needle syringe with a heparin solution (200 U/dL of saline) is used to obtain blood samples. The sample can be collected either in peripheral vascularization or by cardiac puncture, and the sample must be promptly transferred to test tubes positioned under an ice layer.

3.3.3 Preparation of Erythrocyte Concentrate

1. Centrifuge 1.0 mL of heparinized blood at 1100 g for 5 minutes at 4 °C.
2. Separate the erythrocytes and wash twice with 0.15 mol/L sodium chloride. To wash the erythrocytes, add sodium chloride, shake gently and centrifuge at 1100 g for 5 minutes at 4 °C. To reduce the presence of substances present in the plasma, vacuum the supernatant at each centrifugation with a Pasteur pipette.
3. Then, determine the hemoglobin concentration by laboratory use methods.
4. TIP: when vacuuming the supernatant, the 1 mm layer that corresponds to the white blood cells (buffy coat), formed on the concentrate of red blood cells, must also be removed, discarding.

3.3.4 Extraction of Glycogen from Erythrocytes

1. Transfer 200 μL of the erythrocyte concentrate to another flask.
2. Add 600 μL of 0.6 mol/L of a cold perchloric acid solution.
3. Centrifuge at 900 g for 10 min at 4 °C.
4. Transfer 400 μL of the supernatant to a test tube.
5. Add 500 μL of isopropyl alcohol.
6. Shake slowly with the help of a vortex.
7. Incubate at 50 °C, for 1 hour, for precipitation of glycogen.
8. Centrifuge at 1500 g for 10 minutes at room temperature (24 °C).
9. Discard the supernatant and dry the tubes by inversion.
10. Dissolve the precipitated glycogen, by ultrasonication 20 s with 200 μL sodium acetate buffer 0.1 mol/L, pH 4.8.
11. Separate 100 μL of the glycogen test solution in acetate buffer to be used in the control tube.

3.3.5 Preparation of the Standard Curve

1. Prepare a glycogen stock solution at a concentration of 5 mg/dL (50 μg/mL).
2. Dilute the stock solution in the standard proportions indicated below:
   - P1 = 1.25 μg/mL: 10 μL stock solution +390 μL Perchloric acid 0.6 mol/L.
   - P2 = 2.50 μg/mL: 20 μL stock solution +380 μL Perchloric acid 0.6 mol/L.
   - P3 = 5.00 μg/mL: 40 μL stock solution +360 μL Perchloric acid 0.6 mol/L.
   - P4 = 10.00 μg/mL: 80 μL stock solution +320 μL Perchloric acid 0.6 mol/L.
   - P5 = 20.00 μg/mL: 160 μL stock solution +240 μL Perchloric acid 0.6 mol/L.
3. Slowly add 500 μL of isopropyl alcohol to each tube.
4. Incubate at 50 °C, for 60 minutes, for glycogen precipitation.
5. Centrifuge at 1500 g for 10 minutes at room temperature (24 °C).
6. Discard the supernatant and dry the tubes by inversion.
7. Dissolve the precipitated glycogen by ultrasonication 20 s with 100 μL sodium acetate buffer 0.1 mol/L, pH 4.8.

   The combination of high temperatures and less polar alcohol resulted in the successful quantitative recovery of micro amounts of glycogen using a simple alcohol precipitation procedure.

Table 2
Synthesis of the steps of the glycogen dosing technique in erythrocyte

	Alíquot	Water	Amyloglucosidase reagent	Hexolinase reagent
Sample	100 μL	0	5 μL	400 μL
Standards	100 μL	0	5 μL	400 μL
Calibrator	100 μL	5 μL	0	400 μL

3.3.6 Quantitative Analysis of Glycogen

1. Add 5 μL of amyloglucosidase reagent (4 U) to each test tubes with a sample of glycogen and standard solutions.
2. Prepare a calibrator tube containing 100 μL of the glycogen sample solution and 5 μL of distilled water. This solution is used to correct the contaminating free glucose absorbance of the erythrocytes glycogen sample.
3. Homogenize the sample tube solutions, standards, and calibrator.
4. Incubate for 30 minutes at 37 °C. In this step, by a reaction catalyzed by the enzyme amyloglucosidase, glycogen will be hydrolyzed and converted to glucose.
5. Add 1.0 mL of the hexokinase reagent to determine the glucose concentration.
6. Incubate for 10 minutes at 37 °C.
7. Check the absorbance values at 340 nm wavelength, setting the absorbance zero to the calibrator tube.
8. Determine the glycogen concentration in the sample using the standard curve.

   TIP: if the contaminating glucose concentration is high, it is suggested to calibrate the spectrophotometer with distilled water and read the calibrator tube solution's absorbance. Then, discount the absorbance value of the calibrator tube solution from the standard and sample solutions' absorbance values (Table 2)

3.3.7 Calculations

The concentration of glycogen in erythrocyte samples can be determined using the formula below. The concentration of glycogen will be expressed in μg of glycogen in g of hemoglobin.

$$[\text{GLYCOGEN}]\ (\mu g/mL) = \frac{[\text{Standard}] \times \text{Absorbance sample} \times \text{Dilution}}{\text{Standard Absorbance}}$$

1. Calculate the arithmetic mean of the glycogen concentration values in the standard solutions. [Standard] = (1.25 + 2.50 + 5.00 + 10.00 + 20.00)/5 = 7.75 μg/mL.

2. Calculate the mean of the absorbance values verified for the standard solutions. Consider "Standard Absorbance" in the formula described above.
3. A dilution of 16x for the erythrocyte sample should be used for calculation, based on dilution resulting from the addition of perchloric acid and fractionated collection of the precipitated glycogen.
4. Convert the glycogen concentration (μg/mL) to glycogen mass (μg) in 200 μL of sample.
5. Considering the hemoglobin mass in 200 μL of the sample, the glycogen concentration in μg per gram of hemoglobin is determined.

Example:

Red blood cell sample = 200 μL.

Hemoglobin concentration in the erythrocyte sample = 15 g/dL (in 200 μL of the sample, the hemoglobin mass will be 30 g).

The absorbance of the erythrocyte sample = 0.30.

Average concentration of standards = 7.75 μg/mL.

Mean absorbance of standards = 0.35.

Red cell sample dilution = 16

$$[\text{GLYCOGEN}]\ (\mu\text{g/mL}) = \frac{[\text{Standard}] \times \text{Absorbance sample} \times \text{dilution}}{\text{Standard absorbance}}$$

$$[\text{GLYCOGEN}]\ (\mu\text{g/mL}) = \frac{7.75 \times 0.30 \times 16}{0.35} = 106.29\ \mu\text{g/mL}$$

106.29 μg of glycogen in 1 mL of solution.

The glycogen precipitated from the erythrocyte sample was dissolved in 200 μL of the solution,

In 200 μL of the solution, the glycogen mass is 21.26 μg.

In 200 μL of the solution has 30 g of hemoglobin.

Therefore, it corresponds to 0.70 μg of glycogen per gram of hemoglobin.

4 Conclusions

In humans, glycogen is the main storage form of glucose and the primary means of nonoxidative glucose disposal into muscle and liver tissues. Glycogen is a ubiquitous fuel source stored in the cytosol of cells, and almost all tissues contain some glycogen, but the relative amounts of glycogen vary considerably. In addition to human muscle and liver cells, glycogen is stored in small amounts in brain cells, heart cells, smooth muscle cells, kidney cells, red and

white blood cells, and even adipose cells. In muscles and liver, the glycogen concentration analysis is performed by the sulfuric phenol technique after digestion of the tissue with potassium hydroxide and glycogen precipitation with alcohol. The erythrocytes glycogen analysis is performed after isolation with isopropyl alcohol followed by enzymatic reactions and expressed concentration having the ug/g Hb index.

References

1. Adeva-Andany MM, Gonzalez-Lucan M, Donapetry-Garcia C, Fernandez-Fernandez C, Ameneiros Rodriguez E (2016) Glycogen metabolism in humans. BBA Clin 5:85–100
2. Young FG (1957) Claude Bernard and the discovery of glycogen: a century of retrospect. Br Med J 1:1431–1437
3. Cori CF, Colowick SP, Cori GT (1937) The isolation and synthesis of glucose-1-phosphoric acid. J Biol Chem 121:465–477
4. Cori CF, Schmidt G, Cori GT (1939) The synthesis of a polysaccharide from Glucose-1-phosphate in muscle extract. Science 89: 464–465
5. Berthet J, Rall TW, Sutherland EW (1957) The relationship of epinephrine and glucagon to liver phosphorylase. IV. Effect of epinephrine and glucagon on the reactivation of phosphorylase in liver homogenates. J Biol Chem 224: 463–475
6. Rall TW, Sutherland EW, Wosilait WD (1956) The relationship of epinephrine and glucagon to liver phosphorylase. III. Reactivation of liver phosphorylase in slices and in extracts. J Biol Chem 218:483–495
7. Fischer EH, Krebs EG (1955) Conversion of phosphorylase b to phosphorylase a in muscle extracts. J Biol Chem 216:121–132
8. Krebs EG, Kent AB, Fischer EH (1958) The muscle phosphorylase b kinase reaction. J Biol Chem 231:73–83
9. Shulman RG, Rothman DL (2001) 13C NMR of intermediary metabolism: implications for systemic physiology. Annu Rev Physiol 63: 15–48
10. Depre C, Vanoverschelde JJ, Taegtmeyer H (1999) Glucose for the heart. Circulation 99: 578–588
11. Guyton AC, Hall JE (2011) Guyton and Hall textbook of medical physiology. Saunders/ Elsevier, New York
12. Philp A, Hargreaves M, Baar K (2012) More than a store: regulatory roles for glycogen in skeletal muscle adaptation to exercise. Am J Physiol Endocrinol Metab 302:E1343–E1351
13. Fernandez-Elias VE, Ortega JF, Nelson RK et al (2015) Relationship between muscle water and glycogen recovery after prolonged exercise in the heat in humans. Eur J Appl Physiol 115:1919–1926
14. Kreitzman SN, Coxon AY, Szaz KF (1992) Glycogen storage: illusions of easy weight loss, excessive weight regain, and distortions in estimates of body composition. Am J Clin Nutr 56(1 suppl):292S–293S
15. Mul JD, Stanford KI, Hirshman MF, Goodyear LJ (2015) Exercise and regulation of carbohydrate metabolism. Prog Mol Biol Transl Sci 135:17–37
16. Petersen MC, Vatner DF, Shulman GI (2017) Regulation of hepatic glucose metabolism in health and disease. Nat Rev Endocrinol 13: 572–587
17. Duran J, Gruart A, López-Ramos JC, Delgado-García JM, Guinovart JJ (2019) Glycogen in astrocytes and neurons: physiological and pathological aspects. Adv Neurobiol 23: 311–329
18. Ceperuelo-Mallafre V, Ejarque M, Serena C et al (2016) Adipose tissue glycogen accumulation is associated with obesity-linked inflammation in humans. Molec Metab 5:5–18
19. Brown AM, Ransom BR (2007) Astrocyte glycogen and brain energy metabolism. Glia 55: 1263–1271
20. Wasserman DH (2009) Four grams of glucose. Am J Physiol Endocrinol Metab 296:E11–E21
21. Wu L, Wang CP, Swanson RA (2019) Methodological considerations for studies of brain glycogen. J Neurosci Res 97(8):914–922
22. Meléndez R, Meléndez-Hevia E, Cascante M (1997) How did glycogen structure evolve to satisfy the requirement for rapid mobilization of glucose? A problem of physical constraints in structure building. J Mol Evol 45:446–455
23. Goldsmith E, Sprang S, Fletterick R (1982) Structure of maltoheptaose by difference Fourier methods and a model for glycogen. J Mol Biol 156:411–427

24. Cao Y, Mahrenholz AM, DePaoli-Roach AA, Roach PJ (1993) Characterization of rabbit skeletal muscle glycogenin. Tyrosine 194 is essential for function. J Biol Chem 268(20): 14687–14693
25. Smythe C, Cohen P (1991) The discovery of glycogenin and the priming mechanism for glycogen biogenesis. Eur J Biochem 200(3): 625–631
26. Prats C, Graham TE, Shearer J (2018) The dinamic life of the glycogen granule. J Biol Chem 293(19):7089–7098
27. Johnson LN (1992) Glycogen phosphorylase: control by phosphorylation and allosteric effectors. FASEB J 6:2274–2282
28. Agius L, Centelles J, Cascante M (2002) Multiple glucose 6-phosphate pools or channelling of flux in diverse pathways? Biochem Soc Trans 30:38–43
29. Drochmans P (1962) Morphologie du glycogene: etude du miscroscope electronique de colorations negative du glycogene particulaire. J Ultrasctruct Res 6:141–163
30. Sullivan MA, Vilaplana F, Cave RA, Stapleton D, Gray-Weale AA, Gilbert RG (2010) Nature of α and β particles in glycogen using molecular size distributions. Biomacromolecules 11:1094–1100
31. Lo S, Russel JC, Taylor AW (1970) Determination of glycogen in small tissue samples. J Appl Physiol 8(2):45–59
32. Lo S, Russell JC, Taylor AW (1970) Determination of glycogen in small tissue samples. J Appl Physiol 28(2):234–236
33. Giozzet VA, Rafacho A, Boschero AC, Carneiro EM, Bosqueiro JR (2008) Dexamethasone treatment in vivo counteracts the functional pancreatic islet alterations caused by malnourishment in rats. Metabolism 57(5): 617–624
34. Roehrig KL, Allred JB (1974) Direct enzymatic procedure for the determination of liver glycogen. Anal Biochem 58(2):414–421
35. Carr RS, Neff JM (1984) Quantitative semiautomated enzymatic assay for tissue glycogen. Comp Biochem Physiol B 77(3):447–449
36. Uruno A, Yagishita Y, Katsuoka F, Kitajima Y, Nunomiya A, Nagatomi R, Pi J, Biswal SS, Yamamoto M (2016) Nrf2-mediated regulation of skeletal muscle glycogen metabolism. Mol Cell Biol 36(11):1655–1672
37. Kaga AK, Barbanera PO, do Carmo NOL, Rosa LRO, Fernandes AAH (2018) Effect of N-acetylcysteine on Dyslipidemia and carbohydrate metabolism in STZ-induced diabetic rats. Int J Vasc Med 2018:6428630
38. Azevedo MRA (2019) Hematologia Básica: Fisiopatologia e Diagnóstico Laboratorial. Thieme Revinter, 6° edição, Rio de Janeiro
39. Montel-Hagen A, Sitbon M, Taykir N (2009) Erythroid glucose transportes. Curr Opin Hematol 16(3):165–172
40. Yoa RG, Rapin JR, Wiernsperger NF, Martinand A, Belleville I (1993) Demonstration of defective glucose uptake and dependent diabetic patients and effects of metformin storage in erythrocytes from non-insulin. Clin Exp Pharmacol Physiol 20:563–567
41. Jacquez JA (1984) Red blood cell as glucose carrier: significance for placental and cerebral glucose transfer. Am J Phys 246(3 Pt 2): R289–R298
42. Passoneau JV, Lauderdale VR (1974) A comparison of three methods of glycogen measurement in tissues. Anal Biochem 60:405–412
43. Hers HG, Verhue W, Van Hoof F (1967) The determination of amylo-1,6-glucosidase. Eur J Biochem 2:256–264
44. Segers O, Somers G, Sener A, Malaisse WJ (1990) Blood glycogen and metabolic control in diabetes mellitus. Diabet Med 7:207–210
45. Nahorski SR, Rogers KJ (1972) An enzymic fluorometric micro method for determination of glycoen. Anal Biochem 49(2):492–497
46. Ferrannini E, Bjorkman O (1986) Role of red blood cells in the regulation of blood glucose levels in man. Diabetes 35(Suppl. l):39
47. Guarner V, Alvarez-Buylla R (1989) Erythrocytes and glucose homeostasis in rats. Diabetes 38:410–415
48. Guarner V, Alvarez-Buylla R (1990) Compensation by fetal erythrocytes of plasma glucose changes in rats. Diabetes 39:1191–1197
49. Beckman BS, Hollenberg MD (1979) P-adrenergic receptors and adenylate cyclase activity in rat reticulocytes and mature erythrocytes. Biochem Pharmacol 28:239–248
50. Farquharson J, Jamieson EC, MacPhee GB, Logan RW (1990) A new sensitive microassay for the measurement of erythrocyte glycogen. Clin Chim Acta 187:89–94

Chapter 10

Evaluation of the Minerals and Trace Elements in the Biological Samples

Duygu Aydemir and Nuriye Nuray Ulusu

Abstract

Minerals and trace elements are crucial for all organisms' biological functions, including plants, humans, and other mammals. Impairment in the mineral and/or trace element metabolism involves the formation of several diseases, including cancer, obesity, diabetes, cardiovascular diseases, and neurological disorders. ICP-MS (inductively coupled plasma-mass spectrometry) can be described as the most sensitive and effective method to evaluate minerals and trace elements in biological samples. This chapter describes an effective and fast method for validating trace elements and minerals via ICP-MS in the cell lysates, mammalian tissue, and serum samples. Minimum relative standard deviation (RSD) values of ICP-MS measurements are observed in the samples digested with a microwave with the SUPRAPUR® grade 65% nitric acid (HNO_3) at the lower dilution rates. This protocol may guide researchers to evaluate trace elements and minerals in the mammalian samples, including blood, serum, tissue, and cells easily and accurately.

Key words ICP-MS, Acidic digestion, Microwave digestion, Mammalian tissue, Serum, Cell culture

1 Introduction: Importance of the Minerals and Trace Elements in Biology

Minerals and trace elements are essential since they play vital roles in all organisms' biological functions, including plants, humans, and other mammals. They are involved in the structure of various enzymes responsible for the detoxification system, amino acid metabolism, immune system, and DNA metabolism [1]. Organisms require minerals and trace elements to maintain their metabolic processes, biological regulation, synthesis molecules, build up organelles, reproduction, growth, development, energy processing, catalyzing reactions, structural function, life, and death [2–10]. Minerals and trace elements have an optimum concentration for regulating almost all cellular reactions to survive the organism. Every organism has an optimum mineral and trace element range,

Cinthia Baú Betim Cazarin (ed.), *Basic Protocols in Foods and Nutrition*,
Methods and Protocols in Food Science, https://doi.org/10.1007/978-1-0716-2345-9_10,

and this range can be altered due to physiological and biochemical properties of the species, internal and external conditions, gender, aging, pregnancy, and lifestyle [8–15].

The concentration of minerals and trace elements levels must be supplied from the environment according to the species' needs; otherwise, absence, insufficient, or excess amounts can cause various problems and trigger unwanted biochemical, physiological, catalytic, structural, and regulatory reactions and pathways. The optimum concentrations of minerals and trace elements may differ at different compartments of the cell, intracellular, extracellular levels, plasma, tissues, health, and diseases [8–25]. If the minerals and trace element concentrations are lower or higher than the optimum concentrations, that can cause various problems such as failure to thrive, diseases, or death of the species. In general, the minerals and trace elements are necessary for various physiological functions, biochemical reactions, optimal metabolic functions, and deficiency or abundance can cause dyshomeostasis, toxicity and induce localized injury, programmed cell death, apoptosis, and necrosis that leads to various diseases and disorders also may cause the death of the organisms [25–35].

The minerals cannot be catabolized or synthesized via metabolic pathways; they can be used several times for various purposes [4]. These molecules must be taken from the soil, water, or from the food chain because they cannot be synthesized by the organisms [3, 5]. Minerals and trace elements have many specialized biochemical and physiological functions in the body/cell such as: preserve the structural component of numerous proteins and macromolecules, act as a second messenger, play an essential role in the component of primary and tertiary protein structure via disulfide bond as well as role in sulfur-containing enzymes or zinc finger tertiary protein structure, serve as cofactors in enzymatic reactions, function in metabolic pathways and electron transfer reactions and production of high energy phosphates, essential structural component of nucleic acids, regulation of acid-base balance, maintenance of osmotic pressure, fluid balance, transport of gases, oxidative reactions, immune response, membrane integrity and permeability, essential for membrane pumps, formation of hormones, secretion of hormones, nerve conduction, muscle contraction, blood clotting, oxygen transport, action on heart, blood coagulation, structural components of the skeleton, and required for bone formation and remodeling. Deficiencies of minerals may lead to oxidative stress and oxidative damage of biomolecules, tissue damage, health problems, and several diseases. Furthermore, toxic effects are produced if these elements are found in high concentrations [35–45]. These functions of minerals and trace elements can be classified as: structural, physiological, catalytic, regulatory, and the last one is the excess that is toxic to the organism or the cell [15, 33, 46–54].

There are several methods and techniques to measure trace elements and mineral levels in various tissues and serum; however, ICP-MS (inductively coupled plasma-mass spectrometry) is the most sensitive and accurate technique. ICP-MS measures the positively charged ions' mass-to-charge ratios, which pass through a quadrupole mass filter and then a mass detector. It provides isotopic information and mass data of the samples [55–57]. The main advantage of the ICP-MS technique is the lower detection limits in ppt (parts per trillion) which also allows the measurement of ultra-trace elements and can measure 82 elements with a minimized spectral interference. Nevertheless, for ICP-MS systems, even the high matrix samples can be analyzed; they should be diluted before the measurement [55–57]. Furthermore, polyatomic interferences, which are usually encountered in biological fluids, are removed by using an octopole reaction system with helium collision mode in the ICP-MS configuration [58].

Several methods for preparing tissue, blood, and serum samples are used to measure mineral and trace element levels in ICP-MS such as alkali dilution and acidic digestion. Alkali dilution method was used to evaluate trace element and mineral levels in both breast milk and blood samples, but not for tissue samples [59, 60]. Additionally, using suprapur grade of HNO_3 is another critical point during trace element and mineral measurement to avoid possible cross-contaminations of the samples with HNO_3. On the other hand, besides these methods, the dilution rate is one of the most important factors for analyzing mineral and trace element levels. Therefore, this chapter addresses alkali dilution and acid digestion methods' effectiveness and precision to determine minerals and trace elements in biological samples [61–64].

2 Materials

2.1 Sample Materials for Mineral and Trace Element Analysis

The deficiency or excess of trace element and mineral concentrations have various roles in health homeostasis and disease status; thus, the effects of various diseases on mineral and trace elements metabolism should be clarified in detail [65]. The possible effects of the various diseases on minerals and trace elements concentrations can be clarified by using rats, mouse, human, zebrafish disease models such as genomics, various knockout models to investigate alcoholism, diabetes, metabolic syndrome, obesity, neuroscience, spinal cord injury, traumatic brain injury, regenerative medicine, and infectious or from human body fluids and tissues [58–65]. We have evaluated mineral and trace element levels in serum, and tissue samples of Wistar albino rats (*Rattus norvegicus*, Sprague-Dawley), nude human, and cell culture lysates for our research projects. All rats or mice were placed in the glass cages with stainless steel covers

in an air-conditioned room (12 h light/dark cycle with a temperature 21 ± 4 °C and relative humidity of 50 ± 5). Animals were provided *ad libitum* with pellet food and tap water during experimental procedures, as reported previously [61–64].

2.2 Serum Preparation

Blood samples of humans or animals should be drained into additive-free vacutainers (BD vacutainers) used for ICP-MS analysis that allows clotting blood. Blood samples are collected from heart for animals or from veins for human patients. After collecting blood samples in the vacutainers, samples are incubated in the tubes for 10 minutes at room temperature to start clotting. The next step is to centrifuge the samples at 4 °C at 500 g for 10-15 minutes to collect serum accumulated on the top of the clotted blood. Serum samples are separated from blood samples and stored at –80 °C until analysis [61–64].

2.3 Tissue Preparation

Human or animal samples are washed with ice-cold saline solution or phosphate-buffered saline (PBS) three times to get rid of the blood, and tissues are replaced immediately in the liquid nitrogen or dry ice. All samples should be kept at – 80 ° C for long-term storage until experiments are performed [61–64].

2.4 Preparation of Cell Lysates

Cells are grown in the polystyrene cell culture plates, and at the end of experimental procedures, flasks are placed on ice, and cells are washed briefly with ice-cold PBS three times. Then ice-cold 500 μL of Na_2PO_4 buffer (pH 7.4) or PBS containing protease inhibitor cocktail are added onto the cells. Lysed cells are scraped off with a plastic scraper and transferred into the 1.5 mL or 15 mL centrifuge tubes depending on the lysate volume. Samples are sonicated for 10 s and then centrifuged at 105,000 g for 1 h at 4 °C to investigate cytosolic fracture. Otherwise, cells can be used after sonication directly for ICP-MS analysis if cytosolic fractures are not needed particularly. Cell culture lysates are stored at − 80 °C freezer until the analysis is performed [61–65].

2.5 Standard Preparation

The multi-element solution 2A of SPEX CertiPrep was used as the external calibration standard. A suprapur grade HNO_3 5% (v/v) solution is used for the matrix of the solution. The analytical standards are prepared from high purity single element concentrates of individual elements using Class A laboratory ware to give precise concentrations. Standard consists of 10 ppm of Ag, Al, As, Ba, Be, Ca, Cd, Co, Cr, Cs, Cu, Fe, Ga, K, Li, Mg, Mn, Na, Ni, Pb, Rb, Se, Sr, Tl, U, V, and Zn. Two milliliters of 2% suprapur grade HNO_3 (v/v) are used as the blank solution to draw the calibration curve's abacus origin [61–66].

3 Methods

3.1 Microwave Digestion

Tissue, serum, or cell lysate samples are dissolved with the suprapur grade HNO_3 for acidic treatment in the microwave digestion system (Milestone START D). Thirty to eighty milligrams of tissue or 100-200 μL of serum or cell lysate samples are dissolved into 10 mL of 65% suprapur grade HNO_3 (v/v). The microwave digestion process occurs in three steps. As the first step, the temperature increases to 150 °C in 15 min, following that the target temperature is constant for 30 min. The method of microwave digestion was created and optimized after several experimental trials. When a higher temperature of more than 200 °C is applied for the acidic digestion of tissue and serum samples, the machine stopped working. According to our experiments, a medium range of temperature and power (500W) is sufficient to digest biological samples. After taking samples from the machine, they are stored at −20 °C until ICP-MS measurement [61–65].

3.2 ICP-MS

ICP-MS is the most sensitive and accurate method to measure trace elements and minerals in the biological samples, among other techniques including inductively coupled plasma atomic emission spectroscopy (ICP-AES), inductively coupled plasma optical emission spectrometry (ICP-OES), flame atomic emission (flame photometry), flame atomic absorption, graphite furnace atomic absorption, and cold vapor/hydride generation atomic absorption. Disadvantages of ICP-MS can be categorized as high costs of equipment, staff, and laboratory setup. On the other hand, interferences need to be controlled carefully. However, ICP-MS can measure multiple elements in a single sample, thus for a high-volume laboratory, ICP-MS can be considered as more cost-effective [66].

Trace and mineral elements in the tissue, serum, or cell lysate samples are measured by Agilent 7700x ICP-MS (Agilent Technologies Inc., Tokyo, Japan). Ag, Al, As, Ba, Be, Ca, Cd, Co, Cr, Cs, Cu, Fe, Ga, K, Li, Mg, Mn, Na, Ni, Pb, Rb, Se, Sr, Tl, U, V, and Zn elements are investigated via ICP-MS. Helium gas is used in the collision/reaction cell to remove potential polyatomic interferences, and MassHunter WorkStation software is used to create the batch and the data analysis. The Full Quant analysis method was performed for the data quantification. “Spectrum” is chosen for analysis mode and the peak pattern is drawn from 3 points for each sample and the measurements are replicated five times [61–65].

3.3 Nitric Acid Choice and Dilution Rates of the Samples

Suprapur grade HNO_3 should be used to prepare mammalian samples for ICP-MS to avoid cross-contaminations, which is the most critical step for this protocol. We have compared EMSURE grade and SUPRAPUR grade HNO_3 in different mammalian tissues and serum samples (Tables 1, 2, 3, 4, 5, 6, 7 and 8). Another

Table 1
Mineral and trace element concentrations in rat serum samples

Dilution rates										
	Element (mg/L)	1:10	1:20	1:50	1:100	1:200	1:400	1:800	1:1000	1:2000
EMSURE® Grade	Na	74 ± 1,2	76 ± 0,8	77 ± 0,7	81 ± 0,5	85 ± 0,7	91 ± 1	93 ± 1,6	97 ± 1,5	121 ± 0,7
	Mg	0,064 ± 0,01	0,068 ± 0,05	0,080 ± 0,02	1,1 ± 0,01	1,4 ± 0,02	2,2 ± 0,04	3,4 ± 0,09	4 ± 0,12	7 ± 0,2
	K	5,8 ± 0,08	5,9 ± 0,05	6,5 ± 0,04	7,8 ± 0,02	9,8 ± 0,13	13 ± 0,2	22 ± 0,3	26 ± 0,7	45 ± 0,7
	Ca	0,5 ± 0,008	0,5 ± 0,01	0,7 ± 0,03	2 ± 0,04	2,7 ± 0,02	6,1 ± 0,2	6,7 ± 0,3	5,1 ± 0,5	7 ± 0,4
	Fe	0,1 ± 0,004	0,08 ± 0,002	ND	ND	ND	ND	ND	ND	ND
	Cu	0,7 ± 0,006	1,5 ± 0,01	3,8 ± 0,02	7,9 ± 0,06	16 ± 0,12	32 ± 0,28	65 ± 0,24	80 ± 0,94	166 ± 2,1
	Zn	0,44 ± 0,004	0,8 ± 0,008	2,4 ± 0,01	4,7 ± 0,03	8,6 ± 0,05	16,6 ± 0,15	32 ± 0,19	42 ± 0,6	81 ± 0,7
	Se	0,01 ± 0,001	ND	ND	ND	ND	ND	ND	ND	ND
	Rb	0,006 ± 0,0003	0,007 ± 0,0004	0,007 ± 0,0004	0,009 ± 0,0006	0,015 ± 0,001	0,018 ± 0,003	0,03 ± 0,006	0,03 ± 0,006	0,05 ± 0,012
	Sr	0,004 ± 0,0002	0,008 ± 0,0002	0,018 ± 0,0002	0,041 ± 0,0009	0,007 ± 0,002	0,15 ± 0,009	0,29 ± 0,007	0,34 ± 0,011	0,67 ± 0,02
	Pb	0,041 ± 0,0003	0,084 ± 0,0007	0,2 ± 0,001	0,41 ± 0,002	0,83 ± 0,009	1,69 ± 0,015	3,36 ± 0,001	4,2 ± 0,06	8,8 ± 0,09
SUPRAPUR® Grade	Na	41,9 ± 0,61	29,6 ± 0,24	28,6 ± 0,28	26,8 ± 0,32	19,5 ± 0,21	10,4 ± 0,24	14,3 ± 0,48	395 ± 2,8	324 ± 2,2
	Mg	0,21 ± 0,004	0,14 ± 0,004	28,6 ± 0,28	0,11 ± 0,012	0,069 ± 0,007	ND	ND	ND	ND
	K	2,3 ± 0,03	1,5 ± 0,02	1,25 ± 0,04	0,77 ± 0,06	ND	ND	ND	ND	ND
	Ca	0,32 ± 0,011	0,22 ± 0,01	0,23 ± 0,02	0,23 ± 0,007	0,01 ± 0,008	ND	ND	ND	ND
	Cu	0,016 ± 0,0001	0,011 ± 0,0004	0,008 ± 0,0009	0,005 ± 0,001	0,003 ± 0,003	ND	ND	ND	ND
	Zn	0,022 ± 0,001	0,015 ± 0,004	0,13 ± 0,002	0,098 ± 0,01	0,35 ± 0,02	ND	ND	5,1 ± 0,14	11,75 ± 0,18
	Rb	0,002 ± 0,0001	0,002 ± 0,0001	0,002 ± 0,0004	0,002 ± 0,0005	0,003 ± 0,001	0,004 ± 0,002	0,005 ± 0,005	0,01 ± 0,004	0,015 ± 0,02
	Sr	0,001 ± 0,0001	0,002 ± 0,00007	0,003 ± 0,0004	0,007 ± 0,0009	0,01 ± 0,002	0,02 ± 0,005	0,04 ± 0,005	0,07 ± 0,012	0,14 ± 0,011
	Ag	0,015 ± 0,0001	0,008 ± 0,0004	0,004 ± 0,0004	ND	ND	ND	ND	ND	ND

Table 2
Mineral and trace element concentrations in rat kidney samples

	Element (mg/L)	1:10	1:20	1:50	1:100	1:200	1:400	1:800	1:1000	1:2000
EMSURE® Grade	Na	24 ± 0,4	25,5 ± 0,3	33,1 ± 0,2	32,2 ± 0,28	48,8 ± 0,44	37,4 ± 0,21	46,8 ± 0,71	98,1 ± 1,19	83,8 ± 0,72
	Dilution rates									
	Mg	2,5 ± 0,03	2,6 ± 0,026	3,4 ± 0,26	3,1 ± 0,026	3,9 ± 0,029	4,3 ± 0,064	5,2 ± 0,15	9,4 ± 0,14	9,3 ± 0,38
	K	40 ± 0,43	42,2 ± 0,41	44,4 ± 0,58	46 ± 0,32	46,1 ± 0,36	49,8 ± 0,22	56,7 ± 0,86	66,9 ± 1,19	83,8 ± 1,6
	Ca	0,23 ± 0,008	32 ± 0,007	2,9 ± 0,068	1,5 ± 0,03	4 ± 0,089	2,9 ± 0,26	3,5 ± 0,4	17,7 ± 0,81	7,86 ± 1,11
	Mn	0,01 ± 0,0003	0,008 ± 0,0003	0,03 ± 0,001	ND	ND	ND	ND	ND	ND
	Fe	0,91 ± 0,017	0,87 ± 0,012	0,53 ± 0,012	ND	ND	ND	ND	ND	ND
	Co	0,002 ± 0,00007	0,0018±0,0007	ND	ND	ND	ND	ND	ND	ND
	Cu	0,79 ± 0,009	1,62 ± 0,013	4,25 ± 0,034	8,31 ± 0,065	16,6 ± 0,1	33,2 ± 0,12	65,9 ± 0,44	83,3 ± 0,52	163,1 ± 2,18
	Zn	0,6 ± 0,009	1 ± 0,01	3,5 ± 0,003	4,6 ± 0,005	9,6 ± 0,07	16,9 ± 0,25	32,7 ± 0,34	46,6 ± 0,6	81,5 ± 0,85
	Rb	0,07 ± 0,001	0,07 ± 0,001	0,07 ± 0,0009	0,07 ± 0,001	0,07 ± 0,002	0,08 ± 0,003	0,08 ± 0,006	0,09 ± 0,01	0,12 ± 0,008
	Sr	0,041 ± 0,0003	0,084 ± 0,0007	0,2 ± 0,001	0,41 ± 0,002	0,83 ± 0,009	1,69 ± 0,015	3,36 ± 0,001	4,2 ± 0,06	8,8 ± 0,09
	Cs	0,0006 ± $6x10^{-4}$	0,0009 ± $6x10^{-4}$	0,002 ± 0,0001	0,004 ± 0,0006	0,008 ± 0,003	0,01 ± 0,0008	0,03 ± 0,001	0,04 ± 0,004	0,08 ± 0,01
	Pb	0,03 ± 0,0007	0,08 ± 0,0007	0,21 ± 0,002	0,42 ± 0,004	0,84 ± 0,008	1,68 ± 0,01	3,31 ± 0,06	4,17 ± 0,05	8,19 ± 0,03
SUPRAPUR® Grade	Na	6,8 ± 0,11	6,5 ± 0,07	4,2 ± 0,12	1,8 ± 0,07	ND	ND	ND	ND	ND
	Mg	1 ± 0,009	1 ± 0,008	1 ± 0,02	0,96 ± 0,01	0,91 ± 0,04	ND	ND	ND	ND
	K	17,5 ± 0,16	17,8 ± 0,17	16,5 ± 0,26	16,1 ± 0,17	15,3 ± 0,12	13 ± 0,35	9,3 ± 0,75	7,1 ± 0,59	ND
	Ca	0,11 ± 0,004	0,11 ± 0,01	0,11 ± 0,01	0,12 ± 0,014	0,34 ± 0,042	ND	ND	ND	ND
	Mn	0,002 ± 0,0009	0,009 ± 0,0001	ND	ND	ND	ND	ND	ND	ND

(continued)

Table 2
(continued)

Element (mg/L)	1:10	1:20	1:50	1:100	1:200	1:400	1:800	1:1000	1:2000
Fe	0,46 ± 0,007	0,11 ± 0,007	ND	ND	ND	ND	ND	ND	ND
Cu	0,07 ± 0,001	0,07 ± 0,00009	0,07 ± 0,002	0,06 ± 0,003	0,07 ± 0,004	0,41 ± 0,009	0,35 ± 0,02	ND	ND
Zn	0,19 ± 0,002	0,25 ± 0,002	0,52 ± 0,011	0,099 ± 0,011	1,78 ± 0,05	1,09 ± 0,035	1,09 ± 0,048	5,3 ± 0,14	11,6 ± 0,29
Rb	0,029 ± 0,0004	0,029 ± 0,0004	0,029 ± 0,0001	0,028 ± 0,001	0,030 ± 0,002	0,028 ± $8x10^{-4}$	0,024 ± 0,002	ND	ND

Table 3
Mineral and trace element concentrations in rat liver samples

	Element (mg/L)	Dilution rates								
		1:10	1:20	1:50	1:100	1:200	1:400	1:800	1:1000	1:2000
EMSURE® Grade	Na	5,3 ± 0,07	5,5 ± 0,1	7,1 ± 0,09	7,6 ± 0,01	16,8 ± 0,12	20,3 ± 0,21	30,7 ± 0,51	32,6 ± 1,24	61,8 ± 4,3
	Mg	1,24 ± 0,02	1,3 ± 0,01	1,4 ± 0,01	1,6 ± 0,01	2,1 ± 0,04	2,9 ± 0,08	4,1 ± 0,08	4,5 ± 0,2	7,9 ± 0,2
	K	21,5 ± 0,9	22,3 ± 0,25	23,4 ± 0,23	22,9 ± 0,13	25,9 ± 0,2	31,6 ± 0,3	38 ± 1,1	40 ± 0,67	59,8 ± 1,5
	Ca	0,13 ± 0,006	0,3 ± 0,007	0,64 ± 0,017	0,99 ± 0,04	3 ± 0,13	5,8 ± 0,17	6,9 ± 0,33	4,3 ± 0,45	8,3 ± 0,79
	Mn	0,012 ± 0,0001	0,008 ± 0,0003	ND	ND	ND	ND	ND	ND	ND
	Fe	0,6 ± 0,009	0,4 ± 0,007	0,12 ± 0,012	ND	ND	ND	ND	ND	ND
	Cu	0,73 ± 0,01	1,5 ± 0,02	3,9 ± 0,02	7,9 ± 0,08	16,3 ± 0,09	32,6 ± 0,28	65,5 ± 0,49	81,5 ± 0,6	161,7 ± 1,33
	Zn	0,49 ± 0,008	0,87 ± 0,01	2 ± 0,02	4 ± 0,06	8,3 ± 0,06	16,2 ± 0,21	32 ± 0,22	39,5 ± 0,48	79,1 ± 1,22
	Rb	0,05 ± 0,001	0,5 ± 0,0005	0,05 ± 0,001	0,05 ± 0,001	0,06 ± 0,001	0,07 ± 0,004	0,08 ± 0,009	0,09 ± 0,009	0,13 ± 0,85
	Sr	0,003 ± 0,0002	0,007 ± 0,0002	0,019 ± 0,0004	0,037 ± 0,001	0,07 ± 0,002	0,15 ± 0,002	0,29 ± 0,023	0,034 ±6x10^{-4}	0,68 ± 0,034
	Cs	0,0008 ± 5x10^{-5}	0,001 ± 9x10^{-5}	0,003 ± 0,0001	0,006 ± 0,0005	0,012± 7x10^{-3}	0,15 ± 0,002	0,05 ± 0,004	0,006 ± 0,002	0,12 ± 0,007
	Ba	0,0008 ± 0,00007	ND	ND	ND	ND	ND	ND	ND	ND
	Pb	0,039 ± 0,0004	0,08 ± 0,0008	0,2 ± 0,003	0,4 ± 0,005	0,8 ± 0,009	1,7 ± 0,02	3,4 ± 0,02	4,2 ± 0,03	8,3 ± 0,09
	U	0,00008±7X10^{-6}	ND	ND	ND	ND	ND	ND	ND	ND

(continued)

Table 3
(continued)

	Element (mg/L)	Dilution rates								
		1:10	1:20	1:50	1:100	1:200	1:400	1:800	1:1000	1:2000
SUPRAPUR® Grade	Na	6,5 ± 0,09	6,1 ± 0,09	4 ± 0,07	1,8 ± 0,08	ND	ND	ND	ND	ND
	Mg	1,5 ± 0,01	1,5 ± 0,02	1,5 ± 0,01	1,5 ± 0,04	1,3 ± 0,06	0,8 ± 0,09	0,8 ± 0,1	ND	ND
	K	26,2 ± 0,3	26,4 ± 0,2	24,8 ± 0,2	24,6 ± 0,2	11,9 ± 0,19	21,8 ± 0,48	15,6 ± 0,2	14,6 ± 1	3,5 ± 2,1
	Ca	0,2 ± 0,007	0,1 ± 0,015	ND	ND	ND	ND	ND	ND	ND
	Mn	0,01 ± 0,0001	0,01 ± 0,0005	0,01 ± 0,001	0,004 ± 0,0009	ND	ND	ND	ND	ND
	Fe	0,7 ± 0,004	0,8 ± 0,007	ND	ND	ND	ND	ND	ND	ND
	Cu	0,03 ± 0,0003	0,03 ± 0,0003	0,03 ± 0,0009	0,03 ± 0,001	0,02 ± 0,002	0,03 ± 0,002	0,02 ± 0,01	0,04 ± 0,02	ND
	Rb	0,06 ± 0,0006	0,06 ± 0,001	0,06 ± 0,001	0,06 ± 0,001	0,06 ± 0,001	0,06 ± 0,005	0,06 ± 0,008	0,07 ± 0,008	0,09 ± 0,01
	Sr	0,01 ± 0,00009	0,002 ± 0,0002	0,004 ± 0,0003	0,008 ± 0,0009	0,01 ± 0,002	0,02 ± 0,004	0,05 ± 0,005	0,06 ± 0,009	0,12 ± 0,02
	Al	0,8 ± 0,01	0,7 ± 0,009	0,49 ± 0,01	0,18 ± 0,01	ND	ND	ND	ND	ND
	Cr	0,07 ± 0,0001	0,06 ± 0,0002	ND	ND	ND	ND	ND	ND	ND

Table 4
Mineral and trace element concentrations in rat brain samples

		Dilution rates								
	Element (mg/L)	1:10	1:20	1:50	1:100	1:200	1:400	1:800	1:1000	1:2000
EMSURE® Grade	Li	0,03 ± 0,002	0,1 ± 0,04	0,16 ± 0,04	0,18 ± 0,02	0,25 ± 0,08	0,62 ± 0,14	1,2 ± 0,3	1,2 ± 0,4	2,8 ± 1
	Na	24,6 ± 0,32	26,1 ± 0,36	29,6 ± 0,17	30,6 ± 0,36	33,4 ± 2,17	42,3 ± 0,3	53,7 ± 0,74	325 ± 5,25	108 ± 2,9
	K	73,4 ± 0,98	75,3 ± 0,55	77,9 ± 0,36	79,8 ± 0,72	82,7 ± 1,1	84,9 ± 0,62	90,9 ± 0,62	99,5 ± 0,38	112 ± 1,7
	Ca	0,48 ± 0,012	0,79 ± 0,044	1,5 ± 0,03	1,8 ± 0,07	3,2 ± 0,15	5,15 ± 0,21	6,9 ± 0,58	19 ± 0,2	16 ± 0,93
	Mn	0,09 ± 0,0003	0,12 ± 0,031	ND	ND	ND	ND	ND	ND	ND
	Fe	0,57 ± 0,008	0,55 ± 0,021	0,26 ± 0,022	ND	ND	ND	ND	ND	ND
	Cu	0,7 ± 0,007	1,6 ± 0,03	4 ± 0,03	8 ± 0,1	16 ± 0,13	32,4 ± 0,28	64,7 ± 0,4	81,2 ± 0,73	161,7 ± 1,61
	Zn	0,53 ± 0,007	1 ± 0,027	2,2 ± 0,03	4,1 ± 0,06	8,1 ± 0,07	16,5 ± 0,26	32 ± 0,22	45,1 ± 0,59	39,5 ± 0,28
	As	0,02 ± 0,0004	0,5 ± 0,0005	ND	ND	ND	ND	ND	ND	ND
	Rb	0,06 ± 0,0006	0,18 ± 0,03	0,12 ± 0,04	0,08 ± 0,003	0,09 ± 0,004	0,12 ± 0,01	0,3 ± 0,17	0,2 ± 0,014	0,27 ± 0,01
	Sr	0,004 ± 0,0001	0,12 ± 0,029	0,07 ± 0,04	0,04 ± 0,0001	0,07 ± 0,0007	0,15 ± 0,004	0,41 ± 0,15	0,45 ± 0,011	0,69 ± 0,011
	Cs	0,004 ± 0,0003	0,11 ± 0,03	0,064 ± 0,04	0,014 ± 0,0003	0,023 ± 0,001	0,045 ± 0,002	0,21 ± 0,16	0,09 ± 0,002	0,17 ± 0,015
	Ba	0,0016 ± 0,0001	ND	ND	ND	ND	ND	ND	ND	ND
	Ti	ND	ND	ND	0,009 ± 0,0009	0,011 ± 0,001	0,014 ± 0,002	ND	ND	ND

(continued)

Table 4
(continued)

	Element (mg/L)	Dilution rates								
		1:10	1:20	1:50	1:100	1:200	1:400	1:800	1:1000	1:2000
SUPRAPUR® Grade	Pb	0,04 ± 0,0003	0,21 ± 0,03	0,29 ± 0,04	0,46 ± 0,002	0,93 ± 0,004	1,8 ± 0,01	3,17 ± 0,17	4,5 ± 0,05	8,9 ± 0,06
	U	0,007 ± 0,0008	6,1 ± 0,09	4 ± 0,07	1,8 ± 0,08	ND	ND	ND	ND	ND
	Li	0,03 ± 0,005	0,03 ± 0,007	0,06 ± 0,01	0,08 ± 0,06	ND	ND	ND	ND	ND
	Na	9,9 ± 0,13	9,9 ± 0,09	8,6 ± 0,06	9,8 ± 0,08	6,7 ± 0,12	28,9 ± 0,49	15,3 ± 0,52	ND	ND
	Mg	1,21 ± 0,02	1,22 ± 0,004	1,24 ± 0,02	1,2 ± 0,04	1,2 ± 0,04	1,5 ± 0,04	1,1 ± 0,13	0,67 ± 0,12	0,37 ± 0,13
	K	33,1 ± 0,37	33,6 ± 0,46	34,5 ± 0,23	32,5 ± 0,19	32,4 ± 0,21	31,4 ± 0,33	29,1 ± 0,52	26,8 ± 0,65	9,44 ± 0,56
	Ca	0,61 ± 0,019	0,68 ± 0,03	1,14 ± 0,04	0,97 ± 0,036	1,4 ± 0,11	7,3 ± 0,29	6,98 ± 0,59	3,7 ± 0,51	6,29 ± 0,63
	Mn	0,02 ± 0,00009	ND	ND	ND	ND	ND	ND	ND	ND
	Cu	0,02 ± 0,00008	0,02 ± 0,0005	0,03 ± 0,002	0,03 ± 0,003	0,05 ± 0,004	0,11 ± 0,01	0,22 ± 0,01	0,09 ± 0,02	0,12 ± 0,02
	Zn	0,14 ± 0,001	0,37 ± 0,005	0,97 ± 0,014	1,44 ± 0,016	3,19 ± 0,02	3,28 ± 0,073	3,24 ± 0,035	4,5 ± 0,14	5,4 ± 0,24
	Rb	0,02 ± 0,0006	0,02 ± 0,0009	0,03 ± 0,0007	0,03 ± 0,0003	0,05 ± 0,003	0,08 ± 0,0005	0,11 ± 0,007	0,12 ± 0,013	0,19 ± 0,013
	Sr	0,001 ± 0,00008	0,002 ± 0,0001	0,006 ± 0,0003	0,009 ± 0,0006	0,01 ± 0,001	0,07 ± 0,007	0,1 ± 0,009	0,08 ± 0,01	0,16 ± 0,036
	Ag	0,022 ± 0,0007	ND	ND	ND	ND	ND	ND	ND	ND
	Cs	0,002 ± 0,00007	0,002 ± 0,0001	0,005 ± 0,0003	0,008 ± 0,0002	0,01 ± 0,0006	0,02 ± 0,001	0,04 ± 0,005	0,05 ± 0,006	0,09 ± 0,01
	Ti	0,005 ± 0,001	0,001 ± 0,00007	0,002 ± 0,0001	0,003 ± 0,0001	0,004 ± 0,0003	0,006±3x10^{-4}	0,009 ± 0,001	0,01 ± 0,001	0,01 ± 0,001
	U	0,002 ± 0,0001	0,0002 ± 2x10^{-5}	ND	ND	ND	ND	ND	ND	ND

Table 5
Mineral and trace element concentrations in rat testis samples

		Dilution rates								
	Element (mg/L)	1:10	2:10	1:50	1:100	1:200	1:400	1:800	1:1000	1:2000
EMSURE® Grade	Na	26,84 ± 0,3	26,4 ± 0,3	28,25 ± 0,2	29,6 ± 0,2	30 ± 0,1	36,4 ± 0,5	45,6 ± 0,53	61,7 ± 1	99 ± 1,45
	Mg	2,2 ± 0,03	2,2 ± 0,01	2,4 ± 0,03	2,5 ± 0,04	2,9 ± 0,02	3,6 ± 0,08	4,69 ± 0,1	6,18 ± 0,24	8,6 ± 0,22
	K	52,4 ± 0,6	51 ± 0,6	52,8 ± 0,7	53,8 ± 0,3	52,2 ± 0,3	56,8 ± 0,8	63,1 ± 0,6	68,7 ± 0,5	89,3 ± 0,5
	Ca	0,2 ± 0,007	0,5 ± 0,018	1,3 ± 0,03	1,5 ± 0,05	2,5 ± 0,13	3 ± 0,13	3,5 ± 0,2	9,9 ± 0,5	9,1 ± 0,5
	Mn	0,003 ± 0,0002	ND	ND	ND	ND	ND	ND	ND	ND
	Fe	0,6 ± 0,012	0,4 ± 0,009	0,2 ± 0,013	ND	ND	ND	ND	ND	ND
	Cu	0,7 ± 0,008	1,5 ± 0,01	4 ± 0,05	8 ± 0,04	16 ± 0,1	32,6 ± 0,3	65,4 ± 0,5	82,3 ± 0,57	162,9 ± 1,16
	Zn	0,7 ± 0,01	1,1 ± 0,01	2,3 ± 0,01	4,2 ± 0,06	8,2 ± 0,07	16,1 ± 0,2	32 ± 0,1	41,9 ± 0,6	79,6 ± 0,7
	As	0,004 ± 0,0004	0,003 ± 0,0005	ND	ND	ND	ND	ND	ND	ND
	Se	0,017 ± 0,0009	0,019 ± 0,0018	ND	ND	ND	ND	ND	ND	ND
	Rb	0,08 ± 0,001	0,08 ± 0,001	0,08 ± 0,003	0,08 ± 0,001	0,09 ± 0,003	0,11 ± 0,005	0,13 ± 0,003	0,15 ± 0,01	0,21 ± 0,017
	Sr	0,004 ± 0,0001	0,008 ± 0,0002	0,022 ± 0,0007	0,03 ± 0,0008	0,074 ± 0,004	0,145 ± 0,005	0,276 ± 0,008	0,36 ± 0,02	0,67 ± 0,017
	Cs	0,001 ± 0,00005	0,002 ± 0,0002	0,004 ± 0,0002	0,008 ± 0,0004	0,016 ± 0,0002	0,029 ± 0,001	0,058 ± 0,005	0,07 ± 0,003	0,14 ± 0,01
	Pb	0,04 ± 0,0003	0,08 ± 0,0007	0,22 ± 0,002	0,45 ± 0,005	0,9 ± 0,011	1,79 ± 0,01	3,5 ± 0,004	4,4 ± 0,03	8,7 ± 0,004

(continued)

Table 5
(continued)

	Element (mg/L)	Dilution rates								
		1:10	2:10	1:50	1:100	1:200	1:400	1:800	1:1000	1:2000
SUPRAPUR® Grade	Na	10,1 ± 0,12	10,2 ± 0,03	8,4 ± 0,06	6,3 ± 0,05	3 ± 0,12	ND	ND	ND	ND
	Mg	0,8 ± 0,01	0,8 ± 0,008	0,8 ± 0,015	0,7 ± 0,03	0,7 ± 0,03	0,4 ± 0,05	ND	ND	ND
	K	20 ± 0,3	20 ± 0,2	19,8 ± 0,14	19,6 ± 0,12	19 ± 0,2	17 ± 0,14	14 ± 0,39	12 ± 0,9	3,8 ± 1,2
	Ca	0,12 ± 0,008	0,28 ± 0,008	0,35 ± 0,04	0,39 ± 0,03	0,15 ± 0,07	ND	ND	ND	ND
	Cu	0,01 ± 0,0002	0,013 ± 0,0003	0,013 ± 0,001	0,01 ± 0,001	0,009 ± 0,003	ND	ND	ND	ND
	Zn	0,15 ± 0,0009	0,26 ± 0,005	0,29 ± 0,007	0,33 ± 0,007	0,27 ± 0,012	0,12 ± 0,02	0,31 ± 0,05	2,4 ± 0,09	14,5 ± 0,2
	As	0,001 ± 0,0001	0,001 ± 0,0002	ND	ND	ND	ND	ND	ND	ND
	Rb	0,031 ± 0,001	0,32 ± 0,03	0,034 ± 0,001	0,037 ± 0,0006	0,044 ± 0,002	0,05 ± 0,006	0,07 ± 0,007	0,07 ± 0,007	0,12 ± 0,009

Table 6
Mineral and trace element concentrations in rat spleen samples

		Dilution rates								
	Element (mg/L)	1:10	1:20	1:50	1:100	1:200	1:400	1:800	1:1000	1:2000
EMSURE® Grade	Na	7,7 ± 0,09	8,3 ± 0,12	10,7 ± 0,14	18,9 ± 0,17	15,2 ± 0,13	36,4 ± 0,31	36,1 ± 0,22	36,1 ± 0,73	61,7 ± 0,76
	Mg	1,3 ± 0,5	1,4 ± 0,01	1,6 ± 0,028	2,3 ± 0,048	2,4 ± 0,02	3,15 ± 0,08	4,3 ± 0,12	4,9 ± 0,17	8,19 ± 0,24
	K	31,5 ± 0,36	32,4 ± 0,35	34,5 ± 0,44	33,9 ± 0,28	35,8 ± 0,28	40,4 ± 0,31	47,7 ± 0,24	51,8 ± 0,35	71,3 ± 0,24
	Ca	0,13 ± 0,005	0,25 ± 0,015	0,85 ± 0,029	2,6 ± 0,06	5 ± 0,12	5,48 ± 0,13	5,6 ± 0,36	9,7 ± 0,26	11,8 ± 0,65
	Fe	9,1 ± 0,09	9,2 ± 0,12	9 ± 0,08	8,8 ± 0,06	7,8 ± 0,08	5,1 ± 0,12	1,6 ± 0,15	ND	ND
	Cu	0,72 ± 0,01	1,5 ± 0,02	3,9 ± 0,03	7,8 ± 0,08	15,9 ± 0,12	32,3 ± 0,28	64,5 ± 0,73	82 ± 0,86	163,9 ± 1,3
	Zn	0,54 ± 0,007	0,95 ± 0,013	2,4 ± 0,025	5,4 ± 0,046	8,9 ± 0,096	17 ± 0,17	32,5 ± 0,29	41,7 ± 0,49	80,6 ± 0,87
	As	0,004 ± 0,0002	ND	ND	ND	ND	ND	ND	ND	ND
	Rb	0,042 ± 0,0007	0,043 ± 0,0005	0,046 ± 0,0008	0,04 ± 0,001	0,05 ± 0,002	0,06 ± 0,004	0,06 ± 0,01	0,07 ± 0,01	0,09 ± 0,02
	Sr	0,003 ± 0,0001	0,007 ± 0,0002	0,02 ± 0,0007	0,04 ± 0,001	0,08 ± 0,001	0,15 ± 0,008	0,29 ± 0,01	0,37 ± 0,01	0,7 ± 0,02
	Cs	0,0007± 0,0002	0,001 ± 0,00006	0,002 ± 0,0002	0,004 ± 0,0004	0,008 ± 0,0009	0,01 ± 0,0008	0,03 ± 0,005	0,04 ± 0,003	0,07 ± 0,006
	Ba	0,0009 ± 0,00006	ND	ND	ND	ND	ND	ND	ND	ND
	Pb	0,03 ± 0,0002	0,08 ± 0,0005	0,2 ± 0,001	0,41 ± 0,005	0,8 ± 0,009	1,67 ± 0,015	3,3 ± 0,042	4,2 ± 0,05	8,4 ± 0,08

(continued)

Table 6
(continued)

		Dilution rates								
	Element (mg/L)	1:10	1:20	1:50	1:100	1:200	1:400	1:800	1:1000	1:2000
SUPRAPUR® Grade	Na	6,8 ± 0,12	6,7 ± 0,1	4,8 ± 0,13	2,4 ± 0,06	ND	ND	ND	ND	ND
	Mg	1,3 ± 0,01	1,3 ± 0,01	1,3 ± 0,02	1,2 ± 0,03	1,2 ± 0,04	1 ± 0,06	0,8 ± 0,1	0,8 ± 0,1	ND
	K	30,7 ± 0,38	31,5 ± 0,36	32,1 ± 0,4	29,6 ± 0,39	29,3 ± 0,21	26,3 ± 0,3	23,6 ± 0,43	20,6 ± 0,97	10,2 ± 1,5
	Ca	0,15 ± 0,01	0,34 ± 0,009	0,26 ± 0,007	0,22 ± 0,03	ND	ND	ND	ND	ND
	Fe	11,5 ± 0,15	11,4 ± 0,08	10,5 ± 0,23	9 ± 0,04	6,9 ± 0,006	ND	ND	ND	ND
	Cu	0,02 ± 0,0003	0,02 ± 0,0005	0,02 ± 0,0006	0,02 ± 0,002	0,03 ± 0,003	0,02 ± 0,008	0,18 ± 0,01	0,02 ± 0,01	0,014 ± 0,02
	Zn	0,13 ± 0,001	0,19 ± 0,003	0,45 ± 0,005	0,45 ± 0,01	0,8 ± 0,03	0,6 ± 0,02	0,6 ± 0,06	0,8 ± 0,06	ND
	As	0,005 ± 0,0003	0,005 ± 0,0003	0,004 ± 0,001	0,004 ± 0,001	ND	ND	ND	ND	ND
	Rb	0,04 ± 0,0005	0,04 ± 0,0008	0,04 ± 0,0008	0,04 ± 0,001	0,04 ± 0,001	0,04 ± 0,003	0,03 ± 0,001	0,04 ± 0,01	0,04 ± 0,01
	Al	0,1 ± 0,006	0,04 ± 0,007	ND	ND	ND	ND	ND	ND	ND

Table 7
Mineral and trace element concentrations in rat lung samples

		Dilution rates								
	Element (mg/L)	1:10	1:20	1:50	1:100	1:200	1:400	1:800	1:1000	1:2000
EMSURE® Grade	Na	18,1 ± 0,26	17,7 ± 0,16	19,1 ± 0,19	21,1 ± 0,23	22,7 ± 0,19	30,1± 0,39	38,6 ± 0,25	44,5 ± 0,34	70,9 ± 0,7
	Mg	1,1 ± 0,02	1,1 ± 0,01	1,3 ± 0,01	1,4 ± 0,02	1,9 ± 0,07	2,7 ± 0,07	3,9 ± 0,09	4,6 ± 0,17	7,5 ± 0,14
	K	25,1 ± 0,34	24,5 ± 0,25	25,8 ± 0,16	25,2 ± 0,05	27,9 ± 0,13	31,8 ± 0,15	39,3 ± 0,16	44,4 ± 0,56	62,7 ± 0,89
	Ca	0,22 ± 0,004	0,33 ± 0,006	1,14 ± 0,02	1,5 ± 0,04	3,2 ± 0,11	4,8 ± 0,09	5,9 ± 0,5	6,89 ± 0,4	9,3 ± 1,4
	Fe	1,1 ± 0,01	1 ± 0,01	0,6 ± 0,02	0,18 ± 0,01	ND	ND	ND	ND	ND
	Cu	0,7 ± 0,009	1,5 ± 0,01	3,9 ± 0,03	8 ± 0,05	16,1 ± 0,11	32,8 ± 0,22	65,6 ± 0,37	81,3 ± 0,84	162,1 ± 1,8
	Zn	0,52 ± 0,004	0,09 ± 0,01	2,1 ± 0,01	4 ± 0,04	8,1 ± 0,05	16,2 ± 0,12	32,1 ± 0,4	40,2 ± 0,34	79,1 ± 0,98
	As	0,003 ± 0,0003	ND	ND	ND	ND	ND	ND	ND	ND
	Rb	0,003 ± 0,0008	0,03 ± 0,0004	0,03 ± 0,001	0,04 ± 0,001	0,04 ± 0,001	0,05 ± 0,005	0,08 ± 0,005	0,09 ± 0,01	0,13 ± 0,01
	Sr	0,03 ± 0,0008	0,03 ± 0,0004	0,03 ± 0,001	0,04 ± 0,001	0,04 ± 0,001	0,05 ± 0,005	0,08 ± 0,005	0,09 ± 0,01	0,13 ± 0,01
	Cs	0,0009± $4x10^{-5}$	0,001 ± 0,0001	0,003 ± 0,0001	0,007 ± 0,0002	0,01 ± 0,001	0,02 ± 0,0007	0,05 ± 0,005	0,06 ± 0,01	0,12 ± 0,007
	Ba	0,001 ± 0,0001	ND	ND	ND	ND	ND	ND	ND	ND
	Pb	0,04 ± 0,0005	0,08 ± 0,0008	0,21 ± 0,0007	0,43 ± 0,004	0,88 ± 0,007	1,7 ± 0,012	3,5 ± 0,04	4,3 ± 0,06	8,5 ± 0,1

(continued)

Table 7
(continued)

	Element (mg/L)	Dilution rates								
		1:10	1:20	1:50	1:100	1:200	1:400	1:800	1:1000	1:2000
SUPRAPUR® Grade	Na	9,8 ± 0,09	9,5 ± 0,07	7,7 ± 0,11	5,4 ± 0,08	1 ± 0,05	ND	ND	ND	ND
	Mg	0,58 ± 0,004	0,57 ± 0,008	0,5 ± 0,007	0,5 ± 0,01	0,39 ± 0,04	0,18 ± 0,025	ND	ND	ND
	K	14,9 ± 0,22	15,2 ± 0,11	14,3 ± 0,07	13,9 ± 0,2	13 ± 0,15	11,4 ± 0,23	7,3 ± 0,5	4,7 ± 0,5	ND
	Ca	0,14 ± 0,008	0,15 ± 0,019	0,56 ± 0,03	0,4 ± 0,08	0,19 ± 0,07	0,3 ± 0,1	0,3 ± 0,13	ND	ND
	Fe	0,59 ± 0,007	0,22 ± 0,01	ND	ND	ND	ND	ND	ND	ND
	Cu	0,014 ± 0,0003	0,01 ± 0,0005	0,018 ± 0,0007	0,039 ± 0,002	0,03 ± 0,002	0,03 ± 0,008	ND	ND	ND
	Zn	0,11 ± 0,002	0,23 ± 0,004	0,66 ± 0,009	1,3 ± 0,02	2,99 ± 0,04	2,6 ± 0,05	2,5 ± 0,15	12,6 ± 0,2	ND
	As	0,004 ± 0,0003	0,004 ± 0,0005	0,01 ± 0,001	0,007 ± 0,002	0,005 ± 0,001	ND	ND	ND	ND
	Rb	0,02 ± 0,0004	0,02 ± 0,0001	0,02 ± 0,001	0,02 ± 0,0007	0,02 ± 0,002	0,03 ± 0,003	0,04 ± 0,002	0,04 ± 0,005	0,06 ± 0,01
	Sr	0,001 ± 0,00009	0,001 ± 0,0001	ND	ND	ND	ND	ND	ND	ND

Table 8
Mineral and trace element concentrations in rat heart samples

	Element (mg/L)	Dilution rates								
		1:10	1:20	1:50	1:100	1:200	1:400	1:800	1:1000	1:2000
EMSURE® Grade	Na	11,5 ± 0,17	12,5 ± 0,15	13,7 ± 0,13	15,5 ± 0,82	18,2 ± 0,17	22,4 ± 0,18	33,6 ± 0,77	43,5 ± 0,61	65,5 ± 0,84
	Mg	2,29 ± 0,03	2,4 ± 0,02	2,5 ± 0,03	2,7 ± 0,04	3 ± 0,06	3,7 ± 0,11	4,9 ± 0,15	6 ± 0,16	9 ± 0,17
	K	32,2 ± 0,56	33,8 ± 0,39	35,2 ± 0,22	34,2 ± 0,31	36,5 ± 0,37	40,6 ± 0,27	49 ± 0,42	54,4 ± 0,42	74,1 ± 0,48
	Ca	0,13 ± 0,007	0,17 ± 0,009	0,31 ± 0,026	0,66 ± 0,029	1,32 ± 0,11	2,9 ± 0,17	3,1 ± 0,18	6,4 ± 0,08	6,4 ± 0,4
	Mn	0,002 ± 0,0002	ND	ND	ND	ND	ND	ND	ND	ND
	Fe	0,8 ± 0,01	0,8 ± 0,01	0,45 ± 0,01	ND	ND	ND	ND	ND	ND
	Cu	0,77 ± 0,012	1,5 ± 0,01	4 ± 0,04	8 ± 0,1	16,3 ± 0,12	32,6 ± 0,3	65,6 ± 0,7	82,2 ± 0,77	162,5 ± 1
	Zn	0,5 ± 0,006	0,89 ± 0,008	2 ± 0,022	4 ± 0,05	8,2 ± 0,06	16 ± 0,08	32 ± 0,44	41 ± 0,24	79,7 ± 0,44
	Rb	0,04 ± 0,0003	0,04 ± 0,0007	0,04 ± 0,001	0,04 ± 0,002	0,04 ± 0,002	0,05 ± 0,005	0,06 ± 0,003	0,06 ± 0,005	0,09 ± 0,02
	Sr	0,003 ± 0,0001	0,007 ± 0,0002	0,01 ± 0,0002	0,03 ± 0,001	0,07 ± 0,001	0,14 ± 0,005	0,28 ± 0,01	0,36 ± 0,008	0,71 ± 0,03
	Cd	0,00005± $3x10^{-6}$	ND	ND	ND	ND	ND	ND	ND	ND
	Cs	0,0005 ± $5x10^{-5}$	0,0008 ± $8x10^{-5}$	0,001 ± 0,0001	0,003 ± 0,0003	0,009 ± 0,0002	0,01 ± 0,0009	0,04 ± 0,006	0,05 ± 0,02	0,1 ± 0,006
	Ba	0,001 ± 0,00007	ND	ND	ND	ND	ND	ND	ND	ND
	Pb	0,03 ± 0,0003	0,08 ± 0,0008	0,2 ± 0,001	0,41 ± 0,006	0,84 ± 0,008	1,6 ± 0,01	3,3 ± 0,03	4,1 ± 0,002	8,1 ± 0,14

(continued)

Table 8
(continued)

	Element (mg/L)	Dilution rates								
		1:10	1:20	1:50	1:100	1:200	1:400	1:800	1:1000	1:2000
SUPRAPUR® Grade	Na	7,8 ± 0,06	7,5 ± 0,06	5,3 ± 0,07	2,8 ± 0,08	ND	ND	ND	ND	ND
	Mg	1,1 ± 0,01	1,1 ± 0,02	1 ± 0,01	1 ± 0,02	0,9 ± 0,03	0,77 ± 0,09	0,43 ± 0,17	0,17 ± 0,12	ND
	Ca	0,1 ± 0,007	0,1± 0,01	0,08 ± 0,01	ND	ND	ND	ND	ND	ND
	K	15,7 ± 0,18	16,1 ± 0,34	15 ± 0,17	14,5 ± 0,18	13,5 ± 0,23	11,4 ± 0,31	8 ± 0,31	4,9 ± 1	ND
	Fe	0,06 ± 0,002	ND	ND	ND	ND		ND	ND	ND
	Cu	0,03 ± 0,0005	0,03 ± 0,0005	0,03 ± 0,001	0,02 ± 0,001	0,02 ± 0,003	ND	ND	ND	ND
	Zn	0,12 ± 0,001	0,23 ± 0,002	0,25 ± 0,004	0,22 ± 0,009	0,38 ± 0,009	0,001 ± 0,042	1 ± 0,09	13,6 ± 0,14	11 ± 0,35
	Rb	0,02 ± 0,0002	0,02 ± 0,0005	0,019 ± 0,001	0,019 ± 0,0007	0,019 ± 0,002	ND	ND	ND	ND
	Sr	0,001 ± 0,00008	0,002 ± 0,0001	0,004 ± 0,005	0,007 ± 0,001	0,01 ± 0,002	0,02 ± 0,003	0,06 ± 0,006	0,06 ± 0,007	0,12 ± 0,018

critical point is the dilution rates of the microwave digested samples since we have used 65 % HNO_3, which is too concentrated for the tubing system of the ICP-MS device. Also, tissue and serum samples should be diluted before ICP-MS since the device has limitations in evaluating minerals and trace elements. We have found that 1:10 to 1:20 dilutions are the best rates for accurate measurement via ICP-MS following microwave digestion (Tables 1, 2, 3, 4, 5, 6, 7 and 8).

4 Notes

This book chapter explains the most accurate method for analyzing trace elements and minerals in the mammalian tissue, serum, and cell lysates. Overall, 1/10 and 1/20 dilution rates are the most accurate for both methods with the lowest RSD values. Various elements such as Ca, Cu, Zn, Sr, Pb, and Cs were not measured accurately in the EMSURE-digested samples, unlike suprapur-digested samples (Tables 1, 2, 3, 4, 5, 6, 7 and 8). According to the graphs, SUPRAPUR®-digested samples are evaluated more accurately than EMSURE®-digested serum samples (Tables 1, 2, 3, 4, 5, 6, 7 and 8). Moreover, we detected more trace elements and minerals with the EMSURE grade nitric acid than SUPRAPUR® that can result from impurity of the EMSURE-grade nitric acid.

References

1. National Research Council (US) Committee on Diet and Health. Diet and Health: Implications for Reducing Chronic Disease Risk. Washington (DC): National Academies Press (US); 1989. 14, Trace Elements. Available from: https://www.ncbi.nlm.nih.gov/books/NBK218751/
2. Guthrie GD Jr (1997) Mineral properties and their contributions to particle toxicity. Environ Health Perspect 105(Suppl 5):1003–1011
3. Tandogan B, Ulusu NN (2005) Importance of calcium. Turk J Med Sci 35(4):197–201
4. Skoryna SC, Inoue S, Fuskova M (1980) Classification of biological effects of trace elements. In: Santos W, Lopes N, Barbosa JJ, Chaves D, Valente JC (eds) Nutritional biochemistry and pathology. Nutrition and food science (present knowledge and utilization), vol 3. Springer, Boston
5. National Research Council (US) Safe Drinking Water Committee. Drinking Water and Health Volume 3. Washington (DC): National Academies Press (US); 1980. V, The Contribution of Drinking Water to Mineral Nutrition in Humans. Available from: https://www.ncbi.nlm.nih.gov/books/NBK216589/
6. Fairweather-Tait SJ, Cashman K (2015) Minerals and trace elements. World Rev Nutr Diet. 111:45–52. https://doi.org/10.1159/000362296. Epub 2014 Nov 17
7. Ying H, Zhang Y (2019) Systems biology of selenium and complex disease. Biol Trace Elem Res 192(1):38–50
8. Ulusu NN (2009) Possible effect of calcium in the formation of stress granules. Turkish J. Biochem. 34(1):51–52
9. Ulusu NN, Tandoğan B, Tanyel FC (2007) Sarco(endo)plasmic reticulum and plasmalemmal Ca(2+)-ATPase activities in cremaster muscles and sacs differ according to the associated inguinal pathology. Cell Biochem Funct 25(5):515–519
10. Tanyel FC, Ulusu NN, Tezcan EF, Büyükpamukçu N (2003) Total calcium content of sacs associated with inguinal hernia, hydrocele or undescended testis reflects differences dictated by programmed cell death. Urol Int 70(3):211–215

11. Tanyel FC, Ulusu NN, Tezcan EF, Büyükpamukçu N (2002) Less calcium in cremaster muscles of boys with undescended testis supports a deficiency in sympathetic innervation. Urol Int 69(2):111–115
12. Pekiner B, Ulusu NN, Das-Evcimen N, Sahilli M, Aktan F, Stefek M, Stolc S, Karasu C (2002) In vivo treatment with stobadine prevents lipid peroxidation, protein glycation and calcium overload but does not ameliorate Ca2+ -ATPase activity in heart and liver of streptozotocin-diabetic rats: comparison with vitamin E. Biochim Biophys Acta 1588(1): 71–78
13. Dogru Pekiner B, Daş Evcimen N, Ulusu NN, Bali M, Karasu C (2003) Effects of vitamin E on microsomal Ca(2+) -ATPase activity and calcium levels in streptozotocin-induced diabetic rat kidney. Cell Biochem Funct. 21(2): 177–182
14. Das Evcimen N, Ulusu NN, Karasu C, Doğru B (2004) Adenosine triphosphatase activity of streptozotocin-induced diabetic rat brain microsomes. Effect of vitamin E. Gen Physiol Biophys 23(3):347–355
15. Tandoğan B, Ulusu NN (2007) The inhibition kinetics of yeast glutathione reductase by some metal ions. J Enzyme Inhib Med Chem 22(4): 489–495
16. Aydemir D, Karabulut G, Şimşek G, Gok M, Barlas N, Ulusu NN (2018) Impact of the di (2-ethylhexyl) phthalate administration on trace element and mineral levels in relation of kidney and liver damage in rats. Biol Trace Elem Res 186(2):474–488
17. Blaustein MP (1985) Intracellular Calcium as a Second Messenger. In: Rubin RP, Weiss GB, Putney JW (eds) Calcium in biological systems. Springer, Boston
18. Alfarouk KO, Ahmed SBM, Ahmed A, Elliott RL, Ibrahim ME, Ali HS, Wales CC, Nourwali I, Aljarbou AN, Bashir AHH, Alhoufie STS, Alqahtani SS, Cardone RA, Fais S, Harguindey S, Reshkin SJ (2020) The interplay of dysregulated pH and electrolyte imbalance in cancer. Cancers 12:898
19. Gaffney-Stomberg E (2019) The impact of trace minerals on bone metabolism. Biol Trace Elem Res. 188(1):26–34
20. Institute of Medicine (US) Committee to Review Dietary Reference Intakes for Vitamin D and Calcium; Ross AC, Taylor CL, Yaktine AL, et al., editors. Dietary Reference Intakes for Calcium and Vitamin D. Washington (DC): National Academies Press (US); 2011. 2, Overview of Calcium. Available from: https://www.ncbi.nlm.nih.gov/books/NBK56060/
21. Locatelli J, de Assis LV, Isoldi MC (2014) Calcium handling proteins: structure, function, and modulation by exercise. Heart Fail Rev 19(2):207–225
22. Rall JA (2019) Calcium and muscle contraction: the triumph and tragedy of Lewis Victor Heilbrunn. Adv Physiol Educ. 43(4):476–485
23. Velásquez N, Pérez-Ybarra L, Urdaneta CJ, Pérez-Domínguez M (2019) Sialometry and concentration of phosphate and calcium in stimulated whole saliva and gingival crevicular fluid and its association with dental caries in schoolchildren. Asociación de sialometría, fosfato y calcio en saliva total bajo estímulo y en líquido crevicular gingival con caries dental en escolares. Biomedica 39(1):157–169
24. Coate KC, Hernandez G, Thorne CA, Sun S, Le TDV, Vale K, Kliewer SA, Mangelsdorf DJ (2017) FGF21 Is an exocrine pancreas secretagogue. Cell Metab. 25(2):472–480
25. Suttle NF. (2010) Mineral nutrition of livestock. Cabi Publishing; 4 th Edition page 4.
26. Zipkin I (1970) Interrelation of fluoride with other components of calcified tissue. Bibl Nutr Dieta. 15:62–78
27. Paterson PG, Allen OB, Bettger WJ (1987) Effect of dietary zinc deficiency on the endogenous phosphorylation and dephosphorylation of rat erythrocyte membrane. J Nutr 117(12): 2096–2105
28. Karppanen H (1991) Minerals and blood pressure. Ann Med 23(3):299–305
29. Ellison DH, Velázquez H, Wright FS (1987) Mechanisms of sodium, potassium and chloride transport by the renal distal tubule. Miner Electrolyte Metab 13(6):422–432
30. Ulusu NN, Tandogan B (2006) Purification and kinetics of sheep kidney cortex glucose-6-phosphate dehydrogenase. Comp Biochem Physiol B Biochem Mol Biol 143(2):249–255
31. Tandogan B, Kuruüzüm-Uz A, Sengezer C, Güvenalp Z, Demirezer LÖ, Ulusu NN (2011) In vitro effects of rosmarinic acid on glutathione reductase and glucose 6-phosphate dehydrogenase. Pharm Biol 49(6):587–594
32. Tandogan B, Ulusu NN (2006) Effects of cadmium and zinc ions on purified lamb kidney cortex glucose-6-phosphate dehydrogenase activity. J Enzyme Inhib Med Chem 21(2): 225–230
33. Evlice A, Ulusu NN (2017) Glucose-6-phosphate dehydrogenase a novel hope on a blood-based diagnosis of Alzheimer's disease. Acta Neurol Belg 117(1):229–234
34. Ulusu NN, Ozbey G, Tandogan B, Gunes A, Durakoglugil DB, Karasu C, Uluoglu C,

Zengil H (2005) Circadian variations in the activities of 6-phosphogluconate dehydrogenase and glucose-6-phosphate dehydrogenase in the liver of control and streptozotocin-induced diabetic rats. Chronobiol Int. 22(4): 667–677

35. Aydemir D, Öztaşcı B, Barlas N, Ulusu NN (2019) Effects of butylparaben on antioxidant enzyme activities and histopathological changes in rat tissues. Arh Hig Rada Toksikol 70(4):315–324
36. Akbay E, Ulusu NN, Töröner F, Ayvaz G, Taneri F, Aktürk M, Arslan M, Karasu C (2004) Effects of rosiglitazone treatment on the pentose phosphate pathway and glutathione-dependent enzymes in liver and kidney of rats fed a high-fat diet. Curr Ther Res Clin Exp 65(1):79–89
37. Can B, Ulusu NN, Kilinç K, Leyla Acan N, Saran Y, Turan B (2005) Selenium treatment protects diabetes-induced biochemical and ultrastructural alterations in liver tissue. Biol Trace Elem Res 105(1–3):135–150
38. Ulusu NN, Turan B (2005) Beneficial effects of selenium on some enzymes of diabetic rat heart. Biol Trace Elem Res. 103(3):207–216
39. Ulusu N, Acan N, Turan B, Tezcan E (2003) Inhibition of glutathione reductase by cadmium ion in some rabbit tissues and the protective role of dietary selenium. Biol Trace Elem Res. 91(2):151–156
40. Ulusu NN, Tandoğan B (2007) Purification and kinetic properties of glutathione reductase from bovine liver. Mol Cell Biochem. 303(1–2):45–51
41. Tandogan B, Ulusu NN (2010) Comparative in vitro effects of some metal ions on bovine kidney cortex glutathione reductase. Prep Biochem Biotechnol. 40(4):405–411
42. Tandogan B, Ulusu NN (2010) A comparative study with colchicine on glutathione reductase. Protein J. 29(5):380–385
43. Rhodes D, Klug A (1993) Zinc fingers. Sci Am 268(2):56–59. 62–5
44. Tavsan Z, Ayar Kayali H (2013) The effect of iron and copper as an essential nutrient on mitochondrial electron transport system and lipid peroxidation in Trichoderma harzianum. Appl Biochem Biotechnol. 170(7):1665–1675
45. Berridge MJ, Bootman MD, Roderick HL (2003) Calcium signalling: dynamics, homeostasis and remodelling. Nat Rev Mol Cell Biol. 4(7):517–529
46. Tchounwou PB, Yedjou CG, Patlolla AK, Sutton DJ (2012) Heavy metal toxicity and the environment. Exp Suppl 101:133–164
47. Valko M, Morris H, Cronin MT (2005) Metals, toxicity and oxidative stress. Curr Med Chem 12(10):1161–1208
48. Tandogan B, Ulusu NN (2010) Inhibition of purified bovine liver glutathione reductase with some metal ions. J Enzyme Inhib Med Chem 25(1):68–73
49. Armstrong RA (2019) Risk factors for Alzheimer's disease. Folia Neuropathol 57(2): 87–105
50. Ulusu NN (2015) Glucose-6-phosphate dehydrogenase deficiency and Alzheimer's disease: partners in crime? The hypothesis. Med Hypotheses. 85(2):219–223
51. Ulusu NN, Yilmaz G, Erbayraktar Z, Evlice AT, Aras S, Yener G, Avci A (2015) A Turkish 3-center study evaluation of serum folic acid and vitamin B12 levels in Alzheimer disease. Turk J Med Sci. 45(5):1159–1166
52. Ulusu NN (2015) Curious cases of the enzymes. J Med Biochem. 34(3):271–281
53. Barr AJ (2018) The biochemical basis of disease. Essays Biochem. 62(5):619–642
54. Inductively Coupled Plasma Spectrometer (ICP AES / ICP OES) https://www.labcompare.com/Spectroscopy/26-Inductively-Coupled-Plasma-Spectrometer-ICP-AES-ICP-OES/
55. Inductively Coupled Plasma Spectrometer (ICP AES / ICP OES) https://www.labcompare.com/10-Featured-Articles/165450-Lab-Tech-Face-Off-ICP-AES-vs-ICP-OES-vs-ICP-MS/
56. https://www.thermofisher.com/tr/en/home/industrial/environmental/environmental-learning-center/contaminant-analysis-information/metal-analysis/comparison-icp-oes-icp-ms-trace-element-analysis.html
57. E. McCurdy, G. Woods, D. Potter, "Unmatched removal of spectral interferences in ICP-MS using the Agilent octopole reaction system with Helium collision mode", Application, Metals Analysis retrieved from https://www.agilent.com/cs/library/applications/5989-4905EN.pdf
58. Lu Y, Kippler M, Harari F, Grandér M, Palm B, Nordqvist H, Vahter M (2015) Alkali dilution of blood samples for high throughput ICP-MS analysis-comparison with acid digestion. Clin Biochem 48(3):140–147
59. Levi M, Hjelm C, Harari F, Vahter M (2018) ICP-MS measurement of toxic and essential elements in human breast milk. A comparison of alkali dilution and acid digestion sample preparation methods. Clin Biochem. 53:81–87
60. Aydemir D, Simsek G, Ulusu NN (2020) Dataset of the analyzing trace elements and

minerals via ICP-MS: method validation for the mammalian tissue and serum samples. Data Brief 29:105218. https://doi.org/10.1016/j.dib.2020.105218

61. Aydemir D, Hashemkhani M, Acar HY, Ulusu NN (2020) Evaluation of the biocompatibility of the GSH-coated Ag2S quantum dots in vitro: a perfect example for the non-toxic optical probes. Mol Biol Rep 47(6): 4117–4129
62. Aydemir D, Sarayloo E, Ulusu NN (2020) Rosiglitazone-induced changes in the oxidative stress metabolism and fatty acid composition in relation with trace element status in the primary adipocytes. J Med Biochem 39:267–275
63. Aydemir D, Karabulut G, Gok M, Barlas N, Ulusu NN (2019) Data the DEHP induced changes on the trace element and mineral levels in the brain and testis tissues of rats. Data Brief 17(26):104526
64. Aydemir D, Oztasci B, Barlas N, Ulusu NN (2020) Influence of the butylparaben administration on the detoxification organs. Turk J Biochem (Ahead-of-print). https://doi.org/10.1515/tjb-2020-0048
65. Otahal A, Aydemir D, Tomasich E, Minichsdorfer C (2020) Delineation of cell death mechanisms induced by synergistic effects of statins and erlotinib in non-small cell lung cancer cell (NSCLC) lines. Sci Rep 10(1):959
66. Wilschefski SC, Baxter MR (2019) Inductively coupled plasma mass spectrometry: introduction to analytical aspects. Clin Biochemist. Reviews 40(3):115–133. https://doi.org/10.33176/AACB-19-00024

Chapter 11

Microbiome Evaluation

Alba Rodríguez-Nogales, Antonio Jesús Ruiz-Malagón, Jose Alberto Molina-Tijeras, Maria Elena Rodríguez-Cabezas, and Julio Gálvez

Abstract

Various studies suggest that the intestinal microbiome may modulate the risk of developing different chronic diseases, including type 2 diabetes, allergy, cardiovascular disease, and colorectal cancer (CRC). Next-generation sequencing techniques have allowed a better understanding of the metabolic, physiological, and ecological roles of the microbiome. However, different conditions can affect the microbiome analysis, including experimental model, sample processing, sequencing, assembly, binning, annotation, and visualization. Besides, in order to translate microbiome research into clinical application, it is necessary to address host–microbe and microbe–microbe interactions. In this sense, animal models in association with "omics" approaches are indispensable for investigating host–microbiome interactions. Therefore, this chapter reviews the optimal approach to study the gut microbiome in experimental models highlighting their benefits, drawbacks, and limitations, as well as it provides an efficient protocol to determine the gut microbial community diversity and composition from animal stool samples.

Key words Experimental models, Microbiome, Next-generation sequencing, 16S protocol

1 Introduction

Over the past decade, microbiome research has provided valuable information on the microbiome composition and identified possible associations between the gut microbiome and various diseases. In fact, it is becoming evident that the intestinal microbiome modulates the risk of several chronic diseases, including type 2 diabetes, allergy, cardiovascular disease (CVD), low-grade systemic inflammation, inflammatory bowel disease (IBD), and colorectal cancer (CRC), among others. The studies that have been published on the topic, both in humans and in experimental models, display huge variations in the design (intervention, observational, case-control, cross-sectional, cohort), number of participants, control groups, nature and duration, and lack of use of "run-in periods."

Cinthia Baú Betim Cazarin (ed.), *Basic Protocols in Foods and Nutrition*,
Methods and Protocols in Food Science, https://doi.org/10.1007/978-1-0716-2345-9_11,

This inconsistency, together with the multitude of factors that might participate, makes it very difficult to compare and analyze the data so there is a clear need for larger better-designed studies to understand these mechanisms.

The intestinal microbiota is a highly complex ecosystem. The concept of a healthy, resilient gut microbiome relies on its richness and biodiversity, which definitely contribute to the host homeostasis. Even though many human disorders have been associated with microbiota composition changes and/or function, it remains unclear if these changes are a cause or a consequence of the disease. Therefore, one of the main current challenges for microbiome research is to demonstrate the cause-effect relationship between the microbiome and the host status, health, or disease. For this reason, and in order to efficiently translate microbiome research into clinical application, it is necessary to address the causation and molecular mechanisms of host–microbe and microbe–microbe interactions. However, these final aims are difficult to achieve, and will rely on the implementation of interdisciplinary strategies that combine top-down and bottom-up approaches. The use of animal models in association with "omics" procedures is crucial for investigating the causality and functionality of host–microbiome interactions [1–3].

Moreover, the current experience has made evident that microbiome research needs to be based on robust experimental models that allow to test the proposed hypotheses by systemic manipulations of specific variables. For instance, microbiome sample collection and the subsequent processing procedures are heterogeneous and can clearly affect the outcome. Thus, standardization of methods for sample collection and analysis are pivotal to perform data comparison among assays. In addition, high-throughput sequencing and other "omics" technologies have broken new ground, thus allowing microbial community profiling and assessing their functions and metabolic processes at high resolution. However, clinical translation of basic biomedical findings and the subsequent development of new therapeutic strategies, including dietary intervention or fecal microbiota transfer (FMT), are impeded by large interindividual variations, and methodological bias still constitutes one the major challenges in microbiome research. The establishment of standard operating procedures (SOPs) for sample collection and stabilization of microbial profiles, storage, preservation, isolation and sequencing are indispensable for translational biomedical research. Besides, it is essential to provide an inventory of available experimental models and strategies to analyze and validate cause-effect mechanisms involving gut microbiota. With this purpose, this chapter will describe the procedures to study the gut microbiome in experimental models, highlighting their benefits, drawbacks, and limitations.

1.1 Next-Generation Sequencing Technologies

Prior to the emergence of next-generation sequencing (NGS), the accurate identification of most members in a complex microbial community was troublesome. This was especially relevant on the gut microbiome, a highly diverse and dense microbial community with a small percentage of culturable microbes [4]. Initially, microbiome studies were based on the culture of individual bacteria [5], and the analysis of their interactions was performed by coculture of different microbial communities [6]. Although these methods allowed the investigation of basic microbial interactions, they provided little information about community dynamics because those uncultivable microbes were excluded from analysis, and the microorganisms were outside of their natural environment. The new techniques have enabled the study of communities in greater detail without omitting uncultivable microbes. Nowadays, the two most used methodologies for microbial identification and genotyping are based on gene amplicon/marker genes and shotgun metagenomics.

1.1.1 Gene Amplicon Sequencing

Over the past 25 years, gene amplicon sequencing has been one of the most widespread techniques to study phylogeny and taxonomy of complex microbiomes. This method is based on a single genomic locus targeted for polymerase chain reaction (PCR) amplification; the chosen locus must be largely conserved throughout microorganisms of interest but contain sufficient variation to distinguish individual strains or species. The resulting PCR products are sequenced and compared with known reference sequences in a database. For bacteria, archaea, fungi, and mycobacteria, many specific marker/target genes have been identified that are extensively used for amplicon sequencing. The most used target gene for bacterial identification is 16S rRNA (or 16S rDNA).

Interestingly, the prokaryotic 16S rRNA gene is distinct from its eukaryotic homolog, the 18S rRNA gene. The highly conserved 16S rRNA gene implies its crucial role in cellular function and survival and thus forms the basis of obtaining precise genomic classification of known and unknown microbial taxa. Additionally, it is easier to sequence 16S rRNA genes even for exceedingly large sample sizes due to its relatively short size (~1542 bp). The gene sequence consists of highly conserved primer binding sites along with nine variable regions (V1–V9). Most of the 16S rRNA-based genotyping protocols use V5–V6, V3–V4, or V4 hypervariable regions to identify and catalog microbial profiles [7, 8]. Alternatively, V1–V2 and V3–V4 have been utilized for genotyping archaeal species in complex microbial communities [9]. Unlike bacteria, the identification of gene targets in pathologically important yeast and fungi is still not well determined. The fungal rDNA is composed of coding and noncoding spacer regions [10, 11]. The internal transcribed spacers (ITSs) variable regions have been the most frequently used gene target for fungal genotyping. However,

uneven lengths of these ITSs induce errors and biases, such as preferential amplification and sequencing, often leading to an incorrect estimation of abundance [10]. The methods rely on conserved targets of the PCR primers that are adjacent to sequences that are sufficiently variable to differentiate organisms of interest. As the price of sequencing technologies has dropped off, whole-community metagenome sequencing of arbitrary short reads has become more common, and today they can provide billions of sequence reads (many gigabases) per community.

1.1.2 Metagenomics

Metagenomics refers to direct genetic analysis of genomes obtained from different environments and can identify the majority of the organisms (culturable and unculturable bacteria). While 16S rRNA sequencing utilizes a marker gene approach and it does not target the whole genome, on the contrary, the metagenomic procedure is a culture-independent genomic analysis of microbes, which are taken directly from the environment using a genome-wide shotgun sequencing approach [12, 13]. Shotgun metagenomics (a non-targeted sequencing process) can readily resolve species-level and strain-level classification and provide genome content, functional potential, and some genome assembly for organisms of even modest abundance. Metagenomics can be divided into two types: [1] sequence-based screens, which describe the microbial diversity and genomes of a particular environmental sample and [2] functional screens, which identify the functional gene products but do not determine from what species the genetic material is originated [14]. Metagenomics helps in associating function to phylogeny besides creating evolutionary profiles of the microbial community structure. Importantly, it also helps to identify viruses that are otherwise hard to detect through a single-gene targeting approach due to its high genetic diversity and its inability to discern common genetic links [15]. However, it is still more expensive than amplicon sequencing, less tolerant of low biomass or contaminated samples, and it depends upon considerably more complex and costly computationally analytic procedures.

1.1.3 Metatranscriptomics and Metaproteomics

The metatranscriptomic analysis is based on RNA sequencing evaluation of microbial communities, while metaproteomic refers to determining the proteome expressed in such communities. Metatranscriptomic and metaproteomic analyses are still in their infancy. They are still more expensive because of challenging protocols and the scarcity of computational tools, and there is no consensus yet regarding in which settings or for which health-relevant phenotypes transcription from the microbial community will be more useful [16]. Metatranscriptomics allows the characterization and functionality analysis of the microbiome. It provides RNA sequencing-based measures of gene expression and regulation in

the microbial community. The analysis used for metatranscriptomics is the same as in metagenomics [17] and can be carried out through two different approaches: (i) de novo and (ii) reference based.

On the contrary, metaproteomics can be applied to evaluate metabolic pathways and to identify enzymes present in unculturable microbes and communities [14, 17]. The metaproteomic approach has six steps: sample collection, protein extraction, purification and fractionation, mass spectrometric analysis and, finally, protein identification, and further bioinformatics analysis. Besides, there are two approaches for identifying peptides and proteins: direct mass spectra-based or de novo peptide sequence-based; each one is followed by a quantitative step, along with visualization of the complex functional information [18]. Metaproteomics studies can provide deep insights into diverse biological questions regarding health and disease. Emerging technologies should improve metaproteomic approaches to handle the wide dynamic ranges of metaproteomic samples, which could also help to understand protein modification [19]. Thus, metaproteomic has become a complementary approach to metagenomics, aiming at the extensive characterization of proteins from environmental microbiota [20].

2 Experimental Models to Study the Microbiome

To date, most preclinical microbiome research has focused on rodents, mainly mice and rats, as model organisms for delineating the mechanisms that shape the assembly and dynamic operations of microbial communities. In the last few years, important contributions to understanding microbiome complexity have been made by using more simple animal models, including the zebrafish *Danio rerio*, *Drosophila melanogaster* and *Caenorhabditis elegans*. Although these are of great value and allow to conduct cost-effective experiments over short timescales by using simple protocols to manipulate the microbiota, their main limitation is based on the fact that the microbiome associated with invertebrates and lower vertebrates presents lower taxonomic diversity than in mammals [21]. For this reason, rodent models still constitute the primary choice for preclinical proof-of-concept tests, which would allow causal relationships between microbiome and host physiological, metabolic, immune and neurologic phenotypes, as well as for the development of methods to repair or prevent functional abnormalities in the microbiota composition that contribute to disease pathogenesis [22].

Unfortunately, one of the most relevant concerns associated with these experimental models is the lack of complete

reproducibility in laboratory animals, even within an apparently identical host chromosomal background. Consequently, it becomes difficult to design suitable control groups that would reduce the number of animals used. Even though inbred strains display a reduced genetic variance, an array of environmental factors, such as ambient temperature, water treatment, diet and light-dark cycles, can influence mouse phenotypes. In fact, many of these environmental parameters have been linked to alterations in the microbiome. In consequence, there is a clear demand for well-established methods to control host genetic, microbiome, and the effects of their interactions.

2.1 Cohousing

Cohousing of experimental animals is a widely used method in which separate genotypes live in the same cage. During cohousing, animals may feed on feces (also known as coprophagy) or, more likely, ingest feces by self-grooming, thus sharing microbes across co-caged individuals. This technique may be the simplest and most convenient method because independent experimental animal lines can be bred separately and then can be co-caged once weaned [23]. However, the success in this technique could be influenced by a non-standardized method for cohousing, including the duration and time after weaning, which vary and are not well described. Moreover, precise experimental characterization about the impact of cohousing on the mucosa-associated versus fecal microbiota is lacking (Fig. 1).

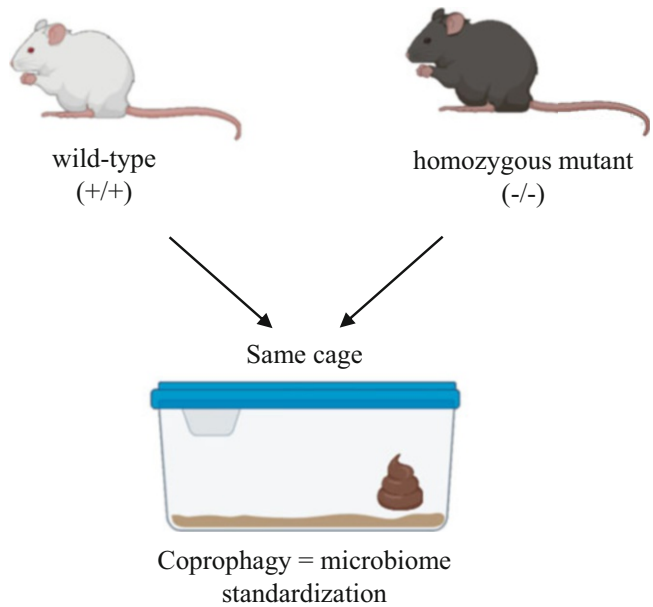

Fig. 1 Cohousing method. During cohousing, animals may feed on feces, thus sharing microbes across co-caged individuals

2.2 Littermates

The use of littermates is considered the gold standard protocol to determine host versus microbiome genes dominance in conferring a phenotype under specific-pathogen-free (SPF) conditions, and can be applied in all animal facilities [24]. The use of littermate controls is a well-recognized alternative to solve the problems mentioned in the cohousing method. Thus, it allows determining if a specific phenotype that was observed prior to standardization of the microbiome was due to the microbiome or the host genetics, or if a genetic modification impacts the microbiota composition. In this context, littermate consists of breeding control (background phenotype) and specific genetically modified experimental animals together to generate a heterozygous generation. Later, breeding heterozygous parents results in all the genotypes required for phenotypic comparison when combined, and experience the same microbial and environmental exposures up to and following birth, avoiding phenotype inheritance via both the maternal and early life effects [25]. However, the disadvantages of this method include the excess production of heterozygotes, the necessity for genotyping and difficulty generating adequate control animals in the case of the mutation of more than one gene (e.g., for double-knockout animals) (Fig. 2).

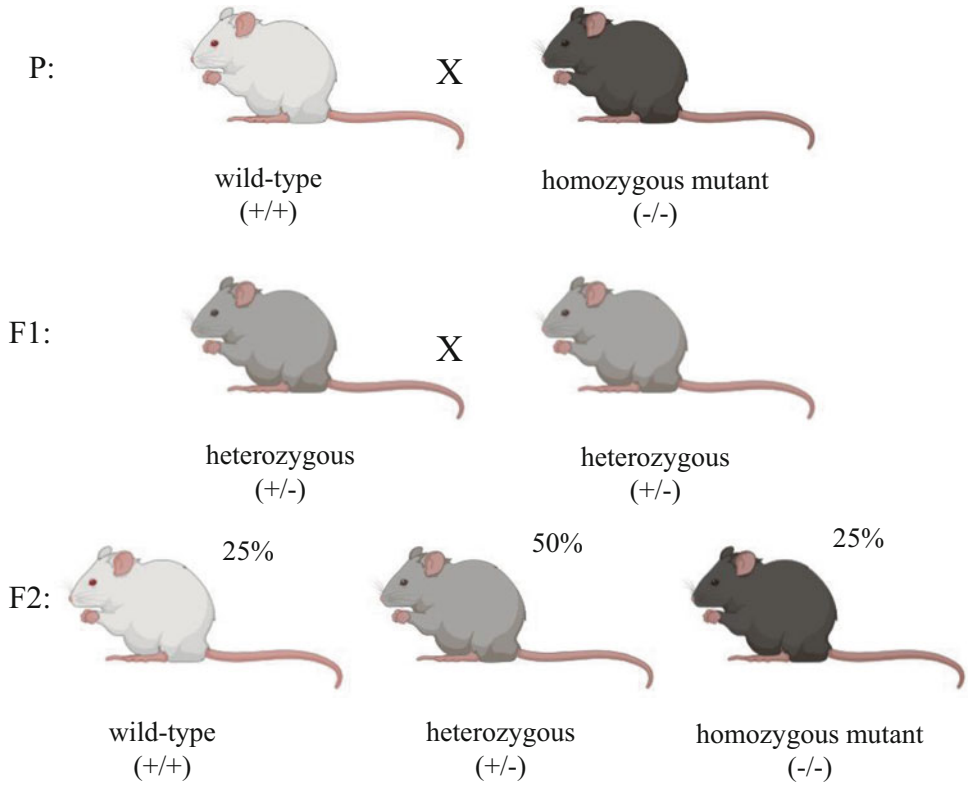

Fig. 2 Littermate-controlled experimental setup. Wild-type (control) animals are crossed to homozygous mutant (experimental) ones (P = parental; F1 = first generation; F2 = second generation)

2.3 Gnotobiotic Animals

Gnotobiology represents an attractive strategy for standardization of the microbiome of animal models. In gnotobiotic animals, the microbiota composition is known, by definition, offering a unique tool to study host–microbiota interactions in more detail. This method describes how to use germ-free (GF) animals, rather than generating littermate controls, as the starting point to standardize the microbiome between control and experimental mice. GF animals do not display colonization resistance and can therefore be colonized with the microbiota of choice. In this context, for designing the consortium of interest, GF animals are conventionalized with a microbiota derived from a donor, which can either be rodent or human, offering a better solution rather than mixing the microbiota of control and mutant strain. Gnotobiotic animals are often used for studying if the microbiome influences the appearance of a determined condition. Thus, donors normally harbor a specific condition or disease, whereas the control donor is healthy, and recipient animals are observed for the appearance of the condition of interest (Fig. 3).

2.4 Antibiotic Treatment

Similar to GF animals, the administration of broad-spectrum antibiotics is commonly used as an alternative and a more basic method for depleting microbiota. Unlike GF conditions, under which complete sterility is maintained throughout life, antibiotics can deplete bacterial populations in animals usually colonized after birth. Furthermore, due to the different mechanisms of action, antibiotics can selectively be chosen to deplete different microbiota members. For example, some antibiotics such as metronidazole and clindamycin specifically target anaerobes, vancomycin is only effective against gram-positive bacteria, and polymyxin B specifically targets gram-negative bacteria [26]. Thus, individual antibiotics can be used to shift the composition of the gut microbiota in order to identify classes of bacteria relevant to different phenotypes. However, and in contrast to GF mice, the antibiotic application does not lead to depleting all microbes, which could be relevant for host phenotype [27].

2.5 Fecal Microbiota Transfer (FMT)

FMT consists of administering a fecal matter solution from a donor into the intestinal tract of a recipient in order to directly change its microbiota composition (Fig. 4) [28]. In this context, FMT could constitute a novel standardization of microbiome in animal models. Then, when a phenotype is observed in an animal strain that has been bred independently from the control wild-type strain, the microbiome from one strain can be transferred to the other strain through fecal transplantation to assess whether the dominant factor responsible for the phenotype is the microbiome or the host genome. Nevertheless, fecal transplants may not efficiently transfer the complete microbial community from the donor animals to the recipients because not all microbial community members may survive the collection and preparation procedure [25].

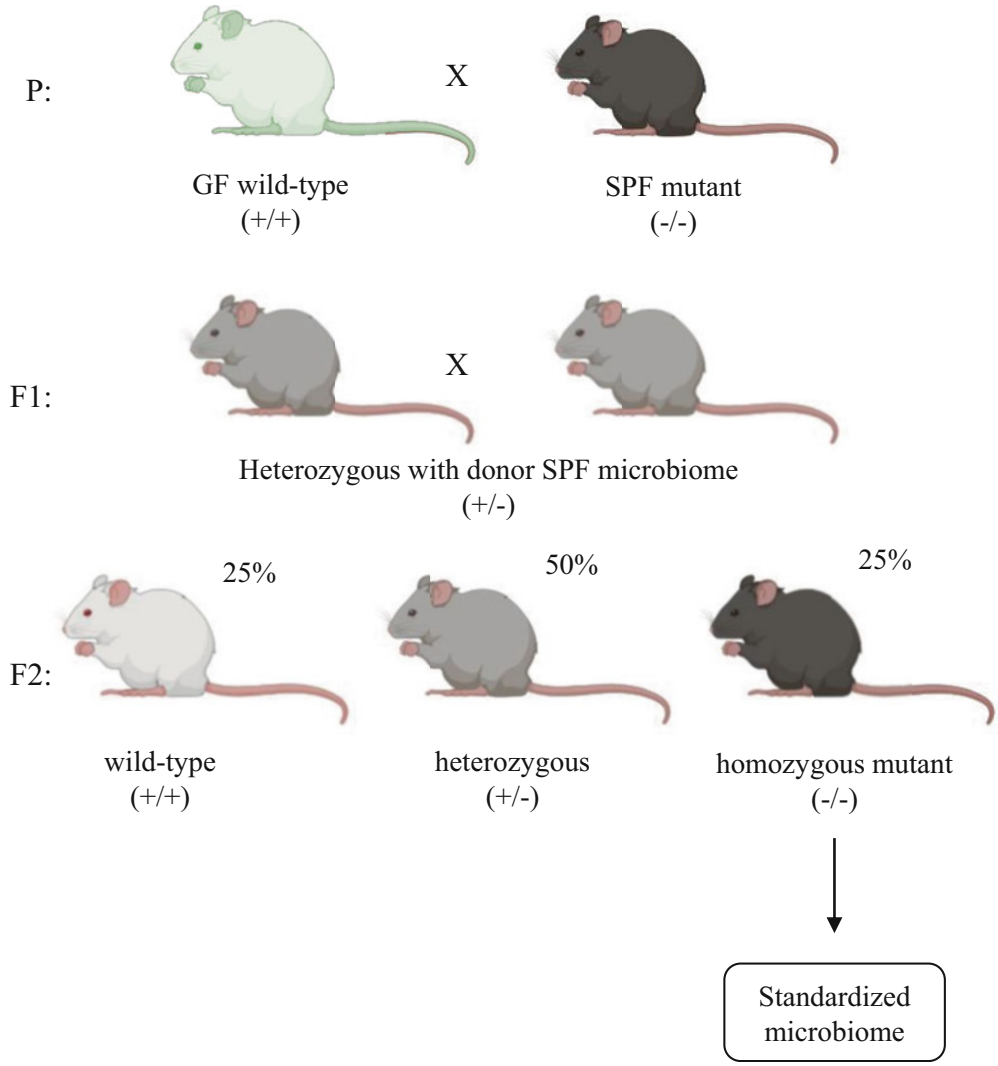

Fig. 3 Experimental setup for colonizing germ-free animals to ensure standardization of gut microbiomes of control and experimental animals. All pups generated from this cross will be heterozygous for the gene of interest and will be colonized with the microbiome originating from the SPF parent (P = parental; F1 = first generation; F2 = second generation)

3 Protocol of Metagenomic Sequencing by 16S rRNA Gene Amplicon Method

Each of the above experimental protocols can provide specific information, so depending on the aim of the study, it is important to choose the one that can deliver the appropriate results to demonstrate our hypothesis. However, the use of a common protocol for DNA isolation can be considered especially relevant. Although many studies have compared DNA extraction protocols for the gut microbiota [28–31], there is no consensus about which extraction

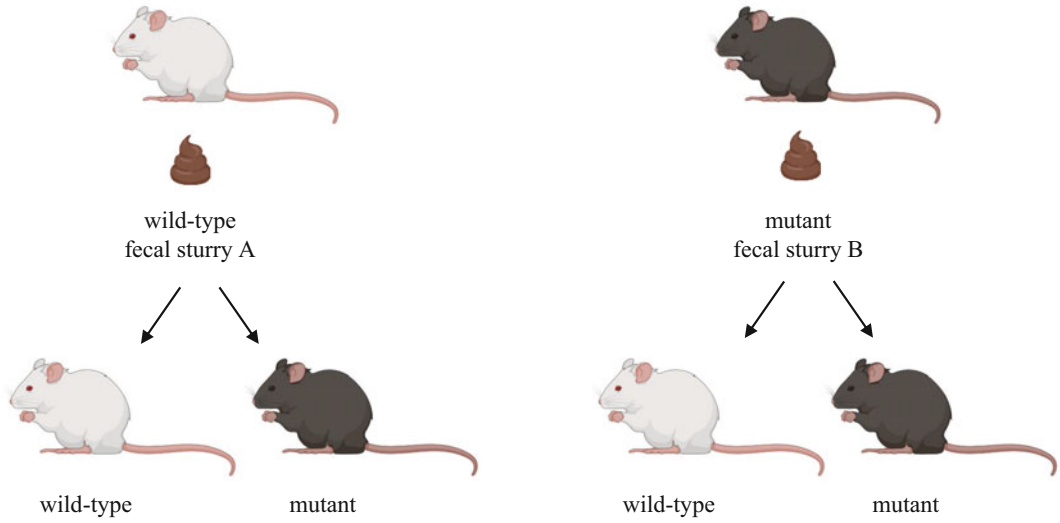

Fig. 4 Fecal transplantation to determine the dominance of the microbiota versus the host genome. Fresh fecal pellets are collected from donors (either wild-type/control or mutant/experimental), and fecal pools are prepared. Fecal pools are then inoculated by oral gavage into wild-type/control and mutant/experimental recipient pups in order to transfer gut microbiome (P = parental; F1 = first generation; F2 = second generation)

method is the most efficient and provides the most representative sample of gut microbial community diversity from stool samples. Nowadays, the published results indicate that most of the observed variations within the model could be attributed to differences between subjects (biological variation), being just a small proportion of variation associated with the DNA extraction method (technical variation) and intra-subject variation. Therefore, although many commercial column-based kits are available, we will focus on phenol:chloroform extraction method in this chapter. The commercial kits are relatively expensive compared to the phenol-chloroform method, and additionally, this method yields up to 93 times more nucleic acids than silica column-based protocols when extracting nucleic acids from small quantities of cells or tissues [32, 33].

3.1 Materials

- Germ-free adult male and female mice (6 to 8 weeks old, e.g., C57BL/6); SPF adult mice of the genetically modified strain; mutant mouse strains.
- Animal housing facility with appropriate sterile food, water, bedding, and environmental enrichments.
- 2 or 1.5 mL sterile microcentrifuge tubes with lockable caps
- 1 mm diameter zirconia/silica sand
- Liquid nitrogen tank and container −80 °C freezer.

- Sterile laminar flow hood.
- Homogenizer with the refrigeration system.
- Nanodrop 2000 Spectrophotometer.
- 96-well PCR plate
- MiSeq Illumina platform.
- AMPure XP beads.
- Bioanalyzer DNA 1000 chip.
- Agilent Technologies 2100 Bioanalyzer.

For animal feces collection, it should be done in sterility as much as possible and place the microcentrifuge tube containing fecal pellets in a −80 °C freezer until further processing.

3.2 Methods

3.2.1 DNA Extraction

1. Collect the fecal samples from the freezer or fresh stool.
2. Use 100–200 mg of fresh or frozen stool.
3. Transfer 100–200 mg of stool to a sterile microcentrifuge tube with zirconia/silica sand.
4. To lysate the fecal samples, add in each tube 1 mL of TN150 buffer (Tris–HCl (10 mM), NaCl (150 mM), pH = 8).
5. Incubate the samples for 30 min at 80 °C in continuous shaking.
6. In the hood, add 150 μL of cold phenol.
7. To homogenize the samples, use the program of 2 cycles of 30 s at maximum speed (5000 rpm) and at 4 °C.
8. After homogenization, add 150 μL of cold chloroform/isoamyl alcohol mix. Mix them.
9. Centrifuge the tubes at 21000×g for 5 min at 4 °C.
10. Transfer the aqueous phase (top) to a new sterile microcentrifuge.
11. Repeat steps 8–10 until the aqueous phase appears completely transparent.
12. Once the aqueous phase appears completely transparent, transfer it to a sterile 2 mL tube.
13. Mix the aqueous phase with 100 μL of cold isopropanol.
14. Add 150 μL of cold chloroform and then mix by inversion.
15. Spin at 21000×g for 5 min at 4 °C.
16. Transfer supernatant to new sterile 2 mL tube.

3.2.2 DNA Purification by Precipitation

1. In order to neutralize molecule charges and facilitate the precipitation of the DNA, add on 100 μL of sodium acetate 3 M pH 5.2. Then, mix by inversion.

2. At this point, it will include 500 μL of cold isopropanol, and the samples will be stored at −20 °C overnight. Thus, maximum precipitation of the DNA will be obtained.
3. Next day, delicately recover the precipitate using a sterile 1 mL tip and transfer it to a new sterile 1.5 mL tube.
4. Once transferred to a new tube, add 0.5–1 mL of cold 70% ethanol to remove the salts.
5. Spin at 21000G for 2 min at 4 °C, then carefully decant the supernatant.
6. Repeat steps 4 and 5.
7. To remove traces of ethanol by evaporation, place the tubes in a thermoblock at 55 °C.
8. Resuspend the pellet in 100 μL of sterile MilliQ water.
9. Finally, the DNA quantification will perform through the NanoDrop 2000 Spectrophotometer.

At this point, the samples are ready to be sequenced. In this sense, and as commented before, different sequencing methods can be applied. This chapter will describe the most used method based on the 16S amplicon, specifically a sequencing method using the MiSeq Illumina platform.

3.2.3 16S Amplicon Sequencing

Sequencing technology has advanced rapidly from the Sanger method to next-generation sequencing (NGS). In fact, nowadays, many sequencing platforms are available; however, among the main international research groups, the most popular technology is the Illumina platform, specifically MiSeq. Therefore, the MiSeq sequencing protocol will be studied in detail in this chapter.

3.2.4 Amplicon Polymerase Chain Reaction (PCR)

This step is characterized by PCRs that amplify the template out of DNA obtained previously.

1. Prepare 5–10 ng/μL of microbial DNA in 10 mM Tris pH 8.5 in one PCR plate.
2. Set up the following reaction of DNA, 2X KAPA HiFi HotStart ReadyMix, and primers (Table 1).
3. Perform PCR in a thermal cycler using the following program:
   (i) 95 °C for 3 min.
   (ii) 25 cycles of:
      - 95 °C for 30 s
      - 55 °C for 30 s
      - 72 °C for 30 s.
   (iii) 72 °C for 5 min
   (iv) Hold at 4 °C.

Table 1
DNA reaction procedure

	Volume
Microbial DNA (5 ng/μL)	2.5 μL
Amplicon PCR forward primer (1 μM)	5 μL
Amplicon PCR reverse primer (1 μM)	5 μL
2X KAPA HiFi HotStart ReadyMix	12.5 μL
Total	**25 μL**

4. Run 1 μL of the PCR product on a Bioanalyzer DNA 1000 chip to verify the size. For example, using V3 and V4 primers pairs, the expected size is ~550 bp.

3.2.5 PCR Cleanup

This step is very important to purify the 16S pair combination of the V1–V9 region amplicon. AMPure XP beads will be used.

1. Vortex the AMPure XP beads for 30 s. Add an appropriate amount of beads depending on the sample number.
2. Add 20 μL of AMPure Xp beads to each well of the Amplicon PCR plate. Then, gently pipette the entire volume up and down.
3. Incubate at room temperature for 5 min.
4. Place the plate on a magnetic stand for 5 min, after which, using a multichannel pipette, remove and discard the supernatant.
5. Wash the beads with 200 μL of 80% ethanol with the PCR plate on the magnetic stand.
6. With the PCR plate still on the magnetic stand, allow the beads to air-dry for 10 min.
7. In this step, remove the plate from the magnetic stand and, with a multichannel pipette, add 52.5 μL of 10 mM Tris pH 8.5 to each sample on the amplicon PCR plate.
8. Gently mix up and down 10 times and make sure the beads are fully resuspended.
9. Incubate at room temperature for 2 min.
10. Once again, put the plate back on the magnetic stand for 5 min.
11. Carefully transfer 50 μL of the supernatant to a new 96-well PCR plate.

Table 2
Preparation of DNA reaction

	Volume
DNA	5 μL
Nextera XT index primer 1 (N7xx)	5 μL
Nextera XT index primer 2 (S5xx)	5 μL
2X KAPA HiFi HotStart ReadyMix	25 μL
PCR grade water	10 μL
Total	**50 μL**

3.2.6 Index PCR

1. From the previous 96-well PCR plate, transfer 5 μL to a new PCR plate. The remaining 45 μL can be stored at −20 °C.
2. In this step, the TruSeq Index Plate Fixture will be used. Therefore, place the 96-well PCR plate with the 5ul of resuspended PCR product DNA in the TruSeq Index Plate Fixture.
3. Prepare the reaction of DNA as described in Table 2.
4. Gently mix up and down 10 times and then cover the plate.
5. Spin the plate at 1000×g for 1 min at 20 °C.
6. Perform PCR using the next program:
   (i) 95 °C for 3 min
   (ii) 8 cycles of:
      - 95 °C for 30 s
      - 55 °C for 30 s
      - 72 °C for 30 s.
   (iii) 72 °C for 5 min
   (iv) Hold at 4 °C.

3.2.7 PCR Cleanup 2

It will also use AMPure XP Beads to clean up the final library.

1. Vortex AMPure XP beads for 30 s and add 56 μL of AMPure Xp beads to each well of the Index PCR plate. Subsequently, mix up and down 10 times.
2. Incubate at room temperature without shaking for 5 min.
3. Place the plate on a magnetic stand for 5 min, and then discard the supernatant.
4. With the Index PCR plate on the magnetic stand, wash the beads with 200 μL of 80% ethanol.

5. With the Index PCR plate still on the magnetic stand, allow the beads to air-dry for 10 min.
6. Remove the plate from the magnetic stand and add 27.5 μL of 10 mM Tris pH 8.5 to each well on the Index PCR plate.
7. Gently mix up and down 10 times and incubate at room temperature for 2 min.
8. Place back the plate on the magnetic stand for 5 min and carefully transfer 25 μL of the Index PCR plate to a new 96-well plate.

3.2.8 Validate the Library

Run 1 μL of a 1:50 dilution of the final library obtained from the last step. For it, a Bioanalyzer DNA 1000 chip will be used.

3.2.9 Library Quantification, Normalizing, and Pooling

1. Quantification of the library by Agilent Technologies 2100 Bioanalyzer trace.
2. Dilute concentrated final library using 10 mM Tris pH 8.5 to 4 nM.
3. Aliquot 5 μL of diluted DNA from each library and mix the aliquots for pooling libraries. Depending on coverage needs, up to 96 libraries can be pooled for one MiSeq run.

3.2.10 Library Denaturing and MiSeq Sample Loading

This step requires that the pooled libraries will be denatured with NaOH, diluted in hybridization buffer, and heat-denatured before the MiSeq sequencing.

(a) DNA denaturation.

1. Mix 5 μL of pooled final DNA library and 5 μL of 0.2 N of NaOH in a new microcentrifuge tube. Subsequently, vortex briefly and centrifuge at 280G for 1 min at 20 °C.
2. Incubate at room temperature 5 min.
3. Add 990 μL of prechilled hybridization buffer and place it on ice.
4. Dilute the denatured DNA to 4 pM (120 μL of 20 pM denatured library +480 μL of prechilled hybridization buffer) and adjust if necessary.
5. Mix by inversion several times and then spin the DNA solution.
6. Place the samples on ice.

(b) PhiX Control denaturation and dilution.

In this step, the control for Illumina sequencing runs will be prepared. Thus, denature and dilute 10 nM PhiX library to the same loading concentration as the Amplicon library, 4 pM.

1. Dilution of the PhiX library to 4 nM:
   (a) 10 nM PhiX library (2 μL) + 10 mM Tris pH 8.5 (3 μL)
2. Combine 5 μL of 4 nM PhiX and 5 μL of 0.2 N NaOH, subsequently vortex briefly.
3. Incubate for 5 min at room temperature to denature the PhiX library into single strands.
4. Add 990 μL of prechilled hybridization buffer to the tube containing denatured PhiX library to result in a 20 pM PhiX library.
5. Dilute the denatured PhiX library to 4 pM (120 μL of 20 pM PhiX +480 μL of prechilled hybridization buffer).
6. Mix by inversion and pulse centrifuge.
7. Put on ice.

(c) Combine Amplicon Library and PhiX Control

1. Combine 30 μL of denatured and diluted PhiX Control and 570 μL of denatured and diluted amplicon library.
2. Set the combination on ice until the heat denaturation is ready. Heat denaturation must be performed immediately before loading the library into the MiSeq platform.
3. With a heat block, incubate the combined library and PhiX Control tube at 96 °C for 2 min.
4. Invert the tubes 3 times to mix and immediately place on ice.
5. Keep the tube on ice for 5 min.

3.3 Illumina MiSeq Analysis

Once the samples are loaded, the MiSeq system provides an analysis tool based on its MiSeq Reporter software. The metagenomics workflow classifies organisms from the selected amplicon primers (pair combination of V1–V9) using a 16S rRNA database, specifically, the Greengenes database (http://greengenes.lbl.gov/). Therefore, the output obtained is a classification of reads at different taxonomic levels from kingdom to species. Moreover, the analysis output provides (i) clusters graph (numbers of raw clusters, clusters passing filters and clusters not associated with index, and duplicates); (ii) sample table that summarizes the sequencing results and (iii) a graphical representation of the classification breakdown for each sample.

Acknowledgments

This work received financial support from Junta de Andalucía (CTS 164), and by Instituto de Salud Carlos III (PI19/1058) with funds from the European Union. CIBER-EHD is funded by Instituto de Salud Carlos III. A. Rodriguez-Nogales is a postdoctoral fellow of

Instituto de Salud Carlos III (Miguel Servet Program); A.J. Ruiz-Malagon is a predoctoral fellow from University of Granada (Programa de Doctorado: Medicina Clínica y Salud Pública); J.A Molina-Tijeras is a predoctoral fellow from Instituto de Salud Carlos III (PFIS program) (Programa de Doctorado: Nutrición y Ciencias de los Alimentos).

References

1. Fritz JV, Desai MS, Shah P, Schneider JG, Wilmes P (2013) From meta-omics to causality: experimental models for human microbiome research. Microbiome 1(1):14
2. Al-Asmakh M, Zadjali F (2015) Use of germ-free animal models in microbiota-related research. J Microbiol Biotechnol 25(10): 1583–1588
3. Lam YY, Zhang C, Zhao L (2018) Causality in dietary interventions-building a case for gut microbiota. Genome Med 10(1):62
4. Eckburg PB, Bik EM, Bernstein CN, Purdom E, Dethlefsen L, Sargent M et al (2005) Diversity of the human intestinal microbial flora. Science (New York, NY) 308(5728):1635–1638
5. Gibbons RJ, Socransky SS, de Araujo WC, van Houte J (1964) Studies of the predominant cultivable microbiota of dental plaque. Arch Oral Biol 9(3):365–370
6. Parker RB, Snyder ML (1961) Interactions of the oral microbiota. I. A system for the defined study of mixed cultures. Proc Soc Exp Biol Med (New York, NY) 108:749–752
7. Tremblay J, Singh K, Fern A, Kirton ES, He S, Woyke T et al (2015) Primer and platform effects on 16S rRNA tag sequencing. Front Microbiol 6:771
8. Woo PCY, Lau SKP, Teng JLL, Tse H, Yuen KY (2008) Then and now: use of 16S rDNA gene sequencing for bacterial identification and discovery of novel bacteria in clinical microbiology laboratories. Clin Microbiol Infect 14(10):908–934
9. Yu H, Braun P, Yildirim MA, Lemmens I, Venkatesan K, Sahalie J et al (2008) High-quality binary protein interaction map of the yeast interactome network. Science (New York, NY) 322(5898):104–110
10. De Filippis F, Parente E, Ercolini D (2017) Metagenomics insights into food fermentations. Microb Biotechnol 10(1):91–102
11. Raja HA, Miller AN, Pearce CJ, Oberlies NH (2017) Fungal identification using molecular tools: a primer for the natural products research community. J Nat Prod 80(3): 756–770
12. Gilbert JA, Dupont CL (2011) Microbial metagenomics: beyond the genome. Annu Rev Mar Sci 3:347–371
13. Escobar-Zepeda A, Vera-Ponce de León A, Sanchez-Flores A (2015) The road to metagenomics: from microbiology to DNA sequencing technologies and bioinformatics. Front Genet 6:348
14. Madhavan A, Sindhu R, Parameswaran B, Sukumaran RK, Pandey A (2017) Metagenome analysis: a powerful tool for enzyme bioprospecting. Appl Biochem Biotechnol 183(2): 636–651
15. Kristensen DM, Mushegian AR, Dolja VV, Koonin EV (2010) New dimensions of the virus world discovered through metagenomics. Trends Microbiol 18(1):11–19
16. Franzosa EA, Morgan XC, Segata N, Waldron L, Reyes J, Earl AM et al (2014) Relating the metatranscriptome and metagenome of the human gut. Proc Natl Acad Sci U S A 111(22):E2329–E2338
17. Simon C, Daniel R (2011) Metagenomic analyses: past and future trends. Appl Environ Microbiol 77(4):1153–1161
18. Wang ZK, Yang YS, Chen Y, Yuan J, Sun G, Peng LH (2014) Intestinal microbiota pathogenesis and fecal microbiota transplantation for inflammatory bowel disease. World J Gastroenterol 20(40):14805–14820
19. Wilmes P, Heintz-Buschart A, Bond PL (2015) A decade of metaproteomics: where we stand and what the future holds. Proteomics 15(20): 3409–3417
20. Petriz BA, Franco OL (2017) Metaproteomics as a complementary approach to gut microbiota in health and disease. Front Chem 5:4
21. Douglas AE (2019) Simple animal models for microbiome research. Nat Rev Microbiol 17(12):764–775
22. Animal Models for Microbiome Research: Advancing Basic and Translational Science: Proceedings of a Workshop. Washington, DC:

2018 by the National Academy of Sciences; 2018.

23. Robertson SJ, Lemire P, Maughan H, Goethel A, Turpin W, Bedrani L et al (2019) Comparison of co-housing and littermate methods for microbiota standardization in mouse models. Cell Rep 27(6):1910–9.e2
24. Stappenbeck TS, Virgin HW (2016) Accounting for reciprocal host–microbiome interactions in experimental science. Nature 534(7606):191–199
25. McCoy KD, Geuking MB, Ronchi F (2017) Gut microbiome standardization in control and experimental mice. Curr Protoc Immunol 117:23.1.1–231.13
26. Kennedy EA, King KY, Baldridge MT (2018) Mouse microbiota models: comparing germ-free mice and antibiotics treatment as tools for modifying gut bacteria. Front Physiol 9:1534
27. Bayer F, Ascher S, Pontarollo G, Reinhardt C (2019) Antibiotic treatment protocols and germ-free mouse models in vascular research. Front Immunol 10:2174
28. Kennedy NA, Walker AW, Berry SH, Duncan SH, Farquarson FM, Louis P, Thomson J, UK IBD Genetics Consortium (2014) The impact of different DNA extraction kits and laboratories upon the assessment of human gut microbiota composition by 16S rRNA gene sequencing. PLoS One 9(2):e88982
29. Peng X, Yu KQ, Deng GH, Jiang YX, Wang Y, Zhang GX, Zhou HW (2013) Comparison of direct boiling method with commercial kits for extracting fecal microbiome DNA by Illumina sequencing of 16S rRNA tags. J Microbiol Methods 95(3):455–462
30. Henderson G, Cox F, Kittelmann S, Miri VH, Zethof M, Noel SJ, Waghorn GC, Janssen PH (2013) Effect of DNA extraction methods and sampling techniques on the apparent structure of cow and sheep rumen microbial communities. PLoS One 8(9):e74787
31. Claassen S, du Toit E, Kaba M, Moodley C, Zar HJ, Nicol MP (2013) A comparison of the efficiency of five different commercial DNA extraction kits for extraction of DNA from faecal samples. J Microbiol Methods 94(2): 103–110
32. Deng MY, Wang H, Ward GB, Beckham TR, McKenna TS (2005) Comparison of six RNA extraction methods for the detection of classical swine fever virus by real-time and conventional reverse transcription-PCR. J Vet Diagn Investig 17(6):574–578
33. Xiang X, Qiu D, Hegele RD, Tan WC (2001) Comparison of different methods of total RNA extraction for viral detection in sputum. J Virol Methods 94(1–2):129–135

Chapter 12

The GSH Colorimetric Method as Measurement of Antioxidant Status in Serum and Rodent Tissues

Milena Morandi Vuolo, Juliana Kelly da Silva-Maia, and Ângela Giovana Batista

Abstract

Aerobic organisms have a wide variety of antioxidants in the biological systems to protect themselves against oxidative stress, GSH being one of the most important component. In this method, GSH reacts with the Ellman's reagent producing 2-nitro-5-mercapto-benzoic acid (TNB), which possesses its absorption maximum at 412 nm, showing a yellow-colored reaction. This assay allows colorimetric detection of almost entire thiol groups in several tissues. This chapter describes optimized conditions for testing rodent tissue homogenates and serum using Ellman's reagent-based GSH method. The Ellman's GSH method is a rapid, inexpensive, and accurate method to measure in vivo antioxidant status.

Key words Thiol, Antioxidant, Glutathione, Dilutions, Oxidative stress

1 Introduction

GSH is a tripeptide composed of the amino acids: glycine, cysteine, and glutamic acid. The GSH synthesis is regulated by its content in the cell [1]. In addition, cysteine also plays a regulating factor in GSH synthesis, being less abundant in relation to glycine and glutamic acid, therefore limiting its synthesis. Glutathione synthesis is a cytosolic process and could enter other cellular compartments, such as mitochondria, nucleus, endoplasmic reticulum, and the extracellular environment [2]. The steps of GSH synthesis are:

1. The enzyme ɣ-glutamyl cysteine synthetase catalyzes the reaction between L-glutamate and L-cysteine forming ɣ-glutamyl cysteine in the presence of Mg^{+2} and Mn^{+2} by hydrolyzing 1 ATP.
2. Glutathione synthetase forms a peptide bond between ɣ-glutamyl cysteine and glycine, originating GSH by hydrolyzing 1 ATP. The thiol of cysteine is a functional moiety of GSH;

Cinthia Baú Betim Cazarin (ed.), *Basic Protocols in Foods and Nutrition*,
Methods and Protocols in Food Science, https://doi.org/10.1007/978-1-0716-2345-9_12,

when oxidized, it forms a dipeptide bond (GSSH), which is not functional and could be recovered by glutathione reductase [3].

GSH is a stock of cysteine that protects it from oxidation, ensuring its integrity and function. GSH has high stability; specific enzymes are required for its degradation, once the γ-glutamyl bond of GSH is not accessed easily by cellular peptidases [4].

GSH is stable inside the cell; however, it can be imported or exported from the cell as reduced, oxidized, or conjugated forms. These forms are transported through two transporters: multidrug resistance-associated protein (MRP) and organic anion transporting polypeptide (OATP). GSH, when exported, is hydrolyzed by ɣ-L-glutamyl transpeptidase (GGT) and dipeptidase present in the outer membrane of cells, resulting in glutamate, cysteine, and glycine to GSH turnover in mammalian cells. GGT is regulated by electrophilic molecules and is responsible for the transference of glutamate from GSH to amino acids and, thus, into the cell [1].

In aerobic life organisms, reactive oxygen species (ROS) formation through the respiratory chain in the mitochondria is a physiologic condition. However, an excess of ROS production can cause an inability of the antioxidant enzymes to scavenge such species. The imbalance between ROS production and antioxidant capacity is named oxidative stress, resulting in many pathological consequences. Aerobic organisms have a wide variety of antioxidants in the biological systems to protect themselves against oxidative stress, GSH being one of the most important components [5].

The SH group of cysteine in GSH possesses a strong nucleophilicity and redox flexibility, giving to GSH the ability to scavenge electrons and conjugate with pollutants and carcinogens. The GSH is the main biological antioxidant in most cells, being responsible for the reduced environment [6]. GSH can donate electrons to glutathione peroxidases and glutathione S-transferases. Furthermore, it can also participate in protein protection, forming disulfide bonds with protein thiols (protecting thiol groups from oxidation and regulating protein activity) and resistance to xenobiotics (Fig. 1) [7, 8]. Thus, GSH has the ability to prevent cellular damage induced by oxidative stress. Therefore, the levels of intracellular GSH can indicate the redox state and cellular health [9].

Dysregulation of GSH homeostasis is present in many pathological conditions, such as diabetes, AIDS, tuberculosis, Alzheimer's disease, myocardial infarction, rheumatoid arthritis, alcoholic liver diseases, and cancer. Thus, the measure of GSH concentration could demonstrate the vulnerability of organisms to the development of metabolic dysfunctions [10]. In this chapter, a GSH quantification method will be described.

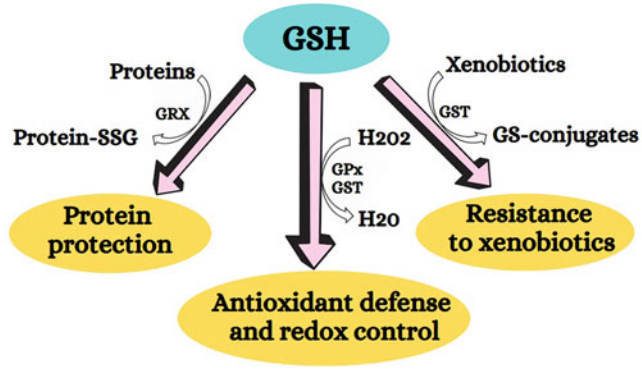

Fig. 1 The main functions of GSH. Protein oxidation protection (GRX); participation in the scavenging of ROS through glutathione peroxidases (GPx) and glutathione S-transferases action (GST); resistance to xenobiotics with GS-conjugates formation

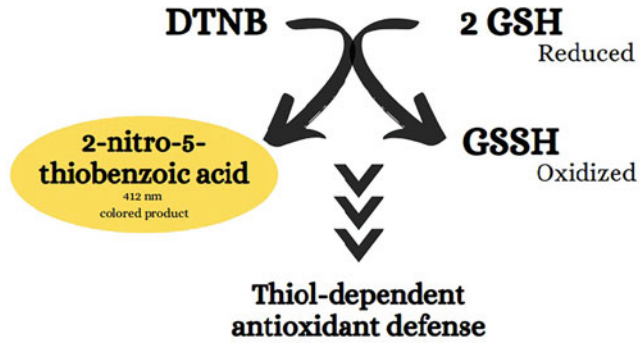

Fig. 2 Principle of the reaction of Ellman's reagent with GSH. 5,5′-dithiobis (2-nitrobenzoic acid) (DTNB)

In the method described in this chapter, GSH reacts with 5,5′-dithiobis (2-nitrobenzoic acid), that is, DTNB, also called the Ellman's reagent. The reagent reacts with 98% of all biological thiols and enables accurate measurement of GSH in most tissues. Samples need deproteination reactions prior to the assay to exclude the reaction of thiol groups in protein. In the DTNB-based reaction, the 5,5′-dithiobis (2-nitrobenzoic acid) is converted into 2-nitro-5-mercapto-benzoic acid (TNB), which possesses its absorption maximum at 412 nm, showing a yellow-colored reaction (Fig. 2) [11]. The Ellman's GSH method is rapid, inexpensive, and accurate [12].

2 Material

Prepare all solutions using distilled water and analytical grade reagents as described.

2.1 Phosphate Buffer Saline (PBS)

Phosphate buffer saline (0.1 M; pH 7.4):

1. Weigh 3.4 g sodium phosphate monobasic and transfer to a glass beaker. Add 200 mL water and mix well. Transfer to a 250 mL volumetric flask and complete the volume.
2. Weigh 3.55 g sodium phosphate dibasic and transfer to a glass beaker. Add 200 mL water and mix well. Transfer to a 250 mL volumetric flask and complete the volume.
3. Adjust the phosphate bibasic solution's pH with a phosphate monobasic solution using a pH meter (*see* **Note 1**). Store in a glass flask at 4 °C.

2.2 Tris/EDTA Buffer

Tris/EDTA buffer (1 mM Tris buffer; pH 8.2):

1. Weigh 12 mg (hydroxymethyl)aminomethane (Tris) and transfer to a glass beaker. Add 100 mL water and homogenize (*see* **Note 2**). Adjust the pH to 8.2 with 1 M HCl. Then, prepare the 2 mM ethylenediaminetetraacetic acid (EDTA) solution.
2. Weigh 37.5 mg EDTA and transfer to a small glass beaker. Add 5 mL distilled water and mix well. Add 100 μL EDTA solution to the Tris–HCl solution. Store in a glass flask at 4 °C.

2.3 Sample Preparation

1. Serum samples: Collect blood and allow it to clot for 30 min at room temperature (24 °C). Centrifuge the clotted blood at 2000 × g for 15 min at 4 °C. Collect the supernatant to a 1.5 mL microtube and store it on ice.
2. Tissue homogenate: For approximately 100 mg tissue (i.e., liver, brain, intestine) in an Eppendorf tube, add 1 mL PBS and homogenate using an appropriated homogenizer. Centrifuge at 10,000 × g for 15 min at 4 °C. Collect the supernatant to a 1.5 mL microtube and store it on ice. Determine protein concentration in the homogenates through Bradford assay [13].

Serum and tissue homogenate deproteination: Add around 3 volumes of cold 5% trichloroacetic acid (TCA) or 0.75 mol/L metaphosphoric acid (MPA) to 1 volume of serum or tissue homogenate supernatant (Note: sometimes use 4:1) and centrifuge at 12,000 × g for 5 min at 4 °C. Collect the supernatant to a 1.5 mL microtube and store it on ice for immediate use, or storage at −80 °C for later use (*see* **Note 3**).

Table 1
Standard curve preparation and concentration points

Standards	GSH's stock solution (μL)	PBS (μL)	Concentration (nmol/mL)
A	0	400	0
B	2	398	2.5
C	5	395	6.25
D	20	380	25
E	50	350	62.5
F	100	300	125
G	200	200	250
H	400	0	500

Dilution before assay: After protein precipitation, samples should be diluted in PBS as appropriated (*see* **Note 4**).

2.4 Standard Curve

Stock solution of L-glutathione reduced (50 μmol/mL): Weigh 154 mg L-glutathione reduced and transfer to a small glass beaker. Add 9 mL distilled water and mix well. Transfer to a 10 mL volumetric flask, complete the volume, and homogenize. In a 1.5 mL microtube, dilute 10 μL this solution into 990 μL PBS (*see* **Note 5**). Then, prepare the standard curve as follows (Table 1):

2.5 DTNB Solution

5,5′-Dithiobis(2-nitrobenzoic acid) – 10 mmol/L DTNB solution: Weigh 20 mg DTNB and transfer to a small glass beaker. Add 5 mL methanol and mix well (*see* **Note 6**).

3 Methods

All procedures should be carried out at room temperature (24 °C) unless otherwise specified (*see* **Note 7**).

3.1 Assay Procedure

- In a 96-well flat-bottom UV-transparent microplate, add 100 μL Tris/EDTA buffer to all wells.
- Add 100 μL standard solution or samples to previously defined well (*see* **Notes 8** and **9**).
- Read at 412 nm in a microplate reader (reading 1).
- Add 20 μL DTNB solution readily prepared to all wells.
- Incubate for 15 min at room temperature (24 °C) (*see* **Note 10**).
- Read again at 412 nm in the microplate reader (reading 2).

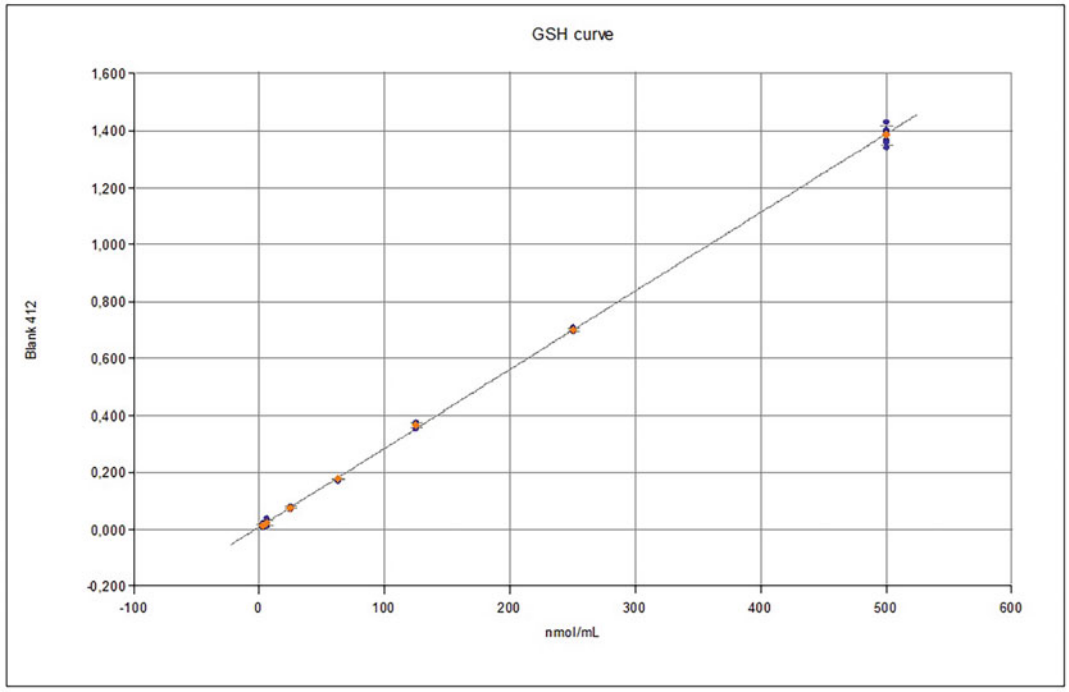

Curve Name	Curve Formula	A	B	R2
GSH (nmol)	Y=A*X+B	0.00276	0.00861	0.999

Fig. 3 GSH standard curve example

3.2 Calculations

- Subtract the standard A (blank) absorbance value from all other values (standards and samples) after readings 1 and 2.
- Calculate the average absorbance for each standard and sample.
- Plot the standard (A-H) curve absorbance by graphing it against the concentration of GSH in the curve (Fig. 3).
- Calculate the standard curve equation (*see* **Note 11**).
- Calculate the total GSH using the linear regression equation and multiplicate by the dilution factor

$$\text{Total GSH} = \left[\frac{(\text{Absorbance at 412 nm}) - (y - \text{intercept})}{\text{Slope}}\right] \times \text{dilution factor} \quad (1)$$

- In serum, express the results as nmol GSH/mL.
- For tissues, divide by the protein concentration in the homogenate.
- Express the results as nmol GSH/mg tissue protein.

4 Notes

1. To prepare PBS, follow the correct order using a pH meter, adding monobasic buffer in the bibasic buffer. The monobasic and bibasic buffers can be stocked separately at 4 °C, and mixed on the day of the assay by calculating how much it will be used daily.
2. Using ultrasound homogenization is the quickest way to dissolve the Tris solution.
3. Samples must always be kept on ice, as well as be defrosted from −80 °C on ice. Depending on how much will be defrosted on ice, it can take a long time, so having small aliquots could help to optimize the time spending on sample preparation.
4. Suggested dilutions for serum samples and tissue homogenates according to methods and species:

Samples	Species	Protein quantification (Bradford)	Deproteination reagent	Dilution in PBS before assay	Ref.
Serum	Swiss mice	–	Dilute 3× in 0.75 mol/L MPA	Dilute homogenate 4×	[14, 15]
Brain	Swiss mice	Dilute homogenate 21×	Dilute 3× in 0.75 mol/L MPA	Dilute homogenate 3.5×	[14, 15]
Liver	Swiss mice	Dilute homogenate 200×	Dilute 3× in 0.75 mol/L MPA	Dilute homogenate 6.5×	[16]
Liver	Sprague-Dawleyrats	Dilute homogenate 10×	Homogenate 10× in 5% TCA	Dilute homogenate 5×	[17]
Pancreas	Sprague-Dawley rats	Dilute homogenate 10×	Homogenate 10× in 5% TCA	Dilute homogenate 5×	[17]
Kidney	Sprague-Dawley rats	Dilute homogenate 10×	Homogenate 10× in 5% TCA	Dilute homogenate 5×	[17]

5. The GSH standard stock solution (50 μmol/mL) can be stored at −80 °C and defrosted together with samples on ice.
6. DTNB is sensible to light. It should be prepared just before use in an aluminum foil-covered glass beaker.
7. All solutions stocked at cold temperatures should reach room temperature (24 °C) before use.
8. Before pipetting samples and standards, prepare a microplate layout. Samples and standards should be made in triplicate.

9. Use a new standard curve for each microplate.
10. Incubate the microplate for the DTNB reaction in dark conditions. You can use aluminum foil or hide the microplate inside a dark chamber.
11. Standard curve linearity is best when R^2 is close to 1.

References

1. Calabrese G, Morgan B, Riemer J (2017) Mitochondrial glutathione: regulation and functions. Antioxidant R Signal 27:1162–1177. https://doi.org/10.1089/ars.2017.7121
2. Okazaki K, Papagiannakopoulos T, Motohashi H (2020) Metabolic features of cancer cells in NRF2 addiction status. Biophys Rev 12:435–441. https://doi.org/10.1007/s12551-020-00659-8
3. Lu SC (2020) Dysregulation of glutathione synthesis in liver disease. Liver Res 4:64–73. https://doi.org/10.1016/j.livres.2020.05.003
4. Bachhawat AK, Kaur A (2017) Glutathione degradation. Antioxidants redox. Signals 27:1200–1216. https://doi.org/10.1089/ars.2017.7136
5. Kwon DH, Cha HJ, Lee H et al (2019) Protective effect of glutathione against oxidative stress-induced cytotoxicity in RAW 264.7 macrophages through activating the nuclear factor erythroid 2-related factor-2/heme oxygenase-1 pathway. Antioxidants 82:1–17. https://doi.org/10.3390/antiox8040082
6. Calabrese G, Morgan B, Riemer J (2017) Mitochondrial glutathione: regulation and functions. Antioxidants Redox Signal 27:1162–1777. https://doi.org/10.1089/ars.2017.7121
7. Mailloux RJ (2020) Protein S-glutathionylation reactions as a global inhibitor of cell metabolism for the desensitization of hydrogen peroxide signals. Redox Biol 32:1–11. https://doi.org/10.1016/j.redox.2020.101472
8. Conrad M, Friedmann Angeli JP (2018) Glutathione peroxidases. In: Comprehensive toxicology, 3rd edn, Tucson, Academic Press
9. Zhou X, He L, Zuo S et al (2018) Serine prevented high-fat diet-induced oxidative stress by activating AMPK and epigenetically modulating the expression of glutathione synthesis-related genes. Biochim Biophys Acta Mol basis Dis 80:488–498. https://doi.org/10.1016/j.bbadis.2017.11.009
10. Coulston AM, Boushey CJ, Ferruzzi MG et al (2017) Nutrition in the prevention and treatment of disease. West Lafayette, eBook ISBN: 9780128029473
11. Ellman GL (1959) Tissue sulfhydryl groups. Arch Biochem Biophys 82:70–77. https://doi.org/10.1016/0003-9861(59)90090-6
12. Giustarini D, Fanti P, Matteucci E et al (2014) Micro-method for the determination of glutathione in human blood. J Chromatogr B Anal Technol Biomed Life Sci 964:191–194. https://doi.org/10.1016/j.jchromb.2014.02.018
13. Bradford MM (1976) A rapid and sensitive method for the quantitation of microgram quantities of protein utilizing the principle of protein-dye binding. Anal Biochem 72:248–254. https://doi.org/10.1016/0003-2697(76)90527-3
14. Batista ÂG, Soares ES, Mendonça MCP et al (2017) Jaboticaba berry peel intake prevents insulin-resistance-induced tau phosphorylation in mice. Mol Nutr Food Res 61:1–10. https://doi.org/10.1002/mnfr.201600952
15. Batista ÂG, Mendonça MCP, Soares ES et al (2020) Syzygium malaccense fruit supplementation protects mice brain against high-fat diet impairment and improves cognitive functions. J Funct Foods. https://doi.org/10.1016/j.jff.2019.103745
16. Batista ÂG, da Silva-Maia JK, Mendonça MCP et al (2018) Jaboticaba berry peel intake increases short chain fatty acids production and prevent hepatic steatosis in mice fed high-fat diet. J Funct Foods 48:266–274. https://doi.org/10.1016/j.jff.2018.07.020
17. Batista ÂG, Lenquiste SA, Cazarin CBB et al (2014) Intake of Jaboticaba peel attenuates oxidative stress in tissues and reduces circulating saturated lipids of rats with high-fat diet-induced obesity. J Funct Foods 50:50–461. https://doi.org/10.1016/j.jff.2013.11.011

Chapter 13

Guidance for Designing a Preclinical Bioavailability Study of Bioactive Compounds

Helena Dias de Freitas Queiroz Barros, Cinthia Baú Betim Cazarin, and Mario Roberto Maróstica Junior

Abstract

The bioavailability of a bioactive compound is a fraction that reaches the systemic circulation and becomes available for its biological fate. This is significant since it provides new insights to understand the possible mechanisms of action. This guide shows some relevant aspects to consider when designing preclinical studies that assess the bioavailability of bioactive compounds in rodents. In this chapter, the following topics will be addressed: choice of animal model, sample size, route of administration of the compound of interest, fasting, blood collection tubes, sample collection, and description of the animal experiment for obtaining blood samples from rodents at six different times.

Key words Experimental design, Bioavailability, Bioactive compounds, Rodents, Plasma

1 Introduction

Each culture has its specific eating habits. The consumption profile of a given population can promote health or increase the risk of chronic diseases. Despite cultural differences in eating habits worldwide, some healthy habits are shared, including fruits and vegetables consumption [1].

Health benefits of fruit consumption may be associated with bioactive compounds. Bioactive compounds are small amounts of extra-nutritional substances in the food matrix [2] that have been widely investigated in epidemiological and biological studies, suggesting their chemopreventive roles in some types of cancers [2, 3] and their control of hyperlipidemia and cardiovascular disease [2, 4].

Bioactive compounds vary widely in chemical structure and function and are grouped accordingly. They are extensively studied due to their role in reducing reactive oxygen and nitrogen species in the pathogenesis of degenerative diseases, such as arteriosclerotic

Cinthia Baú Betim Cazarin (ed.), *Basic Protocols in Foods and Nutrition*,
Methods and Protocols in Food Science, https://doi.org/10.1007/978-1-0716-2345-9_13,

vascular disease, cancer, and chronic inflammation [5, 6]. However, the amount of these substances that reach the target tissues is lower in experimental models than in in vitro studies. These differences could be partially explained by the substance bioaccessibility and chemical modifications during the digestion [7].

Bioavailability was first defined in pharmacology as the rate and extent to which a drug reaches its site of action. Over the years, the definition of bioavailability was updated, and nowadays, it is widely described as "the fraction of an ingested nutrient or compound that reaches the systemic circulation and specific sites where it can exert its biological action" [8].

The bioavailability of bioactive compounds must be evaluated regarding the possible health benefits of these compounds. In fact, since many questions about antioxidants are still unanswered, some bioactive compounds do not have recommended doses of consumption. However, we emphasize that greater doses are not associated with better results, and low concentrations can sometimes positively affect health [9]. In this context, methodologies investigating the bioavailability of bioactive compounds are necessary. This chapter presents some significant considerations when planning a preclinical experimental study, focusing on the characteristics of bioactive compound, choice of animal model, sample size, route of administration, fasting, differences in blood collection tubes, sample collection, experimental design, and sample analysis.

2 Important Considerations

2.1 Characteristics of Bioactive Compounds

A bioactive compound is a chemical substance present in fruits and vegetables that, when ingested, can benefit on health [2–4, 10]. Most bioactive compounds are secondary metabolites produced in plants for protection and survival. These compounds are classified into major groups according to their chemical structure: polyphenols, alkaloids, terpenoids, polyacetylenes, polyenes, miscellaneous pigments, cyanogenic glycosides, glucosinolates, and nonprotein amino acids [11]. Also, they can be classified according to their solubility and physiological absorption properties: hydrophilic and lipophilic.

After consumption, food components undergo many transformations, including gastrointestinal digestion (which may include release from food matrix), absorption, metabolism, tissue distribution, and nutrient/compound bioactivity [12]. All biotransformation in these substances during the digestion and post-absorption can produce metabolites with different activity, which means that the biological effect is not necessarily associated with the native structure found in the food matrix [11].

The structure and physicochemical characteristics of bioactive compounds [10], the particularities related to gastric emptying, and the gastrointestinal transit time [12] directly affect

bioavailability [10, 12]. Indeed, absorption mechanisms for lipophilic compounds depend on micellization (carotenoids and fat-soluble vitamins), whereas hydrophilic compounds do not (polyphenols and hydrophilic vitamins) [13].

Regarding hydrophilic phenolic compounds, once they reach the small intestine, part of them is transformed by enzymatic hydrolysis at the brush border, generating aglycones, which are readily absorbed by the small intestine. The remaining ones transit to the large intestine, where they are biotransformed by gut microbiota. The gut microbiota forms metabolites that are promptly absorbed to exert their benefits. Lipophilic compounds (carotenoids), previously absorbed in the small intestine, must be released from the food matrix and then incorporated into micelles [13].

2.2 Choice of Animal Model

To select the appropriate animal model for the research, one must consider that no model is inherently "good" or "bad." The specificities of a model can only be judged in the context of the research. Therefore, the first consideration should regard the research aim. However, factors such as availability, cost, and ease of maintenance must also be considered [14]. As an example, rodents, such as mice and rats, are widely used because they are relatively small, require less space and resources to maintain, have high reproductive potential, and easily adapt to varied environments and sociability [15].

Furthermore, rodents are similar to humans regarding anatomy and physiology [16, 17]. The mechanisms associated with cellular function and differentiation are similar between humans and mice. Most of the mouse genes (99%) resemble the human genome, making the murine (*Mus musculus*) an ideal model for genomic studies as well as for the modulation of some molecular pathways associated with the development of noncommunicable diseases (cancer, cardiovascular diseases, diabetes, and arthritis) [18].

2.3 How Many Animals per Group?

Experimental studies are radically different from human studies because many have used inbred animals, who have a remarkably similar background. Thus, these studies need fewer animals (when compared to human studies) because variables such as genetic difference [19] and control of environmental conditions (such as breeding and housing) [20] have minimum effects.

Ethically, the principle of 3Rs (Reduction, Refinement, and Replacement) should be considered in all experimental protocols to use fewer animals in each experimental group, to decrease experimental procedures that promote animals' suffering, and to replace substituting the animals for in vitro approaches when possible [21].

The most used scientific method to determine sample size is power analysis [22]. Six major concepts must be prioritized by a researcher when the power analysis approach is considered for sample size:

1. *Effect size:* the minimum difference between two groups which can be considered clinically significant [23].
2. *Standard deviation:* the measure of variability within a sample for a quantitative variable [23].
3. *Type 1 error:* significance level, usually fixed at 5%, which is an arbitrary value that can be decreased or increased according to the research question [22].
4. *Power:* the probability of finding an effect, possibly kept between 80 and even 99% depending on the research question, but usually kept at 80% [22].
5. *Statistical test:* the statistical method that will be applied to the data obtained (parametric or nonparametric tests) must be established [22].
6. *Expected attrition or death of animals:* the final experimental size should be adjusted according to the expected loss in some experimental models. If a 10% animal loss is expected in an experiment, more animals should be considered, dividing the calculated group size by 0.9 [22].

Sample size is a significant parameter for preclinical studies and should be planned ahead of the study [19, 22]. If the researchers choose a smaller number than necessary, it can lead to loss of any significant difference in the population, and if a larger number is chosen, it can lead to resources waste and ethical issues [22].

2.4 Route of Administration

For bioavailability studies, which are the focus of this chapter, the test substance can be administered to rodents by oral gavage or by incorporation into their diet. However, before adding the bioactive compound to diet, interactions with other components should be considered, since they can directly affect the compound's bioaccessibility. On the other hand, oral gavage offers greater control over the dose and administration time, especially in acute studies, in which a single dose of the compound of interest is administered [24]. Moreover, working with fasting animals can reduce the bias associated with the interaction of compounds and diet.

2.5 Fasting

Fasting in rodents—such as mice or rats—is a common procedure which, associated with several types of experiments, reduces the variability of investigative parameters. Fasting stimulation is used to assure that xenobiotics (which include bioactive compounds) are absorbed more consistently and to avoid mixing test compounds with the diet [25]. We emphasize that fasting refers to a state where the animal is completely deprived of food but has access to water for a predetermined time.

Water intake can be affected by fasting in rodents. It increases with greater food intake, since they usually ingest the right volume of water needed for food digestion and excretion of feces.

Table 1
Relative body weight loss in fasting mice and rats

Strain	Age/weight	Duration of fasting (h)	Weight loss (%)	Reference
C57BL/6 J/ male	9 weeks	5	5	Revised by JENSEN et al. [25]
C57BL/6 J/ male	9 weeks	18	16	Revised by JENSEN et al. [25]
Swiss albino/ male	15–18 g	18	17	Revised by JENSEN et al. [25]
Wistar rat/male	10–12 weeks	4	~2	[29]
Wistar rat/male	10–12 weeks	8	~4	[29]
Wistar rat/male	10–12 weeks	16	~8	[29]
Wistar rat/male	10–12 weeks	24	~10	[29]
Wistar rat/male	10–12 weeks	48	~12	[29]
Wistar rat/female	10–12 weeks	4	2	[29]
Wistar rat/female	10–12 weeks	8	~4	[29]
Wistar rat/female	10–12 weeks	16	6	[29]
Wistar rat/female	10–12 weeks	24	~8	[29]
Wistar rat/female	10–12 weeks	48	~11	[29]

However, while fasting, animals tend to ingest less water than when normally fed (ad libitum access to food) because water does not need to be diverted for food digestion [25, 26].

Fasting is an adaptive state of metabolism that stimulates gluconeogenesis (use of noncarbohydrate carbon substrate) to reestablish glucose homeostasis [27]. Therefore, high fasting times affect rodents' weight. Mice significantly lose weight after 12, 18, 24, 48, and 72 h of fasting. After 12 h of fasting, weight loss was stable at a rate of approximately 7% of the mice's weight per day, based on records of a total of 72 h [25]. Table 1 shows the relative body weight loss (%) of fasted mice.

Also, fasting is related to gastrointestinal emptying. Prior et al. [28] assessed the shortest fasting period that could be used to promote gastric emptying and intestinal transit. Four different times were analyzed (0, 3, 6, and 18 h). Then, the stomach and intestine were evaluated. Animals with 6 h fasting showed the same

gastric emptying and intestinal transit as those observed in 18 h fasting. The authors also observed that shortening the fasting period reduced body weight loss, and mice on shorter fasts could be group-housed as the hunger-induced struggle diminished.

2.6 Blood Collection Tubes: How to Choose?

Blood is composed of plasma, a cellular component consisting of red and white blood cells and platelets. The plasma fraction is obtained using tubes with anticoagulants to collect the blood, followed by simple centrifugation to recover the supernatant. However, if no anticoagulant is added, the sample clots, and the supernatant fluid is denominated serum, which is less viscous than plasma, with the absence of fibrinogen, prothrombin, and other clotting proteins [30].

Blood is the most common biofluid used to analyze metabolites since it is easy to obtain and to process and is mostly more homogeneous than urine—which is influenced by the fluid flow rates [31]. Moreover, blood, plasma, and serum show the best correlation between pharmacologic effect and compound concentration [32].

When working with biofluids, metabolite integrity must be maintained. Collect and processing samples exposes the metabolites to degradation and alterations (e.g., enzymatic degradation or oxidation), and the anticoagulant is an important variable to preserve their integrity [33].

Several blood collection tubes are used to sampling plasma, and the main anticoagulants used are ethylenediaminetetraacetic acid (EDTA), heparin, and sodium citrate. EDTA binds to divalent metal cations—such as Ca^{2+} and Mg^{2+}—required for enzyme cofactors. Heparin binds with electrolytes, changing the concentration of free and bound ions. At the same time, sodium citrate chelates cations by inhibiting aspartate aminotransferase and alkaline phosphatase [34]. Paglia et al. [35] assessed the influence of EDTA and citrate collection tubes on the quantitative target metabolomics in plasma and serum samples. They observed that samples collected in plasma citrate seemed to cluster more tightly, suggesting a lower biological variation.

Hemolysis is also another critical part of working with blood collection and processing. It can strongly influence result reliability and is classified as a preclinical factor which causes variation in clinical chemistry testing and as one of the major determinants of preclinical variability [36]. Hemolysis is characterized by the membrane disruption of red blood cells and other blood cells, releasing intracellular components into the serum or plasma [37]. It can be caused by improper sample drawing (i.e., indwelling catheters or tiny needles), handling (i.e., vigorous mixing or shaking blood samples after collection), or sample re-spun after centrifugation [38, 39].

Hemolysis can affect spectrophotometric reading, especially at 415, 540, and 570 nm wavelengths, increasing intracellular components not found in plasma, diluting the sample, or increasing biologically active substances that may activate/inactivate biological pathways [36, 39]. The degree of interference observed depends on the hemolysis level and on the assay methodology [36].

3 Materials and Methods to Collect Samples

3.1 Materials

Before starting any animal experiment, approval from the Animal Use Ethics Committee is required.

List of materials needed for the experiment:

- Clean cages.
- Gavage needle.
- 1 mL syringe
- Anesthetic (e.g., ketamine hydrochloride and xylazine hydrochloride).
- 25G needle to collect blood by cardiac puncture
- Dissecting forceps.
- Dissecting scissors.
- Blood collection tubes.
- 1.5 mL microcentrifuge tubes to store plasma samples
- 2.0 mL microcentrifuge tubes to store tissues samples
- Liquid nitrogen to store tissues.
- Styrofoam box with ice to store blood collection tubes or Styrofoam with dry ice to store plasma tubes.
- Ethanol.
- 200 uL pipette
- 200 uL tips
- Gloves.
- Refrigerated centrifuge.

3.2 Methods

The temperature of the animal's facility should range between 20 and 26 °C [20], with humidity ranging 50–60%. Also, 12 h light/dark cycle must be respected (considering the normal circadian cycle). During acclimatization, food and water should be ad libitum.

1. Rodents (mice or rats) should be randomly selected and housed in three per cage.
2. The animals must be acclimatized for 1 week, or until reaching the desired age or weight.

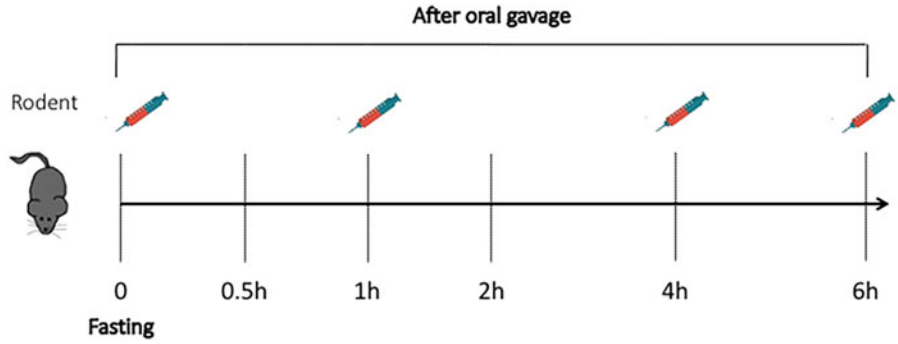

Fig. 1 Experimental design to study the bioavailability of bioactive compounds in rodents

Oral Gavage Hour	Animal 1	Animal 2	Animal 3	Animal 4	Animal 5	Animal 6
10:00 am						
10:05 am						
10:10 am						
10:15 am						
12:30 am						
1:30 pm						
Dissection Hour	4:00 pm	2:05 pm	12:10 am	11:15 am	1:00 pm	1:30 pm

Chart 1 Timetable for oral gavage, blood, and tissues dissection

3. To assess the bioavailability of phenolic compounds, for example, one can use six different time points to collect blood (*see* **Note 1**) just after the oral gavage (time 0), 0.5 h, 1 h, 2 h, 4 h, and 6 h after the gavage, as shown in Fig. 1.
4. On the day of the experiment, animals should be individually identified with marks on the tail and fast for 6 h prior to oral gavage, with water ad libitum.
5. The tested compound must be dissolved in a solution (*see* **Note 2**), and all materials needed for the experiment should be identified and separated (*see* **Note 3**).
6. After 6 h of fasting, the animals should be weighed prior to dose administration to assess the effects of fasting on animal body weight.
7. Collect the blood to start, and then proceed with the gavage. The first animal to receive gavage is the animal who fasted for 6 h. Chart 1 shows a timetable of gavage and dissection (*see* **Note 4**).

8. Blood must be collected by cardiac puncture, using anesthetized mice or rats (chosen model to be described in this chapter).
9. The collected blood should be transferred to a microcentrifuge with anticoagulants (*see* **Note 5**).
10. The tubes must be centrifuged to obtain the plasma, and the plasma must be transferred to new microcentrifuge tubes.
11. After blood collection, the tissues of interest must be collected and stored adequately in microcentrifuge tubes.
12. Biofluids and tissue samples should be stored at −80 °C on ice during processing for further analysis (*see* **Note 6**).

3.3 Analyzing the Plasma Samples

The blood of vertebrate animals is composed of blood cells suspended in blood plasma. Plasma, which represents about 55% of blood fluid (composed mostly of water, 92% by volume), contains dissipated proteins, glucose, mineral ions, hormones, carbon dioxide (since it is the main medium for excretory product transportation), and blood cells [32], some of which can affect target analyte detection [40].

Bioactive compounds, such as polyphenol metabolites, have a high reversible binding affinity to plasma proteins [40]. Therefore, the bond between xenobiotic and protein, among other forms, will depend on their affinity. Generally, acidic compounds tend to bind to albumin, whereas basic compounds bind to α_1-acid glycoprotein (AAG), neutral components can bind to both human serum albumin (HSA) and AAG, and neutral lipophilic compounds bind to lipoproteins [41]. To minimize matrix effects and better identify/quantify the compounds of interest, sample preparation is essential to increase the selectivity of target compounds making the sample suitable to provide reliable and accurate results [32].

Sample preparation is the most time-consuming step of biological analysis [32], and several types of research are conducted to assess methods of biological sample preparation. Before sample injection in the equipment (LC, GC, etc.), sample preparations also: (1) reduce matrix interferences or undesired endogenous compounds; (2) increase selectivity for target analytes; (3) preconcentrate the sample to enhance sensitivity; and (4) stabilize the sample by reconstituting in an inert solvent [42].

Two different analytical techniques are commonly used to detect metabolites in biofluids: nuclear magnetic resonance (NMR) and mass spectrometry (MS), both with positive and negative aspects; however, neither can completely identify and quantify all metabolites in the sample [43, 44]. MS is generally more sensitive than NMR and detects metabolites below the NMR thresholds of detection [45].

MS analysis is usually combined with chromatographic separation of metabolites, using either gas (GC) or liquid chromatography (LC) [46] to improve sensitivity and resolution of metabolite detection [47]. Liquid chromatography (LC-MS) is probably the most used method to detect metabolites since it can separate and detect a wide range of molecules with different physicochemical properties [42, 45]. Moreover, it collects both quantitative and structural information, achieving sensitivities of pg mL^{-1} [45]. GC-MS only analyzes small volatile molecules and molecules that can be made volatile [45]. GC-MS analysis requires sufficient vapor pressure and thermally stable analytes. When polar metabolites are analyzed, functional groups must be derivatized to increase thermal stability and volatility [48].

Since metabolites have an enormous physiochemical diversity, to identify and to quantify them in biological samples can be difficult. The complementation of diverse analytical techniques, including NRM, GC-MS, and LC-MS, can detect a higher number of metabolites, providing new insights to understand biological systems [47].

4 Notes

1. Depending on the compound that you are evaluating, blood samples collection times can vary. You should consider half-life, time of metabolization, and excretion of the compound to be studied.
2. The chemical characteristics of the studied compounds should be considered. If the compound is hydrophilic, for example, it may dissolve in water; however, if the compound is lipophilic, you can use soybean oil or another lipophilic medium.
3. It is recommended to work with a maximum of six animals per day.
4. One can use Chart 1 to plan all steps of the experiment. As an example, animal 1 should receive gavage at 10 am and be dissected 6 h later, at 4 pm. This chart will help you to avoid mistakes.
5. Remember to carefully shake the tubes so that the anticoagulant is incorporated within the sample.
6. Unnecessary freezing/defrost cycles of samples should be avoided. Instead, make aliquots of the samples considering all the analyses planned in your protocol.

Acknowledgments

The authors thank Espaço da Escrita – Pró-Reitoria de Pesquisa – UNICAMP – for the language services provided.

References

1. Kris-Etherton PM et al (2002) Bioactive compounds in foods: their role in the prevention of cardiovascular disease and cancer. Am J Med 113(Suppl 9B):71S–88S
2. Kitts DD (1994) Bioactive substances in food: identification and potential uses. Can J Physiol Pharmacol 72(4):423–434
3. Subramaniam S, Selvaduray KR, Radhakrishnan AK (2019) Bioactive compounds: natural defense against cancer? Biomol Ther 9(12)
4. Casas R et al (2018) Nutrition and cardiovascular health. Int J Mol Sci 19(12):3988
5. Skrovankova S et al (2015) Bioactive compounds and antioxidant activity in different types of berries. Int J Mol Sci 16(10): 24673–24706
6. Karakaya S (2004) Bioavailability of phenolic compounds. Crit Rev Food Sci Nutr 44(6): 453–464
7. Souza JE, Casanova LM, Costa SS (2015) Bioavailability of phenolic compounds: a major challenge for drug development? Revista Fitos 9(1):1–72
8. D'Archivio M et al (2010) Bioavailability of the polyphenols: status and controversies. Int J Mol Sci 11(4):1321–1342
9. Porrini M, Riso P (2008) Factors influencing the bioavailability of antioxidants in foods: a critical appraisal. Nutr Metab Cardiovasc Dis 18(10):647–650
10. Dima C et al (2020) Bioavailability and bioaccessibility of food bioactive compounds; overview and assessment by in vitro methods. Compr Rev Food Sci Food Saf 19(6): 2862–2884
11. Neilson AP, Goodrich KM, Ferruzzi MG (2017) Chapter 15 – Bioavailability and metabolism of bioactive compounds from foods. In: Coulston AM et al (eds) Nutrition in the prevention and treatment of disease, 4th edn. San Diego California, USA, Academic Press, pp 301–319
12. Angelino D et al (2017) Bioaccessibility and bioavailability of phenolic compounds in bread: a review. Food Funct 8(7):2368–2393
13. Barba FJ et al (2017) Bioaccessibility of bioactive compounds from fruits and vegetables after thermal and nonthermal processing. Trends Food Sci Technol 67:195–206
14. Sprott RL (1999) How to choose an animal model. In: Sternberg H, Timiras PS (eds) Studies of aging. Springer, Berlin, Heidelberg, pp 105–110
15. Andersen ML et al (2016) Care and maintenance of laboratory animals. In: Andersen M, Tufik S (eds) Rodent model as tools in ethical biomedical research. Springer, Cham, pp 23–37
16. Gibbs RA et al (2004) Genome sequence of the Brown Norway rat yields insights into mammalian evolution. Nature 428(6982):493–521
17. Chinwalla AT et al (2002) Initial sequencing and comparative analysis of the mouse genome. Nature 420(6915):520–562
18. Dutta S, Sengupta P (2016) Men and mice: relating their ages. Life Sci 152:244–248
19. Serdar CC et al (2021) Sample size, power and effect size revisited: simplified and practical approaches in pre-clinical, clinical and laboratory studies. Biochem Med (Zagreb) 31(1): 010502
20. National Research Council (2011) Guide for the care and use of laboratory animals. 2011 [cited 2021 December 21st, 2021]; Eighth Ed.:Available from: https://www.ncbi.nlm.nih.gov/books/NBK54050/
21. Russell WMS, Burch RL (1959) The principles of humane experimental technique. Methuen, London
22. Charan J, Kantharia ND (2013) How to calculate sample size in animal studies? J Pharmacol Pharmacother 4(4):303–306
23. Arifin WN, Zahiruddin WM (2017) Sample size calculation in animal studies using resource equation approach. Malaysian J Med Sci 24(5): 101–105
24. Singhvi SM et al (1981) Absorption and bioavailability of captopril in mice and rats after administration by gavage and in the diet. J Pharm Sci 70(8):885–888
25. Jensen TL et al (2013) Fasting of mice: a review. Lab Anim 47(4):225–240
26. Kutscher CL (1971) Incidence of food-deprivation polydipsia in the white Swiss mouse. Physiol Behav 7(3):395–399
27. Kinouchi K et al (2018) Fasting imparts a switch to alternative daily pathways in liver and muscle. Cell Rep 25(12):3299–3314.e6
28. Prior H et al (2012) Refinement of the charcoal meal study by reduction of the fasting period. Altern Lab Anim 40(2):99–107
29. Kale VP et al (2009) Effect of fasting duration on clinical pathology results in Wistar rats. Vet Clin Pathol 38(3):361–366
30. Psychogios N et al (2011) The human serum metabolome. PLoS One 6(2):e16957

31. Lundblad R (2003) Considerations for the use of blood plasma and serum for proteomic analysis. Internet J Gen Prot 1(2). Available in: https://print.ispub.com/api/0/ispub-article/3649
32. Niu Z et al (2018) Recent advances in biological sample preparation methods coupled with chromatography, spectrometry and electrochemistry analysis techniques. TrAC Trends Anal Chem 102:123–146
33. Khadka M et al (2019) The effect of anticoagulants, temperature, and time on the human plasma metabolome and lipidome from healthy donors as determined by liquid chromatography-mass spectrometry. Biomol Ther 9(5):200
34. Kennedy AD et al (2021) Global biochemical analysis of plasma, serum and whole blood collected using various anticoagulant additives. PLoS One 16(4):e0249797
35. Paglia G et al (2018) Influence of collection tubes during quantitative targeted metabolomics studies in human blood samples. Clin Chim Acta 486:320–328
36. Simundic AM et al (2020) Managing hemolyzed samples in clinical laboratories. Crit Rev Clin Lab Sci 57(1):1–21
37. Marques-Garcia F (2020) Methods for hemolysis interference study in laboratory medicine - a critical review. EJIFCC 31(1):85–97
38. Koseoglu M et al (2011) Effects of hemolysis interferences on routine biochemistry parameters. Biochem Med (Zagreb) 21(1):79–85
39. Lippi G et al (2019) Blood sample quality. Diagnosis (Berl) 6(1):25–31
40. López-Yerena A et al (2021) Metabolomics technologies for the identification and quantification of dietary phenolic compound metabolites: an overview. Antioxidants (Basel) 10(6):846
41. López-Yerena A et al (2020) Insights into the binding of dietary phenolic compounds to human serum albumin and food-drug interactions. Pharmaceutics 12(11):1123
42. Kohler I, Schappler J, Rudaz S (2013) Microextraction techniques combined with capillary electrophoresis in bioanalysis. Anal Bioanal Chem 405(1):125–141
43. Emwas AH (2015) The strengths and weaknesses of NMR spectroscopy and mass spectrometry with particular focus on metabolomics research. Methods Mol Biol 1277:161–193
44. Bouatra S et al (2013) The human urine metabolome. PLoS One 8(9):e73076
45. Theodoridis GA et al (2012) Liquid chromatography-mass spectrometry based global metabolite profiling: a review. Anal Chim Acta 711:7–16
46. Madsen R, Lundstedt T, Trygg J (2010) Chemometrics in metabolomics—a review in human disease diagnosis. Anal Chim Acta 659(1):23–33
47. Haggarty J, Burgess KEV (2017) Recent advances in liquid and gas chromatography methodology for extending coverage of the metabolome. Curr Opin Biotechnol 43:77–85
48. Dettmer K, Aronov PA, Hammock BD (2007) Mass spectrometry-based metabolomics. Mass Spectrom Rev 26(1):51–78

Part II

Clinical Trials

Chapter 14

Protocols Related to Nutritional Anamnesis in Head and Neck Cancer Patients

Judith Büntzel and Jens Büntzel

Abstract

Problem: What standardized anamnesis tools are available to assess the nutritional status of head and neck cancer patients?

Material and methods: A focused literature research was performed to determine what anamnesis tools to use for appraising the key features for influencing nutritional status in this group of patients. Key factors were defined as following: malnutrition, dysphagia, dysgeusia, cancer diets, loss of appetite, and dental health/hygiene.

Results: For daily application in a clinical setting, we recommend using the following tools: the NRS-2002 (malnutrition), the CiTAS (dysgeusia), a newly proposed screening for cancer diets, the GOHIA (dental health), and the SNAQ (loss of appetite). All tools may easily be used by patients themselves (or with the support of the supervising nursing staff). Clinical trials may resort to more sophisticated screening equipment when analyzing each key factor.

Conclusion: A standardized anamnesis of the nutritional status of patients with head and neck cancer is possible. However, the main problem remains that screening tools are not always available in the patients' mother language.

Key words Nutritional anamnesis, Head and neck cancer, Questionnaires, Cancer survivors, Malnutrition

1 Introduction

Seventy-five percent of all head and neck cancer patients are malnourished or in high danger of malnutrition at the time of diagnosis [1]. The therapeutic approach of surgery followed by adjuvant radiochemotherapy or primary radiochemotherapy leads to acute toxicities like mucositis, loss of taste, a very pronounced xerostomia, and postoperative wound healing problems (including the accompanying postoperative pain). Due to these side effects of cancer therapy, it seems obvious to anticipate a prolonged deficit of nutritional intake in patients undergoing treatment. Long-term side effects like xerostomia are present in 80% of patients, more

Cinthia Baú Betim Cazarin (ed.), *Basic Protocols in Foods and Nutrition*,
Methods and Protocols in Food Science, https://doi.org/10.1007/978-1-0716-2345-9_14,

than 70% suffer from dysphagia, and 42% of survivors report lasting impairments of taste (dysgeusia). We observe scarring stenosis of the esophagus entrance in 21% and a loss of appetite in <10% of patients in follow-up [2].

All these long-term side effects of therapy heavily influence the satisfaction and quality of life of these patients and cancer survivors. Even more important is that the resulting malnutrition directly influences the prognosis of cancer patients [3]. Successfully finishing cancer therapy and thus achieving a favorable prognosis for head and neck cancer patients is only possible when assuring sufficient nutrition, and in consequence, securing a stabilized nutritional status for our patients.

Therefore, we here present protocols assessing nutritional status by simply taking the patients' history. We aim to present equipment of tools that allows assessing the nutritional status of head and neck cancer patients in a standardized, clinical setting. Furthermore, we like to point out areas where more research is yet required and topics that are still a terra incognita yet to be addressed to successfully lead our patients through the therapy and the topic of nutrition. Accompanying and monitoring patients from the point of diagnosis, during and after cancer treatment is a multiprofessional endeavor; therefore, the reader may individually choose part of the proposed equipment for assessing nutritional status he or she applies in daily care.

2 Material

In the following text, we assume that next to the primary disease secondary diagnoses like diabetes mellitus, physicians and caregivers regularly determine diseases of the gastrointestinal tract that may influence nutrition when taking the patient's medical history. Furthermore, in principle, one should take note of radiation therapy and surgery/reconstructive surgery of the gastrointestinal tract. We now aim to introduce standardized screening tools for assessing six important factors influencing nutrition listed above. Under "protocols," we present a detailed description and subsequently discuss the proposed tools.

Factor 1: *Malnutrition*

Kondrup et al. were the first to describe the *Nutritional Risk Screening* (NRS-2002). This screening tool resulted from a meta-analysis of retrospective studies investigating malnutrition, disease burden, and symptoms. The NRS-2002 does not only assess apparent malnutrition but does also identify patients at risk for developing malnutrition [4].

In contrast, the Malnutrition Universal Screening Tool (MUST) and the Mini Nutritional Assessment (MNA) were developed for outpatients (general practitioner) and nursing homes,

respectively [5]. The Subjective Global Assessment (SGA) was described first by Detsky et al. in 1987 and is a mixture of assessing medical history and clinical examination [6]. The derivated PR-SGA is an instrument based on anamnestic questions only [7].

Factor 2: *Swallowing*
The *Modified Swallowing Assessment* (MSA) of Ickenstein et al. contains six anamnestic items that nursing staff may easily assess. If all items are answered with "yes," the MSA includes a swallowing test of water that uses first with a teaspoon-sized portion and later with 90 mL of water [8].

Factor 3: *Dysgeusia*
The *Chemotherapy-induced Taste Alteration Scale* (CiTAS) is a validated questionnaire assessing chemotherapy-induced ageusia or dysgeusia. However, the questionnaire is not used in daily clinical practice. Overall, it contains 18 items [9]. A modified version focusing on metal taste was developed for head and neck cancer patients undergoing radiation therapy by Ijpema et al. in 2016 [10].

Factor 4: *Cancer diets*
So far, questionnaires do only assess foodstuff. This information might be useful for indirectly determining if patients are on a cancer diet without explicitly talking about the topic "cancer diet" itself.

The Diet History Questionnaire (DHQ) of the National Cancer Institute (NCI) contains 112 items that describe the diet of the person questioned [11]. However, to the best of our knowledge, there has not been a systematic assessment of dietary changes undertaken by cancer patients. Therefore, we propose a screening using five items.

Factor 5: *Dental health*
The questionnaire of the WHO about dental health does not seem sufficient and is too extensive for daily application [12]. In fact, we recommend using questionnaires about oral discomfort that assess xerostomia, bleeding, and pain. Further examples are General Oral Health Assessment (GOHA) with 12 items, Dental Health Questions three items [13].

Factor 6: *Loss of appetite*
The AHSP is a validated, Dutch questionnaire including 29 items that were correlated with the (Mini Nutritional Assessment) MNA and seemed to be especially suitable for geriatric patients [14]. Since 2016, the Simplified Nutritional Appetite Questionnaire (SNAQ) offers a four-item tool with similar sensitivity to screen for lost appetite and its reasons [15].

Attention
All these anamnestic tools are not used alone in the clinical setting but require additional clinical information and, if necessary, repetition and then followed by a therapeutic action. An intervention should follow a pathological screening. To explain, if the NRS-2002 yields two points, then a repetition of the screening is indicated a week later. An NRS-2002 score >2 leads to more sophisticated diagnostics in the sense of an assessment and therapy proposal [4].

It makes sense to monitor the daily nutritional intake during wound healing after surgery. The "plate method" is easy and quick to use for this endeavor [16, 17]. Furthermore, a weekly cancer conference is able to evaluate and monitor any acute adverse effects of cancer therapy according to the RTOG/CTC criteria. The team should contain radio oncologists, and oncologists specialized in treating head and neck cancer. It is recommended to adhere to an analogous analysis of late side effects (CTC criteria) during the follow-up period.

Simple clinical diagnostics should complement this nutritional information. Body weight, bioelectrical impedance analysis, and measuring hand strength are recommended. All methods may be repeated during the time of treatment and/or follow-up and add clinically relevant information to the standardized anamnesis.

3 Protocols

We present protocols for each of the fields mentioned above.

Factor 1: ***Malnutrition***
The NRS 2002 by Kondrup et al. has proved its value when screening malnutrition in head and neck cancer patients. Four different questions for prescreen are asked by nursing staff (care anamnesis) at the time point of the initial admission [4]:

- Is BMI 20.5 kg/m^2?
- Has the patient lost weight during the last 3 months?
- Had the patient reduced dietary intake in the last week?
- Is the patient severely ill? (e.g., in intensive therapy)

If one question is answered with "YES," the full screening must be performed (refer to Table 1). The result of the full screening and the following consequences are also described in the last three lines of Table 1. We calculate additional 3–5 min to perform the screening by the staff.

Table 1
Final screening for malnutrition by NRS-2002 [4]

Impaired nutritional status		Severity of disease	
Absent Score 0	**Normal nutritional status**	**Absent Score 0**	**Normal nutritional requirements**
Mild Score 1	Wt loss >5% in 3 months or food intake below 50–75% of normal requirement in the preceding week	Mild Score 1	Hip fracture, chronic patients, in particular with acute complications: cirrhosis, COPD, chronic hemodialysis, diabetes, oncology
Moderate Score 2	Wt loss >5% in 2 months or BMI 18.5–20.5 + impaired general condition or food intake 25–50% of normal requirements in the preceding week	Moderate Score 2	Major abdominal surgery, stroke, severe pneumonia, hematologic malignancies
Severe Score 3	Wt loss >5% in 1 month (>15% in 3 months) or BMI <18.5 + impaired general condition or food intake 0–25% of normal requirements in preceding week	Severe Score 3	Head injury, bone marrow transplantation, intensive care patients (APACHE >10)
Score	+	Score	= Total score
Age	If ≥70 years: add 1 to total score above		= age-adjusted total score
Score ≥3: the patient is nutritionally at risk, and a nutritional care plan is initiated *Score <3*: weekly rescreening of the patient. If the patient is scheduled for a major operation, a preventive nutritional care plan is considered to avoid the associated risk status			

Factor 2: *Swallowing*
Dysphagia is also a symptom easily assessed by nursing staff. The following questions of MSA [8] should be answered by a member of the nursing staff taking the patient's medical history (Part A of MSA):

- Is the patient awake and responding to speech?
- Can the patient cough when asked to?
- Is the patient able to maintain some control of saliva?
- Is the patient able to lick their top and bottom lips?
- Is the patient able to breathe freely (i.e., has no problem in breathing without assistance and maintaining adequate oxygen saturation)?
- Are signs of a wet- or hoarse-sounding voice absent?

If all questions are answered with YES, then the first test of swallowing may follow. In a first step, a teaspoon of water is offered to the upright sitting patient (the trunk is supported). If this volume is consumed without any problem, then a second step

Table 2
Modified Swallowing Assessment (MSA)

B – Swallowing test (1 teaspoon of water) Functional disturbance (PERRY Criteria). Terminate assessment, if *YES* for any function	*YES*	*NO*	Comments
No evident swallowing activity Water leaks out of the mouth Coughing/throat clearing Increase in respiratory rate Wet/gurgly voice within 1 min Do you have doubts or a bad impression?			
C – 90-mL water swallow test Functional disturbance (Suiter and Leder criteria) Terminate assessment if *YES* for any function	*YES*	*NO*	
Coughing after swallowing (1 min)			
Chocking attacks (1 min)			
Change in vocal quality (1 min)			
Test terminated or unable to be performed			
MSA findings (a) MSA pathological in A, B, or C (b) Clinical suspicion of aspiration risk (c) Swallowing therapist informed (d) Doctor informed (e) Swallowing adjusted diet			If *YES*, then c or d If *YES*, then c or d

Adapted from Ref. [8]

follows, where the patient drinks 90 mL of water. Table 2 summarizes both steps (parts B and C of MSA) of the assessment as well as the therapeutic consequences. We calculate 5–10 additional working minutes for the staff.

Factor 3: *Taste*
Internationally, CiTAS assess impairment of tasting. The questionnaire, which patients answered by themselves in a five-point Likert scale, comprises 18 items that assess the following dimensions of taste: quantitative changes in tasting (hypo- or ageusia), qualitative changes in the tasting (dysgeusia), problems concerning dietary intake (fatty and hot dishes) [9].

The alternative questionnaire of Ijpema et al. is based on the CiTAS and altered for patients undergoing radiation therapy. However, 47 items are required. This questionnaire seems not practicable for screening and assessing impairments of tasting [10]. Table 3 shows the items of the CiTAS as a tool for self-assessment by patients. According to our experience, patients need 10–12 min to answer this questionnaire.

Table 3
Chemotherapy-induced Taste Alteration Scale (CiTAS) [18]

	1	2	3	4	5
1. Have difficulty tasting food					
2. Have difficulty tasting the sweetness					
3. Have difficulty tasting the saltiness					
4. Have difficulty tasting the sourness					
5. Have difficulty tasting the bitterness					
6. Have difficulties tasting umami					
7. Unable to perceive the smell or flavor of food					
8. Everything tastes bad					
9. Food does not taste as it should					
10. Have a bitter taste in the mouth					
11. Have bad taste in the mouth					
12. Everything tastes bitter					
13. Feel nauseated or queasy					
14. Bothered by a smell of food					
15. Have difficulty eating hot food					
16. Have difficulty eating oily food					
17. Have difficulty eating meat					
18. Have a reduced appetite					
Likert-Scale Item 1–6: taste normally (1), slightly difficult to taste (2), somewhat difficult to taste (3), quite difficult to taste (4), and unable to taste at all (5)					
Likert-Scale Item 7–18: no (1), slightly (2), somewhat (3), quite (4), and very (5)					

Factor 4: ***Cancer diets***

So far, there has not been a regular procedure to register special *cancer diets*. The focus of our self-report tool is the first question used for screening that requires if a patient changed his or her dietary habits due to the "cancer" diagnosis. If this question is answered with "YES," four additional items assess changes in food products, supplementary agents (e.g., micronutrients, vitamins), or special dietary recommendations. We here introduce a screening tool that usually shows the therapist if a patient requires information. This tool may be used as an app as well as a print version; patients can answer the latter before an appointment with their treating physician (e.g., in the waiting area). Table 4 summarizes this new screening tool, which requires approximately 3–5 min for the patient to fill out the short questionnaire.

Factor 5: ***Dental health***

The first tool for assessing dental health presented here is the general (geriatric) oral health assessment index (GOHAI). The tool comprises 12 questions/symptoms, which are evaluated according to their frequency using a six-step Likert scale ranging from 0 (never) to 5 (always). The items were chosen in a way that is able to mirror problems of dental and oral health in three

Table 4
Self-report cancer diets

Did you change your nutritional habits since you know your cancer diagnosis?		
YES		**NO**
Do you dispense or avoid specific food?	YES: NO	*Before you start a cancer diet, please contact your GP or oncologist.*
Do you prefer specific food?	YES: NO	
Do you take additional supplements?	YES: NO	
Do you follow a specific diet strategy?	YES: NO	
If you answered YES, please specify.		

dimensions: (1) physiological function (including eating, speaking, swallowing); (2) psychosocial functions (comprising fears or concerns about oral health, self-doubt, and dissatisfaction caused by the patients' current situation, and social self-isolation due to dental health) and (3) oral pain/distress or taking pain relievers due to dental pain. The items of the GOHAI tool are listed under Table 5. After filling out the questionnaire, a score between 0 and 60 is calculated. The assessment is suited for both patients with teeth and dental prostheses. The first group has a mean score of 53.1 ± 7.6 and the second of 50.6 ± 8.9 points. Answering the questionnaire takes up to 10 min [13].

Alternatively, we propose to use the three questions of the Rand Health Insurance Study to have a faster way to screen for dental or oral health. These questions focus on the toothache, concerns for teeth, or condition of teeth during the last 3 months. Scoring ranges depend on the answers from 3 (bad) to 12 (very good) [19].

Factor 6: ***Loss of appetite***
The SNAQ is a screening/anamnesis tool that has been proven to assess loss of appetite. It uses four questions that are answered by the patients using a five-step Likert scale. The following dimensions are assessed: appetite, abdominal fullness, taste, and the current food intake compared to the patient's normal food intake. These four pillars of the test and instructions for screening are presented in Table 6 and unmask signs of loss of appetite. The SNAQ is easily applied and more sensitive than more sophisticated protocols [14, 15]. It takes 5 min for patients or nursing staff to complete the screening.

Table 5
General (geriatric) oral health assessment index [13]

	Never	Seldom	Sometimes	Often	Very often	Always
How often did you limit the kinds or amounts of food you eat because of problems with your teeth or dentures?	5	4	3	2	1	0
How often did you have trouble biting or chewing any kind of food, such as firm meat or apples?	5	4	3	2	1	0
How often were you able to swallow comfortably?	0	1	2	3	4	5
How often have your teeth or dentures prevented you from speaking the way you wanted?	5	4	3	2	1	0
How often were you able to eat anything without feeling discomfort?	0	1	2	3	4	5
How often did you limit contact with people because of the condition of your teeth or dentures?	5	4	3	2	1	0
How often were you pleased or happy with the looks of your teeth and gums or dentures?	0	1	2	3	4	5
How often did you use medication to relieve pain or discomfort from around your mouth?	5	4	3	2	1	0
How often were you worried or concerned about the problems with your teeth, gums, or dentures?	5	4	3	2	1	0
How often did you feel nervous or self-conscious because of problems with your teeth, gums, or dentures?	5	4	3	2	1	0
How often did you feel uncomfortable eating in front of people because of problems with your teeth or dentures?	5	4	3	2	1	0
How often were your teeth or gums sensitive to hot, cold, or sweets?	5	4	3	2	1	0

A summary, we present in Fig. 1 all protocols, we proposed including the staff and time required to apply them. A modular use during daily clinical work is possible and reasonable.

4 Notes

The PG-SGA was already presented as a validated clinical tool to assess patients' nutritional status. While this questionnaire already covers some special nutritional aspects of head and neck cancer

Table 6
Short Nutritional Appetite Questionnaire (SNAQ)

Please specify the following sentences!					
	1	**2**	**3**	**4**	**5**
My appetite is	Very poor	Poor	Average	Good	Very good
I feel full after eating …	Few mouthfuls	A third of a meal	Half of a meal	Most of a meal	A meal
The food tastes	Very bad	Bad	Average	Good	Very good
Normally I eat per day	<1 meal	1 meal	2 meals	3 meals	>3 meals

Modified from Ref. [15]

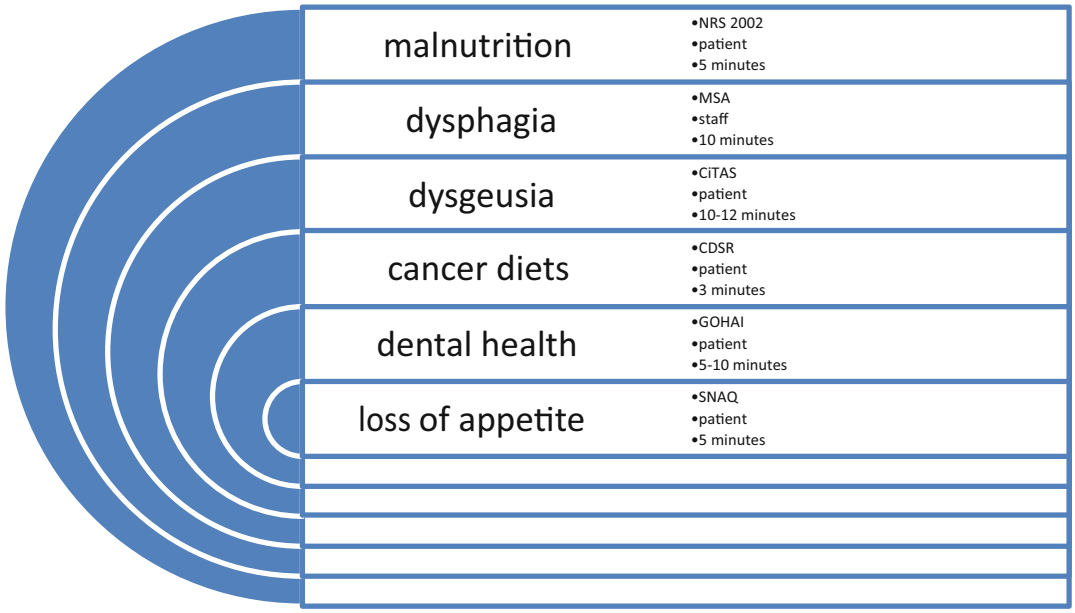

Fig. 1 Parts of nutritional anamnesis

patients (xerostomia, loss of appetite, taste), it does not allow an in-depth assessment of every single patient's individual needs. Furthermore, users of the questionnaire have described several problems of interpreting results, which led to the discussion to publish an additional manual for patients and medical staff [20].

Our proposal of using different anamnesis tools as modules for assessment recognizes the diversity of nutritional problems in head and neck cancer patients. These problems arise either due to cancer itself or due to other impairments and toxicities that develop during our multimodal cancer treatments. On principle, a transfer of our tools to other cancer entities is possible. However, the underlying reason impairing nutrition should be assessed before doing so.

Our second keynote was to choose anamnestic tools that patients themselves can easily answer without additional support. The sole exception is the modified swallowing assessment; here, the assistance of nursing staff is required for completing the questionnaire. In our opinion, daily clinical practice necessitates this simple, time, and resource-saving approach. The patients need approximately 40–45 min to prepare for the whole assessment. The physician is able to prioritize topics by choosing specific modules and is guided by these through the process of nutritional assessment.

The third advantage of our approach is the modular setup of these anamnesis tools. Depending on the patient's individual needs, we can retrace and reassess these topics during treatment. These changes are necessary and of great importance as symptoms are dynamic and changing over time.

Now, on a fourth thought, we like to discuss the limitations of the presented tools. The knowledge of these is crucial for correctly interpreting test results.

The NRS 2002 focuses mainly on the energetic balance of patients [4]. However, this covers only a part of the issue of malnutrition. This tool is able to detect malnutrition in obese or overweight patients. However, the NRS 2002 is less able to detect the dynamic aspects of malnutrition. In this case, we propose to additionally use more sensitive indicators (e.g., bioelectrical impedance analysis). Furthermore, the NRS 2002 does not mirror other facets of malnutrition like a deficit of trace elements or vitamins. Nonetheless, these deficits correlate with individual toxicities. Therefore, it is imperative to monitor the levels of trace elements and vitamins in the blood.

The MSA by Icksenstein [8] reflects well the status of oropharyngeal ingestion. Therefore, this tool is appropriate to use when deciding about individual diet. Nevertheless, the MSA does rarely allow concluding the reason for dysphagia. Additional logopedic and medical examination (endoscopy, cinematography) are able to characterize dysphagia and offer further, therefore, approaches for successful therapy. The gastral and esophageal influence on dysphagia is also insufficiently characterized by the presented tool.

We already pointed out the shortcomings of using the CiTAS [9] to evaluate dysgeusia during or after radiation therapy. An additional item representing metallic taste during food intake would be helpful. An advantage of the CiTAS is the dichotomy of evaluating flavor and the subjective impressions of the patients. It is possible to establish a semiquantitative assessment of taste based on the CiTAS in clinical practice.

For the first time, we here propose a screening tool for cancer diets. However, this tool must be validated in clinical practice. So far, it is used by our medical staff in daily practice and draws the specific eating/nutritional habits into the clinician's focus. We use the tool repetitively during the course of disease to spot and address additional (nutritional) therapy efforts of the patients.

The GOHAI is an established tool in general dental medicine. This tool also seems suitable for the elderly. It assesses nonspecific clues for typical oncological side effects like osteonecrosis or neuropathic afflictions in the oral area. So far, there has not been a validation for head and neck cancer patients. However, this tool is especially suitable for non-dentists to recognize the need for action and transfer patients to a dentist. The Rand Health Insurance Study questions are a tool that reflects the patient's self-care concerning the topic "oral well-being."

The SNAQ [15] is also mainly a tool suitable for screening. Validated for the elderly, the SNAQ should be easy to integrate into clinical practice. Further validation is required before using this tool for clinical trials or documentation over time.

Finally, we like to address common limitations of all presented questionnaires: taking medical history usually occurs in the patient's mother tongue. A translation of a tool for using it in daily clinical practice is sensible and possible. For using these questionnaires in clinical trials, the tools have to be presented to the patient in his or her native language. However, only a few validated questionnaires are available in several languages (e.g., NRS 2002, MSA, CiTAS).

5 Outlook

The presented anamnesis tools are clinically orientated and focused on assessing the whole range of nutritional problems of head and neck cancer patients using mainly patients' self-assessment. It requires the patients to be literate and interested in therapy and communication. Each tool might also be completed by nursing staff or caregivers.

We have pointed out the expansion options for each symptom if single aspects of nutrition are to be investigated by clinical trials. For assessing specific effects, the initiator(s) should use the following single symptoms listed and categorized by the Common Terminology Criteria of the National Cancer Institute under the organ complex "gastrointestinal diseases": cheilitis, dental caries, dry mouth, dysphagia, lip pain, malabsorption, mucositis oral, oral cavity fistula, oral dysesthesia, oral hemorrhage, oral pain, periodontal disease, salivary duct inflammation, salivary gland fistula, tooth discoloration, toothache [21].

Listed at metabolic or nutritional disorders, we may find the keywords "anorexia" and "dehydration"; and under the neurological system, the symptom "dysgeusia." Single symptoms are described on a scale from 0 to 5 (0 equal no adverse event).

We propose to routinely use the following additional features to complement these anamnesis tools in clinical practice: weight, basic laboratory tests, and bioelectrical impedance analysis. After taking medical history and results of the investigation follows an individual therapy recommendation embedded in a multi-professional dialogue between physician, swallowing therapist, and oecotrophologist.

References

1. Büntzel J, Micke O, Kisters K et al (2019) Malnutrition and survival – bioimpedance data in head neck cancer patients. In Vivo Athens Greece 33:979–982. https://doi.org/10.21873/invivo.11567
2. Büntzel J, Glatzel M, Mücke R et al (2007) Influence of amifostine on late radiation-toxicity in head and neck cancer--a follow-up study. Anticancer Res 27:1953–1956
3. van Rijn-Dekker MI, van den Bosch L, van den Hoek JGM et al (2020) Impact of sarcopenia on survival and late toxicity in head and neck cancer patients treated with radiotherapy. Radiother Oncol J Eur Soc Ther Radiol Oncol 147:103–110. https://doi.org/10.1016/j.radonc.2020.03.014
4. Kondrup J, Rasmussen HH, Hamberg O et al (2003) Nutritional risk screening (NRS 2002): a new method based on an analysis of controlled clinical trials. Clin Nutr Edinb Scotl 22:321–336
5. Kondrup J, Allison SP, Elia M et al (2003) ESPEN guidelines for nutrition screening 2002. Clin Nutr Edinb Scotl 22:415–421
6. Detsky AS, McLaughlin JR, Baker JP et al (1987) What is subjective global assessment of nutritional status? JPEN J Parenter Enteral Nutr 11:8–13. https://doi.org/10.1177/014860718701100108
7. Ottery FD (1996) Definition of standardized nutritional assessment and interventional pathways in oncology. Nutr Burbank Los Angel Cty Calif 12:S15–S19. https://doi.org/10.1016/0899-9007(96)90011-8
8. Ickenstein GW, Riecker A, Höhlig C et al (2010) Pneumonia and in-hospital mortality in the context of neurogenic oropharyngeal dysphagia (NOD) in stroke and a new NOD step-wise concept. J Neurol 257:1492–1499. https://doi.org/10.1007/s00415-010-5558-8
9. Simeone S, Esposito MR, Gargiulo G et al (2019) The CiTAS scale for evaluating taste alteration induced by chemotherapy: state of the art on its clinical use. Acta Bio-Medica Atenei Parm 90:17–25. https://doi.org/10.23750/abm.v90i6-S.8278
10. IJpma I, Timmermans ER, Renken RJ et al (2017) Metallic taste in cancer patients treated with systemic therapy: a questionnaire-based study. Nutr Cancer 69:140–145. https://doi.org/10.1080/01635581.2017.1250922
11. Diet History Questionnaire III (DHQ III) | EGRP/DCCPS/NCI/NIH. https://epi.grants.cancer.gov/dhq3/. Accessed 13 Feb 2021
12. Petersen PE, Baez R, Word Health Organisation (2013) Oral health surveys, basic methods. In: Oral health surveys, basic methods, 5th edn. WHO Library Cataloguing-in-Publication Data
13. Atchison KA, Dolan TA (1990) Development of the geriatric oral health assessment index. J Dent Educ 54:680–687. https://doi.org/10.1002/j.0022-0337.1990.54.11.tb02481.x
14. Mathey MF (2001) Assessing appetite in Dutch elderly with the Appetite, Hunger and Sensory Perception (AHSP) questionnaire. J Nutr Health Aging 5:22–28
15. Wilson M-MG, Thomas DR, Rubenstein LZ et al (2005) Appetite assessment: simple appetite questionnaire predicts weight loss in community-dwelling adults and nursing home residents. Am J Clin Nutr 82:1074–1081. https://doi.org/10.1093/ajcn/82.5.1074
16. Volkert D, Schrader E (2013) Dietary assessment methods for older persons: what is the best approach? Curr Opin Clin Nutr Metab Care 16:534–540. https://doi.org/10.1097/MCO.0b013e328363c8d1
17. Ingadottir AR, Hilmisdottir HB, Ramel A, Gunnarsdottir I (2015) Energy- and protein intake of surgical patients after the implementation of energy dense hospital menus. Clin Nutr ESPEN 10:e107–e111. https://doi.org/10.1016/j.clnesp.2015.03.081

18. Kano T, Kanda K (2013) Development and validation of a chemotherapy-induced taste alteration scale. Oncol Nurs Forum 40: E79–E85. https://doi.org/10.1188/13.ONF.E79-E85
19. Brook RH, Ware JE, Davies-Avery A et al (1979) Overview of adult health measures fielded in Rand's health insurance study. Med Care 17:iii–x, 1
20. Balstad TR, Bye A, Jenssen CR et al (2019) Patient interpretation of the patient-generated subjective global assessment (PG-SGA) short form. Patient Prefer Adherence 13: 1391–1400. https://doi.org/10.2147/PPA.S204188
21. U. S. Department of Health and Human Services Common Terminology for Adverse Events, Version 5.0. U. S, Department of Health and Human Services

Chapter 15

Food Diary, Food Frequency Questionnaire, and 24-Hour Dietary Recall

Luisa Saravia, Paula Moliterno, Estela Skapino, and Luis A. Moreno

Abstract

Diet and nutrition have an essential connection to human health. Dietary data provide valuable information about specific associations between exposure to dietary components and health, disease, or mortality. Due to the high daily variability of diet, the accurate assessment of dietary intake in the free-living human population is more challenging than the measurement of other environmental exposures. For most epidemiological studies, exposure to a long-term diet is more relevant than intake on a specific day or a reduced number of days. It is essential to choose a suitable method for assessing diet and interpreting data collected. Dietary intake can be assessed using subjective or objective methods. Subjective methods are based on people's memory, who must answer a self-reporting form, or can be carried out by a trained interviewer, recalling food and food preparations consumed at the previous mealtime, the day before, or for a specified period. Subjective dietary assessment methods include the food frequency questionnaire, 24-hour dietary recall, food record, and weight food record. In recent years, technological innovations have improved data collection methods and subsequent analysis, but the problem of misreporting dietary intake, whether voluntary or involuntary, persists and contributes to data inaccuracy and misinterpretation. Objective dietary assessment methods appeal to nutritional biomarkers to estimate dietary exposures. These markers highly correlated with dietary intake, regardless of the subject's memory and ability to describe the type and quantity of food consumed. These methods are usually expensive and invasive, so their use in large epidemiological studies can be difficult to implement. Some biomarkers have been used to validate dietary questionnaires, which are frequently used in large epidemiological studies; for example, the case of doubly labeled water as a marker of dietary energy. The human validation of this technique included different ages and conditions. Most of the studies show lower values for reported energy intake compared with measured total energy expenditure. This underreporting is usually higher in people with obesity. Biomarkers are also used to measure intake or exposure to a food component; for example, urinary sodium excretion is used as an objective marker of sodium intake or urinary nitrogen, which provides an objective measurement of dietary protein intake. Biomarkers can also be used to assess nutritional status by measuring body fluids like urine, blood, saliva, or tissues or even provide accurate information of dietary intake and new insights into the biological effect of dietary patterns and lifestyle and their impact on health/disease risk. In recent years, omics technologies have been integrated into nutritional epidemiological research to identify novel biomarkers. These scientific advances will help researchers obtain more accurate data and will allow for a better calibration of traditional methods when assessing dietary intake.

Key words Dietary intake assessment methods, Food frequency questionnaire, 24-hour dietary recall, Food records, Doubly labeled water, Biomarkers, Validity

Cinthia Baú Betim Cazarin (ed.), *Basic Protocols in Foods and Nutrition*,
Methods and Protocols in Food Science, https://doi.org/10.1007/978-1-0716-2345-9_15,

1 Introduction

Food consumption is one of the most important determinants of health, disease, and mortality [1]. In order to pinpoint the specific associations between different dietary components and related diseases and disorders, it is critical to make an accurate assessment of dietary intake. Ideally, assessment methods should allow for the amount of food eaten over a long period of time to be precisely estimated, as dietary intake varies from one day to another and diet-related diseases develop following long-lasting exposure to a given dietary risk factor [2]. From the information obtained on food intake and considering the size of the portion eaten, the methods used should allow for the amount of nutrients consumed and non-nutritional components of the foods to be calculated, using some of the available food composition tables. In addition, more and more research is being conducted on the main nutrition determinants of health, focusing on general dietary patterns, such as the Mediterranean diet, the overall quality of the diet, and specific health-related dietary patterns such as the DASH diet [3]. Questionnaires rely on the individual's memory and accuracy to estimate food portions. Recent developments in technology-based dietary assessment allow for the real-time data collection of food consumption. The use of the Internet and smartphones for dietary assessment has expanded traditional methods, allowing for the collection of objective dietary intake and facilitating timely data analysis [4]. However, the technology to support automatic food recognition and estimated portion size is still insufficient to provide fully automated food intake assessment with acceptable precision [5].

Currently, numerous biomarkers allow for the estimation of the intake of specific food components. In the near future, we should be able to combine information from questionnaires and biomarkers to precisely identify the dietary risk factors associated with the diseases and disorders of interest [6]. Recently, a multi-targeted metabolomics platform was suggested for the simultaneous estimation of 450 dietary metabolites in short run times using small volumes of the biological sample, facilitating its application in epidemiological studies [7].

Assessing food and nutrient intakes and their relationship with disease outcomes is critical in defining nutritional guidelines to improve the population's health. For all these reasons, this chapter aims to describe the most widely used subjective and objective methods for assessing dietary intake and their corresponding validity and reliability.

2 Subjective Methods for Assessing Dietary Intake

The impact of dietary intake on the prevention of noncommunicable diseases (NCDs) and the increase of NCDs and micronutrient deficiencies worldwide have stimulated the development and validation of methods to assess food consumption for use in epidemiological studies [8].

Understanding how diet influences health and disease highlights the need for continuous refinement of existing intake assessment tools [9]. For most epidemiological studies, the conceptually relevant exposure is long-term diet rather than intake on a specific day or a reduced number of days, so to consider the daily variation of dietary intake is essential in choosing a suitable method for assessing diet and interpreting data collected using various approaches (Table 1) [10].

Many factors influence an individual's food choice (biological, behavioral, psychological, cultural, economic, social, geographical, political, historical, and environmental, among others) that are repeatedly considered both simultaneously and sequentially in food choice decision-making [11]. Food intake and eating patterns may influence an individual's risk of developing obesity, cardiovascular disease, and other NCDs [12].

One of the most common classifications of dietary intake assessment methods involves objective and subjective methods. In epidemiological studies, the preferred methods are subjective because of their low cost compared to objective methods (biomarkers and doubly labeled water) [11]. Subjective methods are based on people's memory, who must answer a self-reporting form (in paper or technological format), or can be carried out by a

Table 1
Dietary questionnaires to be used according to the type of study

Type of study	Outcome	Questionnaire
Cross-sectional	Nutrients	24-hour recall (3–7 days)
	Nutrients	Food record (3–7 days)
	Food	Food frequency questionnaire
Case-control		Food frequency questionnaire
Cohort		Food frequency questionnaire
		24-hour recall (3–7 days)
		Food record (3–7 days)
Experimental		Food frequency questionnaire
		Food record (3–7 days)

trained interviewer, recalling food and food preparations consumed at the previous mealtime, the day before, or for a specified period of time [11]. Subjective dietary assessment methods that assess an individual's intake include the food frequency questionnaire (FFQ), 24-hour dietary recall (24-hour), food record (FR), and weight food record (WFR). Usually, in these methods, data are collected with the support of a trained interviewer or through self-reporting [13]. Although they are commonly used, they are based on the individuals' memory and, as such, have limitations [11].

2.1 Food Frequency Questionnaire (FFQ)

The FFQ is a checklist asking respondents how often (once in a month, twice or three times in a month, every week, every day, etc.) they ate and how much food they ate over a specific period (1 week, months, or even 1 year) [10]. Usually presenting about 100–150 foods, this questionnaire takes 20–30 min to complete and can be self-reported or collected via interview.

The purpose of developing an FFQ is to provide an accurate method to assess the population's habitual intake and eating patterns, with a limited number of questions. It is not designed to estimate precise individual intakes but instead rank an individual's intake within a population [14]. A qualitative FFQ refers to a questionnaire that does not collect additional information about portion size; a semiquantitative FFQ refers to a questionnaire that collects information about portion size; and a quantitative FFQ refers to a questionnaire that collects information about the usual portion size, using realistic food models or providing pictures of various portion sizes [15].

The underlying principle of the FFQ approach is that the average long-term diet, for example, intake over weeks, months, or years, is conceptually relevant exposure rather than intake over a few specific days [10, 15]. Therefore, the FFQ classifies individuals according to their food intake and not only quantifies food or nutrient intake.

Each FFQ should be created and validated in the specific population in which it will be used. This instrument's development requires special attention in choosing food items, developing accurate background questions, and formatting the frequency response section [10]. Moreover, it is important to consider the number of items that will be included and the method for measuring portion sizes if the FFQ is quantitative [16].

FFQs are especially useful for measuring the intake of a specific nutrient or food group because, due to its format and methodology, it allows for questions to be asked on the intake of the specific food group or nutrient only [17–24].

This method allows for assessing of long-term dietary intakes in a relatively simple, cost-effective, and time-efficient manner [13]. A short FFQ may underestimate the true or real variation in dietary

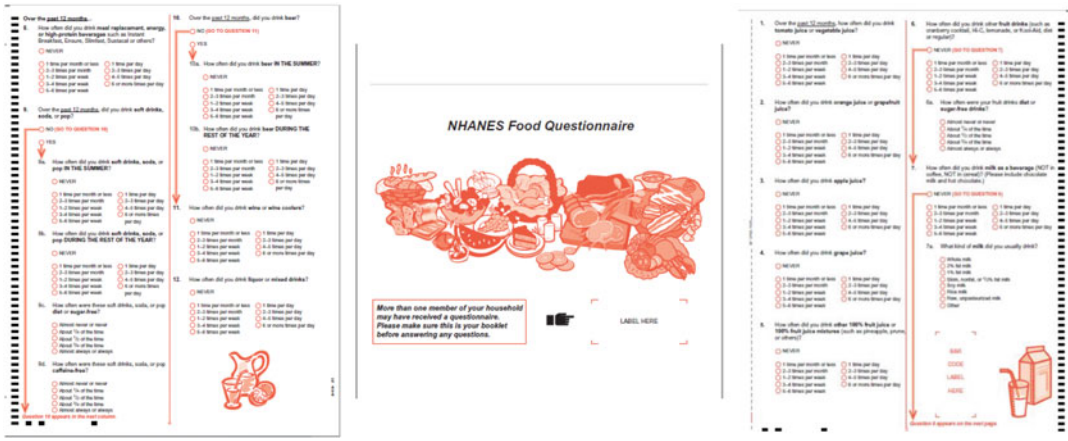

Fig. 1 NHANES FFQ. (https:/epi.grants.cancer.gov/diet/usualintakes/FFQ.English.June0304.pdf)

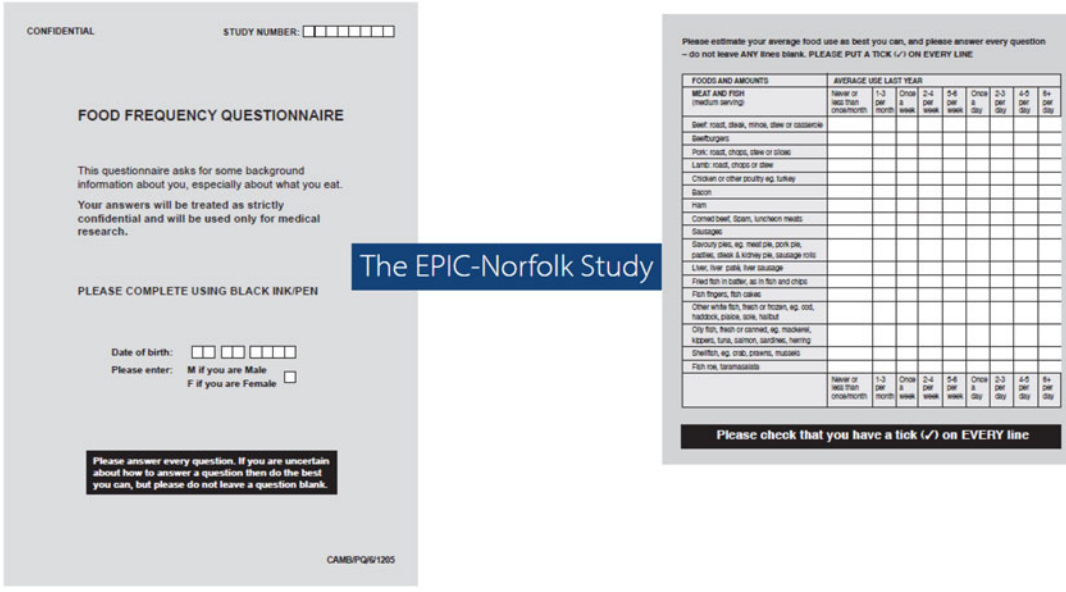

Fig. 2 EPIC FFQ. (https:/www.epic-norfolk.org.uk/wp-content/uploads/2020/11/CAMB-PQ-6-1205a_front.pdf)

intake, but an exceptionally long and detailed one can be time- and resource-consuming, and the burden on the respondent may jeopardize data quality [15]. Some examples of FFQs are shown in Figs. 1 and 2.

2.2 24-Hour Recall

The 24-hour is used to describe the average dietary intake of groups of individuals. Participants are asked to recall and describe in an open-ended manner the foods and beverages consumed over one day, preferably the day before, in detail and depth [10].

This method requires a trained interviewer, usually a nutritionist, to ask the respondents to remember details of all the foods and beverages they consumed over the previous 24 hours [15, 25]. The interviewer asks for detailed information about everything the respondent eats and drinks from midnight to midnight of the previous day and enquires about additional foods, food preparation methods, and ingredients by asking questions in a manner that puts the respondent at ease and facilitates the ability to recall the previous day's intake [10]. The interviewer requires intensive training on obtaining accurate and complete dietary recalls. Detailed information about food preparation methods, recipe ingredients, and brand name identification of commercial products are often required. The interviewer's ability to ask nonjudgmental questions, maintain a neutral attitude toward all responses, use open-ended questions in probing foods and descriptive details, and avoid asking questions in a manner that might influence the participant's responses are important in obtaining complete and accurate information [10].

The U.S. Department of Agriculture developed five sequential passes in the interview through the automated multiple-pass method to facilitate the accurate recall of dietary intake [26]:

1. Asking the participant to start by quickly list the foods consumed the previous day (not respecting time sequences)
2. Asking about any forgotten foods in nine commonly forgotten categories of foods
3. Asking the time and the occasion of consumption for each food
4. Probing for specific details on foods, like amounts consumed and foods consumed between identified eating events
5. Probing for whether anything was forgotten

The requirement of trained interviewers limits the use of the 24-hour in large epidemiological studies though they are usually used in small samples to validate dietary intake assessed with FFQs. Because they require highly trained interviewers, recalls are expensive and impractical for large-scale nutrition research, leading to the use of food frequency questionnaires [27].

The 24-hour is commonly used to study the diet's intrapersonal variability; usually, several 24-hour are used to capture within-person variability [25]. The recommendation for epidemiological studies is that every individual should respond to at least three 24-hour in the data collection period, two on weekdays and one on the weekend; in this way, the variability of weekly intake is covered [10]. The short-term measurement of a 24-hour is sufficient to determine the mean consumption of groups, while two or more 24-hour are recommended for statistical modeling to estimate individuals' usual dietary consumption. Thereby, the application of the 24-hour method for different epidemiological settings improves [28].

Name: Simon ID Number: 008 Sex: M

Date of Birth: 13th July 1989 Date: 18th September 2010

Table D - *A 24-hour recall*

BREAKFAST — Time: 7.15 am — Place: home

NAME	FOOD DESCRIPTION	HOUSEHOLD AMOUNT	AMOUNT (g/mL)	PREPARATION/ INGREDIENTS
Soymilk	Soymilk, plain	1 cup	200ml	Hot soymilk
+ coffee	Espresso (Illy)	1 coffee cup	30ml	+ coffee (without sugar)
Bread	Wholemeal bread, with salt	2 slices, thin	100g	Toasted bread
+ butter	Low fat butter, (Granarolo)	1 level tablespoon	10g	
+ jam	Blueberry jam, (Zuegg)	2 heaped teaspoons	20g	Sugar free jam
Biscuits	Dried, Vanilla biscuits	4/5 pieces	30g	Homemade

SNACK (mid-morning) — Time: 10.00 pm — Place: work

NAME	FOOD DESCRIPTION	HOUSEHOLD AMOUNT	AMOUNT (g/mL)	PREPARATION/ INGREDIENTS
Apple	Fresh apple	1 medium	150g	Fresh apple with peel
Cappuccino	Full cream milk	1 cup	200ml	Hot cappuccino + sugar
	+ espresso (Illy)	1 coffee cup	30ml	
+ sugar, brown, packed		1 pack	7g	
Crackers	Wholemeal crackers, low fat, (Misura)	1 pack	30g	Wholemeal crackers, low fat, without salt

LUNCH — Time: 13.00 pm — Place: work

NAME	FOOD DESCRIPTION	HOUSEHOLD AMOUNT	AMOUNT (g/mL)	PREPARATION/ INGREDIENTS
Dried pasta, (uncooked)	Macaroni (Barilla)	1 cup	60g	Boiled Pasta with pulses (beans)
+ beans, white	with beans, white, mature seeds, canned (Valfruttal	1 cup	150g	
+ e.v. olive oil		1 tablespoon	10ml	+ e.v. olive oil
+ cheese		2 heaped tablespoons	20g	+ parmesan (cheese)
Salad, raw	Lettuce, romaine, fresh, raw	4 leaves	80g	Fresh salad
+ e.v. olive oil	(De Cecco)	2 tablespoons	20ml	+ e.v. olive oil
+ salt		A pinch		+ salt
Water	Natural water	2 glasses	400ml	

Food and Agriculture Organization of the United Nations

Fig. 3 FAO 24-hour dietary recall. (http:/www.fao.org/3/i9940en/I9940EN.pdf)

The interviewees can be adolescents or adults who are part of the study population or, in the case of children, their parents or the people in charge of feeding them [10]. An example of a 24-hour is shown in Fig. 3.

2.3 Food Record (FR)

The FR is a method that consists of a specially designed booklet, or a mobile app, in which individuals list every food and beverage consumed over three, five, or seven consecutive days [29]. Food intake is to be recorded by the participant when the foods are eaten to minimize reliance on memory [10]. The food portions consumed are estimated using household measurements, such as cups or spoons, food photographs, or food models.

Its main limitation is that, because people must record their daily food consumption, they often change their eating behavior during the period in which they record the diet to facilitate observation work. Due to the difficulties of the dietary intake data collection method, FRs are not used in large epidemiological studies.

2.4 Weighted Food Record (WFR)

WFR is similar to the FR method; however, foods and beverages consumed are weighed and recorded by the participants rather than estimated [25]. This method requires a very detailed training program to obtain accurate results. Due to its difficulties and cost, WFR is not used in epidemiological studies, though it may be used to validate other dietary intake methods.

Note: Cross-cultural adaptation The aim of culturally adapting a dietary intake assessment questionnaire is to achieve an equivalent questionnaire to be used in another different cultural context. The adaption cannot involve language translation alone; it must follow a methodology that ensures conceptual and semantic equivalence with the original [30]. If the adaption is not possible, a new questionnaire must be developed and adjusted to the new culture. This adaptation is particularly important in questionnaires used to measure food consumption in people since the variations between countries and regions, the different ways of preparing food, and the way of naming foods are specific to each country or region [31].

2.5 Technological Use of Dietary Intake Assessment Methods

There have been advances in methods of collecting dietary intake data over recent years through technological innovations enhancing existing self-reporting methods (e.g., recalls, FFQs, and records) and developing novel instruments (e.g., wearable devices). These technological advances include computer software and web-based applications that aim to standardize the process of an interviewer-reported or a self-reported dietary report [15]. New technologies for assessing diet can be considered according to the technology used, such as web-based or online tools, mobile systems (apps), camera-based tools, and other developing technologies, such as consumer purchase data and wearable sensors [32]. In particular, the use of the Internet and smartphones for dietary assessment to collect more accurate dietary intake has resulted in the extension of traditional methods, allowing for the collection of detailed dietary intake with lower costs and participant burden and facilitating timely data analysis approaches. If an Internet connection is available, free web-based tools can be accessed at any location, providing real-time data, reducing the impact of inconsistencies related to erroneous data entry, and allowing for the automatic calculation of energy and nutrient intakes. Computer-based questionnaires often offer tutorials; they are faster than annotated data (since the skip patterns rule out certain questions and detailed questions show up only when something is consumed), probe into multiple details of the consumption in a harmonized manner, and provide digital images for food identification and portion-size estimation [15]. However, to be confident of the data collected and inferences made, one must ensure that any methods to be used for research purposes are valid and reliable [9].

A systematic review was conducted by The International Life Sciences Institute (ILSI) Europe Dietary Intake and Exposure Task Force report on a review of tools for the dietary assessment using new technologies which are applicable for use in research, commercial, clinical, and public health contexts. Of the 33 tools used for research or surveillance, $n = 21$ (64%) were web-based for use on a computer; $n = 6$ (18%) were optimized for use on smartphones; $n = 3$ (9%) were for PC only (not web-based); $n = 2$ (6%) used

wearables for data collection; and $n = 1$ (3%) was designed for use on a tablet. Of the 33 tools designed to collect dietary data for research purposes, $n = 16$ (48%) were designed exclusively for adults; $n = 11$ (33%) were for all ages; and $n = 6$ (18%) were exclusively for children and/or adolescents. Among all the tools designed for research purposes, $n = 17$ (52%) collected dietary intake over the previous 24 hours using dietary recalls; $n = 11$ (33%) collected food records, while the remainder collected intakes via food frequency questionnaires ($n = 3$; 9%) or imaging systems ($n = 2$; 6%) [32].

3 Objective Methods for Assessing Dietary Intake

3.1 Doubly Labeled Water Method

As described above, there are several subjective methods for assessing dietary intake. Most of them rely on the reports of foods and drinks consumed over the previous day, weeks, or months. As these methods appeal to the memory of the participants, they are usually not accurate. One of the most common documented errors is the self-reporting of energy intake, which is often less than that of the individual's measured energy expenditure [33]. This situation may be explained due to underrecording, underreporting, or undereating when it comes to self-reports.

Energy intake may be presumed to be equal to energy expenditure when a person's body weight is stable. Given the inaccuracies when reporting energy intake, energy expenditure measurement can provide validation for energy intake measurement. Energy expenditure can be measured by direct calorimetry, based on the measurement of body heat loss in a metabolic chamber over 24 hours [34]. It is a highly precise method but is expensive and not practical for epidemiological studies.

Indirect calorimetry allows for measuring energy expenditure based on the measurement of oxygen consumption, carbon dioxide production, and urine nitrogen loss for energy production from carbohydrates, proteins, and fat and using established equations [35].

The doubly labeled water (DLW) technique is an innovative method for measuring energy expenditure derived from the measurement of carbon dioxide production. It has become the reference method, considered the gold standard for human energy requirements under daily living conditions [36]. It was first developed by Lifson et al. in the late 1940s [37] when they discovered that the oxygen in respiratory carbon dioxide is in isotopic equilibrium with the oxygen in body water. Firstly, they experimented with laboratory mice [38], then with free-range animals [39], and, by 1975, with the advances in analytical devices and reductions in the costs of ^{18}O-enriched water, the method was applied in the field of human energy metabolism. The first validation for the measurement of energy expenditure in humans was in 1982 [40].

The DLW procedure consists of providing participants with water labeled with nonradioactive heavy oxygen and hydrogen isotopes ($^2H_2{}^{18}O$). The two isotopes equilibrate with total body water and then are eliminated differently from the body. Oxygen leaves the body partly in the form of exhaled carbon dioxide (CO_2) and partly in the form of water (H_2O). Deuterium (^2H) only leaves the body in the form of water. Thus, the difference in the rate of oxygen and hydrogen loss provides an estimate of the loss of oxygen in the form of carbon dioxide and, thereby, an estimate of carbon dioxide production and energy expenditure [10].

In practice, the DLW procedure includes collecting two samples of body water (saliva, urine, or blood); usually, urine is chosen. The first sample is collected several hours after dose administration when equilibrium has been established with total body water (4–6 h later). The second sample is collected at the end of the observational interval, usually 14 days later (1–3 weeks). The difference in the oxygen and hydrogen loss rate calculated from these two urine samples allows for calculating energy expenditure over the period studied, using standard indirect calorimetric equations [10, 36].

The DLW technique is the only method to measure energy expenditure in any environment, especially with regard to activity energy expenditure, where there is no interference with the subjects' behavior [36]. Because of this, the method was primarily applied for the measurement of physical activity levels. Additionally, the DLW method has become the gold standard for assessing energy requirements [41] and providing external validation of different dietary assessment methods [42].

This human validation technique included weight stability, overfeeding, underfeeding, intravenous feeding, and heavy exercise [43–46]. These validations showed an accuracy of the method to estimate energy expenditure of 1–2% and an individual precision of 7%, supporting its use as a method to test the accuracy and precision of self-reported energy intake [33].

When comparing energy intake assessed by different traditional instruments and energy expenditure using the DLW technique, most studies show a lower value for reported energy intake than measured total energy expenditure. Prentice conducted one of the first studies in 1986 [47] with young adults obese and lean women. They recorded their food intake by weighing all foods and fluids over 7 days. Energy intake was 34% less than energy expenditure measured by DLW in obese women, while in lean women, there were no differences (2% NS). In 1990, Schoeller summarized the results of nine studies that compared self-reported energy intake with measured energy expenditure by DLW [48]. Lean, nonathletic groups living in industrialized countries demonstrated the smallest mean difference between self-reported energy intakes and expenditure (0–20%), while obese populations demonstrated the largest mean differences (−35 and −50%). Most of the difference

appears to be due to underreporting, but some subjects lost weight during the reporting period, indicating that some of the difference was due to under-eating. More recently, Freedman et al. [49] pooled data from five large studies conducted with different aims and in diverse populations within the United States. These studies validated dietary self-reporting instruments that used DLW as a reference of energy intake to clarify the measurement properties of FFQs and 24-hour. The review, which involved over 2000 participants, confirmed that underreporting of energy intake was observed in each of the five studies. The average rate of underreporting of energy intake was 28% with an FFQ and 15% with a single 24-hour. Participants with obesity (BMI $>$ 30 kg/m^2) underreported energy intake by 7% more than those with a BMI in a healthy range, with no differences between men and women. Having a high school education was also associated with more underreporting of energy intake using either instrument, compared to those who had some college education. Age older than 59 years was associated with less underreporting of energy intake than those aged 50–59. The review also showed that the use of multiple 24-hour substantially increases the correlations when compared with a single 24-hour, but the percent error changed only slightly when more than two 24-hour were averaged. Thus, dietary data were more consistent when two recalls were employed in each participant, but little was gained by further replication. Finally, in a more recent publication, Burrows et al. [50] published a systematic review of 59 studies that included over 6000 adults from different countries on almost every continent. The aim was to evaluate the validity of dietary assessment methods (24-hour, FR including WFR and FFQs) used to estimate adults' energy intake compared with total energy expenditure measured by DLW. The majority of studies reported significant ($P < 0.05$) underreporting of energy intake (average 30–40%) when compared to energy expenditure. The most misreporting was observed for the FFQs and the least for 24-hour. Studies that included a technology-based method (photography, oral recordings) reduced underreporting slightly compared to non-technology methods but still showed underreporting.

The same author carried out a review in children [51] to examine the validity of dietary assessment methods for estimating energy intake in children and adolescents compared with energy expenditure measured using DLW. The most common methods used were FFQ and weighed food records. Child characteristics, including weight status, age, and sex, were not found to influence reported energy intake accuracy consistently. For FFQs, significant underreporting of energy intake ranged from −7 to −23%. Substantial overreporting with FFQ was found in one study, this being greatest when mothers reported their children's intake (+44%), followed by fathers' reporting (+21%), then children's reports of their intakes (+13%).

In a study carried out on independent older people from Brazil with different percentages of body fat [52], the proportion of participants who underreported their energy intake was 31 and 40.5% for the 24-hour and the FFQ, respectively. Underreporting was more frequent in subjects with a higher percentage of body fat and females.

Misreporting dietary intake is a problem for investigators who study relationships between diet, health, and disease. Investigators are, therefore, performing studies that may either reduce misreporting or adjust the self-reported data using techniques to reduce the effect of such misreporting on study outcomes [33, 53].

3.2 Biomarkers

Improving dietary assessment is essential for nutritional epidemiology when attempting to understand the relationship between diet and chronic disease phenotypes, considering that self-reported dietary intake is subject to random and systematic bias [54, 55]. Random error refers to the unpredictable source of error that contributes to variability. It can be considered the difference between an individual's reported intake on a specific administration of the dietary assessment instrument and an individual's long-term average reported intake based on many multiple administrations of the same instrument (Table 2). This variability in measurements can reduce precision and cause a loss of statistical power. However, the impact of random errors can be properly minimized with statistical methodology [56].

Systematic error or bias refers to a measurement that consistently deviates from the true value in the same direction (i.e., always lower or higher) and can be difficult to detect and thus to be corrected [57]. An example of systematic error is intake-related bias, such as the case of underreporting in participants with obesity. A repeat measurement cannot reduce or eliminate energy intake bias, as consumption measurement errors will tend to be positively correlated across assessment instruments [58]. The presence of dietary measurement errors (the difference between "true" and "observed" intake) may interfere with the study of the association between diet and disease [54]. In this sense, biomarkers can objectively measure food consumption without the bias of traditional self-reported dietary instruments and examine their biological effects. However, they are still prone to potential random errors, such as daily diet variation [59].

A biomarker is a biological characteristic that can be objectively measured and serves as an indicator of normal biological processes, pathogenic processes, or responses to therapeutic interventions [60]. In the nutritional field, biomarkers have been referred to as nutritional status indicators related to intake or metabolism of nutrients, dietary patterns, or other dietary components [61]. Unfortunately, biomarkers are usually expensive and invasive [62], so their use in large epidemiological studies can be difficult to implement.

Table 2
Comparison between dietary assessment methods and biomarkers

Method	Characteristics	Strengths	Limitations
FFQ	Large sample Assess intake over long periods Limited resources	Easy to apply Include seasonal variability of food intake It may be applied online Allow for study-specific groups of foods or nutrients Low cost	A short FFQ may underestimate the true variation in dietary intake A long FFQ may cause a respondent burden Require validation of the questionnaire Cross-cultural adaptation
24-hour	Normal size sample Short time period Limited resources	Easy to apply It may be applied online Low cost and respondent burden	Require trained interviewers
FR	Normal size sample Short period Adequate resources	More accurate than FFQ and 24-hour Multiple records can be used to validate the dietary assessment method	Require specific respondent skills Respondents may vary their usual intake to avoid recording complications
WFR	Short sample Short period Adequate resources	More accurate than FFQ, 24-hour, and FR	Require specific respondent skills and motivation Respondents may vary their usual intake to avoid recording complications
DLW	Short sample Measurement of energy expenditure	An accurate method to measure energy expenditure	Very expensive Only measure energy expenditure, not food or nutrients
Biomarkers	Short sample Objective measurement of intake	Measure nutrient consumption without bias It can be used to validate another dietary assessment method	Usually expensive and invasive Require specific and expensive equipment Still not available for many foods and nutrients

Although some biomarkers have been used for a long time in research and clinical settings (e.g., serum cholesterol), identification of new ones and their use is constantly evolving, as laboratory methods develop increasingly sensitive essays that are able to identify subtle changes in biological and molecular processes occurring throughout the continuum between health and disease. An extensive list of biomarkers has already been suggested for nutritional interventions [63]. However, for most identified and validated biomarkers, there is still a lack of clarity regarding the applications, purposes, and, for some indicators, even their physiological mechanisms.

3.3 Classification

In nutritional research, biomarkers may have diverse uses [61, 64]; however, a universal classification has not yet been established.

3.3.1 Biomarkers as a Validation Method

Some biomarkers (e.g., DLW or the use of urinary nitrogen as a marker of dietary protein intake) have been used as a means of validating dietary questionnaires, frequently used in large epidemiological studies [65]. Its use is based on the assumption that a biomarker responds to dose-dependent intake, although this relationship is not always straightforward. Furthermore, it has the advantage that measurement errors are uncorrelated with dietary assessment methods through questionnaires [10].

The use of biomarkers to validate traditional methods of collecting dietary data may differ by application and nutrient. For instance, there are no known specific biomarkers for nutrients, such as fiber or total fat. For others, such as cholesterol or retinol, although their circulating levels may be used as biomarkers, they are so well regulated by homeostasis that they correlate poorly with intake and, therefore, are a poor standard of the performance of the dietary assessment method in a validation study [10]. This is why, in most cases, the use of biomarkers for this purpose is more useful for comparisons across dietary questionnaires [66].

3.3.2 Biomarkers of Intake or Exposure

An intake biomarker reflects the level of extrinsic variables to which an individual is exposed, such as diets or food components, including nutrients and non-nutrient components [67]. In the literature, exposure biomarkers are usually classified as recovery and concentration biomarkers [10]. Exposure biomarkers in urine are termed recovery biomarkers when full dose may be recovered; therefore, they refer to the absolute value of intake considering a specific period (frequently 24 hours). Concentration biomarker is a term used by some authors to name biomarkers measured in plasma. Although well correlated with the intake, concentration biomarkers may not reflect the absolute intake, as the concentration of a nutrient in the blood or tissue is influenced by physiological and environmental interactions apart from the diet. Indeed, individual genetic characteristics may also interact with these processes. One classic example of a recovery biomarker for sodium intake is sodium excretion in 24-hour urine collection. Due to its multiple hidden sources, non-urinary-based dietary sodium assessments are frequently inaccurate. Approximately 93% of sodium intake is excreted in urine [68], which is why urinary sodium excretion has been used as an objective marker of sodium intake.

Both recovery and concentration biomarkers have strengths and limitations. Recovery biomarkers are available for only a few nutrients (24-hour urinary sodium, potassium, and nitrogen) and short periods. For large epidemiological studies where long-term intakes are estimated, the need to take repeat measurements to

compensate day-to-day variability determines the need to combine measurements with total energy expenditure through DLW assessments as a reference measure, which makes this method impractical and expensive [10]. Moreover, the 24-hour urine collection protocol is cumbersome for participants, leading to increased inaccuracy [69].

Recently, Gao et al. proposed three subclasses of exposure biomarkers [70]:

- Food compound intake biomarkers (FCIBs): Divided into nutrient and non-nutrient intake biomarkers (e.g., nitrogen in urine for protein intake) [71].
- Food or food group intake biomarkers (FIBs): Analyzing single (or combined) markers that characterize intake by reflecting a food category. For example, carotenoids with vitamin C are a combined marker candidate for fruit and vegetable intake that has proven to be more accurate than these markers considered separately [59].
- Dietary pattern biomarkers: In general, these markers represent a mixture of FIBs and FCIBs that reflect an individual's average diet consumption. Most research has used them to discriminate consumers from nonconsumers of a specific dietary pattern or categorize relative adherence to a predefined diet [72]. For example, the effect of a Mediterranean Diet on urinary metabolome was assessed by comparing a subsample of participants in the PREDIMED trial at 1 and 3 years of follow-up. Results showed that the most prominent metabolic signatures associated with Mediterranean Diet intervention were related to the metabolism of carbohydrates, creatine, creatinine, amino acids, lipids, and microbial cometabolites [73].

3.3.3 Biomarkers of Effect

Biomarkers of effect reflect the functional response of the body to an exposure [67]. Therefore, they reflect the intake and the metabolism of nutrients and, possibly, the effects on physiological or pathological processes. They are defined in relation to the time course of the response until they reach a steady state or return to baseline levels [64]. Some authors include in this category biomarkers of efficacy when considering indicators of an improvement in a physiologic function or a decrease in risk factors for a disease [64] as a response to a certain diet or dietary exposure. They are often called risk-effect biomarkers; they are widely used in clinical practice, reflecting the different intermediate disease phenotypes or their severity. One example is a change in blood pressure levels as a potential mechanism for a change in cardiovascular disease risk [59].

3.3.4 Biomarkers of Susceptibility or Host Factors

Biomarkers of susceptibility refer to a measurable indicator (including genetic but also intrinsic factors related to the host) that influences an individual's response to dietary exposure [67, 70]. Also called resilience to exposure, they predict, based on the individual's biological background, the intensity of the effect due to exposure.

Considering some of the characteristics previously mentioned, some authors have postulated that the usual classification for biomarkers is ambiguous, and a more flexible definition is needed [67, 70]. A biomarker may fit into more than one category, as it may combine elements of the exposure, functional, or susceptibility classification, depending on the outcome purpose of the measurement or the procedures followed. Qian Gao et al. [70] summarized the diverse classification schemes found in the literature.

3.3.5 Metabolomics for Potential Biomarker Identification

The global analysis techniques called "omics" approaches are a new research area that has opened up over recent decades to discover diet biomarkers or biomarkers' patterns. Omics technologies (which include genomics, transcriptomics, proteomics, and metabolomics) consider the complexity of diet, the synergistic interaction between nutrients or food compounds, and the food matrix's influence [74]. This integrated technology approach generates data at a gene, transcript (RNA), protein, or metabolite level.

Metabolomics consists of studying metabolite or small molecules (<1500 Da) in biological samples such as urine, blood, or saliva, using mainly nuclear magnetic resonance spectroscopy, mass spectroscopy, and mass and liquid chromatography technology along with bioinformatics tools [72, 74]. These small molecules represent a mixture of exogenous and endogenous chemical substances, such as peptides, carbohydrates, organic acids, vitamins, polyphenols, minerals, food additives, and other items that can be ingested, used, or synthesized by a given cell or organism [75]. Metabolites found in biological samples can be influenced by genetics, microbiome, and lifestyle behaviors such as food and exposure to pollutants [76]. For example, differences in metabolite levels may be attributable to differences in the gut microbiota rather than dietary intake differences. Moreover, some other metabolites are synthesized by the organism using its biochemical pathways [74]. By identifying differences in molecular and biological pathways and the consequences when consuming different diets, metabolomics could detect and predict metabolic dysfunctions or the evolution of a healthy state towards a pathologic state related to intake, which may be applied in intervention and observational studies. However, a promising investigation is still incipient. Although computational tools have been created to illustrate route maps of metabolite structure with biochemical pathways, the task is complex as many compounds may be linked to different pathways [74]. Moreover, some metabolites may be related to many different foods. Such is the case of the 3-carboxy-4-methyl-

5-propyl-2-furanpropionate, associated with consumption of fish, alcohol, and wine; or the metabolite pyroglutamine, associated with intake of two food groups: red meat and poultry [77].

Along with the study of metabolites has come the development of metabolomics databases. The Human Metabolome Database (HMDB) is one of the largest databases of organism-specific metabolomics identified in human tissues. It was updated recently and now contains 114,100 human metabolites, along with their chemical structures, biological roles, physiological concentrations, disease associations, and metabolic pathways, among others [78]. MyCompoundID is a library of 8021 known endogenous human metabolites and 375,809 predicted human metabolites [79]. Specific databases, such as PhytoHub (focused on phytochemicals present in commonly consumed foods), Phenol-Explorer (including values for more than 500 different polyphenols contained in foods), or Exposome-Explorer (dedicated to biomarkers of exposure to environmental risk factors for diseases), are available at the web portal developed by the joint project The Food Biomarkers Alliance (FoodBAll) [80].

In epidemiological studies, the use of metabolomics techniques to identify biomarkers in combination with dietary pattern characterization improves the study's value as it provides a less biased estimation of dietary consumption [81].

3.3.6 Considerations When Selecting a Biomarker

Qualities of a promising biomarker include being sensitive, specific, suitable for application to many populations, and easy to measure using preferably noninvasive tissue sampling techniques [63].

In recent decades, multiple biomarkers have been proposed in the literature. These have usually emerged from a single exploratory study or have been established based on knowledge of food composition and human metabolism. These markers, defined as putative by some authors, need to confirm their potential as candidate biomarkers through validation schemes. This process implies the confirmation of their potential, replicating such associations in independent studies. The FoodBAll Consortium has developed a methodology for selecting, reviewing, and reporting potential putative biomarkers related to the consumption of foods. The "Guidelines for Biomarker of Food Intake Reviews (BFIRev)" [82] propose an eight-step scheme that aims to identify and report candidate biomarkers of a specific food or food group and provide available evidence for the systematic evaluation of their quality as biomarkers. So far, reviews on candidate biomarkers for assessing the consumption of dairy and eggs [83]; leafy, bulb, and stem vegetables [84]; tropical fruits [85]; nuts and vegetable oils [86] and berries and grapes [87] have been published. Most conclude that there have only been a limited number of accepted biomarkers of food intake, and databases in food metabolome are still needed.

Additionally, a position paper from the same Consortium [88] was published to outline a validation system not only for candidate biomarkers from the literature search but also as a test strategy for new candidate biomarkers identified from metabolomic studies or from food chemistry. It includes the assessment of eight criteria [88].

Considering those mentioned above, it is understandable that experimental studies to identify new biomarkers (presumably through metabolomics) shall be complemented with comprehensives reviews of the literature on possible preexisting biomarkers. This review will improve the identification of markers in metabolomics and broaden the list of compounds for validation as potential biomarkers.

Another issue of concern is whether one-time measurements can reflect long-term intake or status [10]. Within an individual, some metabolites have significant day-to-day or even overtime variations. For example, recent evidence on long-term studies suggests that sodium achieves a steady state after weeks or months of accumulation and excretion because of immune system regulation and storage in the skin, subcutaneous lymphatic networks, and muscle [89]. Therefore, a single 24-hour urine measurement cannot predict intake [90], and multiple collections should be considered when assessing intake to individual outcome data [69]. At a population level, day-to-day variations in sodium excretion are balanced out when calculating the population average [91]; therefore, a single 24-hour urine collection is suggested. The concern for single measurements relies on the possibility of misrepresenting usual exposure, and, therefore, the potential association between metabolites and health diseases may be poorly detected [92]. If repeat measurements of an indicator are taken, it is possible to assess the metabolites' reproducibility and the greater the likelihood that the indicator is a stable estimate of long-term intake [63].

Researchers should also seek to apply standardized biochemical procedures. Some general considerations when choosing a laboratory were listed by Heidi Michels Blanck et al. [93]. Particularly, in long-term prospective studies, daily as well as long-term quality control planning is important to address time-associated trends, such as sample stability (including the rate of deterioration over time and freeze-thaw effects), possible changes in reagents, analysts, and seasonal variation [93]. Moreover, to optimize and standardize laboratory activities, when reporting results, it is important to detail information related to assays and laboratory practices (e.g., manufacturers and platforms/kits), as well as specimen collection and storage (e.g., seasonality, time of day, analyte stability) [94]. As described recently [66, 94], to promote the validity and reproducibility of clinical and epidemiological research using biomarkers, the definition of complete protocols of specimen collection and handling and laboratory procedures are required.

4 Validity of Dietary Intake Assessment Methods

It has been frequently said that there is no perfect measurement of dietary intake, with the implication that validation studies are not possible. However, the lack of a perfect standard is not unique to dietary intake assessment methods; all measurements involve uncertainty, although they differ in their magnitude. Relative validation studies never compare an operational method with the absolute truth; instead, they compare one method with another [10].

The ideal procedure would be to determine absolute validity, that is, whether the measurement accurately reflects the exact concept it is intended to reflect. For this purpose, a perfect or near-perfect indicator of the target concept referred to as a gold standard (criterion) is needed. However, because of the lack of a gold standard in dietary assessment methodology, the degree of measurement error in the estimation of usual dietary intake cannot be accurately determined [95].

Validation of the dietary intake assessment method is required to show the magnitude and direction of the measurement error, the possible causes, and identify how these errors can be minimized or accounted for in the data's statistical analysis. Validation also provides information on possible misclassification, which is especially relevant when studying diet-disease associations in epidemiological studies [96].

The chosen method and reference methods naturally have some degree of inaccuracy and internal measurement errors, and the two methods must therefore be independent to avoid a correlation of errors. For instance, a quantitative FFQ that relies on memory can be validated against WFR that does not require the subject to recall its intake. However, the test method's poor validity may not necessarily be attributable to errors associated with the method but may also be related to the method's errors. To account for this possibility, a third criterion method, such as a biomarker or doubly labeled water, is often used to triangulate error, but the inclusion of such a criterion method is often expensive and not logistically possible [96]. Once dietary intake data have been generated using both methods, various statistical tests, such as correlation coefficients and Bland-Altman analyses, can be applied in assessing and interpreting the validity of the test method [96].

For the relative validation of FFQs, different reference standard methods have been used. These include other dietary assessment tools, such as 24-hour, FR, WFR or biomarkers for nutrients, and the doubly labeled water method, in the case of energy intake [10, 97]. For FFQs, a correlation coefficient ranging from 0.5 to 0.7 is considered moderate [10].

A meta-analysis performed in children and adolescents to assess dietary intake using FFQs showed that overall relative validity of

energy, macronutrients (CHO, protein, fat, and fiber), certain micronutrients (Ca, Fe, Zn, vitamin A, and vitamin C), and some food item (milk, fruits, and vegetables) intake estimation, using the FFQ, may be considered weak [97].

The U.S. National Cancer Institute's Observing Protein and Energy Nutrition (OPEN) study used intake biomarkers (DLW and urinary nitrogen) to evaluate the extent of misreporting and assess the components of the error introduced when an FFQ or a 24-hour are collected on two occasions in a large sample of groups of free-living individuals, but the magnitude of underreporting varied between foods. According to their results, underreporting of energy was greater than that of protein, possibly indicating a preferential underreporting of fat, carbohydrate, and alcohol. The extent of underreporting was positively associated with intake and higher in the second reporting of methods, probably reflecting the gradual loss of commitment after multiple reports of time-demanding questionnaires. Underreporting, when present, affected all food groups, but the magnitude of underreporting varied between foods. Although the impact of both the FFQ and the 24-hour measurement error on total energy and absolute protein intakes was severe, it was substantially weakened after energy adjustment was applied [15].

5 Concluding Remarks

Diet is a complex, modifiable behavior that influences an individual's health; therefore, its assessment is an important key component for public health surveillance. Traditionally, nutritional epidemiology's main instruments to collect dietary information include food frequency questionnaires, 24-hour recall, and food records. Although they have displayed agreement among them, data on energy and nutrients are prone to systematic misreporting errors, which may interfere with the association between diet and disease. Although they are convenient for implementation in large population studies, these instruments rely on participant memory to recall all foods consumed over the previous days, weeks, or months. Moreover, it is known that people tend to underreport certain types of food that are socially stigmatized or may be tempted to overreport others, given the sociocultural pressure to follow a "healthy" dietary pattern. On the other hand, physiology needs to be considered as it may account for differences in nutrient absorption and metabolism. Dietary validation studies are a necessity when it is considering these aspects.

In this sense, doubly labeled water and nutritional biomarkers can be used as reference instruments. While doubly labeled water is used to measure energy expenditure objectively, biomarkers provide an accurate reflection of dietary intake and new insights into

the biological effect of dietary patterns, lifestyle, and their impact on health. The integration of omics technology into traditional nutritional epidemiology to identify nutritional biomarkers is ongoing. Capable of gathering large amounts of data, metabolomics can help capture the diet's multidimensional nature and enhance our understanding of the role of food in health and disease. However, greater efforts are needed to identify and validate novel biomarkers, as sensitive and specific biomarkers are now available for only a few foods and nutrients. Doubly labeled water and metabolomics assays are expensive, so it is infeasible to use them to assess energy expenditure or dietary habits in large cohort studies with thousands of participants. However, it would be a start to incorporate their use in sub-studies to identify and quantify sources of measurement error in the study's primary dietary assessment instrument.

Particularly, when it comes to biomarker measurements for epidemiological purposes, investigators need to carefully address protocols for collecting samples and laboratory performance to assure optimal processing and storage conditions for the analytes and minimize random error and bias.

In summary, researchers need to focus on efforts to gain more accurate dietary information through the direct use of biomarkers to assess intake, calibration of dietary instruments against doubly labeled water or a nutrient biomarker, or novel statistical approaches to provide novel analyses of data from traditional self-reported dietary instruments.

References

1. Schwingshackl L, Schwedhelm C, Hoffmann G, Lampousi AM, Knüppel S, Iqbal K et al (2017) Food groups and risk of all-cause mortality: a systematic review and meta-analysis of prospective studies. Am J Clin Nutr 105(6):1462–1473
2. Freedman LS, Midthune D, Arab L, Prentice RL, Subar AF, Willett W et al (2018) Combining a food frequency questionnaire with 24-hour recalls to increase the precision of estimation of usual dietary intakes-evidence from the validation studies pooling project. Am J Epidemiol 187(10):2227–2232
3. Gil Á, Martinez de Victoria E, Olza J (2015) Indicators for the evaluation of diet quality. Nutr Hosp 31(Suppl 3):128–144
4. Pendergast FJ, Leech RM, McNaughton SA (2017) Novel online or Mobile methods to assess eating patterns. Curr Nutr Rep 6(3): 212–227
5. Höchsmann C, Martin CK (2020) Review of the validity and feasibility of image-assisted methods for dietary assessment. Int J Obes 44(12):2358–2371
6. Prentice RL, Pettinger M, Neuhouser ML, Tinker LF, Huang Y, Zheng C et al (2020) Can dietary self-reports usefully complement blood concentrations for estimation of micronutrient intake and chronic disease associations? Am J Clin Nutr 112(1):168–179
7. González-Domínguez R, Jáuregui O, Mena P, Hanhineva K, Tinahones FJ, Angelino D et al (2020) Quantifying the human diet in the crosstalk between nutrition and health by multi-targeted metabolomics of food and microbiota-derived metabolites. Int J Obes 44(12):2372–2381
8. Rankin D, Hanekom S, Wright H, MacIntyre U (2010) Dietary assessment methodology for adolescents: a review of reproducibility and validation studies. S Afr J Clin Nutr 23(2): 65–74
9. Rollo ME, Williams RL, Burrows T, Kirkpatrick SI, Bucher T, Collins CE (2016) What

are they really eating? A review on new approaches to dietary intake assessment and validation. Curr Nutr Rep 5(4):307–314
10. Willett W (2013) Nutritional epidemiology. Oxford University Press, New York
11. Saravia L (2018) Desarrollo, validación y medición de la fiabilidad de cuestionarios de frecuencia de consumo de alimentos para niños y adolescentes. Universidad de Zaragoza. https://zaguan.unizar.es/record/90520/files/TESIS-2020-106.pdf
12. Hong TK, Dibley MJ, Sibbritt D (2010) Validity and reliability of an FFQ for use with adolescents in Ho Chi Minh City, Vietnam. Public Health Nutr 13(3):368–375
13. Shim JS, Oh K, Kim HC (2014) Dietary assessment methods in epidemiologic studies. Epidemiol Health 36:e2014009
14. Collins CE, Boggess MM, Watson JF, Guest M, Duncanson K, Pezdirc K et al (2014) Reproducibility and comparative validity of a food frequency questionnaire for Australian adults. Clin Nutr 33(5):906–914
15. Naska A, Lagiou A, Lagiou P (2017) Dietary assessment methods in epidemiological research: current state of the art and future prospects. F1000Research 6:926
16. Henn RL, Fuchs SC, Moreira LB, Fuchs FD (2010) Development and validation of a food frequency questionnaire (FFQ-Porto Alegre) for adolescent, adult and elderly populations from Southern Brazil. Cad Saude Publica 26: 2068–2079
17. Barrat E, Aubineau N, Maillot M, Derbord E, Barthes P, Lescuyer J-F et al (2012) Repeatability and relative validity of a quantitative food-frequency questionnaire among French adults. Food Nutr Res 56. https://doi.org/10.3402/fnr.v56i0.18472
18. De Cock N, Van Camp J, Kolsteren P, Lachat C, Huybregts L, Maes L et al (2017) Development and validation of a quantitative snack and beverage food frequency questionnaire for adolescents. J Hum Nutr Diet 30(2): 141–150
19. Julián Almárcegui C, Huybrechts I, Gómez Bruton A, Matute Llorente Á, González Agüero A, Gómez Cabello A et al (2015) Validity of a food-frequency questionnaire for estimating calcium intake in adolescent swimmers. Nutr Hosp 32:1773–1779
20. Kunaratnam K, Halaki M, Wen LM, Baur LA, Flood VM (2018) Reliability and comparative validity of a Diet Quality Index for assessing dietary patterns of preschool-aged children in Sydney, Australia. Eur J Clin Nutr 72(3): 464–468
21. Moyersoen I, Demarest S, De Ridder K, Tafforeau J, Lachat C, Van Camp J (2017) Fat-soluble vitamin intake from the consumption of food, fortified food and supplements: design and methods of the Belgian VITADEK study. Arch Public Health 75:31
22. Rutishauser IH (2005) Dietary intake measurements. Public Health Nutr 8(7a):1100–1107
23. Saeedi P, Skeaff SA, Wong JE, Skidmore PML (2016) Reproducibility and relative validity of a short food frequency questionnaire in 9–10 year-old children. Nutrients 8(5):271
24. Söderberg L, Lind T, Karlsland Åkeson P, Sandström A-K, Hernell O, Öhlund I (2017) A validation study of an interviewer-administered short food frequency questionnaire in assessing dietary vitamin D and calcium intake in Swedish children. Nutrients 9(7):682
25. Wrieden W, Peace H, Armstrong J, Barton K (2003) A short review of dietary assessment methods used in National and Scottish Research Studies. Working Group on Monitoring Scottish Dietary Targets Workshop ed
26. Conway JM, Ingwersen LA, Vinyard BT, Moshfegh AJ (2003) Effectiveness of the US Department of Agriculture 5-step multiple-pass method in assessing food intake in obese and nonobese women. Am J Clin Nutr 77(5): 1171–1178
27. Subar AF, Thompson FE, Potischman N, Forsyth BH, Buday R, Richards D et al (2007) Formative research of a quick list for an automated self-administered 24-hour dietary recall. J Am Diet Assoc 107(6):1002–1007
28. Eisinger-Watzl M, Straßburg A, Ramünke J, Krems C, Heuer T, Hoffmann I (2015) Comparison of two dietary assessment methods by food consumption: results of the German National Nutrition Survey II. Eur J Nutr 54(3):343–354
29. Visser M, Elstgeest LEM, Winkens LHH, Brouwer IA, Nicolaou M (2020) Relative validity of the HELIUS food frequency questionnaire for measuring dietary intake in older adult participants of the longitudinal aging study Amsterdam. Nutrients 12(7):1998
30. FAO-OPS-OMS (2017) 2016 América Latina y El Caribe. Panorama de la seguridad alimentaria y nutricional. Sistemas alimentarios sostenibles para poner fin al hambre y la malnutrición. Available from: http://www.fao.org/americas/recursos/panorama/es/
31. Saravia L, González-Zapata LI, Rendo-Urteaga T, Ramos J, Collese TS, Bove I et al (2018) Development of a food frequency questionnaire for assessing dietary intake in children

and adolescents in South America. Obesity (Silver Spring) 26(Suppl 1):S31–s40

32. Eldridge AL, Piernas C, Illner AK, Gibney MJ, Gurinović MA, de Vries JHM et al (2018) Evaluation of new technology-based tools for dietary intake assessment-an ILSI Europe dietary intake and exposure task force evaluation. Nutrients 11(1):55
33. Ravelli MN, Schoeller DA (2020) Traditional self-reported dietary instruments are prone to inaccuracies and new approaches are needed. Front Nutr 7:90
34. Kenny GP, Notley SR, Gagnon D (2017) Direct calorimetry: a brief historical review of its use in the study of human metabolism and thermoregulation. Eur J Appl Physiol 117(9): 1765–1785
35. da Rocha EE, Alves VG, da Fonseca RB (2006) Indirect calorimetry: methodology, instruments and clinical application. Curr Opin Clin Nutr Metab Care 9(3):247–256
36. Westerterp KR (2017) Doubly labelled water assessment of energy expenditure: principle, practice, and promise. Eur J Appl Physiol 117(7):1277–1285
37. Lifson N, Gordon GB et al (1949) The fate of utilized molecular oxygen and the source of the oxygen of respiratory carbon dioxide, studied with the aid of heavy oxygen. J Biol Chem 180(2):803–811
38. Lifson N, Gordon GB, Mc CR (1955) Measurement of total carbon dioxide production by means of D2O18. J Appl Physiol 7(6): 704–710
39. Lifson N (1966) Theory of use of the turnover rates of body water for measuring energy and material balance. J Theor Biol 12(1):46–74
40. Schoeller DA, van Santen E (1982) Measurement of energy expenditure in humans by doubly labeled water method. J Appl Physiol Respir Environ Exerc Physiol 53(4):955–959
41. FAO/WHO/UNU (1985) Energy and protein requirements. WHO Technical Report Series 724. Geneva, Switzerland
42. Johnson R, Coward-McKenzie D (2001) Energy requirement methodology. p 31-I
43. Ravussin E, Harper IT, Rising R, Bogardus C (1991) Energy expenditure by doubly labeled water: validation in lean and obese subjects. Am J Phys 261(3 Pt 1):E402–E409
44. Schoeller DA, Kushner RF, Jones PJ (1986) Validation of doubly labeled water for measuring energy expenditure during parenteral nutrition. Am J Clin Nutr 44(2):291–298
45. Schoeller DA, Ravussin E, Schutz Y, Acheson KJ, Baertschi P, Jéquier E (1986) Energy expenditure by doubly labeled water: validation in humans and proposed calculation. Am J Phys 250(5 Pt 2):R823–R830
46. Speakman JR (1998) The history and theory of the doubly labeled water technique. Am J Clin Nutr 68(4):932s–938s
47. Prentice AM, Black AE, Coward WA, Davies HL, Goldberg GR, Murgatroyd PR et al (1986) High levels of energy expenditure in obese women. Br Med J (Clin Res Ed) 292(6526):983–987
48. Schoeller DA, Bandini LG, Dietz WH (1990) Inaccuracies in self-reported intake identified by comparison with the doubly labelled water method. Can J Physiol Pharmacol 68(7): 941–949
49. Freedman LS, Commins JM, Moler JE, Arab L, Baer DJ, Kipnis V et al (2014) Pooled results from 5 validation studies of dietary self-report instruments using recovery biomarkers for energy and protein intake. Am J Epidemiol 180(2):172–188
50. Burrows TL, Ho YY, Rollo ME, Collins CE (2019) Validity of dietary assessment methods when compared to the method of doubly labeled water: a systematic review in adults. Front Endocrinol (Lausanne) 10:850
51. Burrows T, Goldman S, Rollo M (2020) A systematic review of the validity of dietary assessment methods in children when compared with the method of doubly labelled water. Eur J Clin Nutr 74(5):669–681
52. Pfrimer K, Vilela M, Resende CM, Scagliusi FB, Marchini JS, Lima NKC et al (2015) Under-reporting of food intake and body fatness in independent older people: a doubly labelled water study. Age Ageing 44(1): 103–108
53. Bennett DA, Landry D, Little J, Minelli C (2017) Systematic review of statistical approaches to quantify, or correct for, measurement error in a continuous exposure in nutritional epidemiology. BMC Med Res Methodol 17(1):146
54. Kipnis V, Subar AF, Midthune D, Freedman LS, Ballard-Barbash R, Troiano RP et al (2003) Structure of dietary measurement error: results of the OPEN biomarker study. Am J Epidemiol 158(1):14–21; discussion 2–6
55. Kipnis V, Midthune D, Freedman L, Bingham S, Day NE, Riboli E et al (2002) Bias in dietary-report instruments and its implications for nutritional epidemiology. Public Health Nutr 5(6a):915–923
56. Thompson FE, Kirkpatrick SI, Subar AF, Reedy J, Schap TE, Wilson MM et al (2015) The National Cancer Institute's dietary

assessment primer: a resource for diet research. J Acad Nutr Diet 115(12):1986–1995
57. National Institutes of Health (2014) Dietary assessment primer, types of measurement error
58. Prentice RL, Sugar E, Wang CY, Neuhouser M, Patterson R (2002) Research strategies and the use of nutrient biomarkers in studies of diet and chronic disease. Public Health Nutr 5(6a):977–984
59. Picó C, Serra F, Rodríguez AM, Keijer J, Palou A (2019) Biomarkers of nutrition and health: new tools for new approaches. Nutrients 11(5): 1092
60. Raiten DJ, Namasté S, Brabin B, Combs G Jr, L'Abbe MR, Wasantwisut E et al (2011) Executive summary--biomarkers of nutrition for development: building a consensus. Am J Clin Nutr 94(2):633s–650s
61. Potischman N, Freudenheim JL (2003) Biomarkers of nutritional exposure and nutritional status: an overview. J Nutr 133(3):873s–874s
62. Kirkpatrick SI, Collins CE, Keogh RH, Krebs-Smith SM, Neuhouser ML, Wallace A (2018) Assessing dietary outcomes in intervention studies: pitfalls, strategies, and research needs. Nutrients 10:1001
63. Coulston A, Boushey C, Ferruzzi M, Delahanty L (2017) Nutrition in the prevention and treatment of disease, 4th edn. Academic Press, London
64. Biesalski HK, Dragsted LO, Elmadfa I, Grossklaus R, Müller M, Schrenk D et al (2009) Bioactive compounds: definition and assessment of activity. Nutrition 25(11–12): 1202–1205
65. Yuan C, Spiegelman D, Rimm EB, Rosner BA, Stampfer MJ, Barnett JB et al (2018) Relative validity of nutrient intakes assessed by questionnaire, 24-hour recalls, and diet records as compared with urinary recovery and plasma concentration biomarkers: findings for women. Am J Epidemiol 187(5):1051–1063
66. Potischman N (2003) Biologic and methodologic issues for nutritional biomarkers. J Nutr 133(Suppl 3):875s–880s
67. Dragsted LO, Gao Q, Praticò G, Manach C, Wishart DS, Scalbert A et al (2017) Dietary and health biomarkers-time for an update. Genes Nutr 12:24
68. Lucko AM, Doktorchik C, Woodward M, Cogswell M, Neal B, Rabi D et al (2018) Percentage of ingested sodium excreted in 24-hour urine collections: a systematic review and meta-analysis. J Clin Hypertens (Greenwich) 20(9):1220–1229
69. Ginos BNR, Engberink R (2020) Estimation of sodium and potassium intake: current limitations and future perspectives. Nutrients 12(11):3275
70. Gao Q, Praticò G, Scalbert A, Vergères G, Kolehmainen M, Manach C et al (2017) A scheme for a flexible classification of dietary and health biomarkers. Genes Nutr 12:34
71. Hedrick VE, Dietrich AM, Estabrooks PA, Savla J, Serrano E, Davy BM (2012) Dietary biomarkers: advances, limitations and future directions. Nutr J 11:109
72. Guasch-Ferré M, Bhupathiraju SN, Hu FB (2018) Use of metabolomics in improving assessment of dietary intake. Clin Chem 64(1):82–98
73. Vázquez-Fresno R, Llorach R, Urpi-Sarda M, Lupianez-Barbero A, Estruch R, Corella D et al (2015) Metabolomic pattern analysis after Mediterranean diet intervention in a nondiabetic population: a 1- and 3-year follow-up in the PREDIMED study. J Proteome Res 14(1): 531–540
74. Sébédio JL (2017) Metabolomics, nutrition, and potential biomarkers of food quality, intake, and health status. Adv Food Nutr Res 82:83–116
75. Wishart DS (2008) Metabolomics: applications to food science and nutrition research. Trends Food Sci Technol 19(9):482–493
76. Collins C, McNamara AE, Brennan L (2019) Role of metabolomics in identification of biomarkers related to food intake. Proc Nutr Soc 78(2):189–196
77. Langenau J, Oluwagbemigun K, Brachem C, Lieb W, Giuseppe RD, Artati A et al (2020) Blood metabolomic profiling confirms and identifies biomarkers of food intake. Metabolites 10(11):468
78. Wishart DS, Feunang YD, Marcu A, Guo AC, Liang K, Vázquez-Fresno R et al (2018) HMDB 4.0: the human metabolome database for 2018. Nucleic Acids Res 46(D1): D608–Dd17
79. Huan T, Tang C, Li R, Shi Y, Lin G, Li L (2015) MyCompoundID MS/MS search: metabolite identification using a library of predicted fragment-ion-spectra of 383,830 possible human metabolites. Anal Chem 87(20): 10619–10626
80. Food Metabolome Web Portal (2017) The Food Biomarker Alliance. https://foodmetabolome.org/databases
81. Brouwer-Brolsma EM, Brennan L, Drevon CA, van Kranen H, Manach C, Dragsted LO et al (2017) Combining traditional dietary assessment methods with novel metabolomics techniques: present efforts by the Food Biomarker Alliance. Proc Nutr Soc 76(4):619–627

82. Praticò G, Gao Q, Scalbert A, Vergères G, Kolehmainen M, Manach C et al (2018) Guidelines for Biomarker of Food Intake Reviews (BFIRev): how to conduct an extensive literature search for biomarker of food intake discovery. Genes Nutr 13:3
83. Münger LH, Garcia-Aloy M, Vázquez-Fresno R, Gille D, Rosana ARR, Passerini A et al (2018) Biomarker of food intake for assessing the consumption of dairy and egg products. Genes Nutr 13:26
84. Brouwer-Brolsma EM, Brandl B, Buso MEC, Skurk T, Manach C (2020) Food intake biomarkers for green leafy vegetables, bulb vegetables, and stem vegetables: a review. Genes Nutr 15(1):7
85. Vázquez-Manjarrez N, Ulaszewska M, Garcia-Aloy M, Mattivi F, Praticò G, Dragsted LO et al (2020) Biomarkers of intake for tropical fruits. Genes Nutr 15(1):11
86. Garcia-Aloy M, Hulshof PJM, Estruel-Amades S, Osté MCJ, Lankinen M, Geleijnse JM et al (2019) Biomarkers of food intake for nuts and vegetable oils: an extensive literature search. Genes Nutr 14(1):7
87. Ulaszewska M, Garcia-Aloy M, Vázquez-Manjarrez N, Soria-Florido MT, Llorach R, Mattivi F et al (2020) Food intake biomarkers for berries and grapes. Genes Nutr 15(1):17
88. Dragsted LO, Gao Q, Scalbert A, Vergères G, Kolehmainen M, Manach C et al (2018) Validation of biomarkers of food intake-critical assessment of candidate biomarkers. Genes Nutr 13:14
89. Rakova N, Jüttner K, Dahlmann A, Schröder A, Linz P, Kopp C et al (2013) Long-term space flight simulation reveals infradian rhythmicity in human Na(+) balance. Cell Metab 17(1):125–131
90. Birukov A, Rakova N, Lerchl K, Olde Engberink RH, Johannes B, Wabel P et al (2016) Ultra-long-term human salt balance studies reveal interrelations between sodium, potassium, and chloride intake and excretion. Am J Clin Nutr 104(1):49–57
91. Campbell NRC, He FJ, Tan M, Cappuccio FP, Neal B, Woodward M et al (2019) The International Consortium for Quality Research on Dietary Sodium/Salt (TRUE) position statement on the use of 24-hour, spot, and short duration (<24 hours) timed urine collections to assess dietary sodium intake. J Clin Hypertens (Greenwich) 21(6):700–709
92. Sampson JN, Boca SM, Shu XO, Stolzenberg-Solomon RZ, Matthews CE, Hsing AW et al (2013) Metabolomics in epidemiology: sources of variability in metabolite measurements and implications. Cancer Epidemiol Biomarkers Prev 22(4):631
93. Blanck HM, Bowman BA, Cooper GR, Myers GL, Miller DT (2003) Laboratory issues: use of nutritional biomarkers. J Nutr 133(Suppl 3): 888s–894s
94. O'Callaghan KM, Roth DE (2019) Standardization of laboratory practices and reporting of biomarker data in clinical nutrition research. Am J Clin Nutr 112(Suppl 1):453s–457s
95. Gleason PM, Harris J, Sheean PM, Boushey CJ, Bruemmer B (2010) Publishing nutrition research: validity, reliability, and diagnostic test assessment in nutrition-related research. J Am Diet Assoc 110(3):409–419
96. Lombard MJ, Steyn NP, Charlton KE, Senekal M (2015) Application and interpretation of multiple statistical tests to evaluate validity of dietary intake assessment methods. Nutr J 14: 40
97. Saravia L, Miguel-Berges ML, Iglesia I, Nascimento-Ferreira MV, Perdomo G, Bove I et al (2020) Relative validity of FFQ to assess food items, energy, macronutrient and micronutrient intake in children and adolescents: a systematic review with meta-analysis. Br J Nutr:1–27

Chapter 16

The Use of Questionnaires to Measure Appetite

James H. Hollis

Abstract

Overweight and obesity are leading public health problems in many countries, and effective interventions that reduce the number of individuals with these conditions are required. Data indicates that different foods have divergent effects on appetite. Consequently, if foods or food characteristics that promote satiety can be identified, this information could be used to develop new foods or reformulate existing foods to aid weight management. To properly characterize the effect of a food or a food characteristic on appetite, it is essential that a robust methodological approach is used so that the results obtained are reproducible. Due to the human ability to introspect, appetite questionnaires can provide useful information about the effect of foods on appetitive sensations. While appetite questionnaires are relatively straightforward to administer, good experimental procedures are required to produce robust data. This chapter describes how to use appetite questionnaires to determine the effect of foods or food characteristics on appetite.

Key words Appetite, Hunger, Satiety, Satiation, Randomized control trial

1 Introduction: Why Measure Appetite?

In many countries, overweight and obesity are leading public health problems [1]. These conditions arise from a chronic positive energy balance, and a better understanding of the factors that influence food intake could facilitate the development of new approaches to aid weight management. A substantial body of evidence indicates that foods or food characteristics have divergent effects on appetitive sensations [2]. That is, certain foods make people feel fuller for longer after being consumed, which may lead to reduced food intake. In addition, many aspects of food, including its chemical composition [3], its texture [4], or viscosity [5], have been shown to influence postprandial appetite. Moreover, eating styles such as slow eating [6], increasing the number of masticatory cycles before swallowing [7], or taking smaller bites sizes [8] have been demonstrated to reduce postprandial hunger or increase fullness. This information could be used to develop foods that alter eating behavior in a manner that increases satiety (e.g., changing the texture to

Cinthia Baú Betim Cazarin (ed.), *Basic Protocols in Foods and Nutrition*,
Methods and Protocols in Food Science, https://doi.org/10.1007/978-1-0716-2345-9_16,

require more mastication before swallowing), identifying foods that have a high satiety value, and aid the development of new dietary approaches or foods that reduce hunger sensations and aid weight management [9, 10]. However, to establish the effect of an intervention on postprandial appetite, there is the need for a robust and repeatable experimental methodology to substantiate claims.

Appetite cannot be measured directly. Consequently, several indirect measures of appetite have been developed, including food intake, eating behaviors (e.g., eating rate or number of chewing cycles), or the plasma concentration of certain hormones or metabolites [11]. Among the indirect measures of appetite, questionnaires are likely the most common method to measure appetite. A key strength of using appetite questionnaires is that they take advantage of human's ability to introspect and thus provide insights into appetitive feelings that cannot be captured using other methods.

This chapter focuses on the use of questionnaires to assess appetite. It will describe a commonly used approach to studying appetite using questionnaires. The limitations and common decisions that must be made while designing a study are highlighted.

2 Appetite Terminology

Blundell et al. [12] proposed terminology for appetite research that is used throughout this chapter and provides a framework for discussing the methodology to measure appetite. This terminology is briefly described here:

2.1 Appetite

Blundell et al. [12] state that two definitions of appetite are in common use. The first is that appetite "covers the whole field of food intake, selection, motivation, and preference." The second is that appetite "refers specifically to qualitative aspects of eating, sensory aspects or responsiveness to environmental stimulation which can be contrasted with the homeostatic view based on eating in response to physiological stimuli, energy deficit, etc."

2.2 Hunger

Hunger is defined as (a) a "construct or intervening variable that connotes the drive to eat. Not directly measurable but can be inferred from objective conditions" or (b) a "conscious sensation that reflects a mental urge to eat. It can be traced to changes in physical sensations in parts of the body, stomach, limbs, or head. In its strong form may include feelings of light-headedness, weakness or emptiness in the stomach" [12].

2.3 Satiation

Satiation is defined as the "process that leads to the termination of eating; therefore, controls meal size. Also known as inter-meal satiety" [12].

2.4 Satiety

Satiety is defined as the "process that leads to inhibition of further eating, decline in hunger, increase in fullness after a meal has finished. Also known as post-ingestive satiety or inter-meal satiety" [12].

3 Methods

Studying the effect of an intervention (e.g., a food, a specific food characteristic, or change in eating style) on appetite frequently uses a preload study design. The preload study paradigm generally follows this basic procedure:

1. The participant reports to the laboratory and completes an appetite questionnaire to provide a baseline measure of appetite.
2. The participant eats the test food/meal within a specified amount of time (typically 15 min) in the prescribed manner (e.g., at a specified eating rate or using a specified number of chewing cycles before swallowing).
3. Further, appetite questionnaires are completed at regular intervals for a predetermined amount of time (e.g., on the completion of the test meal (t0) and then at t0 + 15 min, 30 min, 45 min, 60 min, 90 min, 120 min, 180 min and 240 min.
4. A test meal is provided, and the amount eaten recorded.

While preload studies appear straightforward, many factors need to be considered when designing these studies if robust and repeatable results are to be obtained. The major decision points will be further discussed.

3.1 The Environmental Context of Appetite Studies

When designing an appetite study, consideration must be given to balancing the internal and external validity of the study. The internal validity of a study relates to the degree to which a study design reduces systematic errors or biases so that robust causal inferences can be made. External validity relates to how the results of a study can be generalized to other situations or populations. Appetite studies are generally conducted in the laboratory. The major strength of conducting studies in the laboratory is that strong control can be exerted over experimental conditions, which increases the internal validity of the study. An individual factor of interest can be isolated and its influence on appetite unambiguously determined free from extraneous environmental factors (e.g., environmental distractions, noises, lighting, or ambience) that may influence the perception of food and appetite [13]. In addition, laboratory studies provide the potential to make measurements that may contribute to a mechanistic explanation for observed differences in appetite. For instance, blood samples can be collected and

assayed for hormones related to appetite, such as cholecystokinin, ghrelin, glucagon-like-peptide-1, peptide YY [14]. Differences in the plasma levels of these hormones (among others) may offer mechanistic support for any observed differences in subjective appetite. Moreover, studies indicate that the microstructure of eating (e.g., eating rate, number of chewing cycles, etc.) may also influence appetite, and these parameters are, at this time, best measured in the laboratory [15].

It is important to recognize that appetite is expressed in environments where both noticed and unnoticed stimuli operate to subtly or strongly influence food intake or appetite. For instance, meal size may be influenced by the label on a bottle of wine [16], the number of people present at a meal [17], or the proximity of food [18, 19]. In addition, nutrition labelling has also been shown to influence appetite or energy intake [20]. The palatability of a meal has a marked influence on food intake [19]. It is noteworthy that seemingly trivial factors such as the weight of the cutlery, background music, or room color influence the rated palatability of a meal and, therefore, may influence food intake [21]. Consequently, a key weakness of laboratory studies is that they do not reflect the environment in which food is typically acquired and eaten. Therefore, results gained in the laboratory may not generalize to normal free-living situations (i.e., low external validity).

Field studies can be conducted to investigate the expression of appetite in natural environments; however, this approach has several weaknesses. First, there is a lack of strong control over experimental procedures, and several extraneous factors may contaminate the relationship between the investigated intervention and appetite. Second, replication of field studies may be difficult as recreating all the environmental factors to allow direct replication of a field study is not feasible. Third, while subjective appetite questionnaires can be administered outside of the laboratory using electronic devices, there may be issues with compliance (e.g., poor response rate). Fourth, it is generally not feasible to collect physiological samples that may provide a mechanistic explanation for the observed differences in appetite.

An innovative approach to study appetite and food intake, which may offer an advance on laboratory studies, is to use immersive virtual reality. A recent study found that users immersed in a virtual restaurant scene could eat while wearing a virtual reality headset and suggested this approach could be used to study eating behavior and appetite [22]. Thus, developing innovative approaches using virtual or augmented reality may bridge the gap between laboratory and free-living studies and provide new insights into how appetite is expressed.

Internal and external validity lies on a continuum, and laboratory studies still provide a certain amount of external validity (e.g., people eat food, at a table using utensils and from plates/bowls) while free-living studies provide some internal validity (e.g., efforts

are made to control experimental conditions). Consequently, all studies are a balance between internal and external validity, and the balance between the two should be dictated by the research question being addressed.

3.2 The Use of Crossover or Parallel-Arm Study Designs

Appetite studies can use a crossover study design or a parallel arm study design. In crossover studies, participants act as their own control and receive all the treatment options. In a parallel arm study, two or more treatments are provided, and each participant only receives one of the treatments. For example, for a study that uses three treatments (A, B, and C), one group only receives treatment A, another group only receives treatment B, and another group only receives treatment C.

A key advantage of crossover study designs is that they have greater statistical power than parallel-arm studies and require a smaller sample size. However, within-subjects studies raise the risk of a carryover effect. A carryover effect is when an effect of one experimental condition "carries over" to the next experimental condition. Consequently, a washout period that is sufficiently long to reduce the risk of a crossover effect should be incorporated into the study. The number of treatments used in a within-subject study can vary; however, issues such as participant's fatigue, participant's attrition, or the time available for the experiment typically limit the number of test sessions to fewer than six.

Parallel-arm studies remove the potential issue of carryover effects and the requirement for washout periods. Consequently, a study could potentially be completed in a shorter period. However, parallel-arm studies have lower statistical power than crossover studies and require more (potentially substantially more) participants. The time required to recruit the extra participants may be larger than the time saved by not having a washout period (this will depend on the length of the washout period). In addition, the extra cost of recruiting and compensating participants may also increase the costs of parallel-arm studies.

While both crossover studies and parallel arm studies have strengths and weaknesses, due to differences in how individuals interpret and respond to questions, it has been recommended that when conducting studies using appetite questionnaires, a within-subject study is employed [12]. However, careful consideration should be given to the possibility of carryover effects.

3.3 Randomization and Treatment Order

All experiments should be fully randomized and balanced to avoid introducing bias. A Latin square design should be used to make a balanced study. A Williams design (a generalized Latin square design), which balances the treatments over subjects and time so that each treatment is preceded by every other treatment an equal number of times, is the preferred method and will take into account a possible carryover effect [12].

3.4 Blinding

Blinding participants and the research team to the purpose of a study or the treatment order is a key part of conducting randomized control trials. A major problem when conducting appetite studies is hiding the experimental manipulation from the research team and the participant so that a double-blind study can be conducted. For instance, changing the macronutrient content of a food would likely influence the appearance, taste, texture, or appearance, which may provide clues to the research team or participants about the experimental manipulation being tested. The participants' expectations may then influence their responses. Thus, true double-blind studies may be difficult when determining the effect of a food or food characteristic on appetite, and the failure to adequately blind studies may lead to inflated effect sizes [23].

In an effort to limit the effects of blinding difficulties, participants in appetite studies are often deceived about the true purpose of the study. Deception strategies include misleading the participant about the study's true purpose by asking the participant to perform tasks unrelated to the study aims (e.g., the participants may be asked to complete cognitive performance tests to make the participant think this is the focus of the study). These procedures are used to remove a demand bias where participants form an impression of the purpose of the study and alter their behavior to fit that interpretation.

While deception has had a prominent role in behavioral studies for over a century, there is an argument that this approach has ethical implications and may infringe on the rights and dignity of the participant [24]. Moreover, it is not clear how well these deceptive practices work, and appetite studies that employ ruses rarely present data to demonstrate that the ruse was successful. Therefore, a post-study interview should be conducted to inform the participant about the study's true purpose and to ask questions whether they were aware of the study purpose. Another consideration is that Institutional Review Boards (IRB) may only allow deception if it is scientifically justified. A debriefing session is provided following the study to inform the participants of the study's true purpose. The participants may then withdraw their consent, and the data from that participant cannot be used.

In addition, these ruses may contaminate normal eating behavior and further reduce the relevance of the collected data to normal eating situations. For example, humans may base eating decisions on several factors based on their information (e.g., taste and visual cues such as portion size). Manipulating these characteristics, and hiding this from the participant, may remove the normal cognitive processes that contribute to eating decisions meaning that the relevance to eating decisions in typical eating situations is reduced.

3.5 Duration of Study

Appetite studies are generally short in duration, typically lasting from less than 1–4 h. It is imperative that the time between the preload and test meal is realistic regarding how the intervention

would be used in normal situations. These short-term studies allow for relatively rapid data collection, but any changes in appetite may be transient and may not persist over the longer term to cause a reduction in body weight. For instance, while a change in food intake may be observed at one meal, the body may compensate by increasing food intake at subsequent meals [25]. This is because appetite may be a dynamic process and is influenced by the body's energetic state.

It has been hypothesized that appetite is part of a physiological system that regulates body fat [26]. While this system only weakly defends against weight gain, it defends strongly against weight loss. Consequently, as fat mass is lost, there is a reduction in plasma leptin [27] which reduces the body's sensitivity to satiation/satiety signals, and a greater amount of food is required to be consumed to reach the same level of satiation/satiety [28]. Consequently, while a short-term study may find that an intervention reduces food intake, its effectiveness may diminish over time. Consuming food with a high satiation value may lead to reduced meal size, which could be measured using a short-term study, but may also lead to a new eating pattern (i.e., increased eating frequency) so that there is no change in daily energy intake. An example of this phenomenon is provided by a study using rodents. Cholecystokinin (CCK) was infused into rodents immediately prior to feeding, which persistently reduced meal size [29]. However, total daily energy intake remained unchanged as feeding frequency increased to compensate for the reduced meal size.

While short-term appetite studies can provide information regarding the factors that influence energy intake, it is not clear that this will be predictive of changes in body weight due to physiological compensatory measures. A greater focus should be placed on longer-term studies (potentially several months) to determine how interventions that reduce meal size influence eating patterns and ultimately body weight. Moreover, it should be determined if reducing meal size leads to unintended deleterious consequences (e.g., increased snacking of low-nutrient-density foods).

3.6 Timing of the Study

Many studies are conducted first thing in the morning. A key reason for this is that it allows participants to fast overnight and start each treatment session in a similar metabolic and appetitive state. However, this may mean that participants eat foods that are not typically eaten at that time. For instance, some studies have provided pizza as a test food for breakfast [7]. While the participants may have found pizza palatable (as determined by asking questions about the participant's rating of pizza palatability before the study began), it is not clear that they found pizza palatable first thing in the morning, which may have influenced their appetitive response or eating parameters.

3.7 Subject Selection

Participants for studies should be chosen carefully and the characteristics of the study group carefully considered so that the results are applicable to the target group of the intervention. For instance, is the food or intervention aimed at people with a certain body mass index, age range, or gender. Many appetite studies are conducted in universities and, while difficult to demonstrate conclusively, students are likely overrepresented in appetite studies. There are several advantages to using students. They are easy to recruit, are willing to take part in studies. College students are also more homogenous regarding factors such as education level, socioeconomic status, and cultural background [30], which allows for smaller sample sizes to be used. However, the study groups for many psychological studies have been described as WEIRD (Western, educated, and from rich, industrialized, and democratic) countries [31]. Thus, these participants do not reflect the wider society, and care should be taken not to extrapolate from studies whose study group does not reflect society [30].

Age has been found to influence appetite. Aging is associated with decreases in appetite and food intake [32]. Moreover, older adults may not respond to internal or external cues in the same manner as younger adults due to sensory losses [33]. While some studies have found that older adults use visual analogue scales (VAS) differently than younger adults, others have suggested that this effect may be due to age-related differences in perception rather than age-related differences in the use of VAS [34]. Therefore, attention should be given to specifying the age range of participants when recruiting for a study, recognizing the potential effects of age on appetite, and factoring this extra variability in when conducting power calculations.

A key issue when recruiting a study is the inclusion of females. Females have historically been underrepresented in clinical research [35]. It should not be assumed that females respond to interventions in the same manner as males, and female participation in appetite research is imperative if health inequalities are eliminated. Also, including equal numbers of females in studies is insufficient. Studies need to recruit enough female participants to draw valid and robust conclusions.

Moreover, the development of inclusion/exclusion criteria that relate specifically to females is required. A priori hypotheses regarding the influence of sex/gender on the outcome measures should be developed rather than just conducting post hoc analysis [36]. Due to its potential effect on appetite, the influence of the menstrual cycle should also be considered, and studies in females need to take into account the four stages of the estrous cycle [37]. Accounting for this in a study may be logistically difficult, requiring females to attend at specific phases of the menstrual cycle and the accurate determination of the phase.

There are several other considerations when setting inclusion/exclusion criteria. Acute illness can impair appetite [38], and individuals who have recently experienced acute illness should be excluded from the study or have their test session rearranged to a later date. Chronic disease, including nonmalignant pain, may also influence appetite, and unless the study specifically targets people with these conditions, they should be excluded [39]. The use of tobacco products, prescription or nonprescription drugs, or alcohol may also influence appetite. Therefore, individuals who use tobacco products are often excluded from studies. It is also prudent to exclude people who use prescription drugs that affect appetite listed as a side effect. Recent strenuous exercise may also influence appetite and should be proscribed for at least 24 h prior to the test day. The participant should also be instructed to use the least strenuous means possible to travel to the laboratory.

3.8 Control for Differences in Antecedent Diets and Energy Balance

It is desirable for all participants to be in a similar energy balance before the start of each test session. Many studies exclude individuals (or rearrange the participant's test session) who have conducted vigorous activity in the 24 h prior to any test session to achieve this criterion. In addition, recent weight changes may be a reason for exclusion from a study. Sometimes, the food intake on the day prior to the test session can potentially reduce the variability in responses [40]. As recent alcohol consumption may affect appetite, it is advisable to exclude participants who have consumed alcohol in the previous 24 h. A diet diary could also be completed before each test session to determine if there were differences in food or macronutrient intake in the lead-up to the test session.

Participants are generally asked to fast for approximately 12 h before a test session. While water may be allowed to be consumed, non-energy beverages that contain caffeine, such as diet colas, tea or coffee, should be prohibited.

3.9 Preload Meal Characteristics and Size

There are different approaches to determining the size of the preload that is served to study participants. First, a standard-sized meal can be served to all study participants (e.g., all participants receive a meal of 500 kcal). However, this does not take into account differences in size between participants, so that 500 kcal is a smaller meal for someone whose daily energy requirements each day are 3000 kcal compared to someone whose daily energy requirements are 2000 kcal. An alternative approach is to estimate energy requirements using equations (e.g., the Harris-Benedict equations or Schofield equations) and multiplying them by an appropriate physical activity level to estimate daily energy requirements. The test meal can be based on a percentage of this value (e.g., 30% of daily estimated energy requirement).

The participant should find the meal palatable. It is possible to confirm this by conducting a screening session and asking the

participant to taste the test food and rate its palatability. So, individuals who do not find the food palatable (for instance, someone who rates the palatability of the food <5 on an 8-point scale) should be excluded.

4 The Use of Questionnaires to Measure Satiation and Satiety

Traditionally, subjective ratings of appetite have been used to capture information about hunger, fullness, and the amount that would be eaten.

4.1 Open-Ended Questionnaires

One approach to obtaining information about appetitive sensations is to use open-ended questionnaires, which encourage a fuller answer regarding current appetitive sensations compared to predefined questions, which provide limited information. Consequently, a strength of open-ended questionnaires is that they may provide novel insights into appetite. While open-ended questionnaires have been used in appetite research to examine the temporal pattern and intensity of appetitive sensations [41, 42], a major limitation of open-ended questionnaires is the large number of responses that are possible. Consequently, the aggregation of data for analysis and its interpretation may be difficult. Open-ended questionnaires will commonly provide reports of sensations from different regions of the body but provide limited quantification of the intensity of these sensations. Further, open-ended questionnaires require more thought and more effort than is needed to complete VAS or category scales, so motivation to complete the questionnaire may become an issue [43].

4.2 Predefined Questions

Generally, questionnaires using predefined questions are used in appetite studies. The general approach is based on that proposed by Hill et al. [44]. Their original questionnaire posed six questions: "How hungry do you feel?" "How full do you feel?" "How strong is your desire to eat?" "How much do you think you could eat right now?" "Urge to eat?" and "Preoccupation with thoughts of food." It is not clear if these questions measure different facets of appetite or appetite reflects the combined responses. Stubbs et al. [45] report that the first component of a PCA analysis explains 85% of the variation observed across the six questions and the first two components over 90% of the variation.

5 Collection of Responses

Multiple methods have been to collect participant responses to appetite questionnaires. The most common methods are visual analogue scales and Likert scales.

5.1 Visual Analogue Scales

Figure 1 provides an example of a VAS. VAS have been used in clinical research to collect information about many subjective sensations, including pain and depression [46, 47]. For example, in appetite studies, responses to appetite questions are typically captured using a VAS. These VAS are typically between 100 mm and 150 mm and are anchored at the ends by the extremes of subjective feelings, for example, not at all hungry and as hungry as I have ever felt (Fig. 1).

Two methods are generally used to present appetite data collected using VAS. First, the average appetite rating at each time point can be calculated and presented using a graph or table [48]. Second, the data may also be presented as an area under the curve (AUC). The AUC is calculated by summarizing the mean scores from adjacent time points and then calculating the weighted mean based on the duration between the two time points [40].

5.2 Category Scales

Figure 2 provides an example of a category scale that may also be used to capture responses to appetite questions. When using category scales, participants are forced to choose a category to report their appetite sensations. There are some limitations to this approach. For instance, the information may be more limited as there are fewer responses that the participant can provide. If the number of categories is very limited (e.g., 3–5), the scale may not allow for sufficient discrimination. However, with a large number of categories (e.g., >13), meaningful discrimination between adjacent categories is also questionable (Fig. 2).

It should be recognized that the scales (VAS or category) are not true ratio scales. That is, the difference between a rating of 2 and a rating of 3 on a VAS or category scale is not the same as a difference between an 8 and 9. Moreover, a rating of 8 should not be interpreted as a feeling twice as intensive as a rating of 4.

Fig. 1 An example of a visual analogue scale

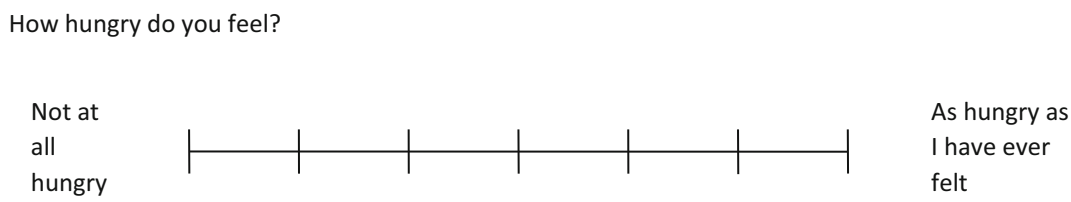

Fig. 2 An example of a category scale

5.3 Methods for Administering Questionnaires

Traditionally, responses to appetite questionnaires were captured using pen/pencil and paper. While this is a cheap and easy to administer method, it also has several drawbacks. First, the participant must not see or have access to their previous responses, contaminating their response. Second, using pen and paper methods means that the data requires transcribing from the paper questionnaires into a statistical package for analysis. This transcription is typically done by measuring where the participant made a line with a ruler and then noting the distance in mm from the left side. Measurement or transcription errors are possible with this approach, and an independent verifier should check data.

A technological advance has been developed that uses handheld computers to collect responses to questionnaires [49] or a wristwatch-based approach [50]. Validation studies show that those responses collected on handheld computers matched those collected by traditional methods [49, 51]. A previous barrier to using electronic methods was the lack of commercially available software and the cost of purchasing handheld computers. However, the widespread ownership of mobile phones and tablets coupled with the availability of software that facilitates the electronic collection of responses to appetite questionnaires (e.g., Qualtrics) can be used. Using electronic questionnaires has several advantages over pen and paper methods. The data can be easily uploaded to a statistical analysis package and does not require transcribing, which eliminates the potential for transcription errors. However, while electronic methods give comparable results to traditional pen and paper methods, these methods should not be used interchangeably.

6 Timing of the Questionnaires

Questionnaires should be administered before the intervention (baseline) and then at regular intervals after the intervention is completed. For example, a typical study may administer questionnaires when the test meal is completed (t0) and then t0 + 15, 30, 45, 60, 90, 120, 180 and 240 min. More measurements will provide additional information about the appetitive response but will put an additional burden on participants. This may lead to participants giving less thought to questionnaires due to fatigue and completing the questionnaire without thinking.

7 Statistical Analysis of Results

There are currently no generally accepted specific guidelines for the statistical analysis of data collected for appetite or food intake studies. However, the statistical analysis should comply with good

practice as used in clinical trials [52, 53]. Good scientific practice demands that the study hypothesis and the statistical analysis plan to test this hypothesis are specified before the study begins. Decisions regarding the chosen endpoints (e.g., appetite ratings, food intake, biomarkers of appetite), outliers, and missing data should be decided before the study begins. Moreover, how data will be presented (e.g., an area under the curve or mean at each time point or average hunger over the study duration) should be determined before the study begins. These decisions should be reported in the methods. A power calculation should be conducted to determine an adequate sample size, and this should be reported in the methods. Studies often use several scales or appetite measures, so the experiment-wide error rate should be controlled for multiple analysis.

8 Notes

This chapter highlights the major decision points when conducting an appetite study using questionnaires. Special attention should be made to the following areas, which may lead to a flawed study. First, a power calculation must be conducted using plausible data to estimate adequate sample size. Responses to appetite questionnaires are highly variable, and small sample sizes increase a type II error risk. Second, the nature of the test meal should be given consideration. If the test meal is too large, hunger may remain low (and fullness high), leading to floor effects (i.e., many participants rate their hunger at the lower extreme and fullness at the upper extreme). Alternatively, if the meal is too small, hunger may be elevated (and fullness low) throughout the test session leading to ceiling effects (i.e., many participants rate their hunger at the upper extreme and fullness at the lower extreme). Third, if pen and paper methods are used to collect appetite data, the participant should not be able to view their previous responses as this may bias their current response (e.g., they rate their hunger where they anticipate it should be based on previous responses). Fourth, if using pen and paper methods, there may be errors in transcribing the data from the questionnaires to a statistical package for analysis. Two independent individuals should check the data for accuracy.

References

1. Blüher M (2019) Obesity: global epidemiology and pathogenesis. Nat Rev Endocrinol 15(5): 288–298
2. Holt SH et al (1995) A satiety index of common foods. Eur J Clin Nutr 49(9):675–690
3. Gibbons C et al (2013) Comparison of postprandial profiles of ghrelin, active GLP-1, and total PYY to meals varying in fat and carbohydrate and their association with hunger and the phases of satiety. J Clin Endocrinol Metab 98(5):E847–E855
4. Zhu Y, Hsu WH, Hollis JH (2013) The effect of food form on satiety. Int J Food Sci Nutr 64(4):385–391
5. Zhu Y, Hsu WH, Hollis JH (2013) The impact of food viscosity on eating rate, subjective

appetite, glycemic response and gastric emptying rate. PLoS One 8(6):e67482
6. Goh AT et al (2021) Increased oral processing and a slower eating rate increase glycaemic, insulin and satiety responses to a mixed meal tolerance test. Eur J Nutr 60:2719–2733
7. Zhu Y, Hsu WH, Hollis JH (2013) Increasing the number of masticatory cycles is associated with reduced appetite and altered postprandial plasma concentrations of gut hormones, insulin and glucose. Br J Nutr 110(2):384–390
8. James LJ et al (2018) Eating with a smaller spoon decreases bite size, eating rate and ad libitum food intake in healthy young males. Br J Nutr 120(7):830–837
9. Hetherington MM et al (2013) Potential benefits of satiety to the consumer: scientific considerations. Nutr Res Rev 26(1):22–38
10. Fillon A et al (2021) A systematic review of the use of the Satiety Quotient. Br J Nutr 125(2): 212–239
11. Mattes RD et al (2005) Appetite: measurement and manipulation misgivings. J Am Diet Assoc 105(5 Suppl 1):S87–S97
12. Blundell J et al (2010) Appetite control: methodological aspects of the evaluation of foods. Obes Rev 11(3):251–270
13. Wansink B (2004) Environmental factors that increase the food intake and consumption volume of unknowing consumers. Annu Rev Nutr 24:455–479
14. Emilien C, Hollis JH (2017) A brief review of salient factors influencing adult eating behaviour. Nutr Res Rev 30(2):233–246
15. Bellisle F (2020) Edograms: recording the microstructure of meal intake in humans-a window on appetite mechanisms. Int J Obes 44(12):2347–2357
16. Wansink B, Payne CR, North J (2007) Fine as North Dakota wine: sensory expectations and the intake of companion foods. Physiol Behav 90(5):712–716
17. Decastro JM, Brewer EM (1992) The amount eaten in meals by humans is a power function of the number of people present. Physiol Behav 51(1):121–125
18. Privitera GJ, Zuraikat FM (2014) Proximity of foods in a competitive food environment influences consumption of a low calorie and a high calorie food. Appetite 76:175–179
19. Wansink B, Painter JE, Lee YK (2006) The office candy dish: proximity's influence on estimated and actual consumption. Int J Obes 30(5):871–875
20. McCann MT et al (2013) Influence of nutrition labelling on food portion size consumption. Appetite 65:153–158
21. Spence C (2015) Multisensory flavor perception. Cell 161(1):24–35
22. Oliver JH, Hollis JH (2021) Virtual reality as a tool to study the influence of the eating environment on eating behavior: a feasibility study. Foods 10(1):89
23. Hróbjartsson A et al (2014) Bias due to lack of patient blinding in clinical trials. A systematic review of trials randomizing patients to blind and nonblind sub-studies. Int J Epidemiol 43(4):1272–1283
24. Baumrind D (1985) Research using intentional deception – ethical issues revisited. Am Psychol 40(2):165–174
25. McKieman F, Hollis JH, Mattes RD (2008) Short-term dietary compensation in free-living adults. Physiol Behav 93(4–5):975–983
26. Speakman JR et al (2011) Set points, settling points and some alternative models: theoretical options to understand how genes and environments combine to regulate body adiposity. Dis Model Mech 4(6):733–745
27. Considine RV et al (1996) Serum immunoreactive leptin concentrations in normal-weight and obese humans. N Engl J Med 334(5): 292–295
28. Baver SB et al (2014) Leptin modulates the intrinsic excitability of AgRP/NPY neurons in the arcuate nucleus of the hypothalamus. J Neurosci 34(16):5486–5496
29. West DB, Fey D, Woods SC (1984) Cholecystokinin persistently suppresses meal size but not food-intake in free-feeding rats. Am J Physiol 246(5):R776–R787
30. Peterson RA (2001) On the use of college students in social science research: insights from a second-order meta-analysis. J Consum Res 28(3):450–461
31. Henrich J, Heine SJ, Norenzayan A (2010) Most people are not WEIRD. Nature 466(7302):29–29
32. Giezenaar C et al (2016) Ageing is associated with decreases in appetite and energy intake-a meta-analysis in healthy adults. Nutrients 8(1): 28
33. Spence C, Youssef J (2021) Aging and the (chemical) senses: implications for food behaviour amongst elderly consumers. Foods 10(1):168
34. Tiplady B et al (1998) Validity and sensitivity of visual analogue scales in young and older healthy subjects. Age Ageing 27(1):63–66
35. Liu KA, Mager NA (2016) Women's involvement in clinical trials: historical perspective and future implications. Pharm Pract (Granada) 14(1):708

36. Bennett JC (1993) Inclusion of women in clinical trials--policies for population subgroups. N Engl J Med 329(4):288–292
37. Dye L, Blundell JE (1997) Menstrual cycle and appetite control: implications for weight regulation. Hum Reprod 12(6):1142–1151
38. Langhans W (2007) Signals generating anorexia during acute illness. Proc Nutr Soc 66(3):321–330
39. Bosley BN et al (2004) Is chronic nonmalignant pain associated with decreased appetite in older adults? Preliminary evidence. J Am Geriatr Soc 52(2):247–251
40. Emilien CH, West R, Hollis JH (2017) The effect of the macronutrient composition of breakfast on satiety and cognitive function in undergraduate students. Eur J Nutr 56(6): 2139–2150
41. Mattes RD, Friedman MI (1993) Hunger. Dig Dis 11(2):65–77
42. Friedman MI, Ulrich P, Mattes RD (1999) A figurative measure of subjective hunger sensations. Appetite 32(3):395–404
43. Flint A et al (2000) Reproducibility, power and validity of visual analogue scares in assessment of appetite sensations in single test meal studies. Int J Obes 24(1):38–48
44. Hill AJ, Rogers PJ, Blundell JE (1995) Techniques for the experimental measurement of human eating behaviour and food intake: a practical guide. Int J Obes Relat Metab Disord 19(6):361–375
45. Stubbs RJ et al (2000) The use of visual analogue scales to assess motivation to eat in human subjects: a review of their reliability and validity with an evaluation of new hand-held computerized systems for temporal tracking of appetite ratings. Br J Nutr 84(4): 405–415
46. Bodian CA et al (2001) The visual analog scale for pain: clinical significance in postoperative patients. Anesthesiology 95(6):1356–1361
47. Ahearn EP (1997) The use of visual analog scales in mood disorders: a critical review. J Psychiatr Res 31(5):569–579
48. Zhu Y, Hollis JH (2014) Gastric emptying rate, glycemic and appetite response to a liquid meal in lean and overweight males. Int J Food Sci Nutr 65(5):615–620
49. Almiron-Roig E et al (2009) Validation of a new hand-held electronic appetite rating system against the pen and paper method. Appetite 53(3):465–468
50. Rumbold PL, Dodd-Reynolds CJ, Stevenson E (2013) Agreement between paper and pen visual analogue scales and a wristwatch-based electronic appetite rating system (PRO-Diary©), for continuous monitoring of free-living subjective appetite sensations in 7–10 year old children. Appetite 69:180–185
51. Whybrow S, Stephen JR, Stubbs RJ (2006) The evaluation of an electronic visual analogue scale system for appetite and mood. Eur J Clin Nutr 60(4):558–560
52. Pocock SJ et al (2002) Subgroup analysis, covariate adjustment and baseline comparisons in clinical trial reporting: current practice and problems. Stat Med 21(19):2917–2930
53. Assmann SF et al (2000) Subgroup analysis and other (mis)uses of baseline data in clinical trials. Lancet 355(9209):1064–1069

Chapter 17

Protocols for the Use of Indirect Calorimetry in Clinical Research

Katherine L. Ford, Camila L. P. Oliveira, Stephanie M. Ramage, and Carla M. Prado

Abstract

Resting energy expenditure (REE) is the largest energy expenditure component and is defined as the body's amount of energy required to maintain vital functions at rest while awake, in a fasting state, and in a thermoneutral environment. Several equations to predict REE have been developed over the years, but indirect calorimetry measurement provides the most accurate value. However, for the REE measurement to be accurate, some requirements apply. In this chapter, the protocols for measuring REE in healthy adults by a selection of four indirect calorimetry devices are described: Vmax® Encore; Q-NRG™ Metabolic Monitor; MedGem®; and FitMate GS.

Key words Indirect calorimetry, Resting energy expenditure, Resting metabolic rate, Protocol, Clinical trial, Energy expenditure, Resting energy metabolism, Calorie needs, Energy needs

1 Introduction

Human energy needs are assessed by measuring an individual's energy expenditure (EE) by calorimetric and noncalorimetric methods [1, 2]. Indirect calorimetry (IC) is an evidence-based calorimetric method that measures the products of respiration: oxygen (O_2) and carbon dioxide (CO_2). Using the volume of O_2 and CO_2 (VO_2 and VCO_2, respectively), the amount of energy released in the combustion of substrates (metabolism) is estimated [3]. Several energy metabolism components can be assessed using IC, such as total energy expenditure (TEE) and its major physiological components (i.e., resting energy expenditure [REE], thermic effect of food [TEF], and activity thermogenesis [AT]). However, this is limited to the availability of a whole-body IC.

More commonly assessed is REE, the largest TEE component, contributing approximately 60–70%, depending on an individual's physical activity levels [4]. This energy metabolism component is

Cinthia Baú Betim Cazarin (ed.), *Basic Protocols in Foods and Nutrition*,
Methods and Protocols in Food Science, https://doi.org/10.1007/978-1-0716-2345-9_17,

defined as the amount of energy required to maintain vital bodily functions while at rest, awake, in a postabsorptive state, and in a thermoneutral environment [5]. Assessment under such conditions ensures that the TEF and AT are not accounted for, providing an accurate REE assessment [6]. Although the terms REE and basal energy expenditure (BEE) are commonly used interchangeably, these energy metabolism components are not synonymous. The difference between REE and BEE relies mainly on how they are measured, and, for this reason, BEE is usually ~10% lower than REE, with the difference representing the energy expended during arousal [1, 7, 8]. Protocols required to measure BEE are beyond this chapter's scope and fully described elsewhere [9]. The focus of this chapter is on the most commonly used protocols to assess REE via IC.

Indirect calorimetry has been used for centuries and is based on the known amounts of heat generated per liter of O_2, and CO_2 consumed and produced when macronutrients are oxidized [1, 10, 11]. Because the oxidation of different macronutrients results in distinct VO_2 and VCO_2, IC estimates substrate oxidation rates, caloric equivalents for macronutrients, and EE [10, 11]. Several scientists have dedicated their work to develop equations for the estimation of EE based on measurements of O_2 and CO_2 [12, 13]. One of the most commonly used equations to estimate REE using IC is the abbreviated Weir equation [12]:

$$\text{REE (kcal/day)} = ((3.941 \times VO_2\,[\text{L}]) + (1.106 \times VCO_2\,[\text{L}])) \times 1440\ \text{min/day}.$$

IC obtains volumes of O_2 and CO_2 through total collection (rigid or flexible system), open-circuit (ventilated or expiratory collection), confinement (respiratory chamber), or closed-circuit systems [1]. Open-circuit calorimeters are a common type of IC devices used to measure REE in both clinical and research settings and include metabolic carts (with a facemask, mouthpiece, or canopy hood to capture gas exchanges) or whole-body calorimetry units, the latter of which, albeit its accuracy and preciseness, will not be discussed in this chapter due to rarity and impracticality in the clinical setting [7, 14]. Techniques and devices commonly used to measure fractional expired oxygen (F_EO_2) and carbon dioxide (F_ECO_2) will be discussed, including the Vmax® Encore and Q-NRG™ Metabolic Monitor. These devices are also compatible with a facemask, although the ventilated hood systems will be discussed. Systems that calculate REE by measuring only F_EO_2 and estimating F_ECO_2 include the FitMate GS (ventilated hood system) and the MedGem® (a mouthpiece/nose clip device) [15–17]. The FitMate GS uses a combination of F_EO_2 and an assumed Respiratory Quotient (RQ), the ratio of CO_2 produced to O_2 consumed, of 0.85 to estimate F_ECO_2 [12, 18, 19]. The

Table 1
Considerations for choosing an indirect calorimetry device

Device	Measures	Calibration (frequency; time required)	Time for warm up	Time for REE measurement	Device cost[a]	Cost per test[b]
Devices measuring O_2 and CO_2						
Vmax® encore	VO_2 VCO_2	Daily ~20 min	60 min	20–30 min	$$$	**
Q-NRG™	VO_2 VCO_2	Monthly ~10 min Pretest (automatic) 1 min	20 min for calibrations 5 min for REE test	10–15 min	$$	***
Devices measuring O_2						
MedGem®	VO_2	Pretest 30 s	~1 min	5–10 min	$	**
FitMate GS	VO_2	Pretest (automatic) ~1 min	N/A	15 min	$	*

Abbreviations: *REE* resting energy expenditure, *min* minutes, VO_2 volume of oxygen, VCO_2 volume of carbon dioxide
[a] $: <$20,000 USD; $$: $20,000–$50,000 USD; $$$: >$50,000 USD
[b] *: <$10; **: $10–$20; ***: >$20

MedGem® uses an abbreviated version of the Weir equation that includes a constant RQ of 0.85 [15]. Overall, considerations for choosing an IC device for the research and/or clinical settings will be dependent on the researcher's needs. Below, various considerations are outlined by the device. A summary of time and cost considerations is shown in Table 1.

1.1 Vmax® Encore Metabolic Cart

Several brands of metabolic carts are available in the marketplace; the Vmax® is one of the most accurate and has been used as a reference method to assess the accuracy of other IC devices [20–22]. The Vmax® requires the most time and expertise to perform an REE test. For a trained user, the calibration process will take between 20 and 30 min and must be completed at the start of every testing day. The time to complete a test will vary from 20 to 30 min, depending on how long it takes a participant to achieve a steady state of breathing. Last, this device requires that the user select the data points for EE calculations, whereas the other devices discussed herein automatically provide EE information. Overall, this device is highly accurate, but access to trained personnel and time should be considered.

1.2 Q-NRG™

The Q-NRG™ is the newest device of those discussed herein and is the most practical for use in spontaneously breathing persons in the clinical setting due to its high accuracy, rapid measurement time,

usability, size, and affordability [23–25]. The Q-NRG+™ is a similar device available for assessing REE in mechanically ventilated populations but will not be discussed herein. The Q-NRG™ device utilizes many disposable components, which increase the cost per test and must be considered for ongoing equipment operation compared to devices with a higher initial investment but are less costly per test (Table 1). However, considering the COVID pandemic, the use of disposables greatly minimizes the risk of contamination, placing less responsibility on the technician for ensuring complete sanitization between participants/patients.

In vitro studies of the Q-NRG™ found accurate concentrations of O_2 and CO_2 (within 2%) [24] and within 1% for $\dot{V}O_2$, $\dot{V}CO_2$, and EE [25]. A study of 15 healthy adults found that the Q-NRG™ had very good interunit precision (coefficient of variation <3% for $\dot{V}O_2$, and $\dot{V}CO_2$) and accuracy (mean difference ± SD (%) between Q-NRG™ and mass spectrometry analysis: 1.61 ± 1.41% for $\dot{V}O_2$, and − 1.53 ± 2.50% for $\dot{V}CO_2$) [25]. Additional studies to assess the accuracy and preciseness of the Q-NRG™ device in various population groups are ongoing [26, 27].

1.3 MedGem®

The MedGem® offers practicality and convenience for measuring REE in the clinical setting due to its size, portability, and the short time required for testing. Compared to the other devices discussed, the MedGem® uses a mouthpiece and a nose clip instead of a ventilated canopy hood; a set-up that may prove more acceptable to participants, depending on their comfort. Compared to a metabolic cart, participants are likely to achieve a steady state of breathing more rapidly when their EE is assessed by the MedGem® [28]. Additionally, this device measures $\dot{V}O_2$ and estimates $\dot{V}CO_2$ based on an assumed respiratory quotient (RQ) of 0.85 rather than measuring both $\dot{V}O_2$ and $\dot{V}CO_2$ [15, 28].

Studies that assessed the accuracy and precision of the MedGem® had returned varying results, including overestimating, underestimating, or validly predicting REE compared to other devices [28]. A systematic review by Hipskind et al. concluded that the MedGem® was an accurate portable IC device used in a healthy population, but the acceptability for its use in hospitalized and/or nutritionally compromised groups requires further research [28]. Most studies reviewed by Hipskind et al. that compared the MedGem® to a metabolic cart in healthy adults found that the MedGem® either overestimated or found no significant difference in REE compared to a metabolic cart. All but one study reviewed found that the MedGem® returned ≤200 kcal/day difference compared to a metabolic cart; the authors suggested that the significant differences observed did not necessarily equate to clinically relevant differences [28–32].

1.4 FitMate GS

Portable IC devices are used in clinical practice in place of predictive equations if they provide accurate and precise EE measures [19, 28]. The FitMate GS is a portable unit that would be practical for the clinical setting, although validation studies conducted in healthy adults across the body mass index (BMI) spectrum returned conflicting results. A study including 60 healthy adults compared REE measured by the FitMate GS (1668 ± 344 kcal/day) and the Douglas Bag (1662 ± 340 kcal/day) and found no statistically significant difference ($p = 0.579$) between devices, concluding that the FitMate GS was a precise and accurate device for REE measurement in healthy adults [17]. Another group compared the FitMate GS to Quark CPET (COSMED) in 30 adults and found the FitMate GS to be highly precise and accurate (mean REE 1779 ± 480 and 1785 ± 409, respectively; $p = 0.55$) [33]. Recently, Purcell et al. compared the FitMate GS to whole-body IC in 77 adults and found good precision (intraclass correlation coefficient: 0.80; 95% CI: 0.70–0.87) upon repeated measures but poor accuracy (1680 ± 420 and 1916 ± 461 kcal/day, respectively; $p < 0.001$) [19]. The device underestimated REE by 240 kcal/day on a group level [19]. Overall, the FitMate GS presents a viable portable IC device, but REE should be interpreted with caution given the heterogeneous results from validations studies.

Regardless of the IC device, to obtain an accurate and precise REE measure, steady-state breathing (metabolic equilibrium) must be achieved. Steady state occurs when VO_2 and VCO_2 remain stable (<10% variation) for 5 consecutive minutes [8, 34]. Several other factors that also impact EE must be considered, and thus, specific protocols should be followed [35]. The most commonly followed requirements for REE assessment are summarized in Fig. 1. Techniques that are device-specific will be discussed in the following sections.

2 Materials

2.1 Metabolic Cart Vmax® Encore

The protocol for the Metabolic Cart Vmax® Encore described in the following section utilizes the following materials:

1. Vmax® Module.
2. Desktop computer with Vmax® software.
3. 3 L syringe for flow sensor calibration.
4. Two compressed gas cylinders for external gas calibration.
   - Recommended gas mixes:
     (i) 4% CO_2, 16% O_2, Balance N_2.
     (ii) 26% O_2, Balance N_2.

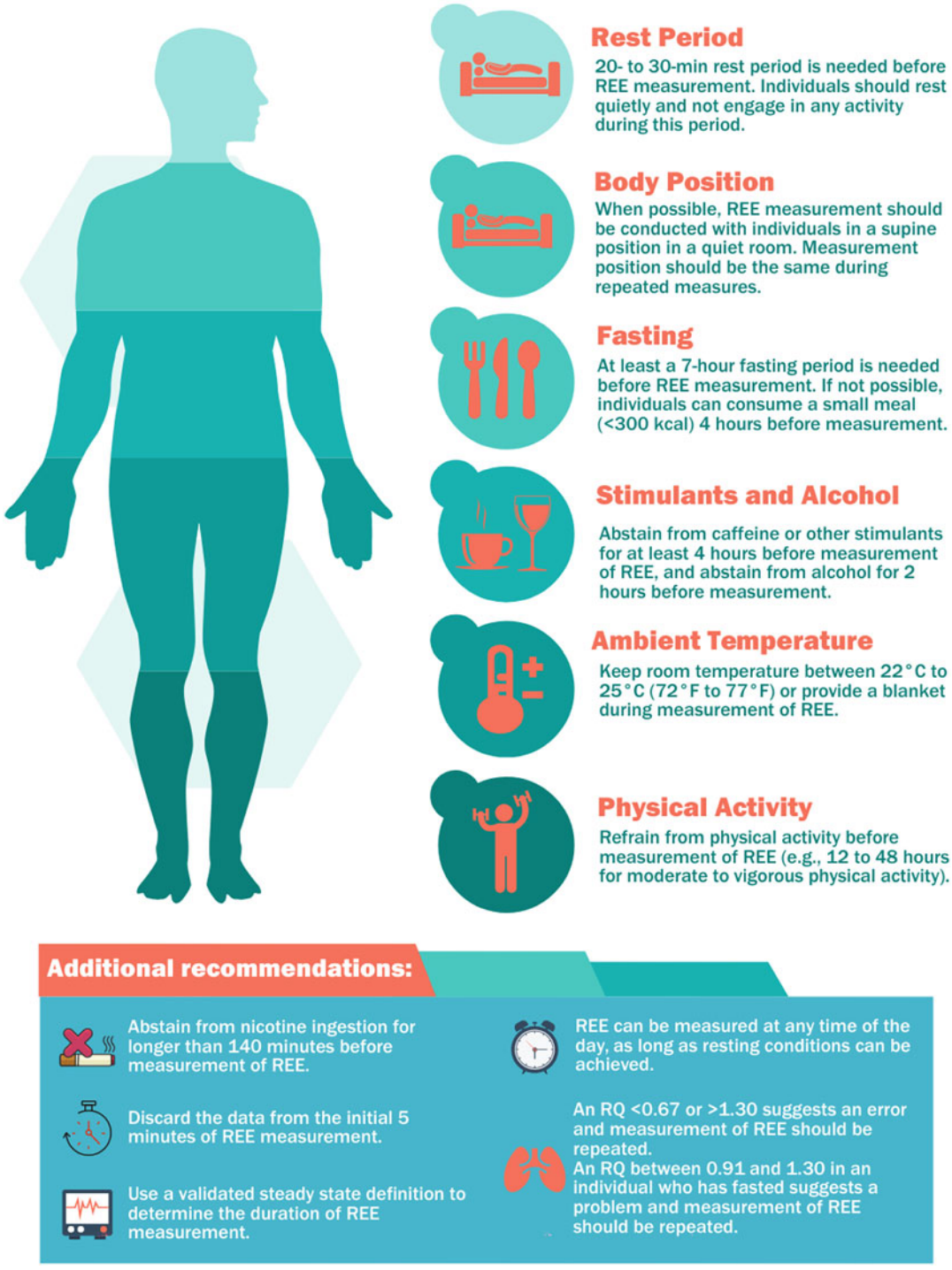

Fig. 1 Guidelines for measuring resting energy expenditure by indirect calorimetry in healthy adults. Abbreviations: min: minutes; REE: resting energy expenditure; RQ: respiratory quotient

5. Ventilated hood with veil.
6. Disposable hose.

2.2 Q-NRG™ Metabolic Monitor

The protocol for the Q-NRG™ described in the following section utilizes the following materials:

1. Q-NRG™ main unit.
2. Laptop computer with OMNIA software.
3. Canopy mode kit that includes a canopy hood and hose.
   - The items are reusable and require cleaning between each test.
4. Canopy veils and antibacterial filters.
   - These items are single use and must be disposed of after each test.
5. 3 L syringe for flow sensor calibration.
6. Compressed gas cylinder and pressure regulator for flow meter calibration.
   - Recommended gas mixture: 16% O_2, 5% CO_2, Balance N_2.

2.3 MedGem®

The protocol for the MedGem® described in the following section utilizes the following materials:

1. MedGem® device and power supply cord.
2. Disposable mouthpieces and nose clips.

2.4 FitMate GS

The protocol for the FitMate GS described in the following section utilizes the following materials:

1. FitMate GS device.
2. Canopy hood with veil.
3. Canopy blower and unit with a connected sampling line.

3 Methods

3.1 Pretest Protocol

Indirect calorimetry, regardless of the device used, requires preparation on behalf of the person being tested, herein referred to as the participant, to ensure that steady-state breathing is achieved (Fig. 1). In brief, prior to measuring REE by IC, individuals should be instructed to fast for at least 7 h, refrain from moderate to vigorous physical activity for 12–48 h, and avoid caffeine for 4 h and nicotine for 2.5 h [35]. Water and essential medication can be consumed, but no calories should be ingested. The participant should minimize daily living activities and physical activity before the measurement by driving or taking public transit to the testing facility and using the elevator instead of the stairs (if applicable).

Fig. 2 Participant resting in the supine position during a ventilated hood indirect calorimetry measurement

The testing environment should be at an ambient room temperature (22–25 °C/72–77 °F) and quiet [35]. The individual should rest, in the supine position, for 20–30 min prior to beginning the IC measurement [35, 36]. It is important that the individual abstains from sitting, standing, reading, listening to music, and/or fidgeting during this period to increase energy expenditure [35, 37–39]. The resting component of the protocol is crucial to ensure accurate measurement and decrease the influence of any activity that occurred leading up to the test [35]. Notably, an IC measurement can be done at any time of the day, given that the above conditions are met [35, 40, 41].

When the participant arrives for their measurement, verification that they followed the pretest protocols is needed. Ask the participant to lay in a supine position (Fig. 2) and rest quietly, without fidgeting, for 20–30 min. During the resting and testing period, the participant should be free from distractions, including any noises, music, reading, cell phone, etc. Indirect calorimetry devices require information about the participant described in the device-specific sections below; it is important to acquire this information before having the participant begin the resting period.

3.2 Vmax® Encore Metabolic Cart

The following methods are based on manufacturer recommendations, training, and the authors' combined clinical experience [42].

3.2.1 Calibration

The flow sensor must be calibrated at the start of every testing day. We recommend powering on the device 1 h prior to starting the calibration process. The calibration takes approximately 20 min to complete and should be completed before the participant arrives. To complete the calibration:

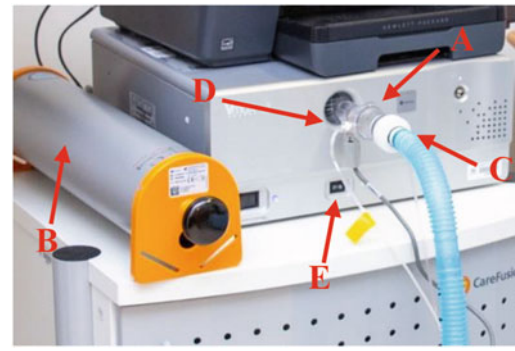

Fig. 3 Components of the Vmax. Arrows point to a specific component of the device, as defined by the letters: Vmax flow sensor (A); 3 L syringe (B); blue hose attached to flow sensor (C); sample line connected to flow sensor (D); flow pump switch (E)

1. Select the VMAX icon from the desktop.
2. Remove the flow sensor from the Vmax® device (silver box) and attach the open end, not the mesh end, to the 3 L syringe (Fig. 3).
3. On the computer, click on "1. Flow Sensor Calibration" in the Vmax® application.
4. Click "F1. Calibration" to begin.
5. Follow the prompts on the screen to zero the mass flow sensor. To do this, the following is needed:
   (a) Pump the syringe by pulling the black handle on the 3 L syringe all the way out and then pushing it all the way back into the syringe. Repeat this process twice, and then press the space bar on the keyboard to zero the machine.
   (b) Wait for the countdown on the screen and wait for the green bar to reach the dialogue box's end.
   (c) A screen with yellow bars will pop up automatically. The yellow bars will turn to green bars once the calibration has passed.
6. Manually calibrate the flow sensor using the 3 L syringe:
   (a) Pump the syringe (as instructed in **step 5a** above) to complete one full circle within each pair of yellow bands on the computer screen. Start with the inner-most bands and work outward.
      - The first 1.5 pumps of the syringe do not register.
      - Pump the syringe slowly at first and then increase speed to work from the inner-most bands toward the outer bands on the screen. Watch the screen while pumping the 3 L syringe and adjust the pumping speed based on the bands on the screen.

(b) A green bar will appear on the right side of each band when each circle is completed.

(c) The time allotted to complete this screen is 5 min and 15 strokes on the syringe. Once completed, the calibration verification screen will pop up.

7. To verify the flow sensor calibration:

(a) Perform five full syringe pumps to draw circles between the different bands on the graph that is on the screen.

- The circles can either all be the same size or of varying sizes that match the circles made in the yellow bands in **step 6a**.

(b) Once the calibration has been accepted, "F2. Verify Calibration" will appear in a gray box at the bottom left of the screen in small a black print.

- If the calibration was not accepted, a dialogue box would appear and prompt a recalibration. Measurement should not be conducted until the calibration has been accepted.

(c) Detach the flow sensor from the 3 L syringe and plug the flow sensor back into the silver box (Vmax® device).

(d) Attach the blue hose from the ventilated hood to the flow sensor (Fig. 3c).

- The end of the hose attached to the ventilated hood should be attached at the chin position (not at the forehead position), as shown in Fig. 4.

Fig. 4 The blue hose is attached to the ventilated hood at the chin position

Fig. 5 Vmax sample line is now connected to the calibration port (A) as shown by the arrow indicating the connection point

(e) Press "F3" to save and exit back to the main menu.

8. The external gas calibration is an optional quality assurance measure that may be performed before the participant arrives to ensure the O_2 and CO_2 analyzers are working properly. We recommend that this step be performed once per testing day. To perform an external gas calibration:
   (a) Remove the flow sensor from the silver box and attach the open end, not the mesh end, to the 3 L syringe.
   (b) Unplug the sample line from the flow sensor and plug it into the calibration port on the silver unit's front, as shown in Figs. 3d and 5.
   (c) Open both gas tanks by turning the top rectangular knob counterclockwise 2–3 half turns.
   (d) Select "Calibrate O_2 CO_2" from the toolbar on the computer screen.
   (e) Press "F1" to begin the calibration.
      - If the first calibration attempt fails, repeat the calibration by starting at **step 8d**. A successful calibration is indicated by a green box in the bottom right-hand corner of the screen that says "PASS."
   (f) Press "F3" to store calibration.
   (g) Close both gas tanks by turning the top rectangular knob clockwise until tightened.
      - This step is very important, or else the gas tanks will continue to release their contents.
   (h) Remove the sample line from the calibration port of the Vmax® device and reinsert the line into the flow sensor (Figs. 3d and 5).

3.2.2 Participant Preparation

1. Measure the participant's height (centimeters) and weight (kilograms). Date of birth and biological sex are also required.
2. Ask the participant to lie down and rest in the supine position for 20–30 min.
3. Before starting the test, inform the participant of the following:
   (a) You must not fall asleep.
   (b) You can use a blanket if they are cold, but this should be put on prior to the resting period to minimize movement.
   (c) The ventilated hood used for the measurement is not airtight, although it may feel stuffy at first. If this feeling persists, the participant can notify the person conducting the test.
   (d) The participant can take the hood off at any time if it becomes uncomfortable, but this will stop the test.
   (e) The sound of the pump will be audible while under the hood.
   (f) Notify the researcher immediately if any medical concerns arise during the test (headache, shortness of breath, etc.).

3.2.3 Device Preparation

1. In the Vmax® application on the computer, click on "2. New Study."
2. Enter the ID, date of birth, sex, height, and weight of the participant.
3. Press "F3" to save and exit to the main menu.
4. Open both gas tanks by turning the top rectangular knob counterclockwise two to three half turns.
5. On the main menu of the computer application, click "4. Exercise/Metabolic Test."
6. Use the default settings and press "F1. Start Test."
7. Press "F1. Analyzer Calibration" to begin calibrating the O_2 and CO_2.
8. A green box will appear in the bottom right-hand corner of the screen when the calibration is complete.
   - Repeat **steps 5** through 7 listed above if the calibration fails. Do not continue until the operator and the participant are ready to start the test.

3.2.4 Running a REE Test

1. On the computer, press "F3" to store and exit the gas calibration screen.
2. Click on "New Study."
   - Double-click on the computer screen if the testing screen does not appear immediately.

3. A dialogue box will appear; follow the prompts.
4. Turn on the flow pump on the Vmax® device. The flow pump is switched on by pressing the black switch at the device's bottom center, where there is a fan symbol, as shown in Fig. 3e.
5. Place the ventilated hood over the participant's head, with the blue tube at the participant's chin, as shown in Fig. 4. Smooth out and press down on the plastic draping around the participant's head to ensure that it is lying as flat as possible on the bed.
   - This step is crucial to prevent air leaks which will affect the measurement.
6. Press the space bar on the keyboard.
7. Press "F8" to start the test and then set the starting pump flow rate:
   - Use the default 30 L/min for adult females and pediatrics.
   - Use 40 L/min for adult males.
8. Monitor the following during the test:
   - F_ECO_2 should be between 0.60% and 0.80%. The most accurate measurement occurs between 0.75% and 0.80%.
     1. Wait for 7–8 min or until the participant is in a steady state of breathing before adjusting the flow rate.
     2. If necessary, adjust the flow rate by two to three units at a time and wait 2–3 min between adjustments.
        - If the F_ECO_2 value is high, increase the pump flow rate to remove CO_2.
        - If the F_ECO_2 value is low, decrease the pump flow rate to remove less CO_2.
   - Steady State
     1. A green box will appear in the bottom right-hand corner that says "Steady State" when the participant is in a steady state of breathing.
     2. Manual annotation of the data points (time intervals) where the participant is in a steady state of breathing is needed. Approximately 15 min of data in a steady state are needed.
        - Typically, it takes about 7 min for a person to enter a steady state. It is normal for a person to move in and out of a steady state during a test.
9. Stop the test once the participant has been in a steady state for at least 15 min. To stop the test:
   - Click "Exit/Pause" on the toolbar at the top of the screen and select "Y/Exit/Pause."

- Remove the ventilated hood from the participant and turn off the flow pump (Fig. 3e).
- Press space the bar on the keyboard to continue (there is no need to enter any comments) and then press "F3" to save the test results. A data analysis screen will appear.
- Turn off gas tanks by turning the rectangular top clockwise until sealed tightly.

10. The participant has now finished the test.
11. On the computer, select the steady-state interval(s) for data analysis:
    - Steady-state data points will be colored black.
        1. Select "1SS" and then mark the first steady-state interval by clicking and dragging the mouse to shade over the desired steady-state intervals that occur consecutively.
        2. Click on the "2SS" tab and then repeat **step 11.1**.
        3. Repeat **step 11.2** for third and fourth sets of steady-state intervals, if necessary.
        4. If only one to three steady-state intervals were used, click on the "SS4" tab and ensure the box "SS4 = average SS1–3" is checked.
        5. Press "F3" to store.
12. Ensure that the flow pump is turned off and that the gas tanks are closed.

3.3 Q-NRG™ Metabolic Monitor

The following methods are based on manufacturer recommendations, training, and the authors' combined clinical experience [43].

3.3.1 Calibration

The gas analyzers must be calibrated monthly. To calibrate the device:

1. Make sure the device has warmed up for 20 min (i.e., device has been powered on for 20 min).
2. Connect the output of the calibration cylinder to the calibration gas port on the back of the device.
3. Adjust gas output pressure to five to six bar (70–90 psi).
4. On the device screen, tap on "Calibration," then select "Gas Analyzers (Cylinder)," and finally, choose "Canopy-Face Mask Mode." Start the calibration procedure by following the on-screen instructions. Calibration will be performed automatically.
5. To calibrate the gas analyzer to room air:

(a) Make sure the device has been warmed up for 20 min.

(b) On the device touch screen, tap on "Calibration," then select "Gas Analyzer (Room Air)," and lastly, select "Canopy/Face Mask Mode."

(c) Start the calibration procedure by following the on-screen instructions. The calibration will be performed automatically.

6. To calibrate the blower/internal flow meter:

(a) Connect the calibration syringe to the canopy inlet port on the screen side of the device using the blower calibration adapter.

(b) On the device touch screen, tap on "Calibration," then select "Flowmeters," and lastly, select "Blower."

(c) Start the calibration procedure by following the on-screen prompts.

(d) Perform the required number of syringe strokes, paying particular attention to cover the whole motion range in 8–12 s.

3.3.2 Participant Preparation

1. Measure the participant's height (centimeters) and weight (kilograms). Date of birth and biological sex are also required.
2. Ask the participant to lie down and rest in the supine position for 20–30 min.
3. Before starting the test, inform the participant of the following:

(a) They must not fall asleep.

(b) They can use a blanket if they are cold, but this should be put on prior to the resting period to minimize movement.

(c) The ventilated hood used for the measurement is not airtight, although it may feel stuffy at first. If this feeling persists, it can notify the person conducting the test.

(d) The participant can take the hood off at any time if they become uncomfortable, but this will stop the test.

(e) The sound of the pump will be audible while under the hood.

(f) Notify the researcher immediately if any medical concerns arise during test (headache, shortness of breath, etc.).

3.3.3 Device Preparation

1. Power on the device by pressing and holding the On/Off button for 2 s. Wait for 5 min before starting the measurements.
2. Set up the canopy by placing the single-use veil over the canopy hood according to the instructions printed on the veil packaging.

Fig. 6 Q-NRG™ canopy hood

3. Connect the canopy hose and the antibacterial filter to the canopy hood, as shown in Fig. 6.
   - It is important to note that the canopy hose and antibacterial filter are connected at the forehead position and not at the canopy hood's chin position.
4. Connect the canopy hose to the "Canopy" port of the Q-NRG™ device, located on the front of the device in the bottom right-hand corner.
5. Select or add a new participant:
   - To enter new participant data:
     (i) Tap "New test" and then "New patient."
     (ii) Enter the participant's last/first name, date of birth (DOB), sex, weight, and height.
       - To ensure confidentiality, we recommend entering the participant ID instead of the person's last name and using a "–" or another symbol for their first name.
       - The device requires the participant's sex (listed as gender in the machine). This information is used to calculate predicted values for REE; thus, we recommend that the person's biological sex be entered instead of their gender identity.
   - To select an existing participant from the device:

(i) Tap "New test" and then "Search patient."

(ii) Select the appropriate participant and tap "Ok" to confirm the selection.

(iii) Edit the person's information, if necessary, then tap "Ok" to confirm.

3.3.4 Running a REE Test

1. To start the test, tap "Canopy" to start and activate the internal blower.
   - The blower must be running before placing the canopy over the participant's head.
2. Carefully place the canopy hood and veil over the participant's head, avoiding air leaks around the veil and bed's surface (Fig. 6).
   - This step is crucial to prevent air leaks which can cause underestimation of $V\mathrm{O}_2$ and $V\mathrm{CO}_2$.
3. The automatic calibration will begin and takes about 1 min to complete. Once the calibration is complete, press the "Start" button on the screen.
4. Measurements will begin appearing on the device screen after about 90 s.
5. Tap "Start recording" to record data immediately. Alternatively, the device will automatically start storing data after 2 min of testing.
6. Adjust the dilution flow to achieve a CO_2% ($F_E\mathrm{CO}_2$) of 0.5–1.5%.
   - Note that measured values taken immediately after dilution flow changes are not reliable.
7. To stop the test, remove the canopy from the participant and tap "Stop Recording" on the device screen.
8. Dispose of the nonreusable items (canopy veil and antibacterial filter).
9. The device screen will display REE, RQ, $V\mathrm{O}_2$, and $V\mathrm{CO}_2$, among others. We recommend noting the variables of interest.
10. To export the data from the device:
    - Insert a USB flash drive into the USB port on the device's left-hand side.
    - On the screen, select "Utility/export test" and tap "CSV to USB" or "PDF to USB." Once the data have been successfully exported, the device will display the message "Test successfully exported."

- Insert the USB flash drive into a computer and access the PDF data file exported from the device. Alternatively, data can be reviewed through a connected computer using the OMNIA software program, which provides additional editing capabilities, for example, customizing data points for inclusion in test results.

3.4 MedGem®

The following methods are based on manufacturer recommendations, training, and the authors' combined clinical experience [15].

3.4.1 Participant Preparation

1. Weigh the participant.
2. Ensure that the participant has been resting quietly for at least 15 min prior to initiating the test.
3. Obtain a new mouthpiece and instruct the participant how to put the mouthpiece in their mouth, with their teeth behind the mouthpiece's ridge and their lips sealed over it.

3.4.2 Device Preparation

1. Plug the MedGem® (Fig. 7) power supply into a wall outlet and connect to the device.
   - The device will beep once, and the indicator light will turn from red to green to amber once the device is warmed up.
   - The device must remain attached to a power supply until the test and data extraction are completed.
2. Offer a pillow to the participant, which can be placed under their dominant arm for support while holding the device throughout the test. Have the participant place the nose clip on their nose and blow air to ensure that no air can escape through their nostrils.

Fig. 7 MedGem® device

3. Wash or sanitize hands and then don medical gloves and attach the mouthpiece firmly to the device. Alternatively, the participant can attach the mouthpiece to the device to minimize any contamination. The larger end of the mouthpiece base should be facing downward.
4. Calibrate the MedGem® by pressing the start (amber-colored) button located on top of device. The MedGem® must be on a solid, flat surface during calibration. Once the indicator light turns from amber to flashing green, the calibration is complete. The self-calibration process takes approximately 30 s.

3.4.3 Running a REE Test

1. Once the indicator light is flashing green, hand the device to the participant and encourage them to relax while ensuring that their mouth remains sealed around the mouthpiece.
   - The test must be started within 1 min of the indicator light begins to flash green.
2. The measurement will begin automatically when the participant begins breathing into the device as shown by the indicator light turning to solid green.
3. After 5–10 min, the test will stop automatically and alert by beeping once. The indicator light will turn from green to amber to indicate completion of the test.
   - The time to complete a test will vary by participants as the time required to reach a steady state of breathing varies widely among individuals.
   - The person's VO_2 will appear on the screen, followed by the REE displayed in kcal/day. This information is available on the device until a new test begins.
4. Dispose of the mouthpiece and nose clip.
   - If completing repeating measures on the same participant, a new mouthpiece is recommended for each measurement to ensure accuracy.

3.5 FitMate GS

The following methods are based on manufacturer recommendations, training, and the authors' combined clinical experience [16].

3.5.1 Calibration

The FitMate GS (Fig. 8) will automatically calibrate the analyzer at the start of every test.

3.5.2 Participant Preparation

1. Have the participant lay down and rest for 20–30 min.
2. Do not place the canopy hood on the participant until prompted to do so.
3. Before starting the test, inform the participant of the following:

Fig. 8 FitMate GS with a canopy hood option

(a) You must not fall asleep.

(b) You can use a blanket if they are cold, but this should be put on prior to the resting period to minimize movement.

(c) The ventilated hood used for the measurement is not airtight, although it may feel stuffy at first. If this feeling persists, you can notify the person conducting the test.

(d) The participant can take the hood off at any time if they become uncomfortable, but this will stop the test.

(e) The sound of the pump will be audible while under the hood.

(f) Notify the researcher immediately if any medical concerns arise during the test (headache, shortness of breath, etc.).

(g) The flow selector may be adjusted throughout the test. This piece of equipment is attached to the canopy hood.

3.5.3 Device Preparation

1. Insert the electrical cord into the external power connector and plug it into an outlet. Insert the green connector tube from the blower and unit into the flow connector on the back of the FitMate GS device. Connect the canopy blower to the hood connector and ensure a secure connection between them.
   - If the blower is not pressed far enough into the canopy hood, an alarm will sound when you start the test. If this occurs, verify that the canopy blower is connected properly.

2. Insert the sampling line from the device into the sampling connector on the hood.
3. Press the on/off button for up to 4 s to turn the unit on.
   - The unit should only be turned on during a test. An alarm will sound if turned on when a test is not running.
4. Select "3.Options" then "3.RMR" and "Canopy." The following default settings are what we recommend using during a test but can be changed if necessary:
   - Initial time interval to discard before the data acquisition: 5 min.
   - The average time interval for the RMR test: 10 min.
   - Automatic print at the end of the test: yes.
   - Print of the RMR graph: no.
   - Automatic detection of the start/end of the test: no.
   - Test mode: Canopy.
5. Preparing the measurement for a new versus existing participant will vary as indicated below:
   - To enter a new participant:
     (i) From the main menu, select "1.New."
     (ii) Update "ID" to participant ID or make a note of the automatically-generated FitMate GS ID for your records.
       - We recommend entering the participant ID and using a "−" or another symbol for their first and last name for research purposes.
     (iii) Enter DOB, sex, height (cm), and weight (kg). Press OK
       - The device requires you to indicate the participant's sex. This information is used to calculate predicted values for REE; thus, we recommend that the person's biological sex be entered instead of their gender identity, as shown on the screen.
   - To select an existing participant:
     (i) Select "2.View/Search" on the main menu.
     (ii) Scroll through the list of subjects to find the relevant participant ID. Select "OK."
6. Adjust the flow selector to line up the participant's weight with the canopy blower's red dot.

3.5.4 Running a REE Test

1. Select "1.Resting Metabolic Rate" from the menu and follow the prompts on the warning messages.
   - If you are testing an existing participant, a warning message may appear asking for a new session to start. Press OK.

- When the canopy is turned on after being prompted, the unit will beep a few times. When the green LED on the front of the unit turns on, the test can be started. If the green LED does not go on, do not proceed with the test.
- Do not place the canopy hood over the participant's head until the blower has been turned on.

2. Once the green LED is on, place the canopy hood over the participant's head. The canopy blower must be placed near the top of the participant's head.
   - It is important to flatten the veil on the bed to prevent air leaks which will affect the measurement.
3. The equipment will automatically calibrate the analyzer.
4. Press "1.Start" to start the test, or the test will automatically begin after 1 min.
   - F_EO_2 should be between 19.50% and 20.25%. Adjust the flow selector on the canopy blower as needed by rotating the selector counterclockwise if the F_EO_2 is too low and clockwise if the F_EO_2 is too high. Wait 30–45 s after adjustments to observe the effect before adjusting further. Continue to observe the F_EO_2 values throughout the test and adjust the flow selector as needed.
5. When the test is over, the device will prompt the removal of the hood from the participant and turn off the canopy unit. Once these steps have been completed, press "OK."
6. The test results will be displayed on the screen and printed by the device automatically.
7. Hold the on/off button to power off the device. Disassemble, sanitize, and store.

4 Notes

4.1 Predictive Equations

Indirect calorimetry offers a precise prediction of REE in the clinical setting but creates challenges due to the accessibility of equipment, cost, time, and required skills associated with performing IC measurements. Predictive equations offer clinicians the ability to predict EE on an individual level during the nutritional assessment, albeit with suboptimal accuracy and preciseness. The most common and clinically relevant predictive equations include those by Harris and Benedict [44], Mifflin-St Jeor [45], Owen [46, 47], and the World Health Organization/Food and Agriculture Organization/United Nations University [48, 49]. In healthy adults, Mifflin-St Jeor is the most precise equation and has been shown to predict REE within 10% of the measured value [45, 48]. In older adults, the Mifflin-St Jeor equation has the least bias (−0.3%), while the Harris–Benedict equation has the highest precision (~70%), suggesting that the

former is best for group-level while the latter is best suited for individual-level predictions of REE [45, 50]. Predictive equations are formulated from regressing data on a group level and thus induce error (of which is often clinically relevant) when utilized on an individual basis [48]. To diminish error when predicting EE, especially on an individual level, IC should be applied using an evidence-based protocol [48]. Portable IC devices that provide a precise EE measure across health conditions are needed in the clinical setting.

4.2 Use of RQ to Detect Measurement Error

RQ's physiological range reported across the fed and fasting state is 0.67–1.30, while an expected fasting RQ is 0.68–0.90 [35]. If the RQ is between 0.91 and 1.30, a problem may have occurred, and the measurement should be repeated [35]. Problems could include an error in calibration, an air leak in the IC system, participant hyper- or hypoventilation, or a pretest protocol deviation such as insufficient fasting time, caffeine intake, or exercise [35]. If problems persist despite secure device connection points and the absence of protocol deviation, technical support for the equipment should be sought.

4.3 COVID-19 Considerations

An indirect calorimetry is an important tool used to guide the early nutritional management that is critical for the therapeutic care of patients with various conditions, including the coronavirus disease 2019 (COVID-19) [51–53]. A report of prospective IC measurements throughout the course of intensive care unit (ICU) admission for COVID-19 revealed increasing measured REE (hypermetabolism) and increased variability in measured REE after one and 3 weeks of ICU admission [53]. Although controversial, IC can be safely performed in patients with COVID-19 and, thus, can continue to be used safely for people not exhibiting the virus if proper protocols are followed [52] with enhanced cleaning procedures and the use of disposables. For example, if measuring REE by Q-NRG™, all device components that contact the person undergoing a measurement can be purchased in disposable format (i.e., one-time use), including the flow meter, sampling lines, FiO_2 adapter, and filter. Additionally, single-use veils for the canopy hood can also be purchased. Upon completion of a measurement, the canopy, flow meter (if not using a disposable option), Q-NRG™, and the canopy hose can all be disinfected with high-efficiency cleaners, while the disposables can be discarded. These safety measures can be translated to the research setting.

4.4 Factors that Affect EE

Several factors affect EE and its major physiological compartments, such as genetics, age, sex, menstrual cycle, body composition, physical activity, diet composition, health status, medications, and environmental stimuli [54]. Generally, REE is higher in men than in women even after adjusting for confounding variables such as age, body composition, and activity levels [55, 56]. Another important factor that affects EE is the menstrual cycle. Webb [57]

demonstrated that TEE was 8% higher in the luteal phase compared to the follicular phase. Similarly, to TEE, a recent meta-analysis including 318 women also found REE to be higher during the luteal phase compared to the follicular phase of the menstrual cycle [58]. External factors such as diet composition are also able to affect EE. In fact, the energy expended to digest, absorb, process, and store dietary protein is 25–30% of the energy content of the meal, followed by carbohydrates (6–8%) and fat (2–3%) [59]. The RQ is a highly sensitive value that is also affected by diet composition. An RQ value <0.67 or >1.30 is physiologically unlikely in a fasted and rested state; thus, RQ can be used as an indicator of pretest protocol adherence [35]. If an RQ value is outside of the anticipated fasting range (0.68–0.90) and cannot be explained by a pretest protocol deviation, then the possibility of an air leak should be considered [35, 60]. In addition to diet composition, medications can affect EE by affecting respiration or heart rate, leading to increased or decreased EE. Anti-asthmatic drugs such as salbutamol have been found to increase $\dot{V}O_2$, $\dot{V}CO_2$, and RQ [61]. Conversely, β-blockers have been shown to decrease EE related to their activity, decreasing skeletal muscle sympathetic nerve activity and resting heart rate [62, 63]. Additionally, antiseizure drugs [64], antidepressants [65, 66], antipsychotics [67], corticosteroids [68], and stimulant medications for attention-deficit/hyperactivity disorder [69] have been found to decrease EE. Therefore, if IC is being used in a research design that includes repeated measures, the above-mentioned factors and strict adherence to pretest protocols should be verified to ensure that captured change is truly representative of the change in EE and that the effect of measurement error is minimized. Depending on the research question and study design, these medications should be considered when defining clinical studies' exclusion criteria measuring EE.

References

1. Levine JA (2005) Measurement of energy expenditure. Public Health Nutr 8: 1123–1132. https://doi.org/10.1079/phn2005800
2. Haugen HA, Chan LN, Li F (2007) Indirect calorimetry: a practical guide for clinicians. Nutr Clin Pract 22:377–388. https://doi.org/10.1177/0115426507022004377
3. Ainslie PN, Reilly T, Westerterp KR (2003) Estimating human energy expenditure a review of techniques with particular reference to doubly labelled water. Sports Med 33:683–698

4. Donahoo WT, Levine JA, Melanson EL (2004) Variability in energy expenditure and its components. Curr Opin Clin Nutr Metab Care 7: 599–605. https://doi.org/10.1097/00075197-200411000-00003
5. Lam YY, Ravussin E (2016) Analysis of energy metabolism in humans: a review of methodologies. Mol Metab 5:1057–1071. https://doi.org/10.1016/j.molmet.2016.09.005
6. Adriaens MPE, Schoffelen PFM, Westerterp KR (2003) Intra-individual variation of basal metabolic rate and the influence of daily habitual physical activity before testing. Br J Nutr 90:419–423. https://doi.org/10.1079/bjn2003895
7. Psota T, Chen KY (2013) Measuring energy expenditure in clinical populations: rewards and challenges. Eur J Clin Nutr 67:436–442. https://doi.org/10.1038/ejcn.2013.38
8. Wooley JA, Sax HC (2003) Indirect calorimetry: applications to practice. Nutr Clin Pract 18:434–439. https://doi.org/10.1177/011542650301800543 4
9. Henry C (2005) Basal metabolic rate studies in humans: measurement and development of new equations. Public Health Nutr 8: 1133–1152. https://doi.org/10.1079/phn2005801
10. Sanchez-Delgado G, Ravussin E (2020) Assessment of energy expenditure: are calories measured differently for different diets? Curr Opin Clin Nutr Metab Care 23:312–318. https://doi.org/10.1097/MCO.0000000000000680
11. Schoffelen PFM, Plasqui G (2018) Classical experiments in whole-body metabolism: open-circuit respirometry—diluted flow chamber, hood, or facemask systems. Eur J Appl Physiol 118:33–49. https://doi.org/10.1007/s00421-017-3735-5
12. Weir JB d V (1949) New methods for calculating metabolic rate with special reference to protein metabolism. J Physiol 109:1–9. https://doi.org/10.1113/jphysiol.1949.sp004363
13. Brouwer E (1957) On simple formulae for calculating the heat expenditure and the quantities of carbohydrate and fat oxidized in metabolism of men and animals, from gaseous exchange (oxygen intake and carbonic acid output) and urine-N. Acta Physiol Pharmacol Neerl 6:795–802
14. Chen KY, Smith S, Ravussin E, Krakoff J, Plasqui G, Tanaka S, Murgatroyd P, Brychta R, Bock C, Carnero E, Schoffelen P, Hatamoto Y, Rynders C, Melanson EL (2020) Room indirect calorimetry operating and reporting standards (RICORS 1.0): a guide to conducting and reporting human whole-room calorimeter studies. Obesity 28:1613–1625. https://doi.org/10.1002/oby.22928
15. Microlife Medical Home Solutions (2009) User manual MedGem. Microlife Medical Home Solutions, Golden
16. COSMED Srl (2012) Fitmate user manual, XIV edn. COSMED Srl
17. Nieman DC, Austin MD, Benezra L, Pearce S, McInnis T, Unick J, Gross SJ (2006) Validation of COSMED's FitMate™ in measuring oxygen consumption and estimating resting metabolic rate. Res Sports Med 14:89–96. https://doi.org/10.1080/15438620600651512
18. Lee J-M, Bassett DR, Thompson D, Fitzhugh E (2011) Validation of the COSMED FitMate for prediction of maximal oxygen consumption. J Strength Cond Res 25:2573–2579
19. Purcell SA, Johnson-Stoklossa C, Braga Tibaes JR, Frankish A, Elliott SA, Padwal R, Prado CM (2020) Accuracy and reliability of a portable indirect calorimeter compared to whole-body indirect calorimetry for measuring resting energy expenditure. Clin Nutr ESPEN 39: 67–73. https://doi.org/10.1016/j.clnesp.2020.07.017
20. Cooper JA, Watras AC, O'Brien MJ, Luke A, Dobratz JR, Earthman CP, Schoeller DA (2009) Assessing validity and reliability of resting metabolic rate in six gas analysis systems. J Am Diet Assoc 109:128–132. https://doi.org/10.1016/j.jada.2008.10.004
21. Reeves MM, Capra S, Bauer J, Davies PSW, Battistutta D (2005) Clinical accuracy of the MedGem™ indirect calorimeter for measuring resting energy expenditure in cancer patients. Eur J Clin Nutr 59:603–610. https://doi.org/10.1038/sj.ejcn.1602114
22. Woo P, Murthy G, Wong C, Hursh B, Chanoine JP, Elango R (2017) Assessing resting energy expenditure in overweight and obese adolescents in a clinical setting: validity of a handheld indirect calorimeter. Pediatr Res 81: 51–56. https://doi.org/10.1038/pr.2016.182
23. Achamrah N, Delsoglio M, De Waele E, Berger MM, Pichard C (2020) Indirect calorimetry: the 6 main issues. Clin Nutr 40:4–14. https://doi.org/10.1016/j.clnu.2020.06.024
24. Oshima T, Dupertuis YM, Delsoglio M, Graf S, Heidegger CP, Pichard C (2019) In vitro validation of indirect calorimetry device developed for the ICALIC project against mass spectrometry. Clin Nutr ESPEN 32:50–55. https://doi.org/10.1016/j.clnesp.2019.05.004

25. Delsoglio M, Dupertuis YM, Oshima T, van der Plas M, Pichard C (2020) Evaluation of the accuracy and precision of a new generation indirect calorimeter in canopy dilution mode. Clin Nutr 39:1927–1934. https://doi.org/10.1016/j.clnu.2019.08.017
26. Clinicaltrials.gov. The ICALIC accuracy validation in Geneva study (ICALIC). ClinicalTrials.gov Identifier: NCT02790697. https://clinicaltrials.gov/ct2/show/NCT02790697
27. Clinicaltrials.gov. The ICALIC 2 international multicentric study (ICALIC2). ClinicalTrials.gov Identifier: NCT03947294. https://clinicaltrials.gov/ct2/show/NCT03947294
28. Hipskind P, Glass C, Charlton D, Nowak D, Dasarathy S (2011) Do handheld calorimeters have a role in assessment of nutrition needs in hospitalized patients?: a systematic review of literature. Nutr Clin Pract 26:426–433
29. Alam DS, Hulshof PJM, Roordink D, Meltzer M, Yunus M, Salam MA, van Raaij JMA (2005) Validity and reproducibility of resting metabolic rate measurements in rural Bangladeshi women: comparison of measurements obtained by Medgem™ and by Deltatrac™ device. Eur J Clin Nutr 59:651–657. https://doi.org/10.1038/sj.ejcn.1602122
30. Stewart CL, Goody CM, Branson R (2005) Comparison of two systems of measuring energy expenditure. J Parenter Enter Nutr 29:212–217. https://doi.org/10.1177/0148607105029003212
31. St-Onge M-P, Rubiano F, Jones A, Heymsfield SB (2004) A new hand-held indirect calorimeter to measure postprandial energy expenditure. Obes Res 12:704–709. https://doi.org/10.1038/oby.2004.82
32. Fares S, Miller MD, Masters S, Crotty M (2008) Measuring energy expenditure in community-dwelling older adults: are portable methods valid and acceptable? J Am Diet Assoc 108:544–548. https://doi.org/10.1016/j.jada.2007.12.012
33. Vandarakis D, Salacinski AJ, Broeder CE (2013) A comparison of COSMED metabolic systems for the determination of resting metabolic rate. Res Sports Med 21:187–194. https://doi.org/10.1080/15438627.2012.757226
34. McClave SA, Spain DA, Skolnick JL, Lowen CC, Kleber MJ, Wickerham PS, Vogt JR, Looney SW (2003) Achievement of steady state optimizes results when performing indirect calorimetry. J Parenter Enter Nutr 27:16–20. https://doi.org/10.1177/014860710302700116
35. Fullmer S, Benson-Davies S, Earthman CP, Frankenfield DC, Gradwell E, Lee PSP, Piemonte T, Trabulsi J (2015) Evidence analysis library review of best practices for performing indirect calorimetry in healthy and non-critically ill individuals. J Acad Nutr Diet 115:1417–1446.e2. https://doi.org/10.1016/j.jand.2015.04.003
36. Frankenfield DC, Coleman A (2009) Recovery to resting metabolic state after walking. J Am Diet Assoc 109:1914–1916. https://doi.org/10.1016/j.jada.2009.08.010
37. Levine JA, Schleusner SJ, Jensen MD (2000) Energy expenditure of nonexercise activity. Am J Clin Nutr 72:1451–1454
38. Sujatha T, Shatrugna V, Venkataramana Y, Begnum N (2000) Energy expenditure on household, childcare and occupational activities of women from urban poor households. Br J Nutr 83:497–503
39. Snell B, Fullmer S, Eggett DL (2014) Reading and listening to music increase resting energy expenditure during an indirect calorimetry test. J Acad Nutr Diet 114:1939–1942
40. Leff M, Hill J, Yates A, Cotsonis G, Heymsfield SB (1987) Resting metabolic rate: measurement reliability. J Parenter Enter Nutr 11:354–359
41. Weststrate J, Weys P, Poortvliet E, Deurenber P, Hautvast J (1989) Diurnal variation in postabsorptive resting metabolic rate and diet-induced thermogenesis. Am J Clin Nutr 50:908–914
42. CareFusion (2018) Vmax series operator's manual. CareFusion, Yorba Linda
43. COSMED The Metabolic Company (2020) Q-NRG metabolic monitor user manual. Edition 4.2. COSMED
44. Harris JA, Benedict FG (1918) A biometric study of human basal metabolism. Proc Natl Acad Sci U S A 4:370–373
45. Mifflin M, St Jeor S, Hill L, Scott B, Daugherty S, Koh Y (1990) A new predictive equation for resting energy expenditure in healthy individuals. Am J Clin Nutr 51:241–247
46. Owen O, Holup J, Dalessio D, Craig E, Polansky M, Smalley J, Kavle E, Bushman M, Owen L, Mozzoli M, Kendrick Z, Boden G (1987) A reappraisal of the caloric requirements of men. Am J Clin Nutr 46:875–885
47. Owen O, Kavle E, Owen R, Polansky M, Caprio S, Mozzoli M, Kendrick Z, Bushman M, Boden G (1986) A reappraisal of caloric requirements in healthy women. Am J Clin Nutr 44:1–19
48. Frankenfield D, Roth-Yousey L, Compher C (2005) Comparison of predictive equations for resting metabolic rate in healthy nonobese and obese adults: a systematic review. J Am

Diet Assoc 105:775–789. https://doi.org/10.1016/j.jada.2005.02.005

49. Food and Agricultural Organization, World Health Organization, United Nations University (1985) Energy and protein requirements. Report of a joint FAO/WHO/UNU expert consultation World Health Organization technical report series 724. Geneva, Switzerland
50. Cioffi I, Marra M, Pasanisi F, Scalfi L (2021) Prediction of resting energy expenditure in healthy older adults: a systematic review. Clin Nutr 40(5):3094–3103. https://doi.org/10.1016/j.clnu.2020.11.027
51. Thibault R, Seguin P, Tamion F, Pichard C, Singer P (2020) Nutrition of the COVID-19 patient in the intensive care unit (ICU): a practical guidance. Crit Care 24:447
52. Singer P, Pichard C, De Waele E (2020) Practical guidance for the use of indirect calorimetry during COVID 19 pandemic. Clin Nutr Exp 33:18–23. https://doi.org/10.1016/j.yclnex.2020.07.002
53. Whittle J, Molinger J, MacLeod D, Haines K, Wischmeyer PE (2020) Persistent hypermetabolism and longitudinal energy expenditure in critically ill patients with COVID-19. Crit Care 24:581. https://doi.org/10.1186/s13054-020-03286-7
54. Lam YY, Ravussin E (2017) Indirect calorimetry: an indispensable tool to understand and predict obesity. Eur J Clin Nutr 71:318–322. https://doi.org/10.1038/ejcn.2016.220
55. Ferraro R, Lillioja S, Fontvieille AM, Rising R, Bogardus C, Ravussin E (1992) Lower sedentary metabolic rate in women compared with men. J Clin Invest 90:780–784. https://doi.org/10.1172/JCI115951
56. Arciero PJ, Goran MI, Poehlman ET (1993) Resting metabolic rate is lower in women than in men. J Appl Physiol 75:2514–2520. https://doi.org/10.1152/jappl.1993.75.6.2514
57. Webb P (1986) 24-hour energy expenditure menstrual. Am J Clin Nutr 44:614–619
58. Benton MJ, Hutchins AM, Dawes JJ (2020) Effect of menstrual cycle on resting metabolism: a systematic review and meta-analysis. PLoS One 15:1–21. https://doi.org/10.1371/journal.pone.0236025
59. Jequier E (1995) Nutrient effects: post-absorptive interactions. Proc Nutr Soc 54: 253–265
60. Compher C, Frankenfield D, Keim N, Roth-Yousey L (2006) Best practice methods to apply to measurement of resting metabolic rate in adults: a systematic review. J Am Diet Assoc 106:881–903. https://doi.org/10.1016/j.jada.2006.02.009
61. Amoroso P, Wilson SR, Ponte J, Moxham J (1993) Acute effects of inhaled salbutamol on the metabolic rate of normal subjects. Thorax 48:882–885. https://doi.org/10.1136/thx.48.9.882
62. Newsom SA, Richards JC, Johnson TK, Kuzma JN, Lonac MC, Paxton RJ, Rynn GM, Voyles WF, Bell C (2010) Short-term sympathoadrenal inhibition augments the thermogenic response to β-adrenergic receptor stimulation. J Endocrinol 206:307–315. https://doi.org/10.1677/JOE-10-0152
63. Monroe MB, Seals DR, Shapiro LF, Bell C, Johnson D, Jones PP (2001) Direct evidence for tonic sympathetic support of resting metabolic rate in healthy adult humans. Am J Physiol Endocrinol Metab 280:740–744. https://doi.org/10.1152/ajpendo.2001.280.5.e740
64. Verrotti A, D'Egidio C, Mohn A, Coppola G, Chiarelli F (2011) Weight gain following treatment with valproic acid: pathogenetic mechanisms and clinical implications. Obes Rev 12: 32–43. https://doi.org/10.1111/j.1467-789X.2010.00800.x
65. Fernstrom MH, Epstein LH, Spiker DG, Kupfer DJ (1985) Resting metabolic rate is reduced in patients treated with antidepressants. Biol Psychiatry 20:692–695. https://doi.org/10.1016/0006-3223(85)90107-6
66. Fernstrom MH (1995) Drugs that cause weight gain. Obes Res 3(Suppl 4):435–439. https://doi.org/10.1002/j.1550-8528.1995.tb00210.x
67. Sharpe JK, Byrne NM, Stedman TJ, Hills AP (2005) Resting energy expenditure is lower than predicted in people taking atypical antipsychotic medication. J Am Diet Assoc 105: 612–615. https://doi.org/10.1016/j.jada.2005.01.005
68. Bowles NP, Karatsoreos IN, Li X, Vemuri VK, Wood JA, Li Z, Tamashiro KLK, Schwartz GJ, Makriyannis AM, Kunos G, Hillard CJ, McEwen BS, Hill MN (2015) A peripheral endocannabinoid mechanism contributes to glucocorticoid-mediated metabolic syndrome. Proc Natl Acad Sci U S A 112:285–290. https://doi.org/10.1073/pnas.1421420112
69. Butte NF, Treuth MS, Voigt RG, Llorente AM, Heird WC (1999) Stimulant medications decrease energy expenditure and physical activity in children with attention-deficit/hyperactivity disorder. J Pediatr 135:203–207. https://doi.org/10.1016/S0022-3476(99)70023-5

Chapter 18

Anthropometric Assessment Methods for Adults and Older People

Thalita Cremonesi Pereira and Cinthia Baú Betim Cazarin

Abstract

Anthropometry is one of the most used methods for evaluating the nutritional status of the human in all stages of life. The nutritional diagnosis of individuals can be determined if combined with other objective and subjective methods. In this chapter, we describe simple, basic, noninvasive, and low-cost instruments to evaluate the nutritional status of adults and older adults. The literature has many indexes, guidelines, and anthropometric indicators; the best methodology and cutoffs in the population evaluated should be defined based on the final objective.

Key words Anthropometry, Nutritional assessment, Adults, Aged, Bedridden

1 Introduction

Anthropometry is a tool for assessing healthy or sick individuals' nutritional status, and it is considered an objective method. However, the real nutritional status of an individual or population group cannot be determined using just one type of assessment tool, as it is being, therefore, recommended to use different types of assessment to obtain more accurate data. The other objective tools for assessing nutritional status are the study of dietary intake and laboratory data, and the subjective tools used to evaluate the nutritional status are the clinical (physical examination) and the subjective global assessment [1].

Nutritional assessment is a systematic process that initiates nutritional assistance and aims to obtain adequate information to identify nutrition problems. The comparison of the collected data with their respective reference values permits that the nutritionist takes preventive or treatment decision-making for such nutritional problems, maintaining the nutritional status and health of individuals. These data can orient public health politics and nutritional interventions to populational groups [1].

Cinthia Baú Betim Cazarin (ed.), *Basic Protocols in Foods and Nutrition*,
Methods and Protocols in Food Science, https://doi.org/10.1007/978-1-0716-2345-9_18,

Anthropometry represents a reliable, low-cost, and noninvasive method and can be performed in any environment. However, it requires examiner training to ensure the quality of the data collected [2].

In this chapter, we will list the main and most used anthropometric indexes adopted for the adult and older population and their methods of measurement.

2 Materials

The materials required for anthropometric evaluation are as follows:

1. Body weight balance—platform or digital, mechanical, or electronics (the most reliable mechanics being electronics), varying until 100 g.
2. Stadiometer or horizontal anthropometer. Both with a maximum variation of 1 mm.
3. Inelastic, flexible metric tape, with a variation of 1 mm.
4. Adipometer or pachymeter with constant pressure and 1 mm variation.

3 Methods

3.1 Weight

Body weight represents the sum of all bodily components (water, lean mass, fat mass, bones, organs, and tissues), and it is expressed in grams (g) or kilograms (kg). This parameter is widely used to classify nutritional status in all life cycles, including from pregnancy until aging. For bedridden individuals, the weight can be estimated by equations (Eq. 1) using the circumferences and skin folds, which we shall see later in this chapter. There are many equations in the literature to estimate the weight of bedridden individuals using different populations as a parameter (*see* **Note 1**). You should select the one that is most representative of your population.

Equation 1: This equation is an example of weight estimation in bedridden individuals based on the American population [3].

$$\begin{aligned}&\textbf{Women}: \text{weight}\,(\text{kg}) = [1.27 \times \text{CC}\,(\text{cm})]+[0.87 \times \text{KH}\,(\text{cm})]+[0.98 \times \text{AC}\,(\text{cm})]+[0.4 \times \text{SS}\,(\text{cm})] - 62.35\\ &\textbf{Men}: \text{weight}\,(\text{kg}) = [0.98 \times \text{CC}\,(\text{cm})]+[1.16 \times \text{KH}\,(\text{cm})]+[1.73 \times \text{AC}\,(\text{cm})]+[0.37 \times \text{SS}\,(\text{cm})] - 81.69\end{aligned} \quad (1)$$

Where CC is calf circumference; KH is knee height; AC is arm circumference; and SS is subscapular skinfold.

Fig. 1 Weight and height measurement. (Source: Created by Servier Medical Art (smart.servier.com))

The weight must be measured with individuals with minimum clothing possible, that is, without any footwear, accessories (e.g., glasses, jewelry, clock, cap, or any other accessory in the hair), and any object in the pockets (Fig. 1). The measurement method varies according to age. Place the scale on a stable and regular surface (avoid carpets) and calibrate the instrument.

The measurement of the weight will be held by placing the individual preferably back to the scales meter, in the middle of the platform, erect, with the feet and legs parallel, and the weight distributed on both feet, arms extended along the body, motionless and looking at the horizon line (Frankfort plane).

Attention should be given to individuals who present edema, tumors, or amputated limbs when evaluating body weight. If edema is observed, assess the possibility of using measures based on upper limbs, since they are generally not affected by this condition.

3.2 Height

Height is the measure that expresses the linear growth of the human body in centimeters (cm) or meters (m). This measurement process is also used to evaluate children and adolescents' growth and to classify nutritional status by estimating body mass index (BMI) in adults, the older adults, and pregnant women. To measure the height, the individuals should be barefoot, without hair, or head accessories (loose hair).

The height is measured with a stadiometer, with the individuals standing on their back to the meter, with parallel legs and feet distant at most in 10 cm and upright head with the chin forming an angle of about 90° with the neck, following the Frankfurt plane (horizontally align the lower edge of the opening of the orbital with the upper margin of the outer auditory conductor). The heel, calf, glutes, shoulder blade, and back should be leaning in the stadiometer ruler. The examiner will raise the stadiometer ruler and support the upper rod at the top of the individual's head, recording the same stature (*see* **Note 2**).

For bedridden individuals, the height can be estimated by predictive equations using another anthropometric measure (Eq. 2), which we shall see later in this chapter. As previously presented for weight estimation, there are many equations for height estimation in literature.

Equation 2: This equation is an example of height estimation in bedridden individuals based on the American population [4].

$$\begin{aligned}&\textbf{Women}: \text{height (cm)} = 84.88 + [1.83 \times \text{knee height (cm)}] - [0.24 \times \text{years}]\\ &\textbf{Men}: \text{height (cm)} = 60.65 + [2.04 \times \text{knee height (cm)}]\end{aligned} \tag{2}$$

3.3 Knee Height

The knee-height measure is very important and used in predictive equations to estimate the height and weight of bedridden individuals.

A tape measure or anthropometer is used as an instrument, with the individual in the supine position or sitting as close as

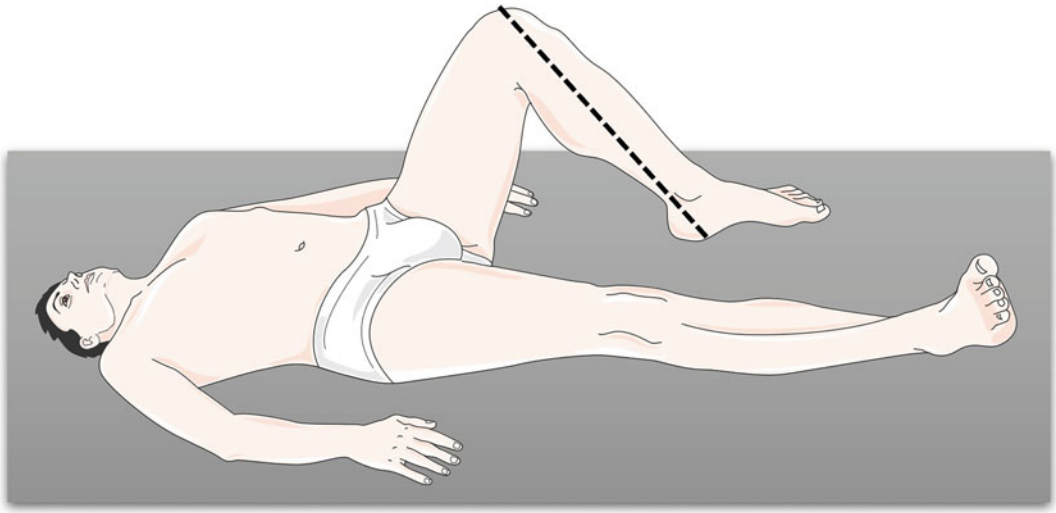

Fig. 2 Measuring the knee length in bedridden individuals. (Source: Created by Servier Medical Art (smart.servier.com))

possible from the chair edge, barefoot, forming a 90-degree angle with the feet and knee. The length of the outer bone point of the knee (tibia head) until the heel (Fig. 2) is measured and expressed in centimeters (cm) [5].

3.4 Circumferences

Circumferences can be used isolated or together with another anthropometric measure to verify sections or dimensions of the body. They are also used to evaluate the body's growth, muscle, or fat distribution, as well as in predictive equations for body composition. The following are the main circumferences used to classify the nutritional status in adults and older people.

3.4.1 Waist Circumference

Waist circumference is an important tool to evaluate the risk of cardiometabolic diseases associated with abdominal adipose tissue accumulation. The cutoff points to evaluate the risk of cardiometabolic diseases using the waist circumference are described in Table 1. Also, from this information, the value of the waist–hip ratio is derived, which will be explained later in this chapter.

Along with the undressed individual, this anthropometric value is measured in the waist area, with the patient standing with arms relaxed and extended along the body, feet together, and the abdomen relaxed (expiration moment).

The individual's waist region is surrounded with a tape measure at the narrower trunk place. If it is difficult to identify the narrower trunk region, the midpoint located between the lower rib (or last palpable rib) and the iliac crest (hip bone) can be used as a reference [7]. This measure is expressed in centimeters (cm).

Table 1
Waist circumference cutoff indicative of cardiometabolic disease risk by International Diabetes Federation, according to the ethnicity

Country/ethnic group	Gender	Waist circumference
Europids		
In the USA, the ATP III values (102 cm male; 88 cm female) are likely to continue to be used for clinical purposes	Male Female	≥94 cm ≥80 cm
South Asians and Japanese		
Based on a Chinese, Malay, and Asian-Indian population	Male Female	≥90 cm ≥80 cm
Ethnic South and Central Americans	Use South Asian recommendations until more specific data are available.	
Sub-Saharan Africans	Use European data until more specific data are available.	
Eastern Mediterranean and Middle East (Arab) populations	Use European data until more specific data are available.	

Source: Adapted from International Diabetes Federation [6]

3.4.2 Hip Circumference

This measure is used in association with waist circumference to estimate the waist–hip ratio (WHR), a simple and useful methodology to check the risk of cardiovascular diseases. The waist–hip ratio is estimated by dividing the waist circumference by the hip circumference. WHR ≥ 0.90 for men and ≥0.85 for women indicate central obesity (visceral obesity or android obesity), which increases the risk of developing cardiometabolic diseases [8].

In the hip area, the hip circumference is measured with the undressed individual (or wearing light clothing made of thin fabric), standing with feet together and arms extended along the body (Fig. 3). The individual's hip region is surrounded with a tape measure in the most protruding place. The measure is expressed in centimeters (cm) [9].

3.4.3 Arm Circumference

Arm circumference or mid-upper arm circumference (MUAC) is widely used to estimate the individual's nutritional status after estimating the percentage of the adequacy of it, with the 50th percentile of the reference tables for children [10]. However, the cutoff of this measure for adults and older individuals is not standardized [11], based on a study performed in Bangladeshi adults, suggested the use of MUAC <25 cm for adult males and <24 cm for adult females as an indication of undernutrition (BMI

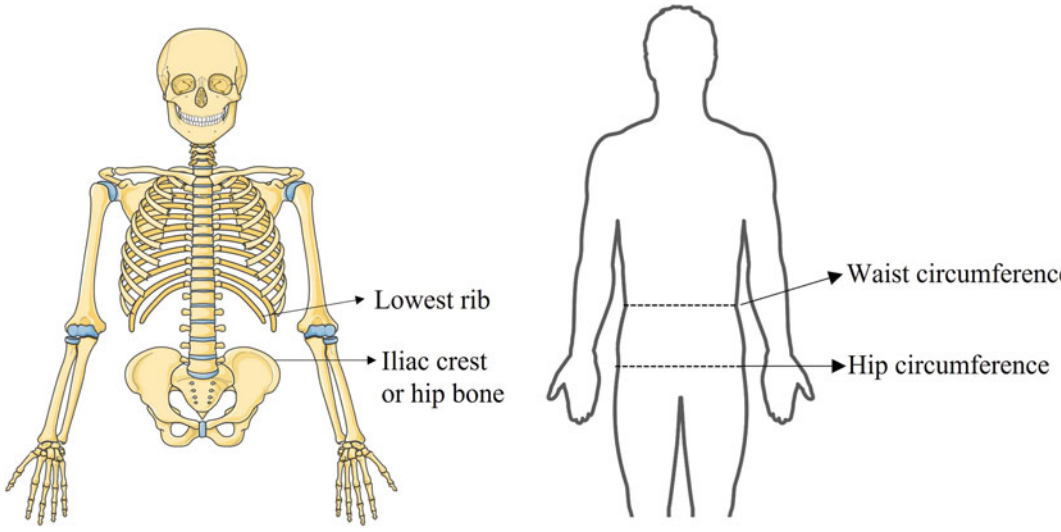

Fig. 3 Circumference of the waist and hip. (Source: Created by Servier Medical Art (smart.servier.com))

<18.5 kg/m^2). Furthermore, Tang et al. [12] observed in a meta-analysis that the MUAC between 23.0 and 25.5 could be acceptable as the cutoff point for malnutrition in communities screening or in clinical environment. This tool can be very useful in edema cases, since this is not a usual problem in upper limbs [13].

Its value can also be applied in mathematical formulas of the triceps skinfold to estimate the arm muscle circumference, arm muscle area, total arm area, and arm fat area. This anthropometric measure is recommended by the World Health Organization for children, adolescents, adults, and older population to predict the protein-energy nutritional status.

With the nondominant unclothed arm positioned at a 90-degree angle to the trunk, the measure is determined at the midpoint between the acromion and the olecranon bone. Moreover, the individual should be asked to extend the arm beside the body with the palm facing the body, arms relaxed, and circle the already marked midpoint with a measuring tape without squeezing the skin (Fig. 4). The measure is expressed in centimeters (cm).

3.4.4 Calf Circumference

The calf circumference is mainly used in older adults to estimate the protein status or the presence of protein malnutrition, as well as in predictive equations to estimate body weight in bedridden individuals.

The individual should preferably be standing, with the legs slightly away, and the tape measure surrounding the most protruding point of the calf, being careful to not to tight excessively. The measure is expressed in centimeters (cm) [14].

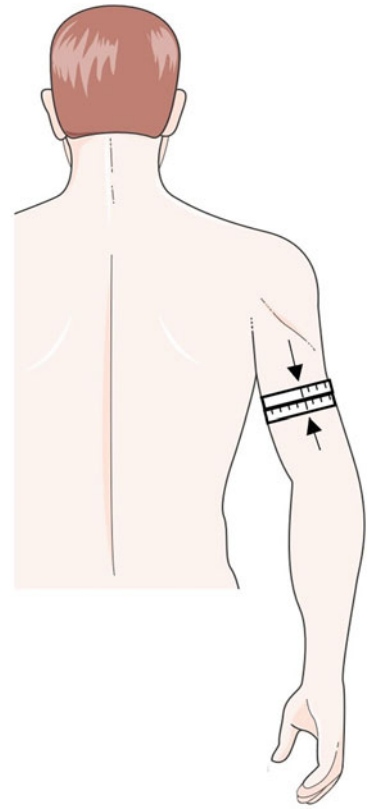

Fig. 4 Measure of the mid-upper arm circumference. (Source: Created by Servier Medical Art (smart.servier.com))

3.4.5 Neck Circumference

The risk of cardiovascular diseases can also be estimated using neck circumference as a parameter. It is performed with the individual preferably sitting, or standing, thus locating the midpoint of the cervical spine, which is surrounded by a tape measure. The measure is expressed in centimeters (cm) [15].

Although neck circumference is a simple tool significantly correlated with waist and BMI circumference, the cutting points for use in standardized methodologies have not yet been defined. However, some studies suggest cutoff values (male 34.0–41.0 and female 32.0–36.1) for neck circumference as a risk indicator for cardiometabolic diseases [16–20].

3.5 Skinfolds

Skinfolds are used to estimate body fat tissue, since about half of the total body fat is located in the subcutaneous tissue. This anthropometric data is important to differentiate the muscle mass from the fat mass, since the weight data do not distinguish the distribution of these tissues in the body. Besides, some of the skinfolds are used in predictive equations to estimate weight, height, and body fat percentage. The techniques described in this chapter follow international standardization [21, 22].

The examiner must be trained to ensure a reliable measurement. The steps to measure the skinfolds are as follows:

- The individual needs to be without clothing, accessories, or any other obstruction in the examined region.
- Preferably, the measures should be determined in the standing individual.
- The examiner presses the individual's skin with the thumb and left index finger, separating the adipose tissue from muscle mass.
- Holding the caliper (adipometer apparatus) with the right hand, it opens enough and carefully releases the pressure exerted in the appliance rods.
- The skinfold should be held with the fingers until the end of the measure.
- The value of the measure in millimeters (mm) should be registered.

It is recommended to repeat the measurement three times at the same point marked and to estimate the mean value to minimize the errors.

More than 90 points in the body are cited in the literature to measure the skinfolds; however, the most predictive equations use up to nine sites to estimate body fat. Therefore, the main skinfolds for adults and older individuals will be presented below (Fig. 5).

3.5.1 Triceps Skinfold

It is performed with the right arm relaxed next to the trunk and the palm of the hand facing the body. After identifying the midpoint between acromion and olecranon, the caliper is placed parallel to the longitudinal axis of the body to perform the measurement.

3.5.2 Biceps Skinfold

It is measured with the right arm relaxed next to the trunk and the palm of the hand facing forward. This skinfold is in the midpiece of the anterior arm between the acromial process of the clavicle and the olecranon process of the ulna (coincides with the marking line of the triceps skinfold). The fold is parallel to the longitudinal axis of the body.

3.5.3 Subscapular Skinfold

This skinfold is measured with one of the arms extended along the body and the palm of the hand facing forward, so the site of the measure is 2 cm below the lower angle of the scapula. The next step is to position the palm of the individual's hand facing the body and to pick up the skinfold obliquely from the longitudinal body axis.

3.5.4 Midaxillary Skinfold

Along with one of the arms folded behind the body, this skinfold is measured in the midpoint between the middle axillary line and the transverse line at the height of the sternum xiphoid process. This is obliquely measured to the body's longitudinal axis.

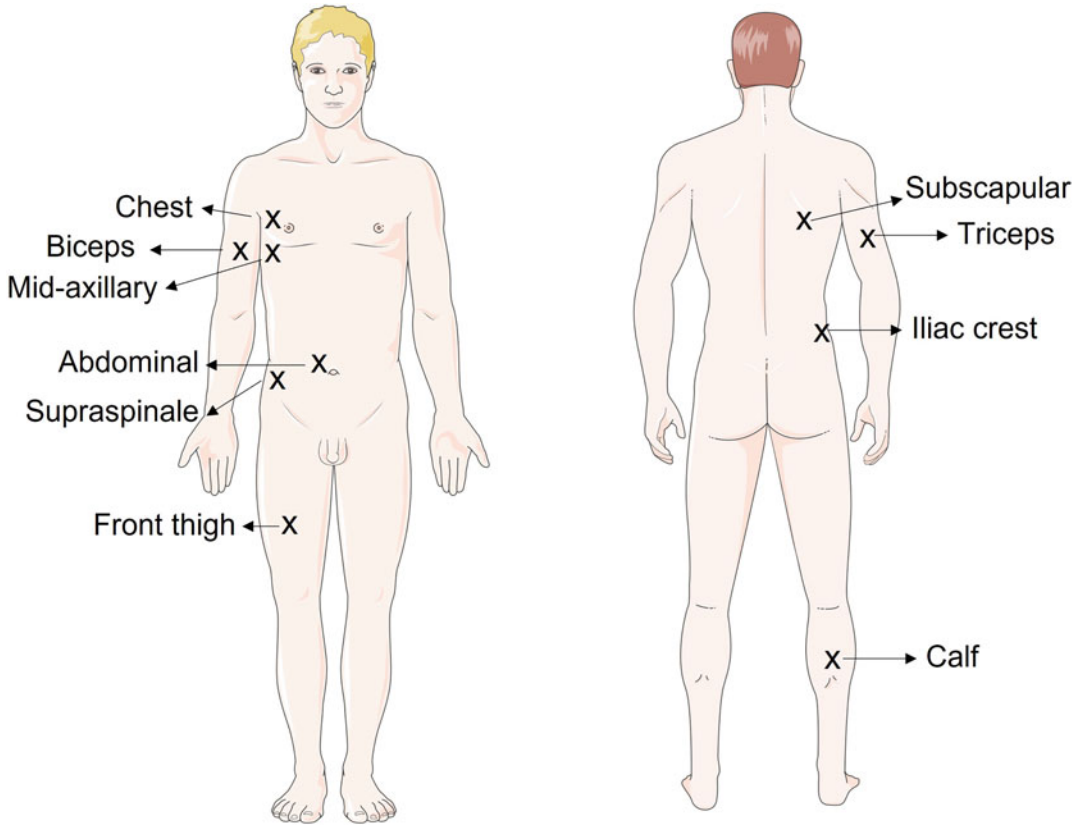

Fig. 5 The main sites used to measure skinfolds. (Source: Created by Servier Medical Art (smart.servier.com))

3.5.5 Supraspinal Cutaneous

It is measured in the intersection between the front part of the iliac crest and the horizontal line from the anterior part of the axilla at 45°, or obliquely 5–7 cm above the anterior iliac spine.

3.5.6 Iliac Skinfold

The arm must be positioned behind the body, and it is selected at the site obliquely to the longitudinal axis of the body, at the midpoint between the last costal arch and the iliac crest, on the middle axillary line.

3.5.7 Chest or Pectoral Skinfold

It is measured with arms extended along the body, obliquely to the longitudinal axis of the body, at the midpoint between the anterior axillary and nipple (for men), or one-third of the anterior axillary line (for women).

3.5.8 Abdominal Skinfold

The arms must be extended along the body, 2 cm the right of the umbilical scar, parallel to the longitudinal axis of the body.

3.5.9 Calf Skinfold

It is measured with the knee joint folded in 90° (supporting the foot on a chair or box), the ankle in anatomical position, and the feet supported or not. Next, the midpoint or more protruding of the calf is picked up, parallel to the longitudinal axis of the body.

3.5.10 Front Thigh or Mid-Thigh Skinfold

It must be performed with the individual standing with the leg to be evaluated relaxed. The skinfold is in the midpoint between the inguinal fold and the upper edge of the patella.

3.6 Nutritional Status Classification in Adults and the Older Adults

Body mass index is an important tool to evaluate the nutritional status of the individuals, which is estimated by dividing the weight by height squared (kg/m^2). To individuals aged 18–59 years old, the anthropometric parameters recommended in the international standards for assessing the nutritional status are BMI (Table 2) and waist–hip ratio according to the WHO [23], associated with the measure of the skinfolds and circumferences according to Frisancho [10], classified by Blackburn and Thornton [24]. From the age of 60, it is considered appropriate to classify BMI for other (Table 3) accepted by the Pan American Health Organization [25] and the other anthropometric parameters by Burr and Philips [26], whose data are accepted internationally.

Table 2
BMI classification for adults

Classification	BMI (kg/m^2)
Underweight	<18.50
Eutrophic (normal weight)	18.50–24.99
Overweight	25.00–29.99
Obese class I	30.00–34.99
Obese class II	35.00–39.99
Obese class III	≥40.00

Source: Adapted from World Health Organization [23]

Table 3
BMI classification for older adults

Classification	BMI (kg/m^2)
Underweight	≤22.00
Eutrophic (normal weight)	22.01–26.99
Overweight	≥27.00

Source: Adapted from Lipschitz [25]

4 Notes

1. The weight measurement can be determined with an adult holding the bedridden individual in the arms, as long as it is safe. The weight can also be measured using a scale coupled to the bed.
2. For bedridden individuals, the height measurement can be predicted by the wingspan: with the arms of the individual stretched forming a 90-degree angle with the body, the distance between the middle finger of one hand until the middle finger of the other hand is measured with a tape measure; therefore, this distance is estimated as the individual's height [27].

Acknowledgments

The authors want to thank Conselho Nacional de Desenvolvimento Científico e Tecnológico (CNPq) for financial support (140816/2019-4). This study was supported in part by the Coordenação de Aperfeiçoamento de Pessoal de Nível Superior—Brasil (CAPES)—Finance Code 001.

References

1. Srinivasan B et al (2017) Precision nutrition – review of methods for point-of-care assessment of nutritional status. Curr Opin Biotechnol 44: 103–108
2. Madden AM, Smith S (2016) Body composition and morphological assessment of nutritional status in adults: a review of anthropometric variables. J Hum Nutr Diet 29(1):7–25
3. Chumlea WC et al (1988) Prediction of body weight for the nonambulatory elderly from anthropometry. J Am Diet Assoc 88(5): 564–568
4. Chumlea WC, Roche AF, Steinbaugh ML (1985) Estimating stature from knee height for persons 60 to 90 years of age. J Am Geriatr Soc 33(2):116–120
5. Chumlea WC, Guo SS, Steinbaugh ML (1994) Prediction of stature from knee height for black and white adults and children with application to mobility-impaired or handicapped persons. J Am Diet Assoc 94(12):1385–1388, 1391; quiz 1389-90
6. International Diabetes Federation. The IDF consensus worldwide definition of the metabolic syndrome. 2006 [cited 10/12/2021]. Available from: https://www.idf.org/e-library/consensus-statements/60-idfconsensus-worldwide-definitionof-the-metabolic-syndrome.html
7. Wang J et al (2003) Comparisons of waist circumferences measured at 4 sites. Am J Clin Nutr 77(2):379–384
8. World Health Organization. Waist circumference and waist-hip ratio: report of a WHO expert consultation. 2008 [cited 12/08/2020]. Available from: https://www.who.int/publications/i/item/9789241501491
9. Taylor RW et al (2000) Evaluation of waist circumference, waist-to-hip ratio, and the conicity index as screening tools for high trunk fat mass, as measured by dual-energy X-ray absorptiometry, in children aged 3-19 y. Am J Clin Nutr 72(2):490–495
10. Frisancho A (1990) Anthropometric standards for the assessment of growth and nutritional status. University of Michigan Press, Michigan
11. Sultana T et al (2015) Assessment of under nutrition of Bangladeshi adults using anthropometry: can body mass index be replaced by mid-upper-arm-circumference? PLoS One 10(4):e0121456

12. Tang AM et al (2020) Determining a global mid-upper arm circumference cut-off to assess underweight in adults (men and non-pregnant women). Public Health Nutr 23(17): 3104–3113
13. Shills ME et al (2009) Modern nutrition in health and disease, 10th edn. Lippincott Williams & Wilkins, Philadelphia
14. Vellas B et al (1999) The Mini Nutritional Assessment (MNA) and its use in grading the nutritional state of elderly patients. Nutrition 15(2):116–122
15. Selvan C et al (2016) Neck height ratio is an important predictor of metabolic syndrome among Asian Indians. Indian J Endocrinol Metab 20(6):831–837
16. Hingorjo MR, Qureshi MA, Mehdi A (2012) Neck circumference as a useful marker of obesity: a comparison with body mass index and waist circumference. J Pak Med Assoc 62(1): 36–40
17. Kumar NV et al (2014) Neck circumference and cardio-metabolic syndrome. J Clin Diagn Res 8(7):MC23–MC25
18. Anothaisintawee T et al (2019) Neck circumference as an anthropometric indicator of central obesity in patients with prediabetes: a cross-sectional study. Biomed Res Int 2019: 4808541
19. Caro P et al (2019) Is neck circumference an appropriate tool to predict cardiovascular risk in clinical practice? A cross-sectional study in Chilean population. BMJ Open 9(11): e028305
20. Espinoza López PA et al (2021) Neck circumference in Latin America and the Caribbean: a systematic review and meta-analysis. Wellcome Open Res 6:13
21. Lean ME, Han TS, Deurenberg P (1996) Predicting body composition by densitometry from simple anthropometric measurements. Am J Clin Nutr 63(1):4–14
22. Lohman TG (1992) Advances in body composition assessment. Human Kinetics, Champaign
23. World Health Organization. Obesity: preventing and managing the global epidemic. 2000 [cited 12/08/2020]. Available from: https://apps.who.int/iris/handle/10665/42330
24. Blackburn GL, Thornton PA (1979) Nutritional assessment of the hospitalized patient. Med Clin North Am 63(5):11103–11115
25. Lipschitz DA (1994) Screening for nutritional status in the elderly. Prim Care 21(1):55–67
26. Burr ML, Phillips KM (1984) Anthropometric norms in the elderly. Br J Nutr 51(2):165–169
27. Bowen M (1995) Respiratory management in scoliosis. In: Lonstein JE et al (eds) Textbook of scoliosis and other spinal deformities. WB Saunders Company, Philadelphia

Chapter 19

MRI-Based Body Composition Analysis

Magnus Borga, André Ahlgren, and Sarah Weston

Abstract

Magnetic resonance imaging (MRI) is considered being state-of-the-art technology for body composition analysis. Compared to other indirect techniques such as scales, calipers, bioimpedance, and dual-energy X-ray absorptiometry (DXA), MRI offers direct and precise measurements of the volumes of different tissue compartments and also enables quantification of diffuse fat infiltration in organs. Here, we describe a protocol for acquiring of fat–water-separated MRI data and the image postprocessing required for the quantification of several body composition biomarkers relevant for metabolic research. This protocol has successfully been used in several clinical studies and also in the large UK Biobank population study.

Key words Body composition analysis, Magnetic resonance imaging, Metabolic imaging biomarkers, Visceral adipose tissue, Subcutaneous adipose tissue, Muscle fat infiltration, Liver fat

1 Introduction

1.1 Body Composition

It is well known that an excessive amount of body fat is related to increased morbidity and mortality but also that the metabolic risk related to fat accumulation is strongly dependent on its distribution [1]. Ectopic fat accumulation, in general, is an important metabolic risk factor [2, 3], and, in particular, visceral adipose tissue (VAT) is related to cardiac risk [4, 5], type 2 diabetes [6, 7], liver disease [8], and cancer [9, 10]. At the same time, high liver fat levels increase the risk for liver disease and type 2 diabetes [11], and increased muscle fat has been associated with increased risk for insulin resistance and type 2 diabetes [12].

Besides fat, skeletal muscles are also of great interest to study, and the balance between the energy-consuming muscles and the energy-storing fat compartments is highly relevant in order to understand the metabolic balance of the body. Cachexia, defined as involuntary loss of body weight, usually with disproportionate muscle wasting, is often related to the progression of a serious underlying disease (e.g., cancer [13]). Sarcopenia, which can be related to cachexia, but is also associated with aging, is commonly

Cinthia Baú Betim Cazarin (ed.), *Basic Protocols in Foods and Nutrition*,
Methods and Protocols in Food Science, https://doi.org/10.1007/978-1-0716-2345-9_19,

defined as reduced physical performance following the loss of muscle mass, usually accompanied by increased fat infiltration of the muscles [14].

These are only a few examples of the need for body composition analysis in studies related to food and nutrition research. This chapter describes a state-of-the-art method for body composition analysis based on magnetic resonance imaging (MRI). The methodology described here has been used in several clinical studies as well as in the large UK Biobank study [15].

1.2 Methods for Body Composition Analysis

There is a range of different methods available for noninvasive body composition analysis. The simplest measures based on tape and scale such as body mass index (BMI), waist circumference, and waist-to-hip ratio do not actually measure body composition but body shape, which does correlate with body composition on a population level, but have all been shown to be poor predictors of metabolic health on an individual level [16–18]. Other methods such as hydrostatic weighing and air displacement plethysmography measure the gross body density, which then, using different body composition models [19, 20], can be used to estimate the total amounts of fat and lean tissue in the body. Bioelectrical impedance analysis (BIA) takes this densitometry approach one step further, measuring the density in the limbs and trunk separately [21, 22]. The model of uniform distribution of fat and water fits better to the extremities than the trunk [23], and while BIA measurements may correlate well with total abdominal AT, BIA cannot be used for measuring VAT [24].

Turning to image methods for body composition analysis, the simplest one is dual-energy X-ray absorptiometry (DXA). DXA uses two X-ray sources with different energies to produce two-dimensional coronal projections of the body. The two energies enable differentiation of bone and soft tissue, and after removing pixels containing bone, the fraction between lean and adipose tissue can be estimated in the remaining voxels. Similar to the methods described above, this technique actually measures the density, and hence, anatomical models are required to transform these density measures to quantitative measures of fat and lean tissue. This technique works well for measuring total amounts of body fat and lean tissue, but for VAT, the agreement with direct methods such as MRI is poor [25]. Furthermore, since BIA is based on a two-dimensional projection of the body, it is not possible to measure diffuse fat infiltration in organs such as the liver or muscles.

In order to obtain direct (and therefore accurate and precise) measures of the distribution of fat and lean tissue, we need to apply tomographic methods, that is, computed tomography (CT) or MRI, which are today considered as the gold standard for body composition analysis [26–28]. Both these techniques are three dimensional, and they also have the capabilities of discriminating

adipose from lean tissue and differentiating between different anatomical locations. However, ionizing radiation in CT limits its use in certain studies, particularly on children and healthy volunteers. Furthermore, due to the exposure to ionizing radiation, the CT-based measurements are often in practice limited to one or a low number of slices rather than the complete three-dimensional volume of interest. This requires an anatomical model of the patient to transform the two-dimensional area measurements to volumetric estimates, thereby reducing them to indirect measurements.

1.3 Theory of MRI-Based Body Composition Analysis

MRI is based on the magnetic properties of different tissues and has excellent soft-tissue contrast for medical imaging. Furthermore, by using proper postprocessing, MRI can be used as a quantitative measurement tool, that is, not only producing contrast images for qualitative radiological reading but calibrated numerical measurements with a physical interpretation. This leaves it as the only direct measurement tool for in vivo body composition analysis that does not use ionizing radiation.

Two different approaches are being used for quantifying fat and lean tissue in MR images. The simplest one is to use some more-or-less automated method for classifying each voxel (three-dimensional pixel) into one of a set of mutually exclusive classes, such as "fat," "lean tissue," and "background." However, this approach has several disadvantages. One is that the measurements will be dependent on the image resolution [29], limiting the reproducibility across different scanners. Another important limitation of this approach is that it does not allow for measurements of diffuse fat infiltration in organs, e.g., muscles and liver. This is because an increased fat infiltration will not change the classification of a voxel until it reaches a specified threshold when it will change completely from one tissue type to another.

The second approach is to use quantitative MRI, where the value in each voxel is proportional, e.g., to the amount of fat in that voxel. This approach reduces the dependence on image resolution and, more importantly, enables quantification of diffuse fat infiltration [29]. This is the approach further described in this chapter.

In the context of body composition analysis, quantitative MRI is obtained using chemical shift-encoded (CSE) MRI. This technology is based on the fact that protons in fat and water have different electromagnetic resonance frequencies (Larmor frequencies). This causes the measured signals ("echoes") from fat and water to have slightly different frequencies leading to a phase shift between those signals. If at least two echoes are acquired, this phase shift allows the scanner's image reconstruction software to separate the fat and water signals from each other, enabling the generation of a perfectly aligned image pair with one image depicting fat and the other image depicting water, which is the dominant substance

in lean tissue. This imaging methodology is known as fat–water-separated MRI [30] and can be performed by most modern MRI scanners.

However, the fat and water images generated by the scanner are not quantitative, that is, the voxel values do not directly correspond to any physical tissue properties, such as the actual amount of fat or water in the tissue. In order to obtain a quantitative image, it needs to be calibrated. One way of calibrating the fat image is to divide it by the sum of the fat and water images. If the fat and water images are proton density (PD) weighted, this fraction is known as proton density fat fraction (PDFF), which is a quantitative measure of the relative amount of fat [31]. However, PDFF quantification is usually based on the 6-echo acquisition and thus requires longer scan times than what is practical for whole-body acquisition. An alternative approach, which allows for more rapid T1-weighted dual-echo imaging, is fat-referenced MRI [32, 33].

Once a quantitative fat image is obtained, it needs to be segmented into different compartments. There are several different, more or less automated, techniques for achieving such segmentations. The method described in this chapter is designed to perform highly reproducible (*see* Subheading 4.1) quantification of VAT, abdominal subcutaneous tissue (ASAT), anterior and posterior thigh muscle volume, thigh muscle fat infiltration, and liver fat fraction, which are imaging biomarkers known to be associated do different metabolic disorders [34].

2 Materials

MRI-based body composition naturally requires an MRI scanner. Table 1 shows examples of MRI scanner models and scanner software versions that are able to acquire MR images appropriate for body composition analysis. Other scanner manufacturers and models than the ones listed below might also work.

The fastest CSE MRI acquisition, also known as a Dixon sequence, uses two symmetrical echoes, and the best results for body composition are obtained using a Dixon sequence with 3D-spoiled gradient-recalled echo (GRE) readout. Some commercial names of this sequence type are given in Table 2. Three-dimensional Dixon sequences are normally included by default on all MRI scanners.

The only measurement 2-point Dixon is not sufficient for in this context is liver fat. Liver fat is commonly measured using multipoint CSE sequences to produce reliable results. Table 2 includes some commercial names also for this sequence type. Multipoint CSE is not available on all MRI scanners, but alternative approaches are possible. Liver imaging is the only part that requires an auxiliary surface coil.

Table 1
Examples of MRI scanner models and scanner software versions suitable for body composition imaging

Manufacturer and type	Model
GE 3T	SIGNA premier, SIGNA architect, SIGNA Pioneer, SIGNA PET/MR, discovery MR750w GEM, discovery MR750, SIGNA HDxt
GE 1.5T	SIGNA artist, SIGNA explorer, SIGNA creator, SIGNA voyager, discovery MR450, optima MR450w GEM, optima MR450w, optima MR360, Brivo MR355, SIGNA HDxt
GE upgraded systems	SIGNA premier lift, SIGNA architect lift, discovery MR750 lift, SIGNA artist lift, SIGNA explorer lift, optima 450
GE software versions	HD16, HD23, SV20, SV23, SV25, DV22, DV23, DV24, DV25, DV26, DV27, PX25, PX26, RX27, MP24, MP26
Philips 3T	Ingenia Elition 3.0T X/S, Ingenia 3.0T CX, Ingenia 3.0T, Achieva 3.0T
Philips 1.5T	Ingenia ambition 1.5T X/S, Ingenia Prodiva 1.5T CX/CS, Ingenia 1.5T CX/S, Ingenia 1.5T, Achieva 1.5T, Multiva 1.5T
Philips upgraded systems	Achieva 3.0T dStream, Achieva 1.5T dStream, Intera Achieva
Philips software versions	Release 5.1, release 5.2, release 5.3, release 5.4, release 5.5, release 5.6, release 5.7, release 6
Siemens 3T	MAGNETOM Vida, MAGNETOM Prisma, MAGNETOM Skyra, MAGNETOM Verio, MAGNETOM Lumina, MAGNETOM spectra, MAGNETOM biograph mMR, MAGNETOM trio
Siemens 1.5T	MAGNETOM Aera, MAGNETOM sola, MAGNETOM Altea, MAGNETOM Amira, MAGNETOM Sempra, MAGNETOM Espree, MAGNETOM Avanto
Siemens upgraded systems	MAGNETOM Vida fit, MAGNETOM Prisma fit, MAGNETOM Skyra fit, MAGNETOM sola fit, MAGNETOM Avanto fit, MAGNETOM symphony TIM
Siemens software versions	B17, B19, B20, D12, D13, E11, XA10, XA11, XA12, XA20

Table 2
Examples of MRI sequences for fat–water-separated imaging

Type of sequence	Examples of commercial names
Dixon sequence with 3D GRE readout (for body composition)	GE: LAVA-flex Philips: mDixon (XD) Siemens: Dixon-VIBE
Multipoint CSE sequence (for liver fat)	GE: Ideal-IQ Philips: mDixon-quant Siemens: LiverLab (qDixon)

3 Methods

This section is divided into three parts: The first part is a step-by-step guide on setting up the MRI protocol. The second part describes how to perform the MRI scan. Finally, the third part describes how the acquired MR images are processed to obtain quantitative measurements of body composition with high repeatability and reproducibility (*see* Subheading 4.1).

3.1 MRI Protocol Set-up

The body composition MRI protocol consists of the following:

Neck-to-Knee Sequences

Coverage is achieved using eight contiguous, overlapping Dixon sequences at preset locations. Suspended expiration breath-hold technique is used over the chest and abdomen while pelvis-to-knee is scanned free-breathing.

Manufacturer-specific parameters for the three most common MRI scanner manufacturers are contained within and are referred to in Subheading 4.3; however, these parameters are translatable to alternate manufactures. Important areas where the scanning technique differs from routine clinical practice are outlined in Table 3.

Liver Sequence

Coverage is achieved using a single sequence with a suspended expiration breath-hold technique. Specific parameters are not required as the manufacturer's quantitative liver sequence is intended to be scanned as per the manufacturer's instructions (LiverLab/Ideal-IQ/mDixon-Quant).

3.1.1 Neck-to-Knee Sequences Set-up

- Select the appropriate 3D Dixon sequence from the scanner protocol library as indicated in Subheading 4.3.
- Activate Dixon reconstructions of fat, water, in-phase (IP), and opposed-phase (OP).
- Label the sequence "Dixon_BH_1."

Table 3
Important differences from routine clinical practice

	Neck-to-knee	Liver
Surface coils	X	✓
Integrated body coil	✓	X
Localizer	X	✓
Planning	X	✓
Knee cushion	X	X

- Remove any parallel imaging acceleration techniques.
- Ensure the integrated scanner body coil is activated and no surface coils are activated.
- Set the sequence according to the Dixon breath-hold parameters (*see* Subheading 4.3)
- Make four copies of the sequence.
- Set the last copy according to the Dixon Thighs (*see* Subheading 4.3).
- Label the last copy "Dixon_Thighs_5."
- Make three copies of the Thigh sequence.
- Enter the manufacturer-specific table positions for each sequence (*see* Subheading 4.3).

3.1.2 Liver Sequence Set-Up

- Add a localizer sequence to cover the liver utilizing surface coils posteriorly and anteriorly.
- Add the manufacturer's quantitative liver sequence and label the sequence "BH_Liver."
- The protocol queue should resemble that of Table 4.
- If parameters cannot be set exactly as per the values in Subheading 4.3, refer to Subheading 4.4 for answers to frequently asked questions.

Table 4
Protocol queue

Protocol
Dixon_BH_1
Dixon_BH_2
Dixon_BH_3
Dixon_BH_4
Dixon_Thighs_5
Dixon_Thighs_6
Dixon_Thighs_7
Dixon_Thighs_8
Liver localizer
BH_Liver

3.2 MRI Protocol Scanning

- Place the patient straight and centered in the headfirst supine position as far as the top of the table as is safely possible.
- Ensure the patient is positioned so that the entire liver is covered posteriorly with a surface coil such as the spine coil.
- Do not use a cushion under the patient's knees.
- Use spacers according to local policies.
- Use a loosely tightened foot-strap to keep the legs and feet together and stabilized.
- Place an anterior surface coil over the abdomen, ensuring the entire liver is covered.
- Place the landmark or centering point at the suprasternal notch.
- A localizer is not required for the neck-to-knee sequences.
- The neck-to-knee sequences require no manual planning as the table and image locations are preset within the sequence.
- The neck-to-knee sequences should be scanned without any modification of the slice positions, slice number, or parameters.
- Ensure no surface or spine coils are activated.
- Ensure the integrated whole-body coil is activated (Siemens: BC, Philips: Q-Body, GE: Body Coil by GE or GE T/R body coil).
- Use manual or automatic breath-hold commands for sequence labeled "BH."
- Expiration breath-holds are recommended for sequences labeled "BH."
- Ensure the anterior and posterior surface coils are activated for the liver sequences.
- Scan the liver localizer with expiration breath-hold technique.
- Manually plan the liver sequence to include as much of the liver as possible, prioritizing the liver dome over the liver tail as per Fig. 1.
- Scan the BH_Liver sequence with expiration breath-hold technique.
- Review neck-to-knee sequences and liver sequence image quality correlating with "Common Image Artefacts and Remedial Actions" under Subheading 4.2 to ensure images are suitable for analysis.
- Ensure a complete set of Dixon reconstructed images are present for all Dixon BH and Thigh sequences, and an example for a Siemens 1.5T & 3T scanner is demonstrated in Table 5.
- Ensure a complete set of reconstructed images are present for the liver sequence; an example for a GE 1.5T & 3T scanner is demonstrated in Table 6.

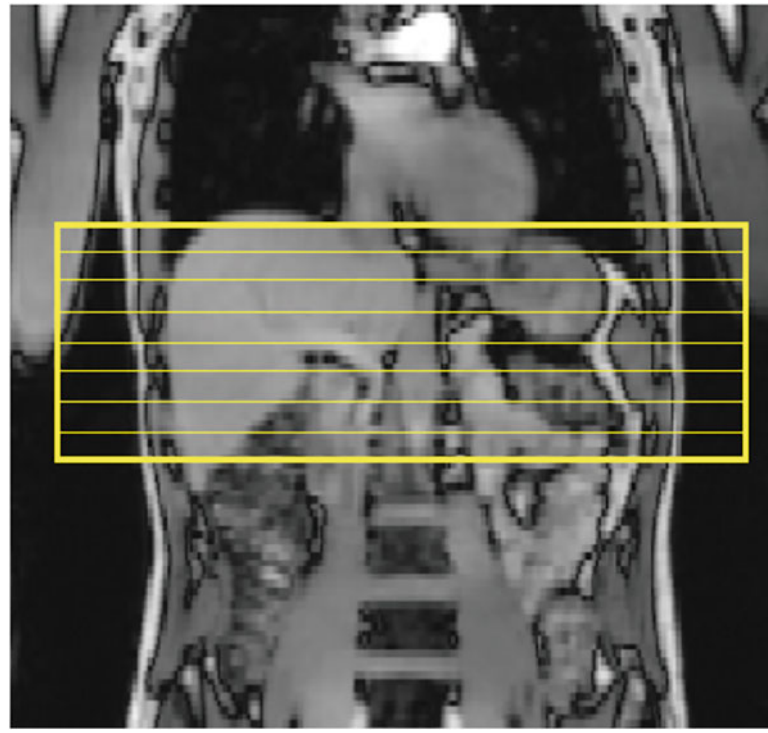

Fig. 1 Planning of liver sequence

Table 5
Complete set of Dixon reconstructed images. Example for Siemens scanners

Dixon protocol	IP image count	OP image count	Fat image count	Water image count
Dixon_BH_1	32	32	32	32
Dixon_BH_2	32	32	32	32
Dixon_BH_3	32	32	32	32
Dixon_BH_4	32	32	32	32
Dixon_Thighs_5	56	56	56	56
Dixon_Thighs_6	56	56	56	56
Dixon_Thighs_7	56	56	56	56
Dixon_Thighs_8	56	56	56	56

Table 6
Complete set of reconstructed images are present for the liver sequence. Example for GE scanners

Liver sequence	IP	OP	Fat	Water	R2*	Fat fraction
IDEAL-IQ	44	44	44	44	44	44

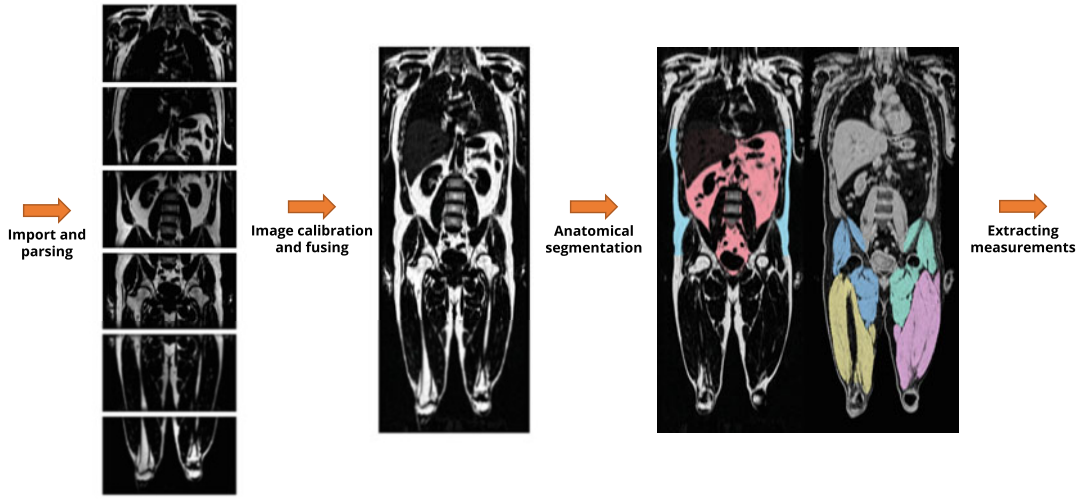

Fig. 2 Schematic overview of the image processing recommended for MRI-based body composition analysis

3.3 Postprocessing

Images are exported from the MRI scanner and imported into an image postprocessing pipeline. It is recommended that the images are exported from the scanner in classic DICOM format, that sensitive patient health information is removed from the image metadata, and that imaging information (such as magnetic field strength, image resolution, and echo times) is preserved in the image metadata. This section describes the different parts of the image postprocessing pipeline required for body composition analysis. See Fig. 2 for a schematic overview. It is advisable to implement some form of quality control of the output from the image postprocessing. In addition, image quality may be reviewed during postprocessing to ensure that the body composition measurements do not contain errors due to imaging issues and artifacts (*see* Subheading 4.2) [35].

3.3.1 Import and Parsing

- Import the image data (image array and metadata) into the pipeline, taking into account the data format/encoding. Save all imaging metadata (also known as DICOM tags) for possible use in image processing and body composition measurements.
- Sort the images based on sequence type (Dixon for body composition, and multipoint CSE for liver fat), as well as on image type (e.g., fat, water, in-phase, opposed-phase, fat fraction, and T2*). The sorting is simplified by using standardized naming of the sequences (found in the "Series Description" tag) and parsing the "Image Type" tag.

3.3.2 Image Calibration and Fusion

- Rescale each image volume according to metadata such as "Rescale Slope" and "Rescale Intercept," or other manufacturer-specific scale factors. Different scanner manufacturers scale the image data differently, so make sure to account for that (it can be handled automatically by reading the Manufacturer's DICOM tag).
- Correct for positive signal bias due to magnitude images (Rician noise) if possible.
- Calibrate the fat and water images to get rid of spurious image inhomogeneities and obtain quantitative fat concentration images using fat-referenced MRI [32, 33, 36]. Apply the same correction to the water volumes.
- Fuse the calibrated image slabs into whole-body volumes. This can be realized by using the image position metadata or by image coregistration. Ensure that the final fused whole-body volume has a consistent voxel size. Ensure that the total amount of calibrated signal is preserved in the fusing algorithm (i.e., do not use the addition of images). The simplest fusion is to crop and stack the image volumes (i.e., stitch them together edge-to-edge), whereas a more precise result will be obtained by performing some form of soft cross-fade (ramp) in the overlap between the slabs.
- Produce a fuzzy soft-tissue concentration image for use in calculating measurements.
- The multipoint CSE liver images are normally sufficient to import the images and account for the scaling factors. The established measurement for liver fat quantification is PDFF, so ensure that the fat fraction image type is imported.

3.3.3 Anatomical Segmentation

- Feed the calibrated and fused image volumes into an anatomical segmentation routine. The segmentation step may be implemented in a variety of ways. Manual segmentation is relatively common in MRI, but it is not recommended for body composition analysis due to being very labor intensive. Better alternatives are automatic or semiautomatic approaches such as atlas-based segmentation, clustering methods, or artificial intelligence methods such as convolutional neural networks.
- Control and, if possible, adjust the segmentation results to conform with predefined clear anatomical definitions.
- For liver fat measurement, whole liver or partial liver measurement may be used. For the latter approach, regions of interest (ROIs) are manually or automatically placed within the liver, avoiding vessels and bile ducts.

3.3.4 Extracting Measurements

- The body composition measurements may now be calculated using the calibrated images and the anatomical segmentations. The standard body composition measurements are as follows:
  - VAT volume: Integrate the fat concentration in the visceral fat compartment (abdominal cavity).
  - ASAT volume: Integrate the fat concentration in the subcutaneous fat around the abdominal region (it is advisable to use standardized landmarks to define the abdominal extent).
  - Thigh muscle volume: Remove the contribution of fat to the muscle region (e.g., by removing fatty voxels or accounting for the fat concentration in every voxel), and sum up the volume of lean muscle tissue. It is recommended to account for cortical bone and other nonlean tissue by also using the soft-tissue concentration image. Muscle volume may be calculated for individual thigh muscle groups as well as the entirety of the thigh muscles.
  - Muscle fat infiltration (MFI): Calculate the relative amount of fat (i.e., fat fraction) within the thigh muscles, for example, by dividing the amount of fat with the muscle mask volume. Ensure to account for any MRI weighting (e.g., T1-weighting) and T2*-induced cross-talk between fat and water.
  - Liver fat: Use the whole liver or ROIs to extract the mean PDFF for the liver.
- Other body composition-related measurements may also be extracted, such as:
  - Total adipose tissue (TAT) volume: Integrate the fat concentration over the entire body (or as much as covered by the imaging protocol). This is similar to what is measured with the DXA technique.
  - Total lean tissue (TLT) volume: Subtract the amount of fat from the total soft-tissue volume over the entire body (or as much as covered by the imaging protocol). This is similar to what is measured with the DXA technique.
  - Thigh subcutaneous adipose tissue (ThighSAT) volume: Calculated in the same way as ASAT volume, but around the thighs instead of the abdomen.
  - Organ volumes (e.g., liver or spleen): Calculate the volume of the segmentation masks over the organs. The volume of fat may be subtracted if lean organ volume is of interest.
- Additional body composition profile measurements may be derived from the standard body composition measurements and complementary patient metadata such as:

  - Fat ratio: Calculated as (VAT + ASAT)/(VAT + ASAT + Total thigh muscle volume)
  - Weight to muscle ratio: Calculated as *Body weight/Total thigh muscle volume*
  - Visceral Fat Ratio: Calculated as *VAT/(VAT + ASAT)*
- Any measurement may be divided by patient height squared to produce normalized indices.
- As part of extracting measurements, any image artifacts or other issues may be reviewed and graded to indicate a potential impact on measurement reliability.

4 Notes

4.1 Repeatability and Reproducibility

The test–retest repeatability and between-scanner reproducibility of body composition analysis performed as described here have been presented in a recent study [37]. The estimated test–retest repeatability coefficients were 13 cl (VAT), 24 cl (ASAT), 17 cl (total thigh muscle volume), 0.53% (MFI), and 1.27–1.37% (liver fat). The corresponding between-scanner reproducibility coefficients were 24 cl (VAT), 42 cl (ASAT), 31 cl (total thigh muscle volume), 1.44% (MFI), and 2.37–2.40% (liver fat).

4.2 Common Image Artifacts and Remedial Actions

Artifacts related to patient positioning are illustrated in Fig. 3.

4.2.1 Positioning

4.2.2 Leg Cushion

Artifacts caused by using a leg cushion are illustrated in Fig. 4.

4.2.3 Coils

Artifact caused by using surface coils in the neck-to-knee acquisition is illustrated in Fig. 5.

4.2.4 Breath-Hold

Artifact caused by breath-hold on inspiration is illustrated in Fig. 6.

4.2.5 Manual Planning

Artifacts caused by manual planning of the scans are illustrated in Figs. 7 and 8.

4.2.6 Movement

Artifact caused by patient movement between sequences is illustrated in Fig. 9.

4.2.7 Metal

Metal artifact is illustrated in Fig. 10.

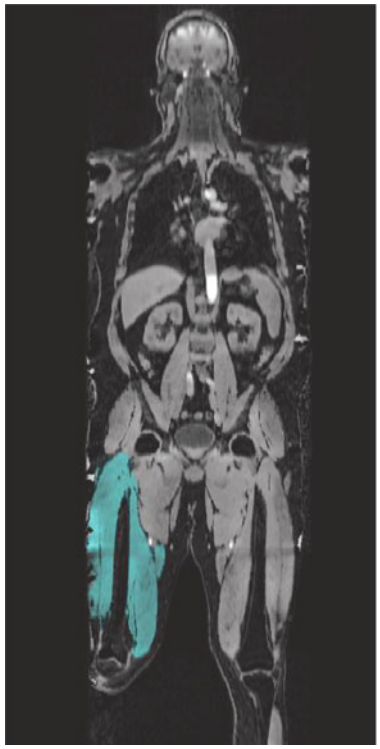

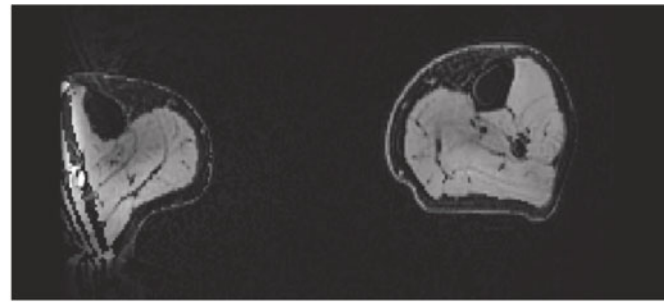

Fault: The patient is off-centre and the legs abducted

Result: Areas of anatomy missing from the field of view

Remedy: Ensure the patient is straight and centred on the scanner table and loosely strap the toes together

Fig. 3 Positioning related artifact

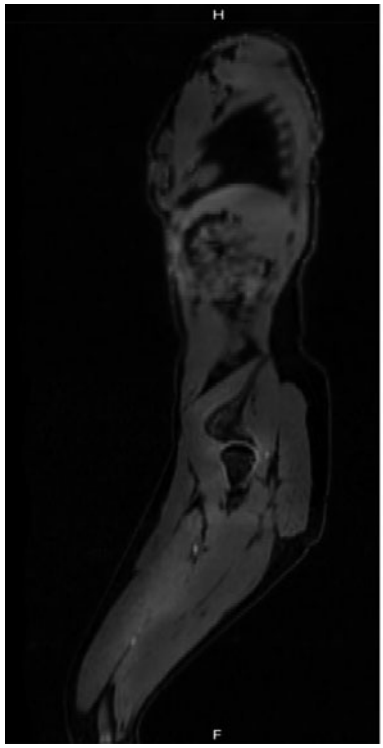

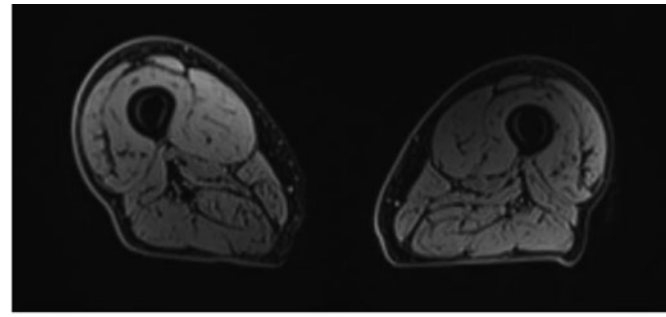

Fault: Areas of anatomy in the posterior thigh region are compressed and the legs elevated

Result: Higher likelihood of complex swaps in the area of compression and missing anatomy from the field of view

Remedy: Ensure cushions/supports are not placed beneath the patient's legs or knees

Fig. 4 Leg cushions should not be used

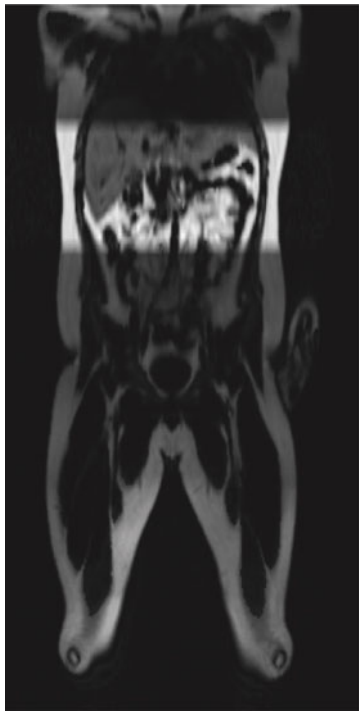

Fault: Inhomogeneous signal throughout merged neck-to-knee acquisition

Result: Image calibration failed

Remedy: Ensure surface coils are not activated for neck-to-knee acquisition. Activate integrated/inherent scanner body coil only (Siemens: BC, Philips: Q-Body, GE: Body Coil by GE or GE T/R body coil)

Fig. 5 Inhomogeneous signal throughout merged neck-to-knee acquisition due to use of surface coils

Fault: Breath-hold on inspiration

Result: Loss of abdominal skin border integrity during post processing

Remedy: Prioritise where possible, suspended expiration, to maintain skin border integrity. If the patient can not comply with suspended expiration, suspended inspiration is acceptable however the breath-hold technique should remain consistent through out

Fig. 6 Breath-hold on inspiration

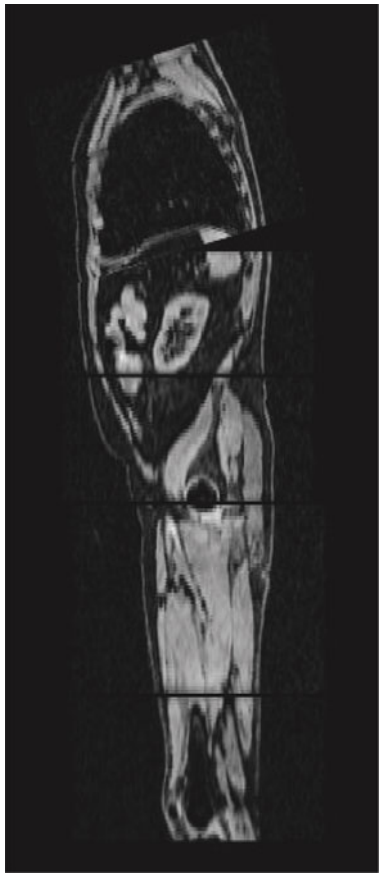

Faults: Dixon_BH_1 undergone manual planning, orientation altered from true axial to oblique. All sequences undergone reduction in number of prescribed slices

Result: Missing anatomy upon reconstruction

Remedy: Ensure sequences are not angled or rotated. Do not reduce the number of prescribed slices or change slice positions

Fig. 7 Missing slices due to manual planning

4.2.8 Complex Fat/Water Swap

Complex fat/water swap artifacts are illustrated in Fig. 11.

4.2.9 Separate-Island Fat/Water Swap

Separate-island swap artifact is illustrated in Fig. 12.

4.2.10 Global Fat/Water Swap

A global fat/water swap is illustrated in Fig. 13.

4.2.11 Unavoidable Artifacts

Unavoidable artifacts typically seen in patients with a larger body habitus are illustrated in Figs. 14 and 15.

4.2.12 Coverage

Wrong anatomical coverage is illustrated in Fig. 16.

4.3 Parameter Tables and Table Locations

Scan parameters and table locations for Siemens scanners are listed in Tables 7 and 8, respectively.

4.3.1 Siemens

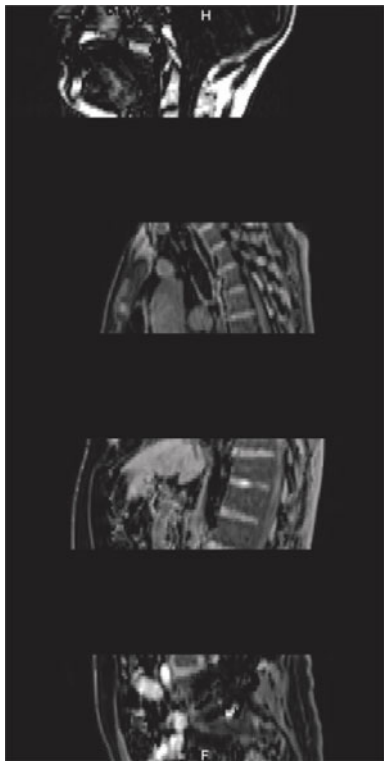

Fault: All sequences have undergone manual planning, pre-defined hard-coded slice coordinates and table positions are lost

Result: Missing anatomy upon reconstruction

Remedy: Ensure sequences are not manually planned, angled or rotated

Fig. 8 Missing slices due to manual planning

4.3.2 Philips

Scan parameters and table locations for Philips scanners are listed in Tables 9 and 10, respectively.

4.3.3 GE

Scan parameters and table locations for GE scanners are listed in Tables 11 and 12, respectively.

4.4 Frequently Asked Questions

- *I cannot set the Frequency FOV to 500 mm/50 cm; what should I do?*

  Choose the maximum FOV possible without exceeding 500 mm/50 cm.
- *The protocol set-up instructions are not perfectly applicable; what should I do?*

  Focus on building a protocol with similar FOV settings as the parameter table with the correct coordinates, then try setting the remaining parameters as close as possible to the parameter table as possible.
- *The scan-assist/conflict-information suggests changes to the protocol or suggests that the protocol settings are incompatible; what should I do?*

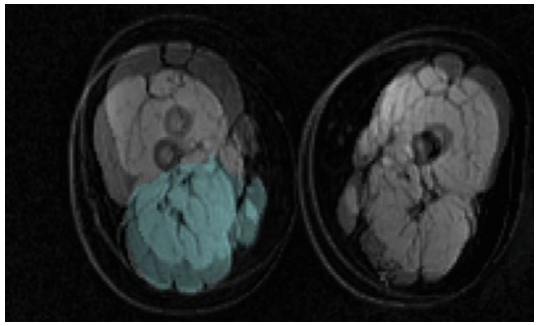

Fault: The patient has changed position in between and/or during sequences

Result: Indistinct anatomical borders

Remedy: If movement artefact is present, the affected sequences should be re-acquired

Fig. 9 Artifact caused by patient movement

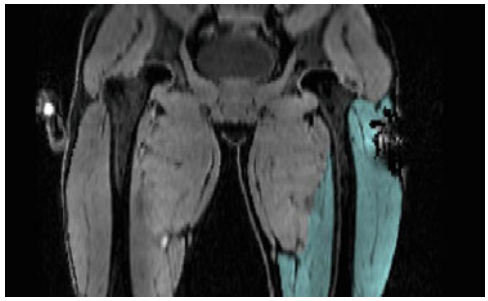

Fault: Metallic jewellery on left hand

Result: Missing anatomy owing to swap and susceptibility artefact

Remedy: Dixon reconstructions rely on a good quality shim resulting in a homogenous magnetic field, this cannot be achieved if metal is present in the scanner bore. Notwithstanding MR compatible metallic prosthesis, remove all metallic objects in and around the scanner bore

Fig. 10 Artifact caused by metal

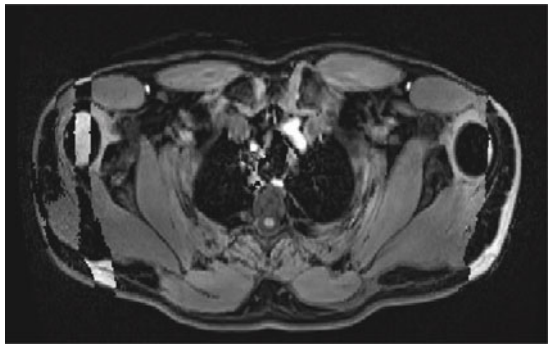

Fault: Complex swap

Result: Inhomogeneous patchy signal

Remedy: Ensure there is no metal in or around the bore and the patient is straight and centred on the scanner table.

Fig. 11 Complex fat/water swap

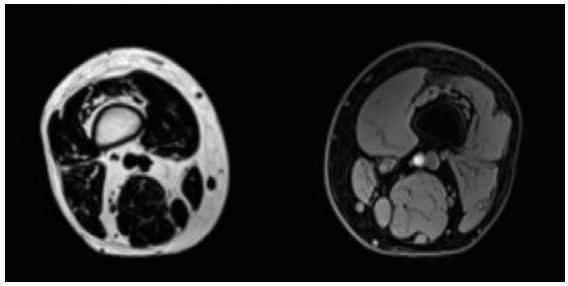

Fault: Separate island swap

Result: An anatomical region disconnected from surrounding tissue associated with the incorrect signal channel

Remedy: Ensure legs and arms are not abducted from the torso and there is no metal in or around the scanner bore

Fig. 12 Separate-island fat/water swap

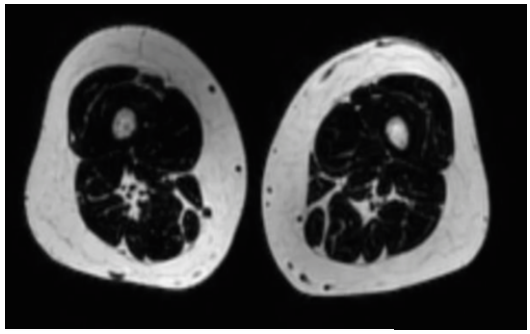

DERIVED\PRIMARY\DIXON\WATER

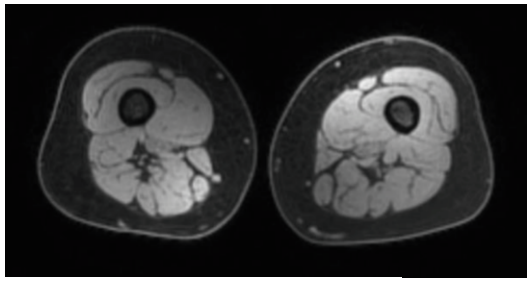

DERIVED\PRIMARY\DIXON\FAT

Fault: Global swap

Result: Entire areas of anatomy are associated with the incorrect signal channel. Pictured here, the 'fat' image is registered as the water channel and vice versa.

Remedy: Repeat the set of neck-to-knee sequences with a new centring point a few millimetres above or below the sternal notch to force a new Dixon reconstruction. Ensure the patient is straight and centred on the scanner table, there is no metal in or around the scanner bore and the arms and legs are not abducted

Fig. 13 Global fat/water swap

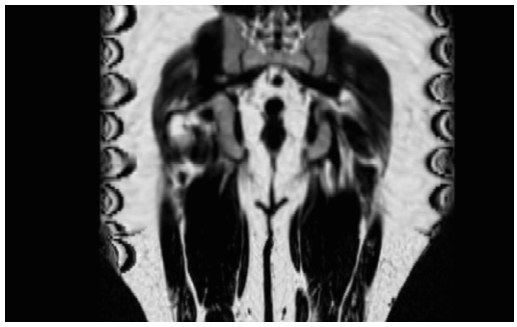

Fault: Swap artefact in lateral most edges of the field of view

Result: Missing anatomy

Remedy: Typically seen in patients with a larger body habitus. To minimise the effect on measurements it is advisable to position the patient as central and straight as possible

Fig. 14 Swap artifacts in lateral edges of the field of view

In general, agree to all automatic modifications of the protocol (e.g., scan-assist suggestions), ignoring any conflict information initially. It is recommended to double-check all parameter settings according to the parameter table once the set-up is complete, especially since automatic modifications may have altered parameters that can be set a second time correctly. If conflicts remain, try to solve them with minimal changes as possible.

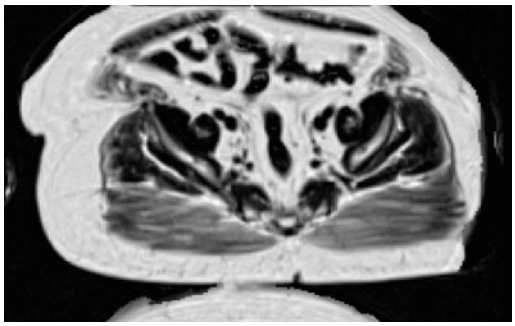

Fault: Anterior anatomy wrapped into posterior

Result: Loss of abdominal skin border integrity

Remedy: Typically seen in patients with a larger body habitus. The wrapped portion of anatomy is measurable, the sequence would not require repeating

Fig. 15 Anterior anatomy wrapped into posterior part of the image

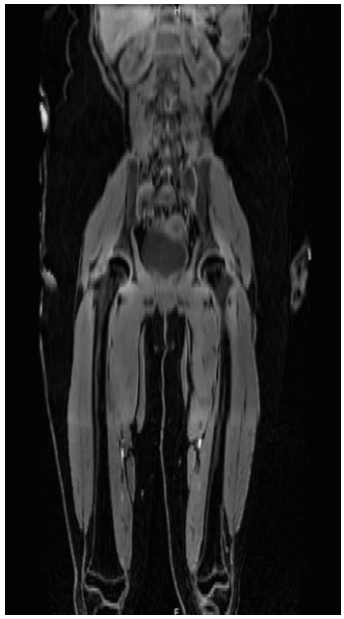

Fault: Centring point positioned below sternal notch

Result: Missing anatomy

Remedy: Ensure the centring point is located at the sternal notch. This centring point is suitable for patients in excess of 2 metres tall and should not be modified to accommodate taller patients. Coverage should include neck-to-knee to ensure all regions are measurable

Fig. 16 Missing anatomy due to centering point positioned below the sternal notch

- *I cannot find all required sequences in the scanner's library; what do I do?*

  The local MR applications specialist or the vendor applications specialist should be able to assist if there is difficulty locating a sequence.
- *What can I do if the anterior–posterior field of view is too small?*

  The AP FOV can be increased by increasing the phase-FOV. To compensate for added scan time, the phase resolution can be decreased. However, nonobese patients should not be scanned with such a modified protocol as the resolution may prove too coarse.

Table 7
Scan parameters for Siemens scanners

	1.5T		3T	
Parameter table	**Dixon-VIBE (breath-hold)**	**Dixon-VIBE (thighs)**	**Dixon-VIBE (breath-hold)**	**Dixon-VIBE (thighs)**
Routine				
Phase oversampling	0	0	0	0
Slice oversampling	18%	22%	0%	22%
Slices per slab	32	56	32	56
FOV read (mm)	500	500	500	500
FOV phase	80%	80%	80%	80%
Slice thickness	5	4	5	4
TE (1/2/3)	–	–	–	–
Averages	1	1	1	1
Contrast				
TR	Min. allowed	Min. allowed	Min. allowed	Min. allowed
Dixon	Fat/water/IP/OP	Fat/water/IP/OP	Fat/water/IP/OP	Fat/water/IP/OP
Flip angle	10	10	10	10
Resolution				
Base resolution	128	224	192	256
Phase resolution	84%	84%	84%	84%
Slice resolution	100%	100%	100%	100%
Phase partial Fourier	6/8	Off	6/8	Off
Slice partial Fourier	5/8	Off	6/8	Off
Interpolation	Off	Off	Off	Off
PAT mode	None	None	None	None
Image filter	Off	Off	Off	Off
Normalize	Off	Off	Off	Off
Distortion correction	On	On	On	On
Mode	2D	2D	2D	2D
Prescan normalize	–	–	–	–

(continued)

Table 7
(continued)

	1.5T		3T	
Parameter table	**Dixon-VIBE (breath-hold)**	**Dixon-VIBE (thighs)**	**Dixon-VIBE (breath-hold)**	**Dixon-VIBE (thighs)**
System				
Coils	Body	Body	Body	Body
Coil select mode	Off—all	Off—all	Off—all	Off—all
Physio				
Resp. control	Breath-hold (expiration)	Off	Breath-hold (expiration)	Off
Sequence				
Contrasts	2	2	2	2
Bandwidth	~470	~470	~1000	~1000
Readout mode	Bipolar	Bipolar	Bipolar	Bipolar
Optimization	Opp/in	Opp/in	Opp/in	Opp/in
Asymmetric echo	Off or weak	Off or weak	Off or weak	Off or weak

Table 8
Table locations for Siemens scanners

Dixon-VIBE table locations	L	P	F
Dixon_1_BH	0	0	50
Dixon_2_BH	0	0	170
Dixon_3_BH	0	0	290
Dixon_4_BH	0	0	410
Dixon_5_Thigh	0	0	560
Dixon_6_Thigh	0	0	740
Dixon_7_Thigh	0	0	920
Dixon_8_Thigh	0	0	1100

- *Can I use surface coils to shorten the breath-hold times?*

  The neck-to-knee protocol does not use surface coils.
- *Must the Dixon neck-to-knee sequences be acquired in the specified order?*

Table 9
Scan parameters for Philips scanners

	1.5T		3T	
Parameter table	**mDixon (breath-hold)**	**mDixon (thighs)**	**mDixon (breath-hold)**	**mDixon (thighs)**
Geometry				
Uniformity	–	–	–	–
Slice orientation	Transversal	Transversal	Transversal	Transversal
FOV RL (mm)	500	500	500	500
FOV AP (mm)	400	400	400	400
FOV FH (mm)	160	208	160	208
ACQ voxel size RL	3.3	2	3.3	2
ACQ voxel size AP	3.6	2.2	3.6	2.2
ACQ voxel size FH	5	4	5	4
Recon voxel sizes	Match ACQ voxel size as close as possible	Match ACQ voxel size as close as possible	Match ACQ voxel size as close as possible	Match ACQ voxel size as close as possible
Image shutter	No	No	No	No
Slice oversampling	1.1	Default	Default	Default
SENSE	No	No	No	No
Slices	32	55	32	55
Fat shift direction	L	L	L	L
Contrast				
Contrast enhancement	T1	T1	T1	T1
Fast imaging mode	None	None	None	None
Echoes	2	2	2	2
TE first	2.2	2.2	1	Shortest
Second/echo-spacing	Shortest	Shortest	Shortest	Shortest
Flyback	No	No	No	No
Flip angle	10	10	10	10
TR	Shortest	Shortest	Shortest	Shortest
Halfscan	No	No	No	No
Water-fat shift	0.35	0.35	0.35	0.35
Motion				
Resp. compensation	Breath-hold	–	Breath-hold	–

(continued)

Table 9
(continued)

	1.5T		3T	
Parameter table	**mDixon (breath-hold)**	**mDixon (thighs)**	**mDixon (breath-hold)**	**mDixon (thighs)**
Breath-hold mode	Expiration	–	Expiration	–
NSA	1	1	1	1
Postprocess				
mDixon images	Fat/water/IP/OP	Fat/water/IP/OP	Fat/water/IP/OP	Fat/water/IP/OP
Coils				
Smart select	Off	Off	Off	Off
Q-body	On (no other coils selected)	On (no other coils selected)	On (no other coils selected)	On (no other coils selected)

Table 10
Table locations for Philips scanners

mDixon table locations	AP	RL	FH
Dixon_1_BH	0	0	−50
Dixon_2_BH	0	0	−170
Dixon_3_BH	0	0	−290
Dixon_4_BH	0	0	−410
Dixon_5_Thigh	0	0	−560
Dixon_6_Thigh	0	0	−740
Dixon_7_Thigh	0	0	−920
Dixon_8_Thigh	0	0	−1100

No, another order can be useful if additional images are acquired at any specific location. However, although breaks in the neck-to-knee protocol can be made to acquire additional images, it is recommended that they are kept to a minimum. As the time between sequences increases, so does the risk that the patient repositions.

Table 11
Scan parameters for GE scanners

	1.5T		3T	
Parameter table	**LAVA-Flex (breath-hold)**	**LAVA-Flex (thighs)**	**LAVA-Flex (breath-hold)**	**LAVA-Flex (thighs)**
ZIP-2/512	No	No	No	No
ARC	No	No	No	No
Scan plane	Axial	Axial	Axial	Axial
Freq. FOV (cm)	50	50	50	50
Phase FOV	0.80	0.80	0.80	0.80
Slice thickness	5	4	5	4
Freq. Dir	R/L	R/L	R/L	R/L
TR	–	–	–	–
# slabs	1	1	1	1
Locs per slab	38	56	48	70
Details				
# of TEs	–	–	–	–
TE (1/2/3)	Min. full	Min. full	Min. full	Min. full
Flip angle	10	10	10	10
Intensity corr.	None	None	None	None
Intensity filter	None	None	None	None
3D geo. corr.	On	On	On	On
Frequency	196	256	196	256
Phase	168	256	140	226
NEX	1	1	1	1
Bandwidth	~83.33	~83.33	~140	~140
In-phase	On	On	On	On
Out-phase	On	On	On	On
Advanced				
RF1 type	–	–	–	–
Turbo mode	1	1	1	1
Centric	–	–	–	–
Multiple TR acq.	0	0	0	0

Table 12
Table locations for GE scanners

	1.5T			3T		
LAVA-Flex table locations	**S/I**	**L/R**	**P/A**	**S/I**	**L/R**	**P/A**
Dixon_1_BH	s40 to i125	0	0	s50 to i165	0	0
Dixon_2_BH	i85 to i250	0	0	i70 to i285	0	0
Dixon_3_BH	i210 to i375	0	0	i190 to i405	0	0
Dixon_4_BH	i335 to i500	0	0	i310 to i525	0	0
Dixon_5_Thigh	i460 to i664	0	0	i430 to i690	0	0
Dixon_6_Thigh	i620 to i824	0	0	i595 to i855	0	0
Dixon_7_Thigh	i780 to i984	0	0	i760 to i1020	0	0
Dixon_8_Thigh	i940 to i1144	0	0	i925 to i1185	0	0

Acknowledgments

Dr. Borga was funded by the Swedish Research Council, grant 2019-04751.

References

1. Hill JH, Solt C, Foster MT (2018) Obesity associated disease risk: the role of inherent differences and location of adipose depots. Horm Mol Biol Clin Investig 33(2). https://doi.org/10.1515/hmbci-2018-0012
2. Britton KA, Fox CS (2011) Ectopic fat depots and cardiovascular disease. Circulation 124(24):e837–ee41
3. Demerath EW, Reed D, Rogers N, Sun SS, Lee M, Choh AC et al (2008) Visceral adiposity and its anatomical distribution as predictors of the metabolic syndrome and cardiometabolic risk factor levels. Am J Clin Nutr 88(5): 1263–1271
4. Liu J, Fox CS, Hickson DA, May WD, Hairston KG, Carr JJ et al (2010) Impact of abdominal visceral and subcutaneous adipose tissue on cardiometabolic risk factors: the Jackson heart study. J Clin Endocrinol Metab 95(12): 5419–5426
5. Neeland IJ, Ayers CR, Rohatgi AK, Turer AT, Berry JD, Das SR et al (2013) Associations of visceral and abdominal subcutaneous adipose tissue with markers of cardiac and metabolic risk in obese adults. Obesity 21(9):E439–EE47
6. Iwasa M, Mifuji-Moroka R, Hara N, Ishidome M, Iwata K, Sugimoto R et al (2011) Visceral fat volume predicts new-onset type 2 diabetes in patients with chronic hepatitis C. Diabetes Res Clin Pract 94(3):468–470
7. Kurioka S, Murakami Y, Nishiki M, Sohmiya M, Koshimura K, Kato Y (2002) Relationship between visceral fat accumulation and anti-lipolytic action of insulin in patients with type 2 diabetes mellitus. Endocr J 49(4): 459–464
8. van der Poorten D, Milner K-L, Hui J, Hodge A, Trenell MI, Kench JG et al (2008) Visceral fat: a key mediator of steatohepatitis in metabolic liver disease. Hepatology 48(2): 449–457
9. Britton KA, Massaro JM, Murabito JM, Kreger BE, Hoffmann U, Fox CS (2013) Body fat distribution, incident cardiovascular disease, cancer, and all-cause mortality. J Am Coll Cardiol 62(10):921–925

10. Doyle SL, Donohoe CL, Lysaght J, Reynolds JV (2011) Visceral obesity, metabolic syndrome, insulin resistance and cancer. Proc Nutr Soc 71(1):181–189
11. Ekstedt M, Franzén LE, Mathiesen UL, Thorelius L, Holmqvist M, Bodemar G et al (2006) Long-term follow-up of patients with NAFLD and elevated liver enzymes. Hepatology 44(4):865–873
12. Goodpaster BH, Kelley DE, Thaete FL, He J, Ross R (2000) Skeletal muscle attenuation determined by computed tomography is associated with skeletal muscle lipid content. J Appl Physiol 89(1):104–110
13. Morley JE, Thomas DR, Wilson M-MG (2006) Cachexia: pathophysiology and clinical relevance. Am J Clin Nutr 83(4):735–743
14. Cruz-Jentoft AJ, Morley JE (2012) Sarcopenia. Wiley-Blackwell, Chichester/Hoboken
15. Linge J, Borga M, West J, Tuthill T, Miller MR, Dumitriu A et al (2018) Body composition profiling in the UK biobank imaging study. Obesity 26(11):1785–1795
16. Prentice AM, Jebb SA (2001) Beyond body mass index. Obes Rev 2(3):141–147
17. Thomas EL, Frost G, Taylor-Robinson SD, Bell JD (2012) Excess body fat in obese and normal-weight subjects. Nutr Res Rev 25:150–161
18. Tomiyama AJ, Hunger JM, Nguyen-Cuu J, Wells C (2016) Misclassification of cardiometabolic health when using body mass index categories in NHANES 2005–2012. Int J Obes 40(5):883–886
19. Baumgartner RN, Heymsfield SB, Lichtman S, Wang J, Pierson RN (1991) Body composition in elderly people: effect of criterion estimates on predictive equations. Am J Clin Nutr 53(6):1345–1353
20. Bergsma-Kadijk JA, Baumeister B, Deurenberg P (1996) Measurement of body fat in young and elderly women: comparison between a four-compartment model and widely used reference methods. Br J Nutr 75(5):649–657
21. Stahn A, Terblanche E, Gunga H-C (2012) Use of bioelectrical impedance: general principles and overview. In: Preedy VR (ed) Handbook of anthropometry: physical measures of human form in health and disease. Springer New York, New York, pp 49–90
22. Khalil SF, Mohktar MS, Ibrahim F (2014) The theory and fundamentals of bioimpedance analysis in clinical status monitoring and diagnosis of diseases. Sensors (Basel) 14(6):10895–10928
23. Kyle UG, Bosaeus I, De Lorenzo AD, Deurenberg P, Elia M, Gómez JM et al (2004) ESPEN GUIDELINES: bioelectrical impedance analysis—part I: review of principles and methods. Clin Nutr 23:1226–1243
24. Browning LM, Mugridge O, Chatfield M, Dixon A, Aitken S, Joubert I et al (2010) Validity of a new abdominal bioelectrical impedance device to measure abdominal and visceral fat: comparison with MRI. Obesity (Silver Spring) 18(12):2385–2391
25. Borga M, West J, Bell JD, Harvey NC, Romu T, Heymsfield SB et al (2018) Advanced body composition assessment: from body mass index to body composition profiling. J Investig Med 66:887–895
26. Cruz-Jentoft AJ, Baeyens JP, Bauer JM, Boirie Y, Cederholm T, Landi F et al (2010) Sarcopenia: European consensus on definition and diagnosis: report of the European Working Group on Sarcopenia in Older People. Oxford University Press
27. Thomas EL, Fitzpatrick JA, Malik SJ, Taylor-Robinson SD, Bell JD (2013) Whole body fat: content and distribution. Prog Nucl Magn Reson Spectrosc 73:56–80
28. Huber FA, Del Grande F, Rizzo S, Guglielmi G, Guggenberger R (2020) MRI in the assessment of adipose tissues and muscle composition: how to use it. Quant Imaging Med Surg 10(8):1636–1649
29. Borga M (2018) MRI adipose tissue and muscle composition analysis—a review of automation techniques. Br J Radiol 91(1089):20180252
30. Dixon W (1984) Simple proton spectroscopic imaging. Radiology 153:189–194
31. Reeder SB, Hu HH, Sirlin CB (2012) Proton density fat-fraction: a standardized MR-based biomarker of tissue fat concentration. J Magn Reson Imaging 36(5):1011–1014
32. Hu HH, Nayak KS (2008) Quantification of absolute fat mass using an adipose tissue reference signal model. J Magn Reson Imaging 28(6):1483–1491
33. Leinhard OD, Johansson A, Rydell J, Smedby O, Nystrom F, Lundberg P et al (2008) Quantitative abdominal fat estimation using MRI. In: 19th International Conference on Pattern Recognition, vols 1–6, pp 2137–2140
34. Linge J, Whitcher B, Borga M, Dahlqvist Leinhard O (2019) Sub-phenotyping metabolic disorders using body composition: an individualized, nonparametric approach utilizing large data sets. Obesity 27(7):1190–1199
35. West J, Dahlqvist Leinhard O, Romu T, Collins R, Garratt S, Bell JD et al (2016) Feasibility of MR-based body composition analysis

in large scale population studies. PLoS One 11(9):e0163332

36. Andersson T, Romu T, Karlsson A, Noren B, Forsgren MF, Smedby O et al (2015) Consistent intensity inhomogeneity correction in water-fat MRI. J Magn Reson Imaging 42(2): 468–476
37. Borga M, Ahlgren A, Romu T, Widholm P, Dahlqvist Leinhard O, West J (2020) Reproducibility and repeatability of MRI-based body composition analysis. Magn Reson Med 84(6): 3146–3156

Chapter 20

Functional Tests for Assessing Human Beta-Cell Function and Insulin Sensitivity

Marcelo Miranda de Oliveira Lima and Bruno Geloneze

Abstract

Glucose homeostasis requires functional tests for assessing pancreatic beta-cell function and insulin sensitivity. The hyperinsulinemic-euglycemic clamp technique is the "gold-standard" method for insulin sensitivity, used to validate other methods. The full comprehension of beta-cell function complexity requires different intravenous or oral tests and the assessment of insulin sensitivity, which can be evaluated simultaneously with insulin secretion by most methods. The selection of the methods of assessing glucose homeostasis in the research settings depends on the aspects of beta-cell function and insulin sensitivity relevant to the proposed hypothesis.

Key words Insulin sensitivity, Insulin secretion, Glucose clamp technique, Glucose tolerance test, Insulin-secreting cells, Insulin, C-peptide

1 Introduction

The study of glucose homeostasis requires functional tests for assessing pancreatic beta-cell function (insulin secretion in response to a given stimulus) and insulin action in tissues (insulin sensitivity). Insulin sensitivity is frequently evaluated independently of insulin secretion, as the former relates to, and is a risk factor for metabolic conditions regardless of glucose tolerance, such as adiposopathy, hypertension, dyslipidemia, cardiovascular disease, systemic inflammation, and polycystic ovarian syndrome, among others [1]. In turn, the beta-cell function has a central role in glucose tolerance and the evaluation of its disorders, particularly diabetes mellitus, requires the assessment of insulin secretion primarily [2]. However, the beta-cell function cannot be correctly interpreted without evaluating the prevailing insulin sensitivity because the maintenance of glucose homeostasis comprises the adaption of the former to the latter [2, 3].

Cinthia Baú Betim Cazarin (ed.), *Basic Protocols in Foods and Nutrition*,
Methods and Protocols in Food Science, https://doi.org/10.1007/978-1-0716-2345-9_20,

The hyperinsulinemic-euglycemic clamp is considered the "gold-standard" method of assessing insulin sensitivity and is used for validation of other methods [1]. Most assessment methods of beta-cell function also permit the estimation of insulin sensitivity in a single experiment [2]. A representative method is a hyperglycemic clamp, in which the insulin sensitivity index is similar to that of the hyperinsulinemic-euglycemic clamp [2, 4]. Other methods estimate insulin sensitivity using empirical formulas and computer-assisted calculations that are freely available and easy to use, or mathematical models that are more reliable but require specific software and expertise [5, 6].

Indexes of beta-cell function or insulin sensitivity must be calculated from independent time periods during the experiment; otherwise, the correlation between these indexes would be biased by collinearity resulting from coincident values of glucose and insulin or C-peptide used in the calculation of both indexes [2].

None of the assessment methods of beta-cell function may be considered "gold standard" because of the multiple aspects of insulin secretory response that cannot be evaluated in a single test [5]. The complexity of the beta-cell function is illustrated by the many possibilities of stimulation or potentiation agents (glucose, other macronutrients, incretins, glucagon, pharmacologic secretagogues, or mixed stimuli), routes of administration (oral versus intravenous, or combined), or standardization of the stimulus.

Intravenous standardized methods like the intravenous glucose tolerance test (IVGTT) and the hyperglycemic clamp have the advantage of not requiring mathematical adjustment of the insulin secretory response to a variable, dynamic stimulus, as do the oral tests, which may be imprecise. The hyperglycemic clamp is one of the preferred methods because it gathers standardized stimulus during the whole experiment and accurate outcomes, and it does not require complex mathematical models for concomitant assessment of insulin sensitivity [2, 4].

Oral stimulation is considered more physiological because it is the natural route of glucose and other nutrients and because a fundamental component of insulin secretory response is the entero-insular axis. It integrates neural pathways involved in glucose homeostasis and gut hormones that markedly potentiate insulin secretion, the so-called incretin effect, particularly glucose-dependent insulinotropic peptide (GIP) and glucagon-like peptide-1 (GLP-1) [7]. For these reasons, oral tests are particularly useful for studying glucose tolerance disorders, bariatric/metabolic surgery, the development of pharmacological and nutrition therapies, and food science. A limitation is that oral tests cannot distinguish intrinsic beta-cell defects from those of the entero-insular axis. In addition, the secretory stimulus cannot be standardized (mostly the variable glucose levels), requiring more complex methods for normalization of insulin secretion to the stimulus [5].

The beta-cell function can be determined from insulin or C-peptide concentrations. Insulin measurements are frequently employed due to facility, but they do not correspond to the full insulin secretion because near half of it undergoes hepatic extraction before reaching the peripheral circulation, a major component of insulin clearance. Changes in hepatic extraction in diverse metabolic conditions may account for much of the variation in peripheral insulin [8]. Nevertheless, peripheral insulinemia correlates well with pancreatic insulin release, particularly during rapid insulin secretion, such as that seen in the first phase secretion elicited by intravenous glucose load.

To overcome the limitations related to hepatic insulin clearance, C-peptide measurements are used in a mathematical model (C-peptide deconvolution) to reconstruct insulin secretion [9]. C-peptide is cosecreted with insulin in equimolar amounts, undergoes negligible hepatic extraction, and has linear and relatively constant kinetics. The beta-cell function index derived from the deconvolution model is the insulin secretion rate (ISR) (pmol/min). The C-peptide levels approach is preferred, but it requires specific software and expertise.

In response to a gradual increase in plasma glucose concentration, insulin secretion is progressively stimulated, and a linear dose-response relationship is observed between glucose concentration and insulin secretion [10]. Based on this principle, beta-cell sensitivity may be calculated. When plasma glucose concentration is sharply increased and maintained at a suprabasal level, as occurs in the hyperglycemic clamp, insulin secretion shows a biphasic pattern, with an initial acute insulin response (AIR), that corresponds to first phase insulin secretion, followed by a gradually increasing secretion that approaches a nearly constant level after about 60–120 min (second-phase insulin secretion) [4]. The magnitude of both first- and second-phase insulin responses relate to the glycemic increment; the magnitude of the second phase relates to the beta-cell dose response. A biphasic response is also observed with the intravenous glucose tolerance test (IVGTT), in which the first-phase acute insulin response (AIR) is followed by a slower and more blunted secretion rise (second phase) [11]. Both first and second phases can be potentiated by previous prolonged exposure to hyperglycemia (beta-cell potentiation) [12]. The beta cells also respond to various nonglucose stimuli. The amino acid arginine is a potent secretagogue. Its acute intravenous administration produces an intense first phase insulin response, potentiated by hyperglycemia, and is considered the “maximal insulin response” [13].

As beta-cell function adapts to the prevailing insulin sensitivity for maintenance of glucose homeostasis, insulin sensitivity must be taken into account in the interpretation of insulin secretion indexes. The most widely used approach is the so-called disposition index (DI), derived from the IVGTT and the minimal model for insulin

sensitivity. The index of beta-cell function corrected for insulin sensitivity (the disposition index) is the product of the acute insulin response (AIR) and the index of insulin sensitivity, derived from the hyperbolic relationship described between AIR and insulin sensitivity index [11]. However, the application of this adjustment requires some caution. The indices of beta-cell function and insulin sensitivity should be based on independent variables (e.g., different functional tests and/or different intervals of the same test), and whether the relationship between them is exactly a hyperbola should be verified in the studied sample. Nevertheless, correlations of other variables with the disposition index may depend on insulin sensitivity rather than the beta-cell function [2, 6].

2 Intravenous Glucose Tolerance Test (IVGTT)

The intravenous glucose tolerance test (IVGTT) is performed by a single glucose infusion in a rapid bolus to stimulate a sharp pattern of the first-phase insulin secretion, followed by a second phase (Fig. 1). For assessment of the first phase, a 10-min IVGTT is sufficient. However, the IVGTT is often used to evaluate insulin sensitivity with the minimal model and the second-phase secretion [11].

The first phase of insulin secretion is assessed in the initial 8–10 min, with frequent samples (at 1–2 min intervals), beginning 2–3 min after time zero. The most widely used first-phase index is

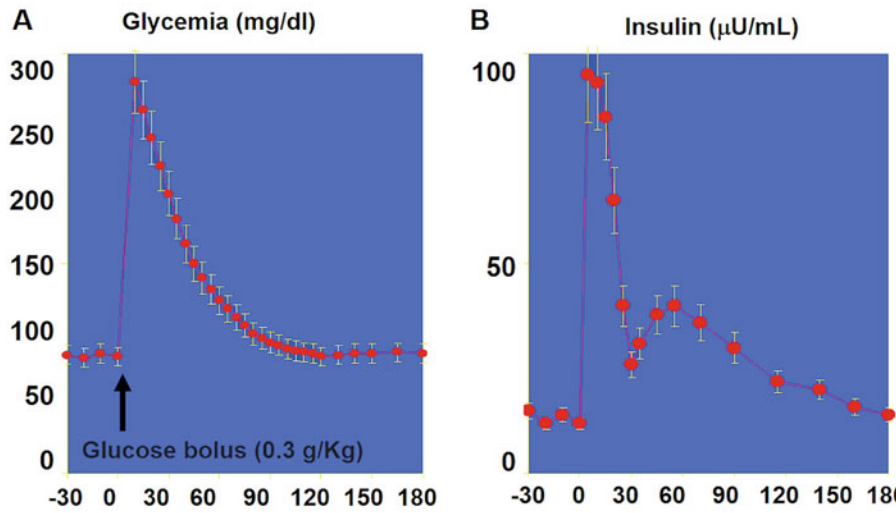

Fig. 1 Intravenous glucose test (IVGTT): (**a**) after an intravenous glucose bolus, (**b**) a biphasic response of insulin secretion is observed. The first-phase acute insulin response (AIR) is followed by a slower and more blunted secretion rise (second phase). Unpublished data

the acute insulin response (AIR), calculated from the insulin concentrations in the first 5–10 min of the test. There are different AIR formulas, including the area under the curve (AUC) of plasma insulin, the average or the sum of stimulated plasma insulin concentration, or the peak of plasma insulin concentration. In any case, the incremental values are preferred, that is, the change from the mean basal value. Optionally, C-peptide may be used instead of insulin to calculate the same indexes or calculation of the insulin secretion rate (ISR) using mathematical modeling (C-peptide deconvolution) [9].

The indexes of second-phase insulin secretion are based on the absolute or incremental areas under the curve (AUC) of insulin or C-peptide concentrations from 10 min (alternatively, from 30 to 60 min) to 180–240 min. The glucose curve must be taken into account, considering that it varies considerably in the second phase and that the insulin secretion depends directly on it. The most widely used index is the insulin AUC ratio (or C-peptide) to the glucose AUC.

It is assumed that the first phase of insulin secretion does not require adjustment to the glucose peak as the bolus dose is standardized. On the other hand, a cornerstone of the interpretation of AIR is its dependence on the prevailing insulin sensitivity. It might be less relevant in individuals with diabetes mellitus, in whom the AIR is virtually abolished, although there may still be a (small) acute response [11].

The frequently sampled IVGTT (FSIGT) is also useful to measure insulin sensitivity along with insulin secretion in a single test, using the software-assisted mathematical modeling (minimal model, MINMOD) [11, 13]. In order to improve the minimal model estimate of insulin sensitivity, intravenous insulin is administered 20 min after the glucose bolus, what is called the insulin-modified minimal model FSIGT. In this protocol, the interpretation of the second-phase insulin secretion may not be appropriate due to the presence of exogenous insulin, which may be partially overcome by the measurement of C-peptide (although some suppression of the endogenous insulin secretion by the exogenous insulin cannot be discarded).

The IVGTT duration is determined by the mathematical model based on the assumption that glucose concentration ends near the basal level. It is particularly relevant for individuals with diabetes, in whom it is expected to take longer to occur [11, 13]. The IVGTT may be shortened if only the first-phase insulin is needed (10-min protocol), usually when another test is chosen to evaluate insulin sensitivity (e.g., euglycemic-hyperglycemic clamp), which is conducted in a different day or 60 min after the IVGTT (Botnia clamp) [14].

2.1 Materials

1. Vein catheters.
2. Large-volume syringes (and a syringe pump, if possible).
3. 20–25% Glucose solution.
4. Regular insulin (100 UI/ml) (for insulin-modified IVGTT).
5. K+-EDTA blood collection tubes (for insulin and C-peptide).
6. Glucose tubes.
7. Ice slurry for lab tubes.
8. Optional (for bedside glucose analysis): glucose Analyzer (YSI 2700, YSI Life Sciences, Yellow Spring, OH, USA) and laboratory centrifuge and centrifuge tubes (for glucose analysis).

2.2 Methods

1. After an overnight fast (8–12 h), a catheter is inserted in an antecubital vein for blood sampling, and a second catheter is inserted in a contralateral antecubital vein for solution infusion. The patency of the venous accesses is maintained by slow saline drip.
2. At least two basal samples are drawn (15–30 min before and at time 0, immediately before glucose infusion) for the average basal measurements.
3. A 20–25% glucose bolus (0.3 g/kg body weight) is injected in a contralateral vein within 0.5–1 min, using a manual large-volume syringe, preferably >20 ml (or a syringe infusion pump, if available) (*see* **Note 1**).
4. After the glucose infusion, blood samples are drawn at frequent intervals over 180–240 min. In the minimal model (MINMOD) frequently sampled IVGTT (FSIGT), which is the most widely used protocol, the samples are drawn at 3, 4, 5, 6, 8, 10, 14, 19, 22, 25, 30, 40, 50, 60, 70, 80, 100, 140, and 180 min.
5. Blood samples for measuring insulin (and optionally, C-peptide) are put in K^+-EDTA tubes and kept in an ice slurry, followed by immediate centrifugation and frozen storage or frozen transportation to the laboratory. The glucose tubes are used for laboratory glucose analysis immediately after the test; optionally, blood samples may be centrifuged immediately for testing in a bedside glucose analyzer.
6. In the insulin-modified minimal model FSIGT, an intravenous insulin dose (0.03–0.05 UI/kg) is administered 20 min after the glucose bolus, over 5 min (between 20 and 25 min).
7. At the end of the test, a meal is offered to the individual.

3 Hyperglycemic Clamp

The hyperglycemic glucose clamp assesses both first- and second-phase insulin secretion and simultaneously evaluates insulin sensitivity [4, 15]. The objective of the hyperglycemic clamp is to achieve a steady hyperglycemic state and a corresponding endogenous insulin response. The most used target glycemia is 180 mg/dl because it is in the range of (near) normal postprandial glycemia and near the threshold of urinary glucose excretion. The usual duration of the hyperglycemic clamp is 180 min (minimum 120 min). It may be longer in some protocols, usually in multi-stepped hyperglycemic levels and/or combined with other stimuli (standard meal or intravenous infusions of insulin secretagogues, such as incretins or arginine) [2, 4].

The first phase of insulin secretion is assessed in the initial 10 min, after an initial priming glucose dose. The first phase secretion index (acute insulin response, AIR) is similar to that obtained with the IVGTT and shares the same physiological interpretation (see the corresponding session). After that, a variable glucose infusion rate (GIR) is required to maintain constant hyperglycemia. In response, the plasma insulin concentration increases gradually (corresponding to the second-phase insulin secretion), and it is expected to plateau in the second or third hour of the test (Fig. 2). At this time, GIR is also expected to be stable (variation <5%). The variation in the glucose infusion rate is essentially dependent on both endogenous insulin production (and clearance) and insulin sensitivity.

The indexes of second-phase insulin secretion are calculated as the absolute or incremental areas under the curve (AUC) of insulin or C-peptide concentrations from 10 min after the start of glucose infusion up to the end of the test or in the last 60 min of the test. Alternatively, the average insulin or C-peptide concentrations in any of these time intervals may be used instead of AUC. In opposition to the IVGTT, the insulin response usually is adjusted to the glucose concentration, because by definition, it is clamped in the same level in all individuals.

The insulin sensitivity index is calculated as the average glucose infusion rate (GIR) during the last hour of the clamp, minus the occasional glucose urinary excretion, adjusted (divided) by the average plasma insulin concentration during the same interval [15]. Under stable conditions of constant hyperglycemia (third hour of the clamp), the amount of glucose infused (GIR) gives an estimate of the glucose disposal in the tissues since endogenous glucose production should be suppressed, similarly to what occurs during the hyperinsulinemic-euglycemic clamp (see the corresponding session below) [15]. The insulin sensitivity index of the hyperglycemic clamp correlates to that of the

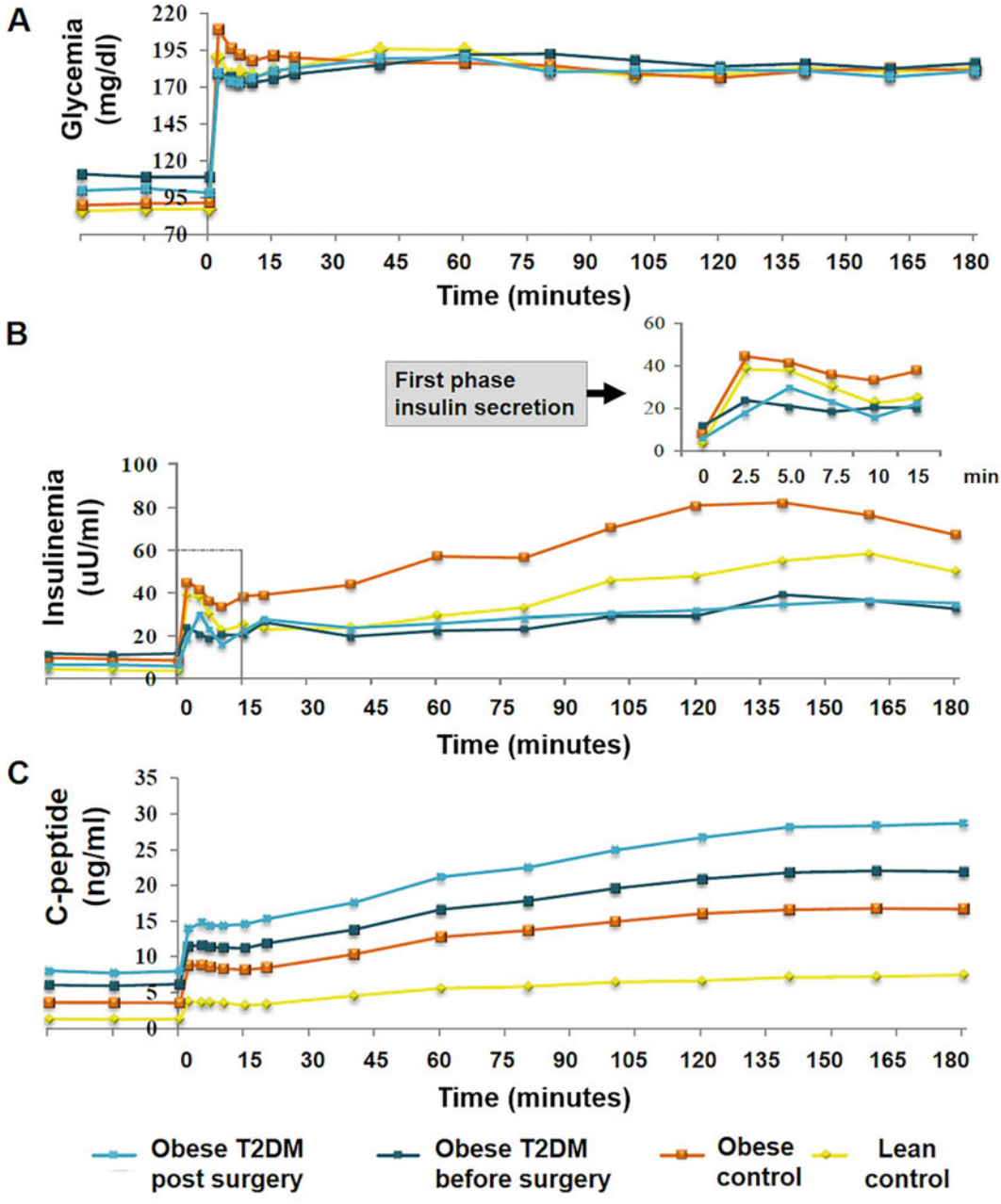

Fig. 2 Hyperglycemic clamp test applied to studying the effects of bariatric/metabolic surgery on glucose homeostasis. (**a**) Plasma glucose sharply raises and is kept at a constant hyperglycemic level, resulting in (**b**) a biphasic pattern of insulin secretion (first and second phases). First phase insulin secretion is typically blunted in type 2 diabetes (T2DM) but may recover after metabolic surgery and increases in obesity with normal glucose tolerance as an adaption to insulin resistance. (**b**, **c**) This adaptation of beta cells is also observed as an increase in second-phase insulin and C-peptide levels. Unpublished data

hyperinsulinemic-euglycemic clamp [15, 16]. However, the hyperglycemic clamp depends on endogenous insulin secretion, and it is not appropriate to study individuals with complete beta-cell failure, as is the case of type 1 diabetes. Comparing subjects with different glucose levels and/or beta-cell capacities (e.g., subjects with normal glucose tolerance and diabetes) require caution [4, 15].

C-peptide may be used to calculate the insulin secretion rate (ISR) in both first and second phases using C-deconvolution and other mathematical modeling methods to estimate beta-cell function and insulin sensitivity [9, 17, 18].

3.1 Materials

1. Heating pad (or warm chamber with heated air, if possible).
2. Vein catheters.
3. High-precision infusion pump.
4. Large-volume syringes (and a syringe infusion pump, if available).
5. 20–25% glucose solution.
6. Laboratory centrifuge and centrifuge tubes (for glucose analysis).
7. Glucose Analyzer (YSI 2700, YSI Life Sciences, Yellow Spring, OH, USA).
8. K^+-EDTA blood collection tubes (for insulin and C-peptide).
9. Ice slurry (for storage of laboratory tubes).

3.2 Methods

1. After an overnight fast (8–12 h), the subject is kept lying on a bed in the supine position. A vein catheter is inserted in an antecubital vein for solution infusion. A second catheter is inserted in a contralateral dorsal hand or wrist vein, in a retrograde fashion, for blood drawing, and this hand is warmed to 50–70 °C using a heating pad, folded around the hand (or a warm chamber with heated air) to obtain arterialized venous blood (*see* **Note 2**). The patency of the venous accesses is maintained by slow saline drip.
2. At least two basal samples are drawn (15–30 min before and at time 0, immediately before glucose infusion) for the average basal measurements (*see* **Note 3**).
3. An infusion pump is installed to administer a 20–25% glucose solution in the antecubital vein throughout the test.
4. A priming glucose bolus is manually injected within 0.5–1 min, using a large-volume syringe (at least 20 ml), or using a syringe infusion pump (if available). This priming dose sharply raises the glucose concentration to the target level of hyperglycemia, usually 180 mg/dl (*see* **Note 4**). The formulas for the calculation of the glucose priming dose are empirical. One of the most used is the following [16]:

$$25\%\ \text{glucose bolus dose (in ml)} = 4 \tilde{n} \text{weight (in kg)} \tilde{n} 1.5 \times [\text{target glycemia (in mg/dl)} - \text{basal glycemia (in mg/dl)}] \tilde{n} 10^{-3}$$

For 50% glucose solution, the equation must be divided by 2. Other solution concentrations require proportional adjustments.

5. After the priming glucose bolus, the hyperglycemic target is maintained by a variable glucose infusion rate (GIR) during the remaining experiment period (usually 180–240 min), using an infusion pump. Blood is sampled frequently and centrifuged immediately for plasma glucose testing using a bedside glucose analyzer. Glucose levels are measured at 2.5-intervals from zero to 10 min, and at intervals of 5 min (eventually, 10 min) from 10 to 180–240 min, and the glucose infusion rate is adjusted accordingly to maintain the hyperglycemic target (*see* **Note 5**). After each adjustment of GIR, plasma glucose concentration should be measured after an interval of 5 min (to permit stabilization of the glucose level in its distribution space), and further adjustments are performed as needed.
6. A steady state is reached in the third hour of the test when the plasma insulin concentrations are expected to plateau, and GIR should be stable (ideally, variation <5–10%) as well as the plasma glucose level (less than 10 mg/dl above or below the target).
7. Blood sampling for measuring insulin (and optionally, C-peptide) is performed at 2.5-min intervals from 0–10 min and intervals of 20 min from 10 to 180–240 min.
8. Blood samples are put in K^+-EDTA tubes on ice, followed by immediate centrifugation and frozen transportation to the laboratory.
9. At the end of the test, a meal is offered to the subject, and bedside glucose levels are measured until 60 min after the end of glucose infusion (*see* **Note 6**).

4 Oral Load Tests: Oral Glucose Tolerance Test (OGTT) and Standard Mixed Meal Tolerance Test (MTT)

The oral glucose tolerance test (OGTT) is the reference method for the assessment of glucose tolerance, despite the poor reproducibility of the test (intra-subject variation of up to 50% for 2 h blood glucose) [19, 21]. In most cases, diabetes is diagnosed by random or fasting plasma glucose concentrations or glycated hemoglobin (HbA1c) without recourse to an OGTT. Patients with intermediate values of fasting glucose (impaired fasting glycemia) or HbA1c

should undergo OGTT. The test also has a particular place in diagnosing gestational diabetes mellitus, where fasting plasma glucose concentrations lack diagnostic sensitivity [19].

In clinical trials, the OGTT is used when the glucose tolerance classification is required. In research settings, it is a method to evaluate the beta-cell function, insulin sensitivity, and the incretin effect, based on the curves of glucose and insulin or C-peptide (Fig. 3); empirical mathematical formulas or more complex mathematical modeling are used for this purpose [5–7, 17]. Another research application of OGTT is the stimulation of gut hormones, although the mixed meal tolerance test (MTT) is usually preferred instead for this purpose (see below) [7].

The typical sampling of OGTT is done at 30-min intervals: zero (preload), 30, 60, 90, and 120 min after the glucose load. Two blood samples are enough for glucose tolerance classification: in the fasting state before the test and 120 min after starting. For gestational diabetes screening, an additional blood sample at 60 min is used [19–21].

The oral load tests typically last 120–180 min to evaluate insulin secretion and insulin sensitivity, but the duration may be up to 240–300 min. The blood collection intervals depend on the mathematical models that are chosen in the research protocol. In the first 30 min after baseline sampling, blood is drawn at 10, 20, and 30 min. Some reduced protocols evaluate 15 and 30 min, or only 30 min. After that, blood is drawn at 15–30 min until 180–240 min, and some extended protocols include a final blood collection at 300 min [5–7, 17].

Mixed meal tolerance tests (MTT) use a mixed meal instead of oral glucose, a more physiological stimulus than glucose alone. Although the MTT is not standardized for glucose tolerance classification and diabetes diagnosis, the combination of carbohydrates, lipids, and protein in mixed meals offer a stronger stimulus for secretion of gastrointestinal hormones, such as glucagon-like peptide 1 (GLP-1) and glucose-dependent insulinotropic polypeptide peptide (GIP) [17]. These hormones are responsible for the incretin effect, that is, the increment in insulin secretion after oral versus intravenous stimulus [7]. Even so, MTT and OGT have nearly the same recommendations, methods, and interpretation.

In the first studies, the mixed meals consisted of a standard meal (usually breakfast) with variable food content. Although still used, they have been extensively replaced by nutrition supplements, mainly ready-to-drink shakes, such as Ensure (Abbott), or a combination of shake and protein bars, used in our research laboratory. The macronutrient composition and calories vary across research protocols. Most standard mixed meals have at least 250–300 kcal and around 40–50 g of carbohydrates. Higher calorie and carbohydrate contents are preferred, although the available commercial products may limit this.

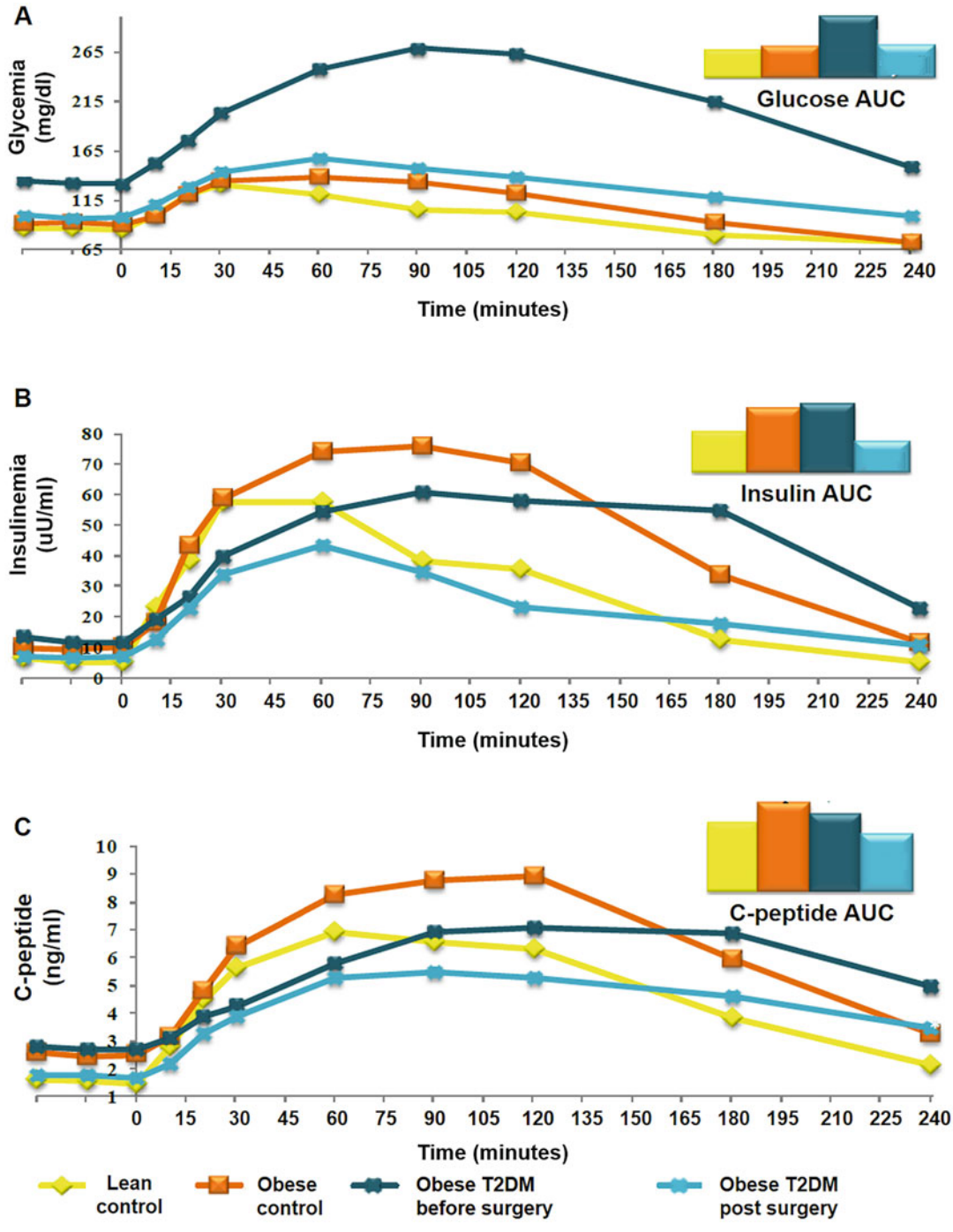

Fig. 3 Oral glucose tolerance test (OGTT) applied to studying the effects of bariatric/metabolic surgery on glucose homeostasis in the absorptive estate. (**a**) The typically increased plasma glucose in type 2 diabetes (T2DM) nearly normalizes after metabolic surgery despite lower levels of (**b**) insulin and (**c**) C-peptide, denoting improved insulin sensitivity. Unpublished data

We have standardized a combination of Ensure shake and a whey protein bar, resulting in 515 kcal (41.8% fat, 40.7% carbohydrates, and 17.5% protein) [22]. Many protocols use only liquid supplements such as Ensure High Protein (360 ml, 391 kcal, 8.5 g of fat, 44 g of carbohydrate, and 17 g of protein) or Ensure Plus (240 ml, 350 kcal, 11 g of fat, 48 g of carbohydrate, and 16 g of protein). An adjustment for body weight may be recommended (e.g., for pediatric population), usually 6 ml/kg body weight to a maximum of 360 ml (as for Ensure Plus, providing 1.1 kcal/ml; 23% fat, 55%, carbohydrate, and 22% protein) [23].

The first 30 min of the oral load tests correlate to the first-phase insulin secretion, and the remaining time corresponds to the second phase [5–7]. The OGTT may be shortened if only the first phase is needed (30-min protocol). However, its interpretation is limited without adjustment to prevailing insulin sensitivity (as discussed IVGTT). In this case, another functional test should be used to evaluate insulin sensitivity (e.g., euglycemic-hyperglycemic clamp), which should be performed on a different day. A surrogate index of insulin sensitivity using basal (preload) parameters (e.g., HOMA-IR) may be acceptable.

The glucose appearance rate is not standardized and is unknown in oral load tests. It means that the insulin concentration and secretion must be adjusted to the prevailing glucose levels in both the first and second phases through empirical indices or mathematical modeling [5–7, 17].

The insulinogenic index is one of the most used, which is the ratio between the supra-basal increments at 30 min of insulin and glucose concentration: [(30-min insulin/basal insulin)/(30-min glucose/basal glucose)]. Similar indexes have been proposed, using 15-min values and/or replacing insulin for C-peptide, or using the ratio between the 30-min incremental area under the curve (AUC) of insulin (or C-peptide) and the incremental glucose AUC [5–7, 24, 25].

The ratio between the incremental areas under the insulin curve (or C-peptide) and glucose may be used as an index of second-phase or total insulin secretion. Empirical formulas have also been derived from intravenous glucose tests [24, 25]. Mathematical modeling, including C-peptide minimal models and C-peptide deconvolution, is based on complex beta-cell function aspects, such as insulin hepatic extraction, beta-cell delay time, and beta-cell sensitivity [17, 24–26].

Oral tests may be used to estimate insulin sensitivity through empirical formulas or complex mathematical modeling using C-peptide levels [27, 28]. The most used formulas are described below.

1. Matsuda's formula [29]: $\mathrm{ISI}_{\mathrm{comp}} = \sqrt{(G_{\mathrm{b}} \tilde{n} I_{\mathrm{b}} \tilde{n} G_{\mathrm{m}} \tilde{n} I_{\mathrm{m}})} \,/\, 1000$, where G_{b} and I_{b} are basal (preload) glucose and insulin,

respectively, and G_m and I_m are the mean concentrations during the OGTT (used sampling protocol: 0, 30, 60, 90, 120 min).

2. Stumvoll's Method [24]: $MCR_{est} = 18.8 - (0.27 \cdot BMI) - (0.0052 \cdot I_{120}) - (0.27 \cdot G_{90})$, where BMI ($kg/m^2$) is the body mass index, I_{120} is insulin at 120 min (pmol/l), and G_{90} is glucose at 90 min (mmol/l). This equation compares results with the last 60-min clamp-derived glucose clearance rate; thus, the units are thus ml/min/kg. Alternative formulas without BMI or for different sampling times have also been provided [24, 25].
3. OGIS Model [27]: $OGIS = f(G_b, G_{90}, G_{120}, I_b, I_{90}, D)$, where G and I are glucose and insulin concentrations at the time indicated by the subscript and D is the oral glucose dose (g/m^2 body surface area). The function (f) is derived from mathematical modeling and is calculated by software that may be accessed at http://webmet.pd.cnr.it/ogis. OGIS is a predictor of the clamp-derived glucose clearance rate adjusted to body surface area; thus, the units are ml/min/kg. Formulas for a 180-min OGTT are also available at the same web address.

4.1 Materials

1. Vein catheters.
2. 0.9% saline solution.
3. K^+-EDTA blood collection tubes (for insulin and C-peptide).
4. Glucose tubes.
5. Ice slurry for lab tubes.
6. Optional (for bedside glucose analysis): laboratory centrifuge and centrifuge tubes (for glucose analysis); glucose Analyzer (YSI 2700, YSI Life Sciences, Yellow Spring, OH, USA).
7. Anhydrous glucose 75 g—for oral glucose tolerance test (OGTT).
8. Standard mixed meal (breakfast style or nutrition supplement, e.g., Ensure Plus or Ensure High Protein)—for standard mixed meal tolerance test (MMTT).

4.2 Methods

1. For 3 days before the test, the subject should be on an unrestricted weight-maintaining diet, with at least 150 g carbohydrate per day, and should exercise normally. On the day of the test, smoking should be avoided. Interpretation may be difficult in subjects taking β-blockers, diuretics, nicotinic acid, or high doses of glucocorticoids or during hospitalization or acute illness [20].
2. After an overnight fast (8–12 h), a vein catheter is inserted in an antecubital vein for blood sampling. The patency of the venous accesses is maintained by slow saline drip.

3. At least two basal samples are drawn (15–30 min before and at time 0, immediately before glucose load) for the average basal measurements (*see* **Note 6**).
4. The subject should remain seated to drink an oral load (75-g anhydrous glucose solution for OGTT, or standard mixed meal for MMTT) within 5 min (if not possible, within less than 10 min). After drinking, the participant should rest sitting or lying down.
5. The typical sampling of OGTT is done at 30-min intervals: zero (preload), 30, 60, 90, and 120 min after the glucose load. Two blood samples are enough for glucose tolerance classification: in the fasting state before the test and 120 min after starting. For gestational diabetes screening, an additional blood sample at 60 min is used. A 60-min collection has also been proposed for glucose intolerance screening in the general population.
6. The test lasts 180–300 min to evaluate insulin secretion and insulin sensitivity, although a 120-min duration may be used. The blood collection intervals depend on the mathematical models that are chosen in the research protocol. In the first 30 min, blood is drawn at 10, 20, and 30 min. Some reduced protocols evaluate 15 and 30 min, or only 30 min. After that, blood is drawn at 15–30 min until 180–240 min, and some extended protocols include a final blood collection at 300 min.

5 Insulin Tolerance Test (ITT)

The original concept of insulin sensitivity was derived from the empirical observation of heterogeneous requirements of exogenous insulin for lowering plasma glucose levels among individuals with insulin-dependent diabetes [1]. Thus, the glucose decay to a standardized insulin bolus seems to be an obvious method to measure insulin sensitivity. In the insulin tolerance test (ITT), a single intravenous insulin bolus provokes a fall in plasma glucose, and the glucose decay rate is used to estimate insulin sensitivity. During the test, plasma glucose quickly decreases to hypoglycemic levels. A short (15 min) protocol is preferred to avoid the confounding factor of hypoglycemia-induced counter-regulatory hormones (cortisol, catecholamines, growth hormone) that slow the glucose disappearance rate and for safety reasons [30].

The most used insulin sensitivity index is the constant (K) rate of glucose decay (Kitt). Kitt represents the percent decline in plasma glucose levels per min (%/min) and is determined by the ratio of $0.693/t^{1/2}$, where the denominator is the half-life of plasma glucose decay, calculated from the slope of the linear regression of the logarithm of blood glucose against time during the

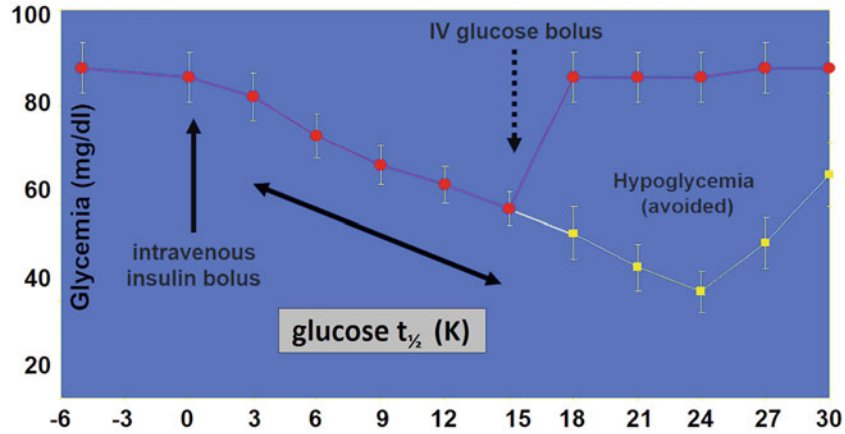

Fig. 4 Insulin tolerance test (ITT): the action of an intravenous insulin bolus on plasma glucose concentration is measured as the constant (K) rate of glucose decay (Kitt). The Kitt index represents the percent decline in plasma glucose levels per min, calculated from glucose half-life ($t_{1/2}$). The test is interrupted after 15 min in order to avoid hypoglycemia. Unpublished data

15 min interval (Fig. 4). An alternative insulin sensitivity index can be calculated by $\Delta G/G_b$, in which ΔG is the difference between baseline glycemia and the final glycemia (after 15 min), divided by baseline glycemia (G_b). Kitt has been validated against the hyperinsulinemic-euglycemic clamp [30]. However, it relies on a very short experiment interval that lacks a steady state, resulting in higher intra-individual variability in comparison to glucose clamps, so it may not be appropriate for small samples.

5.1 Materials

1. Vein catheter.
2. 0.9% saline solution.
3. 20–50% glucose solution.
4. Regular insulin (100 UI/ml).
5. 0.3–0.5 ml insulin syringe with needle.
6. Syringe without needle of 5-ml capacity or larger.
7. Glucose tubes.
8. Ice slurry for lab tubes.
9. Optional (for bedside glucose analysis): laboratory centrifuge and centrifuge tubes (for glucose analysis); glucose Analyzer (YSI 2700, YSI Life Sciences, Yellow Spring, OH, USA).

5.2 Methods

1. After an overnight fast (8–12 h), the subject is kept lying on a bed in the supine position. A vein catheter is inserted in an antecubital vein for insulin infusion and blood sampling. The patency of the venous accesses is maintained by slow saline drip.

2. At least two basal samples are drawn (5 min before and at time 0, immediately before insulin bolus infusion) for the average basal glucose measurements.
3. The regular insulin (0.1 U/kg) is prepared using a 0.3–0.5 ml insulin syringe (for dose precision of 1 IU) and transferred to a larger syringe with saline solution (*see* **Note 7**). The syringe is gently agitated, and the insulin solution is rapidly injected intravenously.
4. After the insulin bolus, blood is drawn at 3, 5, 7, 10, and 15 min for glucose measurement.
5. Immediately after the last blood sampling, the test is interrupted with a slow intravenous bolus of 50% glucose (20 ml) to reverse and prevent hypoglycemia. A meal is offered to the subject, and bedside glucose levels are measured until 30 min after the test.

6 Euglycemic-Hyperinsulinemic Clamp

The euglycemic-hyperinsulinemic clamp technique is traditionally recognized as the "gold-standard" method for assessing insulin sensitivity in vivo [1, 4]. This status is attributable to some technical advantages and the extensive knowledge about the pathophysiology of carbohydrate metabolism derived from glucose clamp studies.

The concept of insulin sensitivity extends to all actions elicited by insulin signaling, including protein synthesis, lipolysis inhibition, activation of growth pathways, among others. However, insulin sensitivity in vivo usually refers to glucose metabolism because of the tight relationship between plasmatic glucose and insulin [1].

One of the main advantages of the euglycemic-hyperinsulinemic clamp is the high reproducibility (intra-individual coefficient of variation of ~10%), which is mostly justified by a long-duration steady-state condition [31]. Other major advantages are the independence of endogenous insulin secretion and its simple conceptual principles (described below), which allow protocol versatility and straightforward interpretation of the experiment results [31]. It does not mean that the measurement of insulin sensitivity from the clamp test is superior to those estimated by other techniques, such as the intravenous glucose tolerance test, and the choice of one method over others is made primarily based on practical issues, including researchers' expertise, available resources and sample size [1, 31]. Despite its complex execution, the main concepts of the euglycemic-hyperinsulinemic clamp are quite simple (Fig. 5). In the normal fasting (postabsorptive) state, glucose homeostasis is maintained in a closed loop in which a relatively low insulin secretion tightly regulates the endogenous glucose output (~95% from the liver).

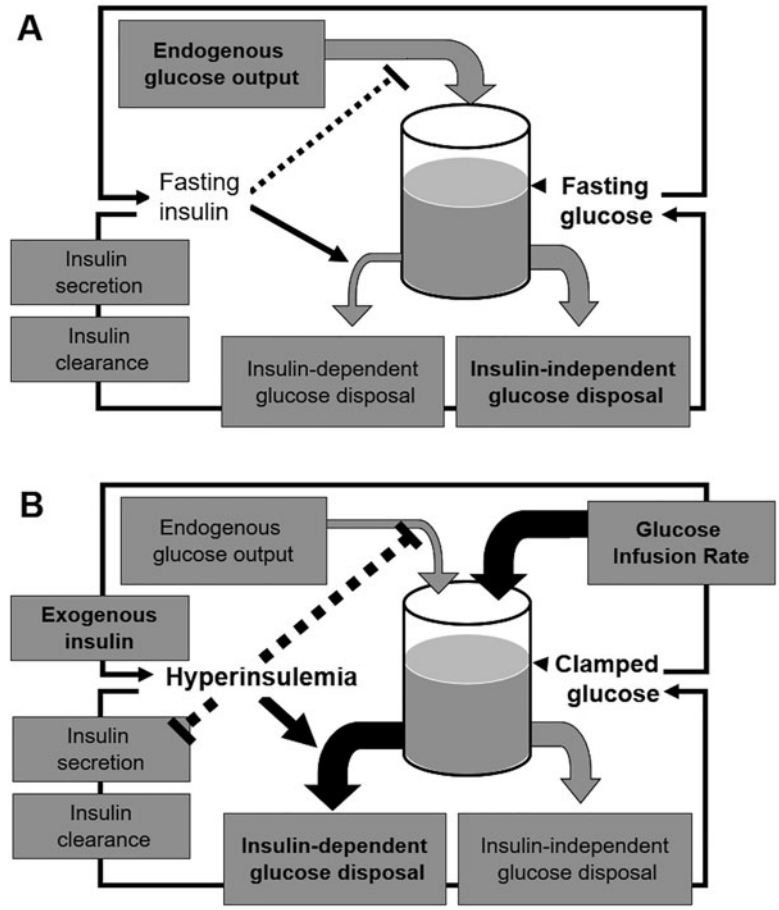

Fig. 5 Schematic diagram of (**a**) normal fasting glucose homeostasis represented in a closed loop. The glucose influx to the glucose space (extracellular fluid) equals the glucose outflux, resulting in constant glycemia. The only source of glucose input comes from endogenous glucose output (mostly from the liver and from kidneys), and the glucose disposal is predominantly insulin-independent. (**b**) The closed-loop is "opened" during the hyperglycemic euglycemic clamp test by a hyperinsulinemic plateau achieved through exogenous insulin infusion, while the endogenous insulin secretion is suppressed. Hyperinsulinemia almost completely suppresses endogenous glucose output, and the exogenous glucose infusion accounts for insulin-dependent, whole-body glucose requirements under these conditions. (Dashed lines in the figure represent suppression)

In contrast, the glucose uptake is mostly independent of insulin action and prevails in insulin-independent tissues (e.g., the brain) (Fig. 5a). In the clamp study, this loop is opened through a constant infusion of exogenous insulin to produce a hyperinsulinemic plateau that suppresses most of the endogenous glucose output and increases the whole-body glucose disposal (~90% in the skeletal muscles), which would result in a decline of plasma glucose concentration.

A second intervention prevents this decline in the loop: an exogenous infusion of glucose that exactly matches the insulin-dependent glucose uptake out of the glucose space (extracellular fluid) into the tissues as well as the reduction of endogenous glucose output (Fig. 5b) [1, 4, 31].

It is impossible to measure the in vivo glucose utilization in the tissues directly in the clamp experiment. However, the amount of exogenous glucose required to maintain constant euglycemia during a hyperinsulinemic state equals the amount of glucose that is taken up from the glucose space to be metabolized; thus, the glucose infusion rate (GIR) is a measurable variable that corresponds to the insulin-stimulated whole-body glucose disposal. For this reason, GIR is the primary insulin sensitivity index of the clamp test, expressed as mg · kg body weight^{-1} · min^{-1}. It is most frequently called the "*M*-value," as it refers to the "metabolized glucose," after mathematical adjustments (see below) [1, 4].

The *M*-value represents the whole-body glucose disposal rate at a specific level of hyperinsulinemia. As with other dynamic studies (despite acknowledging as "gold standard"), there are no broadly accepted cut-off values to define "insulin resistance" or "low insulin sensitivity" for the glucose clamp, and age- and weight-matched control groups are required in the protocols. In large samples, insulin resistance may be considered in the lower quartile of the *M*-value in a heterogeneous or nonselected population [1]. *M*-values below the 95% confidence interval of a healthy, glucose tolerant population may be considered, which grossly would give a cut-off around 5 mg · kg body weight^{-1} · min^{-1}, based on a series of previous studies using the insulin infusion of 40 mU/m^2/min [1].

The hyperinsulinemic-euglycemic clamp technique is sustained by some assumptions that must be fulfilled.

One assumption is that endogenous glucose output is suppressed or negligible during the clamp. As a result, the amount of glucose infused equals the amount of glucose metabolized in peripheral tissues, mainly in the skeletal muscles, giving an index of peripheral insulin sensitivity essentially [4]. However, GIR corresponds to the net effect of insulin on whole-body glucose metabolism in which the endogenous glucose output may not be completely inhibited in some clinical conditions, depending on the hyperinsulinemic level. Therefore, the variable measured in the hyperinsulinemic-euglycemic clamp is more appropriately called a whole-body insulin sensitivity index. The distinction between the hepatic and the peripheral insulin sensitivities requires a tracer-dilution technique with radioisotope-labeled glucose during the hyperinsulinemic-euglycemic clamp. The hepatic glucose production is determined from the difference between tracer-derived glucose disposal and the known exogenous glucose infusion rate in the fasting state, followed by the hyperinsulinemic state

during the glucose clamp. The hepatic insulin sensitivity is calculated as the degree of suppression of the hepatic glucose production and the peripheral insulin sensitivity as the difference between the hepatic and the whole-body insulin sensitivity [1, 31, 32].

A second assumption is the achievement of a stable hyperinsulinemic plateau through a constant intravenous infusion of exogenous insulin. This condition means that the hyperinsulinemic-euglycemic clamp does not depend on pancreatic insulin production, and the method is appropriate in a full range of beta-cell function [1, 4]. This is a major advantage of this method over others to assess insulin sensitivity. The suppression of beta-cell secretion induced by the hyperinsulinemic state is combined with the euglycemic condition that also prevents the stimulation of endogenous insulin secretion that otherwise could alter the desired plasma insulin level, and the hyperinsulinemic state suppresses insulin [1].

A full range of hyperinsulinemic targets have been tested (from ~10 to 1000 mU/m^2/min), including multistep hyperinsulinemic clamps. However, the relationship between insulin sensitivity is not linear and tends to plateau [1]. The standard insulin infusion rate during a hyperinsulinemic-euglycemic clamp test is 40 mU/m^2/min^1, which corresponds approximately to 1 mU/kg/min. The resulting steady plasma insulin concentrations are between 70 and 130 mU/ml [1], within the range of physiological postprandial hyperinsulinemia [33]. This range serves for most research purposes due to a good balance between suppression of endogenous glucose output (which may not be achieved at lower insulin levels) and discrimination of small differences in peripheral insulin sensitivity (which may disappear at higher levels) [1].

The variation in the plasma insulin concentrations for the same insulin infusion rate among individuals or different studies may relate to differences in insulin clearance, fasting plasma insulin concentrations, suppressing endogenous insulin secretion, and even to different insulin assays [1].

A third assumption is the maintenance of constant euglycemia, usually convened as 90 mg/dl (or eventually 100 mg/dl), with a narrow variation around this goal. In some protocols, the individual fasting plasma glucose concentration is clamped, which is termed an isoglycemic hyperinsulinemic clamp. However, the same glycemic goal should be established for all individuals for comparison. Individuals with fasting hyperglycemia should be corrected during the clamp to reach the predetermined euglycemic level.

Finally, another assumption is the achievement of a steady state in which the glucose infusion rate (GIR) and glycemia are constant (variation <5–10%) (Fig. 6). The duration of the clamp test must be long enough to reach this condition for at least 30 min, taking into account that there is considerable variation in glycemia (and consequently in GIR) before reaching the steady state [1, 4].

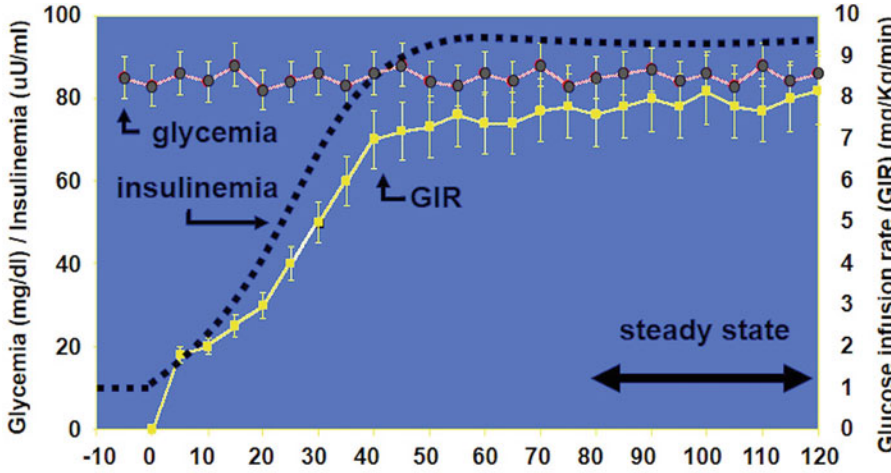

Fig. 6 Curves of plasma glucose and insulin and glucose infusion rate (GIR) during the hyperinsulinemic-euglycemic clamp test. A steady state must be observed in the final 30–60 min of the experiment

In healthy, nonobese individuals without significant metabolic disorders, a clamp test duration of 120 min may be adequate; the steady state is usually reached in the second hour, and the time periods of 60–120 min and 80–120 min are the most used for calculation of the insulin sensitivity index [31]. However, in individuals with dysmetabolic conditions like obesity and diabetes mellitus, a steady state usually will not occur before the third hour, and the time periods of 120–180 or 150–180 min are used. A progressive increase in glucose disposal is generally observed as the duration of the clamp test increases, resulting from increases in glucose oxidation [34]. Thus, the comparison of *M*-values between individuals or groups requires that the same time periods are used to calculate the *M*-values. Therefore, the duration of the clamp test in a study is usually predefined as the least duration that all participants are expected to achieve the steady state (120 or 180 min).

Even in a steady state, plasma glucose levels are not always perfectly constant. The GIR must be adjusted to changes in glycemia that do not represent real glucose uptake using a factor called "space correction" [4]. It is the rate at which glucose was added to or removed from the glucose space independently of changes in glucose uptake.

The *M*-value is calculated considering the space correction: $M = \text{GIR} - \text{SC} - \text{UC}$, where GIR is the glucose infusion rate, *SC* the space correction, and UC the correction for urinary glucose loss (rarely used because glycosuria is negligible in euglycemia). The *M*-value is calculated for each period of 10–20 min during the test, and the final index is the mean of *M*-values during 30–60 min intervals in a steady state. The space correction is calculated as follows: $\text{SC}\ (\text{mg/kg/min}) = (G_2 - G_1) \cdot 0.095$, where G_2 and G_1 are the

plasma glucose concentrations (mg/dl) at the end and the beginning of each 20-min period, respectively. If 10-min periods are used, the result must be multiplied by 2; for any other time periods, the equation must be adjusted. The number 0.095 derives from calculations that comprise the whole-body distribution volume of glucose expressed in liters [0.19 (l/kg body weight)]. The space correction will perform accurately only if glycemia is within a narrow range of the target level (±10 mg/dl). In addition, the time interval between the two measurements of plasma glucose concentrations used for the calculation of the space correction should not exceed 20 min. For any other time interval, the equation must be adjusted.

Further adjustments of the *M*-value are advisable for comparisons. As described above, the whole-body glucose disposal is usually presented per kg body weight ($mg \cdot kg\ body\ weight^{-1} \cdot min^{-1}$). The adjustment of *M*-values to fat-free mass (MFFM) is the most recommended [1, 31]. This correction accounts for gender-related differences in fat mass [8] and prevents underestimating insulin sensitivity in obesity [35]. Other adjustment factors are not usual, such as the resting energy expenditure (MREE) or the steady-state glycemia during the clamp (which yields the metabolic clearance rate, MCR) [1, 31]. The correction for steady-state plasma insulin concentration during the clamp (*M/I*) seems intuitive, but it adds no benefit and increases the dispersion of values [1].

6.1 Materials

1. Heating pad (or warm chamber with heated air, if possible).
2. Vein catheters and plastic three-way stop cock.
3. High-precision volumetric infusion pump and respective infusion set.
4. High-precision syringe infusion pump with fine adjustment of the infusion rates (0.02–0.15 ml/min).
5. Large-volume (50–60 ml) syringe (compatible with the syringe infusion pump).
6. Long extension tube (for connection between syringe pump and vein catheter).
7. Extension tube (for venous access).
8. 20–25% glucose solution bag.
9. 0.9% saline solution.
10. Regular insulin (100 UI/ml).
11. 0.3–0.5 ml insulin syringe with needle.
12. Laboratory centrifuge and centrifuge tubes (for glucose analysis).
13. Glucose Analyzer (YSI 2700, YSI Life Sciences, Yellow Spring, OH, USA).

14. K^+-EDTA blood collection tubes (for insulin and C-peptide).
15. Ice slurry (for storage of laboratory tubes).

6.2 Methods

1. For insulin infusate preparation, a large-volume syringe is filled in with 0.9% saline solution, completing the volume with 2 ml of the individual's blood, added to every 48 ml (for a total of 50 ml). The blood prevents insulin adsorption to plastic surfaces of the syringe and infusion lines, particularly with long extension lines. Then the regular insulin is added using a 0.3–0.5 ml insulin syringe (for dose precision of 1 IU), and the syringe is gently agitated before installation in the infusion pump. The most widely insulin infusion rate is 40 $mU/m^2/min$, proposed in original protocols [1, 4] (*see* **Note 8**).

   To simplify preparation, the infusate volume and the insulin pump infusion rate are predefined, and the insulin dose is calculated as follows:

$$\text{Insulin dose (IU)} = \left[\text{Ins}\left(40\ \text{mU/m}^2/\text{min}\right) \times \text{BSA}\ \left(\text{m}^2\right) \times 60\ \text{min} \times \text{Syringe Vol.}(50\ \text{ml})\right] \times \left[\text{Pump Infusion Rate}\ (11.4\ \text{ml/h}) \times 1000\right]^{-1}$$

   Ins represents insulin infusion rate (per minute), usually adjusted for body surface area (BSA, in square meters). The Syringe Vol. refers to the filled volume in the syringe. The Pump Infusion Rate is the predefined constant rate of an insulin infusion pump (ml/h), here chosen to be 11.4 ml/h. The number 1000 in the denominator converts the insulin units from mU to IU [4] (*see* **Note 9**).
2. After an overnight fast (8–12 h), the subject is kept lying on a bed in the supine position. A vein catheter is inserted in an antecubital vein for solution infusion. In order to avoid possible interference of ipsilateral infusion and blood sampling, a second catheter is inserted in a contralateral dorsal hand or wrist vein, in a retrograde fashion, for blood drawing.
3. The hand used for blood collection is warmed to 50–70 °C using a heating pad, folded around the hand (or a warm chamber with heated air) to obtain arterialized venous blood (*see* **Note 2**). The patency of the venous accesses is maintained by slow saline drip.
4. At least two basal samples are drawn (15–30 min before and at time 0, immediately before glucose infusion) for the average basal measurements.
5. An infusion pump is installed to administer a 20–25% glucose solution in the antecubital vein throughout the test (*see* **Note 10**), and another pump (syringe infusion pump) is installed in parallel in the same vein (using a three-way stopcock) to administer the insulin solution.

Table 1
Simplified protocol of primed insulin infusion for the hyperinsulinemic-euglycemic clamp test (40 mU/m^2/min)

Time (min)	Insulin per body surface are per min (mU/m^2/min)	Infusion rate (ml/h)
0–3	160	45.6
3–7	80	22.8
7–end of test	40	11.4

6. In order to achieve and maintain a constant hyperinsulinemic state, a priming insulin infusion is administered in the first 7–10 min of the test, which acutely raises the plasma insulin to achieve a whole-body saturation of insulin receptors (*see* **Note 11**). The priming is performed in a declining fashion (Table 1) and is followed by a predefined continuous insulin infusion rate to maintain the desired hyperinsulinemic level (*see* **Note 12**). A steady-state insulin concentration is expected after 60 min.
7. During insulin priming (first 7–10 min), the glucose infusion is started following the same time schedule, following an empirical scale of low (though progressive) glucose infusion rates (GIR), which is suitable for insulin-resistant individuals or correction of mild fasting hyperglycemia (~100 mg/dl). Typically, GIR (mg/dl glucose per kg body weight per min) is gradually increased from 0.5 (0–3 min) to 1.0 (3–7 min) and to 1.5 (7–10 min). This protocol should be scaled up for individuals perceived as more insulin sensitive (eumetabolic, physically very active), starting with GIR >1–2 mg · kg^{-1} body weight · min^{-1}. The glucose infusion should not start before reaching euglycemia for higher plasma glucose concentrations (up to ~150 mg/dl) (*see* **Note 13**). An electronic spreadsheet for converting glucose infusion rate (GIR) to volume infusion rate (Fig. 7) may be filled out before the procedure starts, inputting an individual's weight and glucose solution concentration. This is useful to streamline the infusion rate adjustments in the pump.
8. Plasma glucose levels are measured at 5-min intervals until the end of the test using a bedside glucose analyzer (*see* **Note 14**) to adjust the glucose infusion rate to achieve and maintain euglycemia (90 mg/dl). Ten-min intervals may be applied in some periods of the test. After each adjustment of GIR, plasma glucose concentration should be measured after an interval of 5 min (to permit stabilization of the glucose level in its distribution space), and further adjustments are performed as

GIR	Infusion rate (ml per hour)	GIR	Infusion rate (ml per hour)
0.5		6.0	
1.0		6.5	
1.5		7.0	
2.0		7.5	
2.5		8.0	
3.5		8.5	
4.0		9.0	
4.5		9.5	
5.0		10.0	

Fig. 7 Example spreadsheet for conversion of glucose infusion rate (GIR) to volume infusion rate for glucose clamp tests, according to body weight and the weight per volume of the glucose solution. Infusion rate = GIR (mg glucose per kg body weight per min) · body weight (kg) · [glucose weight per volume (mg/ml)]$^{-1}$ · 60 min, where the glucose weight per volume is usually 200 mg/ml (Glucose 20%) or 250 mg/ml (Glucose 25%)

needed. As a result, the glucose measurements are not always performed at exact 5-min intervals. On the other hand, a delay between blood collection and the respective adjustment of GIR may compromise the achievement of a steady state during the clamp test. For this reason, the glucose analyzer must be fast enough to provide measurements within less than a minute from blood sampling. A worksheet helps to track measurements and adjustments during the experiment (Fig. 8).

9. Although there are some proposed algorithms for the adjustment of GIR, the empirical adjustment based on the researcher's experience usually works better and is preferred. A general rule is to increment or decrement GIR by 0.5 mg · kg^{-1} body weight · min^{-1} whenever the glucose level is more than 5% below or above the target, respectively (*see* **Notes 15** and **16**).
10. A steady state is reached in the second or third hour of the test when the variation of GIR should be ideally less than 5–10% for a time period of at least 30 min at the end of the test. At this time, the variation of glycemia should be less than 5–10% above or below the goal (90 mg/dl).

Time (minutes)	Glycemia (mg/dl)	GIR	Infusion rate (ml/hour)	Time (minutes)	Glycemia (mg/dl)	GIR	Infusion rate (ml/hour)
- 60				85			
- 30				90			
- 15				95			
0		*0.5*		100			
3		*1.0*		105			
7		*1.5*		110			
10				115			
15				120			
20				125			
25				130			
30				135			
35				140			
40				145			
45				150			
50				155			
55				160			
60				165			
65				170			
70				175			
75				180			
80							

Fig. 8 Example worksheet for documentation of glycemia and glucose infusion rate (GIR) during glucose clamp tests. Typically, GIR is gradually increased in the first 7–10 min; then, it is empirically adjusted according to plasma glucose concentration, measured at 5-min intervals until the end of the test. Insulin-sensitive individuals will require higher starting rates

11. Blood sampling for insulin is performed at 30-min intervals or more frequently during the test. The plasma insulin analysis generally is not needed for interpretation of the results, but it is useful to evaluate the quality of the procedure, that is, the achievement of the desired constant hyperinsulinemic state, particularly in the second and third hours. C-peptide may be measured in the same schedule for estimating the suppression of endogenous insulin secretion. Blood samples are put in K^+-EDTA tubes on ice, followed by immediate centrifugation and frozen transportation to the laboratory.
12. At the end of the test, the insulin infusion pump is turned off. A meal is offered to the subject and bedside glucose levels are measured until 60 min after the test. In order to prevent hypoglycemia, it is warranted to keep the glucose infusion while waiting for exogenous insulin clearance (~30 min, and up to 60 min) and the glycemic meal load (*see* **Note 17**).

7 Conclusion

The full comprehension of beta-cell function complexity requires different tests and the assessment of insulin sensitivity, which can be evaluated simultaneously with insulin secretion by most methods. In contrast to insulin sensitivity, which has the hyperinsulinemic-euglycemic clamp recognized as the "gold-standard" method, no single beta-cell test fulfills such status, and each one has its advantages and limitations. The possibility of concomitant assessment of insulin sensitivity during procedures primarily dedicated to evaluating insulin secretory response is an advantage. The hyperglycemic clamp, followed by IVGTT, typically represents this possibility. Both intravenous tests have in common standardized insulin secretory stimuli, meaning that interpretation of insulin response is less dependent on mathematical modeling, even though IVGTT does have a nonstandardized portion that depends on modeling for accurate interpretation of second-phase insulin secretion and insulin sensitivity. Nonstandardization of stimuli (most related to unpredictable and variable glucose concentrations) is a typical limitation of oral tests, and then they require complex mathematical interpretation. In turn, they are closer to normal living and enclose the insulin potentiation exerted by gut hormones and are useful in studying glucose intolerance, pharmacological and nutrition therapies, and food science.

The selection of the methods of assessment of glucose homeostasis in the research settings depends on the aspects of beta-cell function and insulin sensitivity that are relevant to the proposed hypothesis, the possibility of assessment of both beta-cell function and insulin sensitivity, and the accuracy of different methods according to the type of interpretation (such as empirical versus mathematical modeling), the sample size and the studied population. It also comprises the experiments' complexity and feasibility, taking into account the available laboratory equipment and computational resources, the previous experience of the researchers, and the possibility of cooperation with other research centers, particularly for the application of mathematical models.

8 Notes

1. Particular attention must be paid to the duration of the glucose bolus because of the narrow interval until the first blood sampling in IVGTT. Some protocols use a higher glucose bolus (0.5 g/kg of body weight), resulting in a larger volume (particularly in individuals with obesity), making it more to infuse the bolus within 1 min. With higher doses, plasma glucose concentrations may take longer to normalize, and they may

not return to basal levels within the specified duration of the experiment, mainly in individuals with diabetes mellitus.

2. The "heated hand technique" for venous blood arterialization is proposed to avoid differences in plasma glucose related to its uptake in distal arm tissues. It may not be a major concern in most cases, and this technique has been considered unnecessary by some authors. However, tissue glucose uptake is higher in insulin-sensitive individuals than in insulin-resistant ones, resulting in arteriovenous differences proportional to insulin sensitivity [1]. Therefore, the venous glucose clamping may have a little but not negligible negative impact in the determination of insulin sensitivity, particularly for comparison of heterogeneous groups.
3. In individuals with diabetes mellitus, basal hyperglycemia near or above the target glucose level may contraindicate the hyperglycemic clamp. In contrast to the euglycemic-hyperinsulinemic clamp, it is not desirable to bring the subjects to euglycemia through intravenous insulin infusion because this would confound the endogenous insulin.
4. The rapid bolus protocol in the hyperglycemic clamp reproduces the shape of the sharp pattern of first-phase insulin secretion obtained in the intravenous glucose tolerance test (IVGTT). The difference between the hyperglycemic clamp and the IVGTT is that the target glucose level is predicted to calculate the glucose bolus in the former but not in the latter. Other priming protocols are based on the classical description of the hyperglycemic clamp [4] and use a priming dose over 15 min in which half of the total glucose mass is infused during the first 5 min and the remainder during the next 10 min.
5. Although there are some proposed algorithms for the adjustment of GIR, the empirical adjustment based on the researcher's experience usually works better and is preferred [1]. In the hyperglycemic clamp, a general rule is to increment or decrement GIR by ~1 mg · kg body weight^{-1} · min^{-1} whenever the glucose level is more than 5–10% below or above the target, respectively.
6. In clinical settings, oral load tests would not be recommended for subjects with fasting plasma glucose ≥126 mg/dl, although it is acceptable in research settings. However, the interpretation of the metabolic responses may be compromised as the basal glycemia approaches 200 mg/dl and definitively should not be performed with fasting plasma glucose ≥200 mg/dl. Glucotoxicity may lead to underestimation of insulin response. On the other hand, higher glucose levels after the oral load may increase the glucose effectiveness, that is, increased glucose concentrations promote its transfer to tissues independently of insulin action, thus overestimating insulin sensitivity.

7. It is advisable to dilute an amount of insulin that is higher than the calculated dose to improve the precision of insulin dosing in insulin tolerance test (ITT), usually in a ratio of 1 UI of insulin per 1 ml of saline solution.
8. In the hyperinsulinemic-euglycemic clamp, the insulin infusion rate may be calculated per kg body weight instead of per body surface area. The frequently used insulin infusion rate of 40 mU per square meter body surface area per minute [1, 4] corresponds to 1 mU per kg body weight per minute. However, calculation per body weight may not be appropriate in samples with different weight ranges or for which significant weight changes are expected, leading to heterogeneous hyperinsulinemic levels.
9. The 50-ml volume of insulin infusate is enough for a 180-min euglycemic hyperglycemic clamp. In protocols of longer duration, however, sequential infusates may be required. Preparing one stem infusate for the whole test before it starts is preferable to guarantee identical insulin concentrations throughout the test.
10. Glucose solutions with concentrations below 20% are not recommended for the hyperinsulinemic-euglycemic clamp because they may cause overhydration during the clamp test.
11. Unprimed insulin infusion protocols are generally not applied because it takes longer to achieve an appropriate plateau of insulin concentration, and there may not be enough time of steady state within the specified duration of the test.
12. Hyperinsulinemia may induce hypokalemia through stimulation of cellular uptake of potassium, and the serum potassium levels tend to decrease dose-dependently, as plasma insulin concentration gradually rises in the first 2 h of the clamp test [36]. However, the hyperinsulinemic levels are similar to those commonly reached in the postprandial state, and serum potassium concentration spontaneously reincreases in the third hour of the clamp [36]. Although some researchers recommend repeated measurement of plasma potassium or even concomitant prophylactic potassium infusion during the clamp test, most recognize that the serum potassium decrease is not clinically relevant, and usually, no specific measures are performed.
13. If the basal glycemia is above 150 mg/dl before the hyperinsulinemic-euglycemic clamp, it may take over an hour to normalize following the start of the protocol-specified insulin infusion. Therefore, it is advisable to reschedule the procedure in most cases because a delay to achieve the steady state may compromise the results. In case of hyperglycemia before or during the glucose clamp, an intravenous insulin bolus is not recommended to reach euglycemia because it would affect the

insulin levels. Even if the researchers wait at least 1 h for plasmatic clearance of the exogenous insulin, changes in insulin signaling (saturation of insulin receptors, sensitization), some suppression of endogenous glucose output, or the endocrine pancreas cannot be ruled out.

14. Laboratory glucose analyzers are recommended due to higher precision for bedside measurements during functional tests. However, they require careful maintenance and frequent calibration and may fail. Although not as precise, a backup portable glucometer may help continue the clamp test until any problem is resolved. Choose the most precise glucometer model and test the same blood sample twice (double-check).
15. Particular attention is recommended in the adjustment of GIR following the first 30 min of the clamp test when an increase in glucose disposal is usually noticed to avoid hypoglycemia. For the same reason, plasma glucose levels above the target may require less correction in the first ~30 min.
16. During the hyperinsulinemic-euglycemic clamp, a greater adjustment of GIR (increment or decrement of $1.0 \cdot kg^{-1}$ body weight $\cdot$ min^{-1}) may eventually be necessary (usually when glycemia is more than 10% off the target), and in case of hyperglycemia (>100 mg/dl) during the procedure, the glucose infusion pump may be turned off temporarily.
17. After the end of the hyperinsulinemic-euglycemic clamp, the glucose infusion rate may be gradually decreased, usually by half, since insulin infusion ends and the meal starts, then again every 10–15 min, for at least 30–45 min.

References

1. Bergman RN, Finegood DT, Ader M (1985) Assessment of insulin sensitivity in vivo. Endocr Rev 6(1):45–86
2. Ahrén B, Pacini G (2004) Importance of quantifying insulin secretion in relation to insulin sensitivity to accurately assess beta cell function in clinical studies. Eur J Endocrinol 150: 97–104
3. Bergman RN, Ader M, Hücking K et al (2002) Accurate assessment of beta-cell function: the hyperbolic correction. Diabetes 51(Suppl 1): S212–S220
4. DeFronzo RA, Tobin JD, Andres R (1979) Glucose clamp technique: a method for quantifying insulin secretion and resistance. Am J Phys 237(3):E214–E223
5. Mari A (2006) Methods of assessment of insulin sensitivity and beta-cell function. Immunol Endocr Metab Agents Med Chem 6:91–104
6. Mari A, Pacini G, Brazzale AR, Ahrén B (2005) Comparative evaluation of simple insulin sensitivity methods based on the oral glucose tolerance test. Diabetologia 48:748–751
7. Creutzfeldt W (2001) The entero-insular axis in type 2 diabetes – incretins as therapeutic agents. Exp Clin Endocrinol Diabetes 109 (Suppl 2):S288–S303
8. Ferrannini E, Natali A, Bell P et al (1997) Insulin resistance and hypersecretion in obesity European Group for the Study of Insulin Resistance (EGIR). J Clin Invest 100:1166–1173
9. Hovorka R, Soons PA, Young MA (1996) ISEC: a program to calculate insulin secretion. Comput Methods Prog Biomed 50: 253–264
10. Byrne MM, Sturis J, Polonsky KS (1995) Insulin secretion and clearance during low–dose graded glucose infusion. Am J Phys 268: E21–E27
11. Kahn SE, Prigeon RL, McCulloch DK et al (1993) Quantification of the relationship between insulin sensitivity and beta-cell

function in human subjects: evidence for a hyperbolic function. Diabetes 42:1663–1672
12. Cerasi E (1981) Differential actions of glucose on insulin release: re-evaluation of a mathematical model. In: Cobelli C, Bergman RN (eds) Carbohydrate metabolism quantitative physiology and mathematical modelling. Wiley, Chichester, pp 3–22
13. Bergman RN (1989) Toward physiological understanding of glucose tolerance: minimal-model approach. Diabetes 38:1512–1527
14. Tripathy D, Wessman Y, Gullström M et al (2003) Importance of obtaining independent measures of insulin secretion and insulin sensitivity during the same test: results with the Botnia clamp. Diabetes Care 26:1395–1401
15. Mitrakou A, Vuorinen-Markkola H, Raptis G et al (1992) Simultaneous assessment of insulin secretion and insulin sensitivity using a hyperglycemia clamp. J Clin Endocrinol Metab 75: 379–382
16. Pimenta WP, Santos ML, Cruz NS et al (2002) Brazilian individuals with impaired glucose tolerance are characterized by impaired insulin secretion. Diabetes Metab 28:468–476
17. Cobelli C, Toffolo GM, Dalla Man C et al (2007) Assessment of beta-cell function in humans, simultaneously with insulin sensitivity and hepatic extraction, from intravenous and oral glucose tests. Am J Physiol Endocrinol Metab 293:E1–E15
18. Cobelli C, Caumo A, Omenetto M (1999) Minimal model SG overestimation and SI underestimation: improved accuracy by a Bayesian two-compartment model. Am J Phys 277:E48–E48
19. American Diabetes Association (2020) 2. Classification and diagnosis of diabetes: standards of medical care in diabetes-2020. Diabetes Care 43(Suppl 1):S14–S31
20. Center of Disease Control (2007) National Health and Nutrition Examination Surveys (NHAES) Oral Glucose Tolerance Test (OGTT) procedures manual. https://www.cdc.gov/nchs/data/nhanes/nhanes_07_08/manual_ogtt.pdf. Accessed 18 Dec 2020
21. Bartoli E, Fra GP, Carnevale Schianca GP (2011) The oral glucose tolerance test (OGTT) revisited. Eur J Intern Med 22:8–12
22. Fellic AC, Lambert G, Lima MM et al (2015) Surgical treatment of type 2 diabetes in subjects with mild obesity: mechanisms underlying metabolic improvements. Obes Surg 25:36–44
23. Oram RA, Jones AG, Besser REJ et al (2014) The majority of patients with long-duration type 1 diabetes are insulin microsecretors and have functioning beta cells. Diabetologia 57: 187–191
24. Stumvoll M, Mitrakou A, Pimenta W et al (2000) Use of the oral glucose tolerance test to assess insulin release and insulin sensitivity. Diabetes Care 23:295–301
25. Stumvoll M, Van Haeften T, Fritsche A, Gerich J (2001) Oral glucose tolerance test indexes for insulin sensitivity and secretion based on various availabilities of sampling times. Diabetes Care 24:796–797
26. Breda E, Cavaghan MK, Toffolo G et al (2001) Oral glucose tolerance test minimal model indexes of beta-cell function and insulin sensitivity. Diabetes 50:150–158
27. Mari A, Pacini G, Murphy E et al (2001) A model-based method for assessing insulin sensitivity from the oral glucose tolerance test. Diabetes Care 24:539–548
28. Dalla Man C, Caumo A, Cobelli C (2002) The oral glucose minimal model: estimation of insulin sensitivity from a meal test. IEEE Trans Biomed Eng 49(5):419–429
29. Matsuda M, DeFronzo RA (1999) Insulin sensitivity indices obtained from oral glucose tolerance testing. Comparison with the euglycemic insulin clamp. Diabetes Care 22: 1462–1470
30. Bonora E, Moghetti P, Zancanaro C et al (1989) Estimates of in vivo insulin action in man: comparison of insulin tolerance tests with euglycemic and hyperglycemic glucose clamp studies. J Clin Endocrinol Metab 68: 374–378
31. Ferrannini E, Mari A (1998) How to measure insulin sensitivity. J Hypertens 16:895–906
32. Cobelli C, Toffolo G (1990) Constant specific activity input allows reconstruction of endogenous glucose concentration in non-steady state. Am J Phys 258:E1037–E1040
33. Singhal P, Caumo A, Carey PE et al (2002) Regulation of endogenous glucose production after a mixed meal in type 2 diabetes. Am J Physiol Endocrinol Metab 283:E275–E283
34. Roden M, Price TB, Perseghin G, Petersen KF, Rothman DL, Cline GW, Shulman GI (1996) Mechanism of free fatty acid-induced insulin resistance in humans. J Clin Invest 97: 2859–2865
35. Bokemark L, Froden A, Attvall S et al (2000) The hyperinsulinemic euglycemic clamp examination: variability and reproducibility. Scand J Clin Lab Invest 60:27–36
36. Minaker KL, Rowe JW (1982) Potassium homeostasis during hyperinsulinemia: effect of insulin level, beta-blockade, and age. Am J Phys 242:E373–E377

Chapter 21

Maximum Oxygen Consumption: $\dot{V}O_{2\ max}$ Laboratory Assessment

Mara Patrícia Traina Chacon-Mikahil, Alex Castro, Danilo dos Santos Caruso, and Arthur Fernandes Gáspari

Abstract

Cardiorespiratory fitness (CRF) is the most widely examined human physiological functional capacity and is commonly assessed by the measurement of maximal oxygen uptake ($\dot{V}O_{2\,max}$) or represented indirectly by maximum power output (PO_{max}) in incremental exercise tests leading to exhaustion. Our aim is to provide objective guidance on how to program, choose, be safe, and apply a protocol for assessing maximum aerobic capacity and, consequently, maximum power output. We present considerations and a flowchart of important key points facilitating the decision-making process and its direct application in the prescription of physical training programs.

Key words Maximum oxygen consumption, Maximum power output, Cardiorespiratory fitness test, $\dot{V}O_{2\,max}$, Stress exercise protocols tests

1 Introduction

Cardiorespiratory fitness (CRF) is commonly assessed by the measurement of maximal oxygen uptake ($\dot{V}O_{2\,max}$) or indirectly by maximum power output (MPO) in incremental exercise tests leading to exhaustion. The $\dot{V}O_{2\,max}$ is considering the gold-standard measurement of maximal aerobic power and reflects the ability of the circulatory and respiratory systems to capture, transport, and supply oxygen to muscles during physical exercise [1–3].

CRF is the most widely examined human physiological functional capacity [4]. Moreover, higher levels of CRF are strongly associated with lower all-cause and cardiovascular disease mortality [5–7].

Large interindividual differences in CRF levels are frequently observed in sedentary individuals without a history of substantial involvement in regular exercise programs [8–12]. In healthy and sedentary adults aged 17–41 years old, the distribution of intrinsic

Cinthia Baú Betim Cazarin (ed.), *Basic Protocols in Foods and Nutrition*,
Methods and Protocols in Food Science, https://doi.org/10.1007/978-1-0716-2345-9_21,

CRF may vary from 14 to 58 mL/kg/min when measured by $\dot{V}O_{2\,max}$, and several factors may contribute to this variation, with heredity explaining 51% of the variation in $\dot{V}O_{2\,max}$ as seen in data from the HERITAGE Family Study [11, 13].

Our aim is to provide objective guidance on how to program, choose, and apply a protocol for assessing maximum aerobic capacity and, consequently, maximum power output, presenting considerations and a flowchart of important key points facilitating the decision-making process.

2 Materials

2.1 Clinical Screening

An initial general assessment of the individual is important to ensure their safety and the appropriate conditions for their reliable assessment according to standard guidelines [3].

It is recommended that a clinical anamnesis be carried out to identify the presence of cardiovascular diseases, which limit physical exercise, risk factors associated with the development of cardiovascular diseases, history of adverse cardiac events, and the individual physical activity level.

This clinical assessment should preferably contain the assessments: pulmonary, cardiac, abdominal, orthopedic, cutaneous, and other clinical conditions that may be limiting for the practice of physical exercises and neurological function tests (reflexes and cognition) when necessary.

Cardiac assessment, especially for individuals that presented symptoms or cardiovascular diseases, age over 30 years old, and an extreme sedentary condition, necessarily be carried out such as the resting electrocardiogram (EKG), the ergometric clinical exercise test, and, if necessary, additional tests such as 24-h Holter home blood pressure monitoring and imaging tests (chest radiography, echocardiography, carotid ultrasound, scintigraphy, and angiography).

For individuals with pulmonary diseases, also at medical criteria, the complementary assessment includes chest radiography, pulmonary function tests, oximetry analysis, and others.

After these assessments and clinical release, the individual performance assessment can be conducted, including the following:

- Body mass, body mass index, waist circumference, and body fat percentage.
- Blood pressure and heart rate at rest.
- Biochemical and metabolic assessment (suggested for an adequate characterization of the metabolic status and complement the assessment of their health conditions).
- CRF test to obtain the $\dot{V}O_{2\,max}$ and MPO and, in some cases, the anaerobic threshold.

3 CRF Tests

3.1 Organization of Procedures

All equipment (cycle ergometer, treadmill, and sphygmomanometer) must be calibrated periodically or before the evaluation, as is particularly the case of the expired gas analysis system (metabolic analyzer of expired gases), which must be calibrated immediately before each evaluation, or minimum before each daily testing period, according to the manufacturers' specifications.

For calibration of the expired gas analysis system, data referring to room temperature, atmospheric pressure, and relative humidity of air must be inserted in the equipment's software before the calibration [3].

For purposes of standardizing the conditions of the effort for environment and reproducibility of data acquisition conditions, the ambient temperature must be kept between 20 and 22 °C, and the relative humidity of the air must not be less than 60% [14]. Before starting the evaluation, it must be verified if the individual rest biological signs, adequate positioning, and environmental conditions. It is important to know the population's characteristics to validate conditions at rest and during exercise. Using a sedentary young man at rest as an example, values around 3.5 mL/kg/min are expected for the VO_2, 75 beats/min for heart rate, 7 L/min for ventilation, and a respiratory quotient of around 0.85 [15].

Additional care must be taken regarding the environment while conducting the test, such as noise, cleaning, and availability of equipment, stretcher, and emergency aid, before starting the assessment procedures, as well as limiting the number of people in the room, which should be the same throughout the entire procedure.

3.2 Subject Preparation to Assessment

An important starting point is that the participant has previously signed the risk assessment term or informed consent form (in case of research projects approved by the Ethics Committee). Their anamnesis record is available to the evaluator at the time of evaluation.

Some general instructions for standardizing the test must be followed to ensure the accuracy and reproducibility of the measurement of the CRF and the individual's safety [3, 16].

Subjects must abstain from ingesting caffeine, alcohol, psychotropic drugs for at least 24 h before the test, and food or tobacco products for at least 3 h. In addition, to ensure normal hydration during the test, abundant fluid consumption, especially water, is recommended 24 h prior to the test.

The following should be oriented in advance:

1. Wear soft and comfortable clothing, as well as appropriate shoes.
2. Instruct on a peaceful night's sleep.

3. Do not do strenuous exercises for at least 24 h before the test.
4. Must be informed that the test can cause fatigue, and the individual can choose personal support to return home safely.

Suppose the exercise test is performed for the diagnosis of ischemia, routine medications, at the discretion of the responsible physician, may be suspended for a period in advance (e.g., β-blockers, which attenuate the heart rate response and blood pressure during exercise) [17]. The return of medication use should be as brief as possible, taking care of possible rebound effects. Any medication used by the individual must be recorded and analyzed later with the test results (related adverse effects are reported).

To strenuous exercise tests for functional assessment purposes (performance, prescription, or follow-up of the CRF), individuals must maintain the use of medication. The evaluator must analyze the results during and after evaluation regarding the consistency and effectiveness of the expected responses. All and any posology of medication use must be registered, and the variations in dosage between subsequent evaluations are important information for analyzing the results.

Monitoring systemic blood pressure before, during, and in recovery after physical exertion should be a standard condition for this type of assessment [18].

Also, in reassessments, important care must be taken into account about keeping the same protocol and time to the previous test to minimize circadian interferences and the subject's daily routine.

3.3 Assessment Protocols and Implications

The most used protocols to obtain $\dot{V}O_{2\,max}$ values are the incremental protocols that lead the individual to exhaustion [3, 17, 19].

Some procedures and precautions can add important results to the procedures before, during, and after applying the ergospirometry evaluation. Therefore, we emphasize that, when preparing the subject for the assessment, in addition to their previous conditions (sleep, not exercising, medications, and food restrictions), one must:

1. Properly position the subject at rest (supine or sitting resting position).
2. Monitor heart rate at rest with EKG or cardiac monitor.
3. Monitor arterial blood pressure at rest.
4. Properly position the subject on the ergometer, adjusting the saddle and pedal height (for cycle ergometer) or starting position on the treadmill without moving the mat.
5. Carry out instructions on the operation of the ergometer (ideally, perform a prior familiarization test with the room and equipment).

6. Carry out instructions on the protocol to be used.
7. Seek clarification on the use of the perceived exertion scale during exercise testing (show the scale in advance).
8. Be able to add signs about symptoms and the need to interrupt the test.
9. Clarify the location on the ergometer (treadmill) and the possibility of using the test interruption device (stop belt—the individual can activate that).

Regarding the use of the gas analyzer, it is important to:

1. Clarify that the evaluated subject will be connected to the equipment and will remain at all times with free breathing of the ambient air in the room.
2. Be aware that only a sample of expired air will be collected automatically by the equipment for analysis during the test.
3. Show the equipment, nozzle, support, and other accessories to be used.
4. Correctly position the equipment, support, and face mask (choose the model and size appropriate to the person evaluated), adjusting and detecting possible leaking locations of the exhaling air—correcting this situation before the start of the gas collection.
5. Position the blood pressure measurement cuff and monitor it correctly throughout the exercise protocol, clarifying the subject about this procedure.

During the development of the protocol, monitors or displays informing the intensity of the ergometer, heart rate, or other information obtained may or may not be made available to the subject, according to the standardization of procedure previously established by the evaluators and informed to the subject.

In general, the exercise protocols can be of two types, ramp or step (Fig. 1). In both cases, the tests start at lower intensities that are progressively increased. There is an increase in the treadmill inclination until the individual is physically exhausted or achieves some criterion for ending the test.

In the step test protocol, the intensity increases, starting from rest or heating intensity, and remains at the new intensity for a certain period (with 1–5 min being the most common intervals) until it increases again. In the ramp test protocol, the intensity constantly increases during the test, also from rest or heating intensity, obeying an increment rate automatically according to standardized programming in the ergometer. These increases in intensities can occur due to the increase in speed and/or inclination if the ergometer is a treadmill (e.g., 0.5 km/h/min). Moreover, the ergometer that simulates cycles (cycle ergometer) increases the power generated in the pedals (e.g., increases 25 W/min).

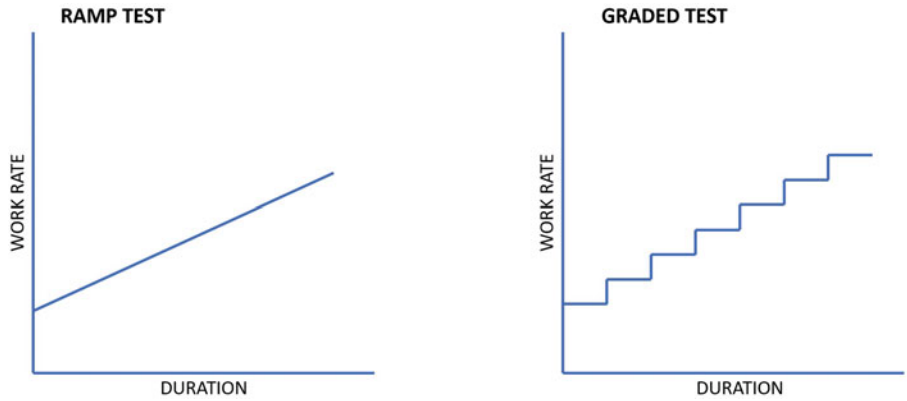

Fig. 1 Hypothetical examples of the two work rate increase mode in the most common incremental exercise tests: ramp and step test protocols

For electromagnetic braking cycle ergometers, rotations per minute (rpm) are necessary to maintain the power developed during pedaling. Therefore, the pedaling cadence may vary, according to the type of ergometer, typically between 60 and 80 rpms [17, 19].

It is also important to point out that there are many ergometers related to the specificity of each sporting gesture. So, the intensity unit can be several among them, ranging from the traditional measures in kilometer per hour or Watts, or even the frequency of ball throws in the tennis table [20].

An important premise for the direct tests to the determination of $\dot{V}O_{2\,max}$ is necessary that it reaches the individual to physical exhaustion. However, this is not always possible. Therefore, submaximal tests can also be used when the evaluated individual has contraindications. Such as older adults, motor limitations, and/or individuals with diseases that may limit it or where the maximum test can become a risk factor [16].

In this case, efforts are performed at submaximal intensities, with heart rate monitoring, and the values obtained are used to estimate the $\dot{V}O_{2\,max}$ from mathematical equations, which is the best way for your prediction [16]. For these cases, please choose the most appropriate exercise protocol; it is recommended to read the specific guidelines for the population to be evaluated [16, 17].

Some criteria must be considered to achieve test parameters that meet the proposed objectives during the execution of the maximum incremental protocol. The initial intensity is one of the factors to be observed to guarantee a total duration of the test between 8 and 12 min. This duration is indicated as ideal to trigger enough physiological systems to exhaustion [19, 21], to reduce the chance of premature fatigue, and to increase the chances that the highest values of $\dot{V}O_2$ are confirmed as $\dot{V}O_{2\,max}$. Attention must also be paid to define this intensity to the individual's functional

capacity. For untrained adults, it is common to start the test near the minimum ergometer speed and or light walking speed, such as values between 4 and 6 km/h or 10–25 W at cycle. This initial speed must be adjusted according to the characteristics of the studied population, and it may be lower for individuals with gait limitations, as observed in lameness. For example, 2 km/h [22] or higher in young individuals with good functionality and recreational populations trained [23], and still extremely high in highly trained endurance athletes such as elite marathon runners who can start the test at 17 km/h [24].

However, the lack of robust data on the initial speed suggested for incremental testing, including recommendations for each population, can be a problem. For example, Dantas and Doria [25] proposed that in trained runners, the initial speed suggested for the test would be 70% of the average speed of a run from 10 to 21 km/h or 80% of the speed of a marathon (42 km), to obtain data related to submaximal intensities thresholds and increase the step by step of an adequate intensity initially. In the absence of a clear reference for choosing the initial intensity of the test, we recommend the observation of the literature containing a similar test and population.

To step protocol, total time spent in the test is directly related to the duration of each step and the magnitude of the increase in intensity. Likewise, in a test considered ramp protocol, the slope of the straight line refers to intensity about time (rate of increment). It is how much the intensity is increased in a given period.

We have observed that protocols with steps lasting 3 min or more are commonly used to obtain submaximal markers of aerobic fitness, such as metabolic thresholds, mainly when these are evaluated through the concentration of lactate, due to the kinetics of removal of this metabolite from muscle cells to the bloodstream [26]. While this is an interesting point of exercise physiology that should be noted by those investigating physical performance, the identification of thresholds and other variables that determine aerobic performance is beyond the scope of this chapter.

Tests with a shorter step, such as 1 min, are usually used to obtain maximum aerobic power values ($\dot{V}O_{2\,max}$) and even metabolic thresholds identified from the gas exchange of O_2 and CO_2 [26]. In this sense, Zhang et al. [27] reported the 1-, 2-, and 3-min step time protocols and a ramp protocol. Both were efficient to obtain the $\dot{V}O_{2\,max}$, which had a maximum duration of approximately 12 min. The test duration seems to be an important characteristic for data validity.

Buchfuhrer et al. [19] compared tests with increments of 15, 30, or 60 W/min, and reported that for the magnitude of load increment per step, or slope of the straight line in the ramp test, the same logic seems to hold, being closely related to the test duration. Zhang et al. [27] also bought increments of 10, 15, and 20 W/min and saw no difference between them in $\dot{V}O_{2\,max}$. It

highlights that the characteristics of the increment will directly affect the final intensity of the test, as protocols with larger increments of intensity per unit of time will result in higher maximum intensity values [28]. Furthermore, when values are to be used for training intensity prescription, as in workouts prescribed by the percentage of maximum intensity, it may result in higher values.

All the details elaborating a protocol to reach an evaluation considered effective directly impact the validity of the values obtained from the $\dot{V}O_{2\,max}$. Some criteria must be used to interrupt the test and validate the data obtained. In general terms, $\dot{V}O_{2\,max}$ values are considered valid when two of the following criteria are met: the presence of a plateau in de $\dot{V}O_2$, being considered increases below 2.1 mL/kg/min in the $\dot{V}O_2$ even with an increase in intensity; respiratory exchange ratio (RER) $\geq$ 1.2; maximum heart rate (HR_{max}) $\geq$ 90% of the HR_{max} predicted by age; and subjective effort perception (PSE) recorded in the last complete stage $\geq$17 points, on a scale of 6–20 [17, 29]. Additionally, for those with access to measurement of blood lactate concentration, lactate concentrations $\geq$8–9 mM for normal subjects can also be used [17, 30].

In addition to being valid, the test needs to be safe. As mentioned earlier, some individuals can put themselves at risk when performing intense activities. Thus, following the recommendations of the ACSM Guideline [ ], the suggested criteria for stopping the test are the onset of symptoms of angina, fall of $\geq$10 mmHg in systolic blood pressure with increased work rate or lower values at the beginning of the test, increase in systolic blood pressure to 250 mmHg and or diastolic to 115 mmHg, shortness of breath, wheezing, leg cramps, or lameness. Other important points to watch out for are signs of deficiency perfusions, such as dizziness, confusion, ataxia, paleness, cyanosis, nausea, cold, and clammy skin. As well as the absence of increases in heart rate, even with the increase in intensity during the test, noticeable change in heart rate by palpation or auscultation, physical or verbal manifestations of severe fatigue, the individual manifestation to asking about the test end, and failure in the test equipment [17].

It is important to know that the test has high reproducibility in young and healthy populations, active or trained. However, in untrained, unmotivated, or sick populations, the inability to reach $\dot{V}O_{2\,max}$ can be observed due to the previous interruption of the test, by lack of capacity, motivation, or symptoms that lead to the end of the test, in which case the maximum value reached is the $\dot{V}O_{2\,max}$, which is a different value from $\dot{V}O_{2\,max}$, since the threshold, in this case, can be multifactorial. Therefore, it does not necessarily represent the maximum oxygen consumption even with an increased workload [21]. Due to the complexity of carrying out an incremental test protocol suitable for each individual and the

need to achieve multiple validation parameters of the $\dot{V}O_{2\,max}$ result and test interruption, which may or may not impact the result succinctly or not, it is suggested that it be performed, after a recovery period (minimum of 48–72 h) the performance of a new test seeking confirmation of the data [21].

The confirmation assessment consists of a constant intensity test to exhaustion, using an intensity approximately 10% greater than the maximum found in the maximum incremental test. It should be considered that, if the actual maximum aerobic power value ($\dot{V}O_{2\,max}$) is reached in the incremental test, in this new test, even an intensity higher than the $\dot{V}O_{2\,max}$, which should be performed for enough exercise time to reach a plateau in the $\dot{V}O_2$ before exhaustion, obtaining the same values of maximum aerobic power [21]. In this evaluation, if the difference is greater than 2.1 mL/kg/min, the exercise test must be repeated another day. If the value is lower, the test will be validated, and the test recorded values considered for analysis [31].

Finally, it should be noted that there are several ergometer options for performing the incremental test, with specific characteristics, advantages, and disadvantages. The treadmill is usually used because the exercise corresponds to the normal movement of walking or running; in contrast, the cycle ergometer brings the possibility of testing individuals with some movement limitations or obesity, for example, and directly quantifying the workload produced [32]. However, it is worth remembering that Buchfuhrer et al. [19] reported that the values of $\dot{V}O_{2\,max}$ found on a cycle ergometer were lower than those observed on the treadmill for the same individuals evaluated. Muscat et al. [33] performed a ramp test in young people in two different ergometers and found different results of $\dot{V}O_{2\,max}$ for the same work rate, probably because of the greater skeletal muscle mass involved in running, consequently higher values of maximum cardiac output, stroke volume, arteriovenous oxygen difference, and greater vascular conductance.

It is noteworthy that in trained individuals, this difference is observed in runners but not in cyclists, indicating that the choice of ergometer should preferably follow the specificity of the training performed [34]. The need for specific ergometers for modalities, or characteristics of a population, has meant that there is a variety of them, for example, paddles and kayaks [35], ergometers for upper limbs (Upper Body Cycle) [36], adapted wheelchairs [37], swim bench ergometers [38], and even vertical ergometers that simulate sport climbing [39].

In treadmill tests, if the results obtained in the incremental test are to be used for training prescription, it is appropriated using a fixed incline of 1% [40] and an increase in intensity to exhaustion employing an increase in speed. This strategy will guarantee speed values referring to running on a flat course, which can be more easily transferred to walking/running training protocols.

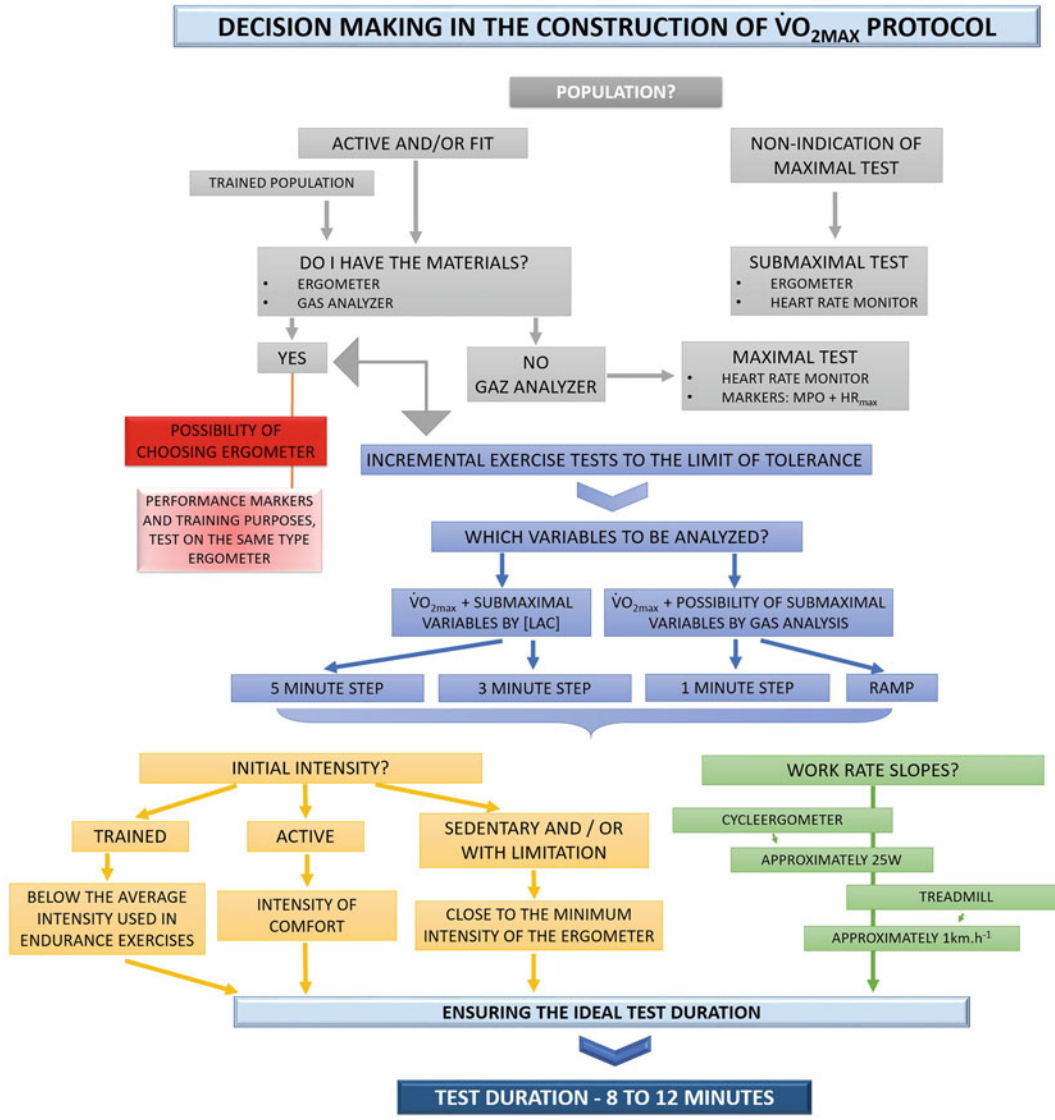

Fig. 2 Flowchart representing the design of the incremental protocol: decision-making tool based on the studied population, available equipment, and possible additional variables of interest. MPO: maximal power output, HR_{max}: maximal heart rate, LAC: blood lactate concentration. (Adapted from [3, 19, 25, 26, 32, 33])

The ventilatory and metabolic results obtained can be interpreted appropriately from interpretation guides and the classification of the level of physical fitness obtained through classification tables established by the compilation of many studies and data.

We present a flowchart (Fig. 2) that addresses the different key points in constructing a maximum incremental protocol and evaluating adequate $\dot{V}O_{2\,max}$ to assist in decision-making when designing the ideal protocol for each population.

3.4 Assessment Reproducibility

In general, the tests to determine the $\dot{V}O_{2\,max}$ show good reproducibility [coefficient of variation (CV) = 5% and intraclass correlation coefficient (ICC) = 0.97] for individuals 17–65 years old of both sexes [41]. However, depending on the population and protocols to be studied, it is important to ensure that the procedures adopted are reproducible, and/or greater familiarization with the test is necessary. In order to know the test reproducibility, through a pilot study, individuals with characteristics similar to the studied population must undergo two runs of the maximum test, with an interval of at least 48 h between them [41].

To determine the CV, first, calculate the typical measurement error (ETM) from the standard deviation of the differences between measurements divided by $\sqrt{2}$. Afterward, divide the ETM by the mean of all observations recorded in both measurements and multiply by 100 to obtain the CV, representing the absolute error between measurements given in percentage [42]. If you do not have software that does it automatically, you can perform the calculations manually to determine the ICC. For this, conduct an analysis of variance to obtain the mean square between individuals (MSr), the mean square within individuals (MSc), and the mean square of the error (MSe). To estimate the ICC between two tests, use the following equation: $\text{ICC} = (\text{MSr} - \text{MSe})/[\text{MSr} + ((k-1) \times \text{MSe}) + k \times (\text{MSc} - \text{Mse})/n]$, where k is the number of tests applied on the same individual and in the number of individuals [43].

Important observations and details in conducting the effort protocol to obtain the $\dot{V}O_{2\,max}$ enhance the veracity, reproducibility, application, and monitoring of information in order to define the good results of the cardiorespiratory assessment.

References

1. Hill AV, Lupton H (1923) Muscular exercise, lactic acid, and the supply and utilization of oxygen. QJM Int J Med os-16: 135–171. https://doi.org/10.1093/qjmed/os-16.62.135
2. Hawkins MN, Raven PB, Snell PG, Stray-Gundersen J, Levine BD (2007) Maximal oxygen uptake as a parametric measure of cardiorespiratory capacity. Med Sci Sports Exerc 39: 103–107. https://doi.org/10.1249/01.mss.0000241641.75101.64
3. Riebe D, Ehrman JK, Liguori G, Magal M (2018) ACSM's guidelines for exercise testing and prescription, 10th edn. Wolters Kluwer, Philadelphia
4. Harber MP, Kaminsky LA, Arena R, Blair SN, Franklin BA, Myers J et al (2017) Impact of cardiorespiratory fitness on all-cause and disease-specific mortality: advances since 2009. Prog Cardiovasc Dis 60(1):11–20. https://doi.org/10.1016/j.pcad.2017.03.001. PMID: 28286137
5. Kodama S, Saito K, Tanaka S, Maki M, Yachi Y, Asumi M et al (2009) Cardiorespiratory fitness as a quantitative predictor of all-cause mortality and cardiovascular events in healthy men and women: a meta-analysis. JAMA 301(19): 2024–2035. https://doi.org/10.1001/jama.2009.681. PMID: 19454641
6. Shah RV, Murthy VL, Colangelo LA, Reis J, Venkatesh BA, Sharma R et al (2016) Association of fitness in young adulthood with survival and cardiovascular risk: the coronary artery risk development in young adults (CARDIA) study.

JAMA Intern Med 176(1):87–95. https://doi.org/10.1001/jamainternmed.2015.6309. PMID: 26618471

7. Fardman A, Banschick GD, Rabia R, Percik R, Segev S, Klempfner R, Grossman E, Maor E (2021) Cardiorespiratory fitness is an independent predictor of cardiovascular morbidity and mortality and improves accuracy of prediction models. Can J Cardiol 37:241–250. https://doi.org/10.1016/j.cjca.2020.05.017
8. Ghosh S, Hota M, Chai X, Kiranya J, Ghosh P, He Z, Ruiz-Ramie JJ, Sarzynski MA, Bouchard C (2019) Exploring the underlying biology of intrinsic cardiorespiratory fitness through integrative analysis of genomic variants and muscle gene expression profiling. J Appl Physiol (1985) 126:1292–1314. https://doi.org/10.1152/japplphysiol.00035.2018
9. Bouchard C, Blair SN, Katzmarzyk PT (2015) Less sitting, more physical activity, or higher fitness? Mayo Clin Proc 90:1533–1540. https://doi.org/10.1016/j.mayocp.2015.08.005
10. Del Coso J, Gu Z, Gerile W, Yang R, Díaz-Peña R, Valenzuela PL, Lucia A, He Z (2020) Interindividual variation in cardiorespiratory fitness: a candidate gene study in Han Chinese people. Genes (Basel) 11:555. https://doi.org/10.3390/genes11050555
11. Bouchard C, Daw EW, Rice T, Pérusse L, Gagnon J, Province MA, Leon AS, Rao DC, Skinner JS, Wilmore JH (1998) Familial resemblance for VO2max in the sedentary state: the HERITAGE family study. Med Sci Sports Exerc 30:252–258. https://doi.org/10.1097/00005768-199802000-00013
12. Castro A, Renata GD, Silva LM, Ferreira MLV, Andrade ALL, Bernardes CF, Cavaglieri CR, Chacon-Mikahil MPT (2021) Understanding the relationship between intrinsic cardiorespiratory fitness and serum and skeletal muscle metabolomics profile. J Proteome Res 20(5):2397–2409. https://doi.org/10.1021/acs.jproteome.0c00905
13. Skinner JS, Jaskólski A, Jaskólska A, Krasnoff J, Gagnon J, Leon AS, Rao DC, Wilmore JH, Bouchard C (2001) Age, sex, race, initial fitness, and response to training: the HERITAGE Family Study. J Appl Physiol (1985) 90:1770–1776. https://doi.org/10.1152/jappl.2001.90.5.1770
14. Kingma B, Frijns A, Van Marken Lichtenbelt W (2012. ISSN 1945-0508) The thermoneutral zone: implications for metabolic studies. Front Biosci (Elite Ed) 4:1975–1985. https://doi.org/10.2741/518
15. Kenney WL, Wilmore JH, Costill DL (2011) Physiology of sport and exercise, 5th edn. Human Kinetics Publishers, Champaign
16. Fletcher GF, Ades PA, Kligfield P, Arena R, Balady GJ, Bittner VA, Coke LA, Fleg JL, Forman DE, Gerber TC, Gulati M, Madan K, Rhodes J, Thompson PD, Williams MA (2013) Exercise standards for testing and training: a scientific statement from the American Heart Association. Circulation 128:873–934. https://doi.org/10.1161/CIR.0b013e31829b5b44
17. Löllgen H, Leyk D (2018) Exercise testing in sports medicine. Dtsch Arztebl Int 115:409–416. https://doi.org/10.3238/arztebl.2018.0409
18. Muntner P, Shimbo D, Carey RM, Charleston JB, Gaillard T, Misra S, Myers MG, Ogedegbe G, Schwartz JE, Townsend RR, Urbina EM, Viera AJ, White WB, Wright JT Jr (2019) Measurement of blood pressure in humans: a scientific statement from the American Heart Association. Hypertension 73(5):e35–e66. https://doi.org/10.1161/HYP.0000000000000087
19. Buchfuhrer MJ, Hansen JE, Robinson TE, Sue DY, Wasserman K, Whipp BJ (1983) Optimizing the exercise protocol for cardiopulmonary assessment. J Appl Physiol 55:1558–1564. https://doi.org/10.1152/jappl.1983.55.5.1558
20. Zagatto AM, Papoti M, Gobatto CA (2008) Validity of critical frequency test for measuring table tennis aerobic endurance through specific protocol. J Sports Sci Med 7:461
21. Poole DC, Jones AM (2017) Measurement of the maximum oxygen uptake VO2max: VO2peak is no longer acceptable. J Appl Physiol 122:997–1002. https://doi.org/10.1152/japplphysiol.01063.2016
22. Tuner SL, Easton C, Wilson J, Byrne DS, Rogers P, Kilduff LP, Kingsmore DB, Pitsiladis YP (2008) Cardiopulmonary responses to treadmill and cycle ergometry exercise in patients with peripheral vascular disease. J Vasc Surg 47:123–130. https://doi.org/10.1016/j.jvs.2007.09.001
23. Machado FA, Kravchychyn AC, Peserico CS, da Silva DF, Mezzaroba PV (2013) Incremental test design, peak aerobic running speed and endurance performance in runners. J Sci Med Sport 16:577–582. https://doi.org/10.1016/j.jsams.2012.12.009
24. Jones AM, Kirby BS, Clark IE, Rice HM, Fulkerson E, Wylie LJ, Wilkerson DP, Vanhatalo A, Wilkins BW (2020) Physiological

demands of running at 2-hour marathon race pace. J Appl Physiol 130(2):369–379. https://doi.org/10.1152/japplphysiol.00647.2020

25. Dantas JL, Doria C (2015) Detection of the lactate threshold in runners: what is the ideal speed to start an incremental test? J Hum Kinet 45:217–224. https://doi.org/10.1515/hukin-2015-0022
26. Bentley DJ, Newell J, Bishop D (2007) Incremental exercise test design and analysis. Sports Med 37:575–586. https://doi.org/10.2165/00007256-200737070-00002
27. Zhang YY, Martin CJ, Chow N, Wasserman K (1991) Effect of exercise testing protocol on parameters of aerobic function. Med Sci Sports Exerc 23:625–630
28. Kuipers H, Rietjens G, Verstappen F, Schoenmakers H, Hofman G (2003) Effects of stage duration in incremental running tests on physiological variables. Int J Sports Med 24:486–491. https://doi.org/10.1055/s-2003-42020
29. Howley ET, Basset DR, Welch HG (1995) Criteria for maximal oxygen uptake: review and commentary. Med Sci Sports Exerc 27:1292–1292. https://doi.org/10.1249/00005768-199509000-00009
30. Poole DC, Wilkerson DP, Jones AM (2008) Validity of criteria for establishing maximal O2 uptake during ramp exercise tests. Eur J Appl Physiol 102:403–410. https://doi.org/10.1007/s00421-007-0596-3
31. Rossiter HB, Kowalchuk JM, Whipp BJ (1985) A test to establish maximum O2 uptake despite no plateau in the O2 uptake response to ramp incremental exercise. J Appl Physiol 100(3):764–770. https://doi.org/10.1152/japplphysiol.00932.2005
32. Nicholas MB, Gibson AL, Janot JM, Kravitz L, Mermier CM, Dalleck LC (2016) Graded exercise testing protocols for the determination of VO2max: historical perspectives, progress, and future considerations. J Sports Med 2016:1–12, Article ID 3968393. https://doi.org/10.1155/2016/3968393
33. Muscat KM, Kotrach HG, Wilkinson-Maitland CA, Schaeffer MR, Mendonca CT, Jensen D (2015) Physiological and perceptual responses to incremental exercise testing in healthy men: effect of exercise test modality. Appl Physiol Nutr Metab 40:1199–1209. https://doi.org/10.1139/apnm-2015-0179
34. Verstappen FT, Huppertz RM, Snoeckx LH (1982) Effect of training specificity on maximal treadmill and bicycle ergometer exercise. Int J Sports Med 3:43–46. https://doi.org/10.1055/s-2008-1026061
35. Borges TO, Bullock N, Aitken D, Cox GR, Coutts AJ (2020) Metabolic cost of paddling on different commercially available kayak ergometers. Int J Sports Physiol Perform 1:1–4. https://doi.org/10.1123/ijspp.2019-0561
36. Baumgart JK, Brurok B, Sandbakk Ø (2020) Comparison of peak oxygen uptake between upper-body exercise modes: a systematic literature review and meta-analysis. Front Physiol 11:412. https://doi.org/10.3389/fphys.2020.00412
37. de Klerk R, Vegter RJ, Goosey-Tolfrey VL, Mason BS, Lenton JP, Vegger DH, van der Woude LH (2019) Measuring handrim wheelchair propulsion in the lab: a critical analysis of stationary ergometers. IEEE Rev Biomed Eng 13:199–211. https://doi.org/10.1109/RBME.2019.2942763
38. Furness J, Bertacchini L, Hicklen L, Monaghan D, Canetti E, Climstein M (2019) A comparison of two commercial swim bench ergometers in determining maximal aerobic power and correlation to a paddle test in a recreational surfing cohort. Sports (Basel) 7:234. https://doi.org/10.3390/sports7110234
39. España-Romero V, Porcel FB, Artero EG, Jiménez-Pavón D, Sainz AG, Garzón MJ, Ruiz JR (2009) Climbing time to exhaustion is a determinant of climbing performance in high-level sport climbers. Eur J Appl Physiol 107:517–525. https://doi.org/10.1007/s00421-009-1155-x
40. Jones AM, Doust JH (1996) A 1% treadmill grade most accurately reflects the energetic cost of outdoor running. J Sports Sci 14:321–327. https://doi.org/10.1080/02640419608727717
41. Skinner JS et al (1999) Reproducibility of maximal exercise test data in the HERITAGE family study. Med Sci Sports Exerc 31(11):1623–1628. https://doi.org/10.1097/00005768-199911000-00020
42. Hopkins WG (2000) Measures of reliability in sports medicine and science. Sports Med 30(1):1–15. https://doi.org/10.2165/00007256-200030010-00001
43. Mcgraw KO, Wong SP (1996) Forming inferences about some intraclass correlation coefficients. Psychol Methods 1(1):30–46. https://doi.org/10.1037/1082-989X.1.1.30

Chapter 22

Muscle and Fat Biopsy and Metabolomics

Cláudia Regina Cavaglieri, Mara Patrícia Traina Chacon-Mikahil, Renata Garbellini Duft, Ivan Luiz Padilha Bonfante, Arthur Fernandes Gáspari, and Alex Castro

Abstract

The analysis of biological fluids and tissues in humans using a metabolomic approach can be somewhat complex if there is not an adequate collection and efficient sample preparation. The adjustment of spectrum acquisition parameters and data analysis are essential both in nuclear magnetic resonance spectroscopy (NMR) and in mass spectrometry (MS). This chapter will focus mainly on the methods and protocols for collecting and preparing biological fluids (blood, saliva, urine) and tissues (adipose and muscle) in humans using ^{1}H NMR.

Key words Metabolomics, Fat biopsy, Muscle biopsy, Blood, Saliva, Urine, Nuclear magnetic resonance

1 Introduction

Since the Human Genome Project, science has been advancing more and more in the area of cellular and molecular biology, expanding a new vision of biology, which is called Systems Biology. Unlike traditional biology that studies genes or proteins individually, Systems Biology seeks a broad and integrated view of systems, metabolic pathways, and their connections to find a comprehensive answer to the functioning of these organisms [1].

General systems theory was introduced in 1920 through researcher Ludwig Von Bertalanffy [2] and later applied by Mihajlo Mesarovic [3, 4], in an attempt to scientifically study the organism in its entirety. The theory found support in mathematical modeling and successfully explored self-regulation systems in biochemical reaction networks, homeostasis, neural, immune, cardiac, and endocrine functions [5].

Cinthia Baú Betim Cazarin (ed.), *Basic Protocols in Foods and Nutrition*,
Methods and Protocols in Food Science, https://doi.org/10.1007/978-1-0716-2345-9_22,

From this advance with Systems Biology, a new approach was explored to understand the interaction between the "omics" sciences (genomics, proteomics, transcriptomics, and metabolomics), using analytical technologies, such as mass spectrometry coupled with other techniques (liquid chromatography or gaseous) and nuclear magnetic resonance. Metabolomics, in particular, identifies and can quantify metabolites, which are small molecules that can be chemically transformed and reflect a functional reading of the physiological state of the organism [6, 7]. Metabolomics offers potential advantages in sensitivity and specificity compared to other omics, classic approaches, and conventional biomarkers measurements [8].

Metabolites are substrates and end products of cellular metabolism that have essential functions such as energy production, storage, signal transduction, and apoptosis [9]. The metabolome represents the set of all metabolites in a cell, biological fluid, tissue, or organism, these substances being considered the end products, which may or may not become a substrate, of cellular processes [10]. It has its roots in investigating global metabolite profiles in biological samples (tissues, cells, fluids, or organisms) under normal conditions compared to altered states promoted by disease, drug treatment, dietary intervention, exercise, or environmental modulation [11]. It has been pointed out as a potential approach for broad classifications and discrimination of various biological states or discovering the origin of these [12].

Due to its prospecting power and a better understanding of biological systems, the interest of the scientific community in metabolomics has been increasing. At the same time, technological advances from chromatographic analytical techniques, from mass spectrometry or hybrids, have facilitated and significantly reduced the cost of data collection [13]. Thus, a huge volume of complex biological data has been generated, which has made it necessary to develop complex computational tools to organize the data, as well as to relate and integrate the interactive molecular networks, since it is necessary to make the dynamic functioning clearer of biological systems [14]. In addition, with the advent of artificial intelligence, there is a need to explore the possibility of discoveries deeply, with machine learning that identifies new patterns and results in helping to make the best decisions, hitherto restricted by limited human capacity [15, 16]. Finally, it is understood that there is a high potential for developing predictive, or prognostic models for more accurate phenotypes, specific conditions or diseases [17, 18] to generate impactful investigations, develop new technologies, and a beneficial change in the paradigms of humanity.

2 Materials

2.1 Biopsy Collection (Muscle and Adipose Tissue)

- Surgical gloves (size dependent on the individual who will use them).
- Nonsurgical gloves.
- Chlorhexidine Digluconate.
- Povidone-iodine (optional as preferred by the physician and nonallergic patient).
- Alcohol 70% (v/v).
- Fenestrated surgical field.
- A surgical field without fenestra (if there is no sterile/autoclaved container for each biopsy).
- Bergstrom needle.
- Tweezers.
- Sterile gauze.
- 1% lidocaine hydrochloride with vasoconstrictor.
- 5 mL syringe.
- Hypodermic needle for 5 mL syringe.
- Scalpel blade (approximately no.11) sterile.
- Autoclave packaging (varied size for Bergstrom needle and tweezers).
- Autoclave masking tape.
- Razorblade.
- Sterile surgical adhesive tape and bandage or material for surgical suture.
- Adhesive tape (occasional needs).
- Bandages (cover for protection and compression can be useful for muscle biopsy recovery).
- Suction Syringe 60 mL (If there is no biological material entering the needle during suction, it can be used more than once in the same day).
- Equipo or extension tube.
- Pipette tip (approximately 200 μL). See the coupling of the suction syringe, equipo, and pipette tip on the Bergstrom needle in Fig. 1.
- Saline solution 0.9% (w/v).
- Microtube for RNAse and DNAse Free to store sample.
- Container with liquid nitrogen for freezing the sample.
- Autoclave, freezer −80 °C and other laboratory facilities.

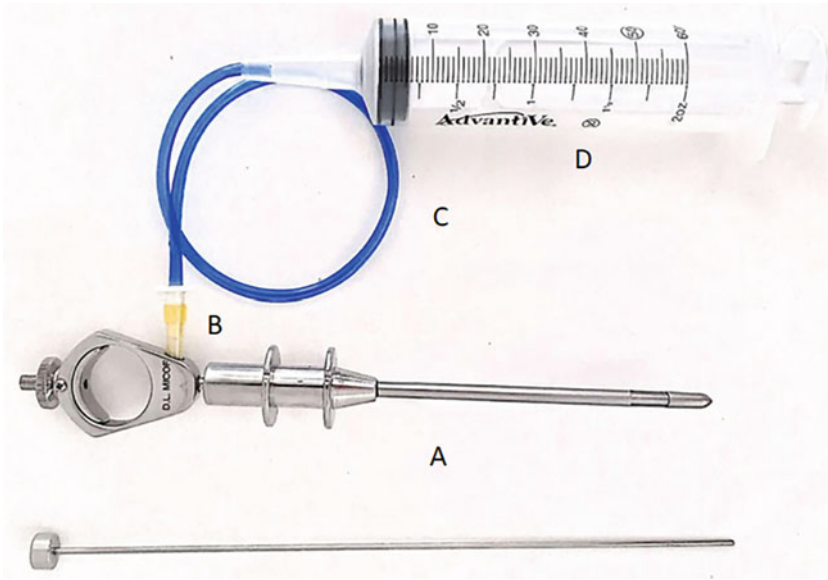

Fig. 1 Bergstrom needle and associated components assembled. A = Bergstrom needle; B = Pipette tip; C = Equipo or extension tube; D = Suction Syringe 60 mL

1. Some materials and procedures to collect blood, urine, and saliva samples are described in Table 1.
2. Consistent use of anticoagulants/Clot Activator additive vacuum containers throughout the study is mandatory.
3. The material of recognized quality is recommended, as contamination even with plastic waste can interfere with the analysis.
4. Paraffin, rubber, or chewing gum paste without coloring and flavor are considered optional materials to stimulate chewing movement saliva collection.

2.2 Preparation of Tissue Samples for NMR

- Mechanical homogenizer.
- Sonicator (VCX 500, Vibra-Cell, Sonics & Material Inc., USA—or similar).
- Milli-Q water (ultrapure water).
- Methanol.
- Chloroform.
- Centrifuge (able to rotate at 20,817 g).
- Vacuum Concentrator (miVac Duo Concentrator, Genevac, UK—or similar).
- Deuterated water (D_2O).
- Electronic precision scale.
- 1 mL and 5 mL tips and their micropipettes.

Table 1
Collection of blood, urine, and saliva

	Blood			
	Serum	**Plasma**	**Urine**	**Saliva**
Tubes and containers	Dry vacuum tubes, with or without serum separator, of 4 mL minimal [1, 2].	Vacuum tubes of 4 mL minimal with EDTA or Heparin [1, 2].	15 mL polypropylene tube (falcon tubes) or bigger commercial containers without special characteristics [2].	15 mL polypropylene tube (falcon tubes) with or without a cotton ball or any absorbent material [2, 3]. Special containers for saliva collection [2, 3].
Sampling materials	Disposable gloves and all personal protection equipment, tourniquet, alcohol 70%, cotton ball or any other absorbent material, needle for vacuum collection devices, bandage for blood collection.			Napkin to clean the participant's residual drool.
Sample storage	1.5 mL polypropylene containers are optimal to store the samples [2]. Liquid nitrogen at −80 °C to immediately freeze and store [4].			
Equipment	Centrifuge (able to rotate at 1500 g), pipettes and tips, −80 °C freezer or liquid nitrogen containers, and other laboratory facilities.			

- Screwcap tubes (polypropylene) with 5–10 mL.
- 2 mL polypropylene microtubes.
- Tweezers and scalpel.
- Petri dish.
- Thermal box.
- Liquid nitrogen.

2.3 Preparation of Serum, Plasma, Saliva, and Urine Samples for NMR

- Filters 3 kDA and its appropriated polypropylene tubes (Amicon Ultra—or similar).
- Centrifuge (able to rotate at 20,817 g).
- Milli-Q water (ultrapure water).
- Deuterated water (D_2O).

2.4 Spectrum Acquisition Solutions

- Phosphate buffer (0.1 M, pH 7.4).
- TMSP-d4 (3-(trimethylsilyl)-2,2′,3,3′-tetradeu-teropropionic acid—0.5 mM (Sigma-Aldrich—or similar).

3 Methods

3.1 Collection Protocol for Muscle and Fat Biopsy

3.1.1 General Aspects of Adipose Tissue Biopsy

The adipose tissue is located in several locations of the organism, from superficial places close to the skin such as the subcutaneous compartments to deeper points such as the intravisceral compartment, ectopic fat, or brown adipose tissue [19].

Usually, a biopsy of visceral and ectopic compartments in the context of clinical research in humans occurs in situations where there is already the presence of a certain surgical procedure, as in the case of bariatric surgery, for example. Biopsies that focus on brown adipocytes analysis are also rare, due to a greater degree of complexity, in terms of being an invasive procedure, as well as the difficulty of the exact location of these adipocytes. Therefore, in addition to the surgical procedure, biopsy of brown adipocytes needs devices such as ultrasound or, for greater reliability, Positron Emission Computed Tomography (PET-CT) in conjunction with the 18F-fluorodeoxyglucose (18FDG) radiopharmaceutical, having its uptake stimulated by exposure to cold [20–22]. Due to the ease of access, manipulation, and less invasive intervention, the subcutaneous adipose compartment, especially the abdominal/waist area, is the most accessed area for adipocyte biopsy in humans.

The main subcutaneous adipocyte biopsy methods are: making a medium incision with the adipose tissue being pulled by tweezers; use of the Punch instrument; and Bergstrom needle [22–24].

The use of a medium incision has as a positive point in a greater amount of tissue collected; however, the need for surgical sutures made up of some stitches and a larger scar is something negative, as it can keep volunteers from research projects. On the other hand, the use of Punch has the advantage of less damage to the skin due to the smaller incision; however, the tissue collected tends to be more superficial (between the skin and above the superficial fascia) and with a significant amount of epithelial tissue. Therefore, we consider the use of the Bergstrom needle the best option since it consists of an intermediary between the positive and negative points of the other two procedures. Bergstrom needle tends to collect an amount of fatty material of higher quality/location than the Punch and with a similar amount of sample, maintaining the need for a small incision and consequently providing a smaller scar, unlike biopsy with a medium incision [22–24]. Thus, we focus below on the biopsy procedure using the Bergstrom needle.

3.1.2 Preparation of the Environment, Materials, and Collection Team

1. The biopsy process must be performed in a room made up of a stretcher and support compartment for additional materials. The room should be a clean place with a pleasant temperature (~23 °C). The stretcher must be covered with a sheet of paper and have a pillow or reclining compartment for head support. For each biopsied individual, the stretcher must be cleaned

with 70% alcohol and coated with paper. It is recommended to use some form of the curtain so that the participant does not maintain eye contact with the procedure, further increasing their anxiety.

2. All material to be used must be sterile, with the Bergstrom needle autoclaved (≥100 °C for 60 min on average, see the cycle time of the used autoclave machine), as well as additional materials such as tweezers for the removal and dissection of tissue samples from the needle. These materials must remain on a sterile surgical field for the operator to use [22–24].
3. The biopsy team must be composed of at least three technicians, or ideally four. Technician 1: A physician who will be the operator responsible for conducting and supervising all aspects of the biopsy procedure. Technician 2: Assistant responsible for assisting the operator in all aspects of tissue extraction, including the application of suction with a sterile syringe. Technician 3: Assistant responsible for receiving, handling, and storing the tissue sample. Technician 4: Assistant responsible for talking and easing the participant's anxiety [24]. All technicians must be dressed in a protective apron. The operator (Technician 1) must wear sterile surgical gloves and the other assistants (Technicians 1 and 2) common gloves.

3.1.3 Preparation of the Participant

1. The individual should abstain from exercise and vigorous physical activity for at least 48 h before the procedure. Fasting for 10–12 h for baseline collections or 90–120 min after a standardized meal before the acute exercise session [25]. The individual should abstain from alcohol for 24 h, caffeine, or any stimulating drink for 12 h. In the case of the use of drugs by the participant, their inclusion in the study must be evaluated considering possibilities of interference with the research objectives and safety issues [22–24]. Other dietary adaptations may be required based on the research objectives.
2. It is advised to standardize the last meal consumed by the participant since the composition of the diet and postprandial time are expected to affect the metabolome [26–29]. It is recommended that this meal be balanced (60% carbohydrate, 25% lipid, and 15% protein), containing 30% or 20% of the estimated individual daily caloric expenditure, for meals offered at dinner and breakfast, respectively [25, 28, 30]. These recommendations can vary depending on research objectives. If it is impossible to offer a standardized meal, the food record must be obtained and the food pattern replicated in subsequent study evaluations.
3. For the biopsy day, the participant must wear flexible clothes to perform the biopsy, such as shorts/shorts and a T-shirt.

4. Before the biopsy starts, the participant must be: asked about possible allergies concerning the materials and substances that will be used (e.g., Iodine and Lidocaine); informed about the procedures described in the research consent form; and alerted about the procedures that will be performed to avoid any problems related to fear or related aspects [22–24].
5. Prior to biopsy, the area to be biopsied should be shaved with razor blades (area of ~15 cm × 15 cm) and cleaned with antiseptic. This cleaning prevents body hair from entering the incision during the procedure and closing, in addition to allowing better contact between the tape closures and the skin.
6. Afterward, the participant must be kept at rest lying down, for at least 15 min, to decrease metabolic demands arising from the displacement to the location, which should be done preferably minimizing the active displacement as much as possible [22–24].
7. For the biopsy of the vastus lateralis muscle, the participant must be positioned lying supine on a stretcher. Place pillows under the leg and the heel so that the knee is fully extended (elevated ~1 cm), thus placing the vastus lateralis in a shortened position. For the adipose tissue, the positioning will depend on the chosen location and should be concentrated in places with a greater amount of subcutaneous fat (abdominal region, hips, and thighs), and that does not have the passage of any nerve/vases, or that may induce damage with the procedure. We recommend a safe place with a good amount of fat in the waist region on the iliac crest; in this case, the participant should lie on the side with the legs slightly flexed.
8. Identify the location to be biopsied. For the vastus lateralis muscle, mark the point immediately anterior to the fascia lata, corresponding to approximately one-third of the distance between the top of the patella and the greater trochanter of the femur (Fig. 2). Then, instruct the participant to momentarily contract the thigh to visualize the muscle to be biopsied. For adipose tissue, the central region over the iliac crest is the place to be objectified (Fig. 2). We recommend that regardless of the material to be biopsied, the chosen side should be standardized among all participants. In the case of a study with an experimental design that has more than one evaluation, we suggest that in addition to the biopsies being performed on the same side, the second is not done on the site/scar of the initial biopsy, since there may be excess fibrous tissue and healing, which can interfere with the results and material collected.
9. Mark ~0.5–1.0 cm below the incision site with a permanent fine-tip marker. Ask the operator to determine the approximate skinfold thickness with the fingers.

Fig. 2 Adipose tissue biopsy: central region over the iliac crest is the place to be objectified

10. Have the operator sterilize the area with prehumidified sterile gauze with a topical antiseptic (iodine-povidone or chlorhexidine gluconate for individuals allergic to iodine/shellfish). Start at the center and work in concentric circles toward the outer edge of the trichotomized area. Repeat this process two more times with new humidified gases.

3.1.4 The Biopsy Procedure

The procedures described below were based on previous literature [23, 24] and adapted according to the guidelines of the surgeon responsible for the biopsies of our research group.

1. Using sterile gloves, with the assistance of technician 2, the operator will place a fenestrated curtain over the site to be biopsied, using an aseptic technique, in order to maintain a sterile field.
2. Technician 2 will present the operator with a 5 mL syringe equipped with a 21 G needle. Then, remove the seal from the lidocaine bottle, clean its top with sterile gauze moistened with antiseptic (iodine-povidone or chlorhexidine gluconate), and position it so that the operator immediately withdraws 5 mL of lidocaine. Afterward, the operator will evacuate the air bubbles from the syringe. Always keep the technique aseptic.
3. The operator will insert the needle into the dermis, approximately horizontally in relation to the thigh or iliac crest, lightly aspirate the needle, and then infiltrate with ~100 μL of lidocaine to produce a 2- to 4-mm diameter "bubble."
4. The operator will then lightly aspirate the syringe to confirm that the needle has not been placed in a blood vessel. If blood appears in the syringe, remove it, dispose of it in a sharps container, and start again.
5. Afterward, the operator will advance the needle into the subcutaneous tissue, aspirate the needle again, and then infiltrate the tissue with ~1 mL of lidocaine to form a blister. Once the bubble has subsided, insert the needle vertically, stopping at the surface of the fascia. In adipose tissue, the insertion of the needle should be concentrated in the dermis and adipose region. The participant may feel a slight sensation of momentary sting on the initial injection of lidocaine (similar to an insect sting).
6. Do not infiltrate muscle tissue with lidocaine because it is myotoxic. For adipose tissue, try to concentrate more anesthesia in the dermis; however, due to the proximity between the dermis and the adipocytes, this interference between anesthetic and tissue is not easy to be controlled.
7. Again, aspirate the needle and then inject the remaining 4 mL of lidocaine while removing the needle from the thigh. In the adipose tissue, the injection of this anesthetic content should

be fan-shaped (directed to form an anesthetized circular region). Afterward, keep a sterile gauze over the injection site while the local anesthetic takes effect.

8. After 2–3 min, technician 2, using aseptic technique, will provide a scalpel blade (No. 11) to the operator, who will lightly examine the biopsy site with the tip of the scalpel to confirm that the area is anesthetized. If necessary, an additional 3–4 mL can be injected into the incision site.
9. The operator will make a straight ~0.5–1.0 cm incision parallel to the femur through the skin, subcutaneous tissues, and muscle fascia. The participant may experience slight discomfort or pressure with the deepest cut if the blade cuts the muscle and fascia. In adipose tissue, we recommend that the straight incision of the same size be made over the central area of the iliac crest.
10. At that time, technician 4 will have a conversation with the participant in order to keep him calm and minimize anxiety.
11. After cutting, the operator will apply sterile gauze pressure directly to the incision site to reduce bleeding.
12. Technician 2 will connect a ~30 cm long plastic tube (serum set) to the end of a 60 mL disposable syringe. For greater sealing, the tape can be used in the tube–syringe junction. Then, the free end of the tube will be connected to the end of the conical connector that comes with the equipment, and it will be connected to the large end of a 200 μL tip with ~15–18 mm of the cut end. The tip cut must be of sufficient size to make a perfect fit with the biopsy needle.
13. After the bleeding subsides, technician 2 will open the envelope containing the sterile biopsy needle. The operator will pick up and assemble the needle and then check its alignment and sliding movement. Keep the technique aseptic throughout the process.
14. The operator will firmly hold the needle assembly (outer cannula and inner trocar) with both hands to prevent the inner trocar from turning. Afterward, technician 2 will firmly insert the cut tip of the tip into the internal trocar of the biopsy needle, promoting a slight twist for a better fit. Make sure technician 2 does not touch the operator or the biopsy needle, just the tip of the tip.
15. The operator will insert the biopsy needle into the tissue through the incision. Locate the fascia with the tip of the biopsy needle. Afterward, advance the needle just beyond the fascia and then tilt it down toward the floor while the needle advances to the muscle. Individuals may experience some discomfort such as “deep pressure” or a cramping sensation, both

mild. In the adipose tissue, the needle should be inserted its initial end slightly downward and later in a parallel way to the skin, looking for the deeper subcutaneous adipose layer (below the superficial fascia and above the iliac crest).

16. Technician 3 will instruct the participant to remain relaxed and not contract the thigh muscles while the operator is advancing the needle into the muscle. For the adipose tissue, ask the participant to remain generally relaxed, especially the abdominal, hip, and thigh regions.
17. When the biopsy needle is in position, the operator will signal technician 2 to prepare to open the 60 mL disposable syringe. At the operator's signal, technician 2 will quickly pull the syringe plunger up to the 40–50 cc mark to create suction inside the biopsy needle.
18. The operator will pull the internal trocar outward (~1 cm) to open the external cannula window, maintaining the position of the external trocar within the muscle. Then, the operator will quickly close the internal trocar to cut (hold) and collect the muscle sample. The operator can rotate the biopsy needle by 90°, and the procedure can be repeated up to a total of four cuts. After collecting the sample, the operator will signal Technician 2 to release the suction, disconnecting the tip with the biopsy needle.
19. When removing the thigh biopsy needle/waist, the operator will apply direct back pressure to the incision site with sterile gauze, always taking care not to trap the fascia or the skin. If there is significant resistance, cut again while applying a twisting motion to the internal trochanter.
20. After removing the biopsy needle from the thigh/waist, the operator will pull the internal trocar (~1 cm) back to visually inspect the lumen on the outer side of the cannula to estimate whether an adequate amount of tissue has been collected.
21. The operator will deliver the biopsy needle to Technician 3, ensuring the aseptic technique. Technician 3 will remove the tissue from the biopsy needle using the plunger and a pair of fine-tipped forceps to ensure that all muscle tissue is removed from the inside of the trocar and outer cannula. For adipose tissue, as sometimes the desired amount of sample may not be sufficient, we recommend that the needle be kept with the operating physician (Technician 1) until the material collected by technician 3 is removed as if the procedure is necessary (**steps 15–20**) can be performed again.
22. The sample collected should be placed on a cold block and bathed with saline to remove excess blood, while carefully and visible connective tissue and fat from muscle samples are dissected as quickly as possible. In the adipose tissue, keep the

same procedure, paying attention to possible excess of connective tissue or fragments of skin along with the sample. Posteriorly, these samples will be immediately stored in cryotubes or microtubes with or without RNase inhibitor and DNase, or prepared for histology when appropriate, and then immersed in liquid nitrogen followed by freezer storage at −80 °C for further analysis. In addition to metabolomics and lipidomics, analysis of gene and protein expression also has this same procedure for sample storage. If the procedure is immunohistochemistry, the collected fragment must be placed in an anti-RNAse and anti-DNAse microtube, but with 4% paraformaldehyde that should be exchanged for 70% alcohol between 24 and 48 h after collection and kept there until the subsequent lamination of the fragment.

23. After reaching the target amount of sample, manual pressure will be applied with sterile gauze for a few minutes over the incision site to prevent bleeding. The closure of the incision will depend on what those responsible for the procedure will choose. It can be through traditional surgical suture using a surgical stitch or sterile surgical adhesive tape after joining the suture edges to be covered with a small bandage to prevent its detachment. In the case of surgical suture, hemostasis is more favorable and decrease the risk of possible subsequent bleeding, being indicated for people with some clotting problem or who use some medication with an anticoagulant effect, or even if the procedure site is subject to high movement, as close to some joint for example. However, the scar tends to look less beautiful, and there is a need for an additional visit to remove the surgical point. With the use of adhesive tape, the scar tends to be better aesthetically, and there is no need for an additional visit to remove the suture. However, there may be the possibility of minor bleeding and the need for further use of an ice pack in the 15 min following this suture to minimize possible edema and bleeding.

3.1.5 Postbiopsy Recommendations

1. In the case of suture via surgical tape, the individual will be instructed to keep the small bandage for 24 h and keep the incision clean and dry for the same period and maintain the surgical tape for 72 h. If the surgical suture is performed, its removal must be done by a qualified professional within ~5 days after the procedure.
2. Provided that all precautions are observed, complications due to this procedure are rare and extend to minor posterior bleeding and local edema, which must be treated with a straightforward application of cold (ice wrapped in a bag) and compression [22–24].

4 Blood, Urine, and Saliva Collection

First, it is necessary to separate and organize all materials used in this procedure before start. A datasheet with names and codes of volunteers, as well as some labels to stick to or a permanent pen to write on tubes, microtubes, and containers is fundamental. Depending on the urine sampling rate protocol of the study, labeled containers have to be given to participants previously. It is also necessary to take notes about everything from the volunteer: fasting state, drugs, date, and time.

4.1 Blood

1. Use vacutainer equipment for blood sampling and appropriate protective equipment. The procedure must follow safety guidelines and be performed by a nurse or trained person. Collect the required amount of blood according to the analyses that will be performed.
2. *Blood serum*: Blood is collected in a red top dry tube (without additives) and with or without a serum separator. Leave the tube around 30 min at room temperature (~24 °C) for clotting (*see* **Notes 9.1**, **step 3**). Then, the tubes are centrifuged at 1500 g for 10 min. Transfer the small serum aliquots to 1.5 mL microtubes using a pipette and store them at −80 °C.
3. *Blood Plasma*: Blood is collected in a purple tube with an anticoagulant EDTA or heparin (green tubes) and gently mixed by inverting the tube 5–6 times. Heparin tubes are advisable to be used for NMR analysis since, unlike EDTA and citrate tubes, no peaks from heparin interfere with peaks from plasma metabolites. Then, the tubes are centrifuged at 1500 g for 10 min. Transfer the small plasma aliquots to 1.5 mL microtubes using a pipette and store them at −80 °C.

4.2 Urine

1. Choose the sampling protocol: Urine samples can be obtained from a single collection or the total urine produced 24 h. For example, for urine collection at "first-morning urine" or 24 h, urine production labeled containers have to be given to participants previously. The metabolic composition of these urine samples is different, and the collection methodology must be standardized and indicated in the study protocol [31–33].
2. Regardless of whether the sample is the result of a single collection or the sum of several collections to compose a single sample with a total urine volume of 24 h, the initial stream of urine should be neglected and the intermediate portion used as a sample [31–33]. Not using the first stream is strongly recommended to minimize contamination with bacteria, cells, and particles of the genital mucosa and urethra [32, 33]. To collect the first urine eliminated in the morning, after resting during

the night, and before eating any food and any physical activity will confer a better and reproducible picture of the urine metabolomics profile [33]. Depending on the research study proposal, urine may be collected after an experimental protocol as ingestions of food products, physical activity, medicines, or another intervention. However, in these cases, a urine sample control pre- and post-experimental protocol are suggested, and more posttime collections may be necessary depending on the research question.

3. After collection, centrifuge at 1500–2000 g for 10–20 min at 4 °C to remove cell debris, bacteria, and suspended materials and store the sample under minimum refrigeration of 4 °C. In studies with 24-h urine using samples collected during this period group the different samples in a single common recipient, it should be taken care to maintain adequate storage of all intermediate samples.
4. Collect and store the urine sample in polypropylene containers. Use the sample, stored at 4 °C, within 48 h after collection [31–33]. Alternatively, aliquot samples and freeze as cold as possible (liquid nitrogen or −80 °C freezer is recommended) to the storage, avoiding refreezing procedures and allowing homogeneous aliquots for subsequent analysis without having to thaw the total amount of urine collected initially (TIP: we suggest 1.5 mL aliquots) [31–33]. Long-term storage at −20 °C for up to 6 months and −80 °C can last as long as years.

4.3 Saliva Collection

1. Choose the sampling protocol: The collection of whole-mouth saliva, nonspecific by the gland, can be unstimulated (topic 2) and stimulated (topic 3). Differences in pH and composition of saliva samples obtained in a stimulated or nonstimulated manner indicate the need for standardization of the collection method and indication in the protocol of which method was used [34]. The saliva sample must be collected at the same time of the day to avoid interference from the circadian rhythm [35, 36], and at an interval of 90–120 min before collection, the donor must not eat, drink, smoke, or brush his teeth [35].
2. The unstimulated collection corresponds to the saliva obtained from the mixture of secretions that enters the mouth in the absence of exogenous stimuli and depends on the daily basal salivary flow rate in the oral cavity. The composition of the unstimulated saliva sample is influenced by hydration, head position, body posture, and circadian rhythm [34].
   (a) For the collection of unstimulated saliva, the individual tilts the head forward and leaves the saliva flows out of the mouth, which is being produced naturally, passively, drop by drop, into a container, for example, graduated 15 mL polypropylene tube. The individual should not make movements with the jaws or tongue or spit [34].

(b) The unstimulated saliva sample can also be obtained by placing a cotton ball or absorbent material in the mouth; some commercial devices are available. The material must not be chewed or moved in the mouth. Then, the absorbent material is centrifuged (600–2000 g for 2–5 min), and the liquid extracted from the absorbent material is used as a sample [34].

(c) Collecting unstimulated saliva may be time-consuming, so instruct the individual to drop the saliva for up to 10 min or until a volume of 6 mL of sample is obtained.

3. The stimulated collection corresponds to the secreted saliva in response to mechanical stimuli of masticatory movements, movements with the jaws or tongue or spit. Some materials such as paraffin, rubber, or chewing gum paste without coloring and flavor can stimulate chewing movement. The masticatory movement increases the flow rate, and the desired volume of the sample is obtained more quickly. Saliva is collected by spit in a polypropylene tube (15 mL falcon tubes), and the sample is centrifuged at 2000 g for 10–15 min to separate the clarified saliva from emulsion (foam), mucin aggregates, and mucosal particles, the stimulating material of the masticatory movement [34].
4. After collection, the saliva sample can be kept at 4–22 °C for up to 6 h or at −20 °C for up to 4 weeks. Saliva samples kept at −80 °C have been tested stable for up to 4 weeks, but the limited time of stability can be much longer (stability time limit unknown) [35].

5 Metabolomics Muscle NMR Protocol

1. Weigh fragments of muscle tissue (~40 mg) still frozen. Keep the cryotubes with the samples in a styrofoam box with liquid nitrogen to be able to promote the immediate freezing of the sample if necessary. The sample weight will be used for data normalization.
2. After weighing, immediately add the sample to a cold methanol/chloroform solution (2:1 v/v, 2.5 mL total). This solution can be stored in falcon or Eppendorf tubes (>5 mL) immersed in ice.
3. Homogenize the tissues while still on ice. Using a mechanical homogenizer, perform 3 cycles of 30 s, interspersed with 10 s of pause. Repeat the process until the fibers in the sample are broken and dispersed in the solution. Be careful not to heat the sample.

4. After ~15 min in contact with the first solvent, add a cold solution of chloroform/Milli-Q water (1:1 v/v, 2.5 mL total) to the sample.
5. Vortex the samples briefly until an emulsion is formed and after centrifuging them at 2000 g, for 30 min at 4 °C. Make sure the tube will withstand centrifugation. Preferably use fixed rotors for a more aligned separation of the mixture in relation to the vertical position of the tube.
6. After centrifuging, the upper phase of the mixture (methanol, water, and polar metabolites) will be collected and must be completely dried in a vacuum concentrator (miVac Duo Concentrator, Genevac, UK) at room temperature (24 °C). For 2 mL of solution, approximately 8–10 h are expected until complete drying.
7. Finally, the remaining solid phase can be rehydrated in 0.6 mL deuterium oxide containing phosphate buffer (0.1 M, pH 7.4) and 0.5 mM TMSP-d4. Be sure to shake the tube sufficiently with the sample to detach from the tube and solubilize it in the solution. Then, add the solution to a 5 mm NMR tube (Wilmad Standard Series 5 mm, Sigma-Aldrich®) for reading and immediate spectra acquisition on the spectrometer.
8. Before starting to acquire the spectra, make sure that there are no bubbles, scratches, and fingerprints on the NMR tube that may interfere with the acquisition of the spectra.

6 Metabolomics Blood, Urine, and Saliva NMR Protocol

1. Thaw samples of serum, plasma, urine, and saliva at room temperature (~24 °C), if stored in the freezer before analysis.
2. To remove proteins and other big molecules from the sample, use filters 3kDA (Amicon Ultra or similar).
3. First, the filters must be washed with 500 μL of H20 Milli-Q and centrifuged at 20,817 g for 10 min at 4 °C five times.
4. After, add 350 μL of the sample inside the filter and centrifuge at the same rotation and temperature for 45 min. The filtered solution can be frozen at −80 °C to use later.
5. The filtered solution (250 μL) was diluted in 290 μL deuterium oxide solution (D_2O, 99.9%; Cambridge Isotope Laboratories Inc., USA) containing 60 μL of phosphate buffer (0.1 M, pH 7.4) with 0.5 mM TMSP-d4 (3-(trimethylsilyl)-2,2′,3,3-′-tetradeu-teropropionic acid from Sigma-Aldrich), completing the volume of 600 μL.
6. The mixture should be transferred to a standard 5 mm NMR tube (Wilmad Standard Series 5 mm, Sigma-Aldrich) for immediate acquisition.

7 Spectra Acquisition—NMR

This set-up is specific for the 600 MHz NMR Varian Inova (*Agilent Technologies* Inc., Santa Clara, CA, EUA).

1. Insert the tube with the sample into the NMR magnet.
2. Create a data parameter file for 1H acquisition. Perform probe and sample tuning with the spectrometer.
3. Perform field-frequency locking using the D_2O signal to prevent fluctuations in the magnetic field generation, stabilizing the measurement.
4. Perform one gradient shimming and then adjust manually to improve the resolution of the signal with the homogenization of the magnetic field used for the sample inside the probe (probe) through the *X*, *Y*, and *Z* axes, making all points of the sample receive the same magnetic field.
5. Set pulse sequence for residual water suppression using presaturation.
6. Set the Parameters: temperature of 298 K (25 °C), 256 scans, 4 s, and relaxation delay intervals between scans of 1.5 s.
7. Adjust offset frequency to the center of the water signal.
8. Adjust receiver gain.
9. Acquire the data.
10. Save the acquisition

8 Metabolites Identification and Quantification—NMR

1. For processing and quantifying the metabolites, it is possible to use Chenomx RMN Suite software (Chenomx Inc., Edmonton, AB, Canada). The first part is done in the Processor module.
2. *Phase adjustment*: Make the spectrum as linear as possible so that the baseline was a horizontal line and not invaded by the peaks.
3. *Baseline correction*: It is necessary to prevent the under or overestimated concentration values. Adjust the baseline, passing it as close as possible to the base of the peaks without invading them.
4. *Line broadening*: Apply a Fourier transformation after multiplying the FID (free induction decay) by exponential multiplication with a line broadening typically of 0.3–0.5 Hz to decrease the noise in the signals and facilitate the fitting of the metabolite signals to the peaks of the spectrum.

5. *Removal of the water signal*: Remove the water region from the spectrum to avoid signal suppression, making it difficult to quantify the metabolites due to the intensity of the water signal.
6. *Reference Signal Adjustment*: Certificate that the TMSP peak is symmetrical because it will serve as a reference to calculate the concentration of the other metabolites.
7. *Spectrum Calibration*: Calibrate the spectrum and save the modifications.
8. The second part is performed in the Chenomx Profiler. The peak profiling should be manually adjusted since this does not automatically occur satisfactorily. After the adjustments, the metabolite concentration is obtained automatically by the software through the use of the concentration TMSP, known as a reference.

8.1 Data Analysis and Interpretation

First, when completing the quantification of spectra in Chenomx, export the raw data in a file configured to have samples in rows and metabolites in columns. This exportation will facilitate data analysis in most statistical software.

1. Afterward, be sure to proceed with the corrections of the concentrations. The raw data obtained in Chenomx are generally related to the concentration of the diluted metabolites in the solution of the NMR tube and not in the biological sample itself. For tissue samples, divide the obtained concentration value of the metabolite by the respectively used tissue mass. For fluid samples, use the following equation: C_I * $V_I = C_F$ * V_F, where C_I is the initial concentration of the metabolite in the sample to be known, V_I is the sample volume used in the preparation (e.g., 250 μL), C_F is the final concentration of the metabolite in the NMR tube (final obtained value after quantification in Chenomx), and V_F is the final volume of the solution (e.g., 600 μL) inserted in the NMR tube.
2. Now, the data can be preprocessed to then be analyzed by multivariate and/or univariate statistics, as well as by bioinformatics techniques, which will be used to extract the relevant information from the large data set obtained.
3. Initially, multivariate techniques can be used to reduce the data amount and facilitate the determination of specific patterns and identify discriminating variables in the data set.
4. The first step in conducting multivariate analyzes is to decrease the heterogeneity of the data due to biological variations and experimental conditions. For this, they can be normalized by average, median, or sum of data, by an internal reference, among other methods. Also, nonlinear transformations such as logarithmic or cubic root can be used [37, 38].

5. The next step is to standardize the variables scale. This procedure adjusts the differences in the concentrations of the metabolites through a relative scale factor, allowing the comparison between them. The techniques most commonly used for this purpose are autoscaling, Pareto scaling, range scaling, and mean centering [37].
6. The best combination between applying data transformation techniques and scaling will be the one that results in the greatest symmetry between the data distribution curves [37].
7. After transformation, standardization of scales, and inspection of missing values in the spreadsheet, the data are ready to analyze data dimensionality reduction and identify significant metabolites. Indeed, countless techniques can be used and paths to be followed depending on the research objectives, which is the subject of an extensive book. In this sense, we present only a summary of techniques that can be used for the analysis until interpreting the data (Fig. 1).
8. For metabolomic analysis, many software can be used. The most cited in the literature with the potential to perform statistical analysis and data visualization are integration of omic data, analysis of pathways and networks are Ingenuity Pathway Analysis, MetaCore, PaVESy, Proteome Software, VisANT, VANTED, MassTrix, ProMeTra, MetaboAnalyst, Paintomics, MetPa, IMPaLa, and InCroMAP e 3Omics [39].
9. Finally, for the interpretation of results, several biological databases are available in the literature, which can contribute to understanding the relationship of metabolites and their pathways, such as the Kyoto Encyclopedia of Genes and Genomes (KEGG) [40], the small molecule pathway database (SMPDB) [41], MetaCyc [42], WikiPathways [43], Human Metabolome Database (HMDB) [44], and others.
10. Before analysis, raw data are preprocessed to produce normalized data for multivariate and univariate statistical analyses. Significantly expressed metabolites are then linked to the biological context through enrichment and pathway analysis and biological network construction. Finally, metabolomics data can be integrated with other "omics" data and prior knowledge to provide a comprehensive view of the molecular processes involved (Fig. 3) [39, 45–47].

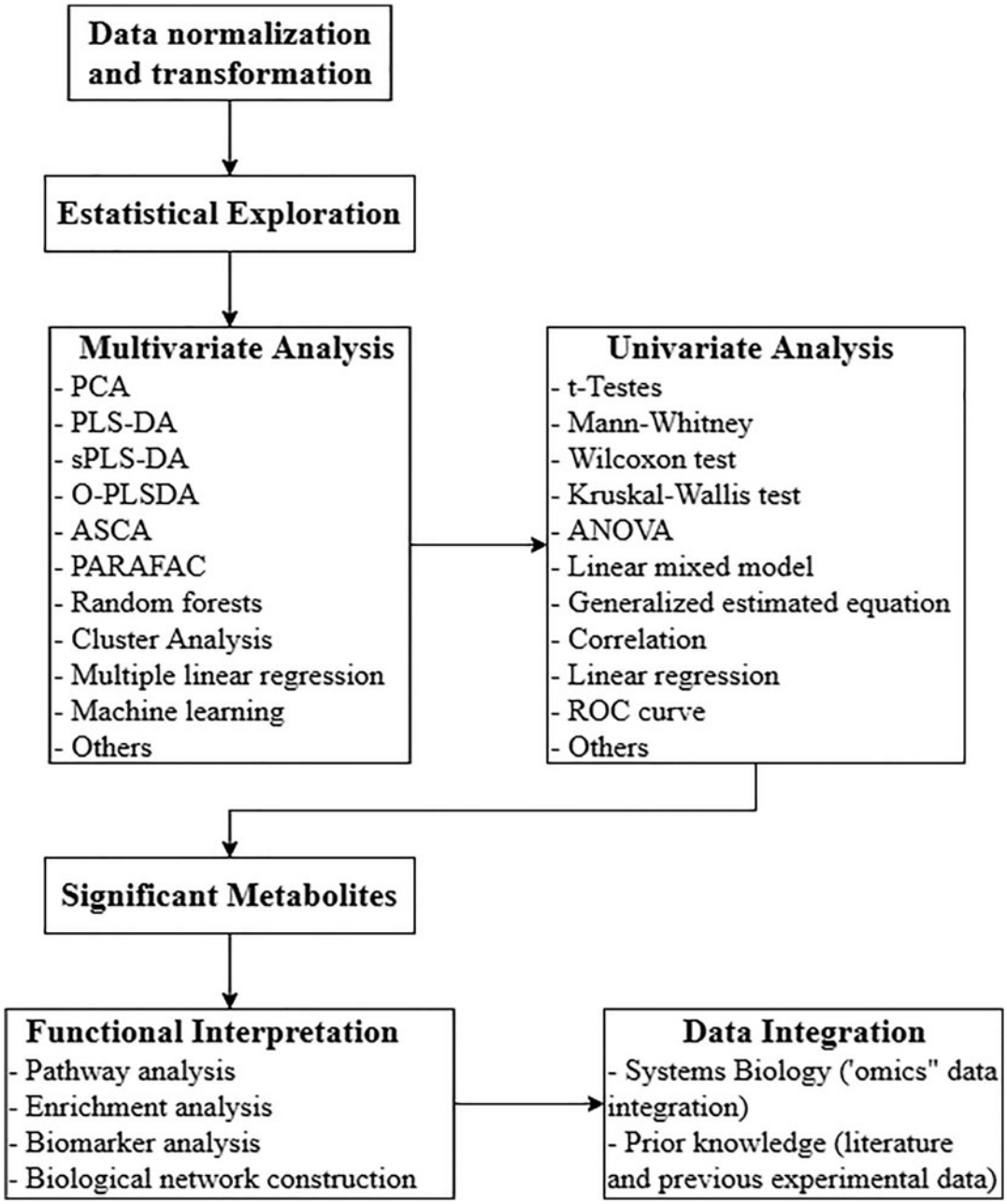

Fig. 3 Flowchart of a typical metabolomics study

9 Notes

9.1 Blood Analysis, Urine, and Saliva

1. Fasting in blood collection procedures in humans is extremely important due to biological and dietary variations, especially for experiments involving metabolomics, where the sensitivity of the equipment requires care and food intake is known to alter sample metabolomics profile. Therefore, it is necessary to have a spreadsheet with all the volunteer's data, check the fasting status, and medications taken in the routine or the day before, among other data.
2. Great care must be taken at the time of blood collection so that hemolysis does not occur, as the rupture of red blood cells will cause the blood to mix with the plasma, altering the subsequent analyses.
3. Samples must be kept resting for at least 30 min to avoid unwanted cellular components, and those that are kept for longer than an hour can have contamination from cell lysis and glycolysis products.
4. The phosphate buffer is used to decrease possible errors in identifying metabolites caused by chemical shifts due to pH variation. This buffer provided stabilization without pH of the protections, keeping it in the range of 7.4.
5. This range of 7.4 is interesting since a Chenomx software library, normally used for the quantification of metabolites, has two pH ranges: 6–9 and another of 4–9. Due to its wide pH variation, this second one contributed to the possible mismatches, which would be an incorrect quantification of the metabolites. The first, which was used, minimized this type of error.
6. The TMSP-d4 of known concentration was used as an internal reference for the quantification of metabolites.

9.2 Biopsy and Muscle Analysis

1. It is recommended that more than one suction accessory be prepared before starting. In case of contamination of the accessory, it can be replaced immediately.
2. To interrupt the metabolic activity in the tissue as quickly as possible after collection, we recommend weighing the sample just when frozen prior to analysis. In a pilot study, become familiar with the tissue size (volume) compatible with the amount of tissue required in the study.
3. In pilot studies, we observed good quality of NMR spectra for samples with mass greater than 30 mg in an experiment with humans. Perform pilot tests to identify the smallest amount of tissue that allows an accurate reading on your equipment.

References

1. Ideker T, Galitski T, Hood L (2001) A new approach to decoding life: systems biology. Annu Rev Genomics Hum Genet 2:343–372. https://doi.org/10.1146/annurev.genom.2.1.343
2. Bertalanffy LV (1972) The history and status of general systems theory. Acad Manag J 15(4): 407–426
3. Mesarović MD (1968) Systems theory and biology – view of a theoretician. In: Mesarović MD (ed) Systems theory and biology. Springer, Berlin, Heidelberg
4. Mesarovic MD, Sreenath SN, Keene JD (2004) Search for organising principles: understanding in systems biology. Syst Biol 1(1):19–27
5. Ederer M, Sauter T, Bullinger E et al (2003) An approach for dividing models of biological reaction networks into functional units. Simulation 79(12):703–716
6. Patti GJ, Yanes O, Siuzdak G (2012) Innovation: metabolomics: the apogee of the omics trilogy. Nat Rev Mol Cell Biol 13(4):263–269
7. Trivedi DK, Hollywood KA, Goodacre R (2017) Metabolomics for the masses: the future of metabolomics in a personalized world. New Horiz Transl Med 3(6):294–305
8. Monteiro MS, Carvalho M, Bastos ML, Guedes P (2013) Metabolomics analysis for biomarker discovery: advances and challenges. Curr Med Chem 20(2):257–271
9. Johnson CH, Ivanisevic J, Siuzdak G (2016) Metabolomics: beyond biomarkers and towards mechanisms. Nat Rev Mol Cell Biol 17(7):451–459. https://doi.org/10.1038/nrm.2016.25. Epub 2016 Mar 16
10. Fiehn O (2002) Metabolomics – the link between genotypes and phenotypes. Plant Mol Biol 48:155–171
11. Klassen A, Faccio AT, Canuto GAB et al (2017) Metabolomics: definitions and significance in systems biology. In: Sussulini A (ed) Metabolomics: from fundamentals to clinical applications. Advances in experimental medicine and biology 965. Springer, Cham, pp 3–17
12. Krastanov A (2010) Metabolomics – the state of art. Biotechnol Biotechnol Equip 24: 1537–1543
13. Pinu FR, Beale DJ, Paten AM et al (2019) Systems biology and multi-omics integration: viewpoints from the metabolomics research community. Metabolites 9(4):76. https://doi.org/10.3390/metabo9040076
14. Subramanian I, Verma S, Kumar S et al (2020) Multiomics data integration, interpretation, and its application. Bioinform Biol Insights 14:1–24. https://doi.org/10.1177/1177932219899051
15. Martorell-Marugán J, Tabik S, Benhammou Y et al (2019) Deep learning in omics data analysis and precision medicine. In: Husi H (ed) Computational biology. Codon Publications, Brisbane
16. Chicco D, Heider D, Facchiano A (2020) Artificial intelligence bioinformatics: development and application of tools for omics and inter-omics studies. Front Genet. https://doi.org/10.3389/fgene.2020.00309
17. Sanchez-Martinez S, Camara O, Piella G, Cikes M, Gonzalez Ballester MA, Miron M, Vellido A, Gomez E, Fraser A, Bijnens B (2019) Machine learning for clinical decision-making: challenges and opportunities. Preprints: 2019110278. https://doi.org/10.20944/preprints201911.0278.v1
18. Tahir UA, Gerszten RE (2020) Omics and cardiometabolic disease risk prediction. Annu Rev Med 71(1):163–175
19. Giralt ME, Villarroya F (2013) White, brown, beige/brite: different adipose cells for different functions? Endocrinology 154(9):2992–3000. https://doi.org/10.1210/en.2013-1403
20. Cypess AM, Lehman S, Williams G et al (2009) Identification and importance of brown adipose tissue in adult humans. N Engl J Med 360:1509–1517. https://doi.org/10.1056/NEJMoa0810780
21. Chondronikola M, Annamalai P, Chao T et al (2015) A percutaneous needle biopsy technique for sampling the supraclavicular brown adipose tissue depot of humans. Int J Obes (Lond) 39(10):1561–1564. https://doi.org/10.1038/ijo.2015.76. Epub 2015 Apr 29
22. Alderete TL, Settler FR, Sheng X et al (2015) A novel biopsy method to increase yield of subcutaneous abdominal adipose tissue. Int J Obes (Lond) 39(1):183–186. https://doi.org/10.1038/ijo.2014.90. Epub 2014 May 21
23. Tarnopolsky MA, Pearce E, Smith K, Lach B (2011) Suction-modified Bergström muscle biopsy technique: experience with 13,500 procedures. Comparative study. Muscle Nerve 43(5):717–725. https://doi.org/10.1002/mus.21945
24. Shanely RA, Zwetsloot KA, Triplett NT et al (2014) Human skeletal muscle biopsy proce-

dures using the modified Bergström technique. J Vis Exp (91):51812. https://doi.org/10.3791/51812

25. Castro A, Duft RG, Zeri ACM et al (2020) Commentary: metabolomics-based studies assessing exercise-induced alterations of the human metabolome: a systematic review. Front Physiol 11:353. https://doi.org/10.3389/fphys.2020.00353
26. Daskalaki E, Blakburn G, Kalna G et al (2015) A study of the effects of exercise on the urinary metabolome using normalisation to individual metabolic output. Metabolites 5(1):119–139. https://doi.org/10.3390/metabo5010119
27. Karimpour M, Surowiec I, Wu J, Gouveua-Figueira S (2016) Postprandial metabolomics: a pilot mass spectrometry and NMR study of the human plasma metabolome in response to a challenge meal. Anal Chim Acta 908:121–131. https://doi.org/10.1016/j.aca.2015.12.009
28. Shrestha A, Mullner E, Poutanen K et al (2017) Metabolic changes in serum metabolome in response to a meal. Eur J Nutr 56(2): 671–681. https://doi.org/10.1007/s00394-015-1111-y
29. Giskeødegård GF, Andreassen T, Bertilsson H et al (2019) The effect of sampling procedures and day-to-day variations in metabolomics studies of biofluids. Anal Chim Acta 1081: 93–102. https://doi.org/10.1016/j.aca.2019.07.026
30. Peake JM, Tan SJ, Markworth JF et al (2014) Metabolic and hormonal responses to isoenergetic high-intensity interval exercise and continuous moderate-intensity exercise. Am J Physiol Endocrinol Metab 307(7): E539–E552. https://doi.org/10.1152/ajpendo.00276.2014
31. González-Domínguez R, González-Domínguez Á, Sayago A, Fernández-Recamales Á (2020) Recommendations and best practices for standardizing the pre-analytical processing of blood and urine. Samples in metabolomics. Metabolites 10(6):229. https://doi.org/10.3390/metabo10060229
32. Bi H, Guo Z, Jia X et al (2020) The key points in the pre-analytical procedures of blood and urine samples in metabolomics studies. Metabolomic 16(6):68. https://doi.org/10.1007/s11306-020-01666-2
33. Emwas AH, Roy R, McKay RT et al (2016) Recommendations and standardization of biomarker quantification using NMR-based metabolomics with particular focus on urinary analysis. J Proteome Res 15(2):360–373
34. Bellagambi FG, Lomonaco T, Salvo P et al (2020) Saliva sampling: methods and devices. An overview. Trends Anal Chem 124: 124115781. https://doi.org/10.1016/j.trac.2019.115781
35. Duarte D, Castro B, Pereira JL et al (2020) Evaluation of saliva stability for NMR metabolomics: collection and handling protocols. Metabolites 10:515. https://doi.org/10.3390/metabo10120515
36. Gardner A, Carpenter G, So PW (2020) Salivary metabolomics: from diagnostic biomarker discovery to investigating biological function. Metabolites 10(2):47. https://doi.org/10.3390/metabo10020047
37. Van Den Berg RA, Hoefsloot HCJ, Westerhuis JA et al (2006) Centering, scaling, and transformations: improving the biological information content of metabolomics data. BMC Genomics 7:142. https://doi.org/10.1186/1471-2164-7-142
38. Duft RG. Castro A, Mikahil MPTC, Cavaglieri CR (2017) Metabolomics and exercise: possibilities and perspectives. Motriz: Rev Educ Fis. Rio Claro 23(2). https://doi.org/10.1590/s1980-6574201700020010
39. Cambiaghi A, Ferrario M, Masseroli M (2017) Analysis of metabolomic data: tools, current strategies and future challenges for omics data integration. Brief Bioinform 18(3):498–510
40. Tanabe M, Kanehisa M (2012) Using the KEGG database resource. Curr Protoc Bioinformatics. Chapter 1:Unit1.12. https://doi.org/10.1002/0471250953.bi0112s38
41. Jewison T, Su Y, Disfany FM et al (2014) SMPDB 2.0: big improvements to the small molecule pathway database. Nucleic Acids Res 42:D478–D484. https://doi.org/10.1093/nar/gkt1067
42. Caspi R, Billingtib R, Ferrer L et al (2016) The MetaCyc database of metabolic pathways and enzymes and the BioCyc collection of pathway/genome databases. Nucleic Acids Res 44 (D1):D471–D480. https://doi.org/10.1093/nar/gkv1164
43. Kelder T, van Iersel MP, Hanspers K et al (2012) WikiPathways: building research communities on biological pathways. Nucleic Acids Res 40:D1301–D1307. https://doi.org/10.1093/nar/gkr1074
44. Wishart DS, Feunang YD, Marcu A et al (2018) HMDB 4.0: the human metabolome database for 2018. Nucleic Acids Res 46(D1): D608–D617. https://doi.org/10.1093/nar/gkx1089

45. Chong J, Soufan O, Caraus I et al (2018) MetaboAnalyst 4.0: towards more transparent and integrative metabolomics analysis. Nucleic Acids Res 46(W1):W486–W494. https://doi.org/10.1093/nar/gky310
46. Lamichhane S, Parthi S, Dickens AM et al (2018) An overview of metabolomics data analysis: current tools and future perspectives. Compr Anal Chem 82:387–413. https://doi.org/10.1016/bs.coac.2018.07.001
47. Chong J, Xia J (2020) Using MetaboAnalyst 4.0 for metabolomics data analysis, interpretation, and integration with other omics data. Methods Mol Biol 2104:337–360

INDEX

A

Animal model 3, 17, 18, 34–36, 39, 40, 44, 49, 54–62, 67, 68, 170, 173, 176, 196, 197
Anthropometric assessment
  body mass index (BMI) 296, 298, 300, 303
  body weight 294, 296, 299
  circumferences 294, 297–300, 303
  height 294–296, 300, 301, 303, 304
  skinfolds 294, 299–303
Antioxidant status 187–194
Appetite
  hunger 249, 258, 261
  satiation 258
  satiety 258
  visual analogue scales (VAS) 256, 258, 259

B

Bile acid
  chenodeoxycholic acid (CDCA) 115–117, 125
  cholic acid (CA) 115–117, 125
  deoxycholic acid (DCA) 116, 118, 124, 126
  lithocholic acid (LCA) 116, 118, 124, 126
Bioavailability
  bioactive compounds 195–204
Biological sample
  bile 108, 115–125
  blood 110, 116, 119–121, 146–148, 238
  feces 116, 119, 120, 122, 125
  intestinal contents 116, 119, 122, 125
  intestinal mucosa 119–121
  liver 110, 115–117, 119–121, 123, 124, 153
  plasma 110, 112, 116, 119–121, 124, 146, 147, 149
  urine 116, 119–121, 124, 238
Blood glucose 35, 39, 41–43, 46–48, 68, 130, 344, 349
Body composition analysis
  magnetic resonance imaging (MRI) 307–330
Body fluid 116, 119, 147
Body weight gain (BWG)
  automated weighing scales (AWS) 25
  manual weighing 23, 24, 26, 27

C

Cardiorespiratory fitness (CRF)
  aerobic performance 367
  maximal oxygen consumption 367

D

Dysgeusia 210, 211, 214, 219, 220

E

Energy efficiency 17–28
Erythrocyte 140–142
Experimental diet
  diet-induced obesity (DIO) 8

F

Fasting 20, 35, 39–41, 43, 44, 47, 48, 56, 68, 130, 138, 196, 198–200, 202, 287, 288, 344, 345, 349, 351–354, 358, 362, 387, 394, 402
Fecal microbiota transfer (FMT) 170, 176
Food intake
  automated weighing scales (AWS) 21
  doubly labeled water method 232
  food consumption 224, 228
  food diary 224–226, 228, 232, 239
  food frequency questionnaire 224–226, 228, 232, 239
  food record 226, 229
  manual weighing 19, 20, 22–24, 26, 27
  pellet dispensers 19, 20, 22–24
  24-hour dietary recall 224–226, 228, 232, 239
  video-based systems 23, 24
  weighted food record (WFR) 226, 229–230, 241

Cinthia Baú Betim Cazarin (ed.), *Basic Protocols in Foods and Nutrition*,
Methods and Protocols in Food Science, https://doi.org/10.1007/978-1-0716-2345-9,

G

Glucose homeostasis 33–49, 199, 335–337, 342, 351, 352, 361
Glucose intolerance 34–37, 40, 43, 45, 56, 349, 361
Glucose tolerance test
  hyperglycemic glucose clamp 341
  intravenous glucose tolerance test 36, 336–338, 351, 362
  oral glucose tolerance test 344–348
  standard mixed meal tolerance test 344–349
Glycogen 39, 129–130

H

High-fat diet (HFD) 4, 5, 8–11, 20, 23, 34, 36, 37, 41–43, 46, 54–57, 59–61
Hypercaloric diets 6

I

Insulin resistance (IR) 5, 11, 34, 36, 37, 40, 41, 44, 54, 94, 307, 342, 353
Insulin sensitivity 35, 37, 39, 41, 43, 44, 335–364
Insulin tolerance test
  euglycemic-hyperinsulinemic clamp 351–360
Intestinal microbiota 74, 76, 170
In vitro studies 45, 73, 76, 196, 268
In vivo studies 73, 76, 90

L

L-glutathione reduced 191
Lipid peroxidation
  malonaldehyde (MDA) 107–109, 111
  oxidative damage 107
Liver 4, 5, 39, 41, 43, 53–58, 60–63, 65, 66, 68, 74, 110, 115–117, 119–121, 123, 124, 129–136, 141, 142, 153, 188, 190, 193, 307–319, 351
Loss of appetite 210, 211, 216, 218–220

M

Metabolic syndrome 4, 5, 54, 58, 63, 147
Metabolic tolerance tests (MTTs) 34–40
Metabolomic
  blood 397–398, 402
  nuclear magnetic resonance spectroscopy 382, 384, 385, 396–398
  saliva 385, 395–398, 402
  tissue biopsy 386, 389
  urine 385, 394–398, 402
Metagenomics 171–173, 177–184
Metatranscriptomic analysis 172
Microbiome
  DNA extraction 177, 179
  DNA purification 179, 180
  gene amplicon sequencing 171, 172, 181
  next-generation sequencing (NGS) 171–173, 180
Minerals
  cell lysates 149, 165
  serum 147, 149, 150, 165
  tissue 147, 149, 165
Muscle 5, 41, 43, 45, 66, 74, 94, 129–136, 141, 142, 146, 240, 288, 297, 299–301, 307–310, 318, 319, 352, 353, 367, 373, 375, 381–402

N

Nonalcoholic fatty liver disease (NAFLD) 53–60, 63, 66–68
Non-esterified fatty acids (NEFA)
  chromatographic analysis 94–96, 98–100, 103
  colorimetric analysis 94, 97–98, 102
  enzymatic kits 97, 99–100
  plasma 93–104
  serum 93–104
  titrimetric analysis 94, 97–98, 101, 102
Normocaloric diet 3, 9
Nutritional anamnesis
  diet history questionnaire (DHQ) 211
  nutritional risk screening (NRS) 210
  simplified nutritional appetite questionnaire (SNAQ) 211, 216, 218, 220

O

Oxidative stress
  reactive oxygen species (ROS) 188
  serum 188
  tissue 146, 188
Oxygen uptake 367

P

Pyruvate tolerance test (PTT) 33–49

R

Resting energy expenditure (REE)
  basal energy expenditure 266
  indirect calorimetry (IC) 265–267, 269, 270, 286, 287

S

Short-chain fatty acids (SCFA)
  acetic acid 73, 74
  butyric acid 73

capillary electrophoresis (CE) 81
gas chromatography (GC) 80
liquid chromatography (LC) 79, 80, 87–89
propionic acid 73
Standard operating procedures (SOPs) 170
Steatohepatitis
nonalcoholic steatohepatitis (NASH) 53–60, 63, 67, 68
Swallowing 211, 213, 214, 216, 219, 221, 249, 251

T

Thiobarbituric acid reactive substances (TBARS) 107–113
Trace elements
cell lysates 165
serum 147, 149, 150, 165
tissue 147, 149, 165